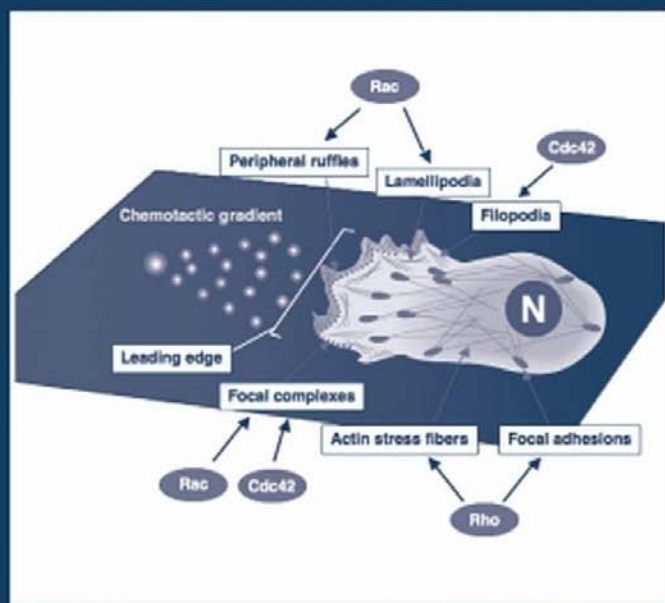


INTERNATIONAL  
REVIEW OF CELL AND  
MOLECULAR BIOLOGY

Edited by  
Kwang W. Jeon



Volume 287





VOLUME TWO EIGHTY SEVEN

INTERNATIONAL REVIEW OF  
**CELL AND MOLECULAR  
BIOLOGY**

# INTERNATIONAL REVIEW OF CELL AND MOLECULAR BIOLOGY

## *Series Editors*

GEOFFREY H. BOURNE 1949–1988  
JAMES F. DANIELLI 1949–1984  
KWANG W. JEON 1967–  
MARTIN FRIEDLANDER 1984–1992  
JONATHAN JARVIK 1993–1995

## *Editorial Advisory Board*

|                     |                     |
|---------------------|---------------------|
| ISAIAH ARKIN        | WALLACE F. MARSHALL |
| PETER L. BEECH      | BRUCE D. MCKEE      |
| ROBERT A. BLOODGOOD | MICHAEL MELKONIAN   |
| DEAN BOK            | KEITH E. MOSTOV     |
| KEITH BURRIDGE      | ANDREAS OKSCHE      |
| HIROO FUKUDA        | MANFRED SCHLIWA     |
| RAY H. GAVIN        | TERUO SHIMMEN       |
| MAY GRIFFITH        | ROBERT A. SMITH     |
| WILLIAM R. JEFFERY  | ALEXEY TOMILIN      |
| KEITH LATHAM        |                     |

VOLUME TWO EIGHTY SEVEN

# INTERNATIONAL REVIEW OF CELL AND MOLECULAR BIOLOGY

*EDITED BY*

**KWANG W. JEON**

*Department of Biochemistry  
University of Tennessee  
Knoxville, Tennessee*



**ELSEVIER**

AMSTERDAM • BOSTON • HEIDELBERG • LONDON  
NEW YORK • OXFORD • PARIS • SAN DIEGO  
SAN FRANCISCO • SINGAPORE • SYDNEY • TOKYO

Academic Press is an imprint of Elsevier



Front Cover Photography: Cover figure by Yoshiyuki Rikitake and Yoshimi Takai

Academic Press is an imprint of Elsevier  
525 B Street, Suite 1900, San Diego, CA 92101-4495, USA  
30 Corporate Drive, Suite 400, Burlington, MA 01803, USA  
32 Jamestown Road, London NW1 7BY, UK  
Radarweg 29, PO Box 211, 1000 AE Amsterdam, The Netherlands

First edition 2011

Copyright © 2011, Elsevier Inc. All Rights Reserved.

No part of this publication may be reproduced, stored in a retrieval system or transmitted in any form or by any means electronic, mechanical, photocopying, recording or otherwise without the prior written permission of the publisher

Permissions may be sought directly from Elsevier's Science & Technology Rights Department in Oxford, UK: phone (+44) (0) 1865 843830; fax (+44) (0) 1865 853333; email: [permissions@elsevier.com](mailto:permissions@elsevier.com). Alternatively you can submit your request online by visiting the Elsevier web site at <http://elsevier.com/locate/permissions>, and selecting *Obtaining permission to use Elsevier material*.

#### Notice

No responsibility is assumed by the publisher for any injury and/or damage to persons or property as a matter of products liability, negligence or otherwise, or from any use or operation of any methods, products, instructions or ideas contained in the material herein. Because of rapid advances in the medical sciences, in particular, independent verification of diagnoses and drug dosages should be made.

#### British Library Cataloguing in Publication Data

A catalogue record for this book is available from the British Library

#### Library of Congress Cataloging-in-Publication Data

A catalog record for this book is available from the Library of Congress

For information on all Academic Press publications  
visit our website at [elsevierdirect.com](http://elsevierdirect.com)

ISBN: 978-0-12-386043-9

PRINTED AND BOUND IN USA

11 12 13 14 10 9 8 7 6 5 4 3 2 1

Working together to grow  
libraries in developing countries

[www.elsevier.com](http://www.elsevier.com) | [www.bookaid.org](http://www.bookaid.org) | [www.sabrc.org](http://www.sabrc.org)

ELSEVIER

BOOK AID  
International

Sabre Foundation

# CONTENTS

*Contributors*

*ix*

|                                                                                                          |           |
|----------------------------------------------------------------------------------------------------------|-----------|
| <b>1. Structure and Functions of Aquaporin-4-Based Orthogonal Arrays of Particles</b>                    | <b>1</b>  |
| Hartwig Wolburg, Karen Wolburg-Buchholz, Petra Fallier-Becker, Susan Noell, and Andreas F. Mack          |           |
| 1. Introduction                                                                                          | 2         |
| 2. General Properties of OAPs and AQP4                                                                   | 3         |
| 3. OAPs and AQP4 in Cells Outside the Central Nervous System                                             | 8         |
| 4. OAPs and AQP4 in Cells of the Central Nervous System                                                  | 13        |
| 5. OAPs and AQP4 in Reactive Astrocytes, Glioma, and Inflammation                                        | 20        |
| 6. Conclusions and Outlook                                                                               | 28        |
| Acknowledgments                                                                                          | 29        |
| References                                                                                               | 29        |
| <b>2. Interpreting the Stress Response of Early Mammalian Embryos and Their Stem Cells</b>               | <b>43</b> |
| Y. Xie, A.O. Awonuga, S. Zhou, E.E. Puscheck, and D.A. Rappolee                                          |           |
| 1. Introduction                                                                                          | 47        |
| 2. Stress and Stress Enzymes                                                                             | 47        |
| 3. Stress Responses                                                                                      | 52        |
| 4. Roles of Stress Enzymes                                                                               | 61        |
| 5. Models and Lessons                                                                                    | 72        |
| 6. Summary, Significance, and Future Studies                                                             | 80        |
| Acknowledgments                                                                                          | 84        |
| References                                                                                               | 84        |
| <b>3. Directional Cell Migration: Regulation by Small G Proteins, Nectin-like Molecule-5, and Afadin</b> | <b>97</b> |
| Yoshiyuki Rikitake and Yoshimi Takai                                                                     |           |
| 1. Introduction                                                                                          | 98        |
| 2. Cell Movement                                                                                         | 99        |
| 3. Small G Proteins and Leading Edge Structures                                                          | 106       |
| 4. Nectins, Necls, and Afadin                                                                            | 111       |

|                                                                                                                  |            |
|------------------------------------------------------------------------------------------------------------------|------------|
| 5. Crosstalk between Growth Factor Receptors and Integrins                                                       | 119        |
| 6. Regulation of Directionality of Cell Movement                                                                 | 122        |
| 7. Regulation of Dynamics of Cyclical Activation and Inactivation of Small G Proteins by Afadin                  | 125        |
| 8. Concluding Remarks                                                                                            | 129        |
| Acknowledgments                                                                                                  | 130        |
| References                                                                                                       | 130        |
| <b>4. Mitochondrial RNA Import: From Diversity of Natural Mechanisms to Potential Applications</b>               | <b>145</b> |
| François Sieber, Anne-Marie Duchêne, and Laurence Maréchal-Drouard                                               |            |
| 1. Introduction                                                                                                  | 146        |
| 2. RNA Import in Protozoa                                                                                        | 149        |
| 3. RNA Import in Plants                                                                                          | 156        |
| 4. RNA Import in Fungi                                                                                           | 161        |
| 5. RNA Import in Metazoa                                                                                         | 166        |
| 6. Potential Applications of Macromolecule Import                                                                | 173        |
| 7. Conclusion and Prospects                                                                                      | 181        |
| References                                                                                                       | 182        |
| <b>5. New Insights into Vinculin Function and Regulation</b>                                                     | <b>191</b> |
| Xiao Peng, Elke S. Nelson, Jessica L. Maiers, and Kris A. DeMali                                                 |            |
| 1. Introduction                                                                                                  | 192        |
| 2. Vinculin Structure                                                                                            | 193        |
| 3. Autoinhibited Conformation and Vinculin Activation                                                            | 196        |
| 4. Biological Functions                                                                                          | 201        |
| 5. Modes of Vinculin Regulation                                                                                  | 211        |
| 6. Emerging Themes and Concepts                                                                                  | 214        |
| 7. Interplay Between Cell–Cell and Cell–Matrix Adhesion: Vinculin in Development and Cardiomyopathy              | 219        |
| 8. Conclusions                                                                                                   | 222        |
| Acknowledgments                                                                                                  | 222        |
| References                                                                                                       | 222        |
| <b>6. Nuclear Pore Complex: Biochemistry and Biophysics of Nucleocytoplasmic Transport in Health and Disease</b> | <b>233</b> |
| T. Jamali, Y. Jamali, M. Mehrbod, and M. R.K. Mofrad                                                             |            |
| 1. Introduction                                                                                                  | 234        |
| 2. What Drives Cargo Transport Through the NPC?                                                                  | 240        |
| 3. Nucleocytoplasmic Transport Pathway                                                                           | 265        |
| 4. NPC and Diseases                                                                                              | 267        |
| 5. Conclusion                                                                                                    | 276        |
| Acknowledgments                                                                                                  | 276        |
| References                                                                                                       | 277        |

---

|                                                                                                |            |
|------------------------------------------------------------------------------------------------|------------|
| <b>7. Dynamic Microtubules and the Texture of Plant Cell Walls</b>                             | <b>287</b> |
| Clive Lloyd                                                                                    |            |
| 1. Introduction                                                                                | 288        |
| 2. Microtubules                                                                                | 294        |
| 3. The Paradoxical Outer Epidermal Wall                                                        | 302        |
| 4. Microtubule Alignment and Twisted Growth                                                    | 304        |
| 5. Microtubule and Microfibril Coalignment                                                     | 306        |
| 6. (Re)interpreting Wall Patterns                                                              | 314        |
| 7. A New Dynamic Model for the Influence of Microtubules<br>on the Texture of Plant Cell Walls | 319        |
| 8. Concluding Remarks                                                                          | 321        |
| Acknowledgments                                                                                | 322        |
| References                                                                                     | 322        |
| <br><i>Index</i>                                                                               | <br>331    |



This page intentionally left blank

# CONTRIBUTORS

## **A.O. Awonuga**

Department of Obstetrics and Gynecology, Wayne State University School of Medicine, Detroit, Michigan, USA

## **Kris A. DeMali**

Department of Biochemistry, University of Iowa Roy J. and Lucille A. Carver College of Medicine, Iowa City, Iowa, USA

## **Anne-Marie Duchêne**

Institut de Biologie Moléculaire des Plantes, UPR 2357-CNRS, Université de Strasbourg, Strasbourg, France

## **Petra Fallier-Becker**

Institute of Pathology, University of Tübingen, Tübingen, Germany

## **T. Jamali**

Department of Bioengineering, University of California, Berkeley, California, USA

## **Y. Jamali**

Department of Bioengineering, University of California, Berkeley, California, USA

## **Clive Lloyd**

Department of Cell and Developmental Biology, John Innes Centre, Norwich, United Kingdom

## **Andreas F. Mack**

Institute of Anatomy, University of Tübingen, Tübingen, Germany

## **Jessica L. Maiers**

Department of Biochemistry, University of Iowa Roy J. and Lucille A. Carver College of Medicine, Iowa City, Iowa, USA

## **Laurence Maréchal-Drouard**

Institut de Biologie Moléculaire des Plantes, UPR 2357-CNRS, Université de Strasbourg, Strasbourg, France

## **M. Mehrbod**

Department of Bioengineering, University of California, Berkeley, California, USA

## **M.R.K. Mofrad**

Department of Bioengineering, University of California, Berkeley, California, USA

**Elke S. Nelson**

Department of Biochemistry, University of Iowa Roy J. and Lucille A. Carver College of Medicine, Iowa City, Iowa, USA

**Susan Noell**

Clinics of Neurosurgery, Medical School, University of Tübingen, Tübingen, Germany

**Xiao Peng**

Department of Biochemistry, University of Iowa Roy J. and Lucille A. Carver College of Medicine, Iowa City, Iowa, USA

**E.E. Puscheck**

Department of Obstetrics and Gynecology, Wayne State University School of Medicine, Detroit, Michigan, USA

**D.A. Rappolee**

CS Mott Center for Human Growth and Development; Department of Obstetrics and Gynecology; Program for Reproductive Sciences; Department of Physiology; Institute for Environmental Health and Safety; Karmanos Cancer Institute, Wayne State University School of Medicine, Detroit, Michigan, USA; and Department of Biology, University of Windsor, Windsor Ontario, Canada

**Yoshiyuki Rikitake**

Department of Biochemistry and Molecular Biology; Department of Internal Medicine, Kobe University, Graduate School of Medicine, Kobe, Japan

**François Sieber**

Institut de Biologie Moléculaire des Plantes, UPR 2357-CNRS, Université de Strasbourg, Strasbourg, France

**Yoshimi Takai**

Department of Biochemistry and Molecular Biology, Kobe University, Graduate School of Medicine, Kobe, Japan

**Karen Wolburg-Buchholz**

Institute of Pathology, University of Tübingen, Tübingen, Germany

**Hartwig Wolburg**

Institute of Pathology, University of Tübingen, Tübingen, Germany

**Y. Xie**

CS Mott Center for Human Growth and Development; Department of Obstetrics and Gynecology, Wayne State University School of Medicine, Detroit, Michigan, USA

**S. Zhou**

CS Mott Center for Human Growth and Development; Program for Reproductive Sciences, Wayne State University School of Medicine, Detroit, Michigan, USA

# STRUCTURE AND FUNCTIONS OF AQUAPORIN-4-BASED ORTHOGONAL ARRAYS OF PARTICLES

Hartwig Wolburg,\* Karen Wolburg-Buchholz,\*  
Petra Fallier-Becker,\* Susan Noell,<sup>†</sup> and Andreas F. Mack<sup>‡</sup>

## Contents

|                                                                                       |    |
|---------------------------------------------------------------------------------------|----|
| 1. Introduction                                                                       | 2  |
| 2. General Properties of OAPs and AQP4                                                | 3  |
| 3. OAPs and AQP4 in Cells Outside the Central Nervous System                          | 8  |
| 4. OAPs and AQP4 in Cells of the Central Nervous System                               | 13 |
| 4.1. Structure of membranes of mammalian astrocytes and related cells <i>in vivo</i>  | 13 |
| 4.2. Structure of membranes of mammalian astrocytes and related cells <i>in vitro</i> | 17 |
| 5. OAPs and AQP4 in Reactive Astrocytes, Glioma, and Inflammation                     | 20 |
| 5.1. Loss of polarity                                                                 | 20 |
| 5.2. AQP4, agrin, and the blood–brain barrier                                         | 21 |
| 5.3. AQP4 and the dystrophin–dystroglycan complex                                     | 24 |
| 5.4. AQP4-driven water flux in brain                                                  | 25 |
| 5.5. AQP4 and brain tumor                                                             | 26 |
| 5.6. AQP4 and inflammation                                                            | 27 |
| 6. Conclusions and Outlook                                                            | 28 |
| Acknowledgments                                                                       | 29 |
| References                                                                            | 29 |

## Abstract

Orthogonal arrays or assemblies of intramembranous particles (OAPs) are structures in the membrane of diverse cells which were initially discovered by means of the freeze-fracturing technique. This technique, developed in the 1960s, was important for the acceptance of the fluid mosaic model of the biological membrane. OAPs were first described in liver cells, and then in

\* Institute of Pathology, University of Tübingen, Tübingen, Germany

<sup>†</sup> Clinics of Neurosurgery, Medical School, University of Tübingen, Tübingen, Germany

<sup>‡</sup> Institute of Anatomy, University of Tübingen, Tübingen, Germany

parietal cells of the stomach, and most importantly, in the astrocytes of the brain. Since the discovery of the structure of OAPs and the identification of OAPs as the morphological equivalent of the water channel protein aquaporin-4 (AQP4) in the 1990s, a plethora of morphological work on OAPs in different cells was published. Now, we feel a need to balance new and old data on OAPs and AQP4 to elucidate the interrelationship of both structures and molecules. In this review, the identity of OAPs as AQP4-based structures in a diversity of cells will be described. At the same time, arguments are offered that under pathological or experimental circumstances, AQP4 can also be expressed in a non-OAP form. Thus, we attempt to project classical work on OAPs onto the molecular biology of AQP4. In particular, astrocytes and glioma cells will play the major part in this review, not only due to our own work but also due to the fact that most studies on structure and function of AQP4 were done in the nervous system.

*Key Words:* Astrocytes, Blood–brain barrier, Freeze-fracturing, Aquaporin-4, Water channel. © 2011 Elsevier Inc.

## 1. INTRODUCTION

The scientific histories of the so-called orthogonal (square) arrays (assemblies) of intramembranous particles (OAPs) on the one hand, and that of the aquaporins on the other hand, have different roots: the OAPs were first described in liver cells (Kreutziger, 1968). Staehelin (1972) described OAPs as a third type of gap junctions in intestinal epithelial cells. This characterization was refuted by Rash et al. (1974) by recognizing OAPs as a structure by its own. The following years were marked by exclusively descriptive morphological work on OAPs in different tissues without any knowledge about the molecular identity. These tissues included muscle cells, epithelial cells in the kidney, stomach, intestine, and in particular, in the nervous system, the macroglial cells such as astrocytes, retinal Müller glial cells, ependymal cells, and tanycytes. In 1986 and 1988, the independent groups of Gheorghe Benga and Peter Agre, respectively, discovered the water channel proteins which later were called aquaporins. It became not immediately clear that the family member aquaporin-4 (AQP4) is being the main constituent of the OAPs. This recognition grew gradually and was still not included in the comprehensive review of the literature on OAPs by Wolburg (1995). Since then, however, we have observed an explosion of data on OAPs and AQP4. In particular, the astrocytes were predominantly addressed as AQP4 and OAP expressing cells. More than 15 years later, we take a second look on the growing literature on OAPs and AQP4.

The detection of water-specific membrane channels in red blood cells belongs to the fundamental discoveries in biology of the twentieth century

(Benga et al., 1986a,b; Denker et al., 1988; Preston et al., 1992). The aquaporins mediate water movements between the intracellular, interstitial, vascular, and ventricular compartments which are under the strict control of osmotic and hydrostatic pressure gradients and can be regulated independently of solute transport (Nase et al., 2008; Pasantes-Morales and Cruz-Rangel, 2010). This function is conserved in animals, plants, and bacteria. At least 13 isoforms of aquaporins have been identified in mammals, designated AQP0 through AQP12 (Zelenina, 2010). Although most aquaporins, including AQP4, are selectively permeable to water, AQP3, AQP7, and AQP9 (aquaglyceroporins) are also permeable to urea and glycerol (Ma et al., 1997b). In mammals, aquaporins are involved in renal water absorption, generation of pulmonary secretions, lacrimation, secretion, and reabsorption of cerebrospinal fluid and aqueous humor, and development of edema (King et al., 2004). At the time of discovery, water channel proteins were named, such as CHIP28 (channel-forming integral membrane protein of 28 kDa; Hasegawa et al., 1994; Nielsen et al., 1993) for AQP1, GLIP (glycerol intrinsic protein; Frigeri et al., 1995) for AQP3, or MIWC (mercurial insensitive water channel; Yang et al., 1996) for AQP4. The major intrinsic protein (MIP) of the lens forms giant lattices in freeze-fracture replicas (Kistler and Bullivant, 1989). It has been identified as a water channel protein as well, now called AQP0 (King et al., 2004), and constitutes about 50% of the proteins in the fiber cells of the lens. Therefore, AQP0 and AQP4 are the only aquaporins to be visualized directly in the electron microscope. It has been pointed out that AQP0 performs not only water transport but also, probably more important, cell-to-cell adhesion in order to mediate lens transparency (Kumari and Varadaraj, 2009).

In the following sections, we will describe OAPs and AQP4 in cells outside and inside the nervous system, but it will be impossible to completely cover the literature due to the overwhelming plethora of data. In particular, many recent studies about AQP4 do not take into consideration or are not aware of the morphological aspect of this water channel as OAPs. Those studies will not be compiled preferentially in this chapter. Due to space limitation, only some selected original papers or prominent reviews will be cited considering cells of the muscle, urinary, intestinal, pulmonary, and auditory systems, before focusing on astrocytes and glioma cells in the CNS.

## 2. GENERAL PROPERTIES OF OAPs AND AQP4

It is now generally accepted that AQP4 constitutes the OAPs. This was shown by several lines of evidence, the absence of OAPs in astrocytes of AQP4-deficient mice (Verbavatz et al., 1997), the formation of OAPs in

Chinese hamster ovary (CHO) cells stably transfected with AQP4 (Yang et al., 1996), and the immunogold fracture-labeling technique directly showing that AQP4 is a component of the arrays (Rash et al., 1998). Moreover, Nielsen et al. (1997) were able to demonstrate by immunogold labeling that the distribution of the AQP4-related immunoreactivity in the retinal Müller glial cells was identical to that of the OAPs and was restricted to glial membranes.

Aquaporins, in general, form tetrameric protein complexes within the membrane plane. On the molecular level, each monomer represents a water channel proper. On the electron microscopical level, a structural subunit of the OAP measuring about  $7 \times 7$  nm represents a tetramer (Fig. 1.1). The number of subunits (tetramers) per OAP can change between 4 and more than 100. AQP4 was described to occur as heterotetramers reflecting the relative expression level of the different splice variants (M1 and M23; Neely et al., 1999, see below). Whereas other aquaporins form single tetramers, AQP0 (see above) and AQP4 are constituted as higher-order complexes arranged in a variable number of tetramers (Engel et al., 2008; Nicchia et al., 2008, 2010; Sorbo et al., 2008). The atomic structure of AQP4 was determined by electron crystallography of double-layered, two-dimensional crystals (Hiroaki et al., 2006; Tani et al., 2009; Fig. 1.1). These studies, together with the analyses of AQP4 mutations, enabled the authors to explain the relationship between the molecular structure of the splice variants and their water gating mechanism.

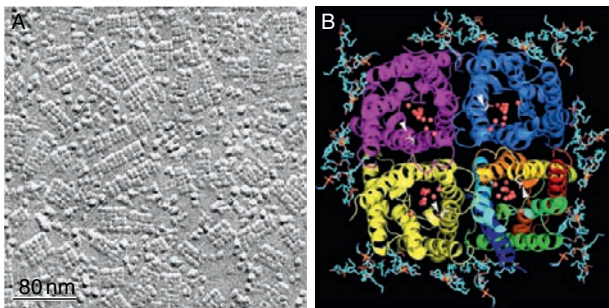


**Figure 1.1** (A) Freeze-fracture replica of a perivascular astrocytic endfoot from the mouse brain (from a collaboration with Dr. C. Betsholtz, Karolinska Institute, Stockholm, Sweden). (B) Structure of the AQP4 molecule. The protein is presented as a tetramer viewed from the cytoplasmic side. The ribbon diagram of the lower-right monomer shows the protein from blue (N-terminus) to red (C-terminus). The water molecules are shown as red spheres. Note that one tetramer corresponds to one particle or subunit in the square array in (A). From Tani et al. (2009), with permission.

The most important splice variants of AQP4 are the M1 isoform (323 amino acids long) and the M23 isoform (22 amino acids shorter at the N-terminus than M1; Jung et al., 1994; Fig. 1.2A). M1 and M23 were also termed AQP4a and AQP4c, respectively (Moe et al., 2008). The other four isoforms are not considered further in this review, because three of them, AQP4b, d, and f, were localized intracellular, and AQP4e expression was not specified in terms of cell type. The M23 isoform exhibits a much stronger water transport capacity than the M1 isoform (Silberstein et al., 2004). Both isoforms elicit distinct OAP morphologies: if CHO-K1 cells were transfected with AQP4 M1, no or very small arrays were found in the membranes, whereas if AQP4 M23 was transfected, large raft-like lattices were formed (Fig. 1.2B). If both isoforms were transfected together, OAPs were formed which strongly resembled those typical for astrocytes *in vivo* (Furman et al., 2003). This would mean that the ratio of the isoforms determines the size of the resulting structure as seen in the freeze-fracture replica, strongly suggesting that both isoforms coexist in one array (Nicchia et al., 2010). However, this did not explain why different lengths of the N-terminus of AQP4 induced different sizes of OAPs.

In an elegant approach using a combination of transfections, mutations, and fracture-immunogold-labeling experiments, Suzuki et al. (2008) reported on the relationship between the length of N-terminal deletion and the ability of the cell to form OAPs. They constructed a series of N-terminal deletion mutants and replaced the last amino acid of the appropriate truncated molecule by methionine, thus getting artificial M6, M11, M16, etc. isoforms. The shortest isoforms (M18 up to M23 and even the artificial mutant M27), if transfected in CHO cells, formed arrays, whereas mutants with deletions of less than 17 residues did not form OAPs. However, if both cysteines at positions 13 and 17 of AQP4 M1 were substituted by alanine (AQP4M1/C13,17A), OAPs were formed readily (Suzuki et al., 2008). The interesting point is that just these cysteine residues are palmitoylated, suggesting that palmitoylation may be involved in the regulation of AQP4 assembly in the membrane. Using the novel technology of quantum dot single particle tracking visualizing AQP4 dynamics in live cells (Crane and Verkman, 2009a; Crane et al., 2008), Crane et al. (2009) supported the view that posttranslational palmitoylation may cause OAP disruption.

The basis of the quantum dot single particle tracking is the evaluation of trajectories of antibody-coated quantum dots recognizing anti-c-myc tagged molecules like AQP4 by means of fluorescence microscopy of cultured cells (Crane et al., 2008). The rationale was the expectation that membrane proteins known to assemble in small clusters like AQP4 M1 would diffuse within the membrane plane with a larger diffusion coefficient than membrane proteins known to assemble in large clusters like AQP4 M23 (Fig. 1.2C and D). Indeed, AQP4 M1 diffused freely with a diffusion coefficient of  $5 \times 10^{-10} \text{ cm}^2/\text{s}$ , corresponding to  $15 \mu\text{m}$  in 5 min.



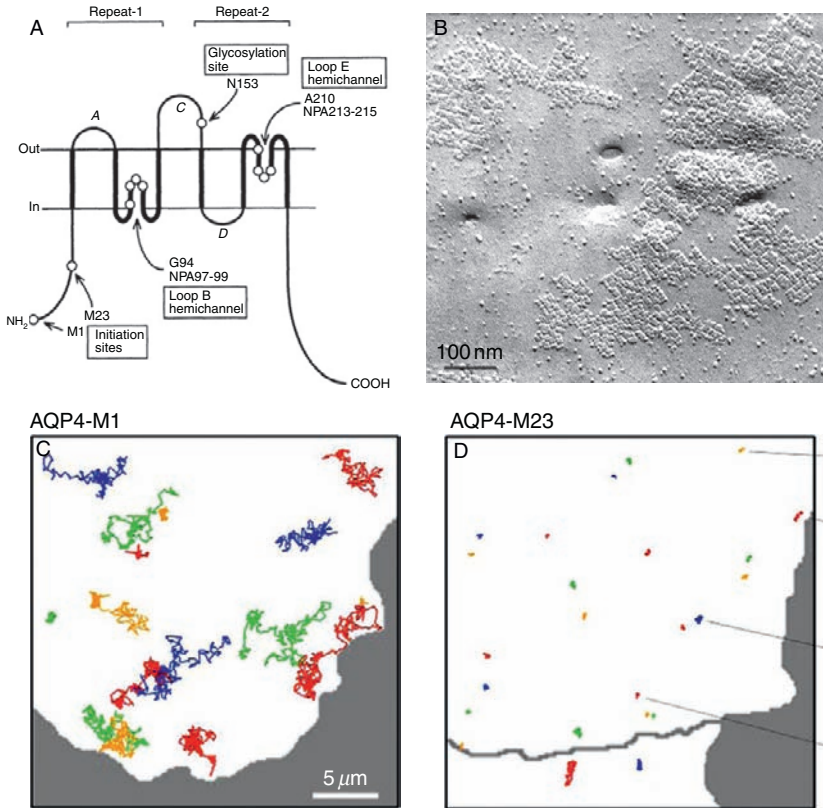


**Figure 1.2** (A) Proposed membrane topology of AQP4, comprising six presumed bilayer-spanning domains and five connecting loops. At the N-terminus, the initiation sites at methionine 1 and 23 are shown. The resulting splice variants M1 and M23 are 323 and 301 amino acids long, respectively. From Jung et al. (1994), with permission. (B) Freeze-fracture replica of an HEK cell transfected with the M23 isoform of AQP4. Huge lattices are formed. From a collaboration with Prof. Vanda Lennon, Mayo Clinics, Rochester, USA. (C and D) Time-lapse single particle tracking of quantum-dot-labeled AQP4 at 1 Hz for 6 min. Representative trajectories superimposed on cellular profiles of COS-7 cells expressing AQP4-M1 (C) and AQP4-M23 (D). The M1 isoform, although longer, does not form large clusters leading to higher mobility in the membrane plane when compared to the M23 isoform which forms large aggregates being much more immobile. From Crane et al. (2008), with permission.

The short AQP4 M23 isoform was found to be much more immobile with a diffusion coefficient of  $6 \times 10^{-11} \text{ cm}^2/\text{s}$ , moving only  $0.6 \mu\text{m}$  in 5 min (Crane et al., 2008). Regarding the palmitoylation as a regulator of AQP4 assembly, Crane et al. (2009) showed a diffusion of AQP4 M1C13A/C17A (the palmitoylation-null mutant due to cysteine-alanine exchange) which

was in the same range as that of native M1, when expressed alone. However, when coexpressed with M23, the M1C13A/C17A mutant became largely immobilized as seen for M23 alone. Thus, palmitoylation deficiency resulted in immobilization of AQP4 (and therefore assembly of OAPs) only in the presence of M23.

However, there was a contradiction between the Fujiyoshi group (Suzuki et al., 2008) and the Verkman group (Crane and Verkman, 2009b; Crane et al., 2009) interpreting the effect of palmitoylation. In the palmitoylation-null mutant (M1C13A/C17A), the first group observed OAPs in freeze-fracture replicas. The second group did not find OAPs (or quantum dot immobility, respectively) at 37 °C, but at reduced temperatures at 10 °C (Crane and Verkman, 2009b). The authors discussed this temperature effect in the way that palmitoylation only partially destabilizes OAPs by affecting the ability of M1 to hinder OAP formation, when M1 and M23 are coexpressed, as in native glial membranes. As the temperature-dependency of OAP formation may be important for fundamental understanding of the biophysics and energetics of the OAP assembly, the relevance for astroglial physiology *in situ* may be questioned. At present, it seems that the results gained with the freeze-fracture and quantum dot technologies do not correspond completely. In addition, there is another method believed to demonstrate square arrays or OAPs, the blue native PAGE (BN-PAGE; Nicchia et al., 2010; Rossi et al., 2010; Sorbo et al., 2008). This method allows evaluating the grade of molecular complexes. However, neither the quantum dot nor the BN-PAGE technology is able to give any information about the OAPs, because the hallmark of this complex is morphological, namely to be orthogonal and to form differently sized arrays. Therefore, the freeze-fracture method is still a valuable method to allow direct statements on the molecular architecture of the OAPs in cell membranes.

Tetrameric AQP4 is not inserted into the membrane as a supramolecular assembly of water channel molecules independently. At least in the case of astrocytes, AQP4 molecules form functional complexes with other membrane proteins such as the dystrophin-dystroglycan complex (DDC; Haenggi and Fritschy, 2006; see below Section 5.3). Whether this is a general property of OAPs in all organs is not clear to date. Nicchia et al. (2008) used two different dystrophin-deficient mice strains, the DP71 KO which lacks the glial dystrophin gene product, and the mdx3cv mice which show a drastic reduction of all dystrophin isoforms. The authors were able to identify a large molecular weight AQP4 pool (>1 MDa) dependent of dystrophin localized in perivascular astrocytes, and a smaller molecular weight AQP4 pool (500 kDa) independent of dystrophin localized in the granular cell layer of the cerebellum and in the subpial astroglial endfeet and ependymal cells. This finding may suggest that the composition of AQP4 pools in glial membranes concerned with the management of the

blood–brain barrier (BBB) is under the control of dystrophin, in contrast to other (subpial) membrane domains not involved in the BBB (see Section 5.2). Nicchia et al. (2010) postulated on the basis of blue native SDS–PAGE analysis of a variety of organs that the differently sized AQP4 pools differ in their M1/M23 ratio by enrichment of M1 in the low molecular and M23 in the high molecular AQP4 pool. This would mean that subpial/perivascular astroglial endfeet would be dominated by an increased/decreased M1/M23 ratio, respectively, and that M23, more than M1, would be of high significance for the stability of the BBB.

### **3. OAPs AND AQP4 IN CELLS OUTSIDE THE CENTRAL NERVOUS SYSTEM**

In *skeletal muscle cells*, OAPs were first detected by Rash and Ellisman (1974). In the sarcolemma of rat diaphragm myofibers, the authors determined the number and distribution of OAPs in the membrane area immediately surrounding a neuromuscular endplate. In the subjunctional membrane, OAPs were not found, but with increasing distance from the junction, the density of OAPs increased to more than  $50 \mu\text{m}^{-2}$ . However, the absence of OAPs in the subjunctional membrane does not appear to be a general feature of skeletal muscle cells. In the frog sartorius muscle, Heuser et al. (1974) found OAPs in muscle membranes beneath nerve terminals. Ellisman et al. (1976) compared fast and slow twitch muscle fibers of the rat and found a higher OAP density in the fast extensor digitorum longus (EDL) muscle than in the slow soleus muscle. The observation that after reinnervation of the slow soleus muscle by the nerve from the fast EDL muscle, the OAP density in the soleus muscle increases to values typical for the EDL muscle, suggested that the OAP density in the sarcolemma is neuronally regulated (Ellisman et al., 1978). However, simple denervation does not induce the disappearance of OAPs (Sirken and Fischbeck, 1985; Tachikawa and Clementi, 1979). Moreover, the decrease of OAP density in Duchenne dystrophy suggested a certain independence of the expression of OAPs from neuronal influences (Schotland et al., 1977, 1981; Wakayama et al., 1984). The same principle was described for the Fukuyama-type congenital muscular dystrophy (Wakayama et al., 1985, 1986), the X chromosome-linked muscular dystrophy (Shibuya and Wakayama, 1991), and the murine muscular dystrophy (Ellisman, 1981).

Frigeri et al. (1995) were the first to correlate the OAPs with the MIWC, which later was identified as the water channel protein AQP4 (Frigeri et al., 1998). In skeletal muscle cells, Shibuya et al. (2006) identified the OAP structure with AQP4 by using anti-AQP4 labeling of freeze-fracture replicas. The decrease of OAPs in muscle diseases as cited above,

and recently summarized by Wakayama (2010), was correlated with a reduction of AQP4 on the protein level in muscle diseases including human Duchenne muscle dystrophy (DMD) and mdx mice, the animal model of DMD (Assereto et al., 2008; Au et al., 2008; Frigeri et al., 2001, 2002; Shibuya et al., 1997; Wakayama et al., 2002). However, whereas in DMD, the reduction of AQP4 protein synthesis was due to decreased AQP4 transcription (Au et al., 2008; Wakayama et al., 2002), the situation in mdx mice seemed to be different: Frigeri et al. (2001) observed a normal level of AQP4 mRNA with reduced amount of AQP4 protein, suggesting that the level of protein synthesis was downregulated independently of the rate of transcription.

In the *urinary system*, Humbert et al. (1975) and Orci et al. (1981) described OAPs in membranes of light (principal) cells of the rat kidney collecting tubules. OAPs were observed only in lateral and basal membranes of these cells. Brown and Orci (1988) reported on a higher density in basal in comparison to lateral membranes. Searching for a possible role of OAPs in principal cells of the kidney collecting tubules, Nakamura and Nagano (1985) observed kidney cells of Brattleboro rats by means of freeze-fracturing. Brattleboro rats are vasopressin-deficient mutants, suffering from diabetes insipidus. The authors reported on an augmentation of OAP number in dehydrated rats and a diminution of OAP number in Brattleboro rats and concluded some role in water transport from the light cell to the basolateral extracellular space. Remarkably, the authors did this parallel to the discovery of aquaporins. However, there were contradictory results regarding the kinetics of OAP formation resulting in stabilization or destabilization depending on different time lengths of vasopressin treatment (Silberstein et al., 2004). This may be explained as the result of complex signaling processes from the vasopressin receptor-binding downstream to the gene expression of various AQP4 splice variants (Van Hoek et al., 2009). However, the main water channel regulated by vasopressin in the kidney is AQP2 (Nielsen et al., 2002). In the basolateral membranes of cells in the distal segment of the lamprey kidney, Hatae (1983) described OAPs which were essentially larger ( $10,000\text{--}40,000\text{ nm}^2$ ) than those in mammalian tissues ( $400\text{--}1300\text{ nm}^2$ ; Neuhaus, 1990). Since the M23 isoform of AQP4 develops such huge lattices after transfection in AQP4-deficient cells (Furman et al., 2003), it would be interesting whether or not these isoforms exist in the lamprey kidney. In any case, water transport in the kidney is not at all regulated by AQP4 alone, including its isoforms, but by other aquaporins as well (Nielsen et al., 2002).

In lateral membranes of *tracheal epithelium* cells of the guinea pig, Inoue and Hogg (1977) described OAPs. Carson et al. (1984) and Gordon (1985) studied OAPs in *bronchiolar epithelial Clara cells* of the golden hamster. In a number of different species, Bartels and Miragall (1986) described OAPs in basal membranes of *pneumocytes*. In contrast, in the comprehensive review

on aquaporins, King et al. (2004) described pneumocytes of both types as AQP4-negative. Instead, Verkman (2007) claimed that pneumocyte type I contained AQP5 and the type II AQP3. However, we observed alveolar cell type I, but not II, expressing both AQP4 and OAPs (Fig. 1.3A–C). The expression of AQP4 was substantially enhanced in nonsmall cell lung cancer cells by in-parallel disappearance of OAPs, suggesting an occurrence of AQP4 also in nonarray form under pathological conditions (Warth and

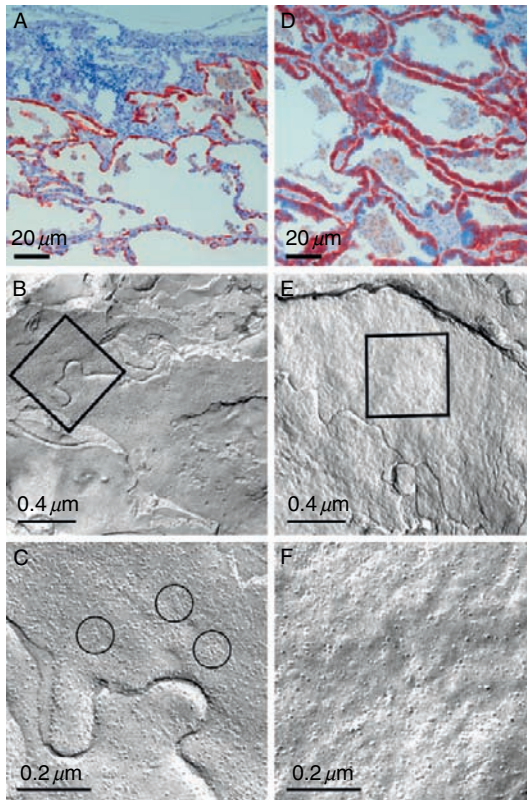


**Figure 1.3** (A) *Anti-AQP4 immunohistochemistry of normal lung tissue.* The water channel protein AQP4 is expressed frequently in alveolar cells. (D) shows a strong anti-AQP4 immunoreactivity in an adenocarcinoma of the same patient. (B), (C), (E), and (F) show freeze-fracture replicas of the same case. (B) and (C) show membranes of an alveolar cell type I of normal lung tissue. (C) is a detail out of (B) illustrating many orthogonal arrays of particles (OAPs). (E) and (F) show membranes of the adenocarcinoma cell membranes of the same patient, as shown in (D). (F) is a detail out of (E), clearly illustrating that in these membranes, no OAPs are present, although the membranes are strongly immunopositive for AQP4. From a collaboration with Dr. Arne Warth (Institute of Pathology, University of Heidelberg, Germany).

Wolburg, unpublished; Fig. 1.3D–F). In cultured airway epithelial cells, Friend (1987) found an irreversible loss of OAPs and concomitantly, an endocytic internalization of OAP-positive membranes. In this case, AQP4 expression is well known from these airway epithelial cells (Nielsen et al., 1997; Verkman, 2007).

In rat *ciliary epithelium*, Hirsch et al. (1988) found OAPs in nonpigmented cells. The comparison of membrane areas in contact and not in contact with the basal lamina showed that OAPs are equally distributed in both membrane domains. This is in obvious contrast to other cells, first of all astrocytes, where a strict correlation of OAP density with the attachment to the basal lamina exists (see below). In any case, AQP4 expression has been detected in ciliary epithelium (Levin and Verkman, 2006), but to a lower degree than AQP1 (Hamann et al., 1998).

Other epithelia known to carry OAPs are the *intestinal cells* in the rat (Staehein, 1972), and the rat *gastric parietal cell* (Bordi and Perrelet, 1978, Bordi et al., 1986). In intestinal epithelial cells of the mouse, we observed a strong AQP4-positive immunoreactivity (Fig. 1.4A), but only extremely few OAPs (Fig. 1.4B), demonstrating that AQP4 can occur in a non-OAP configuration even under physiological conditions. Parietal cells of the stomach and deep crypt epithelium of the ileum have been found to express AQP4 (Koyama et al., 1999; Ma and Verkman, 1999). Carmosino et al. (2001) reported on OAP rearrangements in cultured parietal cells as a response to histamine treatment. Concomitantly with a decrease of water permeability, histamine treatment results in an internalization of AQP4, followed by a phosphorylation of AQP4 (Carmosino et al., 2007).

In addition, even *enteric neurons* have been described to express AQP4 (Thi et al., 2008); however, OAPs were not shown to be formed in these cells so far. In contrast, OAPs were shown in sensory neurons of the olfactory system both of the tiger salamander (Miragall, 1983) and the newt (Usukura and Yamada, 1978), as well as in the rat *vomer nasal sensory neuron* (Miragall, 1983). In the *olfactory epithelium* of the rat, a strong anti-AQP4 staining of basal and supporting cells has been described, together with the secretory acinar and duct cells of the Bowman's glands (Ablimit et al., 2006; Wolburg et al., 2008; Fig. 1.4C). These cells were also positive for OAPs (Wolburg et al., 2008; Fig. 1.4D). The *satellite cells* of sensory and sympathetic ganglia (Elfvin and Forsman, 1978; Gotow et al., 1985; Pannese et al., 1977), and the *supporting cells* of the guinea pig vestibular sensory epithelium (Saito, 1988), were investigated, in the preaquaporin period, for the occurrence of OAPs. Since in the meantime it had been published that the AQP4-knockout mouse suffered from impaired hearing (Li and Verkman, 2001), and age-related changes of AQP4 expression went along with age-related hearing loss (Christensen et al., 2009), we compared the occurrence of AQP4 and OAPs in the organ of Corti of the rat. We found an identical localization of AQP4 and OAPs in the supporting cells of the

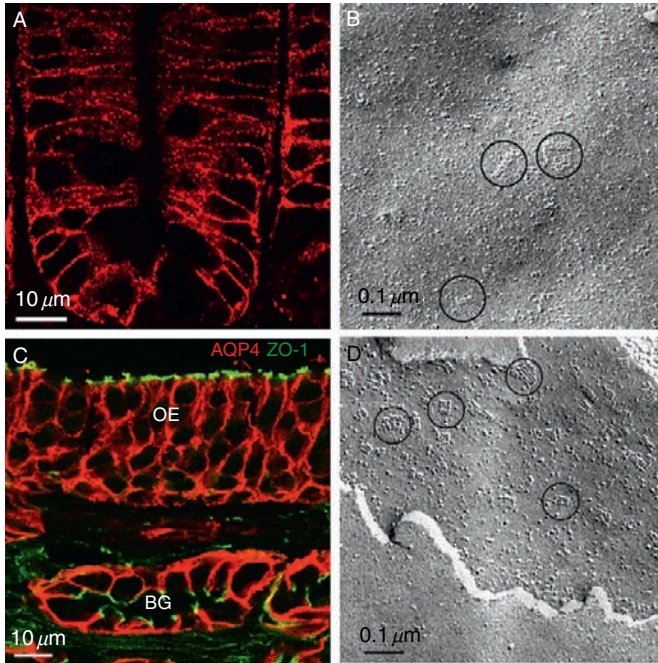


**Figure 1.4** (A) Immunohistochemistry of the epithelium in the jejunum of the mouse stained with an antibody against AQP4. (B) Freeze-fracture replica of the jejunum of the mouse showing only few orthogonal arrays of particles (OAPs; circled). The obvious discrepancy between the strong anti-AQP4 immunoreactivity and the low OAP density speaks in favor of the assumption that in this organ, AQP4 may occur mainly in the non-OAP configuration. (C) Immunohistochemistry of the olfactory epithelium of the rat stained with antibodies against AQP4 (in red) and the tight junction associated protein ZO-1 (in green). Both the olfactory epithelium (OE) and the Bowman's gland cells (BG) are strongly immunopositive for AQP4. (D) Freeze-fracture replica of the olfactory epithelial cells of the rat showing only few OAPs, again suggesting that AQP4 occurs in a non-OAP configuration.

cochlear duct. The medial part of the cochlear duct including the spiral limbus and the inner sulcus was immunoreactive for AQP4. In particular, medial interdental cells showed AQP4 labeling as well as the basal portion of inner sulcus cells. In the lateral part of the cochlear duct including the outer sulcus and the spiral ligament, Hensen cells showed very strong basolateral AQP4 labeling. Claudius cells exhibited basal AQP4-staining as well as outer sulcus cells with root processes protruding into the spiral ligament (Hirt et al., 2010; Lopez et al., 2007). It is highly impressive how the expression patterns of AQP4 and of other aquaporins are finely balanced in order to regulate the water shunt between the perilymphatic and the

endolymphatic spaces in the organ of Corti (Beitz et al., 1999; Hirt et al., 2010; Ishiyama et al., 2010).

## **4. OAPs AND AQP4 IN CELLS OF THE CENTRAL NERVOUS SYSTEM**

### **4.1. Structure of membranes of mammalian astrocytes and related cells *in vivo***

The largest body of data on OAPs has accumulated in the field of glial research. The first descriptions of astrocytic OAPs originated from Dermietzel (1973, 1974) and Landis and Reese (1974). A basic property of astrocytes is the polarized membrane structure; where astrocytic perivascular or subpial endfeet contact the basal lamina, the density of OAPs is very high; where the membrane loses contact with the basal lamina, the density of OAPs drastically drops to zero or at least to low values in the range of  $20 \mu\text{m}^{-2}$  (Figs. 1.5 and 1.6; Anders and Brightman, 1979; Gotow and Hashimoto, 1988; Landis and Reese, 1982; Massa and Mugnaini, 1982; Neuhaus, 1990; Nico et al., 1994; Rohlmann et al., 1992; Wujek and Reier, 1984).

This purely descriptive observation already suggested a mandatory role of the extracellular matrix within the basal lamina for the OAP-based configuration of the perivascular and superficial astrocytic endfeet (Fig. 1.6). This will be described in more detail below. Landis and Reese (1981a) pointed out that during the early postnatal development of the mouse, the number of OAPs in astroglial membranes steadily increases; most glial processes have acquired OAP densities in the adult range by postnatal day 14. Anders and Brightman (1979) quantified OAP densities from prenatal to postnatal stages, and found an increase of OAP number/area between embryonic day 20 and adult from 10 to about 400 OAPs/ $\mu\text{m}^2$ , respectively. These measurements roughly estimated an averaged OAP size of  $1000 \text{ nm}^2$  which seemed to be stable during postnatal development. However, the situation in the mouse brain development is different: in mice, no data concerning OAP densities in astrocytes before, at, and after birth are available in the literature. Noell et al. (2009) found a substantially higher OAP density in marginal endfoot membranes of wild-type C57BL/6 mice at postnatal day 1 in comparison with that in the age-matched rat (Anders and Brightman, 1979).

Also, retinal Müller cells as astroglia-related cells were in the center of neuroscientists' interest as a model system for glial cell physiology and biology (Reichenbach and Bringmann, 2010). The occurrence of Müller cell OAPs was originally described by Reale et al. (1974). Raviola (1977) realized the OAP-related polarity of these cells showing a high OAP density



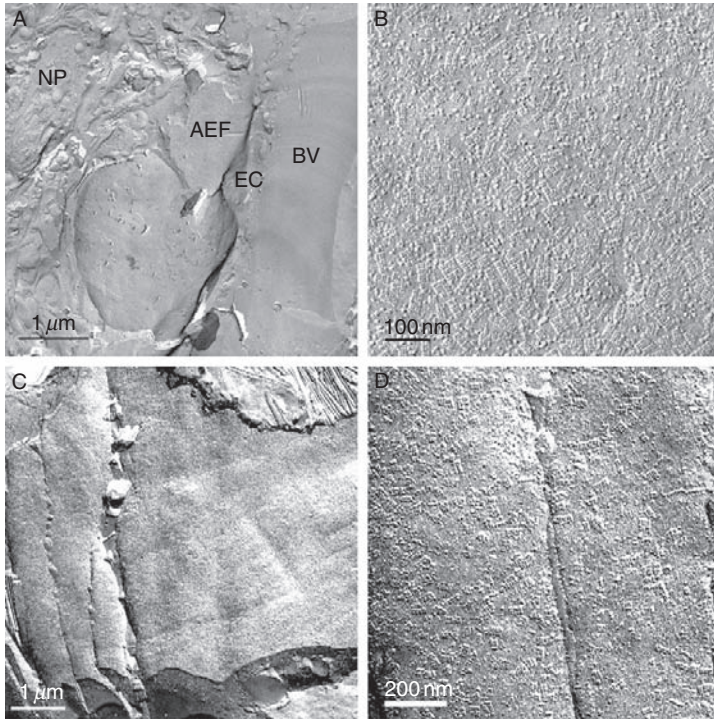


**Figure 1.5** Freeze-fracture replicas of astrocytic superficial (A and B) and perivascular (C and D) endfeet of mouse brain capillaries (A and B) and the rat optic nerve (C and D). NP: neuropil, AEF: astrocytic endfoot. (B) is a high-power view of the astrocytic endfoot indicated in (A) by AEF. EC: endothelial cell, BV: blood vessel. In (C), collagen fibers cover the glial endfeet incompletely, (D) is a detail of (C).

at the inner limiting membrane. Wolburg and Berg (1988) compared rabbit and mouse Müller cell membranes and concluded that a relationship may exist between vascularization of the retina and the amount and distribution of OAPs in the Müller cell. In the vascularized mouse retina, the Müller cell membranes carry OAPs on the entire surface and in higher density, in the paravitreal and perivascular endfeet. In the avascular rabbit retina, OAPs are confined to the paravitreal membranes. This is also true for the Müller cells of the guinea pig (Gotow and Hashimoto, 1989) and two reptile species (lizard and turtle; Sassoè Pognetto and Cantino, 1992). Interesting insights into the possible involvement of OAPs in general neurophysiology came from the comparative investigation of differently fast developing avian retinas.

In the chicken, the first OAPs appeared in the central retina at embryonic day 18, in the pigeon at day 6 after hatching (Bolz and Wolburg, 1992). Both time points of OAP appearance correlated to functional maturation of

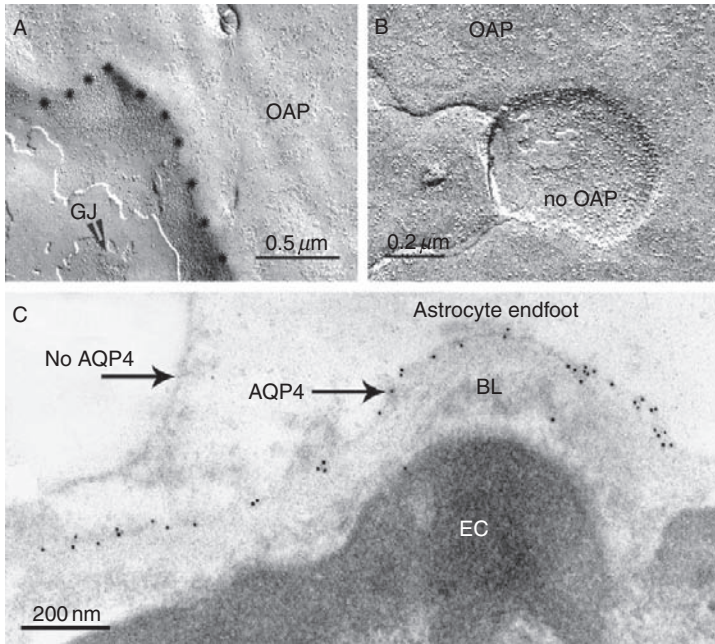


**Figure 1.6** (A) Freeze-fracture replica of a subpial astrocytic endfoot of the rat optic nerve showing the pronounced polarity of the astrocyte. Where the glial membrane contacts the basal lamina (right of the star line), the density of OAPs is high. Where the glial membrane has lost this contact diving into the neuropil (left of the star line) and is interconnected with an adjacent astrocyte by gap junctions (GJ), the density of OAPs is low. (B) Freeze-fracture replica of a paravascular astrocytic endfoot in the central retina of the rabbit. Again, where the glial membrane contacts the inner limiting membrane (ILM), many OAPs are present; where the membrane is displaced by an adjacent glial cell process, the OAP density drops to zero. This directly shows the role of the basal lamina for the architecture of the astrocytic membrane. (C) Electron microscopical immunogold labeling of the gliovascular complex using an antibody against AQP4. Only where the glial cell is in touch with the perivascular basal lamina (BL), immunogold particles are seen; where the glial membrane bends away from this contact, no gold particles indicating AQP4 are seen. EC: endothelial cell.

the respective retina such as the appearance of the electroretinogram. Since the astrocytes of fish and amphibia are devoid of OAPs (Kästner, 1987; Korte and Rosenbluth, 1981; Wolburg et al., 1983; Wujek and Reier, 1984), it appeared plausible that Müller cells of these species would reveal similar membrane architecture. It was therefore unexpected that the goldfish Müller cells were found to carry OAPs (Berg-von der Emde and Wolburg, 1989). To conclude that all Müller cells of vertebrates have OAPs, turned out to be wrong again. Frog (anuran) Müller cells do not reveal OAPs in endfoot membranes, but salamander (urodele) Müller cells

do (Wolburg et al., 1992). This is puzzling, as anuran muscle cells have OAPs (Franzini-Armstrong, 1984; Heuser et al., 1974). Hitherto, these strange heterogeneities just begin to be followed on the AQP4 level; in the zebrafish brain, Grupp et al. (2010) have described radial glial cells expressing AQP4, but lacking OAPs (Table 1.1).

There are other types of macroglial cells related to astroglial cells, namely, ependymal cells, choroid plexus epithelial cells, and tanycytes (Wolburg and Paulus, 2010; Wolburg et al., 2009). As astroglia-related cells, ependymal cells also form OAPs (Privat, 1977; Fig. 1.7A and B) and express AQP4 (Li et al., 2009). Privat (1977) found them in apical and lateral membranes, but not in basal membranes. Mack et al. (1987) contradicted this by showing OAPs also in basal membranes. The lack (or at least inconsistent presence) of both a basal lamina (see Leonhardt, 1970; Reichenbach and Robinson, 1995) and an OAP-related polarity in ependymal cells (without a basal lamina) again accentuates the importance of a basal lamina for polarity formation. Where ependymocytes have contact with a perivascular basal lamina, they are called tanycytes. By means of tight junctions, they form the blood–cerebrospinal fluid barrier in the circumventricular organs which are characterized by leaky blood vessels (Wolburg et al., 2009). Thus, tanycytes are polarized ependymal glial cells (Reichenbach and Wolburg, 2005).

A special study has been devoted to the relationship between OAPs and tight junctions (Mack et al., 1987). The authors observed that both structures are frequently inversely expressed. Fish astrocytes reveal tight junctions and no OAPs, while mammalian astrocytes reveal OAPs and no tight junctions (Wolburg et al., 1983). The olfactory glia of the rat has tight junctions but no OAPs (Mack and Wolburg, 1986; Wolburg et al., 2008). As well, choroid plexus epithelial cells have tight junctions but no OAPs (Fig. 1.7C; Wolburg and Paulus, 2010), and they express no AQP4 but AQP1 (MacAulay and Zeuthen, 2010; Nielsen et al., 1993). In ependymal cells, OAPs, but not (or only few) tight junction strands, are present. In the transitional zone between ependyma and choroid plexus, both structures coexist (Mack et al., 1987). As well, Nakai et al. (1980), Hatton and Ellisman (1982), and Gotow and Hashimoto (1982) showed a polarization of OAP distribution over the cellular surface: the apical and lateral membranes near the tight junctions were free of OAPs, the membranes beneath the basal lamina display a moderate number of OAPs. Thus, both structures seemed to be repelling each other: in tanycytes and pituicytes, the OAP formation was minimized in the area of tight junctions. However, the obvious mutual exclusion of OAPs and tight junctions seems to be a hallmark of astroglia-related cells, since classical epithelial cells such as intestinal cells, kidney collecting tubule cells, or Bowman's glandular cells in the olfactory system allow the coexpression of both structures (Humbert et al., 1975; Staehelin, 1972; Wolburg et al., 2008).

**Table 1.1** Occurrence of OAPs and AQP4 in different tissues

| Tissue/Species                                         | OAPs/<br>AQP4 | Reference                                                         |
|--------------------------------------------------------|---------------|-------------------------------------------------------------------|
| Astroglia fish                                         | -/+           | Wolburg et al. (1983), Grupp et al. (2010)                        |
| Astroglia mammals                                      | +/+           | Dermietzel (1973), Nagelhus et al. (1998)                         |
| Retinal Müller cell fish                               | +/?           | Berg-von der Emde and Wolburg (1989)                              |
| Retinal Müller cell amphibia (urodela)                 | +/?           | Wolburg et al. (1992)                                             |
| Retinal Müller cell amphibia (anura)                   | -/?           | Wolburg et al. (1992)                                             |
| Retinal Müller cell (reptile)                          | +/?           | Sassoè Pognetto and Cantino (1992)                                |
| Retinal Müller cell mammals                            | +/+           | Reale et al. (1974), Nagelhus et al. (1998)                       |
| Ependymal cells amphibia (anura)                       | -/?           | Korte and Rosenbluth (1981)                                       |
| Ependymal cell mammals                                 | +/+           | Privat (1977), Li et al. (2009)                                   |
| Satellite cells, mammals                               | +/?           | Pannese et al. (1977)                                             |
| Skeletal muscle cell, amphibian (anura)                | +/?           | Franzini-Armstrong (1984)                                         |
| Skeletal muscle cell, mammals                          | +/+           | Rash and Ellisman (1974), Frigeri et al. (1998)                   |
| Kidney collecting tubule cell                          | +/+           | Humbert et al. (1975), Nielsen et al. (2002)                      |
| Airway cells, mammals                                  | +/+           | Gordon (1985), Bartels and Miragall (1986), Nielsen et al. (1997) |
| Gastrointestinal system, mammals, epithelial cells     | +/+           | Stachelin (1972), Bordi et al. (1986), Ma and Verkman (1999)      |
| Gastrointestinal system, parietal cells                | +/+           | Bordi and Perrelet (1978), Carmosino et al. (2007)                |
| Olfactory system, mammals, epithelial cells            | +/+           | Ablimit et al. (2006), Wolburg et al. (2008)                      |
| Olfactory system, mammals, olfactory ensheathing cells | -/-           | Wolburg et al. (2008)                                             |
| Corti organ, mammals                                   | +/+           | Hirt et al. (2010)                                                |

#### 4.2. Structure of membranes of mammalian astrocytes and related cells *in vitro*

The most remarkable morphological difference between astrocytes *in vivo* and *in vitro* is the rearrangement of OAPs. In culture, the OAP-related polarity is lost; OAPs are randomly distributed over the surface of the cell

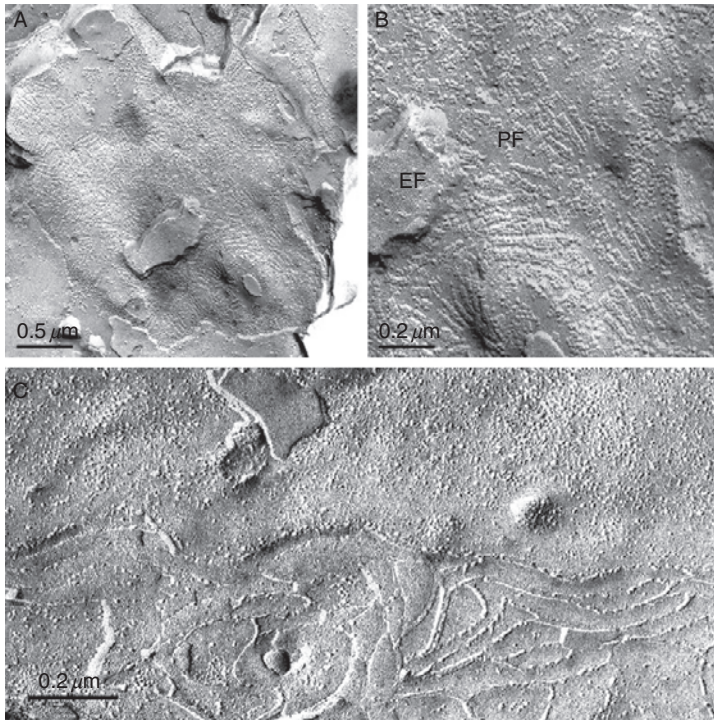


**Figure 1.7** Freeze-fracture replicas of endepidymal cells (A and B) and choroid plexus epithelial cells (C) of the rat. (B) is a detail from (A). The small shred of the E-face (EF) of an adjacent endepidymal cell shows that the P-face (PF) is not associated to a basal lamina; nevertheless, this membrane is extremely occupied by many OAPs. From a collaboration with Dr. Benedicte Dehouk, University of Lille, France. (C) The choroid plexus epithelial cell is tightly interconnected by tight junctions, but these cells do neither express AQP4 nor form OAPs.

(Landis and Weinstein, 1983; Landis et al., 1990, 1991; Massa and Mugnaini, 1985; Neuhaus, 1990; Wolburg et al., 1986). Since cultured astrocytes are devoid of a basal lamina, its absence seems to play a role in the loss of polarity. However, even by culturing astrocytes on laminin, Neuhaus (1990) found only a slight increase of the overall OAP density in astrocytes. Recently, we were able to show that the alteration of the extracellular matrix on which astrocytes were grown in culture, influenced the OAP-related architecture of the astrocyte membrane, but the polarity of astrocytes could not be reestablished (Fallier-Becker et al., 2011; Noell et al., 2007). Even in organotypic slice cultures of the rat visual cortex as used as a simplified model of the brain for testing electrophysiological parameters (Bolz et al., 1992), the astrocytes lost their OAP-related polarity, probably due to the absence of a basal lamina (Schulz-Süchting and Wolburg, 1994).

Wolburg et al. (1986) found a decrease in the OAP density following treatment with the basic fibroblast growth factor. Landis et al. (1990) observed a large variability of OAP expression in cultures grown in different lots of fetal calf serum. Landis et al. (1991) tested the influence of the glucocorticoid dexamethasone on the expression of OAPs in cultured astrocytes. They found that exposure of confluent cultures to 5  $\mu\text{M}$  dexamethasone led to an increase of the OAP density, whereas exposure of rapidly proliferating cells to the same dose did not result in an alteration of the OAP density. Tao-Cheng et al. (1992) investigated the influence of activators of the protein kinases A and C on the membrane architecture in cultured astrocytes and found that augmentation of the intracellular cAMP level by forskolin, isoproterenol, and 8-bromo-cAMP did increase the OAP density, whereas phorbol ester and phosphatidylcholine phospholipase C did not. Taken together, these results show that astrocytes even outside the brain are able to modify their membrane composition in multiple ways, in response to different factors, but that the extremely complex compartmentalization of astrocytes in the brain cannot be imitated in culture.

The stability of astrocytic OAPs has been investigated after circulatory arrest in the rat brain, by Landis and Reese (1981b). The authors reported on structural changes of OAPs in cells frozen 45 s after decapitation. Fifteen minutes after induction of selective cerebral ischemia, Cuevas et al. (1985) found a disappearance of astrocytic OAPs from the pericapillary endfeet membranes. Suzuki et al. (1984) observed an increasing rate of disintegration of OAPs which preceded the swelling of perivascular astrocytic processes following global cerebral ischemia. In contrast to the study of Cuevas et al. (1985), still 11% of astrocytic processes contained large quantities of regular OAPs even after 60 min ischemia. Neuhaus et al. (1990) showed that in pieces of mouse brain which were put in a moist chamber for 2 h at 20 °C, astroglial OAPs remained quite normal. At 37 °C, the OAPs changed their morphology already 40 min after circulatory arrest by forming large lattices.

Taken together, the stability of OAPs does not seem generally to be low as was assumed by Landis and Reese (1981b). Possibly, their sensitivity to energetic depletion increases with their statistical lifetime. Anders and Pagnanelli (1979) and Anders and Brightman (1982) claimed that the biological half-life time of the OAPs is 3 h. Provided that the serious energetic insufficiency produced in the long-lasting incubation of brain tissue outside the body (Neuhaus et al., 1990) or during the cerebral ischemia (Suzuki et al., 1984) may prevent the *de novo* synthesis of AQP4 or the assembly of OAP subunits, respectively, the observed OAPs should be maintained from the time prior to the debilitating event, and therefore be rather stable. The appearance of large lattices, as described by Neuhaus et al. (1990) in hypoxic brain tissue and detected in necrotic areas of human brain tumors as well (Wolburg et al., unpublished observations),

has now attracted novel attention, since the M23 isoform of AQP4, if transfected into OAP-negative cells, formed giant lattices reminiscent of those in hypoxic tissues (Furman et al., 2003, see above). At present, it is not known whether the hypoxia-induced lattices consist of AQP4 M23, or whether there is no causal relationship between oxygen pressure and AQP4 isoform expression.

## **5. OAPs AND AQP4 IN REACTIVE ASTROCYTES, GLIOMA, AND INFLAMMATION**

### **5.1. Loss of polarity**

Reactive astrocytes can be characterized by a number of criteria, including alterations in cell number, cellular shape and size, an increase in the amount of the glial filaments, and multiple changes of the molecular profile (Eddleston and Mucke, 1993; Pekny and Nilsson, 2005; Wilhelmsson et al., 2006). The first report describing the morphological aspect of membrane architecture of reactive astrocytes was published by Anders and Brightman (1979). They reported a higher number of OAPs in deeper layers of a subpial glial scar. The increase of OAP density in parenchymal membranes and the sustained high OAP density in subpial or perivascular membranes of astrocytes lead to a decrease of the OAP-related polarity. This polarity loss, as an additional criterion of reactive astrocytes, was described several times under different conditions: after injury (Anders and Brightman, 1979; Kästner, 1987; Wujek and Reier, 1984), in astrocytomas (Neuhaus, 1990), in epileptic foci (Hatton and Ellisman, 1984), in hypertrophic astrocytes of scrapie mice (Dubois-Dalcq et al., 1977), in the dysmyelinated jimpy mouse mutant (Omlin et al., 1980), in the myelin-deficient rat (Rohlmann et al., 1992), and in the nonmyelinated lamina cribrosa of the rat optic nerve (Bäuerle and Wolburg, 1993). In the cerebellum of the weaver mouse mutant which suffers from the inability of ectopic granule cells to migrate to mature positions in the internal granular layer, Hanna et al. (1976) have shown that parenchymal glial membranes distant from superficial endfeet were crowded with many OAPs. The reduction of OAP-related polarity in reactive astrocytes *in vivo* seems to resemble the complete loss of polarity in cultured astrocytes, with a random distribution of OAPs on their surface. Loss of polarity in reactive glia *in vivo* is commonly associated with an increase of OAP density in parenchymal membranes, but a decrease of OAP density in endfeet membranes can occur as well (Fig. 1.8).

The question as to whether and how this loss of astroglial polarity occurs and which consequences will follow will dominate the rest of this chapter.

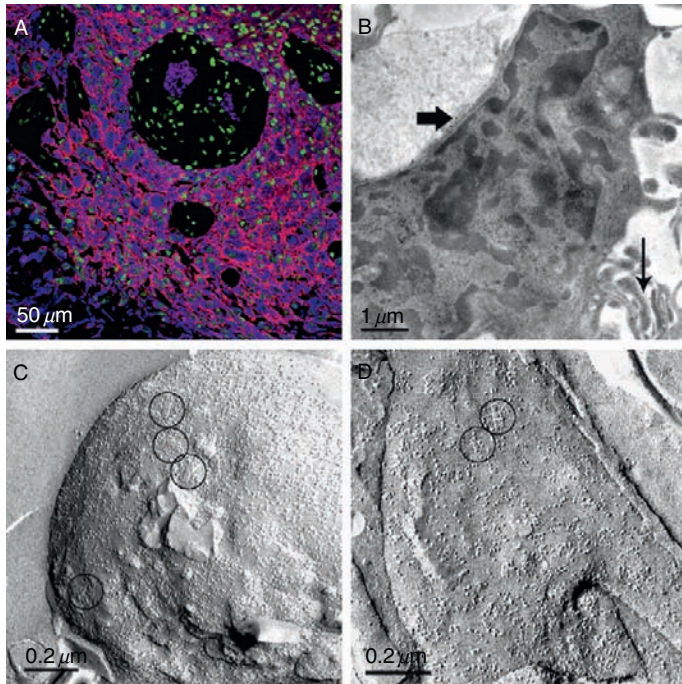


**Figure 1.8** *Human glioblastoma.* (A) Immunohistochemical staining using antibodies against AQP4 (in red) and GFAP (in blue). The glioma cells are not polarized, but AQP4 protein is completely distributed over the whole surface of the cells. (B) On the electron microscopical level as well, the immunogold labeling can be found everywhere on the surface of the glioma cell (thick arrow), also on the slender processes extending from the cell bodies (thin arrow). (C) Freeze-fracture replica of a tip of a slender process as shown in (B) (thin arrow) with OAPs. (D) Freeze-fracture replica of a membrane of the glioma cell body as shown in (B) (thick arrow) with OAPs. The low density of OAPs on glioma cells cannot explain the strong immunoreactivity against AQP4, suggesting what was mentioned before for normal intestinal and olfactory cells (Fig. 1.4) that AQP4 can occur in a non-OAP configuration, in this case, under pathological conditions.

## 5.2. AQP4, agrin, and the blood–brain barrier

The regulation of blood flow and nutrient supply within the CNS need intricate mechanisms and interactive structures which are comprised in the term gliovascular complex. Perfusion parameters differ in specific brain regions and have to be controlled according to local requirements (Ge et al., 2005), the energy supply from blood to neuronal, and synaptic metabolism has to be provided via glial cells, and, most importantly, the nervous parenchyma has to be protected from variabilities in blood



components, in particular from neurotoxic compounds including reactive oxygen species. Protection from neurotoxic compounds and energy supply together results in the dilemma the BBB is faced with. This may be the reason why the network of neurovascular interactions (the “neurovascular unit”) is so complex and involved in manifold metabolic interdependencies between neurons, glial cells, and vascular cells including endothelial cells and pericytes (for overviews on the neurovascular unit, see Carvey et al., 2009; Iadecola, 2004; Simard and Nedergaard, 2004; Zlokovic, 2008).

The direct interface between the neuroglial and the vascular compartment is established by the perivascular glial endfeet (Mathiisen et al., 2010). Astrocytes are believed to play a decisive role in the maintenance of the barrier properties of the brain microcapillary endothelial cells (Abbott et al., 2006; Liebner and Engelhardt, 2005). Astroglial differentiation, as defined in our context by the polarization of astrocytes, and BBB maturation seem to correlate (Brillault et al., 2002; Nico et al., 2001; Wolburg, 1995). Polarity of astrocytes implies a molecular and structural heterogeneity of specific membrane domains of the astroglial surface. Where the astroglial endfeet project to the brain surface or to blood vessels, they contact the superficial or perivascular basal lamina (Fig. 1.6).

Two independent studies have undertaken an approach to test directly the correlation between OAP-related polarity of astrocytes and the quality of the BBB. Zhou et al. (2008) found, in the AQP4-knockout mouse, an altered BBB integrity with a serious increase of permeability and down-regulation of the astrocyte-specific intermediate filament GFAP. In contrast, Saadoun et al. (2009) did not find any difference between wild-type and AQP4-knockout mice concerning the integrity of the BBB. However, it was not tested whether or not, as compensation, another aquaporin isoform was upregulated in response to the deficiency of AQP4. So, it remains unclear which role, if any, AQP4 may play for the integrity of the BBB. But still we can adhere to the statement that each intact BBB in mammals is connected to highly polarized AQP4 in the adjacent astrocytes (Fig. 1.5A and B) and that each disturbed integrity of BBB is responded by reduction or loss of this polarity.

The perivascular basal lamina in the brain is constituted of many components of the extracellular matrix like collagen type IV, laminin, fibronectin, and various proteoglycans (Del Zoppo et al., 2006). Previously, agrin came into the focus of interest, because its presence seemed to correlate to the restriction of AQP4 immunoreactivity at the endfoot membrane of astrocytes (Rascher et al., 2002; Warth et al., 2004; Wolburg et al., 2009). Agrin is an extracellular heparan sulfate proteoglycan which was originally characterized as essential for clustering acetylcholine receptors at the motor endplate (Bezakova and Ruegg, 2003; McMahan, 1990), but has also been described as being important within the CNS, particularly for the integrity of the BBB (Barber and Lieth, 1997; Berzin et al., 2000; Smith and

Hilgenberg, 2002). The agrin-splicing variant A0B0 was reported to be specifically present in the endothelial cell basal lamina of CNS capillaries (Stone and Nikolics, 1995). If agrin were responsible for the AQP4-based polarity of astrocytes, it would be expected that, in the absence of agrin, AQP4 and/or OAPs would lose the polarized distribution. We tested two different conditions of agrin absence: the loss of agrin in human glioblastoma and the agrin deficiency in the agrin knockout mouse. Loss of agrin in glioblastoma went along with a complete redistribution of AQP4 in the glioblastoma cells (Rascher et al., 2002; Warth et al., 2004).

In the agrin-deficient mouse, the OAP density in the astrocyte endfeet membranes was dramatically decreased, when compared with wild type (Noell et al., 2009). However, the anti-AQP4 immunoreactivity of the superficial astrocytic endfeet of the agrin-null mouse was comparable with that in wild-type mice. Thus, agrin seems to play a pivotal role for the clustering of OAPs in the endfoot membranes of astrocytes, while the mere presence of AQP4 is not sufficient for OAP clustering. Since agrin does not bind directly to AQP4, but to  $\alpha$ -dystroglycan (Gee et al., 1994), a close connection between AQP4 and the DDC should be important for the role of agrin to influence the location of AQP4 in the glial membrane. However, an unresolved question concerns the observation that if cells are transfected with AQP4, OAPs are formed without the documented presence of agrin (Furman et al., 2003; Silberstein et al., 2004).

Cell culture experiments showed that in astrocytes grown on agrin, the membrane-associated immunoreactivity of AQP4 increased. In addition, freeze-fracture replicas of such cultures revealed qualitative alterations of the morphological properties of the astrocytic membranes (Noell et al., 2007). Remarkably, cultures treated with the endothelial agrin isoform A0B0 showed OAPs often arranged in small accumulations rather than occurring as single arrays. However, using the neuronal agrin isoform A4B8, the OAP density increased at some places substantially. This suggests that both agrin isoforms (A0B0 and A4B8) induced an aggregation of AQP4 in the astrocytic membrane, but the effect of AQP4 aggregation was more pronounced in agrin A4B8-treated astrocytes. Agrin A0B0 influenced the insertion and/or aggregation of preexisting AQP4 into or within the membrane rather than the expression strength of AQP4. In addition, some raft-like lattices occurred consisting of more than 100 subunits. These lattices were exclusively present in membranes of astrocytes treated with the neuronal agrin isoform A4B8. Additionally, the expression of the AQP4-isoform M23 was upregulated and that for AQP4-M1 downregulated (Noell et al., 2007), resulting in a dramatic increase of the M23/M1 ratio. However, one should be aware of the additional possibility that this ratio can be shifted by the synthesis of M23 directly from the M1 mRNA (Rossi et al., 2010). The authors discussed the option that even in the absence of M23 mRNA, OAPs could be formed.

### 5.3. AQP4 and the dystrophin–dystroglycan complex

Dystrophin is a scaffold protein linking the membrane and the cytoskeleton. Its truncated isoforms such as Dp260, Dp140, Dp116, and Dp71 have also been found in the CNS (Blake and Kröger, 2000; Blake et al., 1999; Haenggi et al., 2004; Lidov et al., 1993). In dystrophin-deficient mice, Nico et al. (2004) observed an increase of the vascular permeability, a loss of some tight junctional components, and a reduction in the expression of AQP4. Dystrophin is connected via its aminoterminal domain to dystroglycan, which consists of  $\alpha$ - and  $\beta$ -subunit and is expressed in astrocytic endfeet (Tian et al., 1996). Both subunits of dystroglycan are encoded by a single gene and are formed by cleavage of a precursor protein into two mature proteins that form a tight noncovalent complex (Holt et al., 2000; Winder, 2001). The astrocyte-selective deletion of the dystroglycan gene was described to cause brain malformations such as disorganization of cortical layering and aberrant migration of granule cells (Moore et al., 2002).

In addition to dystroglycan, the DDC comprises other proteins like dystrobrevins and syntrophins. These are also connected to the C-terminus of dystrophin and enable the DDC to interact with channel molecules. Dystrobrevin was described to be immunolocalized at glial and endothelial cells in the rat retina (Ueda et al., 2000a) and rat cerebellum (Ueda et al., 2000b). A subunit of syntrophin,  $\alpha 1$ -syntrophin, contains a PDZ-binding domain in its C-terminal domain which is both connected to AQP4 (Neely et al., 2001) and to the inward rectifying potassium channel Kir4.1 (Connors et al., 2004). Laminin has been described to induce the aggregation of Kir4.1 and AQP4 via the DDC in cultured astrocytes (Guadagno and Moukhles, 2004).

Thus, as the distribution of Kir 4.1 is similar to that of the DDC and AQP4 (Amiry-Moghaddam and Ottersen, 2003; Blake and Kröger, 2000; Connors et al., 2004; Nagelhus et al., 2004; Warth et al., 2005), it may enable retinal Müller cells to respond to the potassium uptake with water influx (Connors and Kofuji, 2002; Fort et al., 2008; Kofuji et al., 2000; Nielsen et al., 1997; Noël et al., 2005; Pannicke et al., 2004). However, Ruiz-Ederra et al. (2007) showed that the electrophysiological properties of Kir4.1 were unaltered in retinal Müller cells of the AQP4-deficient mouse, suggesting that colocalization of both channels must not imply a functional interdependence. However, knockdown of AQP4 by small interfering RNA is accompanied by a downregulation of volume-regulated anion channels, suggesting that close functional interactions between the water and anion channels play fundamental roles in regulating water homeostasis in the brain (Benfenati et al., 2007).

## 5.4. AQP4-driven water flux in brain

From a neurophysiologic point of view, it is important to stress that in the parenchymal compartment of the brain, the astroglial cell is in close contact with neurons and synapses. Here, the extracellular  $K^+$  concentration strongly increases during synaptic activity which is counterregulated by the spatial buffering system in the astroglial gap junction-connected network (Rash, 2010).  $K^+$  uptake is followed by water entry. This parenchymal water transport is performed by AQP4 channels (MacAulay and Zeuthen, 2010; Tait et al., 2008), but in the parenchymal compartment, these channels are only sparsely present in the glial membrane as demonstrated by anti-AQP4 immunocytochemistry (Amiry-Moghaddam et al., 2003, 2004; Nagelhus et al., 1998, 1999, 2004; Nielsen et al., 1997) and by the low OAP density in freeze-fracture replicas (Neuhaus, 1990; Wolburg, 1995). All the more it is essential to equip this nerve cell-associated domain with fast water channels. Indeed, Noell et al. (2007) showed a strong increase of the expression of the AQP4-M23 isoform (which is a fast water channel; Silberstein et al., 2004), and the accumulation and insertion of AQP4 as a response to the neuronal agrin isoform A4B8 rather than the endothelial agrin isoform A0B0. *In vivo*, the insertion of AQP4-M23 by means of the neuronal agrin isoform A4B8 is restricted to the parenchymal membranes in synaptic regions of the brain. However, under *in vitro* conditions, the entire surface of the astrocyte represents a target for A4B8 activity reacting like the perisynaptic membrane domain *in vivo*. The endothelial and meningeal agrin isoform A0B0 is important for the insertion of AQP4 into the astrocyte endfoot membrane domain and aggregation into the arrays directly adjacent to blood vessels or the subpial space.

The involvement of the astroglial endfeet in the control of water fluxes in the brain was impressively demonstrated by the observation that the AQP4-deficient mouse has a benefit during water intoxication when compared with the wild-type mouse (Manley et al., 2000). Brains from these mice showed a significant reduction of the osmotic water permeability (Ma et al., 1997a; Solenov et al., 2002). Also in another model of brain edema, the middle cerebral artery occlusion-induced ischemia, the AQP4-null mice had an improved neurological outcome (Manley et al., 2000). Inversely, if the amount of astroglia-specific AQP4 was increased in a transgenic approach by using the GFAP promoter, water intoxication resulted in an accelerated cytotoxic brain swelling (Yang et al., 2008). But, since in rodents the AQP4 expression in astrocytes is upregulated in response to cerebral edema caused by brain injury (Ke et al., 2001; Vizuete et al., 1999), focal brain ischemia (Taniguchi et al., 2000), and hyponatremia (Vajda et al., 2000), the question arises as to which is the chicken and which is the egg: is the increase of AQP4 expression the initial reason of, or only the response to injury leading to cytotoxic edema? In any case, the

anchorage of AQP4 to syntrophin (Neely et al., 2001) seems to be important for the correct targeting of the water channel protein at the perivascular site, because syntrophin-deficient mice show a marked loss of AQP4 immunoreactivity (and therefore glial polarity) at perivascular membranes and a substantial swelling of glial endfeet due to a reduced clearance of water (Amiry-Moghaddam et al., 2003). However, in human brain tumors, the common redistribution of AQP4 and  $\alpha$ -syntrophin over the whole surface of glioma cells suggested that  $\alpha$ -syntrophin alone cannot be responsible for the correct targeting of AQP4 to the perivascular membrane (Warth et al., 2004).

### 5.5. AQP4 and brain tumor

In glioblastoma, expression of AQP4 (but also of AQP1; McCoy et al., 2010; Saadoun et al., 2002a), as detected by immunohistochemistry, was increased (Papadopoulos et al., 2001; Saadoun et al., 2002b; Warth et al., 2004). In sharp contrast, OAPs were lost or reduced in gliomatous cells (Hatton and Sang, 1990; Neuhaus, 1990). During upregulation, AQP4 is not only no more strictly targeted to the perivascular endfoot membrane, but also inserted into nonendfoot membrane domains (Fig. 1.8A and B). This redistribution of AQP4 directly corresponds to loss of the water channel-related polarity, leading to water movements not only between the blood and the glia but also between the glia and the brain parenchyma. Here, the water accumulates and decisively contributes to an increased edematous intracranial pressure. Commonly, a distinction is made between cytotoxic edema (cellular water accumulation due to energy failure and/or disturbed volume regulation) and vasogenic edema (extracellular water accumulation due to BBB disruption; Kimelberg, 1995; Klatzo, 1994). However, the frequently mentioned statement of AQP4 as an inducer of cytotoxic edema and a protector against vasogenic brain edema (Papadopoulos and Verkman, 2007) was questioned by the clinical observation that there was no association between survival and WHO grade-dependent AQP4 expression (Warth et al., 2007). In contrast, AQP4 was presented as a tumor progression marker, which is not compatible with the role as a protector against vasogenic edema increasing intracranial pressure.

The apparent contradiction of upregulation of AQP4 (as determined by immunohistochemistry and Western blotting) and loss of OAPs (as determined by freeze fracturing) in glioblastoma cells (Hatton and Sang, 1990; Fig. 1.8C and D) may be resolved by the assumption that in glioma cell membrane, AQP4 exists separated from the OAPs. Since AQP4 M23, but not AQP4 M1, forms lattices (Fig. 1.2B), and a mixture of M1 and M23 typical OAPs (Furman et al., 2003), the disappearance of OAPs during stable expression of the AQP4 protein could indicate a downregulation of M23. However, this was ruled out by demonstrating an unaltered M1/M23

ratio by using Western blotting and PCR analysis (Noell et al., in preparation). Interestingly, the loss of OAP-related polarity and redistribution of AQP4 in human glioblastoma (Fig. 1.8) went along with the focal loss of agrin (Warth et al., 2004). The suggestion of a causal relationship between loss of agrin and reduction of OAP-related polarity was corroborated by the observation that in the agrin-deficient mouse, the OAP formation and not the level of AQP4 protein, was disturbed (Noell et al., 2009). Since agrin is a substrate of the matrix metalloproteinase 3 (MMP-3) (Solé et al., 2004), the loss of agrin can be explained as a result of an observed increase of MMP-3 in human glioblastoma (Noell et al., in preparation).

## 5.6. AQP4 and inflammation

In experimental autoimmune encephalomyelitis (EAE), a presumptive animal model of multiple sclerosis (MS), inflammatory cells breach the endothelial barrier of postcapillary venules and both the endothelial and the glial basal laminae before reaching the CNS parenchyma proper. However, MMP-2 and MMP-9 activities are required to destroy the astroglial basal lamina for leukocyte migration but are dispensable for leukocyte entry across the endothelial BBB and the endothelial basal lamina. Accordingly, MMP-2 and MMP-9 double-knockout mice are resistant to leukocyte migration into the CNS across the glial basal lamina because dystroglycan cleavage is inhibited (Agrawal et al., 2006). This suggests that dystroglycan has a stabilizing anti-inflammatory effect on the glial endfoot membrane.

The study of Wolburg-Buchholz et al. (2009) used SJL/N mice to induce active EAE by immunization with PLP peptide. Three main findings were demonstrated: (i) presence of OAPs in the endfoot membrane as well as in the nonendfoot membrane, thus loss of OAP-related astrocytic polarity, (ii) confirmation of disappearance of  $\beta$ -dystroglycan in the EAE plaque, possibly reflecting activity of MMP-2/9 and suggesting that  $\beta$ -dystroglycan might be responsible for the correct insertion of AQP4 into the endfoot membrane domain, and (iii) decrease of agrin immunoreactivity in the endothelial and not in the glial basal lamina, probably as a result of the MMP-3 activity. It has not been shown so far whether the endothelial agrin isoform might be more sensitive to MMP-3 in comparison to the glial agrin isoform. In any case, in MS patients, MMP-3 was found to be upregulated and its level increased in the serum (Kanesaka et al., 2006; Rosenberg et al., 1996).

A variant of MS is another inflammatory demyelinating disease, the neuromyelitis optica (NMO) affecting selectively the optic nerve and the spinal cord. It has been shown that a serum immunoglobulin autoantibody (NMO-IgG) binds to AQP4 (Hinson et al., 2010; Lennon et al., 2005). Whereas in MS patients, AQP4 expression is enhanced (Aoki-Yoshino et al., 2005; Sinclair et al., 2007), loss of AQP4 in NMO belongs to the

best-known differences between the MS and the NMO (Misu et al., 2006; Roemer et al., 2007; Sinclair et al., 2007). Unfortunately, the mechanism of how the AQP4 autoantibodies affect AQP4 is far from being understood. Numerous questions must be asked: how do antibodies penetrate the BBB? What is the result of antibody binding to AQP4? Why, in NMO, there is no apparent clinical impairment of peripheral organs that have an abundance of AQP4 OAPs such as stomach, kidney, or inner ear? Why is AQP4 lost or downregulated and OAPs are disappearing? Finally, what is the chain of events from antibody–antigen binding up to demyelinating activities in oligodendrocytes? Nevertheless, recent data support the view that AQP4 exclusively in the form of OAPs (M23, not M1) is required to be recognized by the autoantibody (Nicchia et al., 2009). This was interpreted to indicate that the AQP4 protein *per se* does not contain a binding motif for NMO-IgG, but AQP4 has to be assembled into arrays (Rossi et al., 2010). However, data of Hinson et al. (2007) support the view that serum IgG from NMO patients binds to the extracellular domain of AQP4 initiating two potentially competing outcomes, the endocytosis or degradation of AQP4, therefore disappearance of OAPs, and the activation of complement. The authors address the question of demyelination in NMO by stressing the point that OAP-positive paranodal astrocytic processes around the nodes of Ranvier are targets of NMO patients' serum IgG.



## 6. CONCLUSIONS AND OUTLOOK

The intent of this chapter was to review the occurrence of the morphologically defined OAPs in the light of the growing body of data on AQP4 which forms OAPs in certain constellations. Thus, OAPs provide a unique example to bring together morphology, location, and function of a water channel. AQP4 isoforms have been well documented, and new approaches such as quantum dot tracking and BN-PAGE have elucidated some aspects of channel interactions applying to channel assemblies beyond the tetrameric arrangement of individual channels. Nevertheless, the freeze-fracture method remains the only way to detect the square arrays in their morphology and precise location within tissues. This is especially valuable in cases when AQP4 is present without array formation, for example, in glioblastomas, where high AQP4 levels could be detected but no OAPs were found. Other examples are occurrence of AQP4 in the brain before OAPs are formed during the phylogeny (Grupp et al., 2010) and ontogeny (Vollmer, Mack, and Wolburg, unpublished observations), although during phylogeny, OAPs are formed in other tissues earlier, like in hagfish gills or fish Müller cells.

A fundamental and unresolved question about OAPs remains, namely what constitutes the advantage of arranging water channels in a square form. With the exception of AQP0 (earlier called MIP, restricted to the lens), no other water channel or membrane protein is arranged in a similar way. It is still unclear whether clustering of the tetrameric channels into OAPs has any influence on the water transport. The predominant occurrence of OAPs at locations where cells face a basal lamina and the evidence outlined above that extracellular molecules such as agrin play a crucial role in clustering AQP4 to OAPs suggest the involvement of this channel arrangement in establishing and maintaining cell polarity. The polarized localization of the water channels is functionally necessary for fast and directed water movements. Thus, clustered OAP formation in this polarized manner might have functional implications irrespective of possible changes in water conductance of individual channels. The absence of OAPs despite high expression of AQP4 and loss of polarity in glioblastomas are consistent with this view. Clearly, more work and interactive applications of molecular and microscopical techniques are needed to unravel these issues.

## ACKNOWLEDGMENTS

The technical help of Ria Knittel and Yeliz Donat-Krasnici is gratefully acknowledged. The studies cited in this chapter were supported by grants from the Deutsche Krebshilfe (Mildred Scheel foundation; grant numbers 107686 and 109219) and the Hertie foundation (grant number 1.01.1/07/003) to H. W. The last one was given to H. W. together with Prof. Britta Engelhardt (Theodor Kocher Institute, University of Bern, Switzerland). Figure 1.3 is from a collaboration with Dr. Arne Warth (Institute of Pathology, University of Heidelberg, Germany). The improvement of the last section by Prof. Vanda Lennon, Mayo Clinics, Rochester, USA, is gratefully acknowledged.

## REFERENCES

- Abbott, N.J., Rönnbäck, L., Hansson, E., 2006. Astrocyte-endothelial interactions at the blood-brain barrier. *Nat. Rev. Neurosci.* 7, 41–53.
- Ablimit, A., Matsuzaki, T., Tajika, Y., Aoki, T., Hagiwara, H., Takata, K., 2006. Immunolocalization of water channel aquaporins in the nasal olfactory mucosa. *Arch. Histol. Cytol.* 69, 1–12.
- Agrawal, S., Anderson, P., Durbeej, M., Van Rooijen, N., Ivars, F., Opendakker, G., et al., 2006. Dystroglycan is selectively cleaved at the parenchymal basement membrane at sites of leukocyte extravasation in experimental autoimmune encephalomyelitis. *J. Exp. Med.* 203, 1007–1019.
- Amiry-Moghaddam, M., Ottersen, O.P., 2003. The molecular basis of water transport in the brain. *Nat. Rev. Neurosci.* 4, 991–1001.
- Amiry-Moghaddam, M., Williamson, A., Palomba, M., Eid, T., De Lanerolle, N.C., Nagelhus, E.A., et al., 2003. Delayed K<sup>+</sup> clearance associated with aquaporin-4 mislocalization: phenotypic defects in brains of  $\alpha$ -syntrophin-null mice. *Proc. Natl. Acad. Sci. USA* 100, 13615–13620.



- Amiry-Moghaddam, M., Frydenlund, D.S., Ottersen, O.P., 2004. Anchoring of aquaporin-4 in brain: molecular mechanisms and implications for the physiology and pathophysiology of water transport. *Neuroscience* 129, 999–1010.
- Anders, J.J., Brightman, M.W., 1979. Assemblies of particles in the cell membranes of developing, mature and reactive astrocytes. *J. Neurocytol.* 8, 777–795.
- Anders, J.J., Brightman, M.W., 1982. Particle assemblies in astrocytic plasma membranes are rearranged by various agents in vitro. *J. Neurocytol.* 11, 1009–1029.
- Anders, J.J., Pagnanelli, D.M., 1979. The protein nature and arrangement of intramembranous particle assemblies in normal and reactive astrocytes. *Anat. Rec.* 193, 470.
- Aoki-Yoshino, K., Uchihara, T., Duyckaerts, C., Nakamura, A., Hauw, J.-J., Wakayama, Y., 2005. Enhanced expression of aquaporin 4 in human brain with inflammatory diseases. *Acta Neuropathol.* 110, 281–288.
- Assereto, S., Mastrototaro, M., Stringara, S., Gazerro, E., Broda, P., Nicchia, G.P., et al., 2008. Aquaporin-4 expression is severely reduced in human sarcoglycanopathies and dysferlinopathies. *Cell Cycle* 7, 2199–2207.
- Au, C.G., Butler, T.L., Egan, J.R., Cooper, S.T., Lo, H.P., Compton, A.G., et al., 2008. Changes in skeletal muscle expression of AQP1 and AQP4 in dystrophinopathy and dysferlinopathy patients. *Acta Neuropathol.* 116, 235–246.
- Barber, A.J., Lieth, E., 1997. Agrin accumulates in the brain microvascular basal lamina during development of the blood-brain barrier. *Dev. Dyn.* 208, 62–74.
- Bartles, H., Miragall, F., 1986. Orthogonal arrays of particles in the plasma membrane of pneumocytes. *J. Submicrosc. Cytol.* 18, 637–646.
- Bäuerle, C., Wolburg, H., 1993. Astrocytes in the non-myelinated lamina cribrosa of the rat are less polarized than in the optic nerve proper: a freeze-fracture study. *Glia* 9, 238–241.
- Beitz, E., Kumagami, H., Krippeit-Drews, P., Ruppertsberg, J.P., Schultz, J.E., 1999. Expression pattern of AQP water channels in the inner ear of the rat. The molecular basis for a water regulation system in the endolymphatic sac. *Hear. Res.* 132, 76–84.
- Benfenati, V., Nicchia, G.P., Svelto, M., Rapisarda, C., Frigeri, A., Ferroni, S., 2007. Functional down-regulation of volume-regulated anion channels in AQP4 knockdown cultured rat cortical astrocytes. *J. Neurochem.* 1000, 87–104.
- Benga, G., Popescu, O., Pop, V.I., Holmes, R.P., 1986a. *p*-(Chloromercuri)benzenesulfonate binding by membranes proteins and the inhibition of water transport in human erythrocytes. *Biochemistry* 25, 1535–1538.
- Benga, G., Popescu, O., Borza, V., Pop, V.I., Muresan, A., Mocsy, I., et al., 1986b. Water permeability of human erythrocytes. Identification of membrane proteins involved in water transport. *Eur. J. Cell Biol.* 41, 252–262.
- Berg-von der Emde, K., Wolburg, H., 1989. Müller (glial) cells but not astrocytes in the retina of the goldfish possess orthogonal arrays of particles. *Glia* 2, 458–469.
- Berzin, T.M., Zipser, B.D., Rafii, M.S., Kuo-Leblanc, V., Yancopoulos, G.D., Glass, D.J., et al., 2000. Agrin and microvascular damage in Alzheimer's disease. *Neurobiol. Aging* 21, 349–355.
- Bezakova, G., Ruegg, M.A., 2003. New insights into the roles of agrin. *Nat. Rev. Mol. Cell Biol.* 4, 295–308.
- Blake, D.J., Kröger, S., 2000. The neurobiology of Duchenne muscular dystrophy: learning lessons from muscle? *Trends Neurosci.* 23, 92–99.
- Blake, D.J., Hawkes, R., Benson, M.A., Beesley, P.W., 1999. Different dystrophin-like complexes are expressed in neurons and glia. *J. Cell Biol.* 147, 645–657.
- Bolz, S., Wolburg, H., 1992. First appearance of orthogonal arrays of particles in Muller cell membranes depends on retina maturation. *Dev. Neurosci.* 14, 203–209.
- Bolz, J., Novak, N., Götz, M., Bonhoeffer, T., 1992. Formation of target-specific neuronal projections in organotypic slice cultures from rat visual cortex. *Nature* 346, 359–362.

- Bordi, C., Perrelet, A., 1978. Orthogonal arrays of particles in plasma membrane of the gastric parietal cell. *Anat. Rec.* 192, 297–304.
- Bordi, C., Amherdt, M., Perrelet, A., 1986. Orthogonal arrays of particles in the gastric parietal cell of the rat: differences between superficial and basal cells in the gland and after pentagastrin or metiamide treatment. *Anat. Rec.* 215, 28–34.
- Brillault, J., Berezowski, V., Cecchelli, R., Dehouck, M.P., 2002. Intercommunications between brain capillary endothelial cells and glial cells increase the transcellular permeability of the blood-brain barrier during ischemia. *J. Neurochem.* 83, 807–817.
- Brown, D., Orci, L., 1988. Junctional complexes and cell polarity in the urinary tubule. *J. Electron Microsc. Techn.* 9, 145–170.
- Carmosino, M., Procino, G., Nicchia, G.P., Mannucci, R., Verbavatz, J.-M., Gobin, R., et al., 2001. Histamine treatment induces rearrangements of orthogonal arrays of particles (OAPs) in human AQP4-expressing gastric cells. *J. Cell Biol.* 154, 1235–1243.
- Carmosino, M., Procino, G., Tamma, G., Mannucci, R., Svelto, M., Valenti, G., 2007. Trafficking and phosphorylation dynamics of AQP4 in histamine-treated human gastric cells. *Biol. Cell* 99, 25–36.
- Carson, J.L., Collier, A.M., Smith, C.A., 1984. New observations on the ultrastructure of mammalian conducting airway epithelium: application of liquid propane freezing, deep etching, and rotary shadowing techniques to freeze-fracture. *J. Ultrastruct. Res.* 89, 23–33.
- Carvey, P.M., Hendeby, B., Monahan, A.J., 2009. The blood-brain barrier in neurodegenerative disease: a rhetorical perspective. *J. Neurochem.* 111, 291–314.
- Christensen, N., D'Souza, M., Zhu, X., Frisina, R.D., 2009. Age-related hearing loss: aquaporin 4 gene expression changes in the mouse cochlea and auditory midbrain. *Brain Res.* 1253, 27–34.
- Connors, N.C., Kofuji, P., 2002. Dystrophin Dp71 is critical for the clustered localization of potassium channels in retinal glial cells. *J. Neurosci.* 22, 4321–4327.
- Connors, N.C., Adams, M.E., Froehner, S.C., Kofuji, P., 2004. The potassium channel Kir4.1 associates with the dystrophin glycoprotein complex via alpha-syntrophin in glia. *J. Biol. Chem.* 279, 28387–28392.
- Crane, J.M., Verkman, A.S., 2009a. Determinants of aquaporin-4 assembly in orthogonal arrays revealed by live-cell single-molecule fluorescence imaging. *J. Cell Sci.* 122, 813–821.
- Crane, J.M., Verkman, A.S., 2009b. Reversible, temperature-dependent supramolecular assembly of aquaporins-4 orthogonal arrays in live cell membranes. *Biophys. J.* 97, 3010–3018.
- Crane, J.M., Van Hoek, A.N., Skach, W.R., Verkman, A.S., 2008. Aquaporin-4 dynamics in orthogonal arrays in live cells visualized by quantum dot single particle tracking. *Mol. Biol. Cell* 19, 3369–3378.
- Crane, J.M., Bennett, J.L., Verkman, A.S., 2009. Live cell analysis of aquaporins-4 M1/M23 interactions and regulated orthogonal array assembly in glia cells. *J. Biol. Chem.* 284, 35850–35860.
- Cuevas, P., Gutierrez Diaz, J.A., Dujovny, M., Diaz, F.G., Ausman, J.I., 1985. Disturbance of plasmalemmal astrocytic assemblies in focal and selective cerebral ischemia. *Anat. Embryol.* 172, 171–175.
- Del Zoppo, G.J., Milner, R., Mabuchi, T., Hung, S., Wang, X., Koziol, J.A., 2006. Vascular matrix adhesion and the blood-brain barrier. *Biochem. Soc. Trans.* 34, 1261–1266.
- Denker, B.M., Smith, B.L., Kuhajda, F.P., Agre, P., 1988. Identification, purification and partial characterization of a novel  $M_r$  28,000 integral membrane protein from erythrocytes and renal tubules. *J. Biol. Chem.* 263, 15634–15642.

- Dermietzel, R., 1973. Visualization by freeze-fracturing of regular structures in glial cell membranes. *Naturwissenschaften* 60, 208.
- Dermietzel, R., 1974. Junctions in the central nervous system of the cat. III. Gap junctions and membrane-associated orthogonal particle complexes (MOPC) in astrocytic membranes. *Cell Tissue Res.* 149, 121–135.
- Dubois-Dalcq, M., Rodriguez, M., Reese, T.S., Gibbs, C.J., Gajdusek, D.C., 1977. Search for a specific marker in the neural membranes of scrapie mice. A freeze-fracture study. *Lab. Invest.* 36, 547–553.
- Eddleston, M., Mucke, L., 1993. Molecular profile of reactive astrocytes. Implications for their role in neurologic disease. *Neuroscience* 54, 15–36.
- Elfvin, L.G., Forsman, C., 1978. The ultrastructure of junctions between satellite cells and mammalian sympathetic ganglia as revealed by freeze-etching. *J. Ultrastruct. Res.* 63, 261–274.
- Ellisman, M.H., 1981. The membrane morphology of the neuromuscular junction, sarcolemma, sarcoplasmic reticulum and transverse tubule system in murine muscular dystrophy studied by freeze-fracture electron microscopy. *Brain Res.* 214, 261–273.
- Ellisman, M.H., Rash, J.E., Staehelin, L.A., Porter, K.R., 1976. Studies of excitable membranes. II. A comparison of specializations at neuromuscular junctions and non-junctional sarcolemmas of mammalian fast and slow twitch muscle fibers. *J. Cell Biol.* 68, 752–774.
- Ellisman, M.H., Brooke, M.H., Kaiser, K.K., Rash, J.E., 1978. Appearance in slow muscle sarcolemma of specializations characteristic of fast muscle after reinnervation by a fast muscle nerve. *Exp. Neurol.* 58, 59–67.
- Engel, A., Fujiyoshi, Y., Gonen, T., Walz, T., 2008. Junction-forming aquaporins. *Curr. Opin. Struct. Biol.* 18, 229–235.
- Fallier-Becker, P., Sperveslage, J., Wolburg, H., Noell, S., 2011. The impact of agrin on the formation of orthogonal arrays of particles in cultured astrocytes from wild-type and agrin-null mice. *Brain Res.* 1367, 2–12.
- Fort, P.E., Sene, A., Pannicke, T., Roux, M.J., Forster, V., Mornet, D., et al., 2008. Kir4.1 and AQP4 associate with Dp71- and utrophin-DAPs complexes in specific and defined microdomains of Müller retinal glial cell membrane. *Glia* 56, 597–610.
- Franzini-Armstrong, C., 1984. Freeze-fracture of frog slow tonic fibers. Structure of surface and internal membranes. *Tissue Cell* 16, 647–664.
- Friend, D.S., 1987. Loss of square (orthogonal) arrays from cultured airway epithelial cells. *J. Electron Microsc. Techn.* 6, 237–246.
- Frigeri, A., Gropper, M.A., Umenishi, F., Kawashima, M., Brown, D., Verkman, A.S., 1995. Localization of MIWC and GLIP water channel homologs in neuromuscular, epithelial and glandular tissues. *J. Cell Sci.* 108, 2993–3002.
- Frigeri, A., Nicchia, G.P., Verbavatz, J.M., Valenti, G., Svelto, M., 1998. *J. Clin. Invest.* 102, 695–703.
- Frigeri, A., Nicchia, G.P., Nico, B., Quondamatteo, F., Herken, R., Roncali, L., et al., 2001. Aquaporin-4 deficiency in skeletal muscle and brain of dystrophic mdx mice. *FASEB J.* 15, 90–98.
- Frigeri, A., Nicchia, G.P., Repetto, S., Bado, M., Minetti, C., Svelto, M., 2002. Altered aquaporin-4 expression in human muscular dystrophies: a common feature? *FASEB J.* 16, 1120–1122.
- Furman, C.S., Gorelick-Feldman, D.A., Davidson, K.G., Yasumura, T., Neely, J.D., Agre, P., et al., 2003. *Proc. Natl. Acad. Sci. USA* 100, 13609–13614.
- Ge, S., Song, L., Pachter, J.S., 2005. Where is the blood-brain barrier. .really? *J. Neurosci. Res.* 79, 421–427.
- Gee, S.H., Montanaro, F., Lindenbaum, M.H., Carbonetto, S., 1994. Dystroglycan-alpha, a dystrophin-associated glycoprotein, is a functional agrin receptor. *Cell* 77, 675–686.

- Gordon, R.E., 1985. Orthogonal arrays in normal and injured respiratory airway epithelium. *J. Cell Biol.* 100, 648–651.
- Gotow, T., Hashimoto, P.H., 1982. Intercellular junctions between specialized ependymal cells in the subcommissural organ of the rat. *J. Neurocytol.* 11, 363–379.
- Gotow, T., Hashimoto, P.H., 1988. Deep-etch structure of astrocytes at the superficial glia limitans, with special emphasis on the internal and external organization of their plasma membranes. *J. Neurocytol.* 17, 399–413.
- Gotow, T., Hashimoto, P.H., 1989. Orthogonal arrays of particles in plasma membranes of Muller cells in the guinea pig retina. *Glia* 2, 273–285.
- Gotow, T., Yoshikawa, H., Hashimoto, P.H., 1985. Distribution patterns of orthogonal arrays and alkaline phosphatase in plasma membranes of satellite cells in rat spinal ganglia. *Anat. Embryol.* 171, 171–179.
- Grupp, L., Wolburg, H., Mack, A.F., 2010. Astroglial structures in the zebrafish brain. *J. Comp. Neurol.* 518, 4277–4287.
- Guadagno, E., Moukhles, H., 2004. Laminin-induced aggregation of the inwardly rectifying potassium channel, Kir4.1, and the water-permeable channel, AQP4, via a dystroglycan-containing complex in astrocytes. *Glia* 47, 138–149.
- Haenggi, T., Fritschy, J.-M., 2006. Role of dystrophin and utrophin for assembly and function of the dystrophin glycoprotein complex in non-muscle tissue. *Cell. Mol. Life Sci.* 63, 1614–1631.
- Haenggi, T., Soontornmalai, A., Schaub, M.C., Fritschy, J.-M., 2004. The role of utrophin and Dp71 for assembly of different dystrophin-associated protein complexes (DPCs) in the choroid plexus and microvasculature of the brain. *Neuroscience* 129, 403–413.
- Hamann, S., Zeuthen, T., La Cour, M., Nagelhus, E.A., Ottersen, O.P., Agre, P., et al., 1998. Aquaporins in complex tissues: distribution of aquaporins 1–5 in human and rat eye. *Am. J. Physiol.* 274, C1332–C1345.
- Hanna, R.B., Hirano, A., Pappas, G.D., 1976. Membrane specializations of dendritic spines and glia in the weaver mouse cerebellum: a freeze-fracture study. *J. Cell Biol.* 68, 403–410.
- Hasegawa, H., Lian, S.-C., Finkbeiner, W.E., Verkman, A.S., 1994. Extrarenal tissue distribution of CHIP28 water channels by in situ hybridization and antibody staining. *Am. J. Physiol.* 266, C893–C903.
- Hatae, T., 1983. Plasma membrane specializations in the cells of the kidney distal segment of the lamprey. *J. Ultrastruct. Res.* 85, 58–69.
- Hatton, J.D., Ellisman, M.H., 1982. The distribution of orthogonal arrays in the freeze-fractured rat median eminence. *J. Neurocytol.* 11, 335–349.
- Hatton, J.D., Ellisman, M.H., 1984. Orthogonal arrays are redistributed in the membranes of astroglia from alumina-induced epileptic foci. *Epilepsia* 25, 145–151.
- Hatton, J.D., Sang, U.H., 1990. Orthogonal arrays are absent from the membranes of human glioblastomatous tissues. *Acta Anat.* 137, 363–366.
- Heuser, J.E., Reese, T.S., Landis, D.M.D., 1974. Functional changes in frog neuromuscular junctions studied with freeze fracture. *J. Neurocytol.* 3, 109–131.
- Hinson, S.R., Pittcock, S.J., Lucchinetti, C.F., Roemer, S.F., Fryer, J.P., Kryzer, T.J., et al., 2007. Pathogenic potential of IgG binding to water channel extracellular domain in neuromyelitis optica. *Neurology* 69, 2221–2231.
- Hinson, S.R., McKeon, A., Lennon, V.A., 2010. Neurological autoimmunity targeting aquaporin-4. *Neuroscience* 168, 1009–1018.
- Hiroaki, Y., Tani, K., Kamegawa, A., Gyobu, N., Nishikawa, K., Suzuki, H., et al., 2006. Implications of the aquaporin-4 structure on array formation and cell adhesion. *J. Mol. Biol.* 355, 628–639.
- Hirsch, M., Gache, D., Noske, W., 1988. Orthogonal arrays of particles in non-pigmented cells of rat ciliary epithelium: relation to distribution of filipin- and digitonin-induced alterations of the basolateral membrane. *Cell Tissue Res.* 252, 165–173.

- Hirt, B., Penkova, Z.H., Eckhard, A., Liu, W., Rask-Andersen, H., Müller, M., et al., 2010. The subcellular distribution of aquaporin 5 in the cochlea reveals a water shunt at the perilymph-endolymph barrier. *Neuroscience* 168, 957–970.
- Holt, K.H., Crosbie, R.H., Venzke, D.P., Campbell, K.P., 2000. Biosynthesis of dystroglycan: processing of a precursor propeptide. *FEBS Lett.* 468, 79–83.
- Humbert, F., Pricam, C., Perrelet, A., Orci, L., 1975. Specific plasma membrane differentiations in the cells of the kidney collecting tubule. *J. Ultrastruct. Res.* 52, 13–20.
- Iadecola, C., 2004. Neurovascular regulation in the normal brain and in Alzheimer's disease. *Nat. Rev. Neurosci.* 5, 347–360.
- Inoue, S., Hogg, J.C., 1977. Freeze-etch study of the tracheal epithelium of normal guinea pigs with particular reference to intercellular junctions. *J. Ultrastruct. Res.* 61, 89–99.
- Ishiyama, G., Lopez, I.A., Beltran-Parrazal, L., Ishiyama, A., 2010. Immunohistochemical localization and mRNA expression of aquaporins in the macula utriculi of patients with Meniere's disease and acoustic neuroma. *Cell Tissue Res* 340, 407–419.
- Jung, J.S., Bhat, R.V., Preston, G.M., Guggino, W.B., Baraban, J.M., Agre, P., 1994. Molecular characterization of an aquaporin cDNA from brain: candidate osmoreceptor and regulator of water balance. *Proc. Natl. Acad. Sci. USA* 91, 13052–13056.
- Kanesaka, T., Mori, M., Hattori, T., Oki, T., Kuwabara, S., 2006. Serum matrix metalloproteinase-3 levels correlate with disease activity in relapsing-remitting multiple sclerosis. *J. Neurol. Neurosurg. Psychiatr.* 77, 185–188.
- Kästner, R., 1987. Comparative studies on the astrocytic reaction in the lesioned central nervous system of different vertebrates. *J. Hirnforsch.* 28, 221–232.
- Ke, C., Poon, W.S., Ng, H.K., Pang, J.C., Chan, Y., 2001. Heterogeneous responses of aquaporin-4 in oedema formation in a replicated severe traumatic brain injury model in rats. *Neurosci. Lett.* 301, 21–24.
- Kimelberg, H.K., 1995. Current concepts of brain edema: review of laboratory investigations. *J. Neurosurg.* 83, 1051–1059.
- King, L.S., Kozono, D., Agre, P., 2004. From structure to disease: the evolving tale of aquaporin biology. *Nat. Rev. Mol. Cell Biol.* 5, 687–698.
- Kistler, J., Bullivant, S., 1989. Structural and molecular biology of the eye lens membranes. *Crit. Rev. Biochem. Mol. Biol.* 24, 151–181.
- Klatzo, I., 1994. Evolution of brain edema concepts. *Acta Neurochir. Suppl. (Wien)* 60, 3–6.
- Kofuji, P., Ceelen, P., Zahs, K.R., Surbeck, L.W., Lester, H.A., Newman, E.A., 2000. Genetic inactivation of an inwardly rectifying potassium channel (Kir4.1 subunit) in mice: phenotypic impact in retina. *J. Neurosci.* 20, 5733–5740.
- Korte, G.E., Rosenbluth, J., 1981. Ependymal astrocytes in the frog cerebellum. *Anat. Rec.* 199, 267–279.
- Koyama, Y., Yamamoto, T., Tani, T., Nihel, K., Kondo, D., Funaki, H., et al., 1999. Expression and localization of aquaporins in rat gastrointestinal tract. *Am. J. Physiol.* 276, C621–C627.
- Kreutziger, G.O., 1968. Freeze-etching of intercellular junctions of mouse liver. In: *Proceedings of 26th Meeting of the Electron Microscopy Society of America*. Claitors Publishing Division Baton Rouge, Louisiana, pp. 234–235.
- Kumari, S.S., Varadaraj, K., 2009. Intact AQP0 performs cell-to-cell adhesion. *Biochem. Biophys. Res. Commun.* 390, 1034–1039.
- Landis, D.M.D., Reese, T.S., 1974. Arrays of particles in freeze-fractured astrocytic membranes. *J. Cell Biol.* 60, 316–320.
- Landis, D.M.D., Reese, T.S., 1981a. Membrane structure in mammalian astrocytes: a review of freeze-fracture studies on adult, developing, reactive and cultured astrocytes. *J. Exp. Biol.* 95, 35–48.

- Landis, D.M.D., Reese, T.S., 1981b. Astrocyte membrane structure: changes after circulatory arrest. *J. Cell Biol.* 88, 660–663.
- Landis, D.M.D., Reese, T.S., 1982. Regional organization of membrane structure in astrocytes. *Neuroscience* 7, 937–950.
- Landis, D.M.D., Weinstein, L.A., 1983. Membrane structure in cultured astrocytes. *Brain Res.* 276, 31–41.
- Landis, D.M.D., Weinstein, L.A., Skordeles, C.J., 1990. Serum influences the differentiation of membrane structure in cultured astrocytes. *Glia* 3, 212–221.
- Landis, D.M.D., Weinstein, L.A., Skordeles, C.J., 1991. Effects of dexamethasone on the differentiation of membrane structure in cultured astrocytes. *Glia* 4, 335–344.
- Lennon, V.A., Kryzer, T.J., Pittock, S.J., Verkman, A.S., Hinson, S.R., 2005. IgG marker of optic-spinal multiple sclerosis binds to the aquaporin-4 water channel. *J. Exp. Med.* 202, 473–477.
- Leonhardt, H., 1970. Subependymale Basalmembranlabyrinth im Hinterhorn des Seitenventrikels des Kaninchengehirns. *Z. Zellforsch.* 105, 595–604.
- Levin, M.H., Verkman, A.S., 2006. Aquaporins and CFTR in ocular epithelial fluid transport. *J. Membr. Biol.* 210, 105–115.
- Li, J., Verkman, A.S., 2001. Impaired hearing in mice lacking aquaporin-4 water channels. *J. Biol. Chem.* 276, 31233–31237.
- Li, X., Kong, H., Wu, W., Xiao, M., Sun, X., Hu, G., 2009. Aquaporin-4 maintains ependymal integrity in adult mice. *Neuroscience* 162, 67–77.
- Lidov, H.G., Byers, T.J., Kunkel, L.M., 1993. The distribution of dystrophin in the murine central nervous system: an immunocytochemical study. *Neuroscience* 54, 167–187.
- Liebner, S., Engelhardt, B., 2005. Development of the blood-brain barrier. In: De Vries, E., Prat, A. (Eds.), *The Blood-Brain Barrier and Its Microenvironment: Basic Physiology to Neurological Disease*. Taylor and Francis, New York, pp. 1–25.
- Lopez, I.A., Ishiyama, G., Lee, M., Baloh, R.W., Ishiyama, A., 2007. Immunohistochemical localization of aquaporins in the human inner ear. *Cell Tissue Res.* 328, 453–460.
- Ma, T., Verkman, A.S., 1999. Aquaporin water channels in gastrointestinal physiology. *J. Physiol.* 517, 317–326.
- Ma, T., Yang, B., Gillespie, A., Carlson, E.J., Epstein, C.J., Verkman, A.S., 1997a. Generation and phenotype of a transgenic knockout mouse lacking the mercurial-insensitive water channel aquaporin-4. *J. Clin. Invest.* 100, 957–962.
- Ma, T., Yang, B., Verkman, A.S., 1997b. Cloning of a novel water and urea-permeable aquaporin from mouse expressed strongly in colon, placenta, liver, and heart. *Biochem. Biophys. Res. Commun.* 240, 324–328.
- MacAulay, N., Zeuthen, T., 2010. Water transport between CNS compartments: contributions of aquaporins and cotransporters. *Neuroscience* 168, 941–956.
- Mack, A., Wolburg, H., 1986. Heterogeneity of glial membranes in the rat olfactory system as revealed by freeze-fracturing. *Neurosci. Lett.* 65, 17–22.
- Mack, A., Neuhaus, J., Wolburg, H., 1987. Relationship between orthogonal arrays of particles and tight junctions as demonstrated in cells of the ventricular wall of the rat brain. *Cell Tissue Res.* 248, 619–625.
- Manley, G.T., Fujimura, M., Ma, T., Noshita, N., Filiz, F., Bollen, A.W., et al., 2000. Aquaporin-4 deletion in mice reduces brain edema after acute water intoxication and ischemic stroke. *Nat. Med.* 6, 159–163.
- Massa, P.T., Mugnaini, E., 1982. Cell junctions and intramembrane particles of astrocytes and oligodendrocytes: a freeze-fracture study. *Neuroscience* 7, 523–538.
- Massa, P.T., Mugnaini, E., 1985. Cell-cell junctional interactions and characteristic plasma membrane features of cultured rat glial cells. *Neuroscience* 14, 695–709.

- Mathiisen, T.M., Lehre, K.P., Danbolt, N.C., Ottersen, O.P., 2010. The perivascular astroglial sheath provides a complete covering of the brain microvessels: an electron microscopic 3D reconstruction. *Glia* 58, 1094–1103.
- McCoy, E.S., Haas, B.R., Sontheimer, H., 2010. Water permeability through aquaporin-4 is regulated by protein kinase C and becomes rate-limiting for glioma invasion. *Neuroscience* 168, 971–981.
- McMahan, U.J., 1990. The agrin hypothesis. *Cold Spring Harb. Symp. Quant. Biol.* 55, 407–418.
- Miragall, F., 1983. Evidence for orthogonal arrays of particles in the plasma membranes of olfactory and vomeronasal sensory neurons of vertebrates. *J. Neurocytol.* 12, 567–576.
- Misu, T., Fujihara, K., Nakamura, M., Murakami, K., Endo, M., Konno, H., et al., 2006. Loss of aquaporins-4 in active perivascular lesions in neuromyelitis optica: a case report. *Tohoku J. Exp. Med.* 209, 269–275.
- Moe, S.E., Sorbo, J.G., Sogaard, R., Zeuthen, T., Ottersen, O.P., Holen, T., 2008. New isoforms of rat aquaporin-4. *Genomics* 91, 367–377.
- Moore, S.A., Saito, F., Chen, J., Michele, D.E., Henry, M.D., Messing, A., et al., 2002. Deletion of brain dystroglycan recapitulates aspects of congenital muscular dystrophy. *Nature* 418, 422–425.
- Nagelhus, E.A., Veruki, M.L., Torp, R., Haug, F.M., Laake, J.H., Nielsen, S., et al., 1998. Aquaporin-4 water channel protein in the rat retina and optic nerve: polarized expression in Müller cells and fibrous astrocytes. *J. Neurosci.* 18, 2506–2519.
- Nagelhus, E.A., Horio, Y., Inanobe, A., Fujita, A., Haug, F.-M., Nielsen, S., et al., 1999. Immunogold evidence suggests that coupling of K<sup>+</sup> siphoning and water transport in rat retinal Müller cells is mediated by a coenrichment of Kir4.1 and AQP4 in specific membrane domains. *Glia* 26, 47–54.
- Nagelhus, E.A., Mathiisen, T.M., Ottersen, O.P., 2004. Aquaporin-4 in the central nervous system: cellular and subcellular distribution and coexpression with Kir4.1. *Neuroscience* 129, 905–913.
- Nakai, Y., Kudo, J., Hashimoto, A., 1980. Specific cell membrane differentiation in the tanyocytes and glial cells of the organum vasculosum of the lamina terminalis in dog. *J. Electron Microsc.* 29, 144–150.
- Nakamura, T., Nagano, T., 1985. Intramembrane particle distribution in renal collecting tubule cells in normal, dehydrated and hereditary diabetes insipidus rats with particular reference to orthogonal arrays of particles. *J. Electron Microsc.* 34, 364–372.
- Nase, G., Helm, P.J., Enger, R., Ottersen, O.P., 2008. Water entry into astrocytes during brain edema formation. *Glia* 56, 895–902.
- Neely, J.D., Christensen, B.M., Nielsen, S., Agre, P., 1999. Heterotetrameric composition of aquaporin-4 water channels. *Biochemistry* 38, 11156–11163.
- Neely, J.D., Amiry-Moghaddam, M., Ottersen, O.P., Froehner, S.C., Agre, P., Adams, M.E., 2001. Syntrophin-dependent expression and localization of aquaporin-4 water channel protein. *Proc. Natl. Acad. Sci. USA* 98, 14108–14113.
- Neuhaus, J., 1990. Orthogonal arrays of particles in astroglial cells: quantitative analysis of their density, size, and correlation with intramembranous particles. *Glia* 3, 241–251.
- Neuhaus, J., Schmid, E.-M., Wolburg, H., 1990. Stability of orthogonal arrays of particles in murine skeletal muscle and astrocytes after circulatory arrest, and human gliomas. *Neurosci. Lett.* 109, 163–168.
- Nicchia, G.P., Rossi, A., Nudel, U., Svelto, M., Frigeri, A., 2008. Dystrophin-dependent and -independent AQP4 pools are expressed in the mouse brain. *Glia* 56, 869–876.
- Nicchia, G.P., Mastroiuto, M., Rossi, A., Pisani, F., Tortorella, C., Ruggirei, M., et al., 2009. Aquaporin-4 orthogonal arrays of particles are the target for neuromyelitis optica autoantibodies. *Glia* 57, 1363–1373.

- Nicchia, G.P., Rossi, A., Mola, M.G., Pisani, F., Stigliano, C., Basco, D., et al., 2010. Higher order structure of aquaporin-4. *Neuroscience* 168, 903–914.
- Nico, B., Cantino, M., Sassoè Pognetto, M., Bertossi, M., Ribatti, D., Roncali, L., 1994. Orthogonal arrays of particles (OAPs) in perivascular astrocytes and tight junctions in endothelial cells. A comparative study in developing and adult brain microvessels. *J. Submicrosc. Cytol. Pathol.* 26, 103–109.
- Nico, B., Frigeri, A., Nicchia, G.P., Quondamatteo, F., Herken, R., Errede, M., et al., 2001. Role of aquaporin-4 water channel in the development and integrity of the blood-brain barrier. *J. Cell Sci.* 114, 1297–1307.
- Nico, B., Nicchia, G.P., Frigeri, A., Corsi, P., Manieri, D., Ribatti, D., et al., 2004. Altered blood-brain barrier development in dystrophic mdx mice. *Neuroscience* 125, 921–935.
- Nielsen, S., Smith, B.L., Christensen, E.I., Agre, P., 1993. Distribution of the aquaporin CHIP in secretory and resorptive epithelia and capillary endothelia. *Proc. Natl. Acad. Sci. USA* 90, 7275–7279.
- Nielsen, S., Nagelhus, E.A., Amiry-Moghaddam, M., Bourque, C., Agre, P., Ottersen, O.P., 1997. Specialized membrane domains for water transport in glial cells: high-resolution immunogold cytochemistry of aquaporin-4 in rat brain. *J. Neurosci.* 17, 171–180.
- Nielsen, S., Frøklær, J., Marples, D., Kwon, T.H., Agre, P., Knepper, M.A., 2002. Aquaporins in the kidney: from molecules to medicine. *Physiol. Rev.* 82, 205–244.
- Noël, G., Belda, M., Guadagno, E., Micoud, J., Klöcker, N., Moukhles, H., 2005. Dystroglycan and Kir4.1 coclustering in retinal Müller glia is regulated by laminin-1 and requires the PDZ-ligand domain of Kir4.1. *J. Neurochem.* 94, 691–702.
- Noell, S., Fallier-Becker, P., Beyer, C., Kröger, S., Mack, A.F., Wolburg, H., 2007. Effects of agrin on the expression and distribution of the water channel protein aquaporin-4 and volume regulation in cultured astrocytes. *Eur. J. Neurosci.* 26, 2109–2118.
- Noell, S., Fallier-Becker, P., Deutsch, U., Mack, A.F., Wolburg, H., 2009. Agrin defines polarized distribution of orthogonal arrays of particles in astrocytes. *Cell Tissue Res.* 337, 185–195.
- Omlin, F.X., Bischoff, A., Moor, H., 1980. Myelin and glial membrane structures in the optic nerve of normal and jimpy mouse—a freeze-etching study. *J. Neuropathol. Exp. Neurol.* 39, 215–231.
- Orci, L., Humbert, F., Brown, D., Perrelet, A., 1981. Membrane ultrastructure in urinary tubules. *Int. Rev. Cytol.* 73, 183–242.
- Pannese, E., Luciano, L., Iurato, S., Reale, E., 1977. Intercellular junctions and other membrane specializations in developing spinal ganglia: a freeze-fracture study. *J. Ultrastruct. Res.* 60, 169–180.
- Pannicke, T., Iandiev, I., Uckermann, O., Biedermann, B., Kutzera, F., Wiedemann, P., et al., 2004. A potassium-channel-linked mechanism of glial cell swelling in the post-ischemic retina. *Mol. Cell. Neurosci.* 26, 493–502.
- Papadopoulos, M.C., Verkman, A.S., 2007. Aquaporin-4 and brain edema. *Pediatr. Nephrol.* 22, 778–784.
- Papadopoulos, M.C., Saadoun, S., Davies, D.C., Bell, B.A., 2001. Emerging molecular mechanisms of brain tumour edema. *Br. J. Neurosurg.* 15, 101–108.
- Pasantes-Morales, H., Cruz-Rangel, S., 2010. Brain volume regulation: osmolytes and aquaporin perspectives. *Neuroscience* 168, 871–884.
- Pekny, M., Nilsson, M., 2005. Astrocyte activation and reactive gliosis. *Glia* 50, 427–434.
- Preston, G.M., Carroll, T.P., Gugginon, W.B., Agre, P., 1992. Appearance of water channels in *Xenopus* oocytes expressing red cell CHIP28 protein. *Science* 256, 385–387.
- Privat, A., 1977. The ependyma and subependymal layer of the young rat: a new contribution with freeze-fracture. *Neuroscience* 2, 447–457.



- Rascher, G., Fischmann, A., Kröger, S., Duffner, F., Grote, E.-H., Wolburg, H., 2002. Extracellular matrix and the blood-brain barrier in glioblastoma multiforme: spatial segregation of tenascin and agrin. *Acta Neuropathol.* 104, 85–91.
- Rash, J.E., 2010. Molecular disruptions of the panglial syncytium block potassium siphoning and axonal saltatory conduction: pertinence to neuromyelitis optica and other demyelinating diseases of the central nervous system. *Neuroscience* 168, 982–1008.
- Rash, J.E., Ellisman, M.H., 1974. Studies of excitable membranes. I. Macromolecular specializations of the neuromuscular junction and the nonjunctional sarcolemma. *J. Cell Biol.* 63, 567–586.
- Rash, J.E., Staehelin, L.A., Ellisman, M.H., 1974. Rectangular arrays of particles on freeze-cleaved plasma membranes are not gap junctions. *Exp. Cell Res.* 86, 187–190.
- Rash, J.E., Yasumura, T., Hudson, C.S., Agre, P., Nielsen, S., 1998. Direct immunogold labeling of aquaporin-4 in square arrays of astrocyte and ependymocyte plasma membranes in rat brain and spinal cord. *Proc. Natl. Acad. Sci. USA* 95, 11981–11986.
- Raviola, G., 1977. The structural basis of the blood-ocular barriers. *Exp. Eye Res. Suppl.* 27, 27–63.
- Reale, E., Luciano, L., Spitznas, M., 1974. Introduction to freeze-fracture method in retinal research. *Albrecht Von Graefes Arch. Klin. Exp. Ophthalmol.* 192, 73–87.
- Reichenbach, A., Bringmann, A., 2010. Müller cells in the healthy and diseased retina. Springer, New York.
- Reichenbach, A., Robinson, S.R., 1995. Phylogenetic constraints on retinal organisation and development. *Progr. Ret. Eye Res.* 15, 139–171.
- Reichenbach, A., Wolburg, H., 2005. Astrocytes and ependymal glia. In: Kettenmann, H., Ransom, B.R. (Eds.), *Neuroglia*. Oxford University Press, Oxford, pp. 19–35.
- Roemer, S.F., Parisi, J.E., Lennon, V.A., Benarroch, E.E., Lassmann, H., Bruck, W., et al., 2007. Pattern-specific loss of aquaporin-4 immunoreactivity distinguishes neuromyelitis optica from multiple sclerosis. *Brain* 130, 1194–1205.
- Rohlmann, A., Gocht, A., Wolburg, H., 1992. Reactive astrocytes in myelin-deficient rat optic nerve reveal an altered distribution of orthogonal arrays of particles (OAP). *Glia* 5, 259–268.
- Rosenberg, G.A., Navratil, M., Barone, F., Feuerstein, G., 1996. Proteolytic cascade enzyme increase in focal cerebral ischemia in rat. *J. Cereb. Blood Flow Metab.* 16, 360–366.
- Rossi, A., Pisani, F., Nicchia, G.P., Svelto, M., Frigeri, A., 2010. Evidences for a leaky scanning mechanism for the synthesis of the shorter M23 protein isoform of aquaporin-4. Implication in orthogonal array formation and neuromyelitis optica antibody interaction. *J. Biol. Chem.* 285, 4562–4569.
- Ruiz-Ederra, J., Zhang, H., Verkman, A.S., 2007. Evidence against functional interaction between aquaporin-4 water channels and Kir4.1 potassium channels in retinal Müller cells. *J. Biol. Chem.* 282, 21866–21872.
- Saadoun, S., Papadopoulos, M.C., Davies, D.C., Bell, B.A., Krishna, S., 2002a. Increased aquaporin I water channel expression in human brain tumours. *Br. J. Cancer* 87, 621–623.
- Saadoun, S., Papadopoulos, M.C., Davies, D.C., Krishna, S., Bell, B.A., 2002b. Aquaporin-4 expression is increased in oedematous human brain tumours. *J. Neurol. Neurosurg. Psychiatr.* 72, 262–265.
- Saadoun, S., Tait, M.J., Reza, A., Davies, D.C., Bell, B.A., Verkman, A.S., et al., 2009. AQP4 gene deletion in mice does not alter blood-brain barrier integrity or brain morphology. *Neuroscience* 161, 764–772.
- Saito, K., 1988. Orthogonal arrays of intramembrane particles in the supporting cells of the guinea pig vestibular sensory epithelium. *Am. J. Anat.* 183, 338–343.

- Sassoè Pognetto, M., Cantino, D., 1992. Fine structure and plasma membrane organization of retinal Müller cells in two reptiles. *J. Submicrosc. Cytol. Pathol.* 24, 521–531.
- Schotland, D.L., Bonilla, E., Van Meter, M., 1977. Duchenne dystrophy: alteration in muscle plasma membrane structure. *Science* 196, 1005–1007.
- Schotland, D.L., Bonilla, E., Wakayama, Y., 1981. Freeze-fracture studies of muscle plasma membrane in human muscular dystrophy. *Acta Neuropathol.* 54, 189–197.
- Schulz-Stüchtling, F., Wolburg, H., 1994. Astrocytes alter their polarity in organotypic slice cultures of rat visual cortex. *Cell Tissue Res.* 277, 557–564.
- Shibuya, S., Wakayama, Y., 1991. Changes in muscle plasma membranes in young mice with X chromosome-linked muscular dystrophy: a freeze-fracture study. *Neuropathol. Appl. Neurobiol.* 17, 335–344.
- Shibuya, S., Wakayama, Y., Oniki, H., Kojima, H., Saito, M., Etou, T., et al., 1997. A comparative freeze-fracture study of plasma membrane of dystrophic skeletal muscles in dy/dy mice with merosin (laminin 2) deficiency and mdx mice with dystrophin deficiency. *Neuropathol. Appl. Neurobiol.* 23, 123–131.
- Shibuya, S., Wakayama, Y., Inoue, M., Kojima, H., Oniki, H., 2006. The relationship between intramembranous particles and aquaporin molecules in the plasma membranes of normal rat skeletal muscles: a fracture-label study. *J. Electron Microsc.* 55, 63–68.
- Silberstein, C., Bouley, R., Huang, Y., Fang, P., Pastor-Soler, N., Brown, D., et al., 2004. Membrane organization and function of M1 and M23 isoforms of aquaporin-4 in epithelial cells. *Am. J. Physiol. Renal Physiol.* 287, F501–F511.
- Simard, M., Nedergaard, M., 2004. The neurobiology of glia in the context of water and ion homeostasis. *Neuroscience* 129, 877–896.
- Sinclair, C., Kirk, J., Herron, B., Fitzgerald, U., McQuaid, S., 2007. Absence of aquaporin-4 expression in lesions of neuromyelitis optica but increased expression in multiple sclerosis lesions and normal-appearing white matter. *Acta Neuropathol.* 113, 187–194.
- Sirken, S.M., Fischbeck, K.H., 1985. Freeze-fracture studies of denervated and tenotomized rat muscle. *J. Neuropathol. Exp. Neurol.* 44, 147–155.
- Smith, M.A., Hilgenberg, L.G.W., 2002. Agrin in the CNS: a protein in search of a function? *NeuroReport* 13, 1485–1495.
- Solé, S., Petegnief, V., Gorina, R., Chamorro, Á., Planas, A.M., 2004. Activation of matrix metalloproteinase-3 and agrin cleavage in cerebral ischemia/reperfusion. *J. Neuropathol. Exp. Neurol.* 63, 338–349.
- Solenov, E.I., Vetrivel, L., Oshio, K., Manley, G.T., Verkman, A.S., 2002. Optical measurement of swelling and water transport in spinal cord slices from aquaporin null mice. *J. Neurosci. Methods* 113, 85–90.
- Sorbo, J.G., Moe, S.E., Ottersen, O.P., Holen, T., 2008. The molecular composition of square arrays. *Biochemistry* 47, 2631–2637.
- Staehein, A., 1972. Three types of gap junctions interconnecting intestinal epithelial cells visualized by freeze-etching. *Proc. Natl. Acad. Sci. USA* 69, 1318–1321.
- Stone, D.M., Nikolics, K., 1995. Tissue- and age-specific expression patterns of alternatively spliced agrin mRNA transcripts in embryonic rat suggest novel developmental roles. *J. Neurosci.* 15, 6767–6778.
- Suzuki, M., Iwasaki, Y., Yamamoto, T., Konno, H., Yoshimoto, T., Suzuki, J., 1984. Disintegration of orthogonal arrays in perivascular astrocytic processes as an early event in acute global ischemia. *Brain Res.* 300, 141–145.
- Suzuki, H., Nishikawa, K., Hiroaki, Y., Fujiyoshi, Y., 2008. Formation of aquaporin-4 arrays is inhibited by palmitoylation of N-terminal cysteine residues. *Biochim. Biophys. Acta* 1778, 1181–1189.
- Tachikawa, T., Clementi, F., 1979. Early effects of denervation on the morphology of junctional and extrajunctional sarcolemma. *Neuroscience* 4, 437–451.

- Tait, M.J., Saadoun, S., Bell, B.A., Papdopoulos, M.C., 2008. Water movements in the brain: role of aquaporins. *Trends Neurosci.* 31, 37–43.
- Tani, K., Mitsuma, T., Hiroaki, Y., Kamegawa, A., Nishikawa, K., Tanimura, Y., et al., 2009. Mechanism of aquaporin-4's fast and highly selective water conduction and proton exclusion. *J. Mol. Biol.* 389, 694–706.
- Taniguchi, M., Yamashita, T., Kumura, E., Tamatani, M., Kobayashi, A., Yokawa, T., et al., 2000. Induction of aquaporin-4 water channel mRNA after focal cerebral ischemia in rat. *Brain Res. Mol. Brain Res.* 78, 131–137.
- Tao-Cheng, J.-H., Bressler, J.P., Brightman, M.W., 1992. Astroglial membrane structure is affected by agents that raise cyclic AMP and by phosphatidylcholine phospholipase C. *J. Neurocytol.* 21, 458–467.
- Thi, M.M., Spray, D.C., Hanani, M., 2008. Aquaporin-4 water channels in enteric neurons. *J. Neurosci. Res.* 86, 448–456.
- Tian, M., Jacobsen, C., Gee, S.H., Campbell, K.P., Carbonetto, S., Jucker, M., 1996. Dystroglycan in the cerebellum is a laminin  $\alpha 2$  chain binding protein at the glial-vascular interface and is expressed in Purkinje cells. *Eur. J. Neurosci.* 8, 2739–2747.
- Ueda, H., Baba, T., Kashiwagi, K., Iijima, H., Ohno, S., 2000a. Dystrobrevin localization in photoreceptor axon terminals and at blood-ocular barrier sites. *Invest. Ophthalmol. Vis. Sci.* 41, 3908–3914.
- Ueda, H., Baba, T., Terada, N., Kato, Y., Fuji, Y., Takayama, I., et al., 2000b. Immunolocalization of dystrobrevin in the astrocytic endfeet and endothelial cells in the rat cerebellum. *Neurosci. Lett.* 283, 121–124.
- Usukura, J., Yamada, E., 1978. Observations on the cytolemma of the olfactory receptor cell in the newt. 1. Freeze replica analysis. *Cell Tissue Res.* 188, 83–98.
- Vajda, Z., Promeneur, D., Dóczy, T., Sulyok, E., Frøkiaer, J., Ottersen, O.P., et al., 2000. Increased aquaporin-4 immunoreactivity in rat brain in response to systemic hyponatremia. *Biochem. Biophys. Res. Commun.* 13, 495–503.
- Van Hoek, A.N., Bouley, R., Lu, Y.X., Silberstein, C., Brown, D., Wax, M.B., et al., 2009. Vasopressin induced differential stimulation of AQP4 splice variants regulates the in-membrane assembly of orthogonal arrays. *Am. J. Physiol. Renal Physiol.* 296, F1396–F1404.
- Verbavatz, J.-M., Ma, T., Gobin, R., Verkman, A.S., 1997. Absence of orthogonal arrays in kidney, brain and muscle from transgenic knockout mice lacking water channel aquaporin-4. *J. Cell Sci.* 110, 2855–2860.
- Verkman, A.S., 2007. Role of aquaporins in lung liquid physiol. *Respir. Physiol. Neurobiol.* 159, 324–330.
- Vizuete, M.L., Venero, J.L., Vargas, C., Ilundáin, A.A., Echevarría, M., Machado, A., et al., 1999. Differential upregulation of aquaporin-4 mRNA expression in reactive astrocytes after brain injury: potential role in brain edema. *Neurobiol. Dis.* 6, 245–258.
- Wakayama, Y., 2010. Aquaporin expression in normal and pathological skeletal muscles: a brief review with focus on AQP4. *J. Biomed. Biotechnol.*, ID 731569.
- Wakayama, Y., Okayasu, S., Shibuya, S., Kumagai, T., 1984. Duchenne dystrophy: reduced density of orthogonal array subunit particles in muscle plasma membrane. *Neurology* 34, 1313–1317.
- Wakayama, Y., Kumagai, T., Shibuya, S., 1985. Freeze-fracture studies of muscle plasma membrane in Fukuyama-type congenital muscular dystrophy. *Neurology* 35, 1587–1593.
- Wakayama, Y., Kumagai, T., Jimi, T., 1986. Small size of orthogonal array in muscle plasma membrane of Fukuyama type congenital muscular dystrophy. *Acta Neuropathol.* 72, 130–133.
- Wakayama, Y., Jimi, T., Inoue, M., Kojima, H., Murahashi, M., Kumagai, T., et al., 2002. Reduced aquaporin 4 expression in the muscle plasma membrane of patients with Duchenne muscular dystrophy. *Arch. Neurol.* 59, 431–437.

- Warth, A., Kröger, S., Wolburg, H., 2004. Redistribution of aquaporin-4 in human glioblastoma correlates with loss of agrin immunoreactivity from brain capillary basal laminae. *Acta Neuropathol.* 107, 311–318.
- Warth, A., Mittelbronn, M., Wolburg, H., 2005. Redistribution of the water channel protein aquaporin-4 and the K<sup>+</sup> channel protein Kir4.1 differs in low- and high-grade human brain tumors. *Acta Neuropathol.* 109, 418–426.
- Warth, A., Simon, P., Capper, D., Goepfert, B., Tabatabai, G., Herzog, H., et al., 2007. Expression pattern of the water channel aquaporin-4 in human gliomas is associated with blood-brain barrier disturbance but not with patient survival. *Neurosci. Res.* 85, 1336–1346.
- Wilhelmsson, U., Bushong, E.A., Price, D.L., Smarr, B.L., Phung, V., Terada, M., et al., 2006. Redefining the concept of reactive astrocytes as cells that remain within their unique domains upon reaction to injury. *Proc. Natl. Acad. Sci. USA* 103, 17513–17518.
- Winder, S.J., 2001. The complexities of dystroglycan. *Trends Biochem. Sci.* 26, 118–124.
- Wolburg, H., 1995. Orthogonal arrays of intramembranous particles: a review with special reference to astrocytes. *J. Brain Res.* 36, 239–258.
- Wolburg, H., Berg, K., 1988. Distribution of orthogonal arrays of particles in the Müller cell membrane of the mouse retina. *Glia* 1, 246–252.
- Wolburg, H., Paulus, W., 2010. Choroid plexus: biology and pathology. *Acta Neuropathol.* 119, 75–88.
- Wolburg, H., Kästner, R., Kurz-Isler, G., 1983. Lack of orthogonal particle assemblies and presence of tight junctions in astrocytes of the goldfish (*Carassius auratus*). A freeze-fracture study. *Cell Tissue Res.* 234, 389–402.
- Wolburg, H., Neuhaus, J., Pettmann, B., Labourdette, G., Sensenbrenner, M., 1986. Decrease in the density of orthogonal arrays of particles in membranes of cultured rat astroglial cells by the brain fibroblast growth factor. *Neurosci. Lett.* 72, 25–30.
- Wolburg, H., Berg-Von der Emde, K., Naujoks-Manteuffel, C., 1992. Müller (glial) cells in the retina of urodeles and anurans reveal different morphology by means of freeze-fracturing. *Neurosci. Lett.* 138, 89–92.
- Wolburg, H., Wolburg-Buchholz, K., Sam, H., Horvát, S., Deli, M.A., Mack, A.F., 2008. Epithelial and endothelial barriers in the olfactory region of the nasal cavity of the rat. *Histochem. Cell Biol.* 130, 127–140.
- Wolburg, H., Wolburg-Buchholz, K., Mack, A., Reichenbach, A., 2009. Ependymal cells. In: Squire, L. (Ed.), *The New Encyclopedia of Neuroscience*. Academic Press, Oxford, pp. 1133–1140.
- Wolburg-Buchholz, K., Mack, A.F., Steiner, E., Pfeiffer, F., Engelhardt, B., Wolburg, H., 2009. Loss of astrocyte polarity marks blood-brain barrier impairment during experimental autoimmune encephalomyelitis. *Acta Neuropathol.* 118, 219–233.
- Wujek, J.R., Reier, P.J., 1984. Astrocytic membrane morphology: differences between mammalian and amphibian astrocytes after axotomy. *J. Comp. Neurol.* 222, 607–619.
- Yang, B., Brown, D., Verkman, A.S., 1996. The mercurial insensitive water channel (AQP-4) forms orthogonal arrays in stably transfected Chinese hamster ovary cells. *J. Biol. Chem.* 271, 4577–4580.
- Yang, B., Zador, Z., Verkman, A.S., 2008. Glia cell aquaporins-4 overexpression in transgenic mice accelerates cytotoxic brain swelling. *J. Biol. Chem.* 283, 15280–15286.
- Zelenina, M., 2010. Regulation of brain aquaporins. *Neurochem. Int.* 57, 468–488.
- Zhou, J., Kong, H., Hua, X., Xiao, M., Ding, J., Hu, G., 2008. Altered blood-brain barrier integrity in adult aquaporin-4 knockout mice. *NeuroReport* 19, 1–5.
- Zlokovic, B.V., 2008. The blood-brain barrier in health and chronic neurodegenerative disorders. *Neuron* 57, 178–201.

This page intentionally left blank

# INTERPRETING THE STRESS RESPONSE OF EARLY MAMMALIAN EMBRYOS AND THEIR STEM CELLS

Y. Xie,<sup>\*,†</sup> A.O. Awonuga,<sup>†</sup> S. Zhou,<sup>\*,‡</sup> E.E. Puscheck,<sup>†</sup> and  
D.A. Rappolee<sup>\*,†,‡,§,¶,||,★★</sup>

## Contents

|                                                                                                                    |    |
|--------------------------------------------------------------------------------------------------------------------|----|
| 1. Introduction                                                                                                    | 47 |
| 2. Stress and Stress Enzymes                                                                                       | 47 |
| 2.1. Definition                                                                                                    | 47 |
| 2.2. Using null mutants to define essential developmental events                                                   | 51 |
| 3. Stress Responses                                                                                                | 52 |
| 3.1. Cellular stress and essential developmental events in the embryo                                              | 52 |
| 3.2. Dose-dependence in cellular survival and organismal survival responses                                        | 53 |
| 3.3. Time dependence and the switch from cellular to organismal survival                                           | 58 |
| 3.4. Stress response <i>in vitro</i> during reprogramming of adult somatic nuclei to create pluripotent stem cells | 60 |
| 4. Roles of Stress Enzymes                                                                                         | 61 |
| 4.1. Detection of contradictory signals and defining optimal conditions for stem cells                             | 61 |
| 4.2. Difference in homeostatic stress set points                                                                   | 64 |
| 4.3. Effect of maladaptive responses to O <sub>2</sub> stress                                                      | 65 |
| 4.4. Kinetics of the stress responses                                                                              | 66 |

\* CS Mott Center for Human Growth and Development, Wayne State University School of Medicine, Detroit, Michigan, USA

† Department of Obstetrics and Gynecology, Wayne State University School of Medicine, Detroit, Michigan, USA

‡ Program for Reproductive Sciences, Wayne State University School of Medicine, Detroit, Michigan, USA

§ Department of Physiology, Wayne State University School of Medicine, Detroit, Michigan, USA

¶ Institute for Environmental Health and Safety, Wayne State University School of Medicine, Detroit, Michigan, USA

|| Karmanos Cancer Institute, Wayne State University School of Medicine, Detroit, Michigan, USA

★★ Department of Biology, University of Windsor, Windsor Ontario, Canada

|                                                                                                                 |    |
|-----------------------------------------------------------------------------------------------------------------|----|
| 4.5. Practical sequelae of stress response <i>in vitro</i> that can be used to increase the efficacy of IVF/ART | 67 |
| 4.6. Effect of stress on development: Lessons from MRP model of stress                                          | 70 |
| 5. Models and Lessons                                                                                           | 72 |
| 5.1. The “idling car” hypothesis                                                                                | 72 |
| 5.2. Behavior of highly proliferative and lesser proliferative stem cells                                       | 73 |
| 5.3. Preimplantation mouse embryo model for studies of early postimplantation development                       | 74 |
| 5.4. Reversibility of organismal survival mechanisms involving stem cell differentiation                        | 77 |
| 5.5. Lessons from stress that can inform us about mechanisms of normal development                              | 78 |
| 5.6. Stress enzymes and epigenetic memory, a lesson from fruit flies and yeast                                  | 79 |
| 6. Summary, Significance, and Future Studies                                                                    | 80 |
| Acknowledgments                                                                                                 | 84 |
| References                                                                                                      | 84 |

## Abstract

This review analyzes and interprets the normal, pathogenic, and pathophysiological roles of stress and stress enzymes in mammalian development. Emerging data suggest that stem cells from early embryos are induced by stress to perform stress-enzyme-mediated responses that use the strategies of compensatory, prioritized, and reversible differentiation. These strategies have been optimized during evolution and in turn have aspects of energy conservation during stress that optimize and maximize the efficacy of the stress response. It is likely that different types of stem cells have varying degrees of flexibility in mediating compensatory and prioritized differentiation. The significance of this analysis and interpretation is that it will serve as a foundation for yielding tools for diagnosing, understanding normal and pathophysiological mechanisms, and providing methods for managing stress enzymes to improve short- and long-term reproductive outcomes.

**Key Words:** Stress, Stress enzymes, SAPK/JNK, AMPK, Stem cells, Blastocysts, Pluripotency, Differentiation, Transcription factors, Metabolic regulation, Homeostasis. © 2011 Elsevier Inc.

## ABBREVIATIONS

|      |                                                                                             |
|------|---------------------------------------------------------------------------------------------|
| Akt  | protein kinase B (PKB)                                                                      |
| AMPK | AMP-activated protein kinase heterotrimer stress kinase (aka Prkaa1/2 is catalytic subunit) |

|                  |                                                                                                                                                   |
|------------------|---------------------------------------------------------------------------------------------------------------------------------------------------|
| AP1              | activator protein-1 transcription factor dimer                                                                                                    |
| ART              | assisted reproductive technology                                                                                                                  |
| ATF3/4           | activating transcription factor 3 a member of the ATF/CREB family of transcription factors                                                        |
| ATM              | ataxia telangiectasia-mutated serine threonine kinase is activated by binding double-strand DNA breaks                                            |
| BAX              | Bcl-2-associated X protein                                                                                                                        |
| CDKI15/21        | cyclin-dependent kinase inhibitor [CDKI; p15, p21]                                                                                                |
| Cdx2             | caudal-type homeodomain protein 2 transcription factor                                                                                            |
| ER stress        | endoplasmic reticulum-sensed stress                                                                                                               |
| ERK1/3/5         | extracellular receptor kinase 1/3/5                                                                                                               |
| ERR $\beta$      | estrogen receptor-related beta transcription factor                                                                                               |
| ESC              | embryonic stem cells                                                                                                                              |
| FGF4             | fibroblast growth factor 4                                                                                                                        |
| FISH             | fluorescence <i>in situ</i> hybridization                                                                                                         |
| Fos-c            | cellular fos transcription factor                                                                                                                 |
| Foxo             | Fox, a subclass of winged helix DNA-binding proteins (related to Forkhead family)                                                                 |
| GADD45           | growth and DNA damage-induced 45                                                                                                                  |
| Gastrulation     | formation and patterning of the three definitive embryo germ cell layers: endoderm, mesoderm, and ectoderm                                        |
| GATA2            | GATA binding transcription factor 2                                                                                                               |
| GCM1             | glial cells missing 1 transcription factor                                                                                                        |
| Genotoxic stress | nuclear stress affecting DNA integrity                                                                                                            |
| GLYT1            | glycine transporter of the neurotransmitter transporter gene family                                                                               |
| GM-CSF           | granulocyte-monocyte colony stimulating factor                                                                                                    |
| GSK3             | glycogen synthase kinase 3                                                                                                                        |
| Hand1            | heart and mesoderm inducer transcription factor                                                                                                   |
| HDAC             | histone deacetylase enzyme                                                                                                                        |
| HES1             | hairy enhancer of split 1 transcription factor                                                                                                    |
| HIF1             | hypoxia-inducible factor 1 transcription factor                                                                                                   |
| HSP22/68/70      | heat shock proteins 22/68/70.1                                                                                                                    |
| ICC              | immunocytochemistry                                                                                                                               |
| ICM              | inner cell mass of the blastocyst, precursor stem cells of extraembryonic endoderm and mesoderm and of the three germ cell layers at gastrulation |
| Id2              | inhibitor of differentiation 2 dominant negative transcription factor                                                                             |
| iPS cells        | inducible pluripotent stem cells                                                                                                                  |
| ISH              | <i>in situ</i> hybridization                                                                                                                      |
| IVF              | <i>in vitro</i> fertilization                                                                                                                     |



|                                   |                                                                                                                                              |
|-----------------------------------|----------------------------------------------------------------------------------------------------------------------------------------------|
| JunB/C                            | Jun transcription factor in the AP1 family                                                                                                   |
| KSOM                              | potassium (K) simplex optimized media. Least stressful media                                                                                 |
| LDL                               | low-density lipoprotein                                                                                                                      |
| LIF                               | leukemia inhibitory factor necessary for maintaining ESC <i>in vitro</i>                                                                     |
| M16                               | preimplantation culture media, stressful                                                                                                     |
| MAPK/ERK1/3                       | mitogen-activated protein kinase                                                                                                             |
| Maternal recognition of pregnancy | Secreted signal from the mammalian conceptus to keep the implantation site prepared for invasion by and nutrition of the conceptus (aka MRP) |
| MEKK4                             | mitogen-activated protein kinase kinase 4 tyrosine threonine dual protein kinase that activates SAPK and p38MAPK                             |
| MRP                               | maternal recognition of pregnancy                                                                                                            |
| mTOR                              | mammalian target of rapamycin, important signaling protein                                                                                   |
| Myc-c                             | cMyc transcription factor                                                                                                                    |
| NFκβ                              | nuclear factor kappa beta                                                                                                                    |
| Nuclear stress responses          | see genotoxic stress                                                                                                                         |
| Oct4                              | octamer binding transcription factor 4 (aka Pou5f1)                                                                                          |
| P38MAPK                           | p38 mitogen-activated protein kinase (aka MAPK11/12/13/14)                                                                                   |
| P53                               | tumor suppressor factor, (aka TRP53)                                                                                                         |
| PAF                               | platelet-activating factor                                                                                                                   |
| PDGF                              | platelet-derived growth factor                                                                                                               |
| PI3K                              | phosphoinositol 1,3 kinase                                                                                                                   |
| PL1                               | placental lactogen 1 rodent hormone produced by TGC (aka chorionic sommatomammotropin, CSH1)                                                 |
| PLK4                              | polo-like kinase (PLK)4                                                                                                                      |
| PLPM                              | prolactin-like protein M, rodent placental hormone                                                                                           |
| PPAR                              | peroxisome proliferator-activated receptor                                                                                                   |
| SAPK                              | stress-activated protein kinase                                                                                                              |
| SCNT                              | somatic cell nuclear transfer                                                                                                                |
| SGK                               | serum and glucocorticoid-inducible kinase                                                                                                    |
| Stra13                            | mammalian retinoic acid-inducible basic helix-loop-helix protein (aka Sharp2, Dec1)                                                          |
| TEAD4                             | TEA domain family transcription factor                                                                                                       |
| TF                                | transcription factors                                                                                                                        |
| TGC                               | trophoblast giant cells                                                                                                                      |
| TGFβ                              | transforming growth factor beta                                                                                                              |
| TPBPα                             | trophoblast-specific protein α, marker of spongiotrophoblasts in mouse                                                                       |
| TSC                               | trophoblast stem cells                                                                                                                       |

## 1. INTRODUCTION

Our intent is to analyze and interpret data that define the strategy and molecular mechanisms used by mammalian embryos and their stem cells in their response to stress. One key concept is that a unique subset of protein kinases is stress enzymes. These stress enzymes are activated by stress to perform cellular and organismal survival in stem cells and embryos. The strategy early in the stress response and at low stress levels is to first mediate *stem cell survival*. Later in the stress response, but only at higher stress levels, stem cell accumulation decreases and stress enzymes mediate *organismal survival* through stem cell differentiation. We call this compensatory differentiation. Stress-induced stem cell differentiation has unique properties of prioritization of early essential programs and reversibility at lower stress levels. An understanding of stress during early development is significant in diagnosing stress, understanding pathogenic mechanisms, and manipulating stress enzyme activity to improve embryo and stem cell health *in vitro* and *in vivo*.

## 2. STRESS AND STRESS ENZYMES

### 2.1. Definition

Cellular stress results in energy-requiring, cellular responses aimed at homeostasis. But these responses deflect downward the normal ability of the cell to perform adult or embryonic functions. Stress is the basis of pathogenesis, and organismal stress has been studied since early in the 1900s (Selye, 1970, 1971). Here, we will discuss stress effects mediated through stress enzymes in reproductive models; gametes, embryos, and their constituent stem cells.

We first need to define stress enzymes in contrast with other protein kinases. There are 510 protein kinases common to the mouse and human kinomes, 8 unique human protein kinases, and 30 unique mouse protein kinases (Caenepeel et al., 2004; Manning et al., 2002). “Stress enzymes” are a small fraction of the kinome. Stress enzymes can be distinguished from other kinases in that they are not isolated (or causal) as mitogenic mediators in focus-forming assays or from tumor samples, are not activated to high levels by any mitogen tested, but are activated strongly by many types of stressors (Gillis et al., 2001; Kyriakis et al., 1995; Woodgett et al., 1995). In contrast, mitogen-activated protein kinase/extracellular receptor kinases (MAPK/ERKs) are activated by many mitogens to high levels, are found at high levels and in the active state in focus-forming assays and tumor

samples (Mitra and Cote, 2009; Roovers and Assoian, 2000), but they are not activated to high levels by any stressor tested (Gillis et al., 2001; Kyriakis et al., 1995; Woodgett et al., 1995). For example, stress-activated protein kinase/junC terminal kinase (SAPK/JNK, aka MAPK8/9/10, but called SAPK throughout this chapter) and p38 mitogen-activated protein kinase (p38MAPK) (aka MAPK11/12/13/14) are activated to high levels by many stressors, but are not activated to high levels by many mitogenic growth factors.

There are unique characteristics and actions of stress enzymes. Stress kinases are ubiquitously expressed and inactive or active at low levels until the stress stimulus begins (Hardie, 2003; Ip and Davis, 1998; Kyriakis and Avruch, 1996). SAPK and AMP-activated protein kinase (AMPK) fit these criteria as stress enzymes. Thus, stress enzymes are part of a cellular “health insurance policy.” And as it is necessary to buy health insurance before a health crisis, similarly, cells must have an infrastructural stress response prepared before cellular stress initiates.

There are other possible classes of stress enzymes. One class would have a normal function during unstressed development, but this function stops and a separate function arises after stress initiates. A second class is a newly arising enzyme that does not exist before stress but is part of an adaptation to chronic stress. This type does not arise in the immediate phase of the stress response that is primarily posttranslational in regulation and activity (see Section 3.3). Neither of these possible classes will be analyzed here.

Stress enzymes are activated by a broad range of types of stressors, and these stress enzymes share many common substrates and homeostatic effects. Canonical phosphorylation sites on AMPK and SAPK catalytic subunits are allosteric activation sites. These phosphorylation sites also allow experimental detection of enzyme activation by phospho-specific antibodies. As phosphorylation requires relatively little ATP, existing stress mechanisms mediate rapid responses which allow energy to be applied to remediating the stress. Thus, stress enzymes and their substrates are part of a cellular health insurance policy that is in place and ready to function when the stress arrives.

We will next review the role of stress enzymes which mediate stress responses in adult somatic cells. We will consider SAPK and AMPK here, but a number of other stress enzymes will be important in mediating stresses in oocytes, embryos, and their stem cells. The role of stress enzymes and their role in adult somatic cells have been reviewed elsewhere; mammalian target of rapamycin (mTOR) and tuberous sclerosis complex (Di Nardo et al., 2009; Liu et al., 2006), AMPK (Bungard et al., 2010; Liu et al., 2006), SAPK (Goberdhan and Wilson, 1998; Kaneto et al., 2005), p38MAPK (Aouadi et al., 2006; Berra et al., 2000; Blanc et al., 2003), phosphoinositol 1,3 kinase (PI3K) (Abraham, 2004; Chang et al., 2003; Dent et al., 2003; Dreesen and Brivanlou, 2007; Franke, 2008; Okkenhaug and Vanhaesebroeck, 2003; Sedding, 2008; Vanhaesebroeck et al., 2005), and

Akt (Burgering and Medema, 2003; Ceci et al., 2004; Los et al., 2009). During the stress response in development of embryos and stem cells, additional transcription factors that lead to loss of pluripotency and gain of the differentiated states are regulated. These novel regulatory mechanisms will be discussed in this chapter.

Stress enzymes have interactive and unique functions. Stress kinases are unique from one another in performing different functions. For example, AMP responds to the energy status of the cell and corrects high AMP/low ATP status by reducing anabolic processes and increasing catabolic processes (Carling, 2004; Hardie, 2003). Although SAPK reacts to energy status, it does not directly sense AMP/ATP levels, and its chief function is in controlling cellular functions during stress in somatic cells and cell functioning during development (Ip and Davis, 1998; Kyriakis and Avruch, 1996; Rappolee, 2007; Xie et al., 2008). In early mouse embryos, SAPK and p38MAPK control highly distinct subsets of highly changing mRNA during embryo development in M16 media (Maekawa et al., 2005; Xie et al., 2008), which is a stressful media (Wang et al., 2005). Stress enzymes may antagonize one another, as exemplified by p38MAPK blocking SAPK activity (Abell et al., 2009), or stress enzymes may act in synergistic ways, sometimes in a linear sequence where the function of one stress enzyme is dependent on another, as exemplified by p38MAPK-dependent AMPK-induced function (Pelletier et al., 2005; Xi et al., 2001). Compared with SAPK, p38MAPK appears to do more to mediate normal development in the early embryo (Natale et al., 2004; Paliga et al., 2005; Wang et al., 2005; Xie et al., 2006b) and mediates positive adaptive cellular responses such as the induction of aquaporin in response to hyperosmotic stress (Bell et al., 2009). Although aquaporin 8 mRNA was SAPK-dependent in one study in stressful media (Maekawa et al., 2005), aquaporin 3/9 mRNA was not SAPK dependent in response to hyperosmotic stress (Bell et al., 2009). Conversely, hyperosmolar stress induced apoptosis through SAPK but not MAPK. Interestingly, an immediate cellular survival response of the early mouse embryo to hyperosmotic response is intake of GLYT1 osmolytes through cell membrane transporters, which requires no protein synthesis (Steeves et al., 2003). The enzymatic control of upregulation to the cell surface of osmolyte transporters is not known. Other organic osmolytes such as betaine and proline and their transporters are important in the cellular volume regulation response in precompaction mouse embryos (Anas et al., 2007), but postcompaction mouse embryonic development is rescued from hyperosmotic stress by alanine, glutamine, glycine, and beta-alanine (Richards et al., 2010). The coordination and integration of the cellular survival response of aquaporins and osmolyte transporters by stress enzymes in early embryos merits further investigation. Mitogen-activated protein kinase kinase (MEKK)4/SAPK downregulates glial cells missing (GCM)1, SAPK upregulates Hand1 mRNA, and AMPK downregulates

Id2 protein, molecular functions required to activate the placental lactogen 1 (PL1) promoter (Abell et al., 2009; Rappolee et al., 2010; Xie et al., 2010; Zhong et al., 2010). Thus, stress enzymes are unique, but interact with one another to regulate stress-response functions.

Stress can be mediated by organismal signals as well as local signals. For example, organismal stress hormones such as cortisol and adrenaline can diminish stem cell accumulation rates of embryonic stem cells (ESCs) and trophoblast stem cells (TSC) in the early embryo (Rappolee et al., 2010). These hormones or maternal malnutrition can reduce cell number in the peri-implantation embryo. Thus, many indirect signals from the maternal milieu can induce canonical signs of stress such as diminished stem cell accumulation.

Stress-enzyme responses can act at the cell surface, cytoplasm, or nucleus. The nucleus is a key target for the regulation of the stress response for this chapter. Upon activation, stress enzymes work at all positions of the cell. For example, SAPK can act at the cell surface to influence adhesive effects at the cell surface (Almeida et al., 2000; Li et al., 1997). SAPK also contributes to the regulation of mitochondrial activity in the cytoplasm during stress (Kharbanda et al., 2000). Endoplasmic reticulum (ER) stressors of the unfolded protein response initiate in the cytoplasm and also activate stress enzymes like SAPK and pERK (Zhang and Kaufman, 2006). Genotoxic stimuli such as benzopyrene or UV irradiation can initiate in the nucleus where DNA damage repair recognizing genes such as ataxia telangiectasia-mutated serine threonine kinase which binds double-stranded DNA lesions (ATM) can also activate SAPK (Hoffman and Liebermann, 2009; Holbrook et al., 1996; Kharbanda et al., 1998). All these stressors act locally upon the stem cell of the embryo. Thus, despite the stressor initiating signaling at many places within the cell, a single stress enzyme can mediate part of the stress response. After genotoxic stress, SAPK and MAPK directly and indirectly control the activity of hundreds of promoters in the nucleus (Hayakawa et al., 2004; Pokholok et al., 2006). This nuclear control is of interest during the stress response in oocytes, embryos, and their stem cells. Nuclear responses are of key interest, as emerging data suggest that stress enzymes regulate transcription factors and the differentiation programs of stem cells of the early mammalian embryo.

We will next review the role of transcription factors mediating stress responses in adult somatic cells. Stress is known to regulate transcription factors in adult somatic cells. There is a small set of transcription factors that mediate the stress response in somatic cells. These transcription factors and their role in the stress response have been reviewed elsewhere; nuclear factor kappa beta (NF $\kappa$ B) (Bowie and O'Neill, 2000; Mattson et al., 2000; Zhang and Chen, 2004), Forkhead, Foxo (Fox, a subclass of winged helix DNA-binding proteins that share homology with their founding member fork head protein, *Drosophila*.) (Hedrick, 2009; Hoogeboom and Burgering, 2009; Ronnebaum and Patterson, 2010; Sedding, 2008;

van der Horst and Burgering, 2007), activating protein (AP)1 (Karin and Chang, 2001; Karin et al., 2001; Kudo et al., 1999; Shaulian and Karin, 2001), and the glucocorticoid receptor (De Bosscher et al., 2006; Karin and Chang, 2001). These transcription factors mediate the immediate response to the initial stressor and transcription factors like peroxisome proliferator-activated receptor (PPAR) members mediate the resolution of stress response (O'Brien et al., 2005; Yumuk, 2006). These transcription factors are also important in the embryos and stem cells, but transcription factors that control the balance of pluripotency and differentiation are also controlled by stress enzymes during mammalian development.

## 2.2. Using null mutants to define essential developmental events

There are three key deadlines for prenatal developmental events, one near implantation. In the rodent model, null mutants that produce lethal phenotypes elucidate essential roles for protein kinases *in vivo*, and analyses of many null mutant lethals established essential molecular, cellular, and organ function required at specific deadlines for embryonic, fetal, and placental/yolk sac (Copp, 1995; Rappolee, 1999; Stanton et al., 2003). Essential developmental deadlines occur at E5.5 (5.5 days after fertilization), E8.5, and E11. At E5.5, basic cellular processes must be under zygotic control after loss of maternal gene products. Also, the endoderm must acquire nutrients for the embryo. At E8.5, limited diffusion of oxygen requires gene expression that mediates production of a beating heart, closed vascular system, and red blood cells. At E11, a working placenta is required to mediate nutrient and blood-gas transport to the fetus. Thus, the early implanting embryo and its stem cells must expand cell numbers and then differentiate to mediate essential function, as previously reviewed (Rappolee, 2007; Rappolee et al., 2010).

Phenotypes of null lethals are determined in gestational females under unstressed conditions, and more studies are needed for null mutants that may generate lethality only during gestational stress. But, stress kinases may not appear as essential in mouse null mutants where females undergo gestation under a normal, low-stress environment. Under these conditions, there may be no reproductive lethality, or effects of diminished fertility may be subtle. We anticipate, however, that stressed pregnancies would reveal the essential functions of stress enzymes during reproduction. Stress enzymes have not been tested *in vivo* during stressed gestations, but placental hormones have. For example, null mutants of decidual prolactin-related protein (DPRP) and the placental hormone prolactin-like peptide-A (PLPA) have only small fertility problems during normal gestation. But when the female is exposed to hypobaric caging creating gestational hypoxia, these hormonal nulls become lethal (Ain et al., 2004; Alam et al., 2007). This sort

of testing is needed to sort out the mechanisms by which stress enzymes mediate gestational stresses in the conceptus *in vivo*. Thus, gestational stresses such as low oxygen, toxic environmental compounds, or malnutrition may reveal the essential adaptive functions of stress enzymes.

### 3. STRESS RESPONSES

#### 3.1. Cellular stress and essential developmental events in the embryo

Cellular stress has canonical outcomes in adult somatic cells. Cellular stress deflects downward the trajectory of normal unstressed parenchymal function of adult somatic cells. Energy and ATP which would be applied to parenchymal function are diverted to the homeostatic response needed to maintain the cell during stress. The stress response removes the stressor or its cellular sequelae, or readjusts the programs of the cell if the stress is persistent and becomes chronic.

There are additional outcomes of cellular stress that are unique in stem cells and embryos. In the embryo, fetus and placenta, stem cells have no parenchymal function. The first “function” of a stem cell is to retain pluripotency and proliferates to make a stem cell pool sufficient in size. This size must accomplish the parenchymal function upon differentiation that is required by the next essential, developmental deadline. The second function of stem cells is to respond to stimuli, normal or stressful, that regulate the differentiation of sufficient function to mediate survival of the conceptus. Typically, only a subpopulation of stem cells differentiates to a given lineage with a given function. Residual stem cell subpopulations remain after the triggering stimulus for future expansion and differentiation to other lineages. So what developmental deadlines exist in the embryo, placenta, and fetus?

There are three deadlines defined by null mutant lethals, and the deadline at E5.5 for the maternal recognition of pregnancy (MRP) response is a key one for this review. As mentioned in Section 2.2, previous reviews have interpreted mouse knockouts with lethal outcomes to suggest the following developmental deadlines: (1) E5.5, (2) E8.5, and (3) E11. For each of these developmental deadlines, cellular and molecular programs must be in place to mediate sufficient function for organismal survival. The genes leading to lethality in null mutants provide clues to the necessary mechanisms and cellular functions required for organismal survival when the developmental deadline is reached. After these two reviews (Copp, 1995; Rappolee, 1999), other developmentally important events have become obvious. One is the requirement to mediate the antiluteolytic function of MRP at about E6.0, soon after implantation. Another is activation of lung and feeding functions on neonatal day 1. A number of preblastocyst lethal knockouts have

identified genes that mediate blastocyst lineage decision-making and various essential cellular functions (Chapter 7, Matzuk in Knobil and Neill, 2006; Stanton et al., 2003). In particular, MRP function is of significance because placental TSC must produce sufficient hormone to maintain the corpus luteum. This in turn induces sufficient progesterone that activates endometrial secretions necessary to prevent menstrual loss of the implanting conceptus. This is a difficult developmental deadline as the implanting mouse embryo initially has only about 100 TSC, and this pool must expand and then differentiate sufficient trophoblast giant cells (TGC) to produce endocrine hormones that target the corpus luteum. Sufficient multipotent TSC must be held in reserve for differentiate to other placental lineages essential for later development. Stress occurring during implantation would diminish stem cell accumulation rates and diminish the chances of organismal survival for the implanting conceptus. A unique aspect of stress during peri-implantation development is that it diminishes TSC accumulation, but that maternal size does not change. Thus, stressed TSC face a unique problem in that decreased accumulation must be solved by increasing proportional differentiated function from a pool of fewer stem cells.

### 3.2. Dose-dependence in cellular survival and organismal survival responses

Low-zone stress induces stress enzyme-mediated metabolic responses leading to stem cell survival. We define the stress outcomes in two terms for stem cells and embryos. These two outcomes are induced by a low range of stress and a high range of stress. Stress causes metabolic rearrangement, at low dose ranges and short durations. At low doses, apoptosis is not significantly increased and stem cell accumulation rates are not significantly decreased (Fig. 2.1). In our studies using oxygen, sorbitol/extracellular hyperosmolarity, and benzopyrene (BaP)/genotoxic stress, the approximate thresholds for apoptosis/significant cell accumulation decreases (low to moderate stress, Fig. 2.1), and differentiation effects are  $\leq 1\% \text{ O}_2$ ,  $\geq 25$  and  $\leq 200$  mM sorbitol, and  $\geq 1 \mu\text{M}$  BaP. Interestingly, apoptosis occurring via entrance of glucose into the intracellular hexosamine signaling pathway may eventually activate p53 and BAX, at lower levels of glucose at about 25–52 mM (Keim et al., 2001; Pantaleon et al., 2010). Studies from our lab suggest (Zhong et al., 2010) that low doses of stress induce an AMPK-dependent phosphorylation and inactivation of acetyl coA carboxylase (ACC, aka Acaca); (Zhong et al., 2010). This results in an inhibition of fatty acid synthesis and frees the carbons from acetyl coA for use in catabolic production of ATP for cellular homeostasis during the stress response. In the low stress range, stress enzymes do not significantly regulate the transcription factors that mediate stem cell differentiation or the transcription factors that maintain stem cell pluripotency. This low zone metabolic rearrangement and cellular homeostasis are shared by embryos



| <i>Stress</i> , nil to low                                                                  | <i>Stress</i> , low to moderate                                                                                                                                                                                                                | <i>Stress</i> , high                                                                                         | <i>Stress</i> , very high                                                                                                |
|---------------------------------------------------------------------------------------------|------------------------------------------------------------------------------------------------------------------------------------------------------------------------------------------------------------------------------------------------|--------------------------------------------------------------------------------------------------------------|--------------------------------------------------------------------------------------------------------------------------|
| <i>Apoptosis</i> , insignificant                                                            | <i>Apoptosis</i> : low but significant                                                                                                                                                                                                         | <i>Apoptosis</i> , high                                                                                      | <i>Necrosis</i> , not <i>apoptosis</i>                                                                                   |
| <i>Stem cell accumulation</i> may be diminished but not significant                         | <i>Stem cell accumulation</i> : decrease is significant                                                                                                                                                                                        | <i>Stem cell accumulation</i> , decreased to negative.                                                       | <i>Stem cell death</i> in hours                                                                                          |
| <b>Compensatory differentiation doses</b>                                                   |                                                                                                                                                                                                                                                |                                                                                                              |                                                                                                                          |
| <i>Stress enzyme function</i> : Insignificant or metabolic regulation<br>No differentiation | <i>Stress enzyme function</i> : Switch to differentiation, but not dominant<br>Substrates, pluripotency transcription factors destroyed<br>Differentiation transcription factors induced, activated, maintained<br>Differentiation; reversible | <i>Stress enzyme function</i> : Differentiation becomes dominant<br>Differentiation switches to irreversible | <i>Stress enzyme function</i><br>Total protein present<br>Phosphorylation, activation absent<br>Substrates not regulated |
| <i>Hyperosmolar cellular stress</i> :<br>0–25 mM sorbitol                                   | <i>Hyperosmolar cellular stress</i><br>>25 mM, but <200 mM sorbitol                                                                                                                                                                            | <i>Hyperosmolar cellular stress</i><br>400 mM sorbitol                                                       | <i>Hyperosmolar cellular stress</i><br>600–1000 mM sorbitol                                                              |
| <i>Benzopyrene</i> :<br>0 to >0.5 $\mu$ M (>1pack/day)                                      | <i>Benzopyrene</i> :<br>1–1.5 $\mu$ M (2–3 packs/day)                                                                                                                                                                                          | <i>Benzopyrene</i> :<br>2–5 $\mu$ M (4–8 packs/day)                                                          | <i>Benzopyrene</i><br>None                                                                                               |
| <i>Oxygen</i> :<br>2–20%                                                                    | <i>Oxygen</i><br><1%                                                                                                                                                                                                                           | <i>Oxygen</i><br><0.5–0%                                                                                     | <i>Oxygen</i><br>None                                                                                                    |
| ↓                                                                                           | ↓                                                                                                                                                                                                                                              |                                                                                                              |                                                                                                                          |
| Pathology requires multiple day exposure                                                    | Pathology, even after short-term (1 day) exposure                                                                                                                                                                                              |                                                                                                              |                                                                                                                          |

**Figure 2.1** Dose-dependent effects on stem cells include a switch from cellular survival at low doses to organismal survival that requires differentiation at high doses (compensatory differentiation).

and their stem cells and adult somatic cells. The phosphorylation of Acaca in the nil to low dose range occurs in an AMPK-dependent way, but AMPK-Id2 loss does not occur in this stress range (Fig. 2.1).

High doses of stress induce stress enzyme-mediated developmental responses leading to organismal survival through stem cell differentiation. A second set of outcomes in response to stress occurs when stress is at higher levels or durations (low to moderate and high stress ranges, Fig. 2.1). A threshold is passed where stress causes significant decreases in stem cell accumulation rates and significant increases in apoptosis. The threshold for increased apoptosis and decreased proliferation is often similar. The function of stress enzymes encompasses both the regulation of decreased stem cell cycle entry and increased stem cell apoptosis at very high stress levels. Thus, stress enzymes regulate the size of stem cell pools during the stress response, where apoptosis and exit from cell cycle are both SAPK dependent (Zhong et al., 2007). Interestingly, at low stress (or for short period of stress at high stress levels) levels, stress enzymes can inhibit apoptosis (Johnstone et al., 2005; Zhong et al., 2007). This is likely a response aimed at giving the cell and organism time to adapt to the stress (see Section 3.3 for time-dependent changes in the stress response).

Above the nil-low stress range threshold, stem cell accumulation rates are still brisk *in vitro* (Fig. 2.1, low-moderate level) but slightly and significantly lower than in unstressed stem cells. At this higher stress level, stress enzyme activity switches to a function not observed in the low stress range. At higher stress levels, stress enzymes regulate transcription factors that mediate stem cell differentiation. For example, AMPK mediates loss of inhibitor of differentiation (Id)2 at higher stress doses of benzopyrene and hyperosmolar stress (Xie et al., 2010; Zhong et al., 2010). In contrast, SAPK upregulates Eomesodermin and stabilizes Hand1 during stress (Awonuga et al., submitted). Id2 loss occurs normally in mouse and human placental stem cell differentiation, and in both cases, constitutive maintenance of Id2 by transgenesis prevents differentiation (Xie et al., 2010; Zhong et al., 2010, and references therein). Hand1 is necessary for differentiation of placental stem cells into TGC in the mouse soon after implantation, and Hand1 mRNA and protein are regulated by SAPK during stress (Abell et al., 2009; Xie et al., unpublished data). Thus, stress enzymes regulate the transcription factors that positively and negatively regulate differentiation during the response to high stress levels. A high dose stress that activates the maximal level of SAPK also induces *de novo* placental lactogen-1 (PL1) hormone mRNA (Liu et al., 2009). This hormone is the first hormone secreted by TGC and is detected in maternal blood in rodents within 1–2 days after implantation. It is not detected in the blastocyst through the hatched stage just prior to implantation and is not detected in cultured TSC isolated from the blastocyst. But, PL1 mRNA is induced within 24 h of high dose stress (Liu et al., 2009). Thus, stress and stress enzymes mediate placental stem cell differentiation when doses of stress induce stress enzyme-mediated decreases in stem cell accumulation. PL1 is an endocrine hormone

that binds receptors in the corpus luteum and activates progesterone synthesis as part of its antiluteolytic activity (Gregoraszczuk et al., 2000; Spencer et al., 2004; Thordarson et al., 1997; Wierzchos et al., 2000). The progesterone produced by the corpus luteum sustains the endometrium in a receptive state where high levels of secreted glycoproteins are needed to sustain the implanting conceptus. The conceptus implants during a period when oxygen levels are low but the stem cell state requires high levels of carbon to be used to produce ATP. The stem cells in the implanting embryo are virtually all in continuous reentry into S phase. Thus, all stem cell macromolecules in the early embryo must be doubled in every cell cycle, and the ATP needed to mediate this doubling is produced anaerobically by glycolysis with low levels of efficiency. This high zone stress-induced differentiation and organismal homeostasis are unique for embryos and their stem cells, as the capacity of stem cells to proliferate highly and differentiate is unique to stem cells of the embryo, placenta, and fetus. Our theory is that the stem cell responds to high stress with “compensatory differentiation” when an insufficient stem cell proliferation necessitates stem cell differentiation to fulfill an essential need on a developmental deadline. Stress enzymes are well suited to integrate the regulation of metabolic responses, diminished stem cell accumulation, and compensatory differentiation.

The threshold for conversion of stress enzyme function from metabolic to developmental outcomes is affected by two additional inputs, the energy available in the milieu of the embryo and the duration (Section 3.3) of the stress (Fig. 2.2). For example, AMPK is activated by hypoxia much more quickly and to higher levels when the stimulated cells are serum starved (Liu et al., 2006). Serum contains growth factors such as platelet-derived growth factor (PDGF) which activate receptor tyrosine kinases that canonically

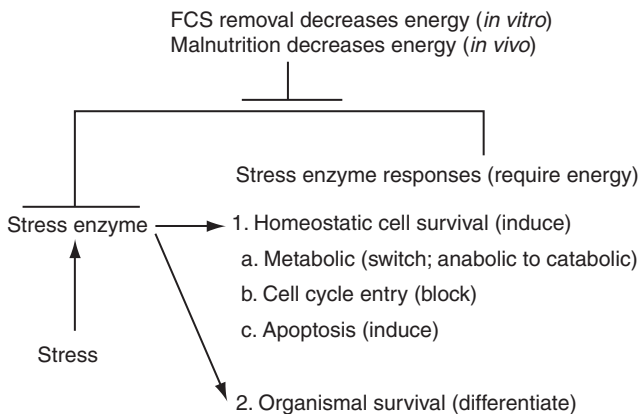


**Figure 2.2** Serum deprivation *in vitro* or malnutrition *in vivo* deplete cells of energy and increase the speed and magnitude of stress induced stress enzyme responses.

activate plasmalemmal distribution of food receptors such as low-density lipoprotein (LDL) receptor and transferring receptor (Rappolee and Werb, 1994 and references therein). Serum also contains additional food molecules such as albumin–fatty acid complexes. Thus, growth factor stimulated cells are able to acquire a larger carbon supply needed when stress depletes ATP.

There are contrasts between the stress response of TSC and ESC. In a previous review, we suggested that stress would induce development to the next essential developmental event (Rappolee, 2007). One would expect that situations throughout development would occur where stem cell accumulation would be diminished by stress and compensatory differentiation would ensue. Are placental stem cells a special case? This stem cell lineage diverges from the ESC lineage in the blastocyst when *Cdx2* becomes dominant in outer epithelial cells and octamer binding transcription factor 4 (*Oct4*) becomes dominant in the inner cell mass (Niwa et al., 2005). ESCs are stress resistant and have increased function for DNA repair and antioxidant function (Saretzki et al., 2004). Also, inner cell mass (ICM) in the day E3.5 embryo can slow cell cycle in response to x-irradiation, presumably during the G2 checkpoint, and undergo DNA repair, but the rapidly dividing embryonic ectoderm during gastrulation cannot (Heyer et al., 2000). An earlier report suggested that the stress of an inflammatory cytokine could induce *oct4* loss and perhaps differentiation (Zou et al., 2006). But other published results and unpublished data from our lab suggest that ESCs do not differentiate in response to stress. In studies using hydrogen peroxide as a stressor mouse ESC did not decrease *Oct4* protein (Guo et al., 2010). And in studies from our lab, transient proteasome-dependent loss of about half of *Oct4* protein at 4 h of cellular stress was followed by regain of *Oct4* protein to baseline levels by 24 h and a further increase by 72 h (Slater et al., unpublished data). Both of these studies are commensurate with a recently discovered stress function and domain on *Oct4* (Kang et al., 2009a,b). Like *Oct1*, *Oct4* appears to be required for the preparation in the unstressed cell of the stress kinome. In addition, once the stress begins, *Oct4*, like *Oct1*, is phosphorylated in the stress domain and is required to mediate the response to stress. *Oct4* loss would diminish the ESC response and appears to not be allowed. Rapid loss of *Id2* protein loss in TSC is not followed by recovery of *Id2* protein but by differentiation (Zhong et al., 2010). Interestingly, *Sox2* and *Nanog* also undergo stress-induced transient loss, but a fourth transcription factor, *Rex1*, undergoes a permanent loss. This suggests that ESCs under stress do not differentiate, but this may mean that they become partially determined. *Rex1* is a transcription factor present in ICM at E3.5 and E4.5 blastocyst but is absent by E5.5 in the primitive ectoderm. It has been shown that *Rex1* negative cells tend to later differentiate to express markers for endoderm and extraembryonic and embryonic mesoderm at gastrulation (Toyooka et al., 2008). So while the function of ESC is to remain

pluripotent and would appear to do so under stress, these stem cells do determine to an intermediate state that may be important for embryo survival as the embryo enters gastrulation.

### 3.3. Time dependence and the switch from cellular to organismal survival

The early global mRNA stress response in TSC is very small and all highly changing mRNAs decrease. When TSC are stressed by the level of hyper-osmolarity that maximizes SAPK activation, there is an interesting global mRNA response (Liu et al., 2009). There is a rapid (Fig. 2.3) highly changing group of mRNA that is small ( $N = 31$ ) and 100% decrease in magnitude. The 30-min time point corresponds to the early SAPK activation peak (Zhong et al., 2007). This time point also corresponds to other studies suggesting that the rapid stress response is to decrease macromolecular synthesis such as translation and transcription (Rappolee et al., 2010). This is linked to the diversion of energy to the homeostatic stress responses and away from the anabolic responses. It is likely that this energy diversion causes a downward deflection from the normal trajectory of high stem cell accumulation rates in the early embryo.

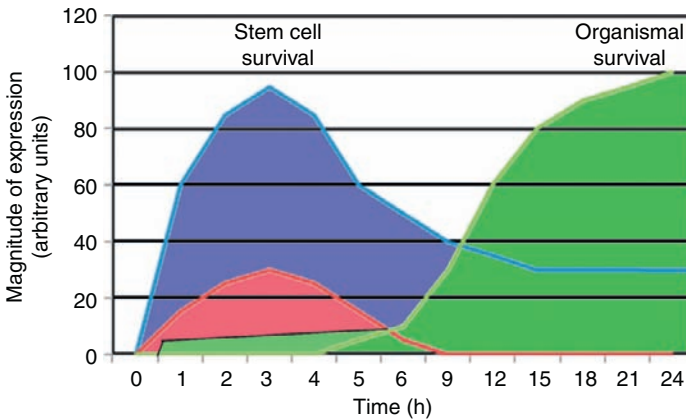


**Figure 2.3** The kinetics of compensatory differentiation. The early response before 6 h is downregulation of a small number of mRNA (relative levels of mRNA loss are shown in dark gray), metabolic stress enzyme activity (e.g., AMPK-dependent pAcaca, SAPK-dependent JunC, MycC, Rb, black), and at high doses preparation for differentiation (as in AMPK-dependent Id2 loss, SAPK-dependent Hand1 stabilization, upregulation, black). The late response after 6 h is 158 new mRNA, many upregulated *de novo* and mediating differentiation to produce markers and secreted placental hormones characteristic of primary/parietal TGC (light gray) while suppressing other placental lineages.

The fate of the early decreasing mRNA is to stay decreased at 24 h of hyperosmolar stress (Liu et al., 2009). We speculate that this is significant in that this response was correct at 30 min and at 24 h. Thus, none of the 31 downregulated genes required a reversal and required an energy-requiring resynthesis at 24 h.

Stress enzyme activity in the early response is regulated by posttranslational changes in TF that are likely to regulate later induction of new, developmental mRNA synthesis. AMPK and SAPK are both active by 15–30 min of hyperosmolar stress, but AMPK activity subsides by 60–120 min and SAPK activity persists as long as about half a day (Xie et al., 2007b, 2010; Zhong et al., 2007, 2010). In this period, AMPK-dependent acetyl CoA carboxylase (Acaca) phosphorylation, inactivation, and suppression of fatty acid anabolism occur to free up carbon usage for catabolism and ATP production (Zhong et al., 2010). In addition at high stress, AMPK-dependent Id2 loss occurs, but Id2 loss does not occur at low stress levels. For SAPK, JunC and MycC are phosphorylated by 30 min in both embryos and TSC (Xie et al., 2007b; Zhong et al., 2007). Hand1 protein is also upregulated and stabilized in a SAPK-dependent manner by 30 min and Hand1 mRNA is induced in a SAPK-dependent manner in cultured TSC (Abell et al., 2009; Rappolee lab, unpublished data). Although stress-induced Id2 loss and Hand1 increase indicates the start of the “organismal survival” response (Fig. 3), the predominant response early after stress is stem cell survival.

After 6–24 h of stress, a large, new set of mRNA is produced that mediate compensatory differentiation of TSC. Following the early response of TSC to the SAPK-maximizing stress dose, a second response has begun by 6 h and significantly increased in magnitude by 24 h of stress (Liu et al., 2009). This second phase of the stress response is largely developed by 24 h when 158/288 of highly changing mRNAs were upregulated. Many of the mRNA upregulated at 24 h were near baseline levels in unstressed TSC, suggesting new transcription had occurred between 6 and 24 h. Not only was there a shift from down- to upregulation of mRNA, but also the quality of the new mRNA program was clearly of developmental as well as homeostatic function. The highly upregulated homeostatic genes included growth and DNA damage-induced (GADD45 $\beta$ / $\gamma$ ), AP1 (junB/junC/activating transcription factor 3 (ATF3/4)), heat shock proteins (HSP22/68), and cyclin-dependent kinase inhibitor (CDKI; p15, p21). The highly induced developmental genes were transcription factors and hormones primarily indicating the induction of differentiated primary parietal TGC: transcription factors (Stra13, hairy enhancer of split 1 (HES1), GATA-binding2) and placental hormones [proliferin, PL-1, prolactin-like protein (PLP)M]. Thus, there is a kinetic aspect to compensatory differentiation similar to the dose-dependent aspect. As the TSC do not have receptors for some of the endocrine hormones induced by stress, these hormones would

not benefit these cells, but would influence maternal progesterone synthesis and benefit the implanting embryo. Although a large number of new mRNA indicate a predominant organismal survival response (Fig. 3, Liu et al., 2009), the stem cell survival response continues at 24hr of stress. The early response to stress cell survival and adaptation to stress is followed by later embryonic survival mediated by genes that regulate differentiation to the essential function needed next during development.

The switch from cellular to organismal survival strategies in stem cells in the implanting embryo is similar to a stress response in adults. For example, an adult organism traveling from low to high altitude initiates a response within hours that insures cellular survival by metabolic adaptation. Specifically, increased 2,3-disphosphoglycerate (DPG) decreases the affinity of hemoglobin in RBC that facilitates hemoglobin transport of  $O_2$  at lower  $pO_2$  (Guyton and Hall, 1997). A second organismal change that requires days is the initiation of hormonal changes that increase the  $O_2$  supply. In this slower change, hypoxia at high altitude induces erythropoietic production, increasing the RBC production that is part of the organismal survival strategy.

### 3.4. Stress response *in vitro* during reprogramming of adult somatic nuclei to create pluripotent stem cells

Somatic cell nuclear transfer (SCNT) leads to stressed blastomeres in reprogramming embryos due to external stress of media mediated by suspected stress mechanisms. The fact that Oct4 function is like Oct1 function in fibroblasts, in mediating preparation for and regulation of the ESC response to stress (Kang et al., 2009a), is important for a number of reasons. One is that media stress during isolation of ESC from embryos derived from oocytes that underwent SCNT is compounded by the transition of the SCNT embryo from a stress response governed by the donor somatic nucleus to the reprogrammed nucleus which is presumably governed by a robust Oct4 response (Gao and Latham, 2004; Vassena et al., 2007), where it is also known that Oct4 can undergo positive feedback (Niwa et al., 2005). The combination of a nucleus that reprograms during a response to stressful and incompatible media with the presence of a stress response governed by Oct4 is likely to lead to hypersensitive blastomeres that overreact to culture stress and lower the efficacy of ESC production.

Oct4 mediates a stress response early during reprogramming after transfection of the “Yamanaka four” reprogramming transcription factors. In addition, during a 16-day study of the ontogeny of induced pluripotent stem (iPS) cells, the first time point studied after reprogramming of an adult somatic cells using the “Yamanaka four” transcription factors was day 4 (Mikkelsen et al., 2008 and citations therein). At this time, the authors noted that a brisk stress kinome induction was detected by analysis of global mRNA microarray. Like the reprogramming of the donor nucleus during SCNT, difficulty in isolating iPS

cells is likely to arise when culture stress is compounded by the overexpression of Oct4 which is needed to reprogram adult somatic nuclei. Overexpression of Oct4 that expresses a stress response domain makes the reprogramming cell hypersensitive to culture stress. Thus, derivation of ESC by SCNT and iPS cells by reprogramming may both benefit from characterizing and managing the stress response mediated by Oct4 and stress enzymes.

## 4. ROLES OF STRESS ENZYMES

### 4.1. Detection of contradictory signals and defining optimal conditions for stem cells

SAPK detects contradictory signals in the milieu of the stem cell and embryo. Much of the initial work indicated that after isolation and IVF culture, embryos were subject to stress and stress enzymes responded proportionally to this stress and created outcomes proportional to this stress (Wang et al., 2005; Xie et al., 2008). But this stress was caused by a multifactorial, multivariable difference in media, so a single stressor, hyperosmolar stress was used by several labs studying stress responses in oocytes and preimplantation embryos (e.g., Downs, Watson, and Baltz labs). The studies of time- and dose-dependent responses of embryos have been reviewed elsewhere (Rappolee, 2007; Xie et al., 2008). One conclusion from these studies is that stress enzymes read from the program of the embryo and detect deviations from the normal milieu of the embryo during culture in complex media. To define this more specifically, we replaced the multiple variables in the milieu with a pair of well-characterized signals in the milieu which are used widely in embryo culture and in the culture of the most prevalent stem cell in the blastocyst, the TSC.

TSC were isolated from blastocysts using fibroblast growth factor 4 (FGF4) plus components of conditioned media from murine embryonic fibroblasts are required to maintain pluripotency and proliferation (Tanaka et al., 1998). FGF4 protein is detected by the late blastocyst stage in cultured embryos and embryo *ex vivo* and is necessary for maintaining pluripotent and proliferating polar trophoblastic TSC (Chai et al., 1998; Rappolee et al., 1994). In addition, low oxygen at 2% partial (p)O<sub>2</sub> has been reported to support cytotrophoblast proliferation and potency, and 20% oxygen favors cessation of proliferation and loss of multipotency in human and rodent placental stem cells (Adelman et al., 2000; Cowden Dahl et al., 2005; Genbacev et al., 1997; Takeda et al., 2007). The implanting blastocyst is derived from a low-oxygen environment close to 2% O<sub>2</sub> (Jauniaux et al., 2001; Rodesch et al., 1992) and thus, FGF4 and 2% oxygen are consonant in maintaining pluripotency and proliferation of TS cells during early peri-implantation embryo development. It was recently reported that FGF4 activates SAPK in TSC and this is required



for maintenance of pluripotency (Abell et al., 2009). However, like almost all reports of TSC *in vitro*, FGF4 was used with ambient oxygen at 20% conditions that would produce contradictory signals favoring TSC pluripotency and differentiation, and favoring and inhibiting TSC proliferation simultaneously. Thus, the contradictory signals of simultaneous FGF4 and 20% O<sub>2</sub> might activate SAPK through stress, not directly activate SAPK through FGF4 signaling alone. As mentioned above, until recently most embryo culture in IVF clinics was performed with O<sub>2</sub> near 20%. Thus, both TSC culture and IVF embryo culture have been done with contradictory signals of 20% O<sub>2</sub> and exogenous of ICM-derived FGF4.

We have found that when either contradictory signal is removed from cultured TSC while retaining the other, activated SAPK decreases about three- to fivefold (Zhou et al., 2011). Stress is relieved when cultured TSC are switched in either of two ways from commonly used 20% O<sub>2</sub>+FGF4: (1) FGF4 is removed but 20% O<sub>2</sub> retained, or (2) 20% O<sub>2</sub> is switched to 2%, but FGF4 is retained. Thus, SAPK detects improper growth factor and oxygen level combinations *in vitro* and presumably would also do so *in vivo*. As high altitude, cigarette smoking, and maternal hypertension could all decrease O<sub>2</sub> below the already low 2% O<sub>2</sub> at the site of implantation, “frank” hypoxia would develop below the 2% level.

The SAPK activation level nadir and stem cell proliferation peak report the optimum culture conditions for a stem cell and this is similar to the *in vivo* optima. The milieu TSC *in vivo* is 2% with FGF4: in the small preimplantation embryo, most TSC are near the FGF4 source which is the ICM. What the function of SAPK is during deviations from ideal milieu *in vivo* is unknown but of great interest. SAPK may play a role in suppressing invasion of TSC-derived cells as this has been reported for the MEKK4 null mutant (Abell et al., 2009). In MEKK4<sup>-/-</sup> mutant TSC, SAPK and p38MAPK stress enzymes are poorly activated. SAPK contributes to choice of TGC and suppression of the alternate lineage (chorionic/syncytiotrophoblasts) in the MEKK4<sup>-/-</sup> mutant (Abell et al., 2009). Stress activating the maximal SAPK levels also induces TGC genes while suppressing the GCM1 chorionic/syncytiotrophoblast cell lineages (Liu et al., 2009). Thus, both these reports suggest that the earliest functioning placental lineage (parietal TGC) is enhanced but a later differentiating lineage (chorionic/syncytiotrophoblast) is suppressed by stress and SAPK. This is a facet of stress-induced “prioritized differentiation.” Like compensatory differentiation, prioritized differentiation appears to be an evolutionarily evolved strategy to produce the next necessary function for a developmental deadline when stress diverts energy from stem cell accumulation.

If the milieu of the TSC in the implanting conceptus is 2% O<sub>2</sub>, one would expect that deviations up or down from this O<sub>2</sub> level would activate SAPK. Such is the case for cultured TSC exposed to suboptimal O<sub>2</sub> levels at 20% O<sub>2</sub> or at 0–0.5% (Fig. 2.4) and suggests that once the stem cell state is set

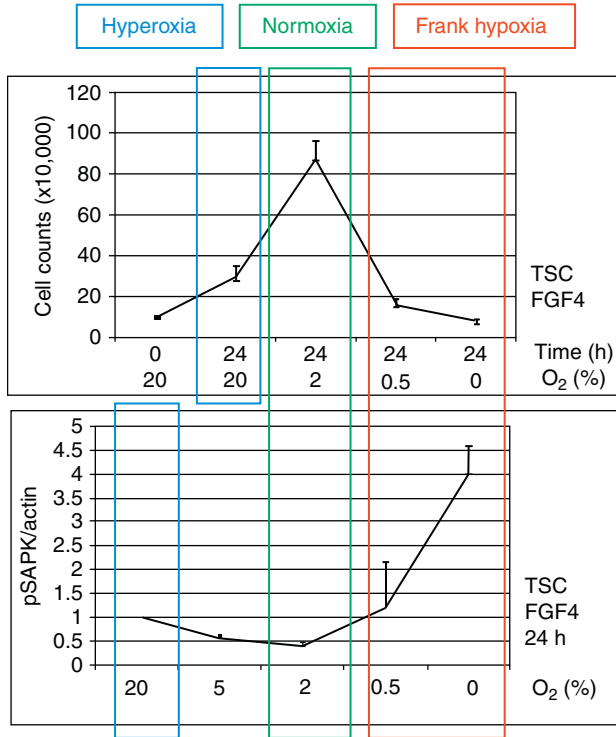


**Figure 2.4** Normoxia for stems cells *in vivo* is 2% O<sub>2</sub> and cultured stem cells are at highest growth rate and lowest stress (as shown by lowest activated stress enzyme) at 2% O<sub>2</sub>.

up, deviations from the O<sub>2</sub> level associated with this state would lead to a homeostatic response by stress enzymes. Interestingly, 2% O<sub>2</sub> is a hypoxic state for adult somatic cells and activates high levels of SAPK. This is the case because the adult somatic cell is in the venous to arterial niche of 5–8% O<sub>2</sub> and hypoxia at 2% requires a homeostatic response at this level for somatic cells. Interestingly, TSC accumulation rates peak at 2% and are less at higher or lower O<sub>2</sub> levels (Zhou et al., 2011). Once again maximal growth of stem cells and minimal stress enzyme activation report the optimal conditions of these stem cells in their milieu *in vivo*.

Stress enzymes can be used to define optimal culture conditions for isolation and maintenance of stem cells for regenerative medicine and for improving IVF/assisted reproductive technology (ART). Taken together, the ability of stress enzymes to detect contradictory signals or to identify optimal growth conditions *in vitro* suggests that the levels of stress enzyme activity can be used as a diagnostic tool for poor stem cell isolation and culture conditions. In addition, manipulating stress enzyme levels may also improve isolation and maintenance. The data from the *in vitro* model may

also be applied to the *in vivo* model where the conceptus adapts to O<sub>2</sub> levels that fluctuate due to a number of phenomena. Altitude changes causes O<sub>2</sub> levels to vary about twofold within the range of mammalian reproduction. Heavy smoking can reduce oxygen transport about 10% by complexing hemoglobin with carbon monoxide. Maternal hypertension may also diminish oxygen delivery to the conceptus. It is likely that stress enzymes play a key role when gestational O<sub>2</sub> fluctuations cause deviation from normal O<sub>2</sub> levels in the milieu of the conceptus and its stem cells.

Historically, IVF embryo culture was initially performed at 20% O<sub>2</sub>, but in recent years 5% have become prevalent. Gene expression in cultured mouse embryos is much closer to age-matched blastocysts after culture at 5% than at 20% (Rinaudo et al., 2006). Thus, optimization of O<sub>2</sub> levels during IVF, with attention to stress enzyme activation and stem cell accumulation rates, should establish an optimum at 5% or 2% compared with 20% O<sub>2</sub>.

## 4.2. Difference in homeostatic stress set points

Thresholds for stress response outcomes for embryos and stem cells are different. We have previously reviewed the differences in thresholds for biological outcomes like apoptosis, cell death, and embryo death (Xie et al., 2007b, 2008; Zhong et al., 2007). It was clear that cultured stem cells derived from the embryo have higher levels of apoptosis after the same duration, magnitude, and type of stress than the same stem cells have in the intact embryo. In fact, intact embryos can withstand the magnitudes of stress for 1–2 days that kill adult somatic cells and placental cell lines within hours. We speculated that this could be due to several mechanistic and teleological reasons. First, the outer epithelium of the embryo is a closed epithelium where all cells have neighbors, whereas ESC (Ezashi et al., 2005) and TSC (unpublished data, our lab) tend to differentiate and/or show greater stress responses at the edge of sheets of cells *in vitro*. Second, compared with single stem cells, the embryo may have supernumerary reservoirs of macromolecules to use during the stress response left from those molecules set during oogenesis and “divided” up among progeny cells during cleavage divisions.

Teleologically, 100 cells undergoing apoptosis in the adult organism is a minor problem, but for the 100 cell blastocyst, it is the end of the organism. Thus, a small embryo will probably have a very flexible molecular survival strategy, particularly among the “decidual” cell lineages that do not participate in the offspring. Stem cells for yolk sac endoderm and placental cell lineages are likely to be able to perform almost any differentiation event needed to preserve the conceptus. However, ESCs appear to be less flexible and can restrict determination, but not overtly differentiate in response to stress (Guo et al., 2010; Slater, unpublished data).

### 4.3. Effect of maladaptive responses to O<sub>2</sub> stress

Maladaptive O<sub>2</sub> responses may lead to clinically relevant outcomes with respect to implantation failure and placental insufficiency. Clinically, reproductive diseases of implantation failure and placental insufficiency such as preeclampsia, and intrauterine growth retardation may initiate and diagnostic markers become apparent in the first trimester. The disease then becomes clinically apparent in the second trimester (Huppertz, 2008; Roberts and Hubel, 2009). The maladaptive maternal response to the implanting conceptus is important in the second stage of pathogenesis. But, it is thought that the first stage of maladaptation to the uterine environment occurs early in the first trimester when TSC undergo incorrect lineage choice during differentiation. Maladaptive TSC responses would lead to improper lineage determination and differentiation that precipitates a second stage pathogenic maternal response. Interestingly, stress-induced differentiation when TSC are cultured in the presence of FGF4 does lead to a lineage imbalance where primary TGC are induced and chorionic/syncytiotrophoblast cells are suppressed, relative to TSC differentiation that occurs when FGF4 is removed without adding stress (Liu et al., 2009 and citations therein).

Similarly, the stress of TSC culture makes it impossible to maintain MEKK4<sup>-/-</sup> TSC that fail to activate SAPK and p38MAPK (Abell et al., 2009). Neither was there any report of a deficit in TSC production *in vivo*, nor do sections of the conceptus show high MEKK4 expression in normal placental lineages have placental lineage failures in MEKK4<sup>-/-</sup> *in vivo*. Thus, it may be a culture stress that the MEKK4<sup>-/-</sup> TSC fail to adapt to that makes the lineage unstable and prone to differentiate. The authors report minor lineage suppression of GCM1 and chorionic-syncytiotrophoblasts and trophoblast-specific protein (TPBP), a spongiotrophoblast that appears to be mediated by SAPK. Thus SAPK mediates lineage imbalance in two reports and in both the imbalance would favor preeclampsia if it occurred in humans.

These findings are somewhat similar to those reported by Liu and colleagues where large stress effects were observed when peak SAPK-activating levels of cellular stress were used in the TSC culture system (Liu et al., 2009). The studies by Liu et al. were on global mRNA outcomes but did not study the enzymes that mediated the stress effects. Preliminary follow-up studies indicate that AMPK mediates Id2 loss (Xie et al., 2010; Zhong et al., 2010) and SAPK does not mediate ID2 loss, but does mediate gain of Hand1 mRNA and protein as well as protein stabilization during stress. The source of culture stress that led to loss of the MEKK4<sup>-/-</sup> TSC is not clear. Improper O<sub>2</sub> levels certainly lead to stress and SAPK activation (Fig. 2.4) and this may contribute to the loss of TSC (Zhou et al., 2011). It is mitogen-activated protein kinase/extracellular receptor kinase (MAPK/ERK), not p38MAPK or SAPK, that are important in maintaining estrogen receptor-related beta (Err $\beta$ ) transcription factor (Abell et al., 2009)

which are necessary for sustaining pluripotency in TSC (Rappolee, 2007; Rappolee et al., 2010). Abell and colleagues found that TSC preferentially differentiate to GCM1+ lineages and have highly enhanced epithelial–mesenchymal transition and invasiveness in Matrigel assays. These appear to be the two major outcomes that would lead to loss of MEKK4<sup>-/-</sup> TSC.

Although SAPK and p38MAPK contribute to the imbalanced choice of TSC differentiation, the role of these two enzymes in suppression of invasion was not tested. Interestingly, it was previously reported that p38MAPK mediates trophoblast invasion in a luminal endometrial epithelial coculture model (Li et al., 2003). While MAPK and PI3K/Akt may mediate growth factor-induced trophoblast migration *in vitro* (Fitzgerald et al., 2005; Gleeson et al., 2001; Qiu et al., 2004), these studies do not address migration of invasion occurring spontaneously during culture. In addition, p38MAPK inhibitors derepress SAPK activation suggesting a role for p38MAPK in TSC may be to suppress SAPK (Abell et al., 2009). *In vivo*, gestational hypobaric O<sub>2</sub> leads to enhanced endovascular invasion of trophoblast cells (Rosario et al., 2008). This suggests that 2% O<sub>2</sub> and slightly lower levels induce some forms of trophoblast invasion, but this may be a different mechanism of invasion than that mediating the invasion into Matrigel. But, the reports suggest those trophoblasts are finely regulated by O<sub>2</sub> levels for many stages and types of invasion. Taken together, the data suggest that an imbalance where stress highly induces SAPK but relatively little p38MAPK could contribute to a suppression of invasion, a hallmark of diseases of placental insufficiency such as preeclampsia.

#### 4.4. Kinetics of the stress responses

Stress enzyme kinetics are dictated by the complementary nature of enzyme–substrate interaction. Long duration, active stress enzymes induce positive TF that mediate differentiation, and short duration, active enzymes mediate loss of differentiation blocking TF. Several stress enzymes are activated during the response of TSCs to a stress high enough to generate an organismal differentiation response. For example, both SAPK and AMPK are induced by cellular stresses such as hyperosmolar sorbitol and genotoxic stresses such as benzopyrene (Rappolee et al., 2010; Xie et al., 2007b, 2008, 2010; Zhong et al., 2007, 2010). However, AMPK is activated rapidly after 10 min of stress and subsides by an hour in TSC, ESC, and blastocysts, but SAPK is activated with a peak of 0.5–4 h with a long activation not subsiding until 10–12 h in TSC and embryos. Interestingly, AMPK mediates rapid proteasome-dependent loss of Id2 protein. However, SAPK mediates a long-term induction of Hand1 mRNA and protein and also Hand1 protein stability is dependent on SAPK (Rappolee lab, unpublished). Although SAPK could mediate Id2 protein downregulation required for

TSC differentiation, the short duration of stress-induced AMPK activity is insufficient to maintain the long-term Hand1 upregulation required for differentiation of TSC to PL1+ TGC *in vitro* and *in vivo* (Hughes et al., 2004; Riley et al., 1998). Thus, the enzyme–substrate kinetics is complementary to the kinetics of transcription factor regulation required for TSC differentiation.

#### 4.5. Practical sequelae of stress response *in vitro* that can be used to increase the efficacy of IVF/ART

All segments of IVF/ART create episodes of stress. IVF/ART provides challenges for the adaptive capabilities of the isolated embryo. Embryos must adapt to changes in O<sub>2</sub> levels, buffered pH in its milieu, complex maternal fluids of the oviduct and uterus, and amino acids. Many protocols in IVF/ART activate stress enzymes and can be interpreted as stressful. Hyaluronidase treatment to isolate the oocyte from surrounding cumulus cells activates AMPK (unpublished data). Pipetting creates shear stress that activates high, transient levels of SAPK (Xie et al., 2007a) although a single round of pipetting does not slow embryonic cell accumulation measured a day after the pipetting.

Stress enzymes diagnose IVF/ART stress. Culture of embryos activates more p38MAPK and SAPK than in age-matched embryos and the more stressful the media the slower the development of the embryo from the 2-cell to blastocyst stages (Wang et al., 2005). In media where more stress is detected (Wang et al., 2005; Xie et al., 2006b), there is a larger number of highly changed mRNA synthesis (114 in suboptimal Whitten's media vs. 29 in optimal KSOMaa) (Rinaudo and Schultz, 2004). The isolation and reimplantation events itself without culture are sufficient to create epigenetic reprogramming (Rivera et al., 2008). Latent TRP53 (aka p53) when activated by culture stress can mediate cell cycle arrest and lower implantation rates (Chandranathan et al., 2006; Li et al., 2007), but this effect is strain-specific in mouse. Therefore, it is likely to be variable in outbred human embryos. Maintenance of latency is mediated by exogenous ligands such as platelet-activating factor (PAF) through activation of PI3K/AKT signaling (Jin et al., 2009). It has been reported that p38MAPK maintains TRP53 mRNA at lower levels and may also contribute to decreased TRP53 activity in mouse embryos (Hickson et al., 2007). This fits with the hypothesis that p38MAPK functions to promote cell survival during stress on cultured embryos (see Section 1). PAF and another survival factor, granulocyte–macrophage colony stimulating factor (GM-CSF), show great promise in optimizing IVF media (Sjoblom et al., 2005). Interestingly, GM-CSF may act to suppress negative aspects of the stress response such as induction of Bax and HSP70 which are induced and may be causal in apoptosis in cultured embryos and stressed TSC (Chandranathan et al.,

2006; Liu et al., 2009) and during hyperosmolar stress (and insulinopathy) due to diabetes *in vivo* (Moley et al., 1998). Similar gene expression files featuring increases in apoptotic genes and increase in cell checkpoint gene expression in mouse and rhesus embryos of low quality judged by morphological means (Jurisicova et al., 1998; Mtango and Latham, 2008). This indicates that interaction of many stress mechanisms will be complex in humans, but that studies in rodents are identifying key nodal mediators of the useful and deleterious parts of the stress response.

Physiological and nonphysiological/nonevolutionary stressors induce stress enzymes and thus stress enzymes are important in IVF/ART protocols. Many of the stressors in IVF/ART are related to physiological or pathophysiological changes experienced by the embryo *in vivo*. Some changes in pH, O<sub>2</sub> levels, nutrient availability, and shear stress are likely to occur *in vivo* and *in vitro*, but at different levels and durations. Other stressors such as cryopreservation may be largely nonphysiological and have not been tested by similar episodes during evolution.

However, nonphysiological stimuli, such as microgravity simulation, also induce pSAPK (Wang et al., 2009). In fact, SAPK is so broad ranging in its response to physiological, toxic, and nonphysiological stressors that it is a good choice to monitor any negative stimulus (Fig. 2.5) to the embryo and its stem cells.

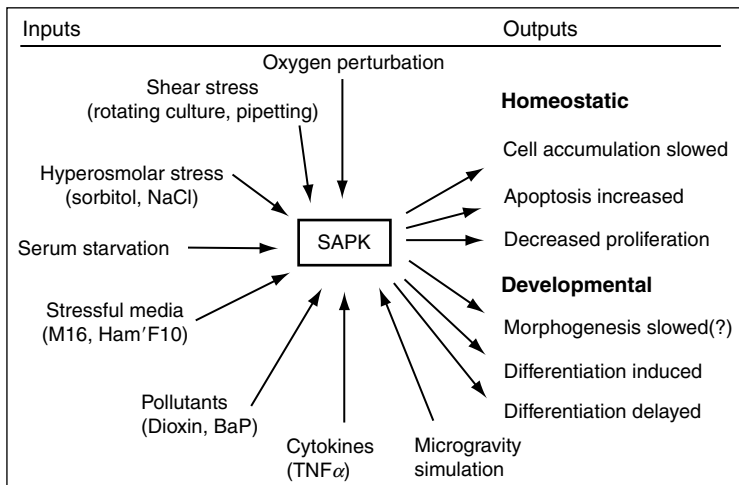


**Figure 2.5** SAPK is activated by a broad range of physiological, nonphysiological nonevolutionary, and toxic stressors and is a choice to measure any novel, experimental stress.

Although AMPK has not been studied as extensively, it is known to regulate oocyte maturation in response to toxic stress, cellular stress, and normal hormonal stimulation (Chen and Downs, 2008; LaRosa and Downs, 2006; LaRosa and Downs, 2007). Stress also induces TSC to prepare to differentiate by AMPK-dependent loss of Id2 (Xie et al., 2010; Zhong et al., 2010) under stress conditions that induce complete differentiation (Liu et al., 2009). Interestingly, AMPK is upregulated during freeze and thaw of a cold weather frog (Rider et al., 2006). So, although cryopreservation of mammalian sperm, oocytes, and embryos is nonphysiological and nonevolutionary, it is likely that AMPK will be activated during freeze and thaw. In addition, both slow and fast (vitrification) cryopreservation protocols use a hyperosmolar cellular dehydration step that is similar to protocols for inducing hyperosmolar stress enzyme activation in oocytes, embryos, and TSC (Liu et al., 2009; Xie et al., 2006b,c, 2007b; Zhong et al., 2007, 2010). Osmotic changes during sperm cryopreservation are likely to affect sperm function and may mimic aspects of capacitation (McCarthy et al., 2010; Pommer et al., 2002; Rutlant et al., 2003). Thus stress enzymes are likely to play a major role in the adaptation of gametes and embryos to cryopreservation.

Episodes of stress reversal may also create stress, even when the new stimulus itself seems intrinsically less stressful to previously unstressed stem cells and embryos. Interestingly, there are conditions of duration and magnitude of stress where removing an exogenous stressor causes greater negative outcomes than maintaining the stress. For both TSC and embryos, high levels of cellular, hyperosmolar stress can lead to a point where removing the stress leads to almost immediate death, whereas maintaining it leads to longer survival, although the stem cells and embryos are morbid (Xie et al., 2007b; Zhong et al., 2007, 2010). The TSC respond with an extensive adaptive program that is induced in response to stress (Liu et al., 2009) and this hypothetically must be reprogrammed to the unstressed state when stress subsides. Thus, isolating, handling, culturing, and reimplanting embryos all create episodes of stress, and we know little of how the embryo responds to multiple episodes of stress.

Stress enzymes make mistakes and adjusting stress enzyme function may aid in multiple protocols in IVF/ART. Stress enzymes may favor some processes while other outcomes are not optimized during the stress response. Or in the case of nonphysiological stresses which stress enzymes have not been tested for during evolution, stress enzymes may make mistakes. For example, SAPK is induced by seven IVF media to different levels and the rate of embryonic development is inversely proportional to the level of stress enzyme induced (Wang et al., 2005). However, in the most stressful media (most stress enzyme activating), SAPK functions to improve the rate of embryogenesis, and in the least stressful media, SAPK slows embryonic development and SAPK inhibitors accelerate development (Xie et al.,



2006a). This suggests that adjustment of SAPK function may improve IVF/ART. More research is needed to test for other effects of SAPK inhibition in optimal media, for long-term effects of SAPK inhibition, and finally to move testing from rodent to primate models.

Adjusting endogenous human responses are part of medicine and medically treating preimplantation gametes and embryos may become part of IVF/ART. It is best to use the array of diagnostic to diagnostics currently available to diagnose stressful segments of IVF/ART. These include spent amino acid turnover assays, metabolomics assays, and potentially assays for single or multiple secreted proteins in the spent media of stressed, cultured IVF embryos (Booth et al., 2007; Seli et al., 2008). A number of the SAPK-dependent mRNA expressed by embryos cultured in M16, a media we identified as stressful (Wang et al., 2005), were for secreted proteins (Maekawa et al., 2005; Rappolee, 2007; Xie et al., 2008). The data suggest that stress enzymes should provide multiple avenues for invasive and non-invasive diagnostics for embryo and stem stress.

#### **4.6. Effect of stress on development: Lessons from MRP model of stress**

Early mammalian development at the lacunar stage of implantation can feature TGC or syncytiotrophoblast, but in mouse, TGC are the primary hormone producers. In the mouse, TSC differentiate into TGC soon after implantation and these cells secrete PL1 into the blood which is detected within 1–2 days after implantation (Ogren et al., 1989) and 5–6 days after fertilization. This time period after implantation is called the “lacunar stage” because of the lacunae of blood surrounding the implanting conceptus (Enders et al., 1997). It is not clear which is the dominant placental cell type during the lacunar stage in different mammals. The predominant cells mediating communication with the maternal vasculature in primates such as rhesus macaques and skunks may be the syncytiotrophoblast, which can be detected as early as the morula stage and participates in endovascular invasion of endometrial arterioles (Enders, 1989; Enders and Mead, 1996; Enders et al., 1997). However, in mouse, the TGC appear to be the dominant cell early after implantation (Bevilacqua and Abrahamsohn, 1988; Chavez et al., 1984). But, in the case of all mammals, it is important to secrete an antiluteolytic hormone to maintain the corpus luteum and the endometrium through luteal progesterone secretion (Roberts et al., 1996).

A model is constructed from several reports that histone deacetylase (HDAC), hypoxia inducible factor 1 (HIF1), and stress enzyme function favor TGC while suppressing chorionic–syncytiotrophoblast and spongiotrophoblast lineages. In the mouse, chorionic trophoblasts arise in

preparation for chorioallantoic fusion and formation of the labyrinthine placenta at E7.5. Mouse TSC in the blastocyst do not express Hand1 or GCM, the essential transcription factors necessary for TGC and chorionic differentiation, respectively (Rappolee et al., 2010). However, during isolation and maintenance in culture, TSC express Hand1 but not GCM1 (Liu et al., 2009; Tanaka et al., 1998). Stress or FGF4 removal induces TSC to upregulate Hand1 to higher levels, but after 24 h of stress, TGC express Hand1 and PL1 but are GCM1 negative. However, after 24 h or FGF4 removal GCM1 positive cells arise (Liu et al., 2009 and citations therein). HIF1 is induced during FGF4 removal or low-oxygen stimulation of TSC and acts to block differentiation of chorionic trophoblast (Maltepe et al., 2005). In addition, HDAC acts to mediate differentiation to TGC and inhibitors of HDAC lead to a switch to the chorionic lineage. As MEKK4 null mutant TSC also enhance chorionic trophoblast and syncytiotrophoblast differentiation (Abell et al., 2009), this suggests that MEKK4/SAPK/p38MAPK HIF1 and HDAC are in a pathway that mediates normal or stressed differentiation to TGC and that SAPK may suppress chorionic differentiation through induction of active HIF1 or independently of HIF1 (Fig. 2.6). As the studies of Maltepe et al. (2005) and Abell et al. (2009) were done with contradictory signals, it is possible that some of the differentiation effects in these models were a product of the stress of culture.

*Common cellular stressors in vitro and in vivo:* Common cellular stressors for cultured cells are sorbitol-mediated hyperosmolarity, culture stress, heat stress, protein translation inhibitors, metabolic poisons such as arsenate, and DNA-damaging reagents such as benzo(a)pyrene (BaP), ultraviolet (UV)-, or gamma-irradiation. Common cellular stressors *in vivo* include malnutrition, hypoxia, toxic stress exposure, and inflammation. These stressors initially signal at different cellular locations where stress sensors initiate the stress response. Inflammatory cytokines like TNF-alpha and hyperosmolar stress initiate at the cell surface and both can activate SAPK, part of a four enzyme cytosolic protein kinase cascade (Ip and Davis, 1998).

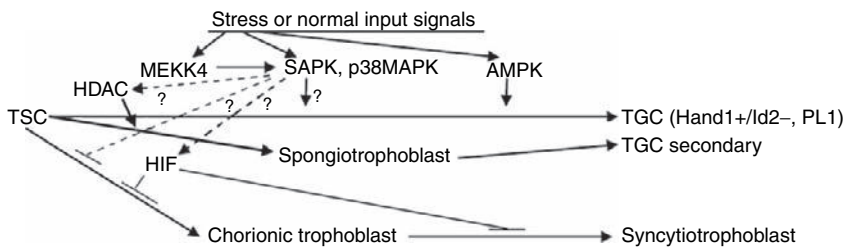


**Figure 2.6** HDAC- and MEKK4/SAPK-mediated induction of TGC differentiation and HIF1- and SAPK-mediated suppression of chorionic trophoblast differentiation.



## 5. MODELS AND LESSONS

### 5.1. The “idling car” hypothesis

Stress slows the preimplantation embryonic development associated with slowing of massive programs of molecular synthesis. The stress response in embryos has many characteristics shared with adult somatic cells. For example, both show time- and dose-dependent effects, although dose thresholds for outcomes can be different. For example, adult somatic cells have a lower threshold dose for initiating apoptosis. A unique effect discussed in this review is the stress-induced differentiation of stem cells to a parenchymal function necessary for a developmental deadline. Another unique aspect of the stress response in embryos is that the effect of the magnitude of stress is related to when the stress response initiates in relationship to the timing of the next developmental deadline.

Throughout this review, the peri-implantation mouse embryo and its TSC have served as models for studying stress-induced developmental control. However, results for the rate of induction of differentiation in embryos and TSC are different. Stress during culture of preimplantation slows developmental rates for four different events over 3 days of culture from the two-cell stage through the hatched blastocyst stage (Wang et al., 2005). Developmental events in the early mouse embryo occur after zygotic genome activation at the two-cell stage. It was established that compaction, the first epithelialization that occurs at the eight-cell stage, requires RNA synthesis between the two- and eight-cell stages (Kidder and McLachlin, 1985; McLachlin and Kidder, 1986). Similarly after compaction, the embryo goes through preparation for adhesion to the uterine epithelium that first requires mRNA synthesis and then protein synthesis (Armant, 2005; Schultz et al., 1997). After zygotic gene activation and compaction, there are very large programs of new mRNA synthesis requiring over 9000 new mRNA species as determined by microarray analysis (Hamatani et al., 2004; Wang et al., 2004). But stress leads to decreases in macromolecular synthesis by inhibiting transcription and translation (Carling, 2004; Hardie, 2003; Kyriakis and Avruch, 1996; Liu et al., 2006) and would thus lead to decreases in cell accumulation rate and developmental rates in stressed preimplantation embryos.

Stress speeds induction of differentiation of TSC where programs of molecular synthesis are largely complete. TSC await initiating signals for differentiation which can be mediated by protein kinases or stress enzymes. In contrast to preimplantation embryos, the TSC are closer to the terminus of preparation for differentiation. Cultured TSC can be re injected into the blastocyst to form a blastocyst chimera. Donor TSC can contribute to all placental lineages and thus are closely related in function to the TSC

endogenous to the blastocyst (Tanaka et al., 1998). However, unlike the TSC in the preimplantation blastocyst, cultured TSC express Hand1 mRNA and protein and thus are more like TSC in postimplantation embryos that are preparing to differentiate to TGC. In a similar model, Hand1 mRNA and protein exist in the Rcho1 rat placental stem cell and mediate differentiation to TGC when serum is removed (Martindill et al., 2007). Interestingly, the enzyme that mediates the derepression of Hand1 protein is polo-like kinase (PLK)4, not SAPK. However, in the Rcho1 and TSC induction models, the data suggest that these stem cells are very far along in preparation for differentiation and may need a small number of derepression events to differentiate. Thus, the cultured TSC represent a stem cell that is near the end of its preparatory macromolecular synthesis and awaiting a normal or stress signal for initiating the final stage of the differentiation program. For the trophectoderm of the implanting blastocyst, extrinsic signals initiate a posttranscriptional and posttranslational adhesion program (Armant, 2005; Khidir et al., 1995; Schultz et al., 1997). Soon after adhesion, the trophectoderm gains access to maternal vasculature during the lacunar stage. We hypothesize that stress could initiate TSC differentiation to PL1-secreting TGC *in vivo* as it does in cultured TSC (Liu et al., 2009 and references therein). In the case of stress for the TSC, induction of PL1 is more rapid than with FGF4 removal that emulates normal differentiation.

So while stress slows development during the large waves of macromolecular synthesis in the preimplantation embryo, it speeds up differentiation in TSC that are past the mRNA synthesis inhibitor- and protein translation inhibitor-sensitive stages of development. We call this the “idling car” hypothesis, as the preimplantation embryo would represent the stages of synthesizing and assembling thousands of car parts and the TSC represent the assembled car, with keys in the ignition, needing only a shift from neutral into gear to initiate the completion of differentiation. Of course, if only a single event is needed to occur to initiate the completion of differentiation, it is likely that stress signals and normal signals would require equal periods of time. It is more likely that stress differentiation includes Hand1 activation and Id2 destruction as well as Err $\beta$  loss and these coupled with all the downstream events they regulate are still complex enough to be prioritized by stress (see Section 4.4). Prioritization may speed up stressed development even though the total amount of energy available during stress may be less.

## 5.2. Behavior of highly proliferative and lesser proliferative stem cells

Highly proliferative stem cells undergo apoptosis rather than cell cycle arrest. In the fastest proliferating stem cells, rapid apoptosis replaces DNA repair. Typically, higher stress levels induce increasing amounts of apoptosis,

but lower stress levels induce less apoptosis but higher levels of cell cycle arrest or cell accumulation rate decreases (Fig. 2.2). During normal gastrulation, extremely high cell doubling rates occur in the embryonic cells. Interestingly, there is also a higher than normal rate of apoptosis in these cells (Manova et al., 1998). But, low levels of genotoxic stress (0.5 Gy) kill rapidly proliferating ESCs during gastrulation through ATM- and p53-dependent apoptosis without cell cycle arrest (Heyer et al., 2000). In the same embryo, however, extraembryonic cells undergo cell cycle arrest after the same stress, despite ATM and p53 expression. Thus, the strategy of the most rapidly growing cells is to undergo apoptosis rapidly without delays of cell cycle arrest and repair. The reason these cells undergo rapid proliferation, with doubling times approaching 3 h, is not clear. But, it is thought that the extraembryonic placental cells may undergo cell cycle arrest and repair including repair failures, because they are ultimately lost at birth. Thus, TSC and their progeny differentiated placental lineages can sustain error and are more flexible to respond to stress compared with cells in the ESC lineage from the ICM to the gastrulation stage embryonic ectoderm.

However, a common theme from blastomeres in the early cleavage stage embryo, through the stem cells in the blastocyst, and the rapidly dividing stem cells in the gastrulating embryo is to preserve DNA integrity. The slower dividing stem cells of the ICM in the blastocyst do not undergo the high rates of apoptosis after 0.5 Gy irradiation compared with the embryonic cells of the gastrulating embryo (Heyer et al., 2000). This suggests that the stress response in the most rapidly dividing stem cells that have progeny in the offspring must have a robust way of insuring apoptosis without relying on possible faulty DNA repair mechanisms that would require G2 checkpoint delays. The slower growing stem cells in the blastocyst, although giving rise to many progeny cells in the offspring, have sufficiently high fidelity DNA repair to overcome DNA lesions without automatic apoptosis.

### 5.3. Preimplantation mouse embryo model for studies of early postimplantation development

Weaknesses in the preimplantation embryo experimental model include small cell number but deficits with biochemical techniques have been overcome over the years. The study of cleavage stage through preimplantation embryos is “incredibly difficult” (Gilbert, 2010). Embryos at these stages are small with few cells and are difficult to study by biochemical techniques. Northern and Western blots are difficult requiring hundreds or thousands of embryos (Bachvarova et al., 1985; Fleming et al., 1989). However, RT-PCR and microarrays have made the study of smaller numbers of embryos and larger numbers of genes possible (Hamatani et al., 2004; Rappolee et al., 1988). For the study of proteins and

posttranslational modifications of proteins, new techniques may also allow the study of single oocytes and embryos (O'Neill et al., 2006). Likewise, new experimental platforms may allow single embryo quantification of multiple mRNA (Spurgeon et al., 2008; Zimmermann et al., 2008).

The preimplantation embryo is translucent and allows for studies of positional information in stem cell lineages in the blastocyst. Positional information is set up when polar, outside cells at the morula stage stabilize Cdx2 expression and determine to the placental lineage (Nishioka et al., 2009; Niwa et al., 2005). Soon after this nonpolar, inner cells where Oct4 is dominant over Cdx2 determine to the embryonic lineage and then express either Nanog (which suppresses endoderm) or Gata6 positive (Chazaud et al., 2006). The Gata6-expressing cells delaminate to form an endoderm that expresses Hex1 at first in all endoderm cells by E4.5, but this restricts to the distal visceral endoderm that is remote from proximal endoderm near the border with extraembryonic endoderm at E5.5 (Chazaud and Rossant, 2006; Thomas et al., 1998) and migrates to become the anterior visceral endoderm by E6.0. Thus, in 2.5 days, the embryo has undergone four events that set up three stem cell lineages and lead to four asymmetries that pattern the embryo.

Like *Caenorhabditis elegans*, the early mouse embryo is translucent, but unlike the *C. elegans*, or other fast genetic developmental research models like *Drosophila* or biochemical models like *Xenopus*, the mouse embryo is regulated in development and does not show overt molecular patterning in the oocyte or cellular patterning during early preimplantation development before the eight-cell stage (Pedersen, 1987). There are hints that the first extraembryonic primitive endoderm in the blastocyst has taken on positional information which will be signaled into the migrating embryonic ectoderm at the start of gastrulation, 2 days after implantation (Donnison et al., 2005; Mesnard et al., 2006; Rappolee, 1999; Tam et al., 2006; Voiculescu et al., 2007). However, the translucence of mouse embryos does afford the use of positional information about proteins, mRNA, and genetic loci of DNA using immunocytochemistry (ICC), *in situ* hybridization (ISH), and (f)luorescence (F)ISH (Nagy et al., 2003; Niwa et al., 2005; Wassarman and DePamphilis, 1993; Wilton, 2005).

Cause-and-effect studies are difficult due to maternal effects, but solid advances have been made and a plethora of experimental techniques exist. However, cause-and-effect methods continue to be difficult. Null mutant embryos are only one of four products of heterozygote mating, but that is the case for studies before and after implantation. However, compounding the problem in preimplantation embryos is the fact that a large number of genes are expressed in the heterozygous oocyte and the wild type, active locus produces sufficient mRNA and protein to delay phenotypes in the null zygote for days after zygote genome activation at the two-cell stage (Rappolee, 1999). Several groups have tried antisense oligonucleotide

injections or incubation (Rappolee et al., 1992; Siddall et al., 2002) or the creation of transient transgenics (Chai et al., 1998; Roelen et al., 1998).

For loss-of-function dominant negative transgenesis, injection of neutralizing antibodies that block maternal and zygotic genes, and zona pellucida (ZP)3 driven Cre-Lox mediated production of loss of maternal effects expression in the oocyte (Georgiades et al., 2007; Rappolee, 1999, 2007; Rossant, 2003; Tam and Rossant, 2003), promises to improve the study of preimplantation development.

Now that stem cells for every lineage in the blastocyst exist (Yamanaka et al., 2006), these stem cells provide biochemical models to corroborate studies of stem cell function in the embryo (Gross et al., 2005; Niwa et al., 2005; Riley et al., 2005). Despite these difficulties, several labs, notably the Rossant and Niwa labs, have used a combination of null preimplantation embryos and stem cells to tease out the complex interactions that determine and allocate ICM/ESC, trophoctoderm/TSC, and primitive endoderm (Chazaud et al., 2006; Ema et al., 2008; Hatano et al., 2003; Nishioka et al., 2009; Niwa et al., 2000, 2005; Ralston et al., 2010; Strumpf et al., 2005; Toyooka et al., 2008; Yamanaka et al., 2010). In the future, it will be important to understand how normal mechanisms are modulated during stress, and what the long-term effects of stress are.

The mouse preimplantation embryo can be cultured serum-free, studied for time- and dose-dependent mechanisms and effects independent of indirect maternal effects, and then reimplanted to assay for long-term effects. One of the slowest developing areas of understanding in mammalian developmental biology is its kinetics and dose-dependence. Relatively little is understood of these effects in the postimplantation developmental models because of expense, difficulty in experimental management of time and dose, and due to indirect maternal effects. The importance of duration of stimuli has been clear from the earliest studies on the stimulus response in adult somatic cells. In these studies, rapid waves of *c-fos* and *c-myc* transcription factors occur sequentially to mediate cell cycle progression (Callahan et al., 1985; Cochran et al., 1983; Kelly et al., 1983, 1984; Muller et al., 1984). In a previous review, we suggested that some data suggest that developmental signals can be rapid although windows of sensitivity are relatively long lived. A relatively well-worked-out example is the dependence of leukemia inhibitory factor (LIF) for blastocyst implantation which has a broad window of about 12 h, a peak window of 3 h, but which can be induced over a period of minutes (Chen et al., 2000; Mohamet et al., 2009; Paria et al., 2002; Rappolee, 2007). Studies on time dependence in the postimplantation model are rare and difficult.

But the mouse preimplantation embryo can be cultured serum free, studied for time- and dose-dependent mechanisms and effects independent of indirect maternal effects. In addition, cohorts of embryos can be reimplanted to assay for long-term effects. Although the preimplantation stem

cell is difficult to study, the motivation and advantages in using this model are strong and as technical difficulties are obviated by emerging technologies, this model should become powerful for studying the role of time- and dose-dependent stimuli in normal and stressed differentiation.

#### 5.4. Reversibility of organismal survival mechanisms involving stem cell differentiation

Stem cell differentiation can reverse when stress subsides. The maternal recognition protein (MRP) response during early postimplantation development exemplifies flexibility and prioritization strategies of TSC during stress-induced differentiation. As the embryo implants and prepares to mount an MRP response, an increase in stress would decrease the expansion of the TSC pool and then prepare and execute a program of differentiation. As we noted previously (Section 4.2), TSC cultured in monolayer are flexible to differentiate, whereas ESC cultured in monolayer are not. The level of flexibility is indicated by several lines of evidence. One is the high stress dose resistance of intact embryos in comparison to cultured TSC, or the lower doses for apoptosis of adult somatic cells compared with stem cells from the embryo (Section 4.2). Another is the high fraction of all stem cells that differentiates in response to stress. Virtually, an entire surviving population of TSC can be induced to lose Id2 and become PL1 positive. However, this creates an impossible situation if permanent. If all TSC differentiated to accomplish sufficient MRP signaling, differentiation of later placental lineages would have insufficient undifferentiated TSC remaining. One strategy to accomplish an essential parenchymal lineage differentiation event and then later differentiation event would be to dedifferentiate to TSC after stress.

This possibility is also indicated by the way stress induces PL1 via Id2 loss. At 400-mM sorbitol, Id2 protein is degraded in a proteasome- and AMPK-dependent manner [(Zhong et al., 2010); a similar AMPK-dependent Id2 loss also occurs with benzopyrene stressor (Xie et al., 2010)], but Id2 mRNA is retained after 24 h at levels similar or slightly higher than in unstressed TSC (Liu et al., 2009). At lower levels of glucose at hyperosmolar stress (100–200 mM sorbitol), significant Id2 loss, apoptosis, and decrease in TSC accumulation occur. But removal of stress leads to an increase in Id2 and decrease in PL1 protein (Zhong et al., 2010). In other words, for durations and magnitudes of stress that are not too high, it is likely that TSC are capable of differentiating to produce PL1 and then dedifferentiating into TSC. It is unclear what the size of subpopulations of stem cells that differentiate and dedifferentiate is, and what the capabilities to the dedifferentiated TSC are. In addition, *in vivo* studies are needed to elucidate how flexible and reversible stem cells are during stressed gestation. Careful studies on the sizes of subpopulations that differentiate and dedifferentiate are needed.



What is clear is the strategy of the TSC under stress shows similarities to responses of adult somatic cells under stress. For example, it is common for stressed somatic cells to disassemble active ribosomes and store mRNA in “stress granules” for use when stress subsides (Anderson and Kedersha, 2008). This strategy is linked to the large savings of energy (precious to the stressed cell) when existing mRNA is saved rather than destroying and then resynthesizing mRNA after stress subsides. Although AMPK has not been characterized in stress granule assembly, it has been characterized as downregulating ribosomal activity during hypoxic stress (Liu et al., 2006), and this in turn is similar to hyperosmolar stress (Patel et al., 2002). Taken together, the data suggest that many transient reproductive stressors will induce a transient differentiation event that is sufficient to mediate an essential lineage differentiation. After essential differentiated function is accomplished some of the cells can dedifferentiate into stem cells once the stress subsides.

## 5.5. Lessons from stress that can inform us about mechanisms of normal development

Duration of stress signaling is short during normal development. In a previous review, we considered the limits to the length of stress signaling in normal development. Although stress signaling could be a part of normal development, the negative aspects of stress-induced changes in metabolism (such as catabolism induction) would not be compatible with normal development if stress signaling was long lasting. AMPK can signal with peak activity at 10 min after stimulation and return to baseline by 30–60 min in response to two stress signals in ESC, TSC, and blastocysts (Xie et al., 2010; Zhong et al., 2010). This longevity of signaling would probably not affect development as 10–15 min of blastocyst pipetting can induce high levels of activated pSAPK, but this does not slow stem cell accumulation 24 h later (Xie et al., 2007a). As mentioned previously (Section 5.3), LIF signaling for 5–10 min is sufficient for essential signaling to the uterine epithelium to mediate implantation. Thus, it is likely that stress enzymes can signal during normal development, but that signaling would be accomplished rapidly, whereas nonstress ERK signaling may continue over extended time periods (Corson et al., 2003; Rappolee, 2007).

Stress enzymes are involved in nodal signaling pathways. Many normal developmental signaling pathways are known to be able to signal through stress enzymes, but these pathways are not well characterized. For example, SAPK can be activated by retinoic acid, wnt (through disheveled-frizzled noncanonical pathway), transforming growth factor beta (TGF $\beta$ ), and estrogen (Rappolee et al., 2010). Whether any of the stress enzymes-mediated signaling is essential or what the regulation shift from major to a more minor stress enzyme signaling is not known.

When duration of differentiation signals exceeds a threshold to establish a new differentiated state, then new regulation can be signaled by previously used growth factors. We have found that reversibility is a key feature of stress signaling, but have also noted that reversal of normal or stress signaling has large acute effects on stress enzymes (Xie et al., 2007b; Zhong et al., 2007, 2010; Zhou et al., 2011). For example, the largest inductions of SAPK occur when FGF4 is removed, pSAPK has rapidly decreased to its lowest point about 4 h after removal and then FGF4 is replenished. We interpret this to mean that a differentiation program must be complete and established for some period of time before the growth factor used to maintain the previous developmental program (in this case TSC pluripotency) can be used again in the new program. For example, FGF4/FGF1 can be used to maintain TSC *in vivo* and *in vitro* in the mouse (Chai et al., 1998; Tanaka et al., 1998), but FGF1 can induce greater PL1 synthesis after FGF4 is removed long enough to induce TGC (Peters et al., 2000). The data to date suggest that FGF4 must be removed for 12–24 h to fully develop the differentiated state before FGF can be added back to upregulate PL1 without dedifferentiating the TGC or causing higher levels of reversal stress in TGC.

## 5.6. Stress enzymes and epigenetic memory, a lesson from fruit flies and yeast

Mammalian ESCs use constantly active mechanisms involving polycomb to maintain open, but silenced genes for multiple, possible differentiation states. Chromatin immunoprecipitation studies suggest that many promoters mediating the differentiated state are open, but silenced in human and mouse ESCs (Boyer et al., 2006; Lee et al., 2006). Polycomb DNA-binding protein is part of this suppressive silenced state that is widespread in ESC and is associated also with promoters occupied by Oct4 and nucleosomes trimethylated at histone H3K27.

Yeast uses stress enzymes on many promoters to regulate large-scale responses. Other chromatin immunoprecipitation studies show that stress enzymes occupy a wide range of promoters in yeast, many of which they are known to regulate (Pokholok et al., 2006) and occupation can occur in a stimulus-dependent manner. Fruit fly uses SAPK to mediate polycomb loss during stress-induced differentiation in two stem cell models. In fruit fly, wounding of imaginal disk stem cells or reactive oxygen species-generated stress of hematopoietic stem cells leads to polycomb loss and stem cell differentiation that depends on SAPK/JNK (Lee et al., 2005; Owusu-Ansah and Banerjee, 2009). This suggests a shared strategy with stem cell strategies that mammalian ESC and TSC use in the stress response.

Mouse, fly, and yeast models discussed above suggest that stress enzymes regulate stemness in mammals. What these models suggest when interpreted

together. Taken together, these data suggest that stress enzymes in mammalian ESC may also respond to stress by activating SAPK/JNK and that this leads to polycomb loss and either differentiation or epigenetic determination of stem cells. As polycomb/extraembryonic deficient (Eed) is important in TSC differentiation (Kalantry et al., 2006; Wang et al., 2001, 2002), some stress enzyme-mediated epigenetic effects may work through this type of stem cell as well.

## 6. SUMMARY, SIGNIFICANCE, AND FUTURE STUDIES

In this review, we have attempted to give a brief analysis and interpretation of stress and stress enzyme responses that help us understand the pathogenic, pathophysiological, and normal strategies during early mammalian development. Key aspects of these strategies include (1) the dose- and time-dependent aspects of compensatory differentiation of stressed stem cells, (2) prioritized development of stressed stem cells, (3) the balance between reversibility and irreversibility of these responses, and (4) the differences in flexibility between different types of stem cells. All these studies are in the category of emerging science and need more detailed experimentation and analysis in rodent, primate, and human *in vitro* and *in vivo* models. The significance of these studies is that they can serve as a basis to diagnose, understand normal and pathophysiological mechanisms, and improve outcomes of early reproduction whether occurring *in vivo* or with *in vitro* segments.

Further studies will include studies of causality of normal and pathological outcomes mediated by stress enzymes. Studies of stress stimuli will include multiple episodes, multiple stressors, and chronic episodes of stress. The causality of stress signaling and its pathogenic mechanisms will be tested with further experiments. One key area to examine is the cyclic nature of stress, and test for the effects of multiple episodes of different qualities, durations, and magnitudes. It is likely that stress quality and episodes are additive in pathogenesis, but it is also possible that some amount of pre-conditioning occurs where early small doses mollifies the severity of the response to a later, larger dose.

To date, much of the testing for stress effects on stem cells and embryos are for hours to days. In the future, longer-term experiments lasting days to weeks should be performed. For longer stress durations, the threshold that divides the cellular survival response from a developmental, organismal response may be much lower. This will be important to understand so that pathogenesis during development can be modeled for many qualities of stress with accurate thresholds for pathogenic responses.

Future studies will translate the studies on cultured stem cells as models for embryos to the embryos themselves and to rodent, human, and primate models. We have put forward data that we have interpreted to suggest that stress induces stem cells to compensatory and prioritized development. These data have largely been developed in culture models for rodent stem cells. So it will be important to test whether compensatory and prioritized development is observed *in vivo*. These questions can be coupled to causality testing by testing whether implanting embryos that carry stress enzyme knockouts can perform stress-induced differentiation when gestational females are stressed.

Much of the pioneering work cited here has been performed in stem cells as an experimental proxy for embryos. Some of the enzyme kinetics and enzyme–substrate couplings appear to be the same for embryos and stem cells but others are not the same. It is important, therefore, to test whether the stress response and its causal effects are similar in embryos and as in stem cells derived from the embryos. In addition, it will be important to test whether these developmental strategies apply to primate and human model systems *in vivo* and *in vitro*. Some basic tenets of normal, early stem cell function for cultured ESC and TSC and for embryos appear to be different for human and primate versus mouse. Thus, translation of data and interpretations from rodent models to humans and primates is very important.

Future studies will test whether stem cells are flexible or inflexible with regard to compensatory differentiation and prioritized differentiation. It is not clear if most stem cells will be similar to TSC, flexible and able to differentiate a large subpopulation of cells under stress. Or most stem cells may be like ESC, where the top hierarchical pluripotency-maintaining transcription factor is tied to the stress response. In this case, that factor and its pluripotency function cannot be lost. For example, many adult stem cells also express Oct4, although this point is debated (Lengner et al., 2008) and these cells may be inflexible and unable to differentiate during their stress response.

It will be important to use flexible and inflexible stem cells to test for outright toxicological effects and for sublethal effects that ramify during the life of the offspring. TSC and ESC will provide models for developmental toxicology, where a nuanced and flexible response or an all-or-nothing response, respectively, are sought after. It is important to find thresholds for outright cellular toxicity. But for a full understanding of a long-term toxic effect, it is important to know how sublethal cellular outcomes may lead to improper organismal outcomes as in the field of fetal origins of adult diseases. It is likely that stress enzymes participate in epigenetic mechanisms that mediate long-term cellular memory developed during embryonic or fetal stress episodes but regulate metabolic programs throughout the lifespan of the offspring.

It is clear that stress enzymes can serve as diagnostics for stem cell culture and embryo culture as indicated by past studies on seven media (Section 4.5) and oxygen dose–response data shown here (Section 4.1). Stress enzymes could be used as diagnostic readouts to perform the kind of simple optimization used to develop the optimized embryo media KSOM (Erbach et al., 1994). Although these studies provide important links from stress dose–responses to stress enzyme mechanisms and outcomes, they do not provide prognostic information about viable embryos. However, data were reviewed that suggest that stress-induced and stress enzyme-dependent mRNA that code for secreted proteins are associated with stress levels. Thus, these could be used to predict the best embryos to reimplant and to build a library of blood-borne proteins that could report the stress status of the first trimester conceptus after implantation (Section 4.5).

Future studies will focus on the use of positive acting growth factors and modulation of stress enzymes to improve IVF/ART. In some small studies, specific transcription factors are regulated by different stress enzymes, and it is now important to test whether these same enzymes regulate global aspects of differentiation choice. If stress enzymes have defined and narrow responses they may be used to direct differentiation to a lineage of choice by using stress enzyme agonists and/or antagonists. In the final analysis, a detailed understanding of the mechanisms of promising modifying agents such as PAF and GM-CSF as positive inputs and stress enzyme antagonists or agonists (e.g., for AMPK and SAPK) may be used in tandem to optimize positive effects and minimize negative effects for short- and long-term health of offspring derived from embryos manipulated during IVF/ART.

Future studies will integrate a larger breadth of molecular mechanisms that mediate low- and high-dose stress responses. We have reviewed how embryos and their stem cells mount cellular survival responses that do not include developmental differentiation responses at low doses. It is important to understand the breadth of cellular survival mechanisms that include maintenance of TRP53 in the latent state, regulation of PPAR activity, regulation of the ER stress and the unfolded protein response, and volume regulation by aquaporins and osmolyte transporters. To date, these efforts to elucidate the dose- and time-dependent response to stress have yielded compelling snapshots of the stress response at low (cellular) and high (developmental) levels. But, an overall understanding of the integration of these low and high stress levels will require a global bioinformatics-based approach along with continuing deep-and-narrow studies of candidate mechanisms.

**Summary Table**

Lessons from studies of stress responses during reproduction: in gametes, stem cells, and embryos (interpretation of these lessons).

- (1) Molecular mechanisms for stress responses are prepared before stress. (Energy must be spent prior to stress so that responses are initiated quickly, without using much energy.)
- (2) Preexisting molecular mechanisms are activated by posttranslational regulation such as phosphorylation or changing the position of the stress protein in the cell. (The allosteric regulation of existing molecular mechanisms maximizes response velocity and minimizes the energy required to regulate it.)
- (3) The initial response to stress is *stem cell survival*. (Dead stem cells cannot function and mediate organismal survival)
- (4) After a sufficient stem cell survival response, a developmental *organismal survival* response can be mounted (compensatory differentiation). (In some cases, this means that the stem cell differentiates but determination-restricted potency-or apoptosis are other choices.)
- (5) Stress enzymes integrate the initial stem cell survival response and the secondary embryonic, organismal survival response of stem cells. (Stress enzymes have been selected through evolution to mediate cell survival and, organismal developmental survival.)
- (6) At low doses, stress enzymes mediate cellular homeostatic/survival response but, at higher doses when stem cell accumulation is insufficient, mediates stem cell differentiation embryonic survival responses (compensatory differentiation, dose dependence).
- (7) pSAPK levels are inversely proportional to stem cell growth (in TSC for low or high oxygen). pSAPK levels are inversely proportional to embryo growth (in preimplantation embryos for culture media stress). (Energy is diverted to stress response from macromolecular synthesis need to replicate cells.)
- (8) pSAPK levels predict optimal culture conditions when stress enzyme activation levels are minimized.
- (9) AMPK (and SAPK) is involved with compensatory differentiation of stem cells at higher stress levels.
- (10) If the adaptation to stress is *incomplete*, then stress reversal can cause the highest levels of stress. (We think this is due to the energy requirements of initial survival and developmental response coupled with a requirement to discontinue the new program and restart the previous program.)
- (11) The kinetic response of TSC to high stress includes a “Small and down” quick response at 30 min. (Energy is conserved by avoiding new macromolecular synthesis in the early response.)

(continued)

**Summary Table** (continued)

- (12) Fate of “small and down” quick response is to stay down. (This as an expected outcome of extensive evolutionary selection where the first responses to stress must be the most robust, correct ones that conserve cellular energy by not having to be reversed as the response matures.)
- (13) As in stroke stress suppresses macromolecular synthesis, including suppression of ribosomal activity but preservation of mRNA for use after stress subsides. (Reuse of existing mRNA saved at the start of stress conserves energy.)
- (14) Stress responses in cultured blastocysts and cultured TSC derived from them are similar. (SAPK-dependent regulation of junC/mycC is similar, and the kinetics of activation of AMPK, ID2 protein loss, and AMPK dependence of ID2 loss are similar.)
- (15) The study of the stress response in reproduction is largely the study of stress enzyme response mechanisms that have been evolutionarily successful.
- (16) The study of reproduction under stress yields global and specific information about what the most important next event is and what molecular mechanisms are needed to mediate it.

**ACKNOWLEDGMENTS**

The research work was supported by grants to D. A. R. from NICHD, NIH, (1R03HD06143101, R01HD40972A) and from the Wayne State University Office of the Vice President for Research.

**REFERENCES**

- Abell, A.N., Granger, D.A., Johnson, N.L., Vincent-Jordan, N., Dibble, C.F., Johnson, G.L., 2009. Trophoblast stem cell maintenance by fibroblast growth factor 4 requires MEKK4 activation of Jun N-terminal kinase. *Mol. Cell. Biol.* 29, 2748–2761.
- Abraham, R.T., 2004. PI 3-kinase related kinases: “Big” players in stress-induced signaling pathways. *DNA Repair (Amst.)* 3, 883–887.
- Adelman, D.M., Gertsenstein, M., Nagy, A., Simon, M.C., Maltepe, E., 2000. Placental cell fates are regulated in vivo by HIF-mediated hypoxia responses. *Genes Dev.* 14, 3191–3203.
- Ain, R., Dai, G., Dunmore, J.H., Godwin, A.R., Soares, M.J., 2004. A prolactin family paralog regulates reproductive adaptations to a physiological stressor. *Proc. Natl. Acad. Sci. USA* 101, 16543–16548.
- Alam, S.M., Konno, T., Dai, G., Lu, L., Wang, D., Dunmore, J.H., et al., 2007. A uterine decidual cell cytokine ensures pregnancy-dependent adaptations to a physiological stressor. *Development* 134, 407–415.

- Almeida, E.A., Ilic, D., Han, Q., Hauck, C.R., Jin, F., Kawakatsu, H., et al., 2000. Matrix survival signaling: from fibronectin via focal adhesion kinase to c-Jun NH(2)-terminal kinase. *J. Cell Biol.* 149, 741–754.
- Anas, M.K., Hammer, M.A., Lever, M., Stanton, J.A., Baltz, J.M., 2007. The organic osmolytes betaine and proline are transported by a shared system in early preimplantation mouse embryos. *J. Cell. Physiol.* 210, 266–277.
- Anderson, P., Kedersha, N., 2008. Stress granules: the Tao of RNA triage. *Trends Biochem. Sci.* 33, 141–150.
- Aouadi, M., Binetruy, B., Caron, L., Le Marchand-Brustel, Y., Bost, F., 2006. Role of MAPKs in development and differentiation: lessons from knockout mice. *Biochimie* 88, 1091–1098.
- Armant, D.R., 2005. Blastocysts don't go it alone. Extrinsic signals fine-tune the intrinsic developmental program of trophoblast cells. *Dev. Biol.* 280, 260–280.
- Bachvarova, R., De Leon, V., Johnson, A., Kaplan, G., Paynton, B.V., 1985. Changes in total RNA, polyadenylated RNA, and actin mRNA during meiotic maturation of mouse oocytes. *Dev. Biol.* 108, 325–331.
- Bell, C.E., Lariviere, N.M., Watson, P.H., Watson, A.J., 2009. Mitogen-activated protein kinase (MAPK) pathways mediate embryonic responses to culture medium osmolarity by regulating aquaporin 3 and 9 expression and localization, as well as embryonic apoptosis. *Hum. Reprod.* 24, 1373–1386.
- Berra, E., Pages, G., Pouyssegur, J., 2000. MAP kinases and hypoxia in the control of VEGF expression. *Cancer Metastasis Rev.* 19, 139–145.
- Bevilacqua, E.M., Abrahamsohn, P.A., 1988. Ultrastructure of trophoblast giant cell transformation during the invasive stage of implantation of the mouse embryo. *J. Morphol.* 198, 341–351.
- Blanc, A., Pandey, N.R., Srivastava, A.K., 2003. Synchronous activation of ERK 1/2, p38mapk and PKB/Akt signaling by H<sub>2</sub>O<sub>2</sub> in vascular smooth muscle cells: potential involvement in vascular disease (review). *Int. J. Mol. Med.* 11, 229–234.
- Booth, P.J., Watson, T.J., Leese, H.J., 2007. Prediction of porcine blastocyst formation using morphological, kinetic, and amino acid depletion and appearance criteria determined during the early cleavage of in vitro-produced embryos. *Biol. Reprod.* 77, 765–779.
- Bowie, A., O'Neill, L.A., 2000. Oxidative stress and nuclear factor-kappaB activation: a reassessment of the evidence in the light of recent discoveries. *Biochem. Pharmacol.* 59, 13–23.
- Boyer, L.A., Plath, K., Zeitlinger, J., Brambrink, T., Medeiros, L.A., Lee, T.I., et al., 2006. Polycomb complexes repress developmental regulators in murine embryonic stem cells. *Nature* 441, 349–353.
- Bungard, D., Fuerth, B.J., Zeng, P.Y., Faubert, B., Mass, N.L., Viollet, B., et al., 2010. Signaling kinase AMPK activates stress-promoted transcription via histone H2B phosphorylation. *Science* 329, 1201–1205.
- Burgering, B.M., Medema, R.H., 2003. Decisions on life and death: FOXO Forkhead transcription factors are in command when PKB/Akt is off duty. *J. Leukoc. Biol.* 73, 689–701.
- Caenepeel, S., Charydczak, G., Sudarsanam, S., Hunter, T., Manning, G., 2004. The mouse kinome: discovery and comparative genomics of all mouse protein kinases. *Proc. Natl. Acad. Sci. USA* 101, 11707–11712.
- Callahan, M., Cochran, B.H., Stiles, C.D., 1985. The PDGF-inducible 'competence genes': intracellular mediators of the mitogenic response. *Ciba Found. Symp.* 116, 87–97.
- Carling, D., 2004. The AMP-activated protein kinase cascade—a unifying system for energy control. *Trends Biochem. Sci.* 29, 18–24.
- Ceci, M., Ross Jr., J., Condorelli, G., 2004. Molecular determinants of the physiological adaptation to stress in the cardiomyocyte: a focus on AKT. *J. Mol. Cell. Cardiol.* 37, 905–912.



- Chai, N., Patel, Y., Jacobson, K., McMahon, J., McMahon, A., Rappolee, D.A., 1998. FGF is an essential regulator of the fifth cell division in preimplantation mouse embryos. *Dev. Biol.* 198, 105–115.
- Chandranathan, V., Li, A., Chami, O., O'Neill, C., 2006. Effects of in vitro fertilization and embryo culture on TRP53 and Bax expression in B6 mouse embryos. *Reprod. Biol. Endocrinol.* 4, 61.
- Chang, F., Lee, J.T., Navolanic, P.M., Steelman, L.S., Shelton, J.G., Blalock, W.L., et al., 2003. Involvement of PI3K/Akt pathway in cell cycle progression, apoptosis, and neoplastic transformation: a target for cancer chemotherapy. *Leukemia* 17, 590–603.
- Chavez, D.J., Enders, A.C., Schlafke, S., 1984. Trophoblast cell subpopulations in the periimplantation mouse blastocyst. *J. Exp. Zool.* 231, 267–271.
- Chazaud, C., Rossant, J., 2006. Disruption of early proximodistal patterning and AVE formation in *Apc* mutants. *Development* 133, 3379–3387.
- Chazaud, C., Yamanaka, Y., Pawson, T., Rossant, J., 2006. Early lineage segregation between epiblast and primitive endoderm in mouse blastocysts through the Grb2-MAPK pathway. *Dev. Cell* 10, 615–624.
- Chen, J., Downs, S.M., 2008. AMP-activated protein kinase is involved in hormone-induced mouse oocyte meiotic maturation in vitro. *Dev. Biol.* 313, 47–57.
- Chen, J.R., Cheng, J.G., Shatzer, T., Sewell, L., Hernandez, L., Stewart, C.L., 2000. Leukemia inhibitory factor can substitute for nidatory estrogen and is essential to inducing a receptive uterus for implantation but is not essential for subsequent embryogenesis. *Endocrinology* 141, 4365–4372.
- Cochran, B.H., Reffel, A.C., Stiles, C.D., 1983. Molecular cloning of gene sequences regulated by platelet-derived growth factor. *Cell* 33, 939–947.
- Copp, A.J., 1995. Death before birth: clues from gene knockouts and mutations. *Trends Genet.* 11, 87–93.
- Corson, L.B., Yamanaka, Y., Lai, K.M., Rossant, J., 2003. Spatial and temporal patterns of ERK signaling during mouse embryogenesis. *Development* 130, 4527–4537.
- Cowden Dahl, K.D., Fryer, B.H., Mack, F.A., Compemolle, V., Maltepe, E., Adelman, D.M., et al., 2005. Hypoxia-inducible factors 1 $\alpha$  and 2 $\alpha$  regulate trophoblast differentiation. *Mol. Cell. Biol.* 25, 10479–10491.
- De Bosscher, K., Vanden Berghe, W., Haegeman, G., 2006. Cross-talk between nuclear receptors and nuclear factor kappaB. *Oncogene* 25, 6868–6886.
- Dent, P., Yacoub, A., Contessa, J., Caron, R., Amorino, G., Valerie, K., et al., 2003. Stress and radiation-induced activation of multiple intracellular signaling pathways. *Radiat. Res.* 159, 283–300.
- Di Nardo, A., Kramvis, I., Cho, N., Sadowski, A., Meikle, L., Kwiatkowski, D.J., et al., 2009. Tuberous sclerosis complex activity is required to control neuronal stress responses in an mTOR-dependent manner. *J. Neurosci.* 29, 5926–5937.
- Donnison, M., Beaton, A., Davey, H.W., Broadhurst, R., L'Huillier, P., Pfeffer, P.L., 2005. Loss of the extraembryonic ectoderm in *Elf5* mutants leads to defects in embryonic patterning. *Development* 132, 2299–2308.
- Dreesen, O., Brivanlou, A.H., 2007. Signaling pathways in cancer and embryonic stem cells. *Stem Cell Rev.* 3, 7–17.
- Ema, M., Mori, D., Niwa, H., Hasegawa, Y., Yamanaka, Y., Hitoshi, S., et al., 2008. Kruppel-like factor 5 is essential for blastocyst development and the normal self-renewal of mouse ESCs. *Cell Stem Cell* 3, 555–567.
- Enders, A.C., 1989. Trophoblast differentiation during the transition from trophoblastic plate to lacunar stage of implantation in the rhesus monkey and human. *Am. J. Anat.* 186, 85–98.
- Enders, A.C., Mead, R.A., 1996. Progression of trophoblast into the endometrium during implantation in the western spotted skunk. *Anat. Rec.* 244, 297–315.

- Enders, A.C., Lantz, K.C., Peterson, P.E., Hendrickx, A.G., 1997. From blastocyst to placenta: the morphology of implantation in the baboon. *Hum. Reprod. Update* 3, 561–573.
- Erbach, G.T., Lawitts, J.A., Papaioannou, V.E., Biggers, J.D., 1994. Differential growth of the mouse preimplantation embryo in chemically defined media. *Biol. Reprod.* 50, 1027–1033.
- Ezashi, T., Das, P., Roberts, R.M., 2005. Low O<sub>2</sub> tensions and the prevention of differentiation of hES cells. *Proc. Natl. Acad. Sci. USA* 102, 4783–4788.
- Fitzgerald, J.S., Busch, S., Wengenmayer, T., Foerster, K., de la Motte, T., Poehlmann, T.G., et al., 2005. Signal transduction in trophoblast invasion. *Chem. Immunol. Allergy* 88, 181–199.
- Fleming, T.P., McConnell, J., Johnson, M.H., Stevenson, B.R., 1989. Development of tight junctions de novo in the mouse early embryo: control of assembly of the tight junction-specific protein, ZO-1. *J. Cell Biol.* 108, 1407–1418.
- Franke, T.F., 2008. PI3K/Akt: getting it right matters. *Oncogene* 27, 6473–6488.
- Gao, S., Latham, K.E., 2004. Maternal and environmental factors in early cloned embryo development. *Cytogenet. Genome Res.* 105, 279–284.
- Genbacev, O., Zhou, Y., Ludlow, J.W., Fisher, S.J., 1997. Regulation of human placental development by oxygen tension. *Science* 277, 1669–1672.
- Georgiades, P., Cox, B., Gertsenstein, M., Chawengsaksophak, K., Rossant, J., 2007. Trophoblast-specific gene manipulation using lentivirus-based vectors. *Biotechniques* 42, 317–318.
- Gilbert, S.F., 2010. *Developmental Biology*. Sinauer Associates, Sunderland, MA.
- Gillis, D., Shrode, L.D., Krump, E., Howard, C.M., Rubie, E.A., Tibbles, L.A., et al., 2001. Osmotic stimulation of the Na<sup>+</sup>/H<sup>+</sup> exchanger NHE1: relationship to the activation of three MAPK pathways. *J. Membr. Biol.* 181, 205–214.
- Gleeson, L.M., Chakraborty, C., McKinnon, T., Lala, P.K., 2001. Insulin-like growth factor-binding protein 1 stimulates human trophoblast migration by signaling through alpha 5 beta 1 integrin via mitogen-activated protein Kinase pathway. *J. Clin. Endocrinol. Metab.* 86, 2484–2493.
- Goberdhan, D.C., Wilson, C., 1998. JNK, cytoskeletal regulator and stress response kinase? A *Drosophila* perspective. *Bioessays* 20, 1009–1019.
- Gregoraszczyk, E.L., Gertler, A., Futoma, E., 2000. Effect of exogenous ovine placental lactogen on basal and prostaglandin-stimulated progesterone production by porcine luteal cells. *Acta Vet. Hung.* 48, 199–208.
- Gross, V.S., Hess, M., Cooper, G.M., 2005. Mouse embryonic stem cells and preimplantation embryos require signaling through the phosphatidylinositol 3-kinase pathway to suppress apoptosis. *Mol. Reprod. Dev.* 70, 324–332.
- Guo, Y.L., Chakraborty, S., Rajan, S., Wang, R., Huang, F., 2010. Effects of oxidative stress on mouse embryonic stem cell proliferation, apoptosis, senescence, and self-renewal. *Stem Cells Dev.* 19(9), 1321–1331.
- Guyton, A.C., Hall, J.E., 1997. *Human Physiology and Mechanisms of Disease*. Saunders, Philadelphia.
- Hamatani, T., Carter, M.G., Sharov, A.A., Ko, M.S., 2004. Dynamics of global gene expression changes during mouse preimplantation development. *Dev. Cell* 6, 117–131.
- Hardie, D.G., 2003. Minireview: the AMP-activated protein kinase cascade: the key sensor of cellular energy status. *Endocrinology* 144, 5179–5183.
- Hatano, N., Mori, Y., Oh-hora, M., Kosugi, A., Fujikawa, T., Nakai, N., et al., 2003. Essential role for ERK2 mitogen-activated protein kinase in placental development. *Genes Cells* 8, 847–856.
- Hayakawa, J., Mittal, S., Wang, Y., Korkmaz, K.S., Adamson, E., English, C., et al., 2004. Identification of promoters bound by c-Jun/ATF2 during rapid large-scale gene activation following genotoxic stress. *Mol. Cell* 16, 521–535.

- Hedrick, S.M., 2009. The cunning little vixen: Foxo and the cycle of life and death. *Nat. Immunol.* 10, 1057–1063.
- Heyer, B.S., MacAuley, A., Behrendtsen, O., Werb, Z., 2000. Hypersensitivity to DNA damage leads to increased apoptosis during early mouse development. *Genes Dev.* 14, 2072–2084.
- Hickson, J.A., Fong, B., Watson, P.H., Watson, A.J., 2007. PP2Cdelta (Ppm1d, WIP1), an endogenous inhibitor of p38 MAPK, is regulated along With Trp53 and Cdkn2a following p38 MAPK inhibition during mouse preimplantation development. *Mol. Reprod. Dev.* 74(7), 821–834.
- Hoffman, B., Liebermann, D.A., 2009. Gadd45 modulation of intrinsic and extrinsic stress responses in myeloid cells. *J. Cell. Physiol.* 218, 26–31.
- Holbrook, N.J., Liu, Y., Fornace Jr., A.J., 1996. Signaling events controlling the molecular response to genotoxic stress. *EXS* 77, 273–288.
- Hooeboom, D., Burgering, B.M., 2009. Should I stay or should I go: beta-catenin decides under stress. *Biochim. Biophys. Acta* 1796, 63–74.
- Hughes, M., Dobric, N., Scott, I.C., Su, L., Starovic, M., St-Pierre, B., et al., 2004. The Hand1, Stra13 and Gcm1 transcription factors override FGF signaling to promote terminal differentiation of trophoblast stem cells. *Dev. Biol.* 271, 26–37.
- Huppertz, B., 2008. Placental origins of preeclampsia: challenging the current hypothesis. *Hypertension* 51, 970–975.
- Ip, Y.T., Davis, R.J., 1998. Signal transduction by the c-Jun N-terminal kinase (JNK)—from inflammation to development. *Curr. Opin. Cell Biol.* 10, 205–219.
- Jauniaux, E., Watson, A., Burton, G., 2001. Evaluation of respiratory gases and acid-base gradients in human fetal fluids and uteroplacental tissue between 7 and 16 weeks' gestation. *Am. J. Obstet. Gynecol.* 184, 998–1003.
- Jin, X.L., Chandrakanthan, V., Morgan, H.D., O'Neill, C., 2009. Preimplantation embryo development in the mouse requires the latency of TRP53 expression, which is induced by a ligand-activated PI3 kinase/AKT/MDM2-mediated signaling pathway. *Biol. Reprod.* 81, 234–242.
- Johnstone, E.D., Mackova, M., Das, S., Payne, S.G., Lowen, B., Sibley, C.P., et al., 2005. Multiple anti-apoptotic pathways stimulated by EGF in cytotrophoblasts. *Placenta* 26, 548–555.
- Juriscova, A., Latham, K.E., Casper, R.F., Varmuza, S.L., 1998. Expression and regulation of genes associated with cell death during murine preimplantation embryo development. *Mol. Reprod. Dev.* 51, 243–253.
- Kalantry, S., Mills, K.C., Yee, D., Otte, A.P., Panning, B., Magnuson, T., 2006. The Polycomb group protein Eed protects the inactive X-chromosome from differentiation-induced reactivation. *Nat. Cell Biol.* 8, 195–202.
- Kaneto, H., Matsuoka, T.A., Nakatani, Y., Kawamori, D., Matsuhisa, M., Yamasaki, Y., 2005. Oxidative stress and the JNK pathway in diabetes. *Curr. Diab. Rev.* 1, 65–72.
- Kang, J., Gemberling, M., Nakamura, M., Whitby, F.G., Handa, H., Fairbrother, W.G., et al., 2009a. A general mechanism for transcription regulation by Oct1 and Oct4 in response to genotoxic and oxidative stress. *Genes Dev.* 23, 208–222.
- Kang, J., Shakya, A., Tantin, D., 2009b. Stem cells, stress, metabolism and cancer: a drama in two Octs. *Trends Biochem. Sci.* 34, 491–499.
- Karin, M., Chang, L., 2001. AP-1—glucocorticoid receptor crosstalk taken to a higher level. *J. Endocrinol.* 169, 447–451.
- Karin, M., Takahashi, T., Kapahi, P., Delhase, M., Chen, Y., Makris, C., et al., 2001. Oxidative stress and gene expression: the AP-1 and NF-kappaB connections. *Biofactors* 15, 87–89.
- Keim, A.L., Chi, M.M., Moley, K.H., 2001. Hyperglycemia-induced apoptotic cell death in the mouse blastocyst is dependent on expression of p53. *Mol. Reprod. Dev.* 60, 214–224.

- Kelly, K., Cochran, B.H., Stiles, C.D., Leder, P., 1983. Cell-specific regulation of the *c-myc* gene by lymphocyte mitogens and platelet-derived growth factor. *Cell* 35, 603–610.
- Kelly, K., Cochran, B., Stiles, C., Leder, P., 1984. The regulation of *c-myc* by growth signals. *Curr. Top. Microbiol. Immunol.* 113, 117–126.
- Kharbanda, S., Yuan, Z.M., Weichselbaum, R., Kufe, D., 1998. Determination of cell fate by *c-Abl* activation in the response to DNA damage. *Oncogene* 17, 3309–3318.
- Kharbanda, S., Saxena, S., Yoshida, K., Pandey, P., Kaneki, M., Wang, Q., et al., 2000. Translocation of SAPK/JNK to mitochondria and interaction with Bcl-x(L) in response to DNA damage. *J. Biol. Chem.* 275, 322–327.
- Khidir, M.A., Stachecki, J.J., Krawetz, S.A., Armant, D.R., 1995. Rapid inhibition of mRNA synthesis during preimplantation embryo development: vital permeabilization by lysolecithin potentiates the action of alpha-amanitin. *Exp. Cell Res.* 219, 619–623.
- Kidder, G.M., McLachlin, J.R., 1985. Timing of transcription and protein synthesis underlying morphogenesis in preimplantation mouse embryos. *Dev. Biol.* 112, 265–275.
- Knobil, E., Neill, J.D., 2006. Knobil and Neill's Physiology of Reproduction. Elsevier, Amsterdam.
- Kudo, N., Taoka, H., Yoshida, M., Horinouchi, S., 1999. Identification of a novel nuclear export signal sensitive to oxidative stress in yeast AP-1-like transcription factor. *Ann. NY Acad. Sci.* 886, 204–207.
- Kyriakis, J.M., Avruch, J., 1996. Protein kinase cascades activated by stress and inflammatory cytokines. *Bioessays* 18, 567–577.
- Kyriakis, J.M., Woodgett, J.R., Avruch, J., 1995. The stress-activated protein kinases. A novel ERK subfamily responsive to cellular stress and inflammatory cytokines. *Ann. NY Acad. Sci.* 766, 303–319.
- LaRosa, C., Downs, S.M., 2006. Stress stimulates AMP-activated protein kinase and meiotic resumption in mouse oocytes. *Biol. Reprod.* 74, 585–592.
- LaRosa, C., Downs, S.M., 2007. Meiotic induction by heat stress in mouse oocytes: involvement of AMP-activated protein kinase and MAPK family members. *Biol. Reprod.* 76, 476–486.
- Lee, N., Maurange, C., Ringrose, L., Paro, R., 2005. Suppression of Polycomb group proteins by JNK signalling induces transdetermination in *Drosophila* imaginal discs. *Nature* 438, 234–237.
- Lee, T.I., Jenner, R.G., Boyer, L.A., Guenther, M.G., Levine, S.S., Kumar, R.M., et al., 2006. Control of developmental regulators by Polycomb in human embryonic stem cells. *Cell* 125, 301–313.
- Lengner, C.J., Welstead, G.G., Jaenisch, R., 2008. The pluripotency regulator Oct4: a role in somatic stem cells? *Cell Cycle* 7, 725–728.
- Li, S., Kim, M., Hu, Y.L., Jalali, S., Schlaepfer, D.D., Hunter, T., et al., 1997. Fluid shear stress activation of focal adhesion kinase. Linking to mitogen-activated protein kinases. *J. Biol. Chem.* 272, 30455–30462.
- Li, H.Y., Chang, S.P., Yuan, C.C., Chao, H.T., Ng, H.T., Sung, Y.J., 2003. Induction of p38 mitogen-activated protein kinase-mediated apoptosis is involved in outgrowth of trophoblast cells on endometrial epithelial cells in a model of human trophoblast-endometrial interactions. *Biol. Reprod.* 69, 1515–1524.
- Li, A., Chandrakanthan, V., Chami, O., O'Neill, C., 2007. Culture of zygotes increases TRP53 [corrected] expression in B6 mouse embryos, which reduces embryo viability. *Biol. Reprod.* 76, 362–367.
- Liu, L., Cash, T.P., Jones, R.G., Keith, B., Thompson, C.B., Simon, M.C., 2006. Hypoxia-induced energy stress regulates mRNA translation and cell growth. *Mol. Cell* 21, 521–531.
- Liu, J., Xu, W., Sun, T., Wang, F., Puscheck, E., Brigstock, D., et al., 2009. Hyperosmolar stress induces global mRNA responses in placental trophoblast stem cells that emulate early post-implantation differentiation. *Placenta* 30, 66–73.

- Los, M., Maddika, S., Erb, B., Schulze-Osthoff, K., 2009. Switching Akt: from survival signaling to deadly response. *Bioessays* 31, 492–495.
- Maekawa, M., Yamamoto, T., Tanoue, T., Yuasa, Y., Chisaka, O., Nishida, E., 2005. Requirement of the MAP kinase signaling pathways for mouse preimplantation development. *Development* 132, 1773–1783.
- Maltepe, E., Krampitz, G.W., Okazaki, K.M., Red-Horse, K., Mak, W., Simon, M.C., et al., 2005. Hypoxia-inducible factor-dependent histone deacetylase activity determines stem cell fate in the placenta. *Development* 132, 3393–3403.
- Manning, G., Whyte, D.B., Martinez, R., Hunter, T., Sudarsanam, S., 2002. The protein kinase complement of the human genome. *Science* 298, 1912–1934.
- Manova, K., Tomihara-Newberger, C., Wang, S., Godelman, A., Kalantry, S., Witty-Blease, K., et al., 1998. Apoptosis in mouse embryos: elevated levels in pregastrulae and in the distal anterior region of gastrulae of normal and mutant mice. *Dev. Dyn.* 213, 293–308.
- Martindill, D.M., Risebro, C.A., Smart, N., Franco-Viseras Mdel, M., Rosario, C.O., Swallow, C.J., et al., 2007. Nucleolar release of Hand1 acts as a molecular switch to determine cell fate. *Nat. Cell Biol.* 9, 1131–1141.
- Mattson, M.P., Culmsee, C., Yu, Z., Camandola, S., 2000. Roles of nuclear factor kappaB in neuronal survival and plasticity. *J. Neurochem.* 74, 443–456.
- McCarthy, M.J., Baumber, J., Kass, P.H., Meyers, S.A., 2010. Osmotic stress induces oxidative cell damage to rhesus macaque spermatozoa. *Biol. Reprod.* 82, 644–651.
- McLachlin, J.R., Kidder, G.M., 1986. Intercellular junctional coupling in preimplantation mouse embryos: effect of blocking transcription or translation. *Dev. Biol.* 117, 146–155.
- Mesnard, D., Guzman-Ayala, M., Constam, D.B., 2006. Nodal specifies embryonic visceral endoderm and sustains pluripotent cells in the epiblast before overt axial patterning. *Development* 133, 2497–2505.
- Mikkelsen, T.S., Hanna, J., Zhang, X., Ku, M., Wernig, M., Schorderet, P., et al., 2008. Dissecting direct reprogramming through integrative genomic analysis. *Nature* 454, 49–55.
- Mitra, A.P., Cote, R.J., 2009. Molecular pathogenesis and diagnostics of bladder cancer. *Annu. Rev. Pathol.* 4, 251–285.
- Mohamet, L., Heath, J.K., Kimber, S.J., 2009. Determining the LIF-sensitive period for implantation using a LIF-receptor antagonist. *Reproduction* 138, 827–836.
- Moley, K.H., Chi, M.M., Knudson, C.M., Korsmeyer, S.J., Mueckler, M.M., 1998. Hyperglycemia induces apoptosis in pre-implantation embryos through cell death effector pathways. *Nat. Med.* 4, 1421–1424.
- Mtango, N.R., Latham, K.E., 2008. Differential expression of cell cycle genes in rhesus monkey oocytes and embryos of different developmental potentials. *Biol. Reprod.* 78, 254–266.
- Muller, R., Bravo, R., Burckhardt, J., Curran, T., 1984. Induction of c-fos gene and protein by growth factors precedes activation of c-myc. *Nature* 312, 716–720.
- Nagy, A., Gertsenstein, M., Vintersten, K., Behringer, R.R., 2003. *Manipulating the Mouse Embryo. A Laboratory Manual.* Cold Spring Harbor Laboratory Press, Cold Spring Harbor.
- Natale, D.R., Paliga, A.J., Beier, F., D'Souza, S.J., Watson, A.J., 2004. p38 MAPK signaling during murine preimplantation development. *Dev. Biol.* 268, 76–88.
- Nishioka, N., Inoue, K., Adachi, K., Kiyonari, H., Ota, M., Ralston, A., et al., 2009. The Hippo signaling pathway components Lats and Yap pattern Tead4 activity to distinguish mouse trophectoderm from inner cell mass. *Dev. Cell* 16, 398–410.
- Niwa, H., Miyazaki, J., Smith, A.G., 2000. Quantitative expression of Oct-3/4 defines differentiation, dedifferentiation or self-renewal of ES cells. *Nat. Genet.* 24, 372–376.

- Niwa, H., Toyooka, Y., Shimosato, D., Strumpf, D., Takahashi, K., Yagi, R., et al., 2005. Interaction between Oct3/4 and Cdx2 determines trophectoderm differentiation. *Cell* 123, 917–929.
- O'Brien, M.L., Spear, B.T., Glauert, H.P., 2005. Role of oxidative stress in peroxisome proliferator-mediated carcinogenesis. *Crit. Rev. Toxicol.* 35, 61–88.
- O'Neill, R.A., Bhamidipati, A., Bi, X., Deb-Basu, D., Cahill, L., Ferrante, J., et al., 2006. Isoelectric focusing technology quantifies protein signaling in 25 cells. *Proc. Natl. Acad. Sci. USA* 103, 16153–16158.
- Ogren, L., Southard, J.N., Colosi, P., Linzer, D.I., Talamantes, F., 1989. Mouse placental lactogen-I: RIA and gestational profile in maternal serum. *Endocrinology* 125, 2253–2257.
- Okkenhaug, K., Vanhaesebroeck, B., 2003. PI3K in lymphocyte development, differentiation and activation. *Nat. Rev. Immunol.* 3, 317–330.
- Owusu-Ansah, E., Banerjee, U., 2009. Reactive oxygen species prime *Drosophila* haematopoietic progenitors for differentiation. *Nature* 461, 537–541.
- Paliga, A.J., Natale, D.R., Watson, A.J., 2005. p38 mitogen-activated protein kinase (MAPK) first regulates filamentous actin at the 8–16-cell stage during preimplantation development. *Biol. Cell* 97, 629–640.
- Pantaleon, M., Tan, H.Y., Kafer, G.R., Kaye, P.L., 2010. Toxic effects of hyperglycemia are mediated by the hexosamine signaling pathway and o-linked glycosylation in early mouse embryos. *Biol. Reprod.* 82, 751–758.
- Paria, B.C., Reese, J., Das, S.K., Dey, S.K., 2002. Deciphering the cross-talk of implantation: advances and challenges. *Science* 296, 2185–2188.
- Patel, J., McLeod, L.E., Vries, R.G., Flynn, A., Wang, X., Proud, C.G., 2002. Cellular stresses profoundly inhibit protein synthesis and modulate the states of phosphorylation of multiple translation factors. *Eur. J. Biochem.* 269, 3076–3085.
- Pedersen, R.A., 1987. *Experimental Approaches to Mammalian Embryonic Development*. Cambridge University Press, Cambridge.
- Pelletier, A., Joly, E., Prentki, M., Coderre, L., 2005. Adenosine 5'-monophosphate-activated protein kinase and p38 mitogen-activated protein kinase participate in the stimulation of glucose uptake by dinitrophenol in adult cardiomyocytes. *Endocrinology* 146, 2285–2294.
- Peters, T.J., Chapman, B.M., Wolfe, M.W., Soares, M.J., 2000. Placental lactogen-I gene activation in differentiating trophoblast cells: extrinsic and intrinsic regulation involving mitogen-activated protein kinase signaling pathways. *J. Endocrinol.* 165, 443–456.
- Pokholok, D.K., Zeitlinger, J., Hannett, N.M., Reynolds, D.B., Young, R.A., 2006. Activated signal transduction kinases frequently occupy target genes. *Science* 313, 533–536.
- Pommer, A.C., Rutlant, J., Meyers, S.A., 2002. The role of osmotic resistance on equine spermatozoal function. *Theriogenology* 58, 1373–1384.
- Qiu, Q., Yang, M., Tsang, B.K., Gruslin, A., 2004. Both mitogen-activated protein kinase and phosphatidylinositol 3-kinase signalling are required in epidermal growth factor-induced human trophoblast migration. *Mol. Hum. Reprod.* 10, 677–684.
- Ralston, A., Cox, B.J., Nishioka, N., Sasaki, H., Chea, E., Rugg-Gunn, P., et al., 2010. Gata3 regulates trophoblast development downstream of Tead4 and in parallel to Cdx2. *Development* 137, 395–403.
- Rappolee, D.A., 1999. It's not just baby's babble/Babel: recent progress in understanding the language of early mammalian development: a minireview. *Mol. Reprod. Dev.* 52, 234–240.
- Rappolee, D.A., 2007. Impact of transient stress and stress enzymes on development. *Dev. Biol.* 304, 1–8.

- Rappolee, D., Werb, Z., 1994. The role of growth factors in early mammalian development. *Adv. Dev. Biol.* 3, 41–71.
- Rappolee, D.A., Brenner, C.A., Schultz, R., Mark, D., Werb, Z., 1988. Developmental expression of PDGF, TGF- $\alpha$ , and TGF- $\beta$  genes in preimplantation mouse embryos. *Science* 241, 1823–1825.
- Rappolee, D.A., Sturm, K.S., Behrendtsen, O., Schultz, G.A., Pedersen, R.A., Werb, Z., 1992. Insulin-like growth factor II acts through an endogenous growth pathway regulated by imprinting in early mouse embryos. *Genes Dev.* 6, 939–952.
- Rappolee, D.A., Basilico, C., Patel, Y., Werb, Z., 1994. Expression and function of FGF-4 in peri-implantation development in mouse embryos. *Development* 120, 2259–2269.
- Rappolee, D.A., Awonuga, A.O., Puscheck, E.E., Zhou, S., Xie, Y., 2010. Benzopyrene and experimental stressors cause compensatory differentiation in placental trophoblast stem cells. *Syst. Biol. Reprod. Med.* 56, 168–183.
- Richards, T., Wang, F., Liu, L., Baltz, J.M., 2010. Rescue of postcompaction-stage mouse embryo development from hypertonicity by amino acid transporter substrates that may function as organic osmolytes. *Biol. Reprod.* 82, 769–777.
- Rider, M.H., Hussain, N., Horman, S., Dilworth, S.M., Storey, K.B., 2006. Stress-induced activation of the AMP-activated protein kinase in the freeze-tolerant frog *Rana sylvatica*. *Cryobiology* 53, 297–309.
- Riley, P., Anson-Cartwright, L., Cross, J.C., 1998. The Hand1 bHLH transcription factor is essential for placental and cardiac morphogenesis. *Nat. Genet.* 18, 271–275.
- Riley, J.K., Carayannopoulos, M.O., Wyman, A.H., Chi, M., Ratajczak, C.K., Moley, K. H., 2005. The PI3K/Akt pathway is present and functional in the preimplantation mouse embryo. *Dev. Biol.* 284, 377–386.
- Rinaudo, P., Schultz, R.M., 2004. Effects of embryo culture on global pattern of gene expression in preimplantation mouse embryos. *Reproduction* 128, 301–311.
- Rinaudo, P.F., Giritharan, G., Talbi, S., Dobson, A.T., Schultz, R.M., 2006. Effects of oxygen tension on gene expression in preimplantation mouse embryos. *Fertil. Steril.* 86 (Suppl. 4), 1252–1265.
- Rivera, R.M., Stein, P., Weaver, J.R., Mager, J., Schultz, R.M., Bartolomei, M.S., 2008. Manipulations of mouse embryos prior to implantation result in aberrant expression of imprinted genes on day 9.5 of development. *Hum. Mol. Genet.* 17, 1–14.
- Roberts, J.M., Hubel, C.A., 2009. The two stage model of preeclampsia: variations on the theme. *Placenta* 30 (Suppl. A), S32–S37.
- Roberts, R.M., Xie, S., Mathialagan, N., 1996. Maternal recognition of pregnancy. *Biol. Reprod.* 54, 294–302.
- Rodesch, F., Simon, P., Donner, C., Jauniaux, E., 1992. Oxygen measurements in endometrial and trophoblastic tissues during early pregnancy. *Obstet. Gynecol.* 80, 283–285.
- Roelen, B.A., Goumans, M.J., Zwijsen, A., Mummery, C.L., 1998. Identification of two distinct functions for TGF- $\beta$  in early mouse development. *Differentiation* 64, 19–31.
- Ronnebaum, S.M., Patterson, C., 2010. The FoxO family in cardiac function and dysfunction. *Annu. Rev. Physiol.* 72, 81–94.
- Roovers, K., Assoian, R.K., 2000. Integrating the MAP kinase signal into the G1 phase cell cycle machinery. *Bioessays* 22, 818–826.
- Rosario, G.X., Konno, T., Soares, M.J., 2008. Maternal hypoxia activates endovascular trophoblast cell invasion. *Dev. Biol.* 314, 362–375.
- Rossant, J., 2003. Targeting mammalian genes—rats join in and mice move ahead. *Nat. Biotechnol.* 21, 625–627.
- Rutllant, J., Pommer, A.C., Meyers, S.A., 2003. Osmotic tolerance limits and properties of rhesus monkey (*Macaca mulatta*) spermatozoa. *J. Androl.* 24, 534–541.

- Saretzki, G., Armstrong, L., Leake, A., Lako, M., von Zglinicki, T., 2004. Stress defense in murine embryonic stem cells is superior to that of various differentiated murine cells. *Stem Cells* 22, 962–971.
- Schultz, J.F., Mayernik, L., Rout, U.K., Armant, D.R., 1997. Integrin trafficking regulates adhesion to fibronectin during differentiation of mouse peri-implantation blastocysts. *Dev. Genet.* 21, 31–43.
- Sedding, D.G., 2008. FoxO transcription factors in oxidative stress response and ageing—a new fork on the way to longevity? *Biol. Chem.* 389, 279–283.
- Seli, E., Botros, L., Sakkas, D., Burns, D.H., 2008. Noninvasive metabolomic profiling of embryo culture media using proton nuclear magnetic resonance correlates with reproductive potential of embryos in women undergoing in vitro fertilization. *Fertil. Steril.* 90, 2183–2189.
- Selye, H., 1970. The evolution of the stress concept. *Stress and cardiovascular disease.* *Am J Cardiol* 26, 289–299.
- Selye, H., 1971. Hormones and resistance. *J Pharm Sci* 60, 1–28.
- Shaulian, E., Karin, M., 2001. AP-1 in cell proliferation and survival. *Oncogene* 20, 2390–2400.
- Siddall, L.S., Barcroft, L.C., Watson, A.J., 2002. Targeting gene expression in the preimplantation mouse embryo using morpholino antisense oligonucleotides. *Mol. Reprod. Dev.* 63, 413–421.
- Sjoblom, C., Roberts, C.T., Wikland, M., Robertson, S.A., 2005. Granulocyte-macrophage colony-stimulating factor alleviates adverse consequences of embryo culture on fetal growth trajectory and placental morphogenesis. *Endocrinology* 146, 2142–2153.
- Spencer, T.E., Burghardt, R.C., Johnson, G.A., Bazer, F.W., 2004. Conceptus signals for establishment and maintenance of pregnancy. *Anim. Reprod. Sci.* 82–83, 537–550.
- Spurgeon, S.L., Jones, R.C., Ramakrishnan, R., 2008. High throughput gene expression measurement with real time PCR in a microfluidic dynamic array. *PLoS ONE* 3, e1662.
- Stanton, J.A., Macgregor, A.B., Green, D.P., 2003. Gene expression in the mouse preimplantation embryo. *Reproduction* 125, 457–468.
- Steeves, C.L., Hammer, M.A., Walker, G.B., Rae, D., Stewart, N.A., Baltz, J.M., 2003. The glycine neurotransmitter transporter GLYT1 is an organic osmolyte transporter regulating cell volume in cleavage-stage embryos. *Proc. Natl. Acad. Sci. USA* 100, 13982–13987.
- Strumpf, D., Mao, C.A., Yamanaka, Y., Ralston, A., Chawengsaksophak, K., Beck, F., et al., 2005. Cdx2 is required for correct cell fate specification and differentiation of trophoctoderm in the mouse blastocyst. *Development* 132, 2093–2102.
- Takeda, T., Sakata, M., Isobe, A., Yamamoto, T., Nishimoto, F., Minekawa, R., et al., 2007. Hypoxia represses the differentiation of Rcho-1 rat trophoblast giant cells. *Gynecol. Obstet. Invest.* 63, 188–194.
- Tam, P.P., Rossant, J., 2003. Mouse embryonic chimeras: tools for studying mammalian development. *Development* 130, 6155–6163.
- Tam, P.P., Loebel, D.A., Tanaka, S.S., 2006. Building the mouse gastrula: signals, asymmetry and lineages. *Curr. Opin. Genet. Dev.* 16, 419–425.
- Tanaka, S., Kunath, T., Hadjantonakis, A.K., Nagy, A., Rossant, J., 1998. Promotion of trophoblast stem cell proliferation by FGF4. *Science* 282, 2072–2075.
- Thomas, P.Q., Brown, A., Beddington, R.S., 1998. Hex: a homeobox gene revealing peri-implantation asymmetry in the mouse embryo and an early transient marker of endothelial cell precursors. *Development* 125, 85–94.
- Thordarson, G., Galosy, S., Gudmundsson, G.O., Newcomer, B., Sridaran, R., Talamantes, F., 1997. Interaction of mouse placental lactogens and androgens in regulating progesterone release in cultured mouse luteal cells. *Endocrinology* 138, 3236–3241.



- Toyooka, Y., Shimosato, D., Murakami, K., Takahashi, K., Niwa, H., 2008. Identification and characterization of subpopulations in undifferentiated ES cell culture. *Development* 135, 909–918.
- van der Horst, A., Burgering, B.M., 2007. Stressing the role of FoxO proteins in lifespan and disease. *Nat. Rev. Mol. Cell Biol.* 8, 440–450.
- Vanhaesebroeck, B., Ali, K., Bilancio, A., Geering, B., Foukas, L.C., 2005. Signalling by PI3K isoforms: insights from gene-targeted mice. *Trends Biochem. Sci.* 30, 194–204.
- Vassena, R., Han, Z., Gao, S., Baldwin, D.A., Schultz, R.M., Latham, K.E., 2007. Tough beginnings: alterations in the transcriptome of cloned embryos during the first two cell cycles. *Dev. Biol.* 304, 75–89.
- Voiculescu, O., Bertocchini, F., Wolpert, L., Keller, R.E., Stern, C.D., 2007. The amniote primitive streak is defined by epithelial cell intercalation before gastrulation. *Nature* 449, 1049–1052.
- Wang, J., Mager, J., Chen, Y., Schneider, E., Cross, J.C., Nagy, A., et al., 2001. Imprinted X inactivation maintained by a mouse Polycomb group gene. *Nat. Genet.* 28, 371–375.
- Wang, J., Mager, J., Schnedier, E., Magnuson, T., 2002. The mouse PcG gene *eed* is required for Hox gene repression and extraembryonic development. *Mamm. Genome* 13, 493–503.
- Wang, Q.T., Piotrowska, K., Ciemerych, M.A., Milenkovic, L., Scott, M.P., Davis, R.W., et al., 2004. A genome-wide study of gene activity reveals developmental signaling pathways in the preimplantation mouse embryo. *Dev. Cell* 6, 133–144.
- Wang, Y., Puscheck, E.E., Lewis, J.J., Trostinskaia, A.B., Wang, F., Rappolee, D.A., 2005. Increases in phosphorylation of SAPK/JNK and p38MAPK correlate negatively with mouse embryo development after culture in different media. *Fertil. Steril.* 83 (Suppl. 1), 1144–1154.
- Wang, Y., Xie, Y., Wygle, D., Shen, H.H., Puscheck, E.E., Rappolee, D.A., 2009. A major effect of simulated microgravity on several stages of preimplantation mouse development is lethality associated with elevated phosphorylated SAPK/JNK. *Reprod. Sci.* 16, 947–959.
- Wassarman, P.M., DePamphilis, M.L., 1993. *Guide to Techniques in Mouse Development*. Academic Press, San Diego.
- Wierzechos, E., Gregoraszczyk, E.L., Zieba, D., Murawski, M., Gertler, A., 2000. Placental lactogen not growth hormone and prolactin regulates secretion of progesterone in vitro by the 40–45 day ovine corpus luteum of pregnancy. *Folia Biol. (Krakow)* 48, 19–24.
- Wilton, L., 2005. Preimplantation genetic diagnosis and chromosome analysis of blastomeres using comparative genomic hybridization. *Hum. Reprod. Update* 11, 33–41.
- Woodgett, J.R., Avruch, J., Kyriakis, J.M., 1995. Regulation of nuclear transcription factors by stress signals. *Clin. Exp. Pharmacol. Physiol.* 22, 281–283.
- Xi, X., Han, J., Zhang, J.Z., 2001. Stimulation of glucose transport by AMP-activated protein kinase via activation of p38 mitogen-activated protein kinase. *J. Biol. Chem.* 276, 41029–41034.
- Xie, Y., Puscheck, E.E., Rappolee, D.A., 2006a. Effects of SAPK/JNK inhibitors on preimplantation mouse embryo development are influenced greatly by the amount of stress induced by the media. *Mol. Hum. Reprod.* 12, 217–224.
- Xie, Y., Puscheck, E.E., Rappolee, D.A., 2006b. Effects of SAPK/JNK inhibitors on preimplantation mouse embryo development are influenced greatly by the amount of stress induced by the media. *Mol. Hum. Reprod.* 12, 217–224.
- Xie, Y., Wang, F., Zhong, W., Puscheck, E., Shen, H., Rappolee, D.A., 2006c. Shear stress induces preimplantation embryo death that is delayed by the zona pellucida and associated with stress-activated protein kinase-mediated apoptosis. *Biol. Reprod.* 75, 45–55.

- Xie, Y., Wang, F., Puscheck, E.E., Rappolee, D.A., 2007a. Pipetting causes shear stress and elevation of phosphorylated stress-activated protein kinase/jun kinase in preimplantation embryos. *Mol. Reprod. Dev.* 74, 1287–1294.
- Xie, Y., Zhong, W., Wang, Y., Trostinskaia, A., Wang, F., Puscheck, E.E., et al., 2007b. Using hyperosmolar stress to measure biologic and stress-activated protein kinase responses in preimplantation embryos. *Mol. Hum. Reprod.* 13, 473–481.
- Xie, Y., Liu, J., Proteasa, S., Proteasa, G., Zhong, W., Wang, Y., et al., 2008. Transient stress and stress enzyme responses have practical impacts on parameters of embryo development, from IVF to directed differentiation of stem cells. *Mol. Reprod. Dev.* 75, 689–697.
- Xie, Y., Abdallah, M.E., Awonuga, A.O., Slater, J.A., Puscheck, E.E., Rappolee, D.A., 2010. Benzo(a)pyrene causes PRKAA1/2-dependent ID2 loss in trophoblast stem cells. *Mol. Reprod. Dev.* 77, 533–539.
- Yamanaka, Y., Ralston, A., Stephenson, R.O., Rossant, J., 2006. Cell and molecular regulation of the mouse blastocyst. *Dev. Dyn.* 235, 2301–2314.
- Yamanaka, Y., Lanner, F., Rossant, J., 2010. FGF signal-dependent segregation of primitive endoderm and epiblast in the mouse blastocyst. *Development* 137, 715–724.
- Yumuk, V.D., 2006. Targeting components of the stress system as potential therapies for the metabolic syndrome: the peroxisome-proliferator-activated receptors. *Ann. NY Acad. Sci.* 1083, 306–318.
- Zhang, Y., Chen, F., 2004. Reactive oxygen species (ROS), troublemakers between nuclear factor-kappaB (NF-kappaB) and c-Jun NH(2)-terminal kinase (JNK). *Cancer Res.* 64, 1902–1905.
- Zhang, K., Kaufman, R.J., 2006. The unfolded protein response: a stress signaling pathway critical for health and disease. *Neurology* 66, S102–S109.
- Zhong, W., Xie, Y., Wang, Y., Lewis, J., Trostinskaia, A., Wang, F., et al., 2007. Use of hyperosmolar stress to measure stress-activated protein kinase activation and function in human HTR cells and mouse trophoblast stem cells. *Reprod. Sci.* 14, 534–547.
- Zhong, W., Xie, Y., Abdallah, M., Awonuga, A.O., Slater, J.A., Sipahi, L., et al., 2010. Cellular stress causes reversible Prkaa1/2- and proteasome-dependent Id2 protein loss in trophoblast stem cells. *Reproduction*, 140(6), 921–930.
- Zhou, S., Xie, Y., Puscheck, E.E., Rappolee, D.A., 2011. Oxygen levels that optimize TSC culture are identified by maximizing growth rates and minimizing stress. *Placenta* (to be resubmitted).
- Zimmermann, B.G., Grill, S., Holzgreve, W., Zhong, X.Y., Jackson, L.G., Hahn, S., 2008. Digital PCR: a powerful new tool for noninvasive prenatal diagnosis? *Prenat. Diagn.* 28, 1087–1093.
- Zou, G.M., Chen, J.J., Ni, J., 2006. LIGHT induces differentiation of mouse embryonic stem cells associated with activation of ERK5. *Oncogene* 25(3), 463–469.

This page intentionally left blank

# DIRECTIONAL CELL MIGRATION: REGULATION BY SMALL G PROTEINS, NECTIN-LIKE MOLECULE-5, AND AFADIN

Yoshiyuki Rikitake<sup>\*,†</sup> and Yoshimi Takai<sup>\*</sup>

## Contents

|                                                                                                 |     |
|-------------------------------------------------------------------------------------------------|-----|
| 1. Introduction                                                                                 | 98  |
| 2. Cell Movement                                                                                | 99  |
| 2.1. Types of cell movement                                                                     | 99  |
| 2.2. Leading edge structures                                                                    | 100 |
| 3. Small G Proteins and Leading Edge Structures                                                 | 106 |
| 3.1. Rho family                                                                                 | 107 |
| 3.2. Rap                                                                                        | 109 |
| 4. Nectins, Necls, and Afadin                                                                   | 111 |
| 4.1. Nectins and related molecules                                                              | 112 |
| 4.2. Roles of nectins, Necls, and afadin in cell movement                                       | 117 |
| 5. Crosstalk between Growth Factor Receptors and Integrins                                      | 119 |
| 5.1. Integrins                                                                                  | 119 |
| 5.2. Crosstalk between growth factor receptors and integrins                                    | 119 |
| 5.3. Role of Necl-5 in crosstalk between growth factor receptors and integrins                  | 120 |
| 6. Regulation of Directionality of Cell Movement                                                | 122 |
| 6.1. PI3-kinase                                                                                 | 123 |
| 6.2. Cell polarity proteins                                                                     | 123 |
| 6.3. Afadin                                                                                     | 124 |
| 6.4. Necl-5 and microtubules                                                                    | 125 |
| 7. Regulation of Dynamics of Cyclical Activation and Inactivation of Small G Proteins by Afadin | 125 |
| 8. Concluding Remarks                                                                           | 129 |
| Acknowledgments                                                                                 | 130 |
| References                                                                                      | 130 |

<sup>\*</sup> Department of Biochemistry and Molecular Biology, Kobe University, Graduate School of Medicine, Kobe, Japan

<sup>†</sup> Department of Internal Medicine, Kobe University, Graduate School of Medicine, Kobe, Japan

## Abstract

Cell movement is a complex and dynamic process that causes changes in cell morphology by reorganizing the actin cytoskeleton and modulating cell adhesions. For directional cell migration, cells must continuously receive the polarized environmental signals and transmit the polarized intracellular signals from a fixed direction, which orient protrusion of the leading edge. The dynamic regulation of cyclical activation and inactivation of the Rho family small G proteins as a result of the crosstalk between small G protein signaling pathways is particularly important for the formation and disassembly of leading edge structures. However, the regulatory mechanisms of directionality and small G protein dynamics have not been fully understood. Recently, it has been found that nectin, an immunoglobulin-like cell adhesion molecule, implicated in a wide variety of fundamental cellular events including cell adhesion, proliferation, movement, and polarity, and its related proteins such as nectin-like molecule-5 and afadin regulate directionality and small G protein dynamics during directional cell movement.

**Key Words:** nectin, Necl-5, afadin, Rho, Rac, Cdc42, Rap1, Leading edge, Cell movement, Integrin, Actin. © 2011 Elsevier Inc.

## 1. INTRODUCTION

Cells sense and respond to a wide variety of external physiological and chemical signals, integrate such complex incoming signals, and change their morphology, dynamics, behavior, function, and fate (Geiger et al., 2009). Cell movement is one of the fundamental features of living cells. Cell movement is a complex process and plays a critical role in diverse physiological and pathological processes, such as embryonic development, wound healing, immune responses, outgrowth and metastasis of cancer cells, and angiogenesis. For example, epithelial cells migrate during wound healing processes, leukocytes migrate to sites of inflammation and infection, vascular endothelial cells migrate to form new capillaries during angiogenesis, and cell sheets migrate to form tissues and organs during development (Gilbert, 2003; Moser et al., 2004; Singer and Clark, 1999). However, deregulation of cell motility is associated with diverse pathological processes, including tumor metastasis and angiogenesis, chronic inflammation, and the dysfunction of immune response (Luster et al., 2005; Yamaguchi et al., 2005). There are a couple of types of cell movement that includes random movement (chemokinesis), directional migration (chemotaxis), and haptotaxis. Chemotaxis is the directed cell movement along a positive concentration gradient of chemoattractants, whereas haptotaxis is the cell motility in response to adhesive substrates such as extracellular matrix (ECM).

In general, cells become polarized in response to an extracellular stimulus that causes cells to move in a unidirectional manner. In the initial step of cell movement, actin-rich membrane protrusions such as filopodia and lamellipodia are extended and peripheral ruffles are formed at the leading edge in the direction of migration that results in the formation of an asymmetric cell front–rear polarity (Andrew and Insall, 2007; Arriemerlou and Meyer, 2005; Dawe et al., 2003; Petrie et al., 2009). Under peripheral ruffles, focal complexes are formed and these immature cell–ECM adhesion structures are transformed into mature cell–ECM adhesion sites called focal adhesions during cell movement.

The Rho family small GTP-binding proteins (small G proteins) play a key role in the formation of protrusive structures (Etienne-Manneville and Hall, 2002; Hall, 1998; Nobes and Hall, 1999). The formation of filopodia and lamellipodia is regulated by Cdc42 and Rac1, respectively. The formation of peripheral ruffles is regulated by Rac1. The formation of focal complexes and focal adhesions is regulated by Rac1 and RhoA, respectively. Evidence is currently accumulated that there is a fine-tuned crosstalk between small G protein signaling pathways for the spatially and temporally coordinated regulation of cell movement machinery. This review highlights crosstalk between small G protein signaling pathways during directional cell movement and summarizes our current knowledge about how the dynamic activation and inactivation of these small G proteins are coordinately regulated, in particular, focusing on nectin, an immunoglobulin-like cell adhesion molecule, as well as on its related proteins such as nectin-like molecule (Nectl)-5 and afadin. These molecules are implicated in a wide variety of fundamental cellular events including cell adhesion, movement, proliferation, differentiation, survival, and polarization (Takai et al., 2008a,b).



## 2. CELL MOVEMENT

Cells show the motile responses to environmental molecules. Cell movement is one of the fundamental cell behaviors critically involved not only in physiological processes such as embryonic development, wound healing, angiogenesis, and immune responses, but also in pathological processes such as outgrowth and metastasis of cancer cells. Here, we will briefly summarize the types of cell movement and specialized leading edge structures formed at the front of cell movement.

### 2.1. Types of cell movement

There are a couple of types of cell movement that include random movement (chemokinesis), directional migration (chemotaxis), and haptotaxis.

### 2.1.1. Chemokinesis

Chemokinesis is a random cell movement that occurs in the absence of a concentration gradient of chemoattractants, chemotactic agents that induce a cell to migrate toward them. In general, chemokinesis has a nonvectorial moiety, in contrast to chemotaxis as described in Section 2.1.2 and does not have a directional component but includes scalar quantities. The speed or frequency of chemokinesis is determined by chemoattractants.

### 2.1.2. Chemotaxis

Chemotaxis is a directional cell movement along a positive concentration gradient of chemoattractants. Chemotaxis is a fundamental form of cell behavior that involves a complex response of a cell to an external stimulus. Sensing and measuring the concentration of the chemoattractant, transmitting the information to biochemical reaction, and exhibiting the motility and adhesive changes associated with the response are critical factors involved in chemotaxis.

### 2.1.3. Haptotaxis

Haptotaxis is a directional cell movement in response to adhesive substrates such as ECM, a complex structural material surrounding and supporting cells, as Carter stated that it was the movement of cells on an adhesion gradient, in the direction of increasing substrate adhesion (Carter, 1965, 1967). Adhesion to the ECM is very important for cell movement, including haptotaxis. Haptotaxis depends on cell–ECM adhesion that is affected by the types of the cells, the ECM composition, the proteolytic degradation process of ECM, and the kinds of integrins expressed in the cells. Integrins are a family of transmembrane glycoproteins that act as receptors for specific ligands that are constituents of the ECM (Aplin et al., 1998). This type of cell movement plays an important role in a number of biological processes such as wound healing and tumor cell invasion.

## 2.2. Leading edge structures

Cell migration is an integrated multistep process that involves the coordination of complex biochemical and biomechanical signals to modulate cell morphology by dynamically rearranging cytoskeleton filaments and to cause cellular traction (Li et al., 2005; Ridley et al., 2003; Schwartz and Horwitz, 2006). Cell migration is a fundamental cellular process that involves the protrusion of the leading edge, the formation of new adhesive structures at the front, the contraction of the cell, and the release of adhesions at the rear (Fig. 3.1). Alteration of cell shape and cytoskeletal organization and modulation of cell adhesions are associated with the actin polymerization in cell protrusion and traction caused by contraction of actin filaments. Rho family

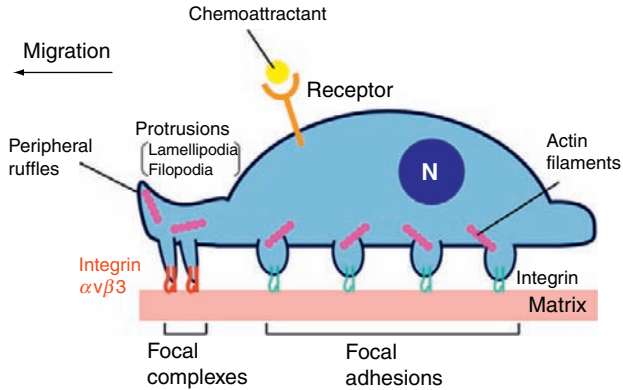


**Figure 3.1** Leading edge structure. In response to chemoattractants, moving cells form specialized structures at the leading edge in the direction of migration. The leading edge structures include protrusions such as filopodia and lamellipodia, and peripheral ruffles. Cells are attached to extracellular matrix through integrin-containing adhesion structures called focal complexes and focal adhesions.

small G proteins are particularly important in these processes, as determinants of how and where actin polymerization and rearrangement occur—Rac and Cdc42 regulate the Arp2/3 complex through the Wiskott–Aldrich syndrome protein (WASP) family proteins, which are composed of WASP, N-WASP, and WAVE1–3 proteins, to promote lamellipodia and filopodia, while Rho regulates the formation of stress fibers and focal adhesions and induces actomyosin contractility (Fig. 3.2) (Raftopoulos and Hall, 2004).

### 2.2.1. Filopodia

During cell migration, finger-like, thin, and transient actin protrusions called filopodia are extended beyond the leading edge of protruding lamellipodia. Filopodia, that sense the environment, contain 15–20 parallel filaments tightly packed into a bundle with their barbed ends facing the membrane (Lewis and Bridgman, 1992). Extension and retraction of filopodia are regulated by actin assembly at the tip and retrograde flow, respectively (Forscher and Smith, 1988; Mallavarapu and Mitchison, 1999; Mitchison and Kirschner, 1988; Okabe and Hirokawa, 1991). Filopodia are particularly prominent in individual cells such as fibroblasts and axonal growth cones, but are also frequently observed at the free front of moving tissue sheets such as dorsal closure in *Drosophila* and ventral enclosure in *Caenorhabditis elegans* during developmental stages as well as wounded edges in which opposing tissue layers approach each other (Wood and Martin, 2002). Filopodia appear to play a role in a diverse number of cellular and developmental processes such as synaptogenesis, dorsal closure in embryos, and viral uptake (Gupton and Gertler, 2007; Mattila and Lappalainen, 2008; Sherer et al., 2007).



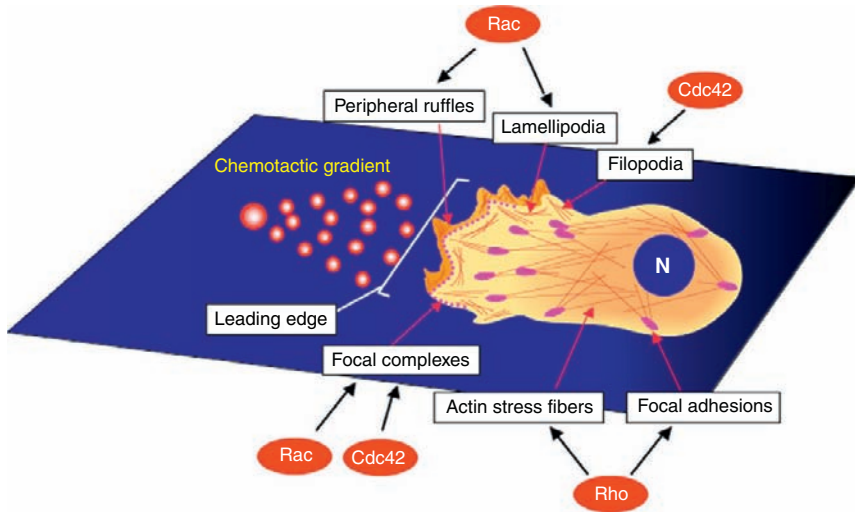


**Figure 3.2** The Rho family small G proteins and formation of leading edge structures. The Rho family small G proteins regulate the formation of leading edge structures. Rac regulates the formation of lamellipodia, peripheral ruffles, and focal complexes. Cdc42 regulates the formation of filopodia and focal complexes. Rho regulates the formation of stress fibers and focal adhesions.

Cdc42, a member of the Rho family small G protein, plays a key role in the formation of filopodia (Nobes and Hall, 1995). The formation of filopodia is regulated by Cdc42 via a number of proteins including IRSp53, Mena, Eps8, and N-WASP (Disanza et al., 2006; Govind et al., 2001; Krugmann et al., 2001; Lim et al., 2008a). Cdc42 appears to recruit IRSp53, which then recruits Mena, Eps8, and N-WASP (Lim et al., 2008a). IRSp53 induces membrane deformation via its I-BAR2,3 domain (Mattila et al., 2007) and its SH3 domain-interacting proteins, Mena, Eps8, and N-WASP, regulate actin dynamics. N-WASP, a member of the WASP family proteins consisting of the WASP subfamily (WASP and N-WASP) and the WAVE subfamily (WAVE1, WAVE2, and WAVE3; Derry et al., 1994; Miki et al., 1996, 1998b; Suetsugu et al., 1999), binds to the Arp2/3 complex, a seven subunit complex containing two actin-related proteins (Arp2 and Arp3), and regulates the Arp2/3 complex-mediated actin nucleation (Takenawa and Suetsugu, 2007). Thus, the Cdc42–N-WASP–Arp2/3 signaling pathway is likely a mechanism that regulates filopodia formation. N-WASP potentiates the ability of Cdc42 to induce filopodia (Miki et al., 1998a), suggesting that N-WASP plays a role in filopodia formation. However, the role of N-WASP in filopodia formation is not directly associated with its ability to activate actin nucleation/polymerization via the Arp2/3 complex (Lim et al., 2008a). In addition, although the Arp2/3 complex appears to exist in filopodia, its function in filopodia has not been well defined, probably because this complex is a relatively minor constituent of filopodia.

A couple of papers suggest the formation of filopodia by the reorganization of the Arp2/3 complex generates actin network (Biyasheva et al., 2004; Svitkina et al., 2003). Proteins such as VASP and formins that mediate the elongation of actin filaments bind to actin filaments in lamellipodia and come together to form a filopodial tip complex that elongates a group of actin filaments to form a filopodium. However, lamellipodia are unlikely essential for filopodia formation, because filopodia formation occurs in the absence of functional WAVE and Arp2/3 complexes (Steffen et al., 2006) and spreading fibroblasts and platelets can form filopodia in the absence of lamellipodia (McCarty et al., 2005; Witkowski and Brighton, 1971). On the other hand, *de novo* nucleation has been suggested to be involved in filopodia assembly (Faix et al., 2009). Filopodia are formed through the establishment of a tip complex of formins, which nucleates long actin filaments that are then bundled. Very recently, Lee et al. (2010) proposed a new clustering-outgrowth model: filopodia form via clustering of Arp2/3 complex activators, self-assembly of filopodia tip complexes on the membrane, and outgrowth of actin buds. The recruitment and clustering of F-BAR domain proteins and N-WASP or other nucleation promoting factors such as VASP and formins at the membrane lead to subsequent recruitment of the Arp2/3 complex and actin. Thus, mechanism of filopodial assembly may vary between different types of cells and different circumstances.

### 2.2.2. Lamellipodia

Lamellipodia are ribbon-like flat cellular protrusions that are formed at the periphery of a moving or spreading cell (Small et al., 2002). Lamellipodia are enriched with a bidimensional dendritic array of a branched network of actin filaments. Fluorescence speckle microscopy revealed two distinct but overlapping actin networks: one is fast-moving and short-lived speckles defined lamellipodia, the other is slow-moving and long-lived speckles defined lamellae (Iwasa and Mullins, 2007; Ponti et al., 2004). Lamellae are sheet-like flat protrusions that are formed behind lamellipodia at the periphery of moving or spreading cells. Lamellae contain a loose array of unbranched actin filaments (Svitkina and Borisy, 1999) that is enriched with tropomyosin and myosin II (DesMarais et al., 2002; Svitkina et al., 1997).

The formation of lamellipodia is controlled by Rac, another member of the Rho family small G protein. The formation of lamellipodia is likely regulated by the Rac-WAVES-Arp2/3 signaling pathway. WAVE proteins are recruited to the plasma membrane by Rac, although WAVE proteins lack a G protein-binding domain. How activation of WAVE proteins is regulated remains unclear. It was recently reported that interactions with prenylated, GTP-bound Rac and acidic phospholipids such as PI(3,4,5)P<sub>3</sub> and phosphorylation are all required for activation of WAVE2 complex (Lebensohn and Kirschner, 2009). IRSp53 that bridges Rac to WAVE2 (Miki et al., 2000) directly binds the plasma membrane and might be able to

sense or induce a specific curvature of the plasma membrane (Scita et al., 2008). WAVE proteins act as powerful switches that lead to maximal actin nucleation through the Arp2/3 complex that plays a role in the generation of branched networks of actin filaments (Takenawa and Miki, 2001; Takenawa and Suetsugu, 2007). The Arp2/3 complex cooperates with proteins such as cofilin and gelsolin that make available actin templates for the Arp2/3 complex to form branches (Pollard and Borisy, 2003). The activation of the Arp2/3 complex increases the binding of this complex to the sides of actin filaments and induces the formation of an actin branch. As each actin branch grows, this generates the force to push the plasma membrane forward, which results in the formation of lamellipodia. Thus, lamellipodial networks are subsequently reorganized so that the cell can form specialized structures for motility.

### 2.2.3. Membrane ruffles

Abercrombie proposed to classify membrane ruffles at lamellipodia into three types: the thin leading edge of the cell that protrudes the membrane along with the substratum, the ruffles formed by the bending upward of the leading edge with occasional transfer behind the anterior edge, and the vertical ruffles that appear directly behind the leading edge on the dorsal surface (Abercrombie et al., 1970). The former two structures formed at the leading edge are simply called peripheral ruffles, while the vertical ruffles are called dorsal ruffles. Peripheral ruffles are proposed to be formed as a result of failed attachment of newly formed lamellipodia to the ECM and are believed to serve as active sites of cytoskeletal reorganization (Borm et al., 2005). Dorsal ruffles are short-lived, dynamic, F-actin-enriched “waves” that occur across the top surface of the cell, and they often form circular structures. It has been thought that dorsal ruffles that develop on the dorsal surface of the cell represent active sites of cytoskeletal reorganization important for invasion, migration, and macropinocytosis (Hedberg and Bell, 1995; Hedberg et al., 1993; Kraynov et al., 2000; Legg et al., 2007; Suetsugu et al., 2003). Rac is a principal regulator of the formation of both peripheral and dorsal ruffles during cell migration. Rac is localized to the leading edge and thereby promotes the spatial activation of the actin polymerization machinery. However, distinct molecules appear to act downstream of Rac. It has been reported in fibroblasts that WAVE1 and N-WASP are required for the formation of dorsal ruffles, while WAVE2 is essential for the formation of peripheral ruffles (Legg et al., 2007; Suetsugu et al., 2003).

### 2.2.4. Focal complexes

Cell adhesion structures can be classified into focal complexes, focal adhesions, and fibrillar adhesions. The classification depends on their size, shape, intracellular localization, molecular composition, and dynamics (Webb et al., 2002; Yamada and Geiger, 1997; Zaidel-Bar et al., 2004; Zamir and Geiger,

2001). Focal complexes are highly dynamic nascent adhesions that disassemble and reassemble at the leading edge in a process called adhesion turnover. Focal complexes appear as small dot-like structures of less than  $1 \mu\text{m}^2$  at the cell periphery of spreading cells or at the leading edge of migrating cells. These structures are associated with a loose actin meshwork (Rottner et al., 1999). Early focal complexes contain integrin  $\beta_3$ , talin, and paxillin, while late focal complexes contain vinculin,  $\alpha$ -actinin, VASP, and focal adhesion kinase (FAK) (Laukaitis et al., 2001; Rottner et al., 1999; Zaidel-Bar et al., 2003, 2004). In moving cells, focal complexes mature into larger (2–5  $\mu\text{m}$  long) focal adhesions (or focal contacts) in response to RhoA signaling.

So far, extensive studies have been carried out to identify the molecular pathways linking integrins to actin assembly at cell adhesion sites. Among various downstream targets of Rac1 that control the formation of focal complexes, the Arp2/3 complex is identified as a potential actin nucleator in nascent focal complexes. It was shown that the Arp2/3 complex is colocalized with vinculin at the leading edge in focal complex-like structures and interacts directly with vinculin, whereas cells transfected with a mutant of vinculin, which does not interact with Arp2/3, show defects in lamellipodium extension and cell spreading (DeMali et al., 2002). However, the Arp2/3 complex is not directly activated by vinculin *in vitro* (DeMali et al., 2002), and the known activators of the Arp2/3 complex (i.e., N-WASP, WAVES, and cortactin) have not been localized at focal complexes. Although the mechanism of actin filament nucleation at focal complexes remains elusive, formins and VASP appear to be good candidates.

### 2.2.5. Focal adhesions

Focal adhesions are dynamic actin–integrin links, are more stable, and display a slower turnover than focal complexes. They are located at the cell periphery and more centrally in less motile regions, associated with the end of stress fibers. Focal complexes are formed underneath lamellipodia, whereas focal adhesions are usually observed at the border between lamellipodia and the lamellae. Focal adhesions contain high levels of vinculin, talin, paxillin, zyxin,  $\alpha$ -actinin, VASP, FAK, phosphotyrosine proteins, and integrin  $\alpha_v\beta_3$  (Zaidel-Bar et al., 2004) and actopaxin (Nikolopoulos and Turner, 2000). Fibrillar adhesions that arise from focal adhesions are elongated structures associated with fibronectin fibrils and located more centrally in cells. In contrast to focal adhesions, fibrillar adhesions are not associated with stress fibers but only with thin actin cables and contain high levels of tensin and integrin  $\alpha_5\beta_1$ , only traces of paxillin, and no vinculin. The elongation of fibrillar adhesions depends on the deformability of the ECM (Zamir et al., 2000).

Focal adhesions functionally interact with stress fibers. Stress fibers are contractile bundles of actin and myosin associated with focal adhesions. These structures contain actin filaments (Cramer et al., 1997), myosin II

(Fujiwara and Pollard, 1976), and several actin filament-binding proteins, including  $\alpha$ -actinin (Lazarides and Burridge, 1975), and are distributed in three classes: ventral stress fibers that are located at the ventral cell surface and associated with focal adhesions at both ends, dorsal stress fibers that are associated with focal adhesions at one end, and transverse arcs that are not associated with focal adhesions (Hotulainen and Lappalainen, 2006; Small et al., 1998). The force applied by stress fibers to focal adhesions is required for the retraction of the rear of the cell. Focal adhesions initiate the elongation of stress fibers, and the tension generated by stress fibers enhances the growth of mechanosensitive focal adhesions (Bershadsky et al., 1996; Chadeneau et al., 1994; Helfman et al., 1999; Kaverina et al., 1999; Pelham and Wang, 1997; Rottner et al., 1999; Volberg et al., 1994).

### 3. SMALL G PROTEINS AND LEADING EDGE STRUCTURES

Small G proteins are monomeric G proteins with molecular masses of 20–40 kDa. Now, more than 100 small G proteins have been identified in eukaryotes from yeast to human, and they comprise a superfamily consisting of the Ras, Rho, Rab, and Ran subfamilies. They act as biotimers that determine the duration of the reactions they control and, at the same time, they also regulate the order in terms of time of sequential downstream reactions so that these occur in this sequence following a single extracellular signal. The biotimers are controlled by the interconversion between the GDP-bound inactive form and the GTP-bound active form. The exchange of GDP for GTP is physiologically facilitated by cytosolic factors, generally indicated as guanine nucleotide exchange factors (GEFs). On the other hand, inactivation occurs through the intrinsic GTPase activity, which converts bound GTP into GDP and is stimulated by regulatory factors called GTPase-activating proteins (GAPs). In this way, one cycle of activation and inactivation is achieved, and small G proteins serve as biotimers that regulate downstream biological responses by controlling the reaction period to transduce upstream signals to downstream effectors.

GDP dissociation inhibitors (GDIs) are another critical regulators of small G proteins (Olofsson, 1999; Sasaki and Takai, 1998; Takai et al., 1993). GDIs inhibit the dissociation of GDP from the GDP-bound small G proteins, which maintains them in an inactive form, and block their activation by GEFs, which prevents their interactions with effector molecules. Also, GDIs interact with the GTP-bound small G proteins to inhibit GTP hydrolysis, which inhibits both intrinsic and GAP-catalyzed GTPase activity. Furthermore, GDIs modulate the cycling of the Rho family small G proteins between cytosol and membranes. GDIs inhibit translocation of the Rho family small G proteins from the cytosol to the plasma membrane and maintain them

as cytosolic proteins by shielding the membrane-targeting moiety of the Rho family small G proteins by the hydrophobic pocket in GDI. So far, Rho GDIs and Rab GDIs have been characterized. RhoGDI constitutes a family with three mammalian members: RhoGDI $\alpha$ , Ly/D4-GDI or RhoGDI $\beta$ , and RhoGDI-3 or  $-\gamma$  (Dovas and Couchman, 2005). RhoGDI $\alpha$  is ubiquitously expressed, while RhoGDI $\beta$  is specifically expressed by hematopoietic cells, particularly by B- and T-lymphocytes. RhoGDI $\gamma$  is preferentially expressed in the brain, pancreas, lung, kidney, and testis.

### 3.1. Rho family

The Rho family small G proteins regulate cytoskeletal reorganization and cell movement. In the early 1990s, Hall and his colleagues showed that Rho regulates the formation of contractile actin–myosin filaments in response to a variety of extracellular stimuli (e.g., lysophosphatidic acid or integrin engagement), Rac induces actin polymerization at the cell periphery to produce lamellipodia in response to platelet-derived growth factor (PDGF) or insulin, and Cdc42 promotes actin filament assembly and filopodia formation at the cell periphery in response to bradykinin and interleukin 1 (IL-1) in Swiss 3T3 cells (Kozma et al., 1995; Nobes and Hall, 1995; Ridley and Hall, 1992; Ridley et al., 1992). At the leading edges of moving cells, the continuous formation and disassembly of these protrusive structures are tightly regulated by the actions of the Rho family small G proteins, including Rho, Rac, and Cdc42. So as to have cells keep moving, each member of the Rho family small G proteins should cyclically be active and inactive as leading edge structures are dynamically formed and disassembled. The cyclical activation and inactivation of the Rho family small G proteins are critical for turnover of the transformation of focal complexes into focal adhesions during cell movement.

#### 3.1.1. Rho

Rho was originally isolated from the mollusk *Aplysia californica* (Madaule and Axel, 1985). To date, its orthologs have been identified in vertebrates, insects, nematode, protozoa, and fungi. The first demonstrated functions of Rho are budding and cytokinesis in *Saccharomyces cerevisiae* (Adams et al., 1990; Bender and Pringle, 1989; Johnson and Pringle, 1990). In addition, the first discovered downstream effectors of Rho1 are a protein kinase C homolog Pkc1 (Nonaka et al., 1995) and a formin protein homolog Bni1 (Kohno et al., 1996) in *S. cerevisiae*. In 1990s, a broad range of cellular functions of Rho has been uncovered. Rho regulates reorganization of the actin cytoskeleton (Johnson and Pringle, 1990), smooth muscle contraction (Hirata et al., 1992), the formation of stress fibers and focal adhesions in fibroblasts (Ridley and Hall, 1992), cell motility (Takaishi et al., 1993), cytokinesis (Kishi et al., 1993), cell cycle progression (Yamamoto et al., 1993), axon

guidance and extension (Jalink et al., 1994), gene expression (Hill et al., 1995), and vesicle trafficking (Komuro et al., 1996).

Rho regulates the formation of stress fibers and focal adhesions (Ridley and Hall, 1992). Rho must be activated at focal adhesions and be inactivated at focal complexes. The ability of Rho to induce actin reorganization and cell movement is likely mediated by two distinct downstream targets, Rho-kinase (ROCK) and the formin homology protein, mDia (Watanabe et al., 1999). Both ROCK and mDia have many downstream targets. ROCK, in particular, the ROCK I isoform (Yoneda et al., 2005), stimulates myosin II-driven contractility in smooth muscle and nonmuscle cells by direct phosphorylation of myosin light chain (Fukata et al., 2001) and by inactivating myosin light chain phosphatase by phosphorylation (Essler et al., 1998). An increase in the levels of phosphorylated myosin light chain leads to cross-linking of myosin II into actin filaments. However, mDia, similarly to other formins, functions as a potent stimulator of actin nucleation and elongation (Higgs, 2005; Zigmond, 2004) and promotes actin polymerization by adopting an open conformation and binding to the barbed ends of actin filaments upon binding active Rho.

It is likely that signals from integrins regulate the activation and inactivation of Rho. A good candidate for signaling molecules that function downstream of integrins is FAK which can activate both GEFs such as p190RhoGEF (Lim et al., 2008b) and GAPs such as p190GAP (Burbelo et al., 1995).

### 3.1.2. Rac

Rac (*Ras*-related C3 botulinum toxin substrate) was originally identified as a substrate for ADP-ribosylation by botulinum toxin C3 ADP-ribosyltransferase from cDNA library of a leukemia cell line HL-60 (Didsbury et al., 1989). Rac regulates the formation of lamellipodia, peripheral ruffles, and focal complexes (Ridley et al., 1992). Studies using dominant-negative Rac revealed that the inhibition of Rac blocks lamellipodial activity and cell movement, suggesting that Rac activity is essential for cell movement (Nobes and Hall, 1999).

At the downstream of Cdc42, WASP interacts directly with the Arp2/3 complex that promotes actin polymerization (Machesky and Insall, 1998; Millard et al., 2004), whereas Rac interacts indirectly with WAVE which can activate Arp2/3 (Eden et al., 2002; Takenawa and Miki, 2001). In spite that both Rac and Cdc42 can activate Arp2/3, it is still not entirely clear why they lead to such morphologically distinct structures, that is, lamellipodia and filopodia, respectively, but it is suggested that *in vitro* reconstitution assays are useful to unravel these processes (Ho et al., 2004; Vignjevic et al., 2003).

Rac can activate p21-activated kinase (PAK), which phosphorylates the focal adhesion protein paxillin at Ser<sup>273</sup>. Phosphorylated paxillin recruits G protein-coupled receptor kinase-interacting proteins 1 and 2 (GIT1 and

GIT2) and  $\beta$ PAK-interactive exchange factor ( $\beta$ PIX), a GEF for Rac, which bind and form another complex that activates Rac, in turn binds the Rac effector PAK (Manser et al., 1998), forming a trimolecular GIT1 (GIT2)– $\beta$ PIX–PAK signaling complex (Manabe et al., 2002). This Rac regulator/effector complex regulates adhesion turnover and protrusion formation at the leading edge (Nayal et al., 2006).

### 3.1.3. Cdc42

Cdc42 was first discovered and characterized in *Saccharomyces cerevisiae* as a protein that regulates growth, cell polarity and normal cell shape during the cell division cycle (Hartwell et al., 1974; Sloat and Pringle, 1978; Sloat et al., 1981; Adams et al., 1990). In 1990, G25K, a 25kDa GTP-binding protein that originally purified from placenta and termed Gp (Evans et al., 1986), was identified as the human homolog of Cdc42 (Munemitsu et al., 1990; Shinjo et al., 1990). Cdc42 regulates the formation of filopodia, peripheral ruffles, and focal complexes (Hall, 1998; Nobes and Hall, 1995). Studies using dominant-negative Cdc42 revealed that the inhibition of Cdc42 destroys a front–rear cell polarity, which results in the partial (50%) inhibition of cell movement. Cdc42 controls the realignment of the Golgi and centrosome to face the direction of movement, a critical feature of cell polarization during cell migration (Nobes and Hall, 1999). The roles of Cdc42 in the regulation of cell polarity will be discussed in Section 6.2.

Cdc42 activates PAK at the leading edge of migrating cells, which limits Rac activity (Cau and Hall, 2005). Cdc42 and PAK are not necessary to activate Rac, but required for localized activation of Rac at the leading edge. Cdc42-dependent polarization of the microtubules and centrosome is independent of the activity of PAK.

Other downstream target of Cdc42 is WASP. WASP interacts directly with the Arp2/3 complex that regulates actin polymerization (Machesky and Insall, 1998; Millard et al., 2004).

## 3.2. Rap

The Rap family proteins were independently discovered by three laboratories in 1988–1989 (Kawata et al., 1988; Kitayama et al., 1989; Pizon et al., 1988) and five different members of this family, namely, Rap1A, Rap1B, Rap2A, Rap2B, and Rap2C, have been identified to date (Bos et al., 2001; Paganini et al., 2006; Takai et al., 2001). During two decades, evidence has been accumulating that Rap plays a pivotal role in regulating a variety of aspects of cellular functions of living cells, such as cell proliferation, differentiation, cell adhesion, cell–cell junction formation, and polarity.

Rap1 is activated in response to a variety of stimuli, including growth factors and G protein-coupled receptor agonists, and transmits signals to several downstream effectors. GEFs for Rap1 are Epac (de Rooij et al.,



1998; Kawasaki et al., 1998), DOCK4 (Yajnik et al., 2003), C3G (Gotoh et al., 1995), and PSD-95-Dlg-1-ZO-1 (PDZ)-GEF (de Rooij et al., 1999; Ohtsuka et al., 1999), while GAPs for Rap1 consist of Rap1GAP family proteins, including Rap1GAPI (Polakis et al., 1991) and Rap1GAPII (Mochizuki et al., 1999), and SPAL family proteins, such as SPA-1 (Kurachi et al., 1997) and E6-TP1a/SPAR/SPAL (Gao et al., 1999).

Recent studies suggested that Rap1 is implicated in the migration of vascular endothelial cells and lymphocytes (Durand et al., 2006; Fujita et al., 2005). Using the fluorescence resonance energy transfer (FRET) technology, Mochizuki's group demonstrated that Rap1 is locally activated at the leading edge of vascular endothelial cells during chemotaxis. Rap1 interacts with regulator of adhesion and cell polarization enriched in lymphoid tissues (RAPL), which is expressed predominantly in lymphoid tissues and mediates integrin adhesion and cell polarization in lymphocytes (Kinashi and Katagiri, 2005). The perturbation of Rap activation or Rap1-RAPL interaction inhibits the directional cell migration. Thus, the directional migration is regulated by Rap1 and its association with RAPL.

In primary lymphocytes, Rap1 is activated by chemokines such as stromal cell-derived factor-1 (SDF-1)/CXCL12 within seconds, and is inactivated rapidly within a few minutes (Shimonaka et al., 2003). Kinashi's group demonstrated that Rap1 is critically involved in cell polarization and migration of lymphocytes, in addition to integrin activation. Independent of spatial cues such as adhesion or chemokine gradients, constitutively active Rap1 can transform lymphocytes into a polarized cell shape with a leading edge and stimulated random migration over intercellular adhesion molecule-1 (ICAM-1) and vascular cell adhesion molecule-1 (VCAM-1; Shimonaka et al., 2003). These phenotypes are unique to Rap1 because although the Rho family G proteins play important roles in cell shape and migration (Sanchez-Madrid and del Pozo, 1999), constitutively active mutants of other Ras/Rho family proteins do not show identical phenotypes (Shimonaka et al., 2003). RAPL is likely the downstream mediator of Rap1 activated by chemokines.

We recently reported that PDGF induces the activation of Rap1, which then induces the activation of Rac1 in NIH3T3 cells (Takahashi et al., 2008). Overexpression of Rap1GAP to inactivate Rap1 as well as knock-down of Rap1 by the use of siRNAs inhibits the PDGF-induced formation of leading edge structures, cell movement, and activation of Rac1 (Takahashi et al., 2008). These observations suggest that the activation of Rap1 and the subsequent activation of Rac1 are important for the PDGF-induced migration of NIH3T3 cells. However, the precise localization of Rap1 that controls crosstalk between Rap1 and the Rho family small G proteins, including Rac1, during cell movement remained unclear. The mechanisms that underlie the Rap1-dependent cell movement raise many interesting questions. How activated Rap1 regulates the PDGF-induced

formation of leading edge structures and cell movement? Whether and how activated Rap1 is recruited to the leading edge? How recruited Rap1 promotes the local activation of Rac1 at the leading edge? We will discuss these questions in Section 6.3.

## 4. NECTINS, NECLS, AND AFADIN

Nectin and Necl are immunoglobulin-like cell adhesion molecules (Fig. 3.3; Takai et al., 2008a,b). Nectin interacts directly with afadin, an F-actin-binding protein, at its cytoplasmic tail, while Necl does not bind afadin. Afadin functions as an adaptor protein by further binding many scaffolding proteins and F-actin-binding proteins and associates nectin with other cell–cell adhesion and intracellular signaling systems. Nectin, Necl, and afadin have been demonstrated to play important roles in the fundamental cellular functions, not only the formation of cell–cell junctions, but also many other cellular activities, such as movement, proliferation, differentiation, survival, and polarization (Takai et al., 2008a,b).

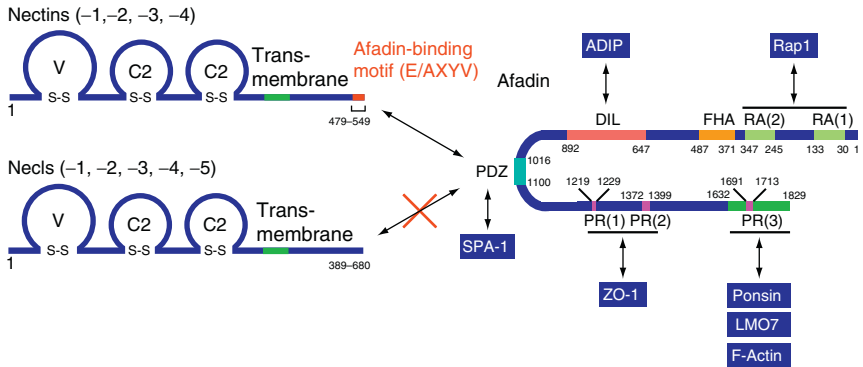


**Figure 3.3** Molecular structures of nectin, Necl, and afadin. Each member of nectin and Necl contains three immunoglobulin-like loops (one V- and two C2-type loops) in the extracellular region, a single transmembrane region, and one cytoplasmic region. A consensus motif of four amino acids (E/AXYV) in nectin is necessary for its binding to afadin. However, Necl does not have this motif and does not bind afadin. Afadin has multiple domains: two Ras-association (RA) domains, a forkhead-associated (FHA) domain, a dilute (DIL) domain, a PSD-95-Dlg-1-ZO-1 (PDZ) domain, three proline-rich (PR) domains, and an F-actin-binding domain at the C-terminus. In addition to interacting with nectin through the PDZ domain, afadin binds Rap1 through the RA domains, afadin DIL-domain-interacting protein (ADIP) through the DIL domain, SPA-1 through the PDZ domain, ZO-1 through the first and second PR domains, ponsin through the third PR domain, and LIM domain only 7 (LMO7) through the C-terminal region containing the F-actin-binding domain.

## 4.1. Nectins and related molecules

### 4.1.1. Nectins

Nectin is a  $\text{Ca}^{2+}$ -independent immunoglobulin-like cell adhesion molecule that comprises a family consisting of four members. Nectin-1, -2, -3 are widely distributed in adult tissues and expressed in various types of cells, such as fibroblasts, epithelial cells, and neurons. Nectin-2 and -3 are also expressed in hematopoietic cells and spermatids, respectively, that lack cadherin (Lopez et al., 1998; Ozaki-Kuroda et al., 2002). In humans, nectin-4 is expressed in the placenta and hair follicle structures, and upregulated in breast cancer (Brancati et al., 2010; Fabre-Lafay et al., 2005; Raymond et al., 2001).

Each member of the nectin family has two or three splicing variants including nectin-1 $\alpha$ , -1 $\beta$ , -1 $\gamma$ , -2 $\alpha$ , -2 $\delta$ , -3 $\alpha$ , -3 $\beta$ , and -3 $\gamma$  (Takai et al., 2008a,b). Nectin-4 has two splicing variants. Except for nectin-1 $\gamma$  that is a secreted protein and lacks the transmembrane and cytoplasmic regions, nectins have an extracellular region with three immunoglobulin-like loops, a single transmembrane region, and a cytoplasmic tail region (Fig. 3.3). The extracellular region of nectins is composed of the V and two C2 types of immunoglobulin-like domains. Nectins other than nectin-1 $\beta$ , -3 $\gamma$ , and -4 have a conserved motif of four amino acids at their carboxyl termini, which serves as a binding motif to the PDZ domain of afadin. Despite a lack of this conserved motif, nectin-4 binds the PDZ domain of afadin at its carboxyl terminus.

Each member of the nectin family initially forms homodimers by *cis*-dimerization through the V-type loop at the extracellular region of nectin, and then *cis*-clustering of homo-*cis*-dimers of nectin takes place (T. Sakisaka and Y. Takai, unpublished data). *Cis*-clusters of nectin homophilically and heterophilically interact in *trans* with each other to form cell-cell adhesion.

In addition, nectin heterophilically interacts in *trans* with other immunoglobulin-like molecules, such as Necl, Tactile/CD96, DNAM-1/CD226, and TIGIT (Bottino et al., 2003; Ikeda et al., 2003; Kakunaga et al., 2004; Seth et al., 2007; Shingai et al., 2003). Nectin-1 interacts in *trans* with nectin-3, -4, Necl-1, and Tactile/CD96; nectin-2 interacts in *trans* with nectin-3, DNAM-1/CD226, and TIGIT; nectin-3 interacts in *trans* with Necl-1, -3, -5.

Tactile/CD96 and DNAM-1/CD226 are very highly homologous with a common structural feature; all extracellular domains are V-like (three V domains for Tactile/CD96 and two V domains for DNAM-1/CD226). Tactile/CD96 and DNAM-1/CD226 are critically involved in natural killer (NK)-mediated recognition of target cells (Fuchs et al., 2004). Tactile/CD96 is expressed on the surface of T and NK cells but not on the majority of B cells, monocytes, and granulocytes (Fuchs et al., 2004). Tactile/CD96 was also described as a tumor marker for leukemia such as

T-cell acute lymphoblastic leukemia (T-ALL) and acute myelogenous leukemia (AML) (Gramatzki et al., 1998; Hosen et al., 2007). Although nectin-1 was reported to bind Tactile/CD96 in mouse (Seth et al., 2007), the significance of the interaction of nectin-1 with Tactile/CD96 remains undetermined. DNAM-1/CD226 is broadly expressed on the surface of peripheral leukocytes including T cells, NK cells, monocytes, and a subset of B cells as well as platelets (Bottino et al., 2003; Kojima et al., 2003; Shibuya et al., 1996). The interaction of nectin-2 with DNAM-1/CD226 plays a role in the T cell- and NK-mediated cytotoxicity, immune response, and tumor immunity (Tahara-Hanaoka et al., 2004, 2006). Further, nectin-2 and DNAM-1/CD226 are expressed in human mast cells and eosinophils and the interaction of nectin-2 with DNAM-1/CD226 is likely involved in allergic reactions through costimulatory receptor–ligand interactions, because blocking nectin-2 expressed on eosinophils by neutralizing antibodies normalizes the hyperactivation in mast cells resulting from IgE-dependent activation of mast cells cocultured with eosinophils (Bachelet et al., 2006). TIGIT (T cell immunoglobulin and immunoreceptor tyrosine-based inhibitory motif (ITIM) domain) is a newly isolated protein expressed by T cells and NK cells (Stanietsky et al., 2009; Yu et al., 2009). This protein contains a V domain, a transmembrane domain, and an ITIM. TIGIT interacts with nectin-2 (Stanietsky et al., 2009) and Necl-5 (Stanietsky et al., 2009; Yu et al., 2009). The affinity of the Necl-5–TIGIT interaction (1–3 nM) is higher than that of the Necl-5–DNAM-1/CD226 interaction (119 nM) (Tahara-Hanaoka et al., 2004). The interaction of TIGIT on T cells with Necl-5 on dendritic cells exhibits immunosuppressive action to increase the secretion of IL-10 and decrease the secretion of proinflammatory cytokines (Yu et al., 2009). The interaction of TIGIT on NK cells with Necl-5 and nectin-2 inhibits NK cell cytotoxicity and decreases the secretion of proinflammatory cytokines (Stanietsky et al., 2009).

Mutations in nectin have been identified in human diseases. The first reported “nectinopathy” is cleft lip/palate–ectodermal dysplasia (CLPED), which includes Zlotogora–Ogur syndrome and Margarita Island ectodermal dysplasia caused by an impaired function of nectin-1 due to mutations of this gene (Sozen et al., 2001; Suzuki et al., 1998, 2000). CLPED appears to be an autosomal recessive disorder that is clinically characterized by cleft lip and/or palate, unusual faces, dental anomalies, hypotrichosis, palmoplantar hyperkeratosis and onychodysplasia, syndactyly, and occasionally mental retardation. The second disease is ectodermal dysplasia–syndactyly syndrome (EDSS) that is characterized by the combination of hair and tooth abnormalities, alopecia, and cutaneous syndactyly. Brancati et al. (2010) identified mutations of nectin-4 in EDSS and reported that mutated nectin-4 lost its capability to bind nectin-1 in patient keratinocytes.

#### 4.1.2. Nectin-like molecules

Necl is a  $\text{Ca}^{2+}$ -independent immunoglobulin-like cell adhesion molecule that comprises a family comprising five members: Necl-1 (TSLL1/SynCAM3), Necl-2 (IGSF4/RA175/SgIGSF/TSLL1/SynCAM1), Necl-3 (similar to Necl3/SynCAM2), Necl-4 (TSLL2/SynCAM4), and Necl-5 (Tage4/PVR (poliovirus receptor)/CD155). Necl-1 homophilically interacts in *trans* and heterophilically interacts in *trans* with nectin-1, nectin-3, and Necl-2, but not nectin-2 or Necl-5 (Kakunaga et al., 2004). Necl-2 also homophilically interacts in *trans* and heterophilically interacts in *trans* with nectin-3 and Necl-1 and another immunoglobulin-like molecule CRTAM, which mediates the cytotoxic activity of NK cells (Boles et al., 2005; Kennedy et al., 2000; Shingai et al., 2003). The binding partners of Necl-3 and Necl-4 have not been identified yet. Necl-5 does not homophilically interact in *trans* but heterophilically interacts in *trans* with nectin-3 and other immunoglobulin-like molecules such as Tactile/CD96, DNAM-1/CD226, and TIGIT (Stanietsky et al., 2009; Yu et al., 2009). Although Tactile/CD96 was cloned in 1992 and known to be a protein of the T-cell activation antigen family (Wang et al., 1992), its function had been unknown until Necl-5 was identified as a ligand for this molecule and the interaction of Tactile/CD96 with Necl-5 was shown to be involved in NK cell adhesion to target cells and cytotoxicity.

Necl, structurally similar to nectin, has an extracellular region with three immunoglobulin-like loops, a single transmembrane region, and a cytoplasmic tail region. However, unlike nectin, Necl does not directly interact with afadin at its C-terminal cytoplasmic tail (Takai and Nakanishi, 2003).

Studies of ours and other laboratories have uncovered the roles of Necl. Necl-1 is selectively expressed in the neural tissue and localizes at the contact sites between two axon terminals, between an axon terminal and an axon shaft, and between an axon terminal and glia cell processes in the cerebellum (Kakunaga et al., 2005). In the peripheral-myelinated nerve fibers, Necl-1 localizes at the contact sites between the cellular processes of Schwann cells at the nodes of Ranvier. Necl-2 is relatively widely expressed in various tissues (Shingai et al., 2003) and acts as a tumor suppressor in human non-small cell lung cancer (Kuramochi et al., 2001). In normal epithelial cells, Necl-2 localizes at the basolateral portion of the cell-cell adhesion sites, but not at the cell-cell junctional apparatus, such as tight junctions, adherens junctions, or desmosomes. It was recently reported that Necl-2 silences the signaling of ErbB3/ErbB2, members of the EGF receptor/ErbB family (Kawano et al., 2009). Necl-2 interacts in *cis* with the extracellular region of ErbB3 and with protein tyrosine phosphatase PTPN13 through its cytoplasmic tail. The interaction of Necl-2 with ErbB3 reduces the ligand-induced, ErbB2-catalyzed tyrosine phosphorylation of ErbB3. Phosphorylation of ErbB3 leads to the inhibition of the

ErbB3-dependent activation of Rac and Akt through the action of PTPN13, resulting in the inhibition of cancer cell movement and survival.

Although the general properties of Necl-3 and Necl-4 remain uncovered, Necl-5 is constitutively expressed at low levels on epithelial and endothelial cells. Human Necl-5 was originally identified as the human PVR (Koike et al., 1990; Mendelsohn et al., 1989), while rodent Necl-5 was originally identified as Tage4, the product of a gene overexpressed in rodent colon carcinoma (Chadeneau et al., 1994). Necl-5 was subsequently shown to be overexpressed in many human cancer cell lines and primary tumors in which this molecule appears to be involved in tumor-cell invasion and migration (Masson et al., 2001; Sloan et al., 2004).

#### 4.1.3. Afadin

Afadin is a nectin- and F-actin-binding protein that is involved in the formation of adherens junctions in cooperation with nectin and cadherin (Mandai et al., 1997). Afadin has multiple domains: two Ras-association (RA) domains, a forkhead-associated domain, a dilute (DIL) domain, a PDZ domain, three proline-rich (PR) domains, and an F-actin-binding domain at the C-terminus (Fig. 3.3). Afadin interacts with nectin through the PDZ domain (Takahashi et al., 1999) and with F-actin through the F-actin-binding domain at the C-terminus. In addition to nectin and F-actin, afadin can bind a variety of proteins such as structural proteins and signaling molecules through the following domains: Rap1 small G protein through the RA domains (Linnemann et al., 1999); afadin DIL-domain-interacting protein (ADIP) through the DIL domain (Asada et al., 2003); a subset of Eph receptor (Buchert et al., 1999; Hock et al., 1998), SPA-1 (Su et al., 2003), Bcr (Radziwill et al., 2003), and c-Src (Radziwill et al., 2007) through the PDZ domain; ZO-1 through the first and second PR domains (Ooshio et al., 2010), although ZO-1 appears to interact with the RA domains (Yamamoto et al., 1997); ponsin through the third PR domain (Mandai et al., 1999); LIM domain only 7 (LMO7) through the C-terminal region containing the F-actin-binding domain (Ooshio et al., 2004). Although Ras small G protein was initially identified as an interacting molecule with the RA domain of afadin (Yamamoto et al., 1997), other studies later demonstrate that afadin binds GTP-bound Rap1 with a higher affinity than GTP-bound Ras or GTP-bound Rap2 (Boettner et al., 2000; Linnemann et al., 1999). Moreover, although the detailed regions for these bindings remain unknown, afadin interacts directly with Fam (Taya et al., 1998), profilin (Boettner et al., 2000), and  $\alpha$ -catenin (Pokutta et al., 2002; Tachibana et al., 2000).

Afadin is phosphorylated by c-Src at Tyr<sup>1237</sup> and the phosphorylation of this tyrosine residue provides a binding site for the SH2 region of the protein tyrosine phosphatase SHP-2 (Nakata et al., 2007).

Afadin is localized to adherens junctions in epithelial cells and plays an important role in the formation of adherens junctions in cooperation with a wide variety of junction proteins, structural proteins, and signaling molecules that include nectins, cadherin, and integrins as described above and summarized in our previously published reviews (Rikitake and Takai, 2008; Takai et al., 2008a,b).

In addition to the significance in the formation of cell–cell junctions, it was recently identified several novel roles of afadin in fibroblasts (Kanzaki et al., 2008; Miyata et al., 2009a,b) and endothelial cells (Tawa et al., 2010). Firstly, afadin plays a critical role in cell survival: embryoid bodies derived from afadin-knockout embryonic stem (ES) cells contained many more apoptotic cells than those derived from wild-type ES cells, and apoptosis induced by serum deprivation or Fas-ligand stimulation was increased in cultured afadin-knockdown fibroblasts (Kanzaki et al., 2008) and endothelial cells (Tawa et al., 2010). Growth factors such as PDGF and vascular endothelial growth factor (VEGF) can activate the phosphatidylinositol 3-kinase (PI3-kinase)–Akt signaling pathway critically involved in cell survival. Knockdown of afadin impaired the activation of this signaling pathway induced by PDGF and VEGF in fibroblasts and endothelial cells, respectively. Further, afadin regulates cell proliferation and tubulogenesis of endothelial cells: knockdown of afadin inhibited the VEGF- or S1P-induced proliferation and tube formation on Matrigel of endothelial cells (Tawa et al., 2010). Moreover, afadin plays a pivotal role in cell movement in fibroblasts and endothelial cells, which will be later discussed in detail (Miyata et al., 2009a,b).

Afadin-knockout mice showed the disorganization of cell–cell junctions during embryogenesis, which leads to the impaired migration and improper differentiation of cells, resulting in embryonic lethality (Ikeda et al., 1999; Zhadanov et al., 1999). Recently, two distinct conditional afadin-knockout mice using the Cre/loxP system have been generated. In neuron-specific afadin-knockout mice which developed by crossing with calcium–calmodulin-dependent kinase II (CaMK) promoter-driven Cre mice, the loss-of-expression of afadin was predominantly observed in the hippocampus (Majima et al., 2009). In the hippocampus of these mice, puncta adherentia junctions were disrupted and the number of perforated synapses was increased, suggesting the instability of synaptic junctions. Thus, afadin is involved in the formation and remodeling of synapses. On the other hand, endothelial cell-specific afadin-knockout mice were developed by crossing with Tie2 promoter-driven Cre mice (Tawa et al., 2010). Most of these mutant mice are embryonically lethal accompanied by impaired lymphangiogenesis (H. Ogita and Y. Takai, unpublished data). Adult mutants showed disturbance of physiological and pathological angiogenesis: vascular network development in the retina, neovessel formation in the Matrigel

implanted into abdominal subcutaneous, and adaptive angiogenesis following hindlimb ischemia (Tawa et al., 2010).

## 4.2. Roles of nectins, Necls, and afadin in cell movement

In addition to the formation of cell–cell adhesion, nectins, Necls, and afadin play roles in cell movement.

### 4.2.1. Roles of nectins and Necls in cell movement

Necl-5 localizes at the leading edge of moving NIH3T3 cells and interacts functionally and physically with integrin  $\alpha_v\beta_3$ , which enhances cell movement (Fig. 3.4; Ikeda et al., 2004; Minami et al., 2007). It had been known that the interaction of integrin  $\alpha_v\beta_3$  with PDGF receptor plays an important role in the PDGF-induced cell movement and intracellular signaling. It has

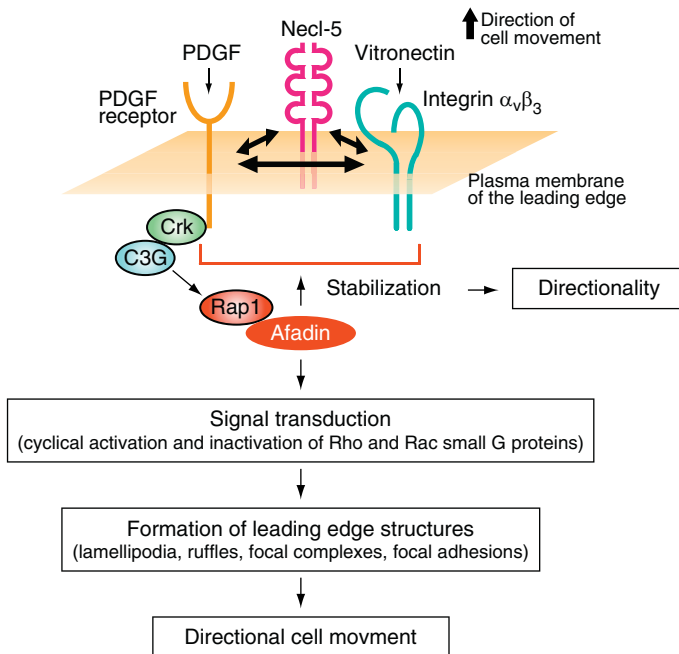


**Figure 3.4** Necl-5 and afadin in intracellular signaling pathways regulating directional cell movement. Necl-5, integrin  $\alpha_v\beta_3$ , and PDGF receptor interact at the leading edge of moving cells such as NIH 3T3 cells. Upon stimulation by PDGF, the complex of these three molecules causes the activation of Rap1, which in turn leads to the activation of Rac and the inhibition of Rho, resulting in enhancement of the formation of leading edge structures contributing cell movement.



been recently clarified that Necl-5 is functionally and physically interacted with integrin  $\alpha_v\beta_3$  and PDGF receptor at the leading edge of the moving cell, and that Necl-5 promotes cell movement by enhancing both integrin  $\alpha_v\beta_3$ - and PDGF receptor-induced signalings. Necl-5 colocalizes with integrin  $\alpha_v\beta_3$  and PDGF receptor at peripheral ruffles and with integrin  $\alpha_v\beta_3$  at focal complexes (Minami et al., 2007). Necl-5 facilitates the PDGF receptor-mediated activation of Rac which regulates the formation of peripheral ruffles and focal complexes.

In addition, it was recently clarified that Necl-5 is involved in the contact inhibition of cell movement and proliferation. When two moving cells collide with each other, Necl-5 on the surface of one cell *trans*-interacts heterophilically with nectin-3 on the adjacent cell surface to initiate the formation of cell-cell junctions (Ikeda et al., 2003). This *trans*-interaction causes the activation of Cdc42 and Rac (Sato et al., 2005), which enhances the reorganization of the actin cytoskeleton and increases the number of cell-cell adhesion sites. However, the *trans*-interaction of Necl-5 with nectin-3 is transient: Necl-5 is downregulated and endocytosed from the cell membrane in a clathrin-dependent manner (Fujito et al., 2005), which leads to reductions in cell movement and proliferation, whereas nectin-3 dissociated from Necl-5 is retained on the cell membrane and subsequently interacts in *trans* with nectin-1, the isoform of nectins that most feasibly interacts in *trans* with nectin-3 (Ikeda et al., 2003), which leads to the recruitment of cadherin to the nectin-based adhesion sites, eventually establishing adherens junctions. Thus, the cell-cell contact-induced *trans*-interaction of Necl-5 with nectin-3 and the subsequent downregulation of Necl-5 are at least one of the mechanisms of the contact inhibition of cell movement and proliferation (Fujito et al., 2005).

#### 4.2.2. Roles of afadin in cell movement

In addition to the functional role of afadin in the organization of cell-cell adhesion in epithelial cells and neurons, afadin plays another novel roles in directional cell movement in NIH3T3 cells. It was recently found that, in NIH3T3 cells which do not form cell-cell junctions, afadin that does not associate with nectin localizes at the leading edges during cell movement (Fig. 3.4; Miyata et al., 2009a). Afadin regulates several features of cell movement (Miyata et al., 2009a,b). Firstly, afadin regulates the formation of leading edge structures; neither lamellipodia, ruffles, nor focal complexes are formed in afadin-knockdown NIH3T3 cells. Secondary, afadin regulates the directionality of cell movement; afadin is involved in their directional, but not random, cell movement. The interaction of afadin with Rap1 at the leading edge is necessary for the PDGF-induced directional movement of NIH3T3 cells. Finally, afadin regulates the cyclical activation and inactivation of small G proteins at the leading edges of moving NIH3T3 cells; the coordinated regulation of the activation and inactivation of Rap1,

Rac1, and RhoA is necessary for cell movement. These novel roles of afadin will be further discussed in the succeeding sections.

## 5. CROSTALK BETWEEN GROWTH FACTOR RECEPTORS AND INTEGRINS

At the molecular level, growth factors and chemokines, as well as interactions between integrins and ECM, act as chemoattractants and provide the signals required for cell movement (Danen et al., 2005; Nishiya et al., 2005; Ridley et al., 2003). It is well known that growth factors are potent chemoattractants for most cells. Also, it has been recognized that integrins, through the integrin–ECM interaction, initiate the signals required for cell motility.

### 5.1. Integrins

Integrins comprise a family of cell adhesion receptors that play a central role in the adhesive interactions between cells and their surrounding ECM (Hynes, 1992). Integrins physically connect the actin cytoskeleton to ECM at focal adhesions and functionally transmit bidirectional (i.e., outside-in and inside-out) signaling across the plasma membrane (Critchley, 2000; Schoenwaelder and Burridge, 1999), which controls not only cell adhesion to ECM but also cell migration, growth, differentiation, and apoptosis that occur in response to the environmental recognition.

Integrins are heterodimers consisting of an  $\alpha$ - and a  $\beta$ -subunit. In mammals, there are 24 canonical integrins formed from combinations of 18  $\alpha$ -subunits and 8  $\beta$ -subunits.

Conformational changes in individual integrin heterodimers and clustering of heterodimers into heterooligomers influence ligand-binding affinity (Carman and Springer, 2003), and therefore both conformational change and clustering of integrins are likely important for integrin function, although their relative contributions appear to vary depending on the types of integrins and cells as well as biological circumstances.

### 5.2. Crosstalk between growth factor receptors and integrins

There is increasing evidence that a coordinated crosstalk between growth factor receptors and integrins is functionally important for an integrated cellular response to the extracellular environment (Blystone et al., 1999; Hynes, 1992; Porter and Hogg, 1997). Particularly under cultured conditions, growth factor-induced cell adhesion, migration, and proliferation depend on specific integrins. The effects of PDGF, insulin, fibroblast

growth factor (FGF), epidermal growth factor (EGF), and VEGF are functionally interacted with integrin  $\alpha_V\beta_3$  (Borges et al., 2000; Brooks et al., 1994; Schneller et al., 1997; Soldi et al., 1999; Woodard et al., 1998). For example, the PDGF-induced DNA synthesis and motility of human fibroblasts are enhanced when cells are plated on the integrin  $\alpha_V\beta_3$  ligand vitronectin compared with plated on the integrin  $\beta_1$  ligand collagen (Schneller et al., 1997). Further, it was reported that integrins can directly associate with growth factor receptors. For example, a vitronectin receptor–integrin  $\alpha_V\beta_3$  physically interacts with PDGF receptor (Borges et al., 2000; Schneller et al., 1997), insulin receptor (Schneller et al., 1997), and VEGF receptor (Borges et al., 2000; Soldi et al., 1999). Integrins  $\alpha_6\beta_4$  and  $\alpha_6\beta_1$  can bind ErbB2/HER-2, a receptor tyrosine kinase closely related to EGF receptor (Falcioni et al., 1997), whereas integrins  $\alpha_6\beta_4$  and  $\alpha_2\beta_1$  can bind hepatocyte growth factor (HGF) receptor/c-Met (McCall-Culbreath et al., 2008; Trusolino et al., 2001). However, the molecular mechanisms of these crosstalks remained mostly undetermined until we discovered the critical role of Necl-5 as discussed below.

### 5.3. Role of Necl-5 in crosstalk between growth factor receptors and integrins

PDGF receptor physically and functionally interacts with integrin  $\alpha_V\beta_3$ , and interaction of these two transmembrane proteins coordinately regulates the signals required for the formation of leading edge structures and cell movement (Woodard et al., 1998). The molecular mechanisms of this crosstalk had remained poorly understood. It was identified that Necl-5 is a key molecule that regulates the crosstalk between PDGF receptor and integrin  $\alpha_V\beta_3$  (Amano et al., 2008; Minami et al., 2007). Necl-5 physically and functionally interacts with PDGF receptor and integrin  $\alpha_V\beta_3$  (Amano et al., 2008; Minami et al., 2007). Although it is practically difficult to prove, Necl-5, PDGF receptor, and integrin  $\alpha_V\beta_3$  might form a ternary complex because these three transmembrane proteins are able to form any combinations of a binary complex.

Necl-5 is essential for the PDGF- and vitronectin-dependent directional cell motility of NIH3T3 cells (Minami et al., 2007). Overexpression of Necl-5 enhances, whereas knockdown of Necl-5 impairs the PDGF-induced migration of NIH3T3 cells that are plated onto vitronectin (Minami et al., 2007). In line with these findings, Necl-5 enhances integrin  $\alpha_V\beta_3$  clustering and the formation of focal complexes at the leading edges of motile cells (Minami et al., 2007). The Necl-5–PDGF receptor–integrin  $\alpha_V\beta_3$  complex localizes at peripheral ruffles over lamellipodia; the Necl-5–integrin  $\alpha_V\beta_3$  complex, but not PDGF receptor, localizes at focal complexes; and integrin  $\alpha_V\beta_3$ , but neither PDGF receptor nor Necl-5, localizes at focal adhesions (Minami et al., 2007; Nagamatsu et al., 2008).

Overexpression of Necl-5 enhances, whereas knockdown of Necl-5 impairs the formation of focal complexes in PDGF-stimulated NIH3T3 cells that are plated onto vitronectin. In fact, the enhancement of the interaction between Necl-5 and integrin  $\alpha_V\beta_3$  by overexpression of Necl-5 results in the augmentation of the PDGF-induced activation of Rac. On the contrary, the reduction of the interaction between these two molecules by knockdown of Necl-5 decreases the activation of Rac.

In addition, Necl-5 regulates the physical interaction between PDGF receptor and integrin  $\alpha_V\beta_3$  (Amano et al., 2008). PDGF receptor, upon binding of PDGF, appears to be internalized and dissociated from Necl-5 and integrin  $\alpha_V\beta_3$ , followed by attachment of peripheral ruffles over the lamellipodia to ECM through the Necl-5–integrin  $\alpha_V\beta_3$  complex and the formation of new focal complexes. Then, Necl-5 is dissociated from the Necl-5–integrin  $\alpha_V\beta_3$  complex during the transformation of focal complexes to focal adhesions. Necl-5 regulates the dissociation of PDGF receptor from the Necl-5–PDGF receptor–integrin  $\alpha_V\beta_3$  complex following stimulation with PDGF as demonstrated by the fact that overexpression of Necl-5 inhibits, whereas knockdown of Necl-5 augments PDGF receptor dissociation. Taken together, Necl-5 regulates the crosstalk between PDGF receptor and integrin  $\alpha_V\beta_3$  and through this crosstalk Necl-5 plays a crucial role in the PDGF- and vitronectin-dependent directional movement of NIH3T3 cells.

Further, Necl-5 regulates the intracellular signaling of PDGF receptor and FGF receptor at the step downstream of the receptors and upstream of Ras small G protein. Necl-5 enhances the activation of the Ras–Raf–MEK–ERK signaling pathway and induces up- or downregulation of cell cycle regulators, such as cyclins D2 and E and cyclin-dependent kinase inhibitor p27<sup>Kip1</sup>, in NIH3T3 cells, resulting in shortening of the G<sub>1</sub> phase of the cell cycle and enhancement of growth factor-induced cell proliferation. Necl-5 interacts with sprouty2, a negative regulator of growth factor-induced signaling for cell proliferation (Christofori, 2003; Kim and Bar-Sagi, 2004), and this interaction prevents tyrosine phosphorylation of sprouty2, resulting in the enhancement of the PDGF-induced activation of Ras (Kajita et al., 2007).

VEGF receptor-2 (VEGFR-2) plays an important role in angiogenesis. It was reported that VEGFR-2 physically and functionally interacts with integrin  $\alpha_V\beta_3$  and this interaction is critical for the VEGF-induced angiogenesis (Borges et al., 2000; Soldi et al., 1999). However, the mechanism involved in this crosstalk is not fully understood. It was reported that c-Src intracellularly regulates this crosstalk because the inhibition of c-Src by its specific inhibitors prevents the VEGF-induced transactivation of integrin  $\alpha_V\beta_3$  signaling (Mahabeleshwar et al., 2007). It was recently identified that Necl-5 extracellularly mediates this crosstalk by regulating the VEGF-dependent binding of integrin  $\alpha_V\beta_3$  with VEGFR-2 (Y. Rikitake

and Y. Takai, unpublished data). Stimulation of cultured endothelial cells with VEGF induces the binding of integrin  $\alpha_V\beta_3$  with VEGFR-2, which is inhibited by knockdown of Necl-5 (Y. Rikitake and Y. Takai, unpublished data). However, we have not determined whether Necl-5 regulates the crosstalk between integrins and growth factor receptors other than PDGF receptor and VEGFR-2. Further studies are required.

The interaction between c-Met and integrin  $\alpha_6\beta_4$  is essential for HGF-dependent invasive growth (Trusolino et al., 2001). Similar to Necl-5, CD151, a member of the transmembrane 4 superfamily, also known as the tetraspanin family, interacts with c-Met and integrin  $\alpha_3/\alpha_6$  (Klosek et al., 2005). In salivary gland carcinoma cells, CD151 forms a structural complex with c-Met and integrin  $\alpha_3/\alpha_6$  and functions as a molecular linker in the formation of the c-Met and integrin  $\alpha_3/\alpha_6$  complex.

## 6. REGULATION OF DIRECTIONALITY OF CELL MOVEMENT

In order to move toward a chemical signal, cells must sense the extracellular attractant gradient and transmit this information inside the cell to elicit changes in cell morphology and produce motility in the direction of the gradient. For directionally persistent cell migration, cells must continuously receive the polarized environmental signals and transmit the polarized intracellular signals from a fixed direction, which orient protrusion of the leading edge. Although it has been shown that a number of molecules are involved in cell movement, molecules that have been identified to regulate directionality are quite limited (Table 3.1).

**Table 3.1** Molecules that regulate motility and directionality during directional cell movement

|                                        | Motility                                                              | Directionality   |
|----------------------------------------|-----------------------------------------------------------------------|------------------|
| Cell polarity proteins                 | Par3, Par6, aPKC                                                      | Par3, Par6, aPKC |
| Small G proteins                       | Rho, Rac, Cdc42, Rap, Arf6                                            | Cdc42            |
| Kinases/<br>Phosphatases               | PI3-kinase, PTEN, SHP1/2, Akt,<br>GSK3 $\beta$ , MAPK, PAK, ROCK, FAK | PI3-kinase       |
| Actin cytoskeleton-associated proteins | WAVE2, N-WASP, Arp2/3, Afadin,<br>Girdin, mDia                        | Afadin           |

## 6.1. PI3-kinase

PI3-kinase regulates a variety of fundamental cellular processes, including cell movement, proliferation, and survival. PI3-kinase phosphorylates the integral membrane lipid PI(4,5)P<sub>2</sub> to generate PI(3,4,5)P<sub>3</sub> at the plasma membrane, leading to recruitment of downstream target proteins to the membrane sites. The action of PI3-kinase is antagonized by phosphatase and tensin homolog deleted on chromosome ten (PTEN), an inositol lipid phosphatase which dephosphorylates PI(3,4,5)P<sub>3</sub> and converts it back into PI(4,5)P<sub>2</sub>. Previous studies using pharmacological inhibitors such as wortmannin and LY294002 and genetic manipulation of PI3-kinase have shown that the PI3-kinase signaling pathway plays an important role in the regulation of the directionality of chemotaxis (Merlot and Firtel, 2003). Studies in both *Dictyostelium* cells and mammalian cells have demonstrated that various chemoattractants induce the localized accumulation of PI(3,4,5)P<sub>3</sub> at the leading edge of moving cells. The polarized, asymmetric localization of PI(3,4,5)P<sub>3</sub> is maintained by positive feedback and negative regulation mechanisms. Positive feedback mechanism is that PI(3,4,5)P<sub>3</sub> stimulates further production of PI(3,4,5)P<sub>3</sub>, probably through a mechanism involving the Rho family small G proteins. Another negative regulation mechanism is that PI(3,4,5)P<sub>3</sub> is dephosphorylated by PTEN and removed from the rear tail region. However, although it is well known that PTEN plays a critical role in the regulation of cell migration, it has become evident that the effects of PTEN are not entirely dependent on the PI3-kinase signaling.

PI(3,4,5)P<sub>3</sub> binds and affects the activity and localization of a variety of the PH domain-containing proteins, which contributes to the establishment of cell polarity and migration. The Rho family small G proteins, such as Cdc42, Rac, and Rho, appear to play important roles in the development of cell polarity. Rac might be a key effector of the PI3-kinase signaling. However, Rac is not a direct target of PI(3,4,5)P<sub>3</sub>. Thus, molecular link between PI(3,4,5)P<sub>3</sub> production and the activation of Rac in development of cell polarity and migration remains to be determined.

## 6.2. Cell polarity proteins

Many important biological processes, including chemotaxis (directional cell movement), require a clearly established cell polarity and the ability of the cell to respond to a directional signal. Cdc42, a member of the Rho family small G proteins, is a key regulator of cell polarization during directional movement (Etienne-Manneville, 2004; Etienne-Manneville and Hall, 2001). Cell polarization influences the formation of the leading edge and the stability of the front-rear axis correlates with the extent of directional movement (Iden and Collard, 2008). Therefore, cell polarity proteins such as the Par complex, consisting of Par3, Par6, and atypical protein kinase C, are recognized to be critically involved in cell polarization during

directional movement (Petrie et al., 2009). Cdc42 links the Par complex to directional movement because the Par complex acts downstream of Cdc42 to stabilize microtubules at the leading edge (Gomes et al., 2005).

In addition to polarity signaling as discussed above, evidence that the crosstalk between small G proteins is important for directional cell movement has been gradually accumulated as reviewed in the recent paper (Petrie et al., 2009). Cdc42 induces the activation of Rac1 locally at the leading edge via at least two signaling pathways, which initiates protrusions and directional movement (Cau and Hall, 2005; Nishimura et al., 2005). Cdc42 directly activates PAK1, which recruits  $\beta$ PIX, a GEF for Rac1, to the leading edge, resulting in the local activation of Rac1 (Cau and Hall, 2005). Cdc42 can directly bind to the Par complex and recruit another Rac1-GEF Tiam1 to the leading edge, resulting in the activation of Rac1 (Nishimura et al., 2005). Active Rac1 might decrease the activity of RhoA through p190RhoGAP, a GAP for RhoA. Conversely, active RhoA can antagonize the activation of Rac1 at the leading edge through the RhoA-mediated activation of Rho-kinase, which disrupts the Par-3-Tiam1 complex and inhibits the Tiam1-increased activity of Rac1 (Nakayama et al., 2008).

### 6.3. Afadin

Despite the importance of the intracellular signaling to operate cell polarization and to control direction of protrusion formation for directional cell movement, the mechanism of how cells can persistently receive the polarized environmental signals, such as soluble factors and ECM, during directional cell movement is largely unknown. We recently discovered that an actin-binding protein afadin plays a key role in persistent directional cell movement by facilitating clustering of the Necl-5-PDGF receptor-integrin  $\alpha_v\beta_3$  complex presumably in a positive feedback amplification manner (Miyata et al., 2009a). Knockdown of afadin in NIH3T3 cells results in reduction of the PDGF-induced directional motility. However, knockdown of afadin does not affect random movement in the presence of PDGF. During directional cell movement of wild-type NIH3T3 cells, the leading edge is continuously formed toward higher concentrations of PDGF and the Necl-5-PDGF receptor-integrin  $\alpha_v\beta_3$  complex localizes at the leading edge. By contrast, the leading edge is transiently formed and immediately disappeared in afadin-knockdown NIH3T3 cells. Thus, afadin stabilizes the Necl-5-PDGF receptor-integrin  $\alpha_v\beta_3$  complex at the leading edge and contributes to initiate persistently the polarized intracellular signals from the leading edge in a fixed direction.

We also demonstrated that the interaction of afadin with Rap1 is necessary for the localization of afadin at the leading edge, the formation of leading edge, and the PDGF-induced directional cell movement (Miyata et al., 2009a). All those phenotypes are blocked by knockdown of afadin and this blockade is rescued by the reexpression of wild-type afadin but not by a

mutant of afadin that lacks the Rap1-binding domain (Miyata et al., 2009a). The interaction of afadin with Rap1 increases the activity of Rap1 (Tawa et al., 2010), which in turn augments the interaction of afadin with Rap1. In addition, the inhibition of the PDGF-induced leading edge formation and directional cell movement by knockdown of afadin is not rescued by a mutant of afadin that lacks the DIL domain, suggesting the critical role of the interaction of afadin with DIL domain-binding protein(s) (H. Ogita and Y. Takai, unpublished data). Since afadin interacts with ADIP through the DIL domain (Asada et al., 2003) and leading edge formation and directional cell movement induced by PDGF is defective in ADIP-knockdown NIH3T3 cells (H. Ogita and Y. Takai, unpublished data), ADIP is likely to be involved in the afadin-mediated regulation of intracellular signaling for cell movement. Further, we also reported that afadin interacts with p85, a regulatory subunit of PI3-kinase, in fibroblasts (Kanzaki et al., 2008) and endothelial cells (Tawa et al., 2010). Rap1 regulates the interaction between afadin and p85 (Tawa et al., 2010). In addition to cell survival, this interaction could also contribute to the PI3-kinase-dependent directional cell movement.

#### 6.4. Necl-5 and microtubules

Microtubules (MTs) are highly dynamic structural components involved in diverse cellular processes such as cell division, cell polarity, cell migration, and vesicular transport. When cells start directional cell movement, MT networks are reorientated and then search for and grow toward the leading edge of moving cells, followed by their stabilization at the rear sites of the leading edge (Wittmann and Waterman-Storer, 2001). We found that Necl-5 regulates the attraction of growing MTs to the plasma membrane of the leading edge of moving cells (Minami et al., 2010). Necl-5 enhances the PDGF-induced growth of MTs and attracts MTs near to the plasma membrane of the leading edge of moving cells in an integrin  $\alpha_v\beta_3$ -dependent manner. Necl-5 also enhances the PDGF-induced attraction of the plus-end tracking proteins (+TIPs), including EB1, CLIP170, an intermediate chain subunit of cytoplasmic dynein, and p150<sup>Glued</sup>, a subunit of dynactin, near to the plasma membrane of the leading edge.



---

## 7. REGULATION OF DYNAMICS OF CYCLICAL ACTIVATION AND INACTIVATION OF SMALL G PROTEINS BY AFDADIN

Cells are moving with dynamically repeating forming and disassembling leading edge structures, such as filopodia, lamellipodia, and peripheral ruffles. The spatially and temporally regulated activation and inactivation of



the Rho family small G proteins, including Rac1, Cdc42, and RhoA, tightly and coordinately regulate these dynamic events in NIH3T3 cells (Fig. 3.5A–D) (Miyata et al., 2009b; Sander et al., 1999). In order to have cells keep moving, each member of the Rho family small G proteins should cyclically become active and inactive as leading edge structures are dynamically formed and disassembled. Rac and Cdc42 are activated and RhoA is inactivated at focal complexes, and *vice versa* at focal adhesions (Ballestrem et al., 2001; Nobes and Hall, 1999; Ridley et al., 1992; Rottner et al., 1999). Thus, the cyclical activation and inactivation of the Rho family small G proteins are critical for turnover of the transformation of focal complexes into focal adhesions during cell movement. So far, the crosstalk between members of the Rho family small G proteins has been reported. For example, the activation of Cdc42 leads to the activation of Rac and subsequently the activation of Rho in Swiss 3T3 fibroblasts (Hall, 1998; Ridley et al., 1992). However, the effects of Rho-like proteins on sequence of activation vary among the cell types. Sander and colleagues reported that the activation of Cdc42 and Rac leads to the downregulation of the activity of Rho in NIH3T3 cells (Sander et al., 1999). The crosstalk between Rac and Rho seems to be unidirectional because the activation of Rho does not affect the activity of Rac. However, it was reported that the RhoA-induced activation of ROCK can lead to inhibition of the activity of Rac at the leading edge (Nakayama et al., 2008). In the process of actin reorganization during adherens junction formation, the activation of Rac controls the inactivation of RhoA by regulating the activity and localization of p190RhoGAP (Wildenberg et al., 2006). However, the regulation mechanism of dynamics underlying the cyclical activation and inactivation of the Rho family small G proteins remains largely unknown.

The crosstalk between the Rho family small G proteins and other families of small G proteins has been gradually uncovered. Arthur and colleagues reported for the first time that, when cells are spreading, Rap1 locally activates Rac1 at the sites of membrane protrusions, resulting in cell spreading by the formation of membrane protrusions adjacent to the ECM (Arthur et al., 2004). We recently reported that stimulation of the cells with PDGF induces the local and transient activation of Rap1 at the leading edge (Takahashi et al., 2008). The activation of Rap1 is mediated by an adaptor protein Crk and the Rap1-GEF C3G through the Necl-5–PDGF receptor–integrin  $\alpha_v\beta_3$  complex (Fig. 3.5A; Takahashi et al., 2008). This spatial and temporal activation of Rap1 has at least three important roles in the formation of leading edge structures (Fig. 3.5B; Miyata et al., 2009b). The first role is to induce the activation of Rac1 by binding to the Rac-GEF Vav2. Activated Rap1 recruits Vav2 to the leading edge and directly binds Vav2, which increases its GEF activity for Rac (Arthur et al., 2004), resulting in the local activation of Rac1 (Fig. 3.5B; Takahashi et al., 2008). Activated Rac1 then induces the

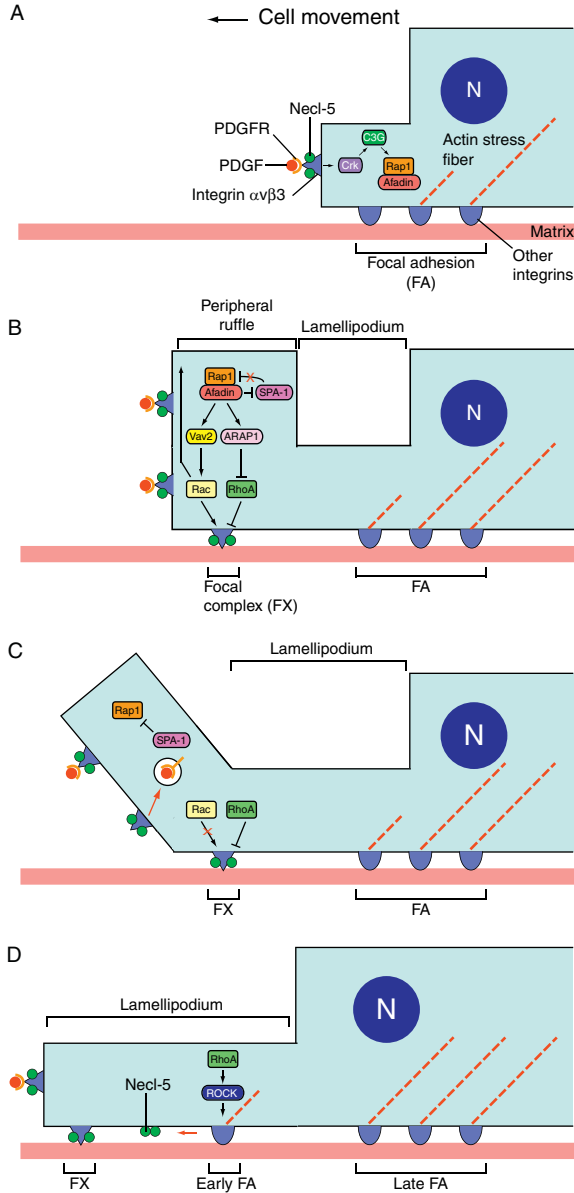


**Figure 3.5** Dynamics of regulation of small G protein activities during directional cell movement. (A) Activation of Rap1 by the Necl-5–PDGF receptor–integrin  $\alpha_v\beta_3$  complex. Upon stimulation by PDGF, the Necl-5–PDGF receptor–integrin  $\alpha_v\beta_3$  complex induces the activation of Rap1 through Crk and the Rap1-GEF C3G locally at the leading edge. Activated Rap1 binds a form of afadin unbound to nectin and recruits it to the leading edge. (B) Activation of Rac and inactivation of RhoA by Rap1. Activated

formation of lamellipodia, peripheral ruffles, and focal complexes. Another role is to induce the inactivation of RhoA by binding to the Rho-GAP ARAP1 (Fig. 3.5B). Activated Rap1 recruits ARAP1 to the leading edge and interacts with ARAP1 through the RA domain. This interaction increases the GAP activity of ARAP1 for RhoA, resulting in the local inactivation of RhoA at the leading edge. Further, activated Rap1 recruits afadin that is not bound to nectins to the leading edge. An active, GTP-bound form of Rap1 directly binds to afadin through the N-terminal RA domains and induces the recruitment of afadin to the leading edge where Rap1 is locally activated. Afadin then recruits SPA-1, a GAP for Rap1, to the leading edge, but because the binding affinity of afadin to active Rap1 is greater than that to SPA-1, afadin preferentially interacts with active Rap1 in the presence of active Rap1, that prevents from inactivating Rap1.

Internalization and downregulation of PDGF receptor from the cell surface may be implicated in the mechanisms of dynamic formation of leading edge structures (Fig. 3.5C). Endocytic downregulation of PDGF receptor terminates the activation of Rap1 with the aid of SPA-1, resulting in the inactivation of Rac1 and activation of RhoA at the leading edge (Miyata et al., 2009b). The activation of RhoA and its downstream ROCK induce the dissociation of Necl-5 from focal complexes and thereby enhance the transformation of focal complexes to focal adhesions (Fig. 3.5D) (Nagamatsu et al., 2008). Collectively, the Necl-5–PDGF receptor–integrin  $\alpha_v\beta_3$  complex-mediated cyclical activation and inactivation of these small G proteins, which are critically regulated by afadin, play a key role in the dynamic formation and disassembly of leading edge structures required for directional cell movement.

---

Rap1 induces the activation of Rac by binding to Vav2, enhancing the formation of lamellipodium, peripheral ruffle, and focal complex (FX). In addition, activated Rap1 also induces the inactivation of RhoA by binding to the Rho-GAP ARAP1, contributing to the formation of FX. The interaction of afadin with activated Rap1 prevents the Rap1-GAP SPA-1 from inactivating Rap1. Note that Necl-5, PDGF receptor, and integrin  $\alpha_v\beta_3$  are observed at peripheral ruffle; however, Necl-5 and integrin  $\alpha_v\beta_3$ , but not PDGF receptor, are concentrated at FX. Focal adhesion (FA) includes other integrins rather than integrin  $\alpha_v\beta_3$ . (C) Inactivation of Rap1 by SPA-1. When PDGF receptor is downregulated by endocytosis, Rap1 is no longer activated and is inactivated by SPA-1, which in turn leads to the inactivation of Rac and activation of RhoA. (D) Enhancement of the transformation of FX into FA by RhoA and Rho-kinase (ROCK). Activated RhoA induces the dissociation of Necl-5 from FX by activating its downstream ROCK and thereby enhances the transformation of FX to FA. N: nucleus.



## 8. CONCLUDING REMARKS

Here, we summarize recent insights into the molecular mechanisms underlying dynamic regulation of the crosstalk between small G protein signaling network, which promotes the formation and disassembly of leading edge structures during directional cell movement. Our currently proposed model of molecular mechanism involving Necl-5 and afadin is addressed in this review. Although this mechanism functions at least in fibroblasts such as NIH3T3 cells, further studies are necessary to analyze whether our model can be applied for other types of cells. In particular, the role and regulation of Cdc42 in NIH3T3 cells is currently unknown. Presumably, the extent of Cdc42 dependency varies among cell types. Regulation mechanisms driving dynamic small G protein signaling crosstalk required for cell movement might be more complicated than those we have currently identified. The crosstalk between small G proteins other than Rap1, RhoA, Rac1, and Cdc42, and its role in directional cell movement are largely unknown. It is possible that regulation mechanisms might vary, depending on types of cells, chemoattractants, ECM, and other environment factors. Therefore, what we discovered might be the tip of an iceberg.

Similar dynamic regulation of small G proteins might play a role in other cellular functions, such as neurite outgrowth that resembles cell movement. Moreover, although not mentioned in this review, dynamic activation of small G proteins might also play a role in the formation of other protrusive structures, such as invadopodia and podosomes (Albiges-Rizo et al., 2009; Nakahara et al., 2003) as well as in the retraction of the tail at the rear side of migrating cells (Alblas et al., 2001; Ridley et al., 2003; Worthylake et al., 2001). Invadopodia and podosomes are actin-rich membrane protrusions, which are considered as cell-matrix adhesion sites. Cdc42 and related small G proteins are likely important for these protrusions although the mechanisms underlying the regulation of invadopodia and podosomes are largely unknown (Albiges-Rizo et al., 2009; Nakahara et al., 2003). Cell movement is regulated by not only front protrusion extension but also by rear tail retraction (Ridley et al., 2003). In migrating cells, integrin adhesions must turn over between assembly and disassembly. It is known that the activities of RhoA and its downstream effector ROCK are required to disassemble integrin adhesions at the rear of the cells to allow detachment from ECM (Alblas et al., 2001; Worthylake et al., 2001). Further studies are needed to clarify if dynamics of the activation and inactivation of the Rho family small G proteins plays a role in the regulation of invadopodia, podosomes, and tail retraction, and if so, what the underlying molecular mechanism is.

## ACKNOWLEDGMENTS

The authors thank Drs. Tadaomi Takenawa, Jun Miyoshi, and Hisakazu Ogita for careful and critical reading of the Chapter. This work was supported by grants-in-aid for Scientific Research and for Cancer Research from the Ministry of Education, Culture, Sports, Science and Technology, Japan (to Y. R. and Y. T.), and grants from Global Center of Excellence (to Y. R. and Y. T.), Hyogo Science and Technology Association, the Mochida Memorial Foundation for Medical and Pharmaceutical Research, Mitsubishi Pharma Research Foundation, Takeda Science Foundation (to Y. R.), and Japan Foundation for Applied Enzymology (Y. T.).

## REFERENCES

- Abercrombie, M., Heaysman, J.E., Pegrum, S.M., 1970. The locomotion of fibroblasts in culture. II. "RRuffling" Exp. Cell Res. 60, 437–444.
- Adams, A.E., Johnson, D.I., Longnecker, R.M., Sloat, B.F., Pringle, J.R., 1990. CDC42 and CDC43, two additional genes involved in budding and the establishment of cell polarity in the yeast *Saccharomyces cerevisiae*. J. Cell Biol. 111, 131–142.
- Albigez-Rizo, C., Destaing, O., Fourcade, B., Planus, E., Block, M.R., 2009. Actin machinery and mechanosensitivity in invadopodia, podosomes and focal adhesions. J. Cell Sci. 122, 3037–3049.
- Alblas, J., Ulfman, L., Hordijk, P., Koenderman, L., 2001. Activation of Rho and ROCK are essential for detachment of migrating leukocytes. Mol. Biol. Cell 12, 2137–2145.
- Amano, H., Ikeda, W., Kawano, S., Kajita, M., Tamaru, Y., Inoue, N., et al., 2008. Interaction and localization of Necl-5 and PDGF receptor beta at the leading edges of moving NIH3T3 cells: implications for directional cell movement. Genes Cells 13, 269–284.
- Andrew, N., Insall, R.H., 2007. Chemotaxis in shallow gradients is mediated independently of PtdIns 3-kinase by biased choices between random protrusions. Nat. Cell Biol. 9, 193–200.
- Aplin, A.E., Howe, A., Alahari, S.K., Juliano, R.L., 1998. Signal transduction and signal modulation by cell adhesion receptors: the role of integrins, cadherins, immunoglobulin-cell adhesion molecules, and selectins. Pharmacol. Rev. 50, 197–263.
- Arriemerlou, C., Meyer, T., 2005. A local coupling model and compass parameter for eukaryotic chemotaxis. Dev. Cell 8, 215–227.
- Arthur, W.T., Quilliam, L.A., Cooper, J.A., 2004. Rap1 promotes cell spreading by localizing Rac guanine nucleotide exchange factors. J. Cell Biol. 167, 111–122.
- Asada, M., Irie, K., Morimoto, K., Yamada, A., Ikeda, W., Takeuchi, M., et al., 2003. ADIP, a novel afadin- and  $\alpha$ -actinin-binding protein localized at cell-cell adherens junctions. J. Biol. Chem. 278, 4103–4111.
- Bachelet, I., Munitz, A., Mankutad, D., Levi-Schaffer, F., 2006. Mast cell costimulation by CD226/CD112 (DNAM-1/Nectin-2): a novel interface in the allergic process. J. Biol. Chem. 281, 27190–27196.
- Ballestrem, C., Hinz, B., Imhof, B.A., Wehrle-Haller, B., 2001. Marching at the front and dragging behind: differential  $\alpha$ V $\beta$ 3-integrin turnover regulates focal adhesion behavior. J. Cell Biol. 155, 1319–1332.
- Bender, A., Pringle, J.R., 1989. Multicopy suppression of the *cdc24* budding defect in yeast by CDC42 and three newly identified genes including the ras-related gene RSR1. Proc. Natl. Acad. Sci. USA 86, 9976–9980.

- Bershadsky, A., Chausovsky, A., Becker, E., Lyubimova, A., Geiger, B., 1996. Involvement of microtubules in the control of adhesion-dependent signal transduction. *Curr. Biol.* 6, 1279–1289.
- Biyasheva, A., Svitkina, T., Kunda, P., Baum, B., Borisy, G., 2004. Cascade pathway of filopodia formation downstream of SCAR. *J. Cell Sci.* 117, 837–848.
- Blystone, S.D., Slater, S.E., Williams, M.P., Crow, M.T., Brown, E.J., 1999. A molecular mechanism of integrin crosstalk:  $\alpha$ v $\beta$ 3 suppression of calcium/calmodulin-dependent protein kinase II regulates  $\alpha$ 5 $\beta$ 1 function. *J. Cell Biol.* 145, 889–897.
- Boettner, B., Govek, E.E., Cross, J., Van Aelst, L., 2000. The junctional multidomain protein AF-6 is a binding partner of the Rap1A GTPase and associates with the actin cytoskeletal regulator profilin. *Proc. Natl. Acad. Sci. USA* 97, 9064–9069.
- Boles, K.S., Barchet, W., Diacovo, T., Cella, M., Colonna, M., 2005. The tumor suppressor TSLC1/NECL-2 triggers NK-cell and CD8+ T-cell responses through the cell-surface receptor CRTAM. *Blood* 106, 779–786.
- Borges, E., Jan, Y., Ruoslahti, E., 2000. Platelet-derived growth factor receptor beta and vascular endothelial growth factor receptor 2 bind to the beta 3 integrin through its extracellular domain. *J. Biol. Chem.* 275, 39867–39873.
- Borm, B., Requardt, R.P., Herzog, V., Kirfel, G., 2005. Membrane ruffles in cell migration: indicators of inefficient lamellipodia adhesion and compartments of actin filament reorganization. *Exp. Cell Res.* 302, 83–95.
- Bos, J.L., de Rooij, J., Reedquist, K.A., 2001. Rap1 signalling: adhering to new models. *Nat. Rev. Mol. Cell Biol.* 2, 369–377.
- Bottino, C., Castriconi, R., Pende, D., Rivera, P., Nanni, M., Carnemolla, B., et al., 2003. Identification of PVR (CD155) and Nectin-2 (CD112) as cell surface ligands for the human DNAM-1 (CD226) activating molecule. *J. Exp. Med.* 198, 557–567.
- Brancati, F., Fortugno, P., Bottillo, I., Lopez, M., Josselin, E., Boudghene-Stambouli, O., et al., 2010. Mutations in PVRL4, encoding cell adhesion molecule nectin-4, cause ectodermal dysplasia-syndactyly syndrome. *Am. J. Hum. Genet.* 87, 265–273.
- Brooks, P.C., Clark, R.A., Chersesh, D.A., 1994. Requirement of vascular integrin  $\alpha$ v $\beta$ 3 for angiogenesis. *Science* 264, 569–571.
- Buchert, M., Schneider, S., Meskenaite, V., Adams, M.T., Canaani, E., Baechli, T., et al., 1999. The junction-associated protein AF-6 interacts and clusters with specific Eph receptor tyrosine kinases at specialized sites of cell–cell contact in the brain. *J. Cell Biol.* 144, 361–371.
- Burbelo, P.D., Miyamoto, S., Utani, A., Brill, S., Yamada, K.M., Hall, A., et al., 1995. p190-B, a new member of the Rho GAP family, and Rho are induced to cluster after integrin cross-linking. *J. Biol. Chem.* 270, 30919–30926.
- Carman, C.V., Springer, T.A., 2003. Integrin avidity regulation: are changes in affinity and conformation underemphasized? *Curr. Opin. Cell Biol.* 15, 547–556.
- Carter, S.B., 1965. Principles of cell motility: the direction of cell movement and cancer invasion. *Nature* 208, 1183–1187.
- Carter, S.B., 1967. Haptotaxis and the mechanism of cell motility. *Nature* 213, 256–260.
- Cau, J., Hall, A., 2005. Cdc42 controls the polarity of the actin and microtubule cytoskeletons through two distinct signal transduction pathways. *J. Cell Sci.* 118, 2579–2587.
- Chadeneau, C., LeMoullac, B., Denis, M.G., 1994. A novel member of the immunoglobulin gene superfamily expressed in rat carcinoma cell lines. *J. Biol. Chem.* 269, 15601–15605.
- Christofori, G., 2003. Split personalities: the agonistic antagonist Sprouty. *Nat. Cell Biol.* 5, 377–379.
- Cramer, L.P., Siebert, M., Mitchison, T.J., 1997. Identification of novel graded polarity actin filament bundles in locomoting heart fibroblasts: implications for the generation of motile force. *J. Cell Biol.* 136, 1287–1305.

- Critchley, D.R., 2000. Focal adhesions—the cytoskeletal connection. *Curr. Opin. Cell Biol.* 12, 133–139.
- Danen, E.H., van Rheenen, J., Franken, W., Huvenceers, S., Sonneveld, P., Jalink, K., et al., 2005. Integrins control motile strategy through a Rho-cofilin pathway. *J. Cell Biol.* 169, 515–526.
- Dawe, H.R., Minamide, L.S., Bamburg, J.R., Cramer, L.P., 2003. ADF/cofilin controls cell polarity during fibroblast migration. *Curr. Biol.* 13, 252–257.
- de Rooij, J., Zwartkruis, F.J., Verheijen, M.H., Cool, R.H., Nijman, S.M., Wittinghofer, A., et al., 1998. Epac is a Rap1 guanine-nucleotide-exchange factor directly activated by cyclic AMP. *Nature* 396, 474–477.
- de Rooij, J., Boenink, N.M., van Triest, M., Cool, R.H., Wittinghofer, A., Bos, J.L., 1999. PDZ-GEF1, a guanine nucleotide exchange factor specific for Rap1 and Rap2. *J. Biol. Chem.* 274, 38125–38130.
- DeMali, K.A., Barlow, C.A., Burridge, K., 2002. Recruitment of the Arp2/3 complex to vinculin: coupling membrane protrusion to matrix adhesion. *J. Cell Biol.* 159, 881–891.
- Derry, J.M., Ochs, H.D., Francke, U., 1994. Isolation of a novel gene mutated in Wiskott–Aldrich syndrome. *Cell* 78, 635–644.
- DesMarais, V., Ichetovkin, I., Condeelis, J., Hitchcock-DeGregori, S.E., 2002. Spatial regulation of actin dynamics: a tropomyosin-free, actin-rich compartment at the leading edge. *J. Cell Sci.* 115, 4649–4660.
- Didsbury J, Weber RF, Bokoch GM, Evans T, Snyderman R., 1989. Rac, a novel ras-related family of proteins that are botulinum toxin substrates. *J Biol Chem.* 264, 16378–16382.
- Disanza, A., Mantoani, S., Hertzog, M., Gerboth, S., Frittoli, E., Steffen, A., et al., 2006. Regulation of cell shape by Cdc42 is mediated by the synergic actin-bundling activity of the Eps8–IRSp53 complex. *Nat. Cell Biol.* 8, 1337–1347.
- Dovas, A., Couchman, J.R., 2005. RhoGDI: multiple functions in the regulation of Rho family GTPase activities. *Biochem. J.* 390, 1–9.
- Durand, C.A., Westendorf, J., Tse, K.W., Gold, M.R., 2006. The Rap GTPases mediate CXCL13- and sphingosine1-phosphate-induced chemotaxis, adhesion, and Pyk2 tyrosine phosphorylation in B lymphocytes. *Eur. J. Immunol.* 36, 2235–2249.
- Eden, S., Rohatgi, R., Podtelejnikov, A.V., Mann, M., Kirschner, M.W., 2002. Mechanism of regulation of WAVE1-induced actin nucleation by Rac1 and Nck. *Nature* 418, 790–793.
- Essler, M., Amano, M., Kruse, H.J., Kaibuchi, K., Weber, P.C., Aepfelbacher, M., 1998. Thrombin inactivates myosin light chain phosphatase via Rho and its target Rho kinase in human endothelial cells. *J. Biol. Chem.* 273, 21867–21874.
- Etienne-Manneville, S., 2004. Cdc42—the centre of polarity. *J. Cell Sci.* 117, 1291–1300.
- Etienne-Manneville, S., Hall, A., 2001. Integrin-mediated activation of Cdc42 controls cell polarity in migrating astrocytes through PKCzeta. *Cell* 106, 489–498.
- Etienne-Manneville, S., Hall, A., 2002. Rho GTPases in cell biology. *Nature* 420, 629–635.
- Evans, T., Brown, M.L., Fraser, E.D., Northup, J.K., 1986. Purification of the major GTP-binding proteins from human placental membranes. *J. Biol. Chem.* 1986, 261, 7052–7059.
- Fabre-Lafay, S., Garrido-Urbani, S., Reymond, N., Goncalves, A., Dubreuil, P., Lopez, M., 2005. Nectin-4, a new serological breast cancer marker, is a substrate for tumor necrosis factor-alpha-converting enzyme (TACE)/ADAM-17. *J. Biol. Chem.* 280, 19543–19550.
- Faix, J., Breitsprecher, D., Stradal, T.E., Rottner, K., 2009. Filopodia: complex models for simple rods. *Int. J. Biochem. Cell Biol.* 41, 1656–1664.

- Falcioni, R., Antonini, A., Nistico, P., Di Stefano, S., Crescenzi, M., Natali, P.G., et al., 1997. Alpha 6 beta 4 and alpha 6 beta 1 integrins associate with ErbB-2 in human carcinoma cell lines. *Exp. Cell Res.* 236, 76–85.
- Forscher, P., Smith, S.J., 1988. Actions of cytochalasins on the organization of actin filaments and microtubules in a neuronal growth cone. *J. Cell Biol.* 107, 1505–1516.
- Fuchs, A., Cella, M., Giurisato, E., Shaw, A.S., Colonna, M., 2004. Cutting edge: CD96 (tactile) promotes NK cell–target cell adhesion by interacting with the poliovirus receptor (CD155). *J. Immunol.* 172, 3994–3998.
- Fujita, H., Fukuhara, S., Sakurai, A., Yamagishi, A., Kamioka, Y., Nakaoka, Y., et al., 2005. Local activation of Rap1 contributes to directional vascular endothelial cell migration accompanied by extension of microtubules on which RAPL, a Rap1–associating molecule, localizes. *J. Biol. Chem.* 280, 5022–5031.
- Fujito, T., Ikeda, W., Kakunaga, S., Minami, Y., Kajita, M., Sakamoto, Y., et al., 2005. Inhibition of cell movement and proliferation by cell–cell contact–induced interaction of Necl-5 with nectin-3. *J. Cell Biol.* 171, 165–173.
- Fujiwara, K., Pollard, T.D., 1976. Fluorescent antibody localization of myosin in the cytoplasm, cleavage furrow, and mitotic spindle of human cells. *J. Cell Biol.* 71, 848–875.
- Fukata, Y., Amano, M., Kaibuchi, K., 2001. Rho–Rho–kinase pathway in smooth muscle contraction and cytoskeletal reorganization of non-muscle cells. *Trends Pharmacol. Sci.* 22, 32–39.
- Gao, Q., Srinivasan, S., Boyer, S.N., Wazer, D.E., Band, V., 1999. The E6 oncoproteins of high-risk papillomaviruses bind to a novel putative GAP protein, E6TP1, and target it for degradation. *Mol. Cell Biol.* 19, 733–744.
- Geiger, B., Spatz, J.P., Bershadsky, A.D., 2009. Environmental sensing through focal adhesions. *Nat. Rev. Mol. Cell Biol.* 10, 21–33.
- Gilbert, S.F., 2003. The morphogenesis of evolutionary developmental biology. *Int. J. Dev. Biol.* 47, 467–477.
- Gomes, E.R., Jani, S., Gundersen, G.G., 2005. Nuclear movement regulated by Cdc42, MRCK, myosin, and actin flow establishes MTOC polarization in migrating cells. *Cell* 121, 451–463.
- Gotoh, T., Hattori, S., Nakamura, S., Kitayama, H., Noda, M., Takai, Y., et al., 1995. Identification of Rap1 as a target for the Crk SH3 domain–binding guanine nucleotide–releasing factor C3G. *Mol. Cell Biol.* 15, 6746–6753.
- Govind, S., Kozma, R., Monfries, C., Lim, L., Ahmed, S., 2001. Cdc42Hs facilitates cytoskeletal reorganization and neurite outgrowth by localizing the 58-kD insulin receptor substrate to filamentous actin. *J. Cell Biol.* 152, 579–594.
- Gramatzki, M., Ludwig, W.D., Burger, R., Moos, P., Rohwer, P., Grunert, C., et al., 1998. Antibodies TC-12 (“unique”) and TH-111 (CD96) characterize T-cell acute lymphoblastic leukemia and a subgroup of acute myeloid leukemia. *Exp. Hematol.* 26, 1209–1214.
- Gupton, S.L., Gertler, F.B., 2007. Filopodia: the fingers that do the walking. *Sci STKE* 2007, re5.
- Hall, A., 1998. Rho GTPases and the actin cytoskeleton. *Science* 279, 509–514.
- Hartwell, L.H., Culotti, J., Pringle, J.R., Reid, B.J., 1974. Genetic control of the cell division cycle in yeast. *Science*. 183, 46–51.
- Hedberg, K.M., Bell, Jr., P.B., 1995. The effect of neomycin on PDGF-induced mitogenic response and actin organization in cultured human fibroblasts. *Exp. Cell Res.* 219, 266–275.
- Hedberg, K.M., Bengtsson, T., Safiejko-Mrocza, B., Bell, P.B., Lindroth, M., 1993. PDGF and neomycin induce similar changes in the actin cytoskeleton in human fibroblasts. *Cell Motil. Cytoskeleton* 24, 139–149.



- Helfman, D.M., Levy, E.T., Berthier, C., Shtutman, M., Rivelino, D., Grosheva, I., et al., 1999. Caldesmon inhibits nonmuscle cell contractility and interferes with the formation of focal adhesions. *Mol. Biol. Cell* 10, 3097–3112.
- Higgs, H.N., 2005. Formin proteins: a domain-based approach. *Trends Biochem. Sci.* 30, 342–353.
- Hill, C.S., Wynne, J., Treisman, R., 1995. The Rho family GTPases RhoA, Rac1, and CDC42Hs regulate transcriptional activation by SRF. *Cell* 81, 1159–1170.
- Hirata, K., Kikuchi, A., Sasaki, T., Kuroda, S., Kaibuchi, K., Matsuura, Y., et al., 1992. Involvement of rho p21 in the GTP-enhanced calcium ion sensitivity of smooth muscle contraction. *J. Biol. Chem.* 267, 8719–8722.
- Ho, H.Y., Rohatgi, R., Lebensohn, A.M., Le, M., Li, J., Gygi, S.P., et al., 2004. Toca-1 mediates Cdc42-dependent actin nucleation by activating the N-WASP-WIP complex. *Cell* 118, 203–216.
- Hock, B., Bohme, B., Karn, T., Yamamoto, T., Kaibuchi, K., Holtrich, U., et al., 1998. PDZ-domain-mediated interaction of the Eph-related receptor tyrosine kinase EphB3 and the ras-binding protein AF6 depends on the kinase activity of the receptor. *Proc. Natl. Acad. Sci. USA* 95, 9779–9784.
- Hosen, N., Park, C.Y., Tatsumi, N., Oji, Y., Sugiyama, H., Gramatzki, M., et al., 2007. CD96 is a leukemic stem cell-specific marker in human acute myeloid leukemia. *Proc. Natl. Acad. Sci. USA* 104, 11008–11013.
- Hotulainen, P., Lappalainen, P., 2006. Stress fibers are generated by two distinct actin assembly mechanisms in motile cells. *J. Cell Biol.* 173, 383–394.
- Hynes, R.O., 1992. Integrins: versatility, modulation, and signaling in cell adhesion. *Cell* 69, 11–25.
- Iden, S., Collard, J.G., 2008. Crosstalk between small GTPases and polarity proteins in cell polarization. *Nat. Rev. Mol. Cell Biol.* 9, 846–859.
- Ikeda, W., Nakanishi, H., Miyoshi, J., Mandai, K., Ishizaki, H., Tanaka, M., et al., 1999. Afadin: a key molecule essential for structural organization of cell-cell junctions of polarized epithelia during embryogenesis. *J. Cell Biol.* 146, 1117–1132.
- Ikeda, W., Kakunaga, S., Itoh, S., Shingai, T., Takekuni, K., Satoh, K., et al., 2003. TAGE4/Nectin-like molecule-5 heterophilically *trans*-interacts with cell adhesion molecule Nectin-3 and enhances cell migration. *J. Biol. Chem.* 278, 28167–28172.
- Ikeda, W., Kakunaga, S., Takekuni, K., Shingai, T., Satoh, K., Morimoto, K., et al., 2004. Nectin-like molecule-5/TAGE4 enhances cell migration in an integrin-dependent, Nectin-3-independent manner. *J. Biol. Chem.* 279, 18015–18025.
- Iwasa, J.H., Mullins, R.D., 2007. Spatial and temporal relationships between actin-filament nucleation, capping, and disassembly. *Curr. Biol.* 17, 395–406.
- Jalink, K., van Corven, E.J., Hengeveld, T., Morii, N., Narumiya, S., Moolenaar, W.H., 1994. Inhibition of lysophosphatidate- and thrombin-induced neurite retraction and neuronal cell rounding by ADP ribosylation of the small GTP-binding protein Rho. *J. Cell Biol.* 126, 801–810.
- Johnson, D.I., Pringle, J.R., 1990. Molecular characterization of CDC42, a *Saccharomyces cerevisiae* gene involved in the development of cell polarity. *J. Cell Biol.* 111, 143–152.
- Kajita, M., Ikeda, W., Tamaru, Y., Takai, Y., 2007. Regulation of platelet-derived growth factor-induced Ras signaling by poliovirus receptor Necl-5 and negative growth regulator Sprouty2. *Genes Cells* 12, 345–357.
- Kakunaga, S., Ikeda, W., Shingai, T., Fujito, T., Yamada, A., Minami, Y., et al., 2004. Enhancement of serum- and platelet-derived growth factor-induced cell proliferation by Necl-5/TAGE4/poliovirus receptor/CD155 through the Ras-Raf-MEK-ERK signaling. *J. Biol. Chem.* 279, 36419–36425.
- Kakunaga, S., Ikeda, W., Itoh, S., Deguchi-Tawarada, M., Ohtsuka, T., Mizoguchi, A., et al., 2005. Nectin-like molecule-1/TSLL1/SynCAM3: a neural tissue-specific

- immunoglobulin-like cell–cell adhesion molecule localizing at non-junctional contact sites of presynaptic nerve terminals, axons and glia cell processes. *J. Cell Sci.* 118, 1267–1277.
- Kanzaki, N., Ogita, H., Komura, H., Ozaki, M., Sakamoto, Y., Majima, T., et al., 2008. Involvement of the nectin-afadin complex in PDGF-induced cell survival. *J. Cell Sci.* 121, 2008–2017.
- Kaverina, I., Krylyshkina, O., Small, J.V., 1999. Microtubule targeting of substrate contacts promotes their relaxation and dissociation. *J. Cell Biol.* 146, 1033–1044.
- Kawano, S., Ikeda, W., Kishimoto, M., Ogita, H., Takai, Y., 2009. Silencing of ErbB3/ErbB2 signaling by immunoglobulin-like Necl-2. *J. Biol. Chem.* 284, 23793–23805.
- Kawasaki, H., Springett, G.M., Mochizuki, N., Toki, S., Nakaya, M., Matsuda, M., et al., 1998. A family of cAMP-binding proteins that directly activate Rap1. *Science* 282, 2275–2279.
- Kawata, M., Matsui, Y., Kondo, J., Hishida, T., Teranishi, Y., Takai, Y., 1988. A novel small molecular weight GTP-binding protein with the same putative effector domain as the ras proteins in bovine brain membranes. Purification, determination of primary structure, and characterization. *J. Biol. Chem.* 263, 18965–18971.
- Kennedy, J., Vicari, A.P., Saylor, V., Zurawski, S.M., Copeland, N.G., Gilbert, D.J., et al., 2000. A molecular analysis of NKT cells: identification of a class-I restricted T cell-associated molecule (CRTAM). *J. Leukoc. Biol.* 67, 725–734.
- Kim, H.J., Bar-Sagi, D., 2004. Modulation of signalling by Sprouty: a developing story. *Nat. Rev. Mol. Cell Biol.* 5, 441–450.
- Kinashi, T., Katagiri, K., 2005. Regulation of immune cell adhesion and migration by regulator of adhesion and cell polarization enriched in lymphoid tissues. *Immunology* 116, 164–171.
- Kishi, K., Sasaki, T., Kuroda, S., Itoh, T., Takai, Y., 1993. Regulation of cytoplasmic division of *Xenopus* embryo by rho p21 and its inhibitory GDP/GTP exchange protein (rho GDI). *J. Cell Biol.* 120, 1187–1195.
- Kitayama, H., Sugimoto, Y., Matsuzaki, T., Ikawa, Y., Noda, M., 1989. A ras-related gene with transformation suppressor activity. *Cell* 56, 77–84.
- Klosek, S.K., Nakashiro, K., Hara, S., Shintani, S., Hasegawa, H., Hamakawa, H., 2005. CD151 forms a functional complex with c-Met in human salivary gland cancer cells. *Biochem. Biophys. Res. Commun.* 336, 408–416.
- Kohno, H., Tanaka, K., Mino, A., Umikawa, M., Imamura, H., Fujiwara, T., et al., 1996. Bni1p implicated in cytoskeletal control is a putative target of Rho1p small GTP binding protein in *Saccharomyces cerevisiae*. *EMBO J.* 15, 6060–6068.
- Koike, S., Horie, H., Ise, I., Okitsu, A., Yoshida, M., Iizuka, N., et al., 1990. The poliovirus receptor protein is produced both as membrane-bound and secreted forms. *EMBO J.* 9, 3217–3224.
- Kojima, H., Kanada, H., Shimizu, S., Kasama, E., Shibuya, K., Nakauchi, H., et al., 2003. CD226 mediates platelet and megakaryocytic cell adhesion to vascular endothelial cells. *J. Biol. Chem.* 278, 36748–36753.
- Komuro, R., Sasaki, T., Takaishi, K., Orita, S., Takai, Y., 1996. Involvement of Rho and Rac small G proteins and Rho GDI in  $Ca^{2+}$ -dependent exocytosis from PC12 cells. *Genes Cells* 1, 943–951.
- Kozma, R., Ahmed, S., Best, A., Lim, L., 1995. The Ras-related protein Cdc42Hs and bradykinin promote formation of peripheral actin microspikes and filopodia in Swiss 3T3 fibroblasts. *Mol. Cell. Biol.* 15, 1942–1952.
- Kraynov, V.S., Chamberlain, C., Bokoch, G.M., Schwartz, M.A., Slabaugh, S., Hahn, K. M., 2000. Localized Rac activation dynamics visualized in living cells. *Science* 290, 333–337.

- Krugmann, S., Jordens, I., Gevaert, K., Driessens, M., Vandekerckhove, J., Hall, A., 2001. Cdc42 induces filopodia by promoting the formation of an IRSp53:Mena complex. *Curr. Biol.* 11, 1645–1655.
- Kurachi, H., Wada, Y., Tsukamoto, N., Maeda, M., Kubota, H., Hattori, M., et al., 1997. Human SPA-1 gene product selectively expressed in lymphoid tissues is a specific GTPase-activating protein for Rap1 and Rap2. Segregate expression profiles from a rap1GAP gene product. *J. Biol. Chem.* 272, 28081–28088.
- Kuramochi, M., Fukuhara, H., Nobukuni, T., Kanbe, T., Maruyama, T., Ghosh, H.P., et al., 2001. TSLC1 is a tumor-suppressor gene in human non-small-cell lung cancer. *Nat. Genet.* 27, 427–430.
- Laukaitis, C.M., Webb, D.J., Donais, K., Horwitz, A.F., 2001. Differential dynamics of alpha 5 integrin, paxillin, and alpha-actinin during formation and disassembly of adhesions in migrating cells. *J. Cell Biol.* 153, 1427–1440.
- Lazarides, E., Burridge, K., 1975. Alpha-actinin: immunofluorescent localization of a muscle structural protein in nonmuscle cells. *Cell* 6, 289–298.
- Lebensohn, A.M., Kirschner, M.W., 2009. Activation of the WAVE complex by coincident signals controls actin assembly. *Mol. Cell* 36, 512–524.
- Lee, K., Gallop, J.L., Rambani, K., Kirschner, M.W., 2010. Self-assembly of filopodia-like structures on supported lipid bilayers. *Science* 329, 1341–1345.
- Legg, J.A., Bompard, G., Dawson, J., Morris, H.L., Andrew, N., Cooper, L., et al., 2007. N-WASP involvement in dorsal ruffle formation in mouse embryonic fibroblasts. *Mol. Biol. Cell* 18, 678–687.
- Lewis, A.K., Bridgman, P.C., 1992. Nerve growth cone lamellipodia contain two populations of actin filaments that differ in organization and polarity. *J. Cell Biol.* 119, 1219–1243.
- Li, S., Guan, J.L., Chien, S., 2005. Biochemistry and biomechanics of cell motility. *Annu. Rev. Biomed. Eng.* 7, 105–150.
- Lim, K.B., Bu, W., Goh, W.I., Koh, E., Ong, S.H., Pawson, T., et al., 2008a. The Cdc42 effector IRSp53 generates filopodia by coupling membrane protrusion with actin dynamics. *J. Biol. Chem.* 283, 20454–20472.
- Lim, Y., Lim, S.T., Tomar, A., Gardel, M., Bernard-Trifilo, J.A., Chen, X.L., et al., 2008b. PyK2 and FAK connections to p190Rho guanine nucleotide exchange factor regulate RhoA activity, focal adhesion formation, and cell motility. *J. Cell Biol.* 180, 187–203.
- Linnemann, T., Geyer, M., Jaitner, B.K., Block, C., Kalbitzer, H.R., Wittinghofer, A., et al., 1999. Thermodynamic and kinetic characterization of the interaction between the Ras binding domain of AF6 and members of the Ras subfamily. *J. Biol. Chem.* 274, 13556–13562.
- Lopez, M., Aoubala, M., Jordier, F., Isnardon, D., Gomez, S., Dubreuil, P., 1998. The human poliovirus receptor related 2 protein is a new hematopoietic/endothelial homophilic adhesion molecule. *Blood* 92, 4602–4611.
- Luster, A.D., Alon, R., von Andrian, U.H., 2005. Immune cell migration in inflammation: present and future therapeutic targets. *Nat. Immunol.* 6, 1182–1190.
- Machesky, L.M., Insall, R.H., 1998. Scar1 and the related Wiskott–Aldrich syndrome protein, WASP, regulate the actin cytoskeleton through the Arp2/3 complex. *Curr. Biol.* 8, 1347–1356.
- Madaule, P., Axel, R., 1985. A novel ras-related gene family. *Cell* 41, 31–40.
- Mahabeleshwar, G.H., Feng, W., Reddy, K., Plow, E.F., Byzova, T.V., 2007. Mechanisms of integrin-vascular endothelial growth factor receptor cross-activation in angiogenesis. *Circ. Res.* 101, 570–580.
- Majima, T., Ogita, H., Yamada, T., Amano, H., Togashi, H., Sakisaka, T., et al., 2009. Involvement of afadin in the formation and remodeling of synapses in the hippocampus. *Biochem. Biophys. Res. Commun.* 385, 539–544.

- Mallavarapu, A., Mitchison, T., 1999. Regulated actin cytoskeleton assembly at filopodium tips controls their extension and retraction. *J. Cell Biol.* 146, 1097–1106.
- Manabe, R., Kovalenko, M., Webb, D.J., Horwitz, A.R., 2002. GIT1 functions in a motile, multi-molecular signaling complex that regulates protrusive activity and cell migration. *J. Cell Sci.* 115, 1497–1510.
- Mandai, K., Nakanishi, H., Satoh, A., Obaishi, H., Wada, M., Nishioka, H., et al., 1997. Afadin: a novel actin filament-binding protein with one PDZ domain localized at cadherin-based cell-to-cell adherens junction. *J. Cell Biol.* 139, 517–528.
- Mandai, K., Nakanishi, H., Satoh, A., Takahashi, K., Satoh, K., Nishioka, H., et al., 1999. Ponsin/SH3P12: an l-afadin- and vinculin-binding protein localized at cell–cell and cell–matrix adherens junctions. *J. Cell Biol.* 144, 1001–1017.
- Manser, E., Loo, T.H., Koh, C.G., Zhao, Z.S., Chen, X.Q., Tan, L., et al., 1998. PAK kinases are directly coupled to the PIX family of nucleotide exchange factors. *Mol. Cell* 1, 183–192.
- Masson, D., Jarry, A., Baurly, B., Blanchardie, P., Laboisse, C., Lustenberger, P., et al., 2001. Overexpression of the CD155 gene in human colorectal carcinoma. *Gut* 49, 236–240.
- Mattila, P.K., Lappalainen, P., 2008. Filopodia: molecular architecture and cellular functions. *Nat. Rev. Mol. Cell Biol.* 9, 446–454.
- Mattila, P.K., Pykalainen, A., Saarikangas, J., Paavilainen, V.O., Vihinen, H., Jokitalo, E., et al., 2007. Missing-in-metastasis and IRSp53 deform PI(4, 5)P<sub>2</sub>-rich membranes by an inverse BAR domain-like mechanism. *J. Cell Biol.* 176, 953–964.
- McCall-Culbreath, K.D., Li, Z., Zutter, M.M., 2008. Crosstalk between the alpha2beta1 integrin and c-met/HGF-R regulates innate immunity. *Blood* 111, 3562–3570.
- McCarty, O.J., Larson, M.K., Auger, J.M., Kalia, N., Atkinson, B.T., Pearce, A.C., et al., 2005. Rac1 is essential for platelet lamellipodia formation and aggregate stability under flow. *J. Biol. Chem.* 280, 39474–39484.
- Mendelsohn, C.L., Wimmer, E., Racaniello, V.R., 1989. Cellular receptor for poliovirus: molecular cloning, nucleotide sequence, and expression of a new member of the immunoglobulin superfamily. *Cell* 56, 855–865.
- Merlot, S., Firtel, R.A., 2003. Leading the way: directional sensing through phosphatidylinositol 3-kinase and other signaling pathways. *J. Cell Sci.* 116, 3471–3478.
- Miki, H., Miura, K., Takenawa, T., 1996. N-WASP, a novel actin-depolymerizing protein, regulates the cortical cytoskeletal rearrangement in a PIP<sub>2</sub>-dependent manner downstream of tyrosine kinases. *EMBO J.* 15, 5326–5335.
- Miki, H., Sasaki, T., Takai, Y., Takenawa, T., 1998a. Induction of filopodium formation by a WASP-related actin-depolymerizing protein N-WASP. *Nature* 391, 93–96.
- Miki, H., Suetsugu, S., Takenawa, T., 1998b. WAVE, a novel WASP-family protein involved in actin reorganization induced by Rac. *EMBO J.* 17, 6932–6941.
- Miki, H., Yamaguchi, H., Suetsugu, S., Takenawa, T., 2000. IRSp53 is an essential intermediate between Rac and WAVE in the regulation of membrane ruffling. *Nature* 408, 732–735.
- Millard, T.H., Sharp, S.J., Machesky, L.M., 2004. Signalling to actin assembly via the WASP (Wiskott–Aldrich syndrome protein)-family proteins and the Arp2/3 complex. *Biochem. J.* 380, 1–17.
- Minami, Y., Ikeda, W., Kajita, M., Fujito, T., Amano, H., Tamaru, Y., et al., 2007. Necl-5/poliiovirus receptor interacts in cis with integrin alphaVbeta3 and regulates its clustering and focal complex formation. *J. Biol. Chem.* 282, 18481–18496.
- Minami, A., Mizutani, K., Waseda, M., Kajita, M., Miyata, M., Ikeda, W., et al., 2010. Necl-5/PVR enhances PDGF-induced attraction of growing microtubules to the plasma membrane of the leading edge of moving NIH3T3 cells. *Genes Cells* 15, 1123–1135.
- Mitchison, T., Kirschner, M., 1988. Cytoskeletal dynamics and nerve growth. *Neuron* 1, 761–772.

- Miyata, M., Ogita, H., Komura, H., Nakata, S., Okamoto, R., Ozaki, M., et al., 2009a. Localization of nectin-free afadin at the leading edge and its involvement in directional cell movement induced by platelet-derived growth factor. *J. Cell Sci.* 122, 4319–4329.
- Miyata, M., Rikitake, Y., Takahashi, M., Nagamatsu, Y., Yamauchi, Y., Ogita, H., et al., 2009b. Regulation by afadin of cyclical activation and inactivation of Rap1, Rac1, and RhoA small G proteins at leading edges of moving NIH3T3 cells. *J. Biol. Chem.* 284, 24595–24609.
- Mochizuki, N., Ohba, Y., Kiyokawa, E., Kurata, T., Murakami, T., Ozaki, T., et al., 1999. Activation of the ERK/MAPK pathway by an isoform of rap1GAP associated with G $\alpha$ (i). *Nature* 400, 891–894.
- Moser, B., Wolf, M., Walz, A., Loetscher, P., 2004. Chemokines: multiple levels of leukocyte migration control. *Trends Immunol.* 25, 75–84.
- Munemitsu, S., Innis, M.A., Clark, R., McCormick, F., Ullrich, A., Polakis, P., 1990. Molecular cloning and expression of a G25K cDNA, the human homolog of the yeast cell cycle gene CDC42. 1990. *Mol Cell Biol.* 10, 5977–5982.
- Nagamatsu, Y., Rikitake, Y., Takahashi, M., Deki, Y., Ikeda, W., Hirata, K., et al., 2008. Roles of Necl-5/poliovirus receptor and Rho-associated kinase (ROCK) in the regulation of transformation of integrin  $\alpha$ (V) $\beta$ (3)-based focal complexes into focal adhesions. *J. Biol. Chem.* 283, 14532–14541.
- Nakahara, H., Otani, T., Sasaki, T., Miura, Y., Takai, Y., Kogo, M., 2003. Involvement of Cdc42 and Rac small G proteins in invadopodia formation of RPMI7951 cells. *Genes Cells* 8, 1019–1027.
- Nakata, S., Fujita, N., Kitagawa, Y., Okamoto, R., Ogita, H., Takai, Y., 2007. Regulation of platelet-derived growth factor receptor activation by afadin through SHP-2: implications for cellular morphology. *J. Biol. Chem.* 282, 37815–37825.
- Nakayama, M., Goto, T.M., Sugimoto, M., Nishimura, T., Shinagawa, T., Ohno, S., et al., 2008. Rho-kinase phosphorylates PAR-3 and disrupts PAR complex formation. *Dev. Cell* 14, 205–215.
- Nayal, A., Webb, D.J., Brown, C.M., Schaefer, E.M., Vicente-Manzanares, M., Horwitz, A.R., 2006. Paxillin phosphorylation at Ser273 localizes a GIT1–PIX–PAK complex and regulates adhesion and protrusion dynamics. *J. Cell Biol.* 173, 587–589.
- Nikolopoulos, S.N., Turner, C.E., 2000. Actopaxin, a new focal adhesion protein that binds paxillin LD motifs and actin and regulates cell adhesion. *J. Cell Biol.* 151, 1435–1448.
- Nishimura, T., Yamaguchi, T., Kato, K., Yoshizawa, M., Nabeshima, Y., Ohno, S., et al., 2005. PAR-6–PAR-3 mediates Cdc42-induced Rac activation through the Rac GEFs STEF/Tiam1. *Nat. Cell Biol.* 7, 270–277.
- Nishiya, N., Kiosses, W.B., Han, J., Ginsberg, M.H., 2005. An  $\alpha$ 4 integrin–paxillin–Arf–GAP complex restricts Rac activation to the leading edge of migrating cells. *Nat. Cell Biol.* 7, 343–352.
- Nobes, C.D., Hall, A., 1995. Rho, rac, and cdc42 GTPases regulate the assembly of multimolecular focal complexes associated with actin stress fibers, lamellipodia, and filopodia. *Cell* 81, 53–62.
- Nobes, C.D., Hall, A., 1999. Rho GTPases control polarity, protrusion, and adhesion during cell movement. *J. Cell Biol.* 144, 1235–1244.
- Nonaka, H., Tanaka, K., Hirano, H., Fujiwara, T., Kohno, H., Umikawa, M., et al., 1995. A downstream target of RHO1 small GTP-binding protein is PKC1, a homolog of protein kinase C, which leads to activation of the MAP kinase cascade in *Saccharomyces cerevisiae*. *EMBO J.* 14, 5931–5938.
- Ohtsuka, T., Hata, Y., Ide, N., Yasuda, T., Inoue, E., Inoue, T., et al., 1999. nRap GEP: a novel neural GDP/GTP exchange protein for rap1 small G protein that interacts with synaptic scaffolding molecule (S-SCAM). *Biochem. Biophys. Res. Commun.* 265, 38–44.

- Okabe, S., Hirokawa, N., 1991. Actin dynamics in growth cones. *J. Neurosci.* 11, 1918–1929.
- Olofsson, B., 1999. Rho guanine dissociation inhibitors: pivotal molecules in cellular signalling. *Cell. Signal.* 11, 545–554.
- Ooshio, T., Irie, K., Morimoto, K., Fukuhara, A., Imai, T., Takai, Y., 2004. Involvement of LMO7 in the association of two cell–cell adhesion molecules, nectin and E-cadherin, through afadin and alpha-actinin in epithelial cells. *J. Biol. Chem.* 279, 31365–31373.
- Ooshio, T., Kobayashi, R., Ikeda, W., Miyata, M., Fukumoto, Y., Matsuzawa, N., et al., 2010. Involvement of the interaction of afadin with ZO-1 in the formation of tight junctions in Madin–Darby canine kidney cells. *J. Biol. Chem.* 285, 5003–5012.
- Ozaki-Kuroda, K., Nakanishi, H., Ohta, H., Tanaka, H., Kurihara, H., Mueller, S., et al., 2002. Nectin couples cell–cell adhesion and the actin scaffold at heterotypic testicular junctions. *Curr. Biol.* 12, 1145–1150.
- Paganini, S., Guidetti, G.F., Catricala, S., Trionfini, P., Panelli, S., Balduini, C., et al., 2006. Identification and biochemical characterization of Rap2C, a new member of the Rap family of small GTP-binding proteins. *Biochimie* 88, 285–295.
- Pelham Jr., R.J., Wang, Y., 1997. Cell locomotion and focal adhesions are regulated by substrate flexibility. *Proc. Natl. Acad. Sci. USA* 94, 13661–13665.
- Petrie, R.J., Doyle, A.D., Yamada, K.M., 2009. Random versus directionally persistent cell migration. *Nat. Rev. Mol. Cell Biol.* 10, 538–549.
- Pizon, V., Chardin, P., Lerosey, I., Olofsson, B., Tavitian, A., 1988. Human cDNAs rap1 and rap2 homologous to the *Drosophila* gene Dras3 encode proteins closely related to ras in the 'effector' region. *Oncogene* 3, 201–204.
- Pokutta, S., Drees, F., Takai, Y., Nelson, W.J., Weis, W.I., 2002. Biochemical and structural definition of the l-afadin- and actin-binding sites of alpha-catenin. *J. Biol. Chem.* 277, 18868–18874.
- Polakis, P.G., Rubinfeld, B., Evans, T., McCormick, F., 1991. Purification of a plasma membrane-associated GTPase-activating protein specific for rap1/Krev-1 from HL60 cells. *Proc. Natl. Acad. Sci. USA* 88, 239–243.
- Pollard, T.D., Borisy, G.G., 2003. Cellular motility driven by assembly and disassembly of actin filaments. *Cell* 112, 453–465.
- Ponti, A., Machacek, M., Gupton, S.L., Waterman-Storer, C.M., Danuser, G., 2004. Two distinct actin networks drive the protrusion of migrating cells. *Science* 305, 1782–1786.
- Porter, J.C., Hogg, N., 1997. Integrin cross talk: activation of lymphocyte function-associated antigen-1 on human T cells alters alpha4beta1- and alpha5beta1-mediated function. *J. Cell Biol.* 138, 1437–1447.
- Radziwill, G., Erdmann, R.A., Margelisch, U., Moelling, K., 2003. The Bcr kinase down-regulates Ras signaling by phosphorylating AF-6 and binding to its PDZ domain. *Mol. Cell Biol.* 23, 4663–4672.
- Radziwill, G., Weiss, A., Heinrich, J., Baumgartner, M., Boisguerin, P., Owada, K., et al., 2007. Regulation of c-Rac by binding to the PDZ domain of AF-6. *EMBO J.* 26, 2633–2644.
- Raftopoulos, M., Hall, A., 2004. Cell migration: rho GTPases lead the way. *Dev. Biol.* 265, 23–32.
- Reymond, N., Fabre, S., Lecocq, E., Adelaide, J., Dubreuil, P., Lopez, M., 2001. Nectin4/PRR4, a new afadin-associated member of the nectin family that *trans*-interacts with nectin1/PRR1 through V domain interaction. *J. Biol. Chem.* 276, 43205–43215.
- Ridley, A.J., Hall, A., 1992. The small GTP-binding protein rho regulates the assembly of focal adhesions and actin stress fibers in response to growth factors. *Cell* 70, 389–399.
- Ridley, A.J., Paterson, H.F., Johnston, C.L., Diekmann, D., Hall, A., 1992. The small GTP-binding protein rac regulates growth factor-induced membrane ruffling. *Cell* 70, 401–410.

- Ridley, A.J., Schwartz, M.A., Burridge, K., Firtel, R.A., Ginsberg, M.H., Borisy, G., et al., 2003. Cell migration: integrating signals from front to back. *Science* 302, 1704–1709.
- Rikitake, Y., Takai, Y., 2008. Interactions of the cell adhesion molecule nectin with transmembrane and peripheral membrane proteins for pleiotropic functions. *Cell. Mol. Life Sci.* 65, 253–263.
- Rottner, K., Hall, A., Small, J.V., 1999. Interplay between Rac and Rho in the control of substrate contact dynamics. *Curr. Biol.* 9, 640–648.
- Sanchez-Madrid, F., del Pozo, M.A., 1999. Leukocyte polarization in cell migration and immune interactions. *EMBO J.* 18, 501–511.
- Sander, E.E., ten Klooster, J.P., van Delft, S., van der Kammen, R.A., Collard, J.G., 1999. Rac downregulates Rho activity: reciprocal balance between both GTPases determines cellular morphology and migratory behavior. *J. Cell Biol.* 147, 1009–1022.
- Sasaki, T., Takai, Y., 1998. The Rho small G protein family-Rho GDI system as a temporal and spatial determinant for cytoskeletal control. *Biochem. Biophys. Res. Commun.* 245, 641–645.
- Sato, T., Irie, K., Okamoto, R., Ooshio, T., Fujita, N., Takai, Y., 2005. Common signaling pathway is used by the *trans*-interaction of Nectin-5/Tage4/PVR/CD155 and nectin, and of nectin and nectin during the formation of cell–cell adhesion. *Cancer Sci.* 96, 578–589.
- Schneller, M., Vuori, K., Ruoslahti, E., 1997.  $\alpha$ v $\beta$ 3 integrin associates with activated insulin and PDGF $\beta$  receptors and potentiates the biological activity of PDGF. *EMBO J.* 16, 5600–5607.
- Schoenwaelder, S.M., Burridge, K., 1999. Bidirectional signaling between the cytoskeleton and integrins. *Curr. Opin. Cell Biol.* 11, 274–286.
- Schwartz, M.A., Horwitz, A.R., 2006. Integrating adhesion, protrusion, and contraction during cell migration. *Cell* 125, 1223–1225.
- Scita, G., Confalonieri, S., Lappalainen, P., Suetsugu, S., 2008. IRSp53: crossing the road of membrane and actin dynamics in the formation of membrane protrusions. *Trends Cell Biol.* 18, 52–60.
- Seth, S., Maier, M.K., Qiu, Q., Ravens, I., Kremmer, E., Forster, R., et al., 2007. The murine pan T cell marker CD96 is an adhesion receptor for CD155 and nectin-1. *Biochem. Biophys. Res. Commun.* 364, 959–965.
- Sherer, N.M., Lehmann, M.J., Jimenez-Soto, L.F., Horensavitz, C., Pypaert, M., Mothes, W., 2007. Retroviruses can establish filopodial bridges for efficient cell-to-cell transmission. *Nat. Cell Biol.* 9, 310–315.
- Shibuya, A., Campbell, D., Hannum, C., Yssel, H., Franz-Bacon, K., McClanahan, T., et al., 1996. DNAM-1, a novel adhesion molecule involved in the cytolytic function of T lymphocytes. *Immunity* 4, 573–581.
- Shimonaka, M., Katagiri, K., Nakayama, T., Fujita, N., Tsuruo, T., Yoshie, O., et al., 2003. Rap1 translates chemokine signals to integrin activation, cell polarization, and motility across vascular endothelium under flow. *J. Cell Biol.* 161, 417–427.
- Shingai, T., Ikeda, W., Kakunaga, S., Morimoto, K., Takekuni, K., Itoh, S., et al., 2003. Implications of nectin-like molecule-2/IGSF4/RA175/SgIGSF/TSLC1/SynCAM1 in cell–cell adhesion and transmembrane protein localization in epithelial cells. *J. Biol. Chem.* 278, 35421–35427.
- Singer, A.J., Clark, R.A., 1999. Cutaneous wound healing. *N. Engl. J. Med.* 341, 738–746.
- Shinjo, K., Koland, J.G., Hart, M.J., Narasimhan, V., Johnson, D.I., Evans, T., et al., 1990. Molecular cloning of the gene for the human placental GTP-binding protein Gp (G25K): identification of this GTP-binding protein as the human homolog of the yeast cell-division-cycle protein CDC42. *Proc Natl Acad Sci USA* 87, 9853–9857.
- Sloan, K.E., Eustace, B.K., Stewart, J.K., Zehetmeier, C., Torella, C., Simeone, M., et al., 2004. CD155/PVR plays a key role in cell motility during tumor cell invasion and migration. *BMC Cancer* 4, 73.

- Sloat, B.F., Pringle J.R., 1978. A mutant of yeast defective in cellular morphogenesis. *Science*. 200, 1171–1173.
- Sloat, B.F., Adams, A., Pringle, J.R., 1981. Roles of the CDC24 gene product in cellular morphogenesis during the *Saccharomyces cerevisiae* cell cycle. *J Cell Biol.* 89, 395–405.
- Small, J.V., Rottner, K., Kaverina, I., Anderson, K.I., 1998. Assembling an actin cytoskeleton for cell attachment and movement. *Biochim. Biophys. Acta* 1404, 271–281.
- Small, J.V., Stradal, T., Vignat, E., Rottner, K., 2002. The lamellipodium: where motility begins. *Trends Cell Biol.* 12, 112–120.
- Soldi, R., Mitola, S., Strasly, M., Defilippi, P., Tarone, G., Bussolino, F., 1999. Role of alphavbeta3 integrin in the activation of vascular endothelial growth factor receptor-2. *EMBO J.* 18, 882–892.
- Sozen, M.A., Suzuki, K., Tolarova, M.M., Bustos, T., Fernandez Iglesias, J.E., Spritz, R.A., 2001. Mutation of PVRL1 is associated with sporadic, non-syndromic cleft lip/palate in northern Venezuela. *Nat. Genet.* 29, 141–142.
- Stanietsky, N., Simic, H., Arapovic, J., Toporik, A., Levy, O., Novik, A., et al., 2009. The interaction of TIGIT with PVR and PVRL2 inhibits human NK cell cytotoxicity. *Proc. Natl. Acad. Sci. USA* 106, 17858–17863.
- Steffen, A., Faix, J., Resch, G.P., Linkner, J., Wehland, J., Small, J.V., et al., 2006. Filopodia formation in the absence of functional WAVE- and Arp2/3-complexes. *Mol. Biol. Cell* 17, 2581–2591.
- Su, L., Hattori, M., Moriyama, M., Murata, N., Harazaki, M., Kaibuchi, K., et al., 2003. AF-6 controls integrin-mediated cell adhesion by regulating Rap1 activation through the specific recruitment of Rap1GTP and SPA-1. *J. Biol. Chem.* 278, 15232–15238.
- Suetsugu, S., Miki, H., Takenawa, T., 1999. Identification of two human WAVE/SCAR homologues as general actin regulatory molecules which associate with the Arp2/3 complex. *Biochem. Biophys. Res. Commun.* 260, 296–302.
- Suetsugu, S., Yamazaki, D., Kurisu, S., Takenawa, T., 2003. Differential roles of WAVE1 and WAVE2 in dorsal and peripheral ruffle formation for fibroblast cell migration. *Dev. Cell* 5, 595–609.
- Suzuki, K., Bustos, T., Spritz, R.A., 1998. Linkage disequilibrium mapping of the gene for Margarita Island ectodermal dysplasia (ED4) to 11q23. *Am. J. Hum. Genet.* 63, 1102–1107.
- Suzuki, K., Hu, D., Bustos, T., Zlotogora, J., Richieri-Costa, A., Helms, J.A., et al., 2000. Mutations of PVRL1, encoding a cell–cell adhesion molecule/herpesvirus receptor, in cleft lip/palate-ectodermal dysplasia. *Nat. Genet.* 25, 427–430.
- Svitkina, T.M., Borisy, G.G., 1999. Arp2/3 complex and actin depolymerizing factor/cofilin in dendritic organization and treadmilling of actin filament array in lamellipodia. *J. Cell Biol.* 145, 1009–1026.
- Svitkina, T.M., Verkhovsky, A.B., McQuade, K.M., Borisy, G.G., 1997. Analysis of the actin–myosin II system in fish epidermal keratocytes: mechanism of cell body translocation. *J. Cell Biol.* 139, 397–415.
- Svitkina, T.M., Bulanova, E.A., Chaga, O.Y., Vignjevic, D.M., Kojima, S., Vasiliev, J.M., et al., 2003. Mechanism of filopodia initiation by reorganization of a dendritic network. *J. Cell Biol.* 160, 409–421.
- Tachibana, K., Nakanishi, H., Mandai, K., Ozaki, K., Ikeda, W., Yamamoto, Y., et al., 2000. Two cell adhesion molecules, nectin and cadherin, interact through their cytoplasmic domain-associated proteins. *J. Cell Biol.* 150, 1161–1176.
- Tahara-Hanaoka, S., Shibuya, K., Onoda, Y., Zhang, H., Yamazaki, S., Miyamoto, A., et al., 2004. Functional characterization of DNAM-1 (CD226) interaction with its ligands PVR (CD155) and nectin-2 (PRR-2/CD112). *Int. Immunol.* 16, 533–538.



- Tahara-Hanaoka, S., Shibuya, K., Kai, H., Miyamoto, A., Morikawa, Y., Ohkochi, N., et al., 2006. Tumor rejection by the poliovirus receptor family ligands of the DNAM-1 (CD226) receptor. *Blood* 107, 1491–1496.
- Takahashi, K., Nakanishi, H., Miyahara, M., Mandai, K., Satoh, K., Satoh, A., et al., 1999. Nectin/PRR: an immunoglobulin-like cell adhesion molecule recruited to cadherin-based adherens junctions through interaction with Afadin, a PDZ domain-containing protein. *J. Cell Biol.* 145, 539–549.
- Takahashi, M., Rikitake, Y., Nagamatsu, Y., Hara, T., Ikeda, W., Hirata, K., et al., 2008. Sequential activation of Rap1 and Rac1 small G proteins by PDGF locally at leading edges of NIH3T3 cells. *Genes Cells* 13, 549–569.
- Takai, Y., Nakanishi, H., 2003. Nectin and afadin: novel organizers of intercellular junctions. *J. Cell Sci.* 116, 17–27.
- Takai, Y., Kaibuchi, K., Kikuchi, A., Sasaki, T., Shirataki, H., 1993. Regulators of small GTPases. *Ciba Found Symp* 176, 128–138 [Discussion: 138–146].
- Takai, Y., Sasaki, T., Matozaki, T., 2001. Small GTP-binding proteins. *Physiol. Rev.* 81, 153–208.
- Takai, Y., Ikeda, W., Ogita, H., Rikitake, Y., 2008a. The immunoglobulin-like cell adhesion molecule nectin and its associated protein afadin. *Annu. Rev. Cell Dev. Biol.* 24, 309–342.
- Takai, Y., Miyoshi, J., Ikeda, W., Ogita, H., 2008b. Nectins and nectin-like molecules: roles in contact inhibition of cell movement and proliferation. *Nat. Rev. Mol. Cell Biol.* 9, 603–615.
- Takaishi, K., Kikuchi, A., Kuroda, S., Kotani, K., Sasaki, T., Takai, Y., 1993. Involvement of rho p21 and its inhibitory GDP/GTP exchange protein (rho GDI) in cell motility. *Mol. Cell Biol.* 13, 72–79.
- Takenawa, T., Miki, H., 2001. WASP and WAVE family proteins: key molecules for rapid rearrangement of cortical actin filaments and cell movement. *J. Cell Sci.* 114, 1801–1809.
- Takenawa, T., Suetsugu, S., 2007. The WASP-WAVE protein network: connecting the membrane to the cytoskeleton. *Nat. Rev. Mol. Cell Biol.* 8, 37–48.
- Tawa, H., Rikitake, Y., Takahashi, M., Amano, H., Miyata, M., Satomi-Kobayashi, S., et al., 2010. Role of afadin in vascular endothelial growth factor- and sphingosine 1-phosphate-induced angiogenesis. *Circ. Res.* 106, 1731–1742.
- Taya, S., Yamamoto, T., Kano, K., Kawano, Y., Iwamatsu, A., Tsuchiya, T., et al., 1998. The Ras target AF-6 is a substrate of the fam deubiquitinating enzyme. *J. Cell Biol.* 142, 1053–1062.
- Trusolino, L., Bertotti, A., Comoglio, P.M., 2001. A signaling adapter function for alpha6-beta4 integrin in the control of HGF-dependent invasive growth. *Cell* 107, 643–654.
- Vignjevic, D., Yarar, D., Welch, M.D., Peloquin, J., Svitkina, T., Borisy, G.G., 2003. Formation of filopodia-like bundles in vitro from a dendritic network. *J. Cell Biol.* 160, 951–962.
- Volberg, T., Geiger, B., Citi, S., Bershadsky, A.D., 1994. Effect of protein kinase inhibitor H-7 on the contractility, integrity, and membrane anchorage of the microfilament system. *Cell Motil. Cytoskeleton* 29, 321–338.
- Wang, P.L., O'Farrell, S., Clayberger, C., Krensky, A.M., 1992. Identification and molecular cloning of tactile. A novel human T cell activation antigen that is a member of the Ig gene superfamily. *J. Immunol.* 148, 2600–2608.
- Watanabe, N., Kato, T., Fujita, A., Ishizaki, T., Narumiya, S., 1999. Cooperation between mDia1 and ROCK in Rho-induced actin reorganization. *Nat. Cell Biol.* 1, 136–143.
- Webb, D.J., Parsons, J.T., Horwitz, A.F., 2002. Adhesion assembly, disassembly and turnover in migrating cells—over and over and over again. *Nat. Cell Biol.* 4, E97–E100.

- Wildenberg, G.A., Dohn, M.R., Carnahan, R.H., Davis, M.A., Lobdell, N.A., Settlemann, J., et al., 2006. p120-catenin and p190RhoGAP regulate cell–cell adhesion by coordinating antagonism between Rac and Rho. *Cell* 127, 1027–1039.
- Witkowski, J.A., Brighton, W.D., 1971. Stages of spreading of human diploid cells on glass surfaces. *Exp. Cell Res.* 68, 372–380.
- Wittmann, T., Waterman-Storer, C.M., 2001. Cell motility: can Rho GTPases and microtubules point the way? *J. Cell Sci.* 114, 3795–3803.
- Wood, W., Martin, P., 2002. Structures in focus—filopodia. *Int. J. Biochem. Cell Biol.* 34, 726–730.
- Woodard, A.S., Garcia-Cardena, G., Leong, M., Madri, J.A., Sessa, W.C., Languino, L.R., 1998. The synergistic activity of alphavbeta3 integrin and PDGF receptor increases cell migration. *J. Cell Sci.* 111, 469–478.
- Worthylake, R.A., Lemoine, S., Watson, J.M., Burrige, K., 2001. RhoA is required for monocyte tail retraction during transendothelial migration. *J. Cell Biol.* 154, 147–160.
- Yajnik, V., Paulding, C., Sordella, R., McClatchey, A.I., Saito, M., Wahrer, D.C., et al., 2003. DOCK4, a GTPase activator, is disrupted during tumorigenesis. *Cell* 112, 673–684.
- Yamada, K.M., Geiger, B., 1997. Molecular interactions in cell adhesion complexes. *Curr. Opin. Cell Biol.* 9, 76–85.
- Yamaguchi, H., Wyckoff, J., Condeelis, J., 2005. Cell migration in tumors. *Curr. Opin. Cell Biol.* 17, 559–564.
- Yamamoto, M., Marui, N., Sakai, T., Morii, N., Kozaki, S., Ikai, K., et al., 1993. ADP-ribosylation of the rhoA gene product by botulinum C3 exoenzyme causes Swiss 3T3 cells to accumulate in the G1 phase of the cell cycle. *Oncogene* 8, 1449–1455.
- Yamamoto, T., Harada, N., Kano, K., Taya, S., Canaani, E., Matsuura, Y., et al., 1997. The Ras target AF-6 interacts with ZO-1 and serves as a peripheral component of tight junctions in epithelial cells. *J. Cell Biol.* 139, 785–795.
- Yoneda, A., Multhaupt, H.A., Couchman, J.R., 2005. The Rho kinases I and II regulate different aspects of myosin II activity. *J. Cell Biol.* 170, 443–453.
- Yu, X., Harden, K., Gonzalez, L.C., Francesco, M., Chiang, E., Irving, B., et al., 2009. The surface protein TIGIT suppresses T cell activation by promoting the generation of mature immunoregulatory dendritic cells. *Nat. Immunol.* 10, 48–57.
- Zaidel-Bar, R., Ballestrem, C., Kam, Z., Geiger, B., 2003. Early molecular events in the assembly of matrix adhesions at the leading edge of migrating cells. *J. Cell Sci.* 116, 4605–4613.
- Zaidel-Bar, R., Cohen, M., Addadi, L., Geiger, B., 2004. Hierarchical assembly of cell–matrix adhesion complexes. *Biochem. Soc. Trans.* 32, 416–420.
- Zamir, E., Geiger, B., 2001. Molecular complexity and dynamics of cell–matrix adhesions. *J. Cell Sci.* 114, 3583–3590.
- Zamir, E., Katz, M., Posen, Y., Erez, N., Yamada, K.M., Katz, B.Z., et al., 2000. Dynamics and segregation of cell–matrix adhesions in cultured fibroblasts. *Nat. Cell Biol.* 2, 191–196.
- Zhadanov, A.B., Provance Jr., D.W., Speer, C.A., Coffin, J.D., Goss, D., Blixt, J.A., et al., 1999. Absence of the tight junctional protein AF-6 disrupts epithelial cell–cell junctions and cell polarity during mouse development. *Curr. Biol.* 9, 880–888.
- Zigmond, S.H., 2004. Formin-induced nucleation of actin filaments. *Curr. Opin. Cell Biol.* 16, 99–105.

This page intentionally left blank

# MITOCHONDRIAL RNA IMPORT: FROM DIVERSITY OF NATURAL MECHANISMS TO POTENTIAL APPLICATIONS

François Sieber, Anne-Marie Duchêne, and  
Laurence Maréchal-Drouard

## Contents

|                                                                                                            |     |
|------------------------------------------------------------------------------------------------------------|-----|
| 1. Introduction                                                                                            | 146 |
| 2. RNA Import in Protozoa                                                                                  | 149 |
| 2.1. Imported tRNAs                                                                                        | 149 |
| 2.2. Selectivity and extent of the process                                                                 | 150 |
| 2.3. Mechanism of tRNA import                                                                              | 152 |
| 3. RNA Import in Plants                                                                                    | 156 |
| 3.1. How is the imported tRNA population determined in plant mitochondria?                                 | 156 |
| 3.2. Evolutionary aspects and mitochondrial translation                                                    | 157 |
| 3.3. Mechanism of tRNA import                                                                              | 158 |
| 4. RNA Import in Fungi                                                                                     | 161 |
| 4.1. Imported tRNA species in <i>S. cerevisiae</i> mitochondria                                            | 162 |
| 4.2. Import of the nuclear-encoded tRNA <sup>Lys</sup> (CUU), tRK1, into <i>S. cerevisiae</i> mitochondria | 162 |
| 5. RNA Import in Metazoa                                                                                   | 166 |
| 5.1. Import of tRNAs                                                                                       | 166 |
| 5.2. Import of 5S rRNA into mammalian mitochondria                                                         | 166 |
| 5.3. Import of the RNA components of RNase MRP and RNase P into human mitochondria                         | 170 |
| 5.4. miRNA import in mammalian mitochondria                                                                | 172 |
| 6. Potential Applications of Macromolecule Import                                                          | 173 |
| 6.1. Protein import                                                                                        | 173 |
| 6.2. DNA import                                                                                            | 176 |
| 6.3. RNA import                                                                                            | 179 |
| 7. Conclusion and Prospects                                                                                | 181 |
| References                                                                                                 | 182 |

Institut de Biologie Moléculaire des Plantes, UPR 2357-CNRS, Université de Strasbourg, Strasbourg, France

*International Review of Cell and Molecular Biology*, Volume 287

ISSN 1937-6448, DOI: 10.1016/B978-0-12-386043-9.00004-9

© 2011 Elsevier Inc.

All rights reserved.

## Abstract

Mitochondria, owing to their bacterial origin, still contain their own DNA. However, the majority of bacterial genes were lost or transferred to the nuclear genome and the biogenesis of the “present-day” mitochondria mainly depends on the expression of the nuclear genome. Thus, most mitochondrial proteins and a small number of mitochondrial RNAs (mostly tRNAs) expressed from nuclear genes need to be imported into the organelle. During evolution, macromolecule import systems were universally established. The processes of protein mitochondrial import are very well described in the literature. By contrast, deciphering the mitochondrial RNA import phenomenon is still a real challenge. The purpose of this review is to present a general survey of our present knowledge in this field in different model organisms, protozoa, plants, yeast, and mammals. Questions still under debate and major challenges are discussed. Mitochondria are involved in numerous human diseases. The targeting of macromolecule to mitochondria represents a promising way to fight mitochondrial disorders and recent developments in this area of research are presented.

**Key Words:** Mitochondrial RNA import, Transfer RNA, Macromolecule import, Gene therapy, Mitochondrial genetic manipulation. © 2011 Elsevier Inc.

## 1. INTRODUCTION

Mitochondria are organelles found in nearly all eukaryotes. They originate from the endosymbiosis of  $\alpha$ -proteobacteria into ancestral proto-eukaryotes. Classical mitochondria have retained a vestige of the genome of the ancestral bacteria. This genome is now highly reduced in size and gene content. Consequently, not only most mitochondrial proteins but also numerous tRNAs have to be imported from the cytosol to mitochondria. Mitochondria are considered as the energetic center of the cell, generating ATP by oxidative phosphorylation, but they are involved in many more biological processes. In a nonexhaustive manner, they play a crucial role in cellular processes such as lipid or amino acid metabolism, FeS clusters biogenesis, calcium homeostasis, and apoptosis. It is worth noting that a few microbial eukaryotes living under anaerobic conditions do not contain classical mitochondria, rather they possess mitochondria-like organelles called hydrogenosomes. Hydrogenosomes produce ATP by fermentation of acetate and do not usually contain a genome (Boxma et al., 2005). A few other anaerobic or microaerophilic organisms contain another type of mitochondria-like organelles called mitosomes. Mitosomes do not contain DNA and do not produce ATP, their only known function being the synthesis of FeS clusters (Goldberg et al., 2008). Biogenesis of these organelles mainly (for mitochondria) or totally relies (for hydrogenosomes and mitosomes) on the expression of the nuclear genome. While

mitochondrial protein import occurs in all types of mitochondria, it is not known if an RNA import process exists in hydrogenosomes or mitosomes.

The establishment of mitochondrial protein import system must have occurred very rapidly after the acquisition of the “proto-mitochondria” and very likely has a common ancestral origin among eukaryotic cells. Mitochondrial protein import has been mainly studied in the yeast *Saccharomyces cerevisiae* (Chacinska et al., 2009; Neupert and Herrmann, 2007; Schmidt et al., 2010). Several recent and excellent reviews described the refined mechanisms required to import proteins into mitochondria in various evolutionary divergent organisms (Lithgow and Schneider, 2010).

While most mitochondrial proteins are nuclear-encoded, a few remaining proteins encoded by mitochondrial genomes are essential and a mitochondrial translation machinery is required for their expression. Depending on the genetic code and on the wobble rules, in many mitochondrial genomes, the number of tRNA genes is insufficient for proper protein synthesis to occur, and the import of nuclear-encoded tRNAs has been shown to compensate this lack. Based on both predictions from *in silico* bioinformatic analysis of complete mitochondrial genome sequences and on experimental proofs, the import of tRNA molecules into mitochondria, first thought to be restricted to a few eukaryotes, is in reality a widespread phenomenon. Since its discovery in *Tetrahymena pyriformis* about 40 years ago (Suyama, 1967), mitochondrial tRNA import is now considered as an essential process of mitochondrial biogenesis and is likely occurring in all eukaryotic kingdoms (Lithgow and Schneider, 2010; Salinas et al., 2008; Schneider and Maréchal-Drouard, 2000). If we look at the phylogenetic distribution of tRNA import, it is clear that even among closely related species, some contain a full set of mitochondrial tRNA genes whereas others have lost part or all of them. The ancestral bacterial genome at the origin of mitochondria had a complete set of tRNA genes. As loss of mitochondrial tRNA genes is very likely irreversible, tRNA import must have occurred independently several times in the course of evolution. On a mechanistic point of view, this observation has an obvious repercussion: although we cannot exclude that the ancestral proto-mitochondria had the innate ability to import nucleic acids and that common core components of tRNA import machinery do exist, it is likely that independent molecular mechanisms have been invented several times during the evolution of eukaryotes. Transfer RNA molecules represent large and negatively charged macromolecules. Characterizing these mechanisms implies to answer several major questions (Fig. 4.1): Where and how is the selectivity of the import process accomplished? What are the protein factors involved in tRNA targeting to the surface of mitochondria? What are the components of the tRNA import channels? What are the forces that drive them against the electrochemical gradient generated at the level of the inner mitochondrial membrane? Is the process regulated and how?

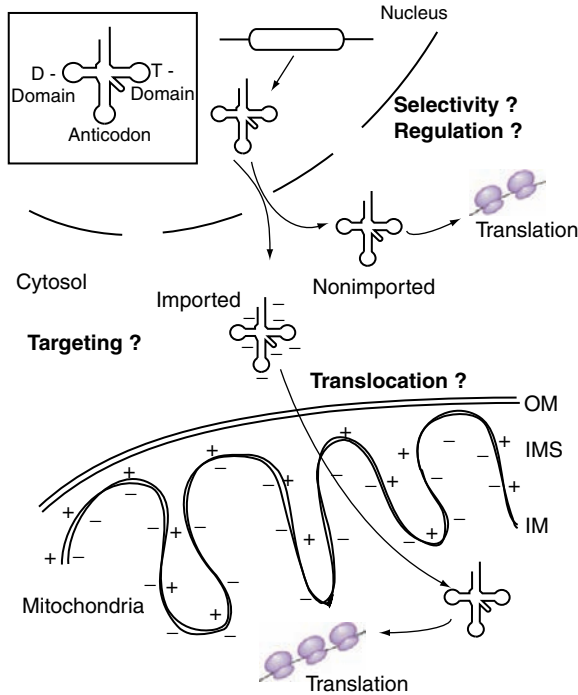


**Figure 4.1** Overview of the fundamental questions of RNA mitochondrial import. Transfer RNA is a very large (25 kDa) negatively charged macromolecule. To understand how some nuclear-encoded tRNAs can enter the mitochondria, we need to address several questions. The major ones are the following: How tRNAs are targeted from the nucleus to the mitochondrial surface? How are they translocated, against the mitochondrial electrochemical gradient, through the double mitochondrial membranes? What is the basis of the selectivity and is the process regulated? In the box (upper left), the different regions of the secondary structure of a tRNA are written.

Finally, in addition to tRNAs, a few other cytosolic RNAs were found in mammalian mitochondria. The most studied one is the human 5S rRNA, but the RNA components of the RNase P or of the RNase MRP as well as some microRNAs (miRNAs) were also found into mammalian organelles. Our present knowledge on their mitochondrial import will also be discussed. In all cases, only structural RNA and no nuclear-encoded mRNA were found in mitochondria yet.

Here, we first present the major developments obtained during the past decade on RNA mitochondrial import in four model organisms: protozoa, plants, yeast, and mammals. Then, in the last part, we focus on the potential applications that we can expect to exploit from our present knowledge not only of RNA but also of protein and DNA mitochondrial import.

## 2. RNA IMPORT IN PROTOZOA

As emphasized in the introduction, it is presently impossible to have a very precise view of the phylogenetic distribution of tRNA mitochondrial import. Experimental proofs have been obtained only for few organisms, and bioinformatic analysis, although of invaluable interest, has its own limits. Nevertheless, the process of tRNA mitochondrial import is much more widespread than previously thought and the protozoan world nicely reflects the importance of this process in the mitochondrial biogenesis. The delivery of cytosolic tRNAs into mitochondria has been first discovered in *T. pyriformis* in 1967 (Suyama, 1967). Since then, several protozoans were used as model organisms to study the tRNA import mechanism. So far, no RNAs other than tRNAs were shown to be imported into protozoan mitochondria. The major outcomes of these studies are presented below.

### 2.1. Imported tRNAs

Based on bioinformatic prediction on complete mitochondrial genome sequences, import of nuclear-encoded tRNAs into mitochondria is likely to occur in most, if not all protozoans (Lithgow and Schneider, 2010). However, according to the very different number of tRNA genes found on the mitochondrial genomes, we can easily speculate that the number and the identity of tRNAs imported into mitochondria greatly vary from one protozoan to the other. In *Reclinomonas americana*, a freshwater protozoa, 26 tRNA genes are encoded by the mitochondrial genome and only one tRNA gene, a *trnT* gene, is apparently missing. The mitochondrial genome of this protist is one of the closest representatives of the ancestral proto-mitochondrial genome. Although a compensation via tRNA import has not been experimentally demonstrated yet, if it is the case, it suggests that the possibility for mitochondria to acquire foreign cytosolic tRNAs has been possible soon during evolution. In *T. pyriformis*, only seven mitochondrial genes encode a tRNA and it has been shown using several approaches (northern hybridization, two-dimensional gel electrophoresis) that at least 15 nuclear-encoded tRNAs are imported into mitochondria of this organism (Chiu et al., 1975; Suyama, 1986). The most extreme situation is found in kinetoplastid protozoa such as *Trypanosoma brucei* and *Leishmania* species or in apicomplexa such as *Toxoplasma gondii* where there is a complete lack of tRNA genes in the mitochondrial genome (Esseiva, 2004). Consequently, all tRNAs needed for mitochondrial translation have to be imported into the organelle. Indeed, it has been proven that at least 14 and 17 cytosolic tRNA species are imported into *T. brucei* and *Leishmania tarentolae* mitochondria, respectively (Kapushoc et al., 2002; Tan et al., 2002a).



## 2.2. Selectivity and extent of the process

It must be stressed out that not all cytosolic tRNAs are found in mitochondria of these organisms, implying that the process is highly specific (Fig. 4.2). For example, neither the nuclear-encoded selenocysteine tRNA (tRNA<sup>Sec</sup>) nor the initiator tRNA<sup>Meti</sup> are present in *T. brucei* mitochondria (Bouzaidi-Tiali et al., 2007), and only one out of three tRNA<sup>Gln</sup> isoacceptors is imported into *Tetrahymena thermophila* mitochondria (Rusconi and Cech, 1996b). Why do a few nuclear-encoded tRNAs remain cytosol specific? In most cases, the presence of a cytosolic tRNA inside a mitochondrion compensates the loss of an essential mitochondrial tRNA and there are two main reasons to explain why not all cytosolic tRNAs go into mitochondria. The first reason is that this tRNA is not required in the organelle. This is, for example, the case for the tRNA<sup>Sec</sup> as no selenoproteins are synthesized in *T. brucei* mitochondria. In the case of tRNA<sup>Meti</sup>, translation initiation is very different between eukaryotes and prokaryotes. In contrast to eukaryotic translation machinery, a formylated methionine tRNA is usually required in translation systems of bacterial origin. As most eukaryotic tRNA<sup>Meti</sup> cannot be formylated, they cannot be used to initiate mitochondrial translation and this tRNA is not addressed to the mitochondria. Quite surprisingly, it has been shown that the elongator tRNA<sup>Met-e</sup> only functions

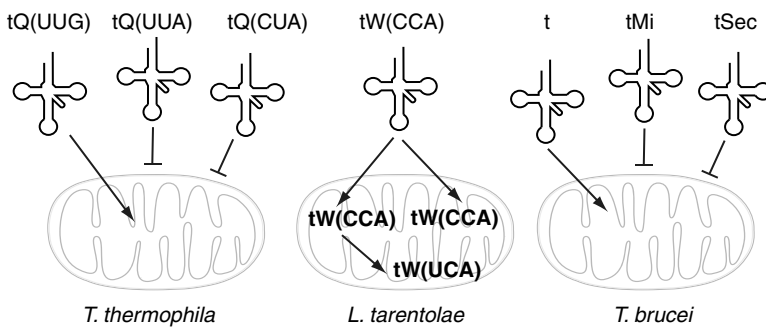


**Figure 4.2** Specificity of tRNA import into protozoan mitochondria. In *Tetrahymena thermophila*, only one out of three tRNA<sup>Gln</sup> (tQ) isoform is imported into mitochondria. The anticodon (UUG) is a major import determinant. In *Leishmania tarentolae*, only one tRNA<sup>Trp</sup> (tW) with a CCA anticodon is encoded by the nucleus and decode the classical UGG tryptophan codon used in nuclear genes. Once imported into mitochondria, the anticodon is partially edited into UCA, thus allowing the decoding of both UUG and UGA (normally a stop codon) as tryptophan in protozoan mitochondria. In *Trypanosoma brucei*, all elongator tRNAs (t) are imported into mitochondria, except the selenocysteine tRNA (tSec). The initiator methionine tRNA (tMi) is also not imported. Both tMi and tSec are not used by the mitochondrial translation machinery in this organism.

as an elongator in the cytosol but, once imported into *T. brucei* mitochondria, it can play a dual role in both elongation and initiation, thanks to its formylation by an unusual formyl-transferase in the organelle (Tan et al., 2002b). The second valuable reason why a tRNA is not entering the mitochondrion is that it can be deleterious for the organelle. The most striking example to illustrate this concerns the case of the tRNA<sup>Gln</sup> isoacceptors in *T. thermophila*. Three tRNA<sup>Gln</sup>, with anticodons UUA, CUA, and UUG, are expressed from nuclear genes. Each of these tRNAs functions in cytosolic translation due to the reassignment of the stop codon UAA and UAG to glutamine in the nucleus. In the mitochondrial genetic code, UAA and UAG are classical stop codons and only tRNA<sup>Gln</sup>(UUG) is imported into mitochondria and has the capacity to be used by the mitochondrial translation machinery while the two other tRNAs need to be excluded to avoid misincorporation of amino acids (Rusconi and Cech, 1996b).

Finally, another interesting situation comes from the import of the tRNA<sup>Trp</sup> in *L. tarentolae* mitochondria (Fig. 4.2). In *Leishmania* (as in many eukaryotes, except plants and a few protists), the mitochondrial genetic code deviates from the universal code in that the UGA stop codon is used as a tryptophan codon. Only one tRNA<sup>Trp</sup> with a CCA anticodon is expressed from the nuclear genome. This tRNA can decode the classical UGG tryptophan codon used in nuclear genes but cannot read the UGA tryptophan codon reassigned in the mitochondrial genome. Alfonzo et al. (1999) showed that, once imported into mitochondria, the nuclear-encoded tRNA<sup>Trp</sup> can be edited at the first position of the anticodon to generate a tRNA with a UCA anticodon then allowing the decoding of UGA codon as tryptophan in the organelle. The cytosolic tryptophanyl-tRNA synthetase can only aminoacylate the cytosolic nonedited tRNA<sup>Trp</sup>. To cope with the problem of the editing event, trypanosomatids mitochondria import a specific mitochondrial tryptophanyl-tRNA synthetase that, unlike its cytosolic counterpart, can recognize both the edited and nonedited version of tRNA<sup>Trp</sup> (Charriere et al., 2006). This represents a nice illustration of how the mitochondrial translation machinery had to adapt during evolution to allow the integration of functional eukaryotic-type cytosolic tRNAs in mitochondria.

The tRNA mitochondrial import process is selective, but is also regulated. Not only cytosolic tRNAs are present or not in mitochondria but the extent of mitochondrial localization also varies from one tRNA to the other. In *L. tarentolae*, preferential import of some tRNAs has been observed and tRNAs were classified into three groups: mainly cytosolic, mainly mitochondrial, and shared between the two compartments (Kapushoc et al., 2002; Shi et al., 1994). In another trypanosomatid, *T. brucei*, the extent of mitochondrial localization varies from 1% to 7.5% for the 15 nuclear-encoded tRNA species analyzed (Tan et al., 2002a). In both cases, the extent of mitochondrial localization is not correlated with the

abundance of tRNAs in the cytosol. It has been shown in several organisms that the tRNA population is adjusted to the codon usage (Duret, 2000), but at least in *T. brucei*, the abundance of imported tRNAs fails to correlate with the mitochondrial codon usage (Tan et al., 2002a). The reasons and the mechanisms why there is a differential extent of mitochondrial localization among imported tRNAs still need to be investigated. Is that at the level of the targeting and/or translocation steps or is there a different stability between the imported tRNA species within the mitochondria? In *T. brucei*, no significant differences in the kinetics of degradation of several tRNAs were observed (Tan et al., 2002a) and these questions remain presently open.

We can also wonder whether the steady-state level of the imported tRNAs is regulated during the cell life. *T. brucei* constitutes an interesting model to answer this question. During its life cycle, *T. brucei* alternates between two forms: the procyclic form during its insect stage and the bloodstream form in the mammalian host. Mitochondria of the procyclic form are highly active, whereas they are more reduced and less active in the bloodstream form of *T. brucei*. Quite surprisingly, the abundance of imported tRNAs is essentially the same, demonstrating that the tRNA import process is constitutive, at least between these two stages (Cristodero et al., 2010). In agreement with these data, we can mention that in another trypanosomatid, *Trypanosoma evansi*, tRNAs are imported although they are not required as there is no translation in the mitochondria of this organism. Again, this suggests that mitochondrial translation and tRNA import are not tightly coupled (Cristodero et al., 2010).

### 2.3. Mechanism of tRNA import

As compared to protein mitochondrial import, RNA mitochondrial import is still poorly understood and as recently stated by Alfonzo and Söll, “the challenge to understand has just begun” (Alfonzo and Söll, 2009). This is the case whatever the organism considered and this is particularly true in protozoa where controversial data exist. There are several reasons to explain the difficulties encountered by researchers working in this field. First, contrary to protein import, tRNA import is usually considered as a process having a polyphyletic origin and various import mechanisms are expected. Second, and most importantly, depending on the strategy used (i.e., *in vitro* vs. *in vivo*; biochemical vs. genetic approaches), the data obtained and their interpretation might be different. Two examples of controversial data are given below. While Scherrer et al. (2003) showed the importance of the 5' flanking sequence of a precursor tRNA<sup>Leu</sup> for its abundance into *T. brucei* mitochondria, the mitochondrial import of the same tRNA<sup>Leu</sup> was demonstrated to be independent of the genomic context in the same organism by Tan et al. (2002a). In another protozoan, *L. tarentolae*, the importance of the

D-arm for tRNA<sup>Tyr</sup> mitochondrial import was shown *in vitro* (Mahapatra et al., 1998) but no consensus sequence within the D-domain exists (Suyama et al., 1998), and this region cannot solely be responsible for tRNA mitochondrial import. Indeed, two types of tRNA classified according to distinct import motifs (D-arm or anticodon for type I and T-arm or variable loop for type II) were proposed by Bhattacharyya et al. (2002). Nevertheless, we will try to give below the best overview we can on the mechanistic aspect of tRNA import in protozoa.

Basically, tRNA import can be divided into two main steps: first, the targeting of tRNAs from the nucleus to the mitochondria and second, their translocation through the double mitochondrial membranes to reach the matrix side where mitochondrial translation occurs. At both levels, we can also expect to address the question of selectivity and/or regulation of the process.

In protozoa, there are two systems where the tRNA import signals have been studied in details. In *T. thermophila*, as described above, only one out of three tRNA<sup>Gln</sup> is imported into mitochondria. *In vivo* analysis (Fig. 4.2) showed that the UUG anticodon of the imported tRNA<sup>Gln</sup> (as compared to the two other cytosol-specific tRNA<sup>Gln</sup> with UUA and CUA anticodon, respectively) is essential and sufficient (Rusconi and Cech, 1996a). No import factor specifically interacting with tRNA<sup>Gln</sup>(UUG) has been found yet and the step (targeting and/or translocation) at which the selectivity occurs is not known. In *T. brucei*, only two tRNAs (tRNA<sup>Meti</sup> and tRNA<sup>Sec</sup>) are not imported into the organelle and remain in the cytosol. *In vivo* studies showed that the nature of the T-stem nucleotide pair 51:63 is essential for the determination of the localization of tRNAs in this organism (Fig. 4.3). While the U51:A63 pair found in tRNA<sup>Meti</sup> specifies its cytosolic localization, any other base pair at this position determines the mitochondrial localization of all the other elongator tRNAs (except the cytosol-specific tRNA<sup>Sec</sup>). Interestingly, the U51:A63 pair in tRNA<sup>Meti</sup> is the major antideterminant for elongation factor 1 $\alpha$  (eEF1 $\alpha$ ) binding and Bouzaidi-Tiali and colleagues demonstrated that, *in vivo*, eEF1 $\alpha$  binding is essential for tRNA targeting to the surface of mitochondria (Bouzaidi-Tiali et al., 2007). In addition to tRNA<sup>Meti</sup>, there is another tRNA, the tRNA<sup>Sec</sup>, that does not bind to eEF1 $\alpha$  and remains in the cytosol. In that case, this tRNA does not possess the U51:A63 pair responsible of the cytosolic localization, but rather contains another antideterminant, the U8-U66 base pair. Thus, in *T. brucei*, in addition to its classical role in translation elongation, eEF1 $\alpha$  plays a crucial role in targeting cytosolic tRNAs to the surface, an essential prerequisite prior to their translocation through the double mitochondrial membranes. This protein represents the first factor shown to be involved in the tRNA targeting step in a protozoa. Whether the same factor is used in other protozoa or is coupled to other protein factors involved in the specificity of the process will need to be addressed in the future.

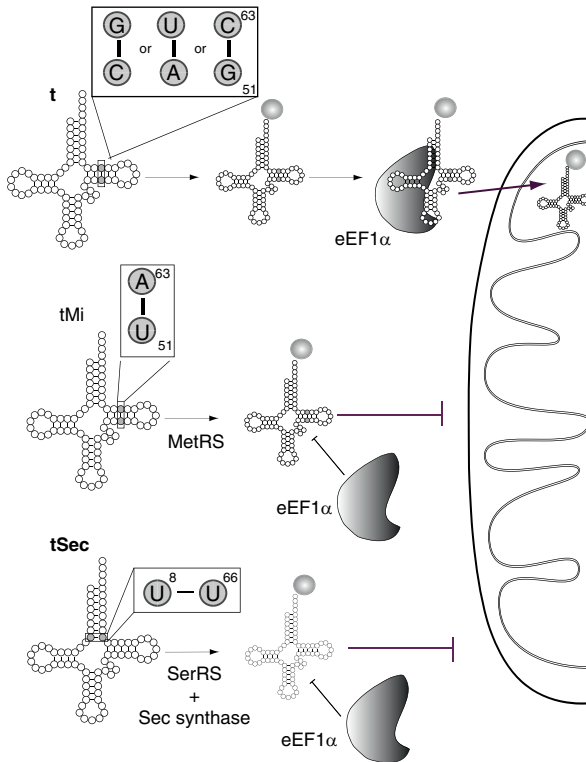


**Figure 4.3** A schematic model for the selectivity of tRNA targeting to the surface of *T. brucei* mitochondria. In *T. brucei*, the cytosolic elongation factor eEF1 $\alpha$  can bind all aminoacylated elongator tRNAs (t), thanks to the nature of the T-stem nucleotide pair 51:63 (C:G, A:U, or G:C), and target them towards the mitochondrial surface. Elongator tRNAs are subsequently transported into the organelle by a still unknown process. The aminoacylated initiator tRNA<sup>Met</sup> (tMi) that cannot bind to eEF1 $\alpha$  owing to the presence of the antideterminant U51-A63 base pair is not targeted to the mitochondrial surface and is therefore cytosol-specific. In a similar manner, tRNA<sup>Sec</sup> (tSec) cannot bind to eEF1 $\alpha$  owing to the presence of the antideterminant U8-U66 base pair and, as tMi, is thus not targeted to the mitochondrial surface.

We can also wonder whether tRNAs need to be aminoacylated to be imported. For example, the interaction between tRNAs and eEF1 $\alpha$  in *T. brucei* implies that tRNAs are charged before their import into the organelle. Also, in the apicomplexa, *T. gondii*, aminoacyl-tRNA synthetases are absent from mitochondria and cytosolic tRNAs are likely imported in their aminoacylated form (Pino et al., 2010). However, an unspliced nonaminoacylated version of a tRNA<sup>Tyr</sup> mutant is imported into *T. brucei* mitochondria, thus showing that aminoacylation can be uncoupled to tRNA mitochondrial import (Schneider et al., 1994).

Once a tRNA has been targeted to the surface of mitochondria, this hydrophilic polyanionic macromolecule of about 25 kDa must cross the outer and inner mitochondrial membranes against the electrochemical gradient generated at the level of the respiratory chain complexes. Thus, it is not surprising that, as mentioned in recent reviews, the tRNA import process is not a passive process but rather requires ATP in protozoa as well as in other organisms studied so far (Entelis et al., 2001b; Lithgow and Schneider, 2010; Salinas et al., 2008). Another common aspect is that, *in vitro*, tRNA import is sensitive to protease pretreatment of mitochondria, meaning that at least one protein receptor is required at the surface of the organelle. However, such receptor has not yet been identified in protozoa, although it has been looked for (Mahapatra and Adhya, 1996).

Up to now and contrary to the situation found for the import of yeast tRNA<sup>Lys</sup> (see below), protozoan cytosolic tRNAs seem imported *in vitro* through a pathway distinct to the protein import channel and without any added cytosolic protein as carrier (Nabholz et al., 1999; Rubio et al., 2000; Yermovsky-Kammerer and Hajduk, 1999). What are the components of the tRNA import apparatus in this case? The group of Adhya (Calcutta, India) has studied the tRNA import pathway in details in *Leishmania tropica*. A summary of its work already described elsewhere (Adhya, 2008; Duchêne et al., 2009; Lithgow and Schneider, 2010; Mirande, 2007) is presented below. However, the published data raise several questions, they are usually in contradiction with the data obtained by other groups working on protozoa and most importantly were recently the subject of an Editorial Expression of Concern by PNAS (Schekman, 2010). Adhya's group showed the presence of a multisubunit RNA Import Complex (called RIC) of about 600 kDa on the inner mitochondrial membrane of *L. tropica*. This complex, biochemically characterized, is composed of 11 subunits and 4 of these subunits are identical to subunits of the respiratory chain. On one hand, an RNA import activity in liposomes has been reconstituted with recombinant RIC subunits isolated from SDS gels and on the other hand, conditional ablation by antisense knockdown of each essential subunit seems to abolish tRNA import. Both approaches represent very difficult tasks (Lithgow and Schneider, 2010) and the RIC has never been identified in any other related organism. Strikingly, in *T. brucei*, a protozoa closely related to *Leishmania*, it was shown that (i) the knock down of the Rieske protein, an essential subunit of the RIC, does not lead to tRNA import inhibition (Paris et al., 2009) and (ii) in the bloodstream stage of the parasite, orthologues of three RIC subunits are not expressed but mitochondria still import tRNAs (Cristodero et al., 2010). Taken together, it is presently difficult to have a precise view of the tRNA mitochondrial import mechanism in protozoa and further biochemical and genetic data are needed to reveal the whole set of protein factors implicated in the process.

### 3. RNA IMPORT IN PLANTS

Up to now, RNA import into plant mitochondria is restricted to tRNAs. The three mitochondrial rRNAs are encoded by the mitochondrial genome. Some cytosolic mRNAs were shown to be targeted to the mitochondrial surface but none to be imported into mitochondria (Michaud et al., 2010). By contrast, one-third to one-half of the mitochondrial tRNAs is imported from the cytosol.

Three types of tRNAs are found in plant mitochondria. Two correspond to mitochondrial-encoded tRNAs. These are the “native” tRNAs originating from the ancestral bacterium at the origin of mitochondria and the chloroplast-like tRNAs whose genes come from the chloroplastic genome that were inserted into the mitochondrial DNA during evolution (Maréchal-Drouard et al., 1993). The last type of tRNAs corresponds to cytosolic tRNAs which are imported into mitochondria. The number of tRNAs of each type greatly varies from one plant species to another (e.g., Kumar et al., 1996), so extrapolation from one plant to the other should be performed with caution.

#### 3.1. How is the imported tRNA population determined in plant mitochondria?

A first approach to determine the imported tRNA population is to determine the whole mitochondrial tRNA pool. Transfer RNAs are first extracted from highly purified mitochondria and separated on a 2D-gel. Each spot is then determined by hybridization, aminoacylation, or RNA sequencing. This strategy was used to evaluate the potato and the wheat mitochondrial tRNA populations. In these two plants, respectively, 16 and 14 tRNA species were proven to be imported into mitochondria (Glover et al., 2001; Maréchal-Drouard et al., 1990a,b). However, it does not allow the detection of rare tRNAs. Moreover, it is not easy to differentiate low import from cytosolic contamination. Last, some tRNAs, such as tRNA<sup>Thr</sup> in wheat, can escape detection (Glover et al., 2001).

Knowledge on mitochondrial genome sequence and its expression is also a great tool to evaluate the imported tRNA population. As translation occurs in plant mitochondria and as the universal genetic code is used, a complete set of tRNAs is needed. When some *tm* genes are missing in the mitochondrial genome, it can be speculated that the corresponding nuclear-encoded tRNA is imported from the cytosol (e.g., Notsu et al., 2002; Sugiyama et al., 2005). But the presence of a gene does not mean the presence of its product. So a more accurate analysis is to look at the expression of mitochondrial *tm* genes. This has been performed in

*Arabidopsis thaliana* and has shown that the “chloroplast-like” *trnW* present on the mitochondrial genome is not expressed and tRNA<sup>Trp</sup> is imported from the cytosol into mitochondria (Duchêne and Maréchal-Drouard, 2001). Also, in sunflower mitochondria, the “native” *trnS*(GCT) is not expressed and all tRNA<sup>Ser</sup> isoacceptors present in the organelle are nuclear-encoded (Ceci et al., 1996). However, such an analysis only gives a minimal number of imported tRNAs.

A last approach is to systematically check the mitochondrial import status of every nuclear-encoded tRNA. This is only possible when the full set of nuclear tRNA genes is available. Since the first complete sequence of a plant genome, that of *A. thaliana* (Initiative, 2000), a number of other plant (and algal) genomes have been completely or almost completely sequenced, thus allowing such an analysis. A detailed study of the mitochondrial tRNA population was recently performed in the green alga *Chlamydomonas reinhardtii* by Northern blot (Vinogradova et al., 2009). Only three *trn* genes are found and expressed in the mitochondrial genome (Michaelis et al., 1990). So most of mitochondrial tRNAs are nuclear-encoded. Among the 49 nuclear-encoded isoacceptor families, 15 are considered to be cytosol-specific, and 34 to be shared between the cytosol and mitochondria. Once again, the distinction between low import and cytosolic contamination is problematic. However, the association of a systematic analysis of expressed mitochondrial *trn* genes with the evaluation of import of each cytosolic tRNA family gives the most accurate determination of the whole mitochondrial tRNA population.

### 3.2. Evolutionary aspects and mitochondrial translation

Transfer RNA gene loss and tRNA import acquisition have occurred very early during evolution of plant mitochondria. Indeed, huge tRNA import is observed in the green alga *C. reinhardtii* (Vinogradova et al., 2009) and tRNA<sup>Ile</sup> import was shown in the bryophyte *Marchantia polymorpha* (Akashi et al., 1996). Some evolutionary characteristics can be drawn, but “accidents” in one particular species are also observed. As examples, tRNAs specific for alanine, arginine, leucine, threonine, or valine are imported into all known angiosperm mitochondria, tRNAs<sup>Gly</sup> are imported into monocot mitochondria, tRNA<sup>Phe</sup> and tRNA<sup>His</sup> into mitochondria of Brassicales and Triticeae, respectively (Duchêne et al., 2010; Small et al., 1999). By contrast, tRNA<sup>Trp</sup> is known to be imported only into *A. thaliana* mitochondria (Duchêne and Maréchal-Drouard, 2001) and tRNA<sup>Ser</sup> in *Helianthus annuus* (Ceci et al., 1996).

Acquisition of tRNA import appears mostly correlated with the loss of the corresponding mitochondrial *trn* gene. In terms of evolution, import of one tRNA species should be a prerequisite for the loss of the corresponding mitochondrial genes to allow the mitochondria translation system to



function. So, in theory, we must be able to identify plant species that are able to import a cytosolic tRNA even though its mitochondrial counterpart is still expressed. However, at the level of the 20 tRNA families corresponding to each amino acid, the imported tRNA population is mostly complementary to the mitochondrial-encoded one: import of cytosolic tRNAs for one amino acid is associated with mitochondrial *tm* gene loss for the same amino acid. At the level of isoacceptors, the link is less obvious. In dicots, tRNA<sup>Gly</sup>(GCC) is mitochondrial-encoded and import of tRNA<sup>Gly</sup>(UCC) was demonstrated. This import seems necessary for the decoding of GGG and GGA codons. However, why is tRNA<sup>Gly</sup>(CCC) also imported (Brubacher-Kauffmann et al., 1999; Salinas et al., 2005), as it is apparently not necessary? Another example is that of tRNA<sup>Leu</sup>. Three isoacceptors (with CAA, TAA, and TAG anticodons) seem sufficient for translation and are found in the mitochondrial genome of *Physcomitrella patens*, *Mesostigma viride*, or *M. polymorpha* (Terasawa et al., 2007). No tRNA<sup>Leu</sup> genes are found in *C. reinhardtii* mitochondrial genomes, and tRNA<sup>Leu</sup> import is expected. It appears that the five cytosolic tRNA<sup>Leu</sup> (CAG, CAA, UAA, UAG, and AAG anticodons) are imported into mitochondria (Vinogradova et al., 2009). Eukaryotic tRNAs have a high level of modified nucleosides as compared to the prokaryotic ones, in particular at the first position of the anticodon. For example, plant tRNA<sup>Leu</sup>(CAA) contains a hypermodified nucleoside at position 34 (Green et al., 1987; Maréchal-Drouard et al., 1990a,b). These modified nucleosides may restrict the codon/anticodon recognition. Consequently, it is likely that more eukaryotic-type tRNA isoacceptor species are required to read all codons of a family as compared to the number of isoacceptors required in bacterial-type translation system.

### 3.3. Mechanism of tRNA import

This question is difficult to take up in plants because in one plant species some cytosolic tRNAs are mitochondrial imported and others are not or are imported at different levels. Moreover, the imported pool is different from one species to the other. For example, a tRNA with an identical primary sequence can be imported in one plant but not in the other, as tRNA<sup>Gly</sup>(GCC) in potato versus wheat (Brubacher-Kauffmann et al., 1999). Two aspects of tRNA import mechanism have been studied. The first goal was to identify tRNA mitochondrial receptors and channels. The second one was to understand the specificity of import.

#### 3.3.1. Identification of mitochondrial membrane proteins implicated in tRNA Import

First, an *in vitro* import system was set up. Radioactive tRNAs can be imported into isolated potato mitochondria in the presence of ATP and mitochondrial membrane potential but without any cytosolic factors

(Delage et al., 2003a). Components of the TOM complex (translocase of the outer membrane) were shown to be involved in tRNA binding to the surface of mitochondria (Salinas et al., 2006). Moreover, both ruthenium red, which induces the closure of VDAC, and antibodies against VDAC are able to inhibit *in vitro* import of tRNA, showing that the voltage-dependent anion channel (VDAC) is involved in tRNA import (Fig. 4.4). However, selectivity of import was partially lost in the *in vitro* import system (Delage et al., 2003a; Salinas et al., 2005), and VDAC was shown to interact with different RNA and DNA substrates (Salinas et al., 2006). Moreover, even if the imported tRNA's pool changes from one plant species to the other, it is difficult to correlate this variation with species-specific adaptation of the import machinery core and specificity-regulating factors are still unknown.

### 3.3.2. Selectivity of the process

Selectivity of import was studied *in vivo*, by generating transgenic plant cell lines expressing different tRNA variants in order to identify import determinants or antideterminants. Two couples of imported versus nonimported tRNAs have been extensively studied in BY2 cells: tRNA<sup>Val</sup>(AAC)/tRNA<sup>Mct-c</sup>(CAU) (Delage et al., 2003b; Laforest et al., 2005) and tRNA<sup>Gly</sup>(UCC)/tRNA<sup>Gly</sup>(GCC) (Salinas et al., 2005). Sequence exchanges between tRNAs in each couple were performed in the anticodon stem, D- or T-domains, and identity elements (Table 4.1). All mutant

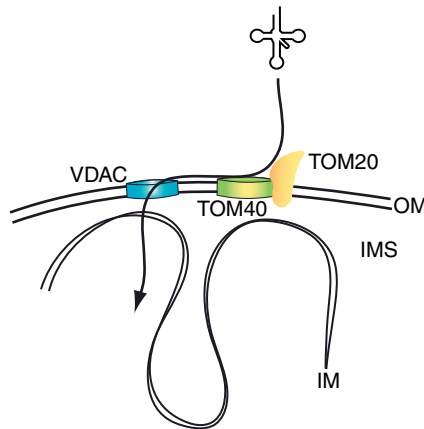


**Figure 4.4** Mitochondrial outer membrane (OM) components involved in tRNA import into plant mitochondria. Two components of the translocase of the mitochondrial outer membrane TOM20 and TOM40 implicated in the protein import machinery are also involved in tRNA binding to the OM. The voltage-dependent anion channel (VDAC) is involved in the tRNA translocation step through the OM. Nothing is known about the protein factors required for tRNA translocation through the inner membrane (IM). IMS: inter membrane space.

**Table 4.1** Specificity of mitochondrial import

| tRNA                        | Natural status                              | Mutation                                                                      | Aminoacylation | <i>In vivo</i> import | Reference        |
|-----------------------------|---------------------------------------------|-------------------------------------------------------------------------------|----------------|-----------------------|------------------|
| tRNA <sup>Val</sup> (AAC)   | Imported in all angiosperms                 | Anticodon stem                                                                | Yes            | Yes                   | – <sup>a,b</sup> |
|                             |                                             | D-domain (Val → Met)                                                          | Yes            | No                    |                  |
|                             |                                             | T-domain (Val → Met)                                                          | Yes            | No                    |                  |
|                             |                                             | Anticodon AAC(Val) → CAU(Met)                                                 | No by ValRS    | no                    |                  |
| tRNA <sup>Met-e</sup> (CAU) | Nonimported in tobacco                      | Anticodon CAU(Met) → CAC(Val)                                                 | No             | No                    | – <sup>a,b</sup> |
|                             |                                             | Anticodon CAU(Met) → CAC(Val) + D-domain (Met → Val)                          | No             | No                    |                  |
| tRNA <sup>Gly</sup> (UCC)   | Imported in all angiosperms                 | Anticodon stem                                                                | Yes            | Yes                   | – <sup>c</sup>   |
|                             |                                             | D-domain (tRNA UCC → GCC)                                                     | Yes            | No                    |                  |
|                             |                                             | Anticodon UCC → GCC                                                           | Yes            | No                    |                  |
| tRNA <sup>Gly</sup> (GCC)   | Nonimported in dicots, imported in monocots | Anticodon stem                                                                | Yes            | No                    | – <sup>c</sup>   |
|                             |                                             | D-domain (tRNA GCC → UCC)                                                     | Yes            | No                    |                  |
|                             |                                             | Anticodon GCC → UCC                                                           | Yes            | No                    |                  |
| tRNA <sup>Leu</sup> (CAA)   | Imported in all angiosperms                 | Insertion of four nucleotides in the anticodon                                | Yes            | Yes                   | – <sup>d</sup>   |
| tRNA <sup>Ala</sup> (UGC)   | Imported in all angiosperms                 | Insertion of four nucleotides in the anticodon                                | Yes            | Yes                   | – <sup>e</sup>   |
|                             |                                             | Insertion of four nucleotides in the anticodon + U70 → C70 (identity element) | No             | No                    |                  |

Mutated tRNAs were expressed in transgenic tobacco plants, except tRNA<sup>Leu</sup> which was expressed in potato.

<sup>a</sup> Delage et al. (2003b).

<sup>b</sup> Laforest et al. (2005).

<sup>c</sup> Salinas et al. (2005).

<sup>d</sup> Small et al. (1992).

<sup>e</sup> Dietrich et al. (1996).

tRNAs are highly expressed. Concerning mitochondrial import, anticodon stem mutations are silent and do not affect the imported or nonimported status of tRNAs. All other sequence exchanges inhibit import of the naturally imported tRNA but do not allow import of the naturally non imported tRNA. Mutations in the D- or T-domain probably affect the tertiary structure of the tRNA suggesting that the 3D structure or tRNA flexibility could be important for efficient import into plant mitochondria. Aminoacylation by the cognate aminoacyl-tRNA synthetase appears to be essential but not sufficient for import, and this is in accordance with a previous work with tRNA<sup>Ala</sup>(UGC) (Dietrich et al., 1996). Mutations in the anticodon were also performed, but no general rules can be observed: GCC mutation in tRNA<sup>Gly</sup>(UCC) background inhibits import, but UCC mutation in tRNA<sup>Gly</sup>(GCC) background does not allow import. By contrast, insertion of four nucleotides in tRNA<sup>Leu</sup>(CAA) and tRNA<sup>Ala</sup>(UGC) anticodons does not affect import (Dietrich et al., 1996; Small et al., 1992). In conclusion, the control of tRNA import selectivity appears complex. Some features (3D structure of the tRNA, aminoacylation) appear essential for import and conserved from one tRNA model to the other, but particular species or tRNA characteristics also influence import (i.e., for tRNA<sup>Gly</sup>).

Another aspect of import regulation is the control of the steady-state level for each tRNA. As in protozoa, this level greatly changes from one tRNA to the other. In *Chlamydomonas*, the percentage of imported tRNAs relative to its cytosolic abundance varies from 0.2% to 98%, and a good correlation between extent of import and codon usages both in mitochondria and in the cytosol was observed (Vinogradova et al., 2009).

## 4. RNA IMPORT IN FUNGI

Based on the lack of essential mitochondrial tRNA genes, import is predicted to occur in some fungi. Indeed, the mitochondrial genome of *Spizellomyces punctatus* only encodes eight tRNA genes (Laforest et al., 1997). Although mitochondrial tRNA editing has been found in this organism that could have explained why tRNA gene escapes detection, the import of nuclear-encoded tRNAs is strongly suggested in this fungus to compensate the lack of mitochondrial tRNA genes. In *Harpochytrium* species, a similar situation is found (Schneider and Maréchal-Drouard, 2000). In contrast to protozoa, plants, and fungi mentioned above, the *S. cerevisiae* mitochondrial genome encodes an apparently full set of tRNA genes. Based on bioinformatic sequence analysis, no tRNA import would be predicted, as the 24 mitochondrial tRNA genes are in theory sufficient to read all sense codons used by the mitochondrial translation system (Foury et al., 1998; Maréchal-Drouard et al., 1992). However, three tRNAs were reported to

be imported into *S. cerevisiae* mitochondria, two nuclear-encoded tRNAs<sup>Gln</sup> and one tRNA<sup>Lys</sup>.

#### 4.1. Imported tRNA species in *S. cerevisiae* mitochondria

Report about mitochondrial tRNA<sup>Gln</sup> import was done by Rinehart (2005). The authors aimed to decipher the aminoacylation pathway of tRNA<sup>Gln</sup> in mitochondria. They showed that, *in vitro*, tRNA<sup>Gln</sup> import is ATP dependent and does not require any protein factor to be targeted into isolated mitochondria. However, import of the two tRNA<sup>Gln</sup> isoacceptors was affirmed in a recent work by Frechin et al. (2009). The latter work unambiguously resolves the aminoacylation process of mitochondrial tRNA<sup>Gln</sup> in *S. cerevisiae* and showed by northern experiments that mitochondria are deprived of any nuclear-encoded tRNA<sup>Gln</sup>. Thus, additional data on tRNA<sup>Gln</sup> mitochondrial import are required to assess whether, under certain conditions, these tRNAs are imported or not into *S. cerevisiae* mitochondria. While tRNA<sup>Gln</sup> mitochondrial import is still subject to debate, the import of one of the two nuclear-encoded tRNA<sup>Lys</sup> into *S. cerevisiae* is clearly demonstrated and its import process has been analyzed in detail. This work is presented below.

#### 4.2. Import of the nuclear-encoded tRNA<sup>Lys</sup>(CUU), tRK1, into *S. cerevisiae* mitochondria

Yeast cells contain three tRNA<sup>Lys</sup> species, called tRK1(CUU), tRK2(UUU), and tRNAK3(UUU), respectively. The two tRNA<sup>Lys</sup> isoacceptors tRK1 and tRK2 are coded for by the nuclear genome. While tRK2 is cytosol-specific, about 3–5% of the total cellular amount of tRK1 is associated with the mitochondrial matrix (Entelis et al., 1996). The third tRNA<sup>Lys</sup>, tRK3(UUU), is encoded by the mitochondrial DNA and restricted to the organelle.

##### 4.2.1. Function of tRK1 in *S. cerevisiae* mitochondria

The import of tRK1 was first demonstrated almost 30 years ago (Martin et al., 1979), its function in mitochondria was uncovered 3 years ago. Due to a modified uridine at the wobble position of the anticodon (5-carboxymethylamino-methyl-2-thiouridine, cmnm5s2U), mitochondrial-encoded tRK3(UUU) is capable, according to classical wobble rules, of recognizing both lysine codons AAA and AAG. Thus, the role of the imported tRK1(CUU) in the organelle seems redundant with regard to the decoding capacity of tRK3. Why should yeast mitochondria import tRK1, as in addition, this tRNA cannot be aminoacylated by the mitochondrial lysyl-tRNA synthetase Msk1p? Is this tRNA involved in another function than protein synthesis?

As a first step toward answering this question, the possibility to import mis-aminoacylated versions of tRK1 was used. Using *in vitro* import assays into yeast- isolated mitochondria, it has been possible to import a tRK1 version with a CAU methionine anticodon in its methionylated form (Kolesnikova et al., 2000). Upon import of this charged  $^{35}\text{S}$ -methionine tRNA, *in organello* protein synthesis permitted the incorporation of radiolabeled methionine in the neo-synthesized polypeptides, thus demonstrating the functionality of modified version of tRK1 in mitochondrial protein synthesis. This functionality in translation was confirmed in human mitochondria, as imported mutated version of yeast tRK1 was capable to complement a mutation in the mitochondrial-encoded human tRNA<sup>Lys</sup>, resulting in a partial restoration of mitochondrial translation.

Then, the direct evidence that tRK1 plays a fundamental role *in vivo* in mitochondrial protein synthesis came from an elegant genetic work. Abolishing import of tRK1 in yeast had no detectable mitochondrial effect under normal conditions of culture at 30 °C, in agreement with the idea that tRK1 import is not absolutely necessary because of the presence of tRK3 (Kamenski et al., 2007). However, strong inhibition of tRK1 import leads to perturbation in mitochondrial translation at 37 °C, notably on two mitochondrial-encoded proteins, Var1p and Cox2p. The corresponding genes are the only ones harboring AAG lysine codons (two on *VAR1* and one on *COX2*) in yeast. Therefore, it has been supposed that, at 37 °C, tRK3(UUU) failed to recognize AAG lysine codons, explaining tRK1 import necessity to perform mitochondrial translation. Investigating the modification status of the tRK3 anticodon under heat stress condition, Tarassov and colleagues showed that the wobble position of tRK3 is under-modified at 37 °C such that this tRNA can no longer recognize the AAG codon, thus preventing an efficient elongation during translation. Taken together, import of tRK1 into yeast mitochondria has been explained as an adaptation mechanism to heat stress condition, to thwart the decoding defect of lysine AAG codons by the under-modified tRK3 (UUU) and to permit an efficient mitochondrial translation.

#### 4.2.2. Selectivity of tRNA<sup>Lys</sup> import into yeast mitochondria

Only one of the two nuclear-encoded tRNA<sup>Lys</sup> is imported into mitochondria, implying a very specific process. tRK1(CUU) and tRK2(UUU) differ in 21 positions. Two major import determinants have been characterized: the first position of the anticodon (C34) and positions localized in the aminoacceptor stem. As a matter of fact, residues C34, G1:C72, and U73, once introduced into tRK2, confer to this normally nonimported tRNA the ability to be targeted to the matrix, both *in vitro* and *in vivo* (Entelis et al., 1998).

Neither the presence of modified nucleotides (Entelis et al., 1996) nor the other nucleotidic differences observed between tRK1 and tRK2 significantly influence the import process, unless the changes are affecting the

conformation of the tRNA. Indeed, one crucial condition that a tRNA needs to satisfy to be imported into the organelle is a substantial affinity to the precursor form of Msk1p (pre-Msk1p) (Tarassov et al., 1995a,b).

Interestingly, while aminoacylation of tRK1 by the cytosolic lysyl-tRNA synthetase, Krs1p, is a prerequisite for import, it is not absolutely necessary. Mutant versions of tRK1 and tRK2 that are not charged in lysine but are still recognized by pre-Msk1p can be imported. It seems that the role of aminoacylation is to induce a conformational change in the tRNA to facilitate its essential binding to pre-Msk1p. Indeed, the aminoacylation identity does not influence the import drastically, as methionylated or alanylated mutant versions of tRK1 and tRK2 bearing import identity elements can be targeted into the mitochondrial matrix (Kolesnikova et al., 2000). As a whole, the major discrimination signal primarily relies on nucleotides identity determining the tertiary conformation of the tRNA and its affinity to pre-Msk1p.

#### 4.2.3. Targeting and translocation steps of tRK1 into *S. cerevisiae* mitochondria

To study the import mechanism of tRK1 into yeast mitochondria (Fig. 4.5), two main complementary approaches were developed: *in vitro* and *in vivo* import assays (Tarassov and Entelis, 1992). The initial studies consisted in establishing an *in vitro* import system to recreate, in an artificial but controlled physiological environment, the import of tRK1 transcript into isolated mitochondria. This strategy first showed that tRK1 import into yeast mitochondria is dependent on ATP hydrolysis and on the electrochemical membrane potential. Furthermore, aminoacylation of tRK1 is essential, as already stated above. In addition, a soluble cytosolic protein extract must be added and at least one protein associated with the outer mitochondrial membrane is important (Tarassov et al., 1995a). Then, during the past decade, the group of Tarassov (Strasbourg, France) went into more depth in the import mechanism and identified several protein components.

The proposed pathway of tRK1 import into yeast mitochondria is shown in Fig. 4.5. Aminoacylation of tRK1 by the cytosolic lysyl-tRNA synthetase Krs1p is a prerequisite for tRK1 import. Then the lysyl-tRK1 is either used by the cytosolic translation machinery or binds the targeting factor enolase-2 (Eno2p). Eno2p is a glycolytic enzyme with multiple roles (Entelis et al., 2006). This protein, in its soluble form, interacts specifically with the aminoacylated tRK1 and targets it to the surface of mitochondria. At this level, the Eno2-lysyl-tRNA is destabilized. Eno2p reaches the glycolytic complex located at the surface of mitochondria, whereas the lysyl-tRNA binds to the mitochondrial precursor form of its cognate mitochondrial lysyl-tRNA synthetase, pre-Msk1p, which is translated by cytosolic ribosomes at the surface of the organelles (Entelis et al., 2006). Finally, pre-Msk1p triggers its translocation across mitochondrial

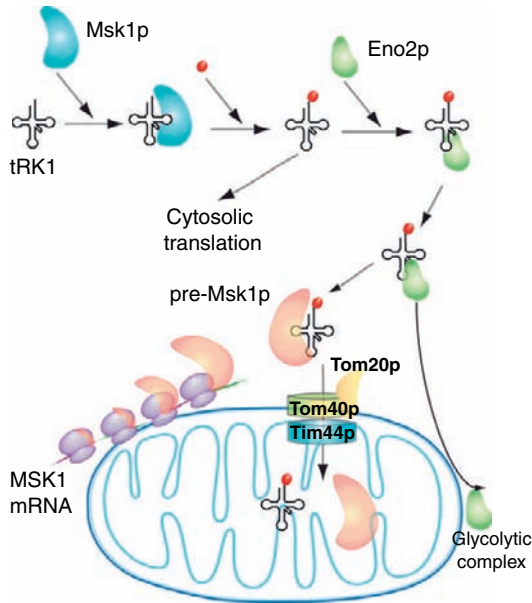


**Figure 4.5** A schematic model for tRK1 import into yeast mitochondria. The nuclear-encoded tRNA<sup>Lys</sup>(CUU), tRK1, is aminoacylated (lysine: red ball) by the cytosolic lysyl-tRNA synthetase Msk1p (in blue). It is either used for the cytosolic translation or is recognized by enolase Eno2p (in green) that acts as a carrier and targets the lysyl-tRK1 to the surface of mitochondria. At this level, Eno2p promotes the interaction between the lysyl-tRK1 and the precursor form of the mitochondrial lysyl-tRNA synthetase pre-Msk1p (in orange) synthesized by cytosolic polysomes localized at the surface of mitochondria. By interacting with the lysyl-tRK1, pre-Msk1p triggers its translocation across the mitochondrial membranes. This mitochondrial translocation step requires at least three components, Tom20p, Tom40p, and Tim44p of the yeast protein import machinery localized at the level of the outer (Tom) and inner (Tim) membranes, respectively.

membranes. This tRK1–pre-Msk1p interaction is absolutely necessary for tRK1 import and seems to proceed in an equimolar ratio.

*In vitro* experiments revealed the central role of the protein import machinery in this process, as blocking the Tim/Tom complexes (translocase of the inner/outer membrane) abolished import of tRK1. Furthermore, quantification by Northern blot of mitochondrial tRK1 in yeast lines depleted in components of the protein import complexes confirmed the implication of Tom20p and Tim44p in the import process, two proteins of the major protein import pathway (Tarassov et al., 1995a). Altogether, the data strongly suggest that pre-Msk1p acts as a specific carrier for lysyl-tRK1 and both partners are translocated through the double mitochondrial membranes via the protein import channel. However, this model is confronted



with the paradigm that proteins need to unfold during translocation (Eilers and Schatz, 1986). If this is the case, it is difficult to imagine how an unfolded aminoacyl-tRNA synthetase can retain its interaction with a tRNA during translocation through the mitochondrial membranes. Answering this question is an important challenge in the future.

## 5. RNA IMPORT IN METAZOA

### 5.1. Import of tRNAs

Based on bioinformatic prediction, a large number of mammals apparently contain a full set of mitochondrial tRNA genes, in particular in most mammals. However, it is worth to note that in *Opossum*, a marsupial, the mitochondrial-encoded tRNA<sup>Lys</sup> is not functional and is compensated by the import of the nuclear-encoded tRNA<sup>Lys</sup> species (Dörner et al., 2001). There are also a large variety of Metazoan species such as the Cnidaria *Metridium senile* or the Mollusca *Crassostrea gigas* that have retained only a few (1–4) tRNA genes on their mitochondrial genomes (Lithgow and Schneider, 2010; Schneider and Maréchal-Drouard, 2000). In these organisms, import of cytosolic tRNAs is likely to occur, again showing that tRNA mitochondrial import is a widespread process. In human, as in the yeast *S. cerevisiae*, the mitochondrial genome encodes a set of 22 tRNAs that are, in theory, sufficient to read all sense codons used by the human mitochondrial translation machinery. However, there is recent evidence that the two cytosolic tRNA<sup>Gln</sup> isoacceptors (with CUG or UUG anticodons) are present in highly purified rat and human mitochondria (Rubio et al., 2008). As the human mitochondrial-encoded tRNA<sup>Gln</sup> is functional (Nagao et al., 2009), there is no need of nuclear-encoded tRNA<sup>Gln</sup> species in human mitochondria. As for the imported tRNA<sup>Lys</sup> present in *S. cerevisiae* mitochondria, one interesting question will be to define the role of these tRNAs in the organelle.

As mentioned above, while only few cases of tRNA import have been reported into mammalian mitochondria so far, paradoxically the mitochondrial import of other types of RNAs has been described mainly in these organisms. It concerns the ribosomal 5S rRNA, the RNA components of the RNase P and RNase MRP, respectively, and more recently miRNAs. Our present knowledge concerning the import of these various nuclear-encoded RNAs is present below.

### 5.2. Import of 5S rRNA into mammalian mitochondria

Cytosolic 5S rRNA was first detected by northern experiment in highly purified and RNase-treated bovine, chicken, and rabbit mitoplasts (Yoshionari et al., 1994). It was then detected in human and rat

mitochondria by Magalhaes et al. (1998). Because 5S rRNA is not encoded by the mitochondrial genome in mammals, the import of this RNA seems to be a conserved feature. Thus, a portion of cytosolic 5S rRNA escapes the classical route to the large cytosolic ribosomal subunits and is directed to the mitochondrial surface where it is translocated through the mitochondrial membranes to reach the matrix side.

### 5.2.1. Role of the cytosolic 5S rRNA in human mitochondria

While 5S rRNA is usually a structural component of the large ribosomal subunit, the three-dimensional structure of the mammalian mitochondrial ribosome was resolved by cryo-electron microscopy and confirmed the absence of 5S rRNA in the large subunit (Sharma et al., 2003), raising the question about its role in mitochondria. Mitoribosome preparations, lacking 5S rRNA, are active in poly(U)-directed phenylalanine polymerization *in vitro* but fail to direct translation of natural mRNAs (Cahill et al., 1995). It was hypothesized that proteins could assume and compensate some of the roles of the 5S rRNA (Sharma et al., 2003). However, we cannot exclude that 5S rRNA is a component of fully functional mitoribosome that is lost during ribosome isolation.

Even if 5S rRNA was never found to be associated with mitoribosomes yet, the first demonstration of the functional importance of 5S rRNA in mitochondrial translation was obtained recently (Smirnov et al., 2010). As discussed later on, inhibition of the expression of rhodanese by gene silencing, a mitochondrial thiosulfate sulfurtransferase, affects the 5S rRNA import into human mitochondria. It also significantly affects mitochondrial translation *in vivo*. Is this effect on translation due to the absence of rhodanese or of 5S rRNA? In yeast, there is a mitochondrial-encoded 5S rRNA, no import of its cytosolic counterpart, and deletion of rhodanese does not produce a respiratory phenotype. Thus, the activity of human mitochondrial translation apparatus appears to be likely linked to the level of cytosolic 5S rRNA inside mitochondria and rules out a possible role of rhodanese in translation. A next challenge will be to precisely define the role of this ribosomal RNA in mitochondrial translation, as a structural component of the ribosome, as a component involved in its assembly, or as part of a regulatory complex.

### 5.2.2. Import mechanism of 5S rRNA into human mitochondria

Studies on 5S rRNA import mechanism into human mitochondria were mainly conducted by the group of Tarassov (Strasbourg, France). As for the tRK1 import study in yeast, they first made use of an *in vitro* import assay into isolated human mitochondria. It is interesting to note that human 5S rRNA has no posttranscriptional modification (Szymanski et al., 2003) and transcript corresponding to 5S rRNA is as efficiently imported into mitochondria as the endogenous 5S rRNA *in vivo*. Using this approach, it was

first demonstrated that the import of 5S rRNA transcript requires energy of ATP hydrolysis, a transmembrane electrochemical potential, the protein import apparatus, and is directed by at least two soluble components (Entelis et al., 2001a; Smirnov et al., 2010). These requirements are strikingly similar to that needed for the import of transcripts corresponding to tRNA<sup>Lys</sup> or derivatives into isolated yeast mitochondria (see above).

Recently, rhodanese has been identified as one of the cytosolic soluble factors involved in 5S rRNA mitochondrial import (Smirnov et al., 2010). Rhodanese is a mitochondrial thiosulfate sulfurtransferase that belongs to a protein superfamily involved in diverse processes, including cyanide detoxification, Fe/S clusters formation, redox reactions as well as intracellular transport, and regulatory pathways (Cipollone et al., 2007). To identify rhodanese as an essential 5S rRNA import factor, several approaches were used. First, using *in vitro* import assays into isolated human mitochondria, Tarassov and colleagues have identified the 5S rRNA import determinants. Two distinct structural elements of 5S rRNA were identified as signals of mitochondrial localization, the  $\alpha$  and  $\gamma$  subdomains (Fig. 4.6). It was shown that these import determinants correspond to binding sites with rhodanese. Then, studies on the interaction between rhodanese and 5S rRNA revealed that the  $\alpha$  domain site functions as the main rhodanese-binding platform, whereas the gamma-domain may contain a region allowing a more tight binding. Further interaction assays using *in-gel* FRET technique allowed to demonstrate that the 5S rRNA–rhodanese interaction is dependent on the RNA conformation, especially involving the  $\alpha$  domain. Silencing of rhodanese genes leads to a strong inhibition of 5S rRNA mitochondrial import. Interestingly, rhodanese in its misfolded form interacts more strongly with the rRNA (Smirnov et al., 2010). In fact, it was shown that this interaction occurs cotranslationally, indicating that 5S rRNA interacts with the protein

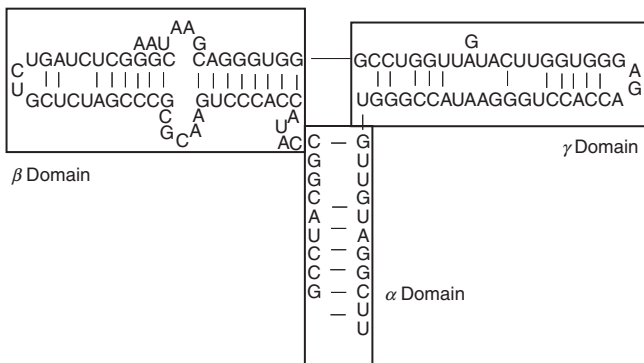


**Figure 4.6** Secondary structure of human 5S rRNA (adapted from Smirnov et al., 2008b). The  $\alpha$ ,  $\beta$ , and  $\gamma$  domains of the human 5S rRNA are boxed.

as soon as its synthesis occurs. In this way, the 5S rRNA plays a role of a chaperone to keep rhodanese in an inactive nonaggregative “misfolded” form.

Taken together, the following model of 5S rRNA trafficking in a human cell can be proposed (Fig. 4.7). In general, the 5S rRNA is integrated in the large subunit of cytosolic ribosomes. However, a small portion of 5S rRNA can escape this main road. In that case, once in the cytosol, rather than to

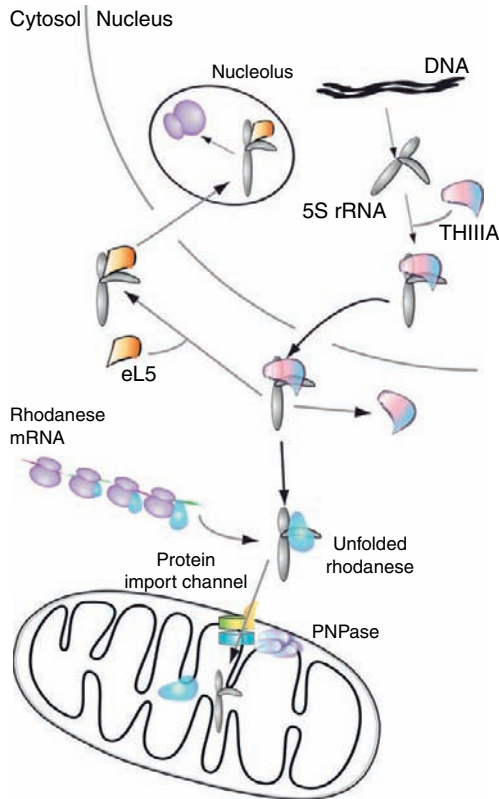


**Figure 4.7** A schematic model for 5S rRNA import into human mitochondria. First, contrary to 18S and 26S rRNAs that are usually transcribed in the nucleolus, the 5S rRNA is transcribed in the nucleoplasm (Haeusler and Engelke, 2006). Then, the transcription factor TFIIIA binds newly synthesized 5S rRNA and triggers its export from the nucleus to the cytosol. Once in the cytosol, the 5S rRNA can have two different fates. Either it interacts with the ribosomal protein eL5 and penetrates into the nucleolus where it becomes part of large subunit of ribosomes, or it binds newly synthesized and unfolded rhodanese, a mitochondrial thiosulfate sulfurtransferase that triggers its import into mitochondria. The protein import channel and the PNPASE, shown to be involved in the 5S rRNA import process, are indicated (Entelis et al., 2001a; Wang et al., 2010).

bind the ribosomal protein eL5 and be redirected to the nucleolus, 5S rRNA interacts with neo-synthesized rhodanese. It is targeted first to the surface of mitochondria and then translocated through the mitochondrial membranes. Smirnov et al. showed that 5S rRNA can interact with another mitochondrial protein, the aldehyde dehydrogenase (Smirnov et al., 2010) but whether or not this protein is really involved in 5S rRNA mitochondrial import remains to be established.

Finally, it must be stressed that based on both *in vivo* and *in vitro* experiments, the mitochondrial polynucleotide phosphorylase (PNPASE) seems to be involved in the regulation of the 5S rRNA import process in human mitochondria (Wang et al., 2010). The precise role of this protein will be discussed in more details in Section 5.3. In contrast to the data obtained by the group of Tarassov, *in vitro* import experiments showing the involvement of the PNPASE were conducted in the absence of any added cytosolic soluble proteins. As a whole, this suggests that the 5S rRNA might use two different pathways to enter human mitochondria.

### 5.3. Import of the RNA components of RNase MRP and RNase P into human mitochondria

Besides tRNA and 5S rRNA mitochondrial import, data supporting the import of the RNA components of the RNase P and of the RNase MRP have been obtained. In both cases, controversial data exist and will be presented as well. The first RNA suggested to be targeted to human mitochondria is the RNA component of the RNase P. The RNase P is involved in the processing of precursor tRNAs (pre-tRNA) by precisely cleaving those molecules to produce mature 5'-ends. Until recently, this endonuclease was thought to be a ribonuclease consisting in protein subunits and a catalytically active RNA component in all domains of life (Evans et al., 2006). In organelles, the RNA component of RNase P is encoded in a number of mitochondrial genomes; however, no such gene was ever found in mammalian mitochondrial DNA. The activity of partially purified RNase P of human HeLa cells mitochondria was found to be micrococcal nuclease sensitive and the RNA component was suspected to be imported into mammalian mitochondria to obtain a functional RNase P activity (Doersen et al., 1985). Furthermore, a mitochondrial-associated RNase P RNA species of 340 nucleotides was described to be identical in sequence to the H1 RNA component of the HeLa cell nuclear RNase P (Puranam and Attardi, 2001). However, the protein content of this ribonucleoprotein complex was never determined. No nuclear-related RNase P proteins could ever be found in human mitochondrial proteome analysis. In contrast, the group of Rossmannith (Vienna, Austria) reported that human mitochondria-associated RNase P activity was RNA-independent (Rossmannith and Karwan, 1998). Very recently, they now reconstituted *in vitro* a human

mitochondrial RNase P activity. This tRNA processing activity relies on the presence of a heterocomplex essentially constituted by three proteins (named MRPP 1–3 for mitochondrial RNase P protein) without any requirement of a transacting RNA (Holzmann et al., 2008).

Interestingly, similar observation was now done in plant mitochondria and chloroplasts where a single protein called PRORP1 (for proteinaceous RNase P) is sufficient to perform the endonucleolytic cleavage of tRNA precursor molecules, without need of any RNA subunit (Gobert et al., 2010). According to these new data, human mitochondrial RNase P activity seems to require only proteins. A more recent work rather proposes the existence of two types of RNase P activities in human mitochondria, one without any RNA component and one containing an RNA subunit (Wang et al., 2010). One of the reasons why such controversial data are obtained can be the amount of the potential nuclear-encoded RNase P RNA in the mitochondria. As already emphasized in the section dealing with RNA import into plant mitochondria, if the amount of an RNA is low, it is then difficult to make a difference between the contamination threshold and a real mitochondrial localization. Furthermore, we cannot exclude that a “passive” nonspecific process permitting the mitochondrial import of various nucleic acids at a low rate exists *in vivo*.

The second RNA proposed to be imported into human mitochondria is the RNA component of the RNase MRP. The ribonucleoprotein complex MRP (mitochondrial RNA processing) is an endoribonuclease that was identified as a nuclear complex but which function was initially studied in the context of isolated mouse mitochondria (Chang and Clayton, 1987). RNase MRP RNA and RNase P RNA are structurally and evolutionary related. RNase P RNA is found in all domains of life, whereas MRP RNA seems to be confined to eukaryotes. In mammalian mitochondria, RNase MRP cleaves RNA transcripts complementary to the origin of replication, forming the RNA primers for the leading strand of mitochondrial DNA replication (Chang and Clayton, 1987). It is important to note that evidence has been put forward to argue against a mitochondrial localization of MRP RNA. Kiss and Filipowicz showed that the MRP RNA is present in mitochondria in a very low and insufficient amount to sustain its function (Kiss and Filipowicz, 1992). However, Topper and colleagues believe that such amount, at the level of detectability, is sufficient to promote an RNase MRP activity (Topper et al., 1992). *In situ* hybridization analysis showed that this RNA is primarily located in the nucleolus but also confirmed the presence of low amounts of MRP RNA in mitochondria (Li et al., 1994).

Wang and collaborators went one step further in identifying a protein factor involved in the mitochondrial import of several RNAs, including the RNA components of a potential RNase P and of the RNase MRP. This import factor is the mitochondrial PNPASE. PNPASE is a protein targeted to mitochondria and in human, contrary to other organisms, this enzyme

has been localized in the intermembrane space (Chen et al., 2007). PNPASE depletion decreases the mitochondrial amount of RNase P RNA, which results in a decrease in mitochondrial tRNA processing. Given that human mitochondrial tRNA genes are encoded between open reading frames of OXPHOS components, failure in tRNA excision also impairs maturation of the OXPHOS subunit transcripts. Thus, depletion of PNPASE affects oxidative phosphorylation to generate ATP. Data suggest that this protein is capable to interact specifically with a stem loop domain of the RNase P or RNase MRP RNAs. When grafted onto another RNA, it triggers its import into yeast mitochondria containing human PNPASE (Wang et al., 2010).

In addition to the potential import of both RNA components of RNase P and RNase MRP, the import of 5S rRNA (see Section 5.2.2) seems also regulated by PNPASE (Wang et al., 2010). Intriguingly, the *in vitro* import assay they performed into isolated mammalian mitochondria permitted the import of the cytosolic 5S rRNA without any added cytosolic soluble proteins. This fully contrasts with the data presented above where two protein factors, including rhodanese, are necessary (Smirnov et al., 2010). It is worth to note that *in vitro* import assays of cytosolic tRNA<sup>Gln</sup> into human mitochondria revealed that the import process is ATP dependent, and does not require any soluble cytosolic protein factors (Rubio et al., 2008). Indeed, Rubio and colleagues support that ATP is the key parameter for mitochondrial ability to import tRNA<sup>Gln</sup>(CUG).

Taken together, one major challenge in the future is to clearly define whether such controversial data reflects differential experimental procedures or whether it corresponds to the existence of several RNA mitochondrial import pathways within the same organism.

#### 5.4. miRNA import in mammalian mitochondria

Two reports mention the detection of miRNAs in rat liver derived mitochondria (Bian et al., 2010; Kren et al., 2009). Fifteen miRNAs and at least 20 miRNAs were identified by microarray analysis in both papers, respectively. Kren et al. showed that the miRNA species they identified are targeted neither against mitochondrial mRNAs nor against nuclear mRNA encoding mitochondrial proteins. They hypothesized that these mitochondria-associated miRNAs are rather involved in apoptosis, cell proliferation, or differentiation. Mitochondria play a central role in apoptosis via disruption of the membrane potential resulting in an increased permeability to small molecules (Kroemer et al., 2007). Authors propose that this increased permeability may represent a mechanism by which miRNAs sequestered in the mitochondria are released into the cell. Nevertheless, direct demonstration of the import of miRNAs into mitochondria as well as their potential role remains to be clarified. As a whole, it is clear that much deeper work is

needed to clearly establish which RNAs are imported into human mitochondria, in which amount, and for which reasons.

## 6. POTENTIAL APPLICATIONS OF MACROMOLECULE IMPORT

Mitochondrial genomes undergo numerous mutations, insertions, deletions, and recombinations. These modifications can result in mitochondrial dysfunctions, which are often dramatic for the cell viability. For example, in human, such mitochondrial disorders can be at the center of neurodegenerative and neuromuscular diseases, diabetes, aging, and also cancers (Bonnet et al., 2008; Florentz et al., 2003; Trifunovic et al., 2004). In plants, mitochondrial disorders can originate from the unusual presence of chimeric sequences in mitochondrial genomes, which in turn lead to cytoplasmic male sterility (CMS). CMS affects plants in a way that they become incapable of producing functional pollen. This aspect constitutes a valuable tool in agronomy to produce hybrid plants that are more vigorous in culture (Budar and Pelletier, 2001). Mitochondrial transformation is thus of great interest, both for the study of mitochondrial disorders, and as a biotechnological tool, for example, in agronomy. Finally, mitochondrial gene expression is still largely unknown and awaits reverse genetics tool for a better knowledge.

To date, studying mitochondrial biogenesis, establishing tools to produce exogenous proteins in mitochondria, or elaborating gene therapy strategies related to the organelles are hampered by the difficulty to manipulate mitochondrial genomes. Only the yeast *S. cerevisiae* (Fox et al., 1988) and the unicellular algae *C. reinhardtii* (Remacle et al., 2006) are amenable for stable mitochondrial transformation using a biolistic approach. Otherwise, no mean exist to stably transform mitochondrial DNA of higher eukaryotes. The main strategies to rescue mitochondrial disorders rely on the import of macromolecules (proteins, DNA, RNA) into organelles (Rustin et al., 2007). The imported macromolecule should rescue a non-functional target originating from a mutated gene, modify the expression of a target gene, or prevent replication of mutated mitochondrial DNA copies. In the following sections, the present state of the art concerning not only RNA import but also protein and DNA import strategies to study, manipulate, and/or correct mitochondrial biogenesis is introduced (Table 4.2).

### 6.1. Protein import

In order to complement a mutation in a mitochondrial protein coding gene, it is in theory possible to express the corresponding protein fused to a mitochondrial sequence from a nuclear transgene (called allotopic



**Table 4.2** The different techniques used to import nucleic acids into mitochondria and the objectives they reached

|                 | Macromolecule | Approach                           | Organism                                        | Aim/effect            | Reference                                         |                |
|-----------------|---------------|------------------------------------|-------------------------------------------------|-----------------------|---------------------------------------------------|----------------|
| <i>In vitro</i> | RNA           | 5S rRNA–tRNAs                      | Direct uptake                                   | Various               | Study of the tRNA import process                  | — <sup>a</sup> |
|                 |               | mRNA                               | Electroporation                                 | Plant                 | Study of mitochondrial RNA processing             | — <sup>b</sup> |
|                 | DNA           |                                    | Direct uptake                                   | Plant, human          | RNA expression for processing studies             | — <sup>c</sup> |
|                 |               |                                    | Electroporation                                 | Plant, human          | RNA expression for processing studies             | — <sup>d</sup> |
|                 |               |                                    | Bacterial conjugation                           | Mouse                 |                                                   | — <sup>e</sup> |
| <i>In vivo</i>  | RNA           | 5S rRNA and tRNA derivatives       | Natural import                                  | Human                 | Complementation of a tRNA <sup>Lys</sup> mutation | — <sup>f</sup> |
|                 |               | tRNA derivatives or antisense RNAs | RIC                                             | Human                 | Complementation of a tRNA <sup>Lys</sup> mutation | — <sup>g</sup> |
|                 | DNA           |                                    | Biolistic                                       | <i>S. cerevisiae</i>  | Inhibition of translation                         | — <sup>h</sup> |
|                 |               |                                    |                                                 | <i>C. reinhardtii</i> | Complementation of mutants—                       |                |
|                 |               |                                    | PNA conjugated to lipophilic cations<br>DQosome | Human                 | Complementation of mutants                        | — <sup>i</sup> |
|                 |               |                                    |                                                 | Rat, human            |                                                   |                |

<sup>a</sup> Entelis et al. (1996, 1998, 2001a).<sup>b</sup> Hinrichsen et al. (2009).<sup>c</sup> Muratovska et al. (2001), Placido et al. (2005, 2009).<sup>d</sup> Castandet et al. (2010), Collombet et al. (1997), Estévez et al. (1999), Staudinger et al. (2005).<sup>e</sup> Yoon and Koob (2005).<sup>f</sup> Entelis et al. (2001a, 2002), Kolesnikova et al. (2004), Smirnov et al. (2008b).<sup>g</sup> Mahata et al. (2006).<sup>h</sup> Bonnefoy and Fox (2007), Remacle et al. (2006).<sup>i</sup> D'Souza et al. (2003), Muratovska et al. (2001).

expression). The expressed protein will then be targeted to mitochondria via the protein import pathway (Chacinska et al., 2009). However, the major drawback of this allotopic expression is that the few proteins still encoded by mitochondrial genomes are localized at the membrane level (e.g., the 13 polypeptides encoded by the human mitochondrial DNA are integral components of the respiratory chain complexes) and are often very hydrophobic. Hydrophobicity constitutes an important barrier and the use of an appropriate mitochondrial targeting sequence may not be sufficient to correctly and efficiently target proteins to mitochondria (Claros et al., 1995).

To bypass this problem, a powerful strategy is to address an mRNA at the surface of mitochondria. This mRNA is then translated at the level of mitochondrial membranes by cytosolic ribosomes and thereby facilitates the correct subsequent mitochondrial localization of the protein. Indeed, it was shown in *S. cerevisiae*, in human, as well as in plants that some mRNAs from nuclear origin encoding mitochondrial proteins are enriched at the surface of mitochondria (Margeot et al., 2002; Michaud et al., 2010; Sylvestre et al., 2003). The role of 3' UTR in the targeting of mRNAs to the surface of mitochondria was established and derivatives were engineered to optimize the allotopic expression of proteins intended for an organellar localization in mammals. For example, versions of ND4 and ND1 mRNAs normally encoded by the mitochondrial genome were recoded for cytosolic translation and designed to harbor RNA targeting sequences. The resulting mRNAs were successfully translated by cytosolic ribosomes at the surface of rat mitochondria, followed by their correct localization in mitochondria (Ellouze et al., 2008). In the same manner, this approach allowed to rescue the phenotype of human cells affected by a mutation of mitochondrial ND4 or ATP6 genes, by restoring their aptitude to grow on galactose rich media thanks to a partial reestablishment of ATP production and of complex I activity (Bonnet et al., 2007, 2008). Examples of direct rescue of mitochondrial defective enzymes by a functional version of the protein are still rare because of trafficking obstacles (Cwerman-Thibault et al., 2010; Rustin et al., 2007).

Another strategy to rescue defects in the respiratory chain is to make use of particular proteins that can shunt and rescue the activity of whole complexes of the respiratory chain which functionality is affected by a defective mutated component (called xenotropic expression). For example, a single polypeptide enzyme rotenone-insensitive NADH-quinone oxidoreductase (Ndi1) of *S. cerevisiae* is able to carry out the electron transport function of complex I. Another example is the cyanide-insensitive alternative oxidase from *Ciona intestinalis* that can replace the activity of complex III. The expression of those enzymes and the correct mitochondrial localization were obtained *in vivo* in mammalian cells or tissues and were shown to take part in the electron transport (Bai et al., 2001; Hakkaart et al., 2006;

Seo et al., 1998, 2004). This strategy constitutes a very promising therapeutic tool in the treatment of respiratory chain complexes impairments.

Among the mitochondrial DNA mutations causing mitochondrial diseases (MITOMAP: A Human Genome Database. <http://www.mitomap.org>), several affect rRNA or tRNA genes. An indirect way to remedy to this kind of defects would be to specifically influence either the replication or the maintenance of organellar genomes. Human mitochondrial DNA is heteroplasmic and mitochondrial diseases show a threshold effect. Thus, by influencing the replication process, it would be possible to favor the propagation of healthy mitochondrial DNA versions against mutated ones. How the replication process occurs in mitochondria of most model organisms is still very unclear and only a few factors were indentified (Wanrooij and Falkenberg, 2010). These factors are sufficient neither to specifically favor the replication of healthy versions of mitochondrial DNA nor to prevent replication of mutated ones. However, it has been proposed to address restriction enzymes to mitochondria that would target restriction sites emerging from a mutated locus in the mitochondrial genome. For example, the T8399G mutation that causes neuropathy, ataxia, and retinitis pigmentosa (NARP) creates a unique *Pst*I restriction site that is not present in healthy versions of mitochondrial DNA sequence. Thus, a protein consisting in a mitochondrial targeting sequence fused to the *Pst*I enzyme has been expressed in cultured human cells (Srivastava and Moraes, 2001). Imported into mitochondria, this enzyme triggered the degradation of mutated DNA versions. This resulted in a shift of the mitochondrial heteroplasmy toward a prevalence of the wild-type genome.

Another approach to prevent the accumulation of mutated DNA is to increase the DNA repair capacity of mitochondria. The 8-oxoguanine DNA glycosylase/apurinic lyase (OGG1) is known to play a role in the repair of oxidative damaged DNA (Nakabeppu, 2001). In a similar manner as described above, this enzyme fused to a mitochondrial targeting peptide has been expressed in human cells. This resulted in an increased cellular survival following oxidative stresses (Druzhyzna et al., 2005; Rachek et al., 2002). A similar approach successfully increased protection of mitochondrial DNA against alkylation using mitochondrially targeted O<sup>6</sup>-methylguanine-DNA methyltransferase (MGMT) (Cai et al., 2005; Rasmussen and Rasmussen, 2005). Considering the role of mitochondrial DNA in the aging process (Weber and Reichert, 2010), approaches aimed at increasing mitochondrial DNA maintenance are meaningful.

## 6.2. DNA import

Other approaches to rescue or influence mitochondrial biogenesis consist in addressing exogenous nucleic acids into the matrix. First, historical attempts aimed to import antisense DNA sequences hybridizing specifically to a

mutated region of mitochondrial DNA in the hope of preventing its replication. Short single-stranded DNA sequences covalently fused to a precursor mitochondrial protein were imported into yeast isolated mitochondria using the protein import machinery (Vestweber and Schatz, 1989) but no effect on replication was obtained. With the same objective, PNA molecules (for peptide nucleic acids) were used, as they mimic DNA molecules with enhanced stability due to their different nature from DNA that protects them against nucleases (Taylor et al., 2000). In addition, they present a better affinity and specificity for DNA complementary sequences than a traditional DNA molecule. PNA molecules fused to a mitochondrial targeting peptide could be targeted into human cells mitochondria *in vivo*. However, several reasons make this technique difficult to use. In particular, there are the difficulty to produce PNA-peptide bonds, the protease sensitivity of the resulting compound and the need to permeabilize cells to allow targeting of PNA-Peptide molecule (Chinnery et al., 2000; Taylor et al., 1997). To circumvent these disadvantages, Muratovska and colleagues fused PNA molecules to lipophilic phosphonium cations (Muratovska et al., 2001). Triphenylphosphonium cations translocate through the cellular membranes and concentrate onto mitochondria. PNA/cation conjugates are imported into mammalian mitochondria both *in vitro* and *in vivo* by the mean of the membrane potential. A PNA/cation conjugate has been designed to selectively inhibit the replication of mitochondrial DNA containing the A8344G point mutation that causes the human disease “myoclonic epilepsy and ragged red fibers” (MERRF) but not the wild-type sequence that differs at a single nucleotide position. When MERRF cells were incubated with the PNA/cation conjugate, the ratio of MERRF to wild-type mitochondrial DNA was unaffected, even though the PNA/cation content of the mitochondria was sufficient to inhibit MERRF mitochondrial DNA replication in a cell-free system. Although this approach allowed the correct targeting of the antisense molecule into mitochondria, the absence of effect on replication of the mutated mitochondrial DNA molecules reveals that the antisense strategy may not be sufficient to prevent the replication machinery to perform its function.

Another strategy involving carrier molecules makes use of dequalinium vesicles (DQAsomes). They constitute promising candidates to mediate delivery of nucleic acids to mitochondria in the cell. Dequalinium is a positively charged amphiphilic molecule. It can self-assemble into liposome-like cationic vesicles that present a tropism for energized mitochondria. It was shown that DQAsomes bind DNA and release DNA toward the surface of isolated mitochondria (D’Souza et al., 2003; Weissig and Torchilin, 2001; Weissig et al., 1998, 2001). In contact with erythrocytes, DQAsomes were shown to enter the cells by endocytosis and to escape from endosomes (D’Souza et al., 2003). Then, they seem attracted by mitochondria where they are capable to salt out the inside bound DNA. However,

internalization of DNA was not observed. D'Souza and colleagues used DQAsomes to investigate whether a mitochondrial localization peptide (MLS) bound to DNA could facilitate this last step of translocation through mitochondrial membranes (D'Souza et al., 2005). This strategy allowed to confirm that DQAsomes are capable to mediate the association of a mitochondrial leader sequence—plasmid DNA conjugate with mitochondria in living cells. Up to now, no transgene could be expressed inside human mitochondria and this constitutes a strong barrier towards nucleic acid delivery studies.

*In vitro* DNA uptake into isolated mitochondria has been obtained in various organisms following different strategies. Introduction and subsequent transcription of DNA have been obtained via electroporation on mammalian (Collombet et al., 1997), trypanosomatids (Estévez et al., 1999), and plant-isolated mitochondria (Castandet et al., 2010; Farré and Araya, 2001; Staudinger et al., 2005). In plant mitochondria, this approach allowed to study *in organello* important gene expression processes such as RNA editing or intron splicing (e.g., Farre and Araya, 2002; Farre et al., 2001). Interestingly, isolated plant, mammalian, and yeast mitochondria were shown to be competent in importing linear DNA via the VDAC (Koulintchenko et al., 2003, 2006; Weber-Lotfi et al., 2009). Using this natural DNA mitochondrial uptake, several mitochondrial gene expression studies were performed. In rat mitochondria, the imported DNA can act as a template for DNA synthesis or transcription and the resulting polycistronic RNA is correctly processed (Koulintchenko et al., 2006). In plant mitochondria, direct DNA uptake followed by subsequent *in organello* transcription, thanks to the presence of a mitochondrial promoter, permitted to show that a defective unedited tRNA precursor molecule is degraded through a polyadenylation-dependent pathway (Placido et al., 2005). This strategy was also used to detect a previously unreported tRNA<sup>His</sup>-dependent guanylyl transferase activity in plant mitochondria (Placido et al., 2010). Finally, a third approach has been described by Yoon and Koob (2005). They used the natural capacity of bacteria to transfer DNA by conjugation to target a plasmid into the mitochondrial matrix of isolated mice mitochondria and to obtain T7-mediated transcription of the construct within the organelle. However, so far, none of these three approaches (electroporation, direct uptake, and conjugation) allowed the detection of any translation of an exogenous gene.

The only report of mitochondrial translation of exogenous genes was obtained by stable genetic transformation of mitochondrial DNA in yeast (Cohen and Fox, 2001; Steele et al., 1996). The method consists in delivering DNA molecules by microprojectile bombardment (biolistic transformation) and their subsequent homologous recombination into the mitochondrial DNA. Indeed, highly active homologous recombination machinery exists in organelles. This strategy allows to insert defined

mutations into endogenous mitochondrial genes or to insert new genes (e.g., the green fluorescent protein [GFP]) into mitochondrial DNA. Mitochondrial biolistic transformation based on homologous recombination was also successful in the unicellular green alga *Chlamydomonas* (Bonnefoy et al., 2007; Remacle et al., 2006). However, no translation of exogenous gene has yet been described in this organism. An important aspect in the development of mitochondrial transformation resides in finding valuable selection markers for mitochondrial transformants. Both *S. cerevisiae* and *C. reinhardtii* mitochondrial transformants can be selected by their ability to grow on selective media requiring active mitochondrial function. In practice, mitochondrial DNA mutations are rescued by the transfected DNA construct and lead to complementation of the respiratory defect on selective media. Beside the fact that these two models offer a large variety of viable mitochondrial mutants that can be complemented, it has also been possible to transfect DNA pieces in the yeast mitochondrial genome so as to express foreign proteins allowing a visible screening. This serves as a mitochondrial genetic marker independently of respiration function. For example, the expression of a GFP recoded gene expressed in yeast mitochondria can be visualized by fluorimetry (Cohen and Fox, 2001). Another example is a synthetic gene ARG8<sup>m</sup> that allows nuclear *arg8* yeast mutants to grow without arginine (Steele et al., 1996). Another selection principle relies on the use of several inhibitors of bacterial protein synthesis that can impair respiratory growth of wild-type yeast. In that context, mutations conferring resistance can serve as genetic markers. For example, mutations in the mitochondrial ribosomal RNA genes can lead to resistance to chloramphenicol, erythromycin, or paromomycin (Bonnefoy et al., 2007). In *Chlamydomonas*, the cytochrome *b* mutation *Mu* confers resistance to myxothiazol and mucidine (Remacle et al., 2006). Taken together, this shows that stable mitochondrial transformation is accessible in lower eukaryotic organisms such as yeast and *Chlamydomonas*. Many attempts to stably transform plant or mammalian mitochondria have failed so far and this constitutes one of the biggest challenges in the next future.

### 6.3. RNA import

Natural import of RNA into mitochondria may represent another promising strategy for manipulating mitochondrial genetics. As reported here, the vast majority of nuclear-encoded RNAs that are imported into mitochondria are tRNAs. Nearly 80 known pathogenic point mutations affect mitochondrial tRNAs in human. These mutations cause poor aminoacylation, hypomodification, or low stability of the tRNA, and result in disorders in mitochondrial protein synthesis (Florentz et al., 2003).

Two strategies were developed to partially rescue the absence of a functional tRNA<sup>Lys</sup> in human mitochondria affected by the MERRF

(myoclonic epilepsy and red ragged fibers) syndrome. This neurodegenerative disease is due to a mutation in the mitochondrial tRNA<sup>Lys</sup> gene (A8344G) that causes a premature termination of translation at some lysine codons (Enriquez et al., 1995). Kolesnikova and colleagues have shown that tRNA<sup>Lys</sup> derivatives expressed in patient-derived fibroblasts bearing the MERRF mutation are imported into mitochondria (Kolesnikova et al., 2000). Imported tRNAs are correctly aminoacylated and able to participate in translation, which allowed a partial rescue of mitochondrial translation, restoration of respiratory complexes activity, and associated respiration rate. In a second approach, targeting of human cytosolic tRNA<sup>Lys</sup> was mediated using *L. tropica* RIC after its reconstitution on mitochondrial membranes when incubated with human cells (Mahata et al., 2006).

Using the RIC, small antisense RNAs bearing tRNA import signals of *Leishmania* were also targeted to mitochondria of HepG2 cells. These antisense RNAs hybridize specifically to the 5'-terminal mitochondrial mRNAs coding regions spanning the 5–6 first codons. Although efficient import of the antisense transcripts triggered specific degradation of mitochondrial RNA targets (Mukherjee et al., 2008), a recent editorial expression of concern (Schekman, 2010) regarding some work of this team leads us to consider the present data with caution.

The use of naturally imported RNA molecules other than tRNAs as vehicles to deliver sequences with therapeutic activities is also interesting to consider. Indeed a tRNA structure can limit the size and the nature of the associated RNA sequences to be targeted to mitochondria. Another candidate is the 5S rRNA, that is, naturally imported into human mitochondria (Magalhaes et al., 1998). Several 5S rRNA derivatives with additional oligonucleotidic extensions or insertions were targeted to mitochondria *in vivo* without losing the mitochondrial import capacity (Smimov et al., 2008a,b, 2010). This data has been obtained in frame of the study on 5S rRNA import determinants, thus the additional sequences tested were not designed to add any specific activity on mitochondrial genetics. The use of this RNA as delivery vector is still to be investigated. Similarly, the RNA targeting signal sequences identified on the RNA components of RNase P and RNase MRP during the characterization of the human PNPASE as a mitochondrial RNA import receptor (Wang et al., 2010) open a new field of research.

Finally, electroporation of mRNAs into isolated plant mitochondria has been described and allowed the study of the processing of mRNA precursors (Hinrichsen et al., 2009). All these approaches are promising, but still present major drawbacks. This can be either the instability of the molecule involved or the difficulty in its internalization or expression. Integrity of mitochondria or toxicity can also represent high limitations in exploiting RNA or DNA mitochondrial import for applied research. However, the different approaches presented above hold great promise and very likely will offer new area of research in a close future.

## 7. CONCLUSION AND PROSPECTS

Mitochondria fulfill important functions in essential cellular processes. The “present-day” mitochondrial genome only encodes a subset of macromolecules, and the import of nuclear-encoded proteins and RNAs (mostly tRNAs) represents key processes in the organelle biogenesis. More than 1000 nuclear-encoded proteins are imported into mitochondria. Since the first studies on mitochondrial protein import in 1977 (Harmey et al., 1977), numerous genetics and biochemical studies combined to more recent proteomic analysis now permit to have a very precise idea of the different pathways involved in mitochondrial protein sorting (Schmidt et al., 2010) and on their evolution in the different eukaryotic branches (Lithgow and Schneider, 2010). Contrary to proteins, only few cytosolic RNAs have yet been identified in the organelle. Nevertheless, the import of these RNAs, in particular tRNAs, is essential, as they represent key elements of the mitochondrial translation machinery. It is, however, surprising to see that in organisms which lack mitochondrial DNA and a translation machinery, such as in the protozoa *T. evansi*, nuclear-encoded tRNAs are still imported (Cristodero et al., 2010). Whether this is the reflect of a recent loss of functional mitochondrial DNA with a still constitutive import of tRNA species or the fact that cytosolic tRNAs may play other functions within the organelle is an open question. Another major difference with proteins is that our knowledge on RNA mitochondrial import is still very poor. Most of the mechanistic data were obtained during the past decade: import determinants, protein factors, and RNA import channels. As described here and in the recent literature, there seem to be major differences between the currently known RNA import models. For example, the protein import pathway and/or the presence of protein carriers do not always seem required, reinforcing the idea of a polyphyletic origin of mitochondrial RNA import. However, it must be stressed that this observation mainly relies on fragmentary and sometimes controversial information. As RNA mitochondrial import is more universal than first believed, it is tempting to speculate that in the next decade a common evolutionary origin of RNA import will emerge. Further experimental work not only will help to better and more carefully address the fundamental question of the RNA import mechanism but also will provide new tools to incorporate foreign RNA molecules in the organelle. In this field also, the various approaches presented in this review are promising, nevertheless they also present important drawbacks. Mitochondria are involved in many human diseases that cannot be ignored anymore. The development and optimization of RNA mitochondrial import strategies to cure mitochondrial diseases represent a major challenge to fight mitochondrial disorders.



## REFERENCES

- Adhya, S., 2008. *Leishmania* mitochondrial tRNA importers. *Int. J. Biochem. Cell Biol.* 40, 2681–2685.
- Akashi, K., Sakurai, K., Hirayama, J., Fukuzama, H., Ohyama, K., 1996. Occurrence of nuclear-encoded tRNA<sup>Leu</sup> in mitochondria of the liverwort *Marchantia polymorpha*. *Curr. Genet.* 30, 181–185.
- Alfonzo, J.D., Söll, D., 2009. Mitochondrial tRNA import—the challenge to understand has just begun. *Biol. Chem.* 390, 717–722.
- Alfonzo, J.D., Blanc, V., Estevez, A.M., Rubio, M.A., Simpson, L., 1999. C to U editing of the anticodon of imported mitochondrial tRNA(Trp) allows decoding of the UGA stop codon in *Leishmania tarentolae*. *EMBO J.* 18, 7056–7062.
- Bai, Y., Hájek, P., Chomyn, A., Chan, E., Seo, B.B., Matsuno-Yagi, A., et al., 2001. Lack of complex I activity in human cells carrying a mutation in MtDNA-encoded ND4 subunit is corrected by the *Saccharomyces cerevisiae* NADH-quinone oxidoreductase (NDI1) gene. *J. Biol. Chem.* 276, 38808–38813.
- Bhattacharyya, S.N., Chatterjee, S., Adhya, S., 2002. Mitochondrial RNA import in *Leishmania tropica*: aptamers homologous to multiple tRNA domains that interact cooperatively or antagonistically at the inner membrane. *Mol. Cell. Biol.* 22, 4372–4382.
- Bian, Z., Li, L.M., Tang, R., Hou, D.X., Chen, X., Zhang, C.Y., et al., 2010. Identification of mouse liver mitochondria-associated miRNAs and their potential biological functions. *Cell Res.* 20, 1076–1078.
- Bonnefoy, N., Fox, T.D., 2007. Directed alteration of *Saccharomyces cerevisiae* mitochondrial DNA by biolistic transformation and homologous recombination. *Methods Mol. Biol.* 372, 153–166.
- Bonnefoy, N., Remacle, C., Fox, T.D., 2007. Genetic transformation of *Saccharomyces cerevisiae* and *Chlamydomonas reinhardtii* mitochondria. *Methods Cell Biol.* 80, 525–548.
- Bonnet, C., Kaltimbacher, V., Ellouze, S., Augustin, S., Benit, P., Forster, V., et al., 2007. Allotopic mRNA localization to the mitochondrial surface rescues respiratory chain defects in fibroblasts harboring mitochondrial DNA mutations affecting complex I or v subunits. *Rejuvenation Res.* 10, 127–144.
- Bonnet, C., Augustin, S., Ellouze, S., Bénit, P., Bouaita, A., Rustin, P., et al., 2008. The optimized allotopic expression of ND1 or ND4 genes restores respiratory chain complex I activity in fibroblasts harboring mutations in these genes. *Biochim. Biophys. Acta* 1783, 1707–1717.
- Bouzaidi-Tiali, N., Aeby, E., Charriere, F., Pusnik, M., Schneider, A., 2007. Elongation factor 1a mediates the specificity of mitochondrial tRNA import in *T. brucei*. *EMBO J.* 26, 4302–4312.
- Boxma, B., de Graaf, R.M., van der Staay, G.W., van Alen, T.A., Ricard, G., Gabaldon, T., et al., 2005. An anaerobic mitochondrion that produces hydrogen. *Nature* 434, 74–79.
- Brubacher-Kauffmann, S., Maréchal-Drouard, L., Cosset, A., Dietrich, A., Duchêne, A.M., 1999. Differential import of nuclear-encoded tRNA<sup>Gly</sup> isoacceptors into *Solanum tuberosum* mitochondria. *Nucleic Acids Res.* 27, 2037–2042.
- Budar, F., Pelletier, G., 2001. Male sterility in plants: occurrence, determinism, significance and use. *C. R. Acad. Sci. III Sci. Vie* 324, 543–550.
- Cahill, A., Baio, D.L., Cunningham, C.C., 1995. Isolation and characterization of rat liver mitochondrial ribosomes. *Anal. Biochem.* 232, 47–55.
- Cai, S., Xu, Y., Cooper, R.J., Ferkowicz, M.J., Hartwell, J.R., Pollok, K.E., et al., 2005. Mitochondrial targeting of human O6-methylguanine DNA methyltransferase protects against cell killing by chemotherapeutic alkylating agents. *Cancer Res.* 65, 3319–3327.
- Castandet, B., Choury, D., Bégu, D., Jordana, X., Araya, A., 2010. Intron RNA editing is essential for splicing in plant mitochondria. *Nucleic Acids Res.* 38, 7112–7121.

- Ceci, L.R., Veronico, P., Gallerani, R., 1996. Identification and mapping of tRNA genes on the *Helianthus annuus* mitochondrial genome. *DNA Seq.* 6, 159–166.
- Chacinska, A., Koehler, C.M., Milenkovic, D., Lithgow, T., Pfanner, N., 2009. Importing mitochondrial proteins: machineries and mechanisms. *Cell* 138, 628–644.
- Chang, D.D., Clayton, D.A., 1987. A mammalian mitochondrial RNA processing activity contains nucleus-encoded RNA. *Science* 235, 1178–1184.
- Charriere, F., Helgadottir, S., Horn, E.K., Soll, D., Schneider, A., 2006. Dual targeting of a single tRNA(Trp) requires two different tryptophanyl-tRNA synthetases in *Trypanosoma brucei*. *Proc. Natl. Acad. Sci. USA* 103, 6847–6852.
- Chen, H.W., Koehler, C.M., Teittel, M.A., 2007. Human polynucleotide phosphorylase: location matters. *Trends Cell Biol.* 17, 600–608.
- Chinnery, P., Taylor, R., Diekert, K., Lill, R., Turnbull, D., Lightowlers, R., 2000. Peptide nucleic acid and delivery to human mitochondria. *Gene Ther.* 7, 813.
- Chiu, N., Chiu, A., Suyama, Y., 1975. Native and imported transfer RNA in mitochondria. *J. Mol. Biol.* 99, 37–50.
- Cipollone, R., Ascenzi, P., Visca, P., 2007. Common themes and variations in the rhodanese superfamily. *IUBMB Life* 59, 51–59.
- Claros, M.G., Perea, J., Shu, Y., Samatey, F.A., Popot, J.L., Jacq, C., 1995. Limitations to in vivo import of hydrophobic proteins into yeast mitochondria. The case of a cytoplasmically synthesized apocytochrome b. *Eur. J. Biochem.* 228, 762–771.
- Cohen, J.S., Fox, T.D., 2001. Expression of green fluorescent protein from a recoded gene inserted into *Saccharomyces cerevisiae* mitochondrial DNA. *Mitochondrion* 1, 181–189.
- Collombet, J.M., Wheeler, V.C., Vogel, F., Coutelle, C., 1997. Introduction of plasmid DNA into isolated mitochondria by electroporation. A novel approach toward gene correction for mitochondrial disorders. *J. Biol. Chem.* 272, 5342–5347.
- Cristodero, M., Seebeck, T., Schneider, A., 2010. Mitochondrial translation is essential in bloodstream forms of *Trypanosoma brucei*. *Mol. Microbiol.* 78, 757–769.
- Cwerman-Thibault, H., Sahel, J.A., Corral-Debrinski, M., 2010. Mitochondrial medicine: to a new era of gene therapy for mitochondrial DNA mutations. *J. Inherit. Metab. Dis.* (in press).
- Delage, L., Dietrich, A., Cosset, A., Maréchal-Drouard, L., 2003a. *In vitro* import of a nuclearly encoded tRNA into mitochondria of *Solanum tuberosum*. *Mol. Cell. Biol.* 23, 4000–4012.
- Delage, L., Duchêne, A.-M., Zaepfel, M., Maréchal-Drouard, L., 2003b. The anticodon and the D-domain sequences are essential determinants for plant cytosolic tRNA(Val) import into mitochondria. *Plant J.* 34, 623–633.
- Dietrich, A., Maréchal-Drouard, L., Carneiro, V., Cosset, A., Small, I.D., 1996. A single base change prevents import of cytosolic tRNA(Ala) into mitochondria in transgenic plants. *Plant J.* 10, 913–918.
- Doersen, C., Guerrier-Takada, C., Altman, S., Attardi, G., 1985. Characterization of an RNase P activity from HeLa cell mitochondria. Comparison with the cytosol RNase P activity. *J. Biol. Chem.* 260, 5942–5949.
- Dörner, M., Altmann, M., Pääbo, S., Mörl, M., 2001. Evidence for import of a lysyl-tRNA into marsupial mitochondria. *Mol. Biol. Cell* 12, 2688–2698.
- Druzhyina, N.M., Musiyenko, S.I., Wilson, G.L., LeDoux, S.P., 2005. Cytokines induce nitric oxide-mediated mtDNA damage and apoptosis in oligodendrocytes. Protective role of targeting 8-oxoguanine glycosylase to mitochondria. *J. Biol. Chem.* 280, 21673–21679.
- D'Souza, G.G., Rammohan, R., Cheng, S.M., Torchilin, V.P., Weissig, V., 2003. DQA-some-mediated delivery of plasmid DNA toward mitochondria in living cells. *J. Control. Release* 92, 189–197.

- D'Souza, G.G., Boddapati, S.V., Weissig, V., 2005. Mitochondrial leader sequence–plasmid DNA conjugates delivered into mammalian cells by DQAsomes co-localize with mitochondria. *Mitochondrion* 5, 352–358.
- Duchêne, A.-M., Maréchal-Drouard, L., 2001. The chloroplast-derived *trnW* and *trnM*-e genes are not expressed in *Arabidopsis* mitochondria. *Biochem. Biophys. Res. Commun.* 285, 1213–1216.
- Duchêne, A.-M., Pujol, C., Maréchal-Drouard, L., 2009. Import of tRNAs and aminoacyl-tRNA synthetases into mitochondria. *Curr. Genet.* 55, 1–18.
- Duchêne, A.M., El Farouk-Ameqrane, S., Sieber, F., Maréchal-Drouard, L., 2010. Import of RNAs into plant mitochondria. In: Kempken, F. (Ed.), *Plant Mitochondria, Advances in Plant Biology*, vol. 1. Springer Science, Berlin 241–260.
- Duret, L., 2000. tRNA gene number and codon usage in the *C. elegans* genome are co-adapted for optimal translation of highly expressed genes. *Trends Genet.* 16, 287–289.
- Eilers, M., Schatz, G., 1986. Binding of a specific ligand inhibits import of a purified precursor protein into mitochondria. *Nature* 322, 228–232.
- Ellouze, S., Augustin, S., Bouaita, A., Bonnet, C., Simonutti, M., Forster, V., et al., 2008. Optimized allotopic expression of the human mitochondrial ND4 prevents blindness in a rat model of mitochondrial dysfunction. *Am. J. Hum. Genet.* 83, 373–387.
- Enriquez, J.A., Chomyn, A., Attardi, G., 1995. MtDNA mutation in MERRF syndrome causes defective aminoacylation of tRNA(Lys) and premature translation termination. *Nat. Genet.* 10, 47–55.
- Entelis, N.S., Krasheninnikov, I.A., Martin, R.P., Tarassov, I., 1996. Mitochondrial import of a yeast cytoplasmic tRNA (Lys): possible roles of aminoacylation and modified nucleosides in subcellular partitioning. *FEBS Lett.* 384, 38–42.
- Entelis, N.S., Kieffer, S., Kolesnikova, O.A., Martin, R.P., Tarassov, I., 1998. Structural requirements of tRNALys for its import into yeast mitochondria. *Proc. Natl. Acad. Sci. USA* 95, 2838–2843.
- Entelis, N.S., Kolesnikova, O.A., Dogan, S., Martin, R.P., Tarassov, I., 2001a. 5 S rRNA and tRNA import into human mitochondria. Comparison of *in vitro* requirements. *J. Biol. Chem.* 276, 45642–45653.
- Entelis, N.S., Kolesnikova, O.A., Martin, R.P., Tarassov, I., 2001b. RNA delivery into mitochondria. *Adv. Drug Deliv. Rev.* 49, 199–215.
- Entelis, N.S., Kolesnikova, O., Kazakova, H., Brandina, I., Kamenski, P., Martin, R.P., et al., 2002. Import of nuclear encoded RNAs into yeast and human mitochondria: experimental approaches and possible biomedical applications. *Genet. Eng. (N.Y.)* 24, 191–213.
- Entelis, N.S., Brandina, I., Kamenski, P., Krasheninnikov, I.A., Martin, R.P., Tarassov, I., 2006. A glycolytic enzyme, enolase, is recruited as a cofactor of tRNA targeting toward mitochondria in *Saccharomyces cerevisiae*. *Genes Dev.* 20, 1609–1620.
- Esseiva, A.C., 2004. Mitochondrial tRNA Import in *Toxoplasma gondii*. *J. Biol. Chem.* 279, 42363–42368.
- Estévez, A.M., Thiemann, O.H., Alfonso, J.D., Simpson, L., 1999. T7 RNA polymerase-driven transcription in mitochondria of *Leishmania tarentolae* and *Trypanosoma brucei*. *Mol. Biochem. Parasitol.* 103, 251–259.
- Evans, D., Marquez, S.M., Pace, N.R., 2006. RNase P: interface of the RNA and protein worlds. *Trends Biochem. Sci.* 31, 333–341.
- Farre, J.C., Araya, A., 2002. RNA splicing in higher plant mitochondria: determination of functional elements in group II intron from a chimeric *cox II* gene in electroporated wheat mitochondria. *Plant J.* 29, 203–213.
- Farré, J.-C., Araya, A., 2001. Gene expression in isolated plant mitochondria: high fidelity of transcription, splicing and editing of a transgene product in electroporated organelles. *Nucleic Acids Res.* 29, 2484–2491.

- Farre, J.C., Leon, G., Jordana, X., Araya, A., 2001. Cis recognition elements in plant mitochondrion RNA editing. *Mol. Cell. Biol.* 21, 6731–6737.
- Florentz, C., Sohm, B., Tryoen-Tóth, P., Pütz, J., Sissler, M., 2003. Human mitochondrial tRNAs in health and disease. *Cell. Mol. Life Sci.* 60, 1356–1375.
- Foury, F., Roganti, T., Lecrenier, N., Purnelle, B., 1998. The complete sequence of the mitochondrial genome of *Saccharomyces cerevisiae*. *FEBS Lett.* 440, 325–331.
- Fox, T.D., Sanford, J.C., McMullin, T.W., 1988. Plasmids can stably transform yeast mitochondria lacking endogenous mtDNA. *Proc. Natl. Acad. Sci. USA* 85, 7288–7292.
- Frechin, M., Senger, B., Brayé, M., Kern, D., Martin, R.P., Becker, H.D., 2009. Yeast mitochondrial Gln-tRNA(Gln) is generated by a GatFAB-mediated transamidation pathway involving Arc1p-controlled subcellular sorting of cytosolic GluRS. *Genes Dev.* 23, 1119–11130.
- Glover, K.E., Spencer, D.F., Gray, M.W., 2001. Identification and structural characterization of nucleus-encoded transfer RNAs imported into wheat mitochondria. *J. Biol. Chem.* 276, 639–648.
- Gobert, A., Gutmann, B., Taschner, A., Gössringer, M., Holzmann, J., Hartmann, R.K., et al., 2010. A single *Arabidopsis* organellar protein has RNase P activity. *Nat. Struct. Mol. Biol.* 17, 740–744.
- Goldberg, A.V., Molik, S., Tsaousis, A.D., Neumann, K., Kuhnke, G., Delbac, F., et al., 2008. Localization and functionality of microsporidian iron-sulphur cluster assembly proteins. *Nature* 452, 624–628.
- Green, G., Maréchal, L., Weil, J.H., Guillemaut, P., 1987. A *Phaseolus vulgaris* mitochondrial tRNA<sup>Leu</sup> is identical to its cytoplasmic counterpart: sequencing and in vivo transcription of the gene corresponding to the cytoplasmic tRNA<sup>Leu</sup>. *Plant Mol. Biol.* 10, 13–19.
- Haeusler, R.A., Engelke, D.R., 2006. Spatial organization of transcription by RNA polymerase III. *Nucleic Acids Res.* 34, 4826–4836.
- Hakkaart, G.A.J., Dassa, E.P., Jacobs, H.T., Rustin, P., 2006. Allotopic expression of a mitochondrial alternative oxidase confers cyanide resistance to human cell respiration. *EMBO Rep.* 7, 341–345.
- Harmey, M.A., Hallermayer, G., Korb, H., Neupert, W., 1977. Transport of cytoplasmically synthesized proteins into the mitochondria in a cell free system from *Neurospora crassa*. *Eur. J. Biochem.* 81, 533–544.
- Hinrichsen, I., Bolle, N., Paun, L., Kempken, F., 2009. RNA processing in plant mitochondria is independent of transcription. *Plant Mol. Biol.* 70, 663–668.
- Holzmann, J., Frank, P., Löffler, E., Bennett, K.L., Gerner, C., Rossmannith, W., 2008. RNase P without RNA: identification and functional reconstitution of the human mitochondrial tRNA processing enzyme. *Cell* 135, 462–474.
- Initiative, T.A.G., 2000. Analysis of the genome sequence of the flowering plant *Arabidopsis thaliana*. *Nature* 408, 796–815.
- Kamenski, P., Kolesnikova, O.A., Jubenot, V., Entelis, N.S., Krashennikov, I.A., Martin, R.P., et al., 2007. Evidence for an adaptation mechanism of mitochondrial translation via tRNA import from the cytosol. *Mol. Cell* 26, 625–637.
- Kapushoc, S., Alfonzo, J.D., Simpson, L., 2002. Differential localization of nuclear-encoded tRNAs between the cytosol and mitochondrion in *Leishmania tarentolae*. *RNA* 8, 57–68.
- Kiss, T., Filipowicz, W., 1992. Evidence against a mitochondrial location of the 7-2/MRP RNA in mammalian cells. *Cell* 70, 11–26.
- Kolesnikova, O.A., Entelis, N.S., Mireau, H., Fox, T.D., Martin, R.P., Tarasov, I., 2000. Suppression of mutations in mitochondrial DNA by tRNAs imported from the cytoplasm. *Science* 289, 1931–1933.
- Kolesnikova, O.A., Entelis, N.S., Jacquin-Becker, C., Goltzene, F., Chrzanowska-Lightowlers, Z.M., Lightowlers, R.N., et al., 2004. Nuclear DNA-encoded tRNAs

- targeted into mitochondria can rescue a mitochondrial DNA mutation associated with the MERRF syndrome in cultured human cells. *Hum. Mol. Genet* 13, 2519–2534.
- Koulintchenko, M., Konstantinov, Y., Dietrich, A., 2003. Plant mitochondria actively import DNA via the permeability transition pore complex. *EMBO J.* 22, 1245–1254.
- Koulintchenko, M., Temperley, R.J., Mason, P.A., Dietrich, A., Lightowers, R.N., 2006. Natural competence of mammalian mitochondria allows the molecular investigation of mitochondrial gene expression. *Hum. Mol. Genet.* 15, 143–154.
- Kren, B.T., Wong, P.Y.-P., Sarver, A., Zhang, X., Zeng, Y., Steer, C.J., 2009. MicroRNAs identified in highly purified liver-derived mitochondria may play a role in apoptosis. *RNA Biol.* 6, 65–72.
- Kroemer, G., Galluzzi, L., Brenner, C., 2007. Mitochondrial membrane permeabilization in cell death. *Physiol. Rev.* 87, 99–163.
- Kumar, R., Maréchal-Drouard, L., Akama, K., Small, I.D., 1996. Striking differences in mitochondrial tRNA import between different plant species. *Mol. Gen. Genet.* 252, 404–411.
- Laforest, M.J., Roewer, I., Lang, B.F., 1997. Mitochondrial tRNAs in the lower fungus *Spizellomyces punctatus*: tRNA editing and UAG ‘stop’ codons recognized as leucine. *Nucleic Acids Res.* 25, 626–632.
- Laforest, M., Delage, L., Maréchal-Drouard, L., 2005. The T-domain of cytosolic tRNA-Val, an essential determinant for mitochondrial import. *FEBS Lett.* 579, 1072–1078.
- Li, K., Smagula, C.S., Parsons, W.J., Richardson, J.A., Gonzalez, M., Hagler, H.K., et al., 1994. Subcellular partitioning of MRP RNA assessed by ultrastructural and biochemical analysis. *J. Cell Biol.* 124, 871–882.
- Lithgow, T., Schneider, A., 2010. Evolution of macromolecular import pathways in mitochondria, hydrogenosomes and mitosomes. *Philos. Trans. R. Soc. Lond. Biol. Sci.* 365, 799–817.
- Magalhaes, P., Andreu, A., Schon, E., 1998. Evidence for the presence of 5S rRNA in mammalian mitochondria. *Mol. Biol. Cell* 9, 2375–2382.
- Mahapatra, S., Adhya, S., 1996. Import of RNA into *Leishmania* mitochondria occurs through direct interaction with membrane-bound receptors. *J. Biol. Chem.* 271, 20432–20437.
- Mahapatra, S., Ghosh, S., Bera, S.K., Ghosh, T., Das, A., Adhya, S., 1998. The D arm of tRNA<sup>Tyr</sup> is necessary and sufficient for import into *Leishmania* mitochondria *in vitro*. *Nucleic Acids Res.* 26, 2037–2041.
- Mahata, B., Mukherjee, S., Mishra, S., Bandyopadhyay, A., Adhya, S., 2006. Functional delivery of a cytosolic tRNA into mutant mitochondria of human cells. *Science* 314, 471–474.
- Maréchal-Drouard, L., Guillemaut, P., Cosset, A., Arbogast, M., Weber, F., Weil, J.H., et al., 1990a. Transfer RNAs of potato (*Solanum tuberosum*) mitochondria have different genetic origins. *Nucleic Acids Res.* 18, 3689–3696.
- Maréchal-Drouard, L., Neuburger, M., Guillemaut, P., Douce, R., Weil, J.H., Dietrich, A., 1990b. A nuclear-encoded potato (*Solanum tuberosum*) mitochondrial tRNA(Leu) and its cytosolic counterpart have identical nucleotide sequences. *FEBS Lett.* 262, 170–172.
- Maréchal-Drouard, L., Dietrich, A., Weil, J.H., 1992. Adaptation of transfer RNA population to codon usage in cellular organelles. In: Hatfield, D., Lee, B.J., Pirtle, R.M. (Eds.), *Transfer RNA in Protein Synthesis*. CRC Press, Boca Raton, pp. 125–140.
- Maréchal-Drouard, L., Weil, J.H., Dietrich, A., 1993. Transfer RNAs and transfer RNA genes in plants. *Annu. Rev. Plant Physiol.* 44, 13–32.
- Margeot, A., Blugeon, C., Sylvestre, J., Vialette, S., Jacq, C., Corral-Debrinski, M., 2002. In *Saccharomyces cerevisiae*, ATP2 mRNA sorting to the vicinity of mitochondria is essential for respiratory function. *EMBO J.* 21, 6893–6904.

- Martin, R.P., Schneller, J.M., Stahl, A., Dirheimer, G., 1979. Import of nuclear deoxyribonucleic acid coded lysine accepting transfer ribonucleic acid (anticodon CUU) into yeast mitochondria. *Biochemistry* 18, 4600–4605.
- Michaelis, G., Vahrenholtz, C., Pratje, E., 1990. Mitochondrial DNA of *Chlamydomonas reinhardtii*: the gene for apocytchrome b and the complete functional map of the 15.8 kb DNA. *Mol. Gen. Genet.* 223, 211–216.
- Michaud, M., Maréchal-Drouard, L., Duchêne, A.M., 2010. RNA trafficking in plant cells: targeting of cytosolic mRNAs to the mitochondrial surface. *Plant Mol. Biol.* 73, 697–704.
- Mirande, M., 2007. The ins and outs of tRNA transport. *EMBO Rep.* 8, 547–549.
- Mukherjee, S., Mahata, B., Mahato, B., Adhya, S., 2008. Targeted mRNA degradation by complex-mediated delivery of antisense RNAs to intracellular human mitochondria. *Hum. Mol. Genet.* 17, 1292–1298.
- Muratovska, A., Lightowlers, R.N., Taylor, R.W., Turnbull, D.M., Smith, R.A., Wilce, J.A., et al., 2001. Targeting peptide nucleic acid (PNA) oligomers to mitochondria within cells by conjugation to lipophilic cations: implications for mitochondrial DNA replication, expression and disease. *Nucleic Acids Res.* 29, 1852–1863.
- Nabholz, C., Horn, E.K., Schneider, A., 1999. tRNAs and proteins are imported into mitochondria of *Trypanosoma brucei* by two distinct mechanisms. *Mol. Biol. Cell* 10, 2547–2557.
- Nagao, A., Suzuki, T., Katoh, T., Sakaguchi, Y., 2009. Biogenesis of glutamyl-tRNA<sup>Gln</sup> in human mitochondria. *Proc. Natl. Acad. Sci. USA* 106, 16209–16214.
- Nakabeppu, Y., 2001. Regulation of intracellular localization of human MTH1, OGG1, and MYH proteins for repair of oxidative DNA damage. *Prog. Nucleic Acid Res. Mol. Biol.* 68, 75–94.
- Neupert, W., Herrmann, J., 2007. Translocation of proteins into mitochondria. *Annu. Rev. Biochem.* 76, 723–749.
- Notsu, Y., Masood, S., Nishikawa, T., Kubo, N., Akiduki, G., Nakazono, M., et al., 2002. The complete sequence of the rice (*Oryza sativa* L.) mitochondrial genome: frequent DNA sequence acquisition and loss during the evolution of flowering plants. *Mol. Genet. Genomics* 268, 434–445.
- Paris, Z., Rubio, M.A., Lukes, J., Alfonzo, J.D., 2009. Mitochondrial tRNA import in *Trypanosoma brucei* is independent of thiolation and the Rieske protein. *RNA* 15, 1398–1406.
- Pino, P., Aeby, E., Foth, B.J., Sheiner, L., Soldati, T., Schneider, A., et al., 2010. Mitochondrial translation in absence of local tRNA aminoacylation and methionyl tRNA formylation in Apicomplexa. *Mol. Microbiol.* 76, 706–718.
- Placido, A., Gagliardi, D., Gallerani, R., Grienberger, J., Maréchal-Drouard, L., 2005. Fate of a larch unedited tRNA precursor expressed in potato mitochondria. *J. Biol. Chem.* 280, 33573–33579.
- Placido, A., Regina, T.M., Quagliariello, C., Volpicella, M., Gallerani, R., Ceci, L.R., 2009. Mapping of 5' and 3'-ends of sunflower mitochondrial nad6 mRNAs reveals a very complex transcription pattern which includes primary transcripts lacking 5'-UTR. *Biochimie* 91, 924–932.
- Placido, A., Sieber, F., Gobert, A., Gallerani, R., Giegé, P., Maréchal-Drouard, L., 2010. Plant mitochondria use two pathways for the biogenesis of tRNA<sup>His</sup>. *Nucleic Acids Res.* 38, 7711–7717.
- Puranam, R.S., Attardi, G., 2001. The RNase P associated with HeLa cell mitochondria contains an essential RNA component identical in sequence to that of the nuclear RNase P. *Mol. Cell. Biol.* 21, 548–561.
- Rachek, L.I., Grishko, V.I., Musiyenko, S.I., Kelley, M.R., LeDoux, S.P., Wilson, G.L., 2002. Conditional targeting of the DNA repair enzyme hOGG1 into mitochondria. *J. Biol. Chem.* 277, 44932–44937.

- Rasmussen, A.K., Rasmussen, L.J., 2005. Targeting of O6-MeG DNA methyltransferase (MGMT) to mitochondria protects against alkylation induced cell death. *Mitochondrion* 5, 411–417.
- Remacle, C., Cardol, P., Coosemans, N., Gaisne, M., Bonnefoy, N., 2006. High-efficiency biolistic transformation of *Chlamydomonas* mitochondria can be used to insert mutations in complex I genes. *Proc. Natl. Acad. Sci. USA* 103, 4771–4776.
- Rinehart, J., 2005. *Saccharomyces cerevisiae* imports the cytosolic pathway for Gln-tRNA synthesis into the mitochondrion. *Genes Dev.* 19, 583–592.
- Rossmannith, W., Karwan, R.M., 1998. Characterization of human mitochondrial RNase P: novel aspects in tRNA processing. *Biochem. Biophys. Res. Commun.* 247, 234–241.
- Rubio, M.A., Liu, X., Yuzawa, H., Alfonso, J.D., Simpson, L., 2000. Selective importation of RNA into isolated mitochondria from *Leishmania tarentolae*. *RNA* 6, 988–1003.
- Rubio, M., Rinehart, J., Krett, B., Duvezin-Caubet, S., Reichert, A., Soll, D., et al., 2008. Mammalian mitochondria have the innate ability to import tRNAs by a mechanism distinct from protein import. *Proc. Natl. Acad. Sci. USA* 105, 9186–9191.
- Rusconi, C.P., Cech, T.R., 1996a. The anticodon is the signal sequence for mitochondrial import of glutamine tRNA in *Tetrahymena*. *Genes Dev.* 10, 2870–2880.
- Rusconi, C.P., Cech, T.R., 1996b. Mitochondrial import of only one of three nuclear-encoded glutamine tRNAs in *Tetrahymena thermophila*. *EMBO J.* 15, 3286–3295.
- Rustin, P., Jacobs, H.T., Dietrich, A., Lightowlers, R.N., Tarassov, I., Corral-Debrinski, M., 2007. Targeting allotopic material to the mitochondrial compartment: new tools for better understanding mitochondrial physiology and prospect for therapy. *Med. Sci. (Paris)* 23, 519–525.
- Salinas, T., Schaeffer, C., Maréchal-Drouard, L., Duchêne, A.-M., 2005. Sequence dependence of tRNA(Gly) import into tobacco mitochondria. *Biochimie* 87, 863–872.
- Salinas, T., Duchêne, A.-M., Delage, L., Nilsson, S., Glaser, E., Zaepfel, M., et al., 2006. The voltage-dependent anion channel, a major component of the tRNA import machinery in plant mitochondria. *Proc. Natl. Acad. Sci. USA* 103, 18362–18367.
- Salinas, T., Duchêne, A.-M., Maréchal-Drouard, L., 2008. Recent advances in tRNA mitochondrial import. *Trends Biochem. Sci.* 33, 320–329.
- Schekman, R., 2010. Editorial expression of concern. *Proc. Natl. Acad. Sci. USA* 107, 9476.
- Scherrer, R., Yermovsky-Kammerer, A., Hadjuk, S., 2003. A sequence motif within trypanosome precursor tRNAs influences abundance and mitochondrial localization. *Mol. Cell. Biol.* 23, 9061–9072.
- Schmidt, O., Pfanner, N., Meisinger, C., 2010. Mitochondrial protein import: from proteomics to functional mechanisms. *Nat. Rev. Mol. Cell Biol.* 11, 655–667.
- Schneider, A., Maréchal-Drouard, L., 2000. Mitochondrial tRNA import: are there distinct mechanisms? *Trends Cell Biol.* 10, 509–513.
- Schneider, A., Martin, J., Agabian, N., 1994. A nuclear-encoded tRNA of *Trypanosoma brucei* is imported into mitochondria. *Mol. Cell. Biol.* 14, 2317–2322.
- Seo, B.B., Kitajima-Ihara, T., Chan, E.K., Scheffler, I.E., Matsuno-Yagi, A., Yagi, T., 1998. Molecular remedy of complex I defects: rotenone-insensitive internal NADH-quinone oxidoreductase of *Saccharomyces cerevisiae* mitochondria restores the NADH oxidase activity of complex I-deficient mammalian cells. *Proc. Natl. Acad. Sci. USA* 95, 9167–9171.
- Seo, B.B., Nakamaru-Ogiso, E., Cruz, P., Flotte, T.R., Yagi, T., Matsuno-Yagi, A., 2004. Functional expression of the single subunit NADH dehydrogenase in mitochondria *in vivo*: a potential therapy for complex I deficiencies. *Hum. Gene Ther.* 15, 887–895.
- Sharma, M.R., Koc, E.C., Datta, P.P., Booth, T.M., Spremulli, L.L., Agrawal, R.K., 2003. Structure of the mammalian mitochondrial ribosome reveals an expanded functional role for its component proteins. *Cell* 115, 97–108.

- Shi, X., Chen, D.T.C., Suyama, Y., 1994. A nuclear tRNA gene cluster in the protozoan *Leishmania tarentolae* and differential distribution of nuclear-encoded tRNAs between the cytosol and mitochondria. *Mol. Biochem. Parasitol.* 65, 23–37.
- Small, I.D., Maréchal-Drouard, L., Masson, J., Pelletier, G., Cosset, A., Weil, J.H., et al., 1992. In vivo import of a normal or mutagenized heterologous transfer RNA into the mitochondria of transgenic plants—towards novel ways of influencing mitochondrial gene expression. *EMBO J.* 11, 1291–1296.
- Small, I., Akashi, K., Chapron, A., Dietrich, A., Duchêne, A.-M., Lancelin, D., et al., 1999. The strange evolutionary history of plant mitochondrial tRNAs and their aminoacyl-tRNA synthetases. *J. Hered.* 90, 333–337.
- Smirnov, A., Entelis, N.S., Krashennikov, I.A., Martin, R., Tarassov, I., 2008a. Specific features of 5S rRNA structure—its interactions with macromolecules and possible functions. *Biochemistry (Mosc)* 73, 1418–1437.
- Smirnov, A., Tarassov, I., Mager-Heckel, A.-M., Letzelter, M., Martin, R.P., Krashennikov, I.A., et al., 2008b. Two distinct structural elements of 5S rRNA are needed for its import into human mitochondria. *RNA* 14, 749–759.
- Smirnov, A., Comte, C., Mager-Heckel, A.-M., Addis, V., Krashennikov, I.A., Martin, R.P., et al., 2010. Mitochondrial enzyme rhodanese is essential for 5S ribosomal RNA import into human mitochondria. *J. Biol. Chem.* 285, 30792–30803.
- Srivastava, S., Moraes, C.T., 2001. Manipulating mitochondrial DNA heteroplasmy by a mitochondrially targeted restriction endonuclease. *Hum. Mol. Genet.* 10, 3093–3099.
- Staudinger, M., Bolle, N., Kempken, F., 2005. Mitochondrial electroporation and in organello RNA editing of chimeric atp6 transcripts. *Mol. Genet. Genomics* 273, 130–136.
- Steele, D.F., Butler, C.A., Fox, T.D., 1996. Expression of a recoded nuclear gene inserted into yeast mitochondrial DNA is limited by mRNA-specific translational activation. *Proc. Natl. Acad. Sci. USA* 93, 5253–5257.
- Sugiyama, Y., Watase, Y., Nagase, M., Makita, N., Yagura, S., Hirai, A., et al., 2005. The complete nucleotide sequence and multipartite organization of the tobacco mitochondrial genome: comparative analysis of mitochondrial genomes in higher plants. *Mol. Gen. Genet.* 272, 603–615.
- Suyama, Y., 1967. The origins of mitochondrial ribonucleic acids in *Tetrahymena pyriformis*. *Biochemistry* 6, 2829–2839.
- Suyama, Y., 1986. Two dimensional polyacrylamide gel electrophoresis analysis of *Tetrahymena* mitochondrial tRNA. *Curr. Genet.* 10, 411–420.
- Suyama, Y., Wong, S., Campbell, D.A., 1998. Regulated tRNA import in *Leishmania* mitochondria. *Biochim. Biophys. Acta* 1396, 138–142.
- Sylvestre, J., Margeot, A., Jacq, C., Dujardin, G., Corral-Debrinski, M., 2003. The role of the 3' untranslated region in mRNA sorting to the vicinity of mitochondria is conserved from yeast to human cells. *Mol. Biol. Cell* 14, 3848–3856.
- Szymanski, M., Barciszewska, M.Z., Erdmann, V.A., Barciszewski, J., 2003. 5 S rRNA: structure and interactions. *Biochem. J.* 371, 641–651.
- Tan, T., Pach, R., Crausaz Esseiva, A., Ivens, A., Schneider, A., 2002a. tRNAs in *Trypanosoma brucei*: genomic organization, expression, and mitochondrial import. *Mol. Cell. Biol.* 22, 3707–3717.
- Tan, T.H.P., Bochud-Allemann, N., Schneider, A., 2002b. Eukaryotic-type elongator tRNAMet of *Trypanosoma brucei* becomes formylated after import into mitochondria. *Proc. Natl. Acad. Sci. USA* 99, 1152–1157.
- Tarassov, I.A., Entelis, N.S., 1992. Mitochondrially-imported cytoplasmic tRNA(Lys) (CUU) of *Saccharomyces cerevisiae*: in vivo and in vitro targeting systems. *Nucleic Acids Res.* 20, 1277–1281.



- Tarassov, I., Entelis, N.S., Martin, R.P., 1995a. An intact protein translocating machinery is required for mitochondrial import of a yeast cytoplasmic tRNA. *J. Mol. Biol.* 245, 315–323.
- Tarassov, I., Entelis, N.S., Martin, R.P., 1995b. Mitochondrial import of a cytoplasmic lysine-tRNA in yeast is mediated by cooperation of cytoplasmic and mitochondrial lysyl-tRNA synthetases. *EMBO J.* 14, 3461–3471.
- Taylor, R.W., Chinnery, P.F., Turnbull, D.M., Lightowers, R.N., 1997. Selective inhibition of mutant human mitochondrial DNA replication in vitro by peptide nucleic acids. *Nat. Genet.* 15, 212–215.
- Taylor, R.W., Chinnery, P.F., Turnbull, D.M., Lightowers, R.N., 2000. *In vitro* genetic modification of mitochondrial function. *Hum. Reprod.* 15 (Suppl. 2), 79–85.
- Terasawa, K., Odahara, M., Kabeya, Y., Kikugawa, T., Sekine, Y., Fujiwara, M., et al., 2007. The mitochondrial genome of the moss *Physcomitrella patens* sheds new light on mitochondrial evolution in land plants. *Mol. Biol. Evol.* 24, 699–709.
- Topper, J.N., Bennett, J.L., Clayton, D.A., 1992. A role for RNAase MRP in mitochondrial RNA processing. *Cell* 70, 16–20.
- Trifunovic, A., Wredenberg, A., Falkenberg, M., Spelbrink, J.N., Rovio, A.T., Bruder, C. E., et al., 2004. Premature ageing in mice expressing defective mitochondrial DNA polymerase. *Nature* 429, 417–423.
- Vestweber, D., Schatz, G., 1989. DNA-protein conjugates can enter mitochondria via the protein import pathway. *Nature* 338, 170–172.
- Vinogradova, E., Salinas, T., Cognat, V., Remacle, C., Maréchal-Drouard, L., 2009. Steady-state levels of imported tRNAs in *Chlamydomonas* mitochondria are correlated with both cytosolic and mitochondrial codon usages. *Nucleic Acids Res.* 37, 1521–1528.
- Wang, G., Chen, H.-W., Oktay, Y., Zhang, J., Allen, E.L., Smith, G.M., et al., 2010. PNPASE regulates RNA import into mitochondria. *Cell* 142, 456–467.
- Wanrooij, S., Falkenberg, M., 2010. The human mitochondrial replication fork in health and disease. *Biochim. Biophys. Acta* 1797, 1378–1388.
- Weber, T.A., Reichert, A.S., 2010. Impaired quality control of mitochondria: aging from a new perspective. *Exp. Gerontol.* 45, 503–511.
- Weber-Lotfi, F., Ibrahim, N., Boesch, P., Cosset, A., Konstantinov, Y., Lightowers, R.N., et al., 2009. Developing a genetic approach to investigate the mechanism of mitochondrial competence for DNA import. *Biochim. Biophys. Acta* 1787, 320–327.
- Weissig, V., Torchilin, V.P., 2001. Towards mitochondrial gene therapy: DQAsomes as a strategy. *J. Drug Target.* 9, 1–13.
- Weissig, V., Lasch, J., Erdos, G., Meyer, H.W., Rowe, T.C., Hughes, J., 1998. DQAsomes: a novel potential drug and gene delivery system made from Dequalinium. *Pharm. Res.* 15, 334–337.
- Weissig, V., D'Souza, G.G., Torchilin, V.P., 2001. DQAsome/DNA complexes release DNA upon contact with isolated mouse liver mitochondria. *J. Control. Release* 75, 401–408.
- Yermovsky-Kammerer, A., Hajduk, S., 1999. *In vitro* import of a nuclear encoded tRNA into the mitochondrion of *Trypanosoma brucei*. *Mol. Cell. Biol.* 19, 6253–6259.
- Yoon, Y.G., Koob, M.D., 2005. Transformation of isolated mammalian mitochondria by bacterial conjugation. *Nucleic Acids Res.* 33, e139.
- Yoshionari, S., Koike, T., Yokogawa, T., Nishikawa, K., Ueda, T., Miura, K., et al., 1994. Existence of nuclear-encoded 5S-rRNA in bovine mitochondria. *FEBS Lett.* 338, 137–142.

# NEW INSIGHTS INTO VINCULIN FUNCTION AND REGULATION

Xiao Peng, Elke S. Nelson, Jessica L. Maiers, *and* Kris A. DeMali

## Contents

|                                                                                                     |     |
|-----------------------------------------------------------------------------------------------------|-----|
| 1. Introduction                                                                                     | 192 |
| 2. Vinculin Structure                                                                               | 193 |
| 2.1. Global structure                                                                               | 193 |
| 2.2. Vinculin head domain                                                                           | 195 |
| 2.3. Proline-rich linker                                                                            | 196 |
| 2.4. Vinculin tail domain                                                                           | 196 |
| 3. Autoinhibited Conformation and Vinculin Activation                                               | 196 |
| 3.1. Autoinhibited conformation                                                                     | 196 |
| 3.2. Activation of vinculin                                                                         | 198 |
| 3.3. Activation by IpaA                                                                             | 200 |
| 3.4. Activation <i>in vivo</i>                                                                      | 200 |
| 4. Biological Functions                                                                             | 201 |
| 4.1. Modulation of cell adhesion and migration                                                      | 201 |
| 4.2. Modulation of apoptosis                                                                        | 209 |
| 4.3. Regulation of bacterial entry                                                                  | 209 |
| 5. Modes of Vinculin Regulation                                                                     | 211 |
| 5.1. Regulation of conformational changes: Tyrosine phosphorylation                                 | 211 |
| 5.2. Regulation of vinculin expression                                                              | 212 |
| 6. Emerging Themes and Concepts                                                                     | 214 |
| 6.1. Vinculin in adherens junctions                                                                 | 214 |
| 6.2. Vinculin recruitment to adhesion sites                                                         | 218 |
| 7. Interplay Between Cell–Cell and Cell–Matrix Adhesion: Vinculin in Development and Cardiomyopathy | 219 |
| 8. Conclusions                                                                                      | 222 |
| Acknowledgments                                                                                     | 222 |
| References                                                                                          | 222 |

Department of Biochemistry, University of Iowa Roy J. and Lucille A. Carver College of Medicine, Iowa City, Iowa, USA

## Abstract

Vinculin is a cytoplasmic actin-binding protein enriched in focal adhesions and adherens junctions that is essential for embryonic development. Much is now known regarding the role of vinculin in governing cell–matrix adhesion. In the past decade that the crystal structure of vinculin and the molecular details for how vinculin regulates adhesion events have emerged. The recent data suggests a critical function for vinculin in regulating integrin clustering, force generation, and strength of adhesion. In addition to an important role in cell–matrix adhesion, vinculin is also emerging as a regulator of apoptosis, *Shigella* entry into host cells, and cadherin-based cell–cell adhesion. A close inspection of this work reveals that there are similarities between vinculin’s role in focal adhesions and these processes and also some intriguing differences.

**Key Words:** Vinculin, Integrins, Cadherins, Cell adhesion, Force generation, Cell migration and Actin. © 2011 Elsevier Inc.

## 1. INTRODUCTION

Vinculin was originally isolated from chicken gizzard smooth muscle in 1979 as a molecule that copurified with  $\alpha$ -actinin (Geiger, 1979). Initial characterization revealed that this protein was localized at regions where the ends of actin bundles terminated in membrane attachment sites (Burrige and Feramisco, 1980; Geiger et al., 1980). Thus, the protein was named vinculin from the Latin word *vinculum*—meaning a bond signifying a union or unity. The subsequent cloning of full-length chicken vinculin in 1988 paved the way for numerous experiments aimed at better understanding this protein’s function. We now know that vinculin is a 116-kDa cytoplasmic protein that is a component of the membrane-associated adhesion complexes that tether cells to the extracellular matrix (cell–matrix adhesions or focal adhesions) and adjacent cells (cell–cell adhesions or adherens junctions). Vinculin has no enzymatic activity; consequently, its function is governed by protein–protein interactions that are highly regulated, in part by conformational changes. The nature of these conformational changes and how they are regulated is emerging. These insights, together with information from other functional assays, have established a role for vinculin in regulating many aspects of cell–matrix adhesion, including the assembly, turnover, and strength of focal adhesions, as well as the transmission of force by these cellular structures. In addition to its more established role in cell–matrix adhesion, vinculin is also emerging as a functional regulator of cadherin-based cell–cell adhesions. Indeed, recent studies have shown that vinculin is important for surface expression and the mechanosensing of cadherins. These observations are corroborated by

*in vivo* studies illustrating vinculin's vital roles in embryogenesis and diseased states. This chapter highlights recent progress and the emerging models for how vinculin function and regulation are governed.

## 2. VINCULIN STRUCTURE

### 2.1. Global structure

For many years, vinculin has been known to be a compact globular protein (Isenberg et al., 1982) that undergoes a conformational change that exposes a 90-kDa N-terminal globular head (residues 1–811), a short flexible proline-rich linker (residues 811–881), and a 27-kDa C-terminal, extended, rod-shaped tail (residues 881–1066) (Coutu and Craig, 1988; Eimer et al., 1993; Milam, 1985; Molony and Burridge, 1985). The vinculin head domain is further divided into three globular protein masses of similar size, organized in a trilobed planar arrangement associated with a short stem (Winkler and Jockusch, 2001; Winkler et al., 1996). Similar to the head, the tail is also globular. It possesses four distinct masses arranged like pearls on a string (Winkler and Jockusch, 2001; Winkler et al., 1996). The proline-rich linker between the head and tail domains of vinculin is flexible, allowing for sharp kinks in the molecule (Winkler and Jockusch, 2001; Winkler et al., 1996).

More recently, the crystal structures of full-length chicken vinculin (Bakolitsa et al., 2004), full-length human vinculin (Borgon et al., 2004), and a fragment of the human vinculin head (1–258) in complex with a fragment encompassing residues 879–1066 of the tail (Izard et al., 2004) have been solved. All three structures share striking similarities with the original structure deduced from electron micrograph images described above (Winkler and Jockusch, 2001; Winkler et al., 1996). They reveal that vinculin is comprised of eight, antiparallel,  $\alpha$ -helical bundles organized into five distinct domains that are denoted domains 1–5 (D1–D5) by Bakolitsa et al. (2004), and vinculin head 1–3 (Vh1–3) and vinculin tail 1–2 (Vt1–2) by Izard et al. (Borgon et al., 2004). For the remainder of this chapter, we will use the D1–D5 nomenclature to discuss the vinculin structure. With the exception of small differences in vinculin D2 and D3, the two full-length crystal structures are very similar (Fig. 5.1A).

The observation that vinculin comprises almost exclusively helical bundles is not surprising, given the prevalence of helical bundles in cytoskeletal proteins, with examples including (but not limited to) talin (Fillingham et al., 2005; Papagrigoriou et al., 2004),  $\alpha$ -catenin (Pokutta et al., 2002; Yang et al., 2001), and focal adhesion kinase (Ceccarelli et al., 2006; Prutzman et al., 2004). However, unlike most helical bundles,

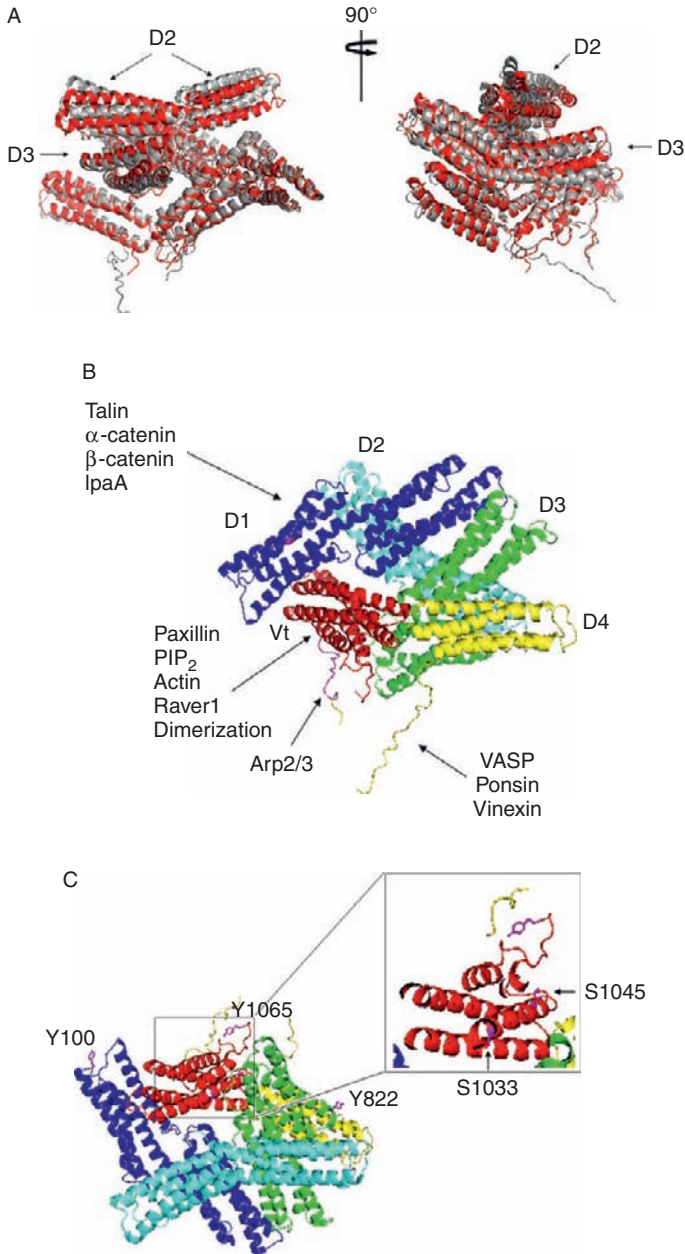


**Figure 5.1** Structure of full-length vinculin in the autoinhibited state. (A) Overlay of two published full-length vinculin structures. Chicken vinculin structure as solved by Bakolitsa et al. (2004) is colored in light gray, and the human vinculin structure

which are structurally rigid and retain their conformation upon ligand binding, vinculin's helical bundle, D1, undergoes remarkable conformational changes upon ligand binding (a process termed helical-bundle conversion; Borgon et al., 2004; Izard et al., 2004). Hence, despite being structurally similar to other cytoskeletal proteins, vinculin possesses some dynamic properties.

## 2.2. Vinculin head domain

The full-length crystal structures of vinculin reveal that the region previously known as the vinculin head (residues 1–811) comprises D1–D3 and a small portion of D4. The D1–D3 region contains two four-helix bundles connected by a long, centrally shared  $\alpha$ -helix (Bakolitsa et al., 2004; Borgon et al., 2004). This region resembles the amino-terminal fragment of  $\alpha$ -catenin; consequently, it has been referred to as a “vinculin/ $\alpha$ -catenin repeat” (Bakolitsa et al., 2004). Several proteins bind to the vinculin head domain. These include talin (Burrige and Mangeat, 1984),  $\alpha$ -catenin (Weiss et al., 1998),  $\beta$ -catenin (Hazan et al., 1997),  $\alpha$ -actinin (Geiger, 1979), and IpaA (Tran Van Nhieu et al., 1997) (Fig. 5.1B). Among these, only talin binds to vinculin exclusively in cell–matrix adhesions (Burrige and Mangeat, 1984), both  $\alpha$ - and  $\beta$ -catenins bind vinculin exclusively in adherens junctions (Drenckhahn and Franz, 1986; Geiger, 1979; Hazan et al., 1997; Watabe-Uchida et al., 1998). The crystal structures of the talin:vinculin D1 and  $\alpha$ -actinin:vinculin D1 complexes reveal that both of these binding partners interact with vinculin by inserting an  $\alpha$ -helix between helices 1 and 2 of the N-terminal helical bundle of vinculin D1 (Bois et al., 2005; Izard and Vonnrhein, 2004; Izard et al., 2004). However, they insert their  $\alpha$ -helices in opposite orientations suggesting that D1 has remarkable flexibility and takes on distinct conformations when bound to different ligands (Bois et al., 2005; Izard and Vonnrhein, 2004; Izard et al., 2004).

---

reported by Borgon et al. (2004) is colored in dark gray. These two structures overlap in most domains except for domain 2 (D2) and part of the domain 3 (D3). Two different views are shown. (B) Binding partners to different regions of vinculin. Vinculin domains are labeled: D1, residues 1–252; D2, residues 253–485; D3, residues 486–717; D4, 718–837; and Vt 891–1066. The proline region is partly disordered and contains a strap (residues 878–890). Binding partners to the vinculin head, linker, and tail region are indicated. This figure is adapted from the paper published by Bakolitsa et al. (2004). (C) Vinculin phosphorylation sites. Vinculin phosphorylation sites Y100, Y822, S1033, S1045, and Y1065 are labeled.

## 2.3. Proline-rich linker

Based on the full-length crystal structure of vinculin, the proline-rich linker has been redefined as residues 838–878 (Bakolitsa et al., 2004). Following the linker is a strap (residues 878–890) that packs against the first two helices of the vinculin tail. Ligands that interact with the proline-rich region include vasodilator-stimulated phosphoprotein (VASP) (Brindle et al., 1996), the Arp2/3 complex (DeMali et al., 2002), vinexin (Kioka et al., 1999), and ponsin (Mandai et al., 1999; Fig. 5.1B). At the N-terminus of the proline-rich linker is an FPPPPP motif (residues 842–847), which is essential for vinculin binding to VASP, vinexin, and ponsin. The C-terminal end of the proline-rich linker contains a PPPP motif (residues 875–878), which mediates Arp2/3 complex recruitment to vinculin (DeMali et al., 2002).

## 2.4. Vinculin tail domain

Like the head domain, the vinculin tail (Vt, D5) is mostly  $\alpha$ -helical. It contains five antiparallel  $\alpha$ -helices (H1–H5) (Bakolitsa et al., 1999, 2004; Borgon et al., 2004) and features two basic elements on the domain surface: a basic ladder formed primarily by the H3 side chains and a basic collar that surrounds a C-terminal, five-residue hairpin. A number of proteins bind to the vinculin tail, including paxillin (Turner et al., 1990; Wood et al., 1994), F-actin (Johnson and Craig, 1995b), phosphatidylinositol-4,5-bisphosphate (PIP<sub>2</sub>) (Johnson and Craig, 1995a), protein kinase C $\alpha$  (PKC $\alpha$ ) (Weekes et al., 1996), and raver1 (Huttelmaier et al., 2001; Fig. 5.1B). The tail domain also contains two serine residues, S1033 and S1045, that are highly phosphorylated by protein kinase C (Fig. 5.1C) (Schwienbacher et al., 1996; Weekes et al., 1996; Ziegler et al., 2002).

# 3. AUTOINHIBITED CONFORMATION AND VINCULIN ACTIVATION

## 3.1. Autoinhibited conformation

The isolated vinculin head domain readily binds to several ligands. However, binding to two of these, talin and  $\alpha$ -actinin, is significantly reduced in full-length vinculin (Chen et al., 2006; Groesch and Otto, 1990; Johnson and Craig, 1994; Kroemker et al., 1994). Similarly, the ability of the isolated vinculin tail domain to bind paxillin (Turner et al., 1990), bind PIP<sub>2</sub> (Johnson and Craig, 1995a), or cosediment and cross-link actin filaments are lost in the full-length molecule. Binding of a number of proteins to the proline-rich linker, including vinexin (Takahashi et al., 2005), VASP (Huttelmaier et al., 1998), and the Arp2/3 complex (DeMali et al., 2002)

are also blocked in full length vinculin. Moreover, the recruitment of some of these binding partners, including talin and actin, could be promoted by addition of phospholipids (Gilmore and Burridge, 1996). These observations led to a model whereby vinculin exists in two conformations: an autoinhibited or inactive conformation in which the binding sites for a number of ligands are masked and an open or active conformation in which the binding sites are exposed (Bakolitsa et al., 2004). It is important to note that although the open conformation is often referred to as the “active conformation,” vinculin has no enzymatic activity.

The recent descriptions of the crystal structures of full-length vinculin in its autoinhibited and talin-bound active states revealed the intricacies of the intramolecular interaction (Bakolitsa et al., 2004; Borgon et al., 2004): the head domains D1–D3 form a pair of pincers, which together with D4, make contact and hold the vinculin tail in an autoinhibited state. The crystal structure of the autoinhibited state also revealed why PIP<sub>2</sub>, the Arp2/3 complex, and F-actin bind only to the open conformation (Bakolitsa et al., 2004). In the case of PIP<sub>2</sub>, this is because it binds to the two basic surfaces on the vinculin tail (the above-described basic ladder and basic collar) (Bakolitsa et al., 1999), but in the autoinhibited conformation the collar is partially obscured by the strap. Binding of the Arp2/3 complex is inhibited because the proline residue (P878) that is critical for its recruitment is present in the strap; P878 packs against the vinculin tail, consistent with the low affinity of autoinhibited vinculin for the Arp2/3 complex (DeMali et al., 2002). Binding by F-actin to vinculin depends on two regions in the vinculin tail, one of which is partially blocked by the vinculin head in the closed conformation.

How the head–tail intramolecular interaction is maintained has been the subject of intense scrutiny. Early biochemical analyses showed that the strong intramolecular interaction can be partially explained by the complementary pI's for the two domains: the head domain has a pI of 5.5 and the tail has a pI of 9.6 (Miller et al., 2001). The crystal structures also revealed that the vinculin head–tail interaction is maintained by (1) hydrophobic interactions and hydrogen bonds formed at the D1–D5 interface, (2) polar interactions between D3 and D5, and (3) hydrogen bonds and electrostatic interactions between D4 and D5. Of these, the D1–D5 interface is thought to be the most critical for maintaining the autoinhibited state (Miller et al., 2001). Biochemical analyses tested which of these interactions maintain the autoinhibited conformation (Cohen et al., 2005). These studies established that D5 interacts with D1–D4 with a higher affinity ( $10^{-7}$  M) than with D1 alone ( $10^{-5}$  M) (Cohen et al., 2005); this finding not only underscored the importance of the D1–D5 interaction but also suggested that other domains play a role in promoting the autoinhibited conformation. Mutagenesis of charged residues to alanines revealed a series of D5 mutants that disrupt the D4–D5, but not the D1–D5 interface (Cohen et al., 2005). The importance



of the D4 interface was verified by reciprocal mutation of residues in D4 that contact D5. In these experiments, the head–tail interaction was reduced by about 100-fold and talin binding was permitted (Cohen et al., 2005). Moreover, these effects do not appear to be limited to interactions *in vitro*. In cells expressing mutant versions of vinculin with a disrupted D4–D5 interaction, the number and size of focal adhesions were increased and residency times were longer (Cohen et al., 2006). Collectively, these data suggest that not only a D1–D5 interaction but also a D4–D5 interaction is required to maintain vinculin in an autoinhibited state. The contribution of the D3–D5 interaction to maintaining the autoinhibited conformation of vinculin has not been tested by biochemical assays.

## 3.2. Activation of vinculin

### 3.2.1. Combinatorial activation

As vinculin lacks enzymatic activity and functions by interacting with other proteins, it is important to understand how the autoinhibited conformation is disrupted. From the crystal structures and biochemical analyses, we have learned that vinculin is held in the autoinhibited conformation by at least two head–tail interfaces and that the conformational changes in the vinculin head, tail, and linker are structurally and thermodynamically linked (Bakolitsa et al., 2004; Cohen et al., 2005). Based on the fact that no known vinculin ligands bind to full-length vinculin with an affinity comparable to that of the head–tail interaction ( $<1$  nM), it has been proposed that two ligands are required to disrupt both interfaces leading to vinculin activation (Bakolitsa et al., 2004). To directly test this hypothesis, the Craig laboratory developed a Förster resonance energy transfer (FRET) system that reports on vinculin conformational changes (Chen et al., 2005, 2006). The FRET probe is a vinculin construct tagged with CFP at the N-terminus and a YFP inserted immediately proceed D5. When vinculin is in the autoinhibited conformation, the two fluorophores are in close proximity and produce a high FRET signal; upon vinculin activation, the two fluorophores are separated and the FRET signal is reduced. This system has been used extensively to study conformational changes in vinculin (Chen et al., 2005, 2006; Grashoff et al., 2010), as well as to test the ability of talin to activate vinculin (Chen et al., 2006). Neither the talin rod (which contains at least three vinculin-binding sites) nor a short talin peptide containing a single vinculin-binding site induced a change in FRET (Chen et al., 2006). These findings were consistent with the notion that two or more ligands are required for vinculin activation. Indeed, when F-actin was applied alongside either the talin rod or the peptide, vinculin was activated in a dose-dependent manner (Chen et al., 2006). These data support a mechanism whereby at least two proteins, talin and F-actin, are required to activate vinculin (Fig. 5.2).

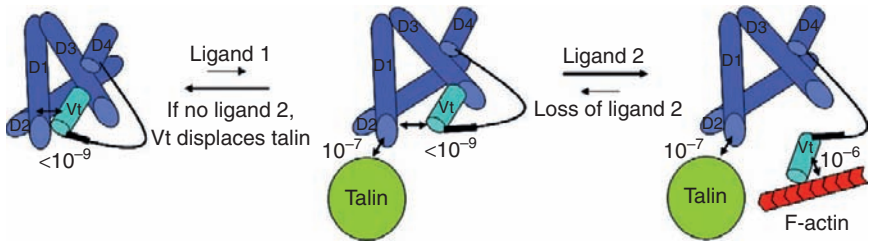


**Figure 5.2** A proposed model for combinatory activation of vinculin by talin and F-actin. Vinculin has a strong head–talin interaction with a  $K_d$  less than  $10^{-9}$  M. A small fraction of vinculin in the open conformation binds talin. As talin’s affinity for vinculin is  $\sim 10^{-7}$  M, talin alone cannot effectively compete with the vinculin tail and little vinculin–talin complex is formed. F-actin binding to vinculin–talin complexes captures vinculin in an active conformation. This figure is adapted from the paper published by Chen et al. (2006).

### 3.2.2. Activation by a single ligand

Notwithstanding the data described above, several lines of evidence support the notion that a single ligand can activate vinculin (Bois et al., 2005, 2006; Izard and Vornrhein, 2004; Izard et al., 2004). First, upon binding of vinculin D1 to either a talin or an  $\alpha$ -actinin peptide containing a single vinculin-binding site, D1 undergoes helical-bundle conversion (Bois et al., 2005; Izard and Vornrhein, 2004; Izard et al., 2004), an event that could in theory produce tail dissociation (Bois et al., 2005; Izard and Vornrhein, 2004; Izard et al., 2004). In further support of the helical bundle conversion, the addition of head ligands to full length vinculin increases its sensitivity to proteases and perturbs its NMR chemical shift patterns. (Bois et al., 2006). However, it remains to be determined if these conformational changes are similar to those that occur when these proteins are present at physiological concentrations in a cell. The second line of evidence supporting the ability of a single ligand to activate vinculin is that the binding sites for talin and  $\alpha$ -actinin are not occluded by the vinculin head–tail interaction (Bakolitsa et al., 2004; Borgon et al., 2004). However, unless the affinity of these ligands for the vinculin head is greater than that of the vinculin tail, it is unlikely that this interaction alone is sufficient to unfurl the molecule. This possibility was tested by adding a peptide containing a single vinculin-binding site to preformed D1:D5 or D1–D4:D5 vinculin complexes and measuring its ability to interact with these complexes. Both peptides were able to compete with the vinculin tail for vinculin head binding supporting the notion that single ligand can activate vinculin (Bois et al., 2006; Izard and Vornrhein, 2004). However, these experiments employed vinculin fragments which have a 10,000-fold (D1:D5, lacks the D4–V5 interface) or 100-fold

(D1–D4:D5) weaker affinity than the full-length molecule, due to the lack of a covalent linkage between the vinculin head and tail. Further studies tested if a peptide containing a binding site can activate the full-length molecule (Bois et al., 2005, 2006). Based on surface plasmon resonance analysis, the affinity of vinculin-binding site peptides for the full-length molecule was calculated to be  $\sim 70\text{--}80$  nM, which is comparable to the affinity of the head for the tail in the absence of linker (Bois et al., 2006). The  $\alpha$ -actinin peptide binds to full-length vinculin or D1 with a  $K_d$  of  $\sim 2$  nM, suggesting that this vinculin-binding site peptide can sever the interaction between the vinculin head and talin (Bois et al., 2005). However, these effects may potentially be accounted for by artificial vinculin activation as a consequence of its immobilization to a solid surface. Consistent with this notion, full-length vinculin absorbed to nitrocellulose, but not vinculin in solution, bound a vinculin-binding site peptide (Adey and Kay, 1997; Steimle et al., 1999). Similarly, in solution-phase binding studies, a talin vinculin-binding-site peptide failed to bind the full-length molecule but readily bound the isolated vinculin head domain (Chen et al., 2006).

### 3.3. Activation by IpaA

One emerging concept regarding the mechanism employed by talin to activate vinculin is that it may not apply to all ligands. In FRET studies using a full-length vinculin probe, Chen et al. (2006) showed that application of the *Shigella* invasin, IpaA, is sufficient to decrease FRET. This finding suggests that unlike talin, IpaA has the ability to activate vinculin independently of F-actin. However, adding F-actin to the IpaA-treated FRET probe further increased vinculin activation, suggesting that F-actin also plays a role (Chen et al., 2006). It remains unclear how IpaA coordinately disrupts both the D1:D5 and D4:D5 interfaces. Unlike talin or  $\alpha$ -actinin, whose vinculin-binding sites are buried inside helical bundles (Bois et al., 2005; Fillingham et al., 2005; Gingras et al., 2006; Papagrigoriou et al., 2004; Ylanne et al., 2001), those of IpaA are exposed and accessible for binding (Hamiaux et al., 2006). Moreover, each of these vinculin-binding sites simultaneously binds two vinculin D1 domains. Hence, it is possible that the accessibility of these sites contributes to IpaA activation of vinculin (Hamiaux et al., 2006).

### 3.4. Activation *in vivo*

The *in vitro* biochemical studies that have been carried out on vinculin have significantly advanced our understanding of its activation. However, the relevance of these findings to cellular events has not been evident until recently. The Craig group has pioneered the study of vinculin conformation at focal adhesions in live cells, using the FRET-based probes described

above (Chen et al., 2005). Their initial examination of these probes confirmed the original model with regard to vinculin at focal adhesions being in the open conformation, and vinculin in the cytoplasm being in the closed conformation. Strikingly, however, their data also revealed that vinculin conformations *in vivo* are much more complicated than predicted in this simplified model (Chen et al., 2005). While most of the vinculin at focal adhesions exists in an open conformation, there is a fraction in the closed conformation: immediately following its recruitment to focal adhesions and later as the adhesions disassemble and the membrane retracts (Chen et al., 2005). These data indicate that vinculin recruitment to focal adhesions is distinct from its activation and that vinculin is inactivated preceding the disassembly of focal adhesions. Additional work is needed to establish which physiological ligands other than talin activate vinculin and to identify the signal transduction pathways that regulate these events *in vivo*.

## 4. BIOLOGICAL FUNCTIONS

### 4.1. Modulation of cell adhesion and migration

Vinculin's function is best understood at sites of cell–matrix adhesion. Cell adhesion to the extracellular matrix regulates numerous basic biological processes, including cell growth, migration, differentiation, and survival (Berrier and Yamada, 2007; Huveneers and Danen, 2009; Schwartz and DeSimone, 2008). The most pronounced adhesion complexes in cultured cells are focal adhesions; they are flat, elongated structures rich in heterodimeric ( $\alpha$  and  $\beta$ ) cell-surface adhesion receptors known as integrins. The cytoplasmic tails of integrins bind with a wide array of proteins that regulate the activation of integrins and their interaction with the extracellular matrix. These focal adhesion proteins also send and respond to extracellular cues and physical properties of the extracellular matrix and provide physical linkage between integrins and the actin cytoskeletal network. Vinculin is recruited to the cytoplasmic tails of  $\beta$  integrin proteins, via its interaction with talin (BurrIDGE and Mangeat, 1984; Horwitz et al., 1986).

A significant body of evidence suggests that vinculin's presence in focal adhesions is critical for integrin-mediated cell adhesion and migration. For example, cells devoid of vinculin have fewer and smaller adhesions and close a wound more rapidly than vinculin-positive cells (Coll et al., 1995; Saunders et al., 2006; Volberg et al., 1995; Xu et al., 1998b). Conversely, in vinculin-overexpressing cells, the number and size of focal adhesions are increased and cell motility is reduced (Rodriguez Fernandez et al., 1992). Hence, vinculin negatively regulates cell motility via its effects on cell adhesion.

#### 4.1.1. Clustering of integrins and turnover of focal adhesions

Despite its well-established role in modulating focal adhesion stability and cell migration, the molecular mechanisms underlying vinculin's effects remained elusive until recently. Cohen et al. (2006) showed that the residency of both vinculin and talin in focal adhesions is increased in cells expressing a mutant vinculin in which head–tail interactions are reduced. When the talin-binding site is ablated, this mutant vinculin exhibits enhanced dynamics in focal adhesions (Cohen et al., 2006). Hence, conformational changes in vinculin regulate the formation and lifetime of talin–vinculin complexes in cells. This observation combined with knowledge that talin regulates integrin activation led to the notion that vinculin could regulate integrin dynamics (Calderwood et al., 1999). The effect of vinculin on integrin dynamics was directly examined using real-time interference reflection microscopy (Saunders et al., 2006). Focal adhesions are smaller and less abundant in vinculin-null cells than in their wild-type counterparts and turnover more rapidly (Saunders et al., 2006). Using mutant versions of vinculin that lack the tail domain to mimic the open vinculin conformation, Humphries et al. (2007) showed that vinculin regulates integrin dynamics and clustering. Importantly, talin must bind vinculin to exert these effects (Humphries et al., 2007). These findings have led to a new model for the mechanism, whereby vinculin regulates cell–matrix adhesions (Carisey and Ballestrem, 2010; Humphries et al., 2007). According to this model, the stability of adhesion complexes is dependent on vinculin activation; when vinculin is activated, the vinculin–talin complexes stabilize the focal adhesions and enhance integrin clustering (Fig. 5.3A). Further support of a role for vinculin in regulating integrin clustering comes from a more recent study showing that small hairpin RNA-based inhibition of vinculin decreases the number of active integrins on the cell surface (Ohmori et al., 2010).

How is the stabilizing effect of vinculin on cell–matrix adhesions relieved? The evidence to date suggests that vinculin binding to PIP<sub>2</sub> regulates the release of vinculin from focal adhesions. Evidence of a role for PIP<sub>2</sub> comes from a vinculin mutant defective for lipid binding, that is, the putative vinculin–PIP<sub>2</sub> interaction surfaces on D5 are disrupted (K952Q, K956Q, R963Q, K966Q, R1060Q, K1061Q) (Chandrasekar et al., 2005). This mutant ablates the majority of PIP<sub>2</sub> binding but preserves the vinculin–actin and the D1:D5 interaction. When expressed in embryonic fibroblasts derived from vinculin-null mice, this mutant localized to focal adhesions at wild-type levels, but did not rescue the spreading defects characteristic of these cells. The lack of spreading suggested that perturbing the vinculin–PIP<sub>2</sub> interaction may lead to more stable focal adhesions. Indeed, the assembly, breakdown, and retrograde transport of focal adhesions in cells expressing the vinculin lipid-binding mutant are all greatly

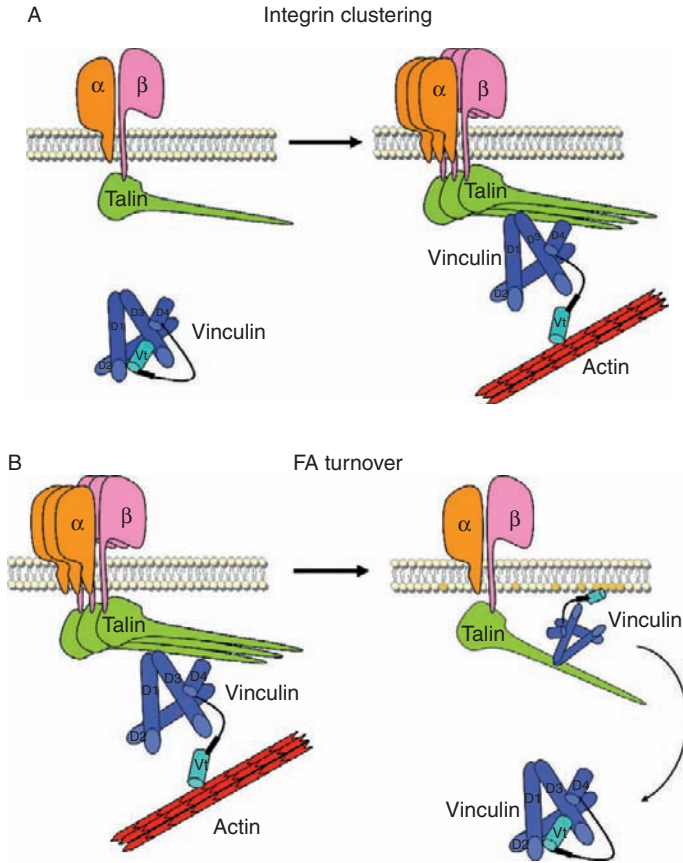


**Figure 5.3** *Vinculin regulates integrin clustering and focal adhesion turnover.* (A) Vinculin–talin interaction regulates integrin clustering. In the absence of vinculin (left panel), talin bound–active integrins form small focal adhesions with few clustered integrins. Upon activation by talin and F-actin (right panel), vinculin regulates integrin dynamics by clustering integrins in an active conformation. (B) The vinculin–PIP<sub>2</sub> interaction regulates focal adhesion turnover. Recent data suggest that stable adhesions (left panel) disassemble when vinculin is lost from focal adhesions when increased phosphoinositide levels causes PIP<sub>2</sub> to bind and displace F-actin from vinculin (right panel) (Chandrasekar et al., 2005; Saunders et al., 2006).

impaired compared to the same processes in their wild-type counterparts (Saunders et al., 2006). Consistent with the reduction in focal adhesion turnover, cells expressing the lipid-binding mutant also exhibit increased adhesion and reduced cell migration (Chandrasekar et al., 2005). These data

have led to a model in which the vinculin–PIP<sub>2</sub> interaction regulates the turnover of focal adhesions (Chandrasekar et al., 2005; Saunders et al., 2006; Ziegler et al., 2006). According to this model, cues for focal adhesion disassembly increase phosphoinositide levels, resulting in competition of PIP<sub>2</sub> with F-actin for binding to vinculin (Fig. 5.3B). The observation that overexpression of PtdInsP 5-kinase  $\alpha$  (but not a kinase-dead mutant) increases PIP<sub>2</sub> levels and stimulates the loss of focal adhesions lends further support to a role of vinculin binding to PIP<sub>2</sub> in the disassembly of focal adhesions (Chandrasekar et al., 2005).

#### 4.1.2. The strength of cell–matrix adhesion

In addition to regulating the dynamics of focal adhesions, vinculin is important for adhesive strength. Adhesive strength is established by the initial integrin–ligand binding step, and is then rapidly enhanced by the clustering of integrins and the recruitment of focal adhesions proteins (Lotz et al., 1989). The latter contributes to adhesive strength by distributing bond forces along the cell–substrate interface (Gallant et al., 2005; Lotz et al., 1989). The role of vinculin in regulating adhesion strength is illustrated by the observation that its recruitment correlates with the formation of focal complexes, and by the fact that its loss results in the weakening of adhesion (Galbraith et al., 2002). Recently, Gallant et al. systematically analyzed the effects of vinculin in adhesion strength. Vinculin-deficient F9 cells exhibit adhesive strength values 20% lower than parental F9 cells (Gallant et al., 2005). These effects are not limited to the F9 cells, as the silencing of vinculin in NIH3T3 cells produced a 25% loss in adhesive strength (Gallant et al., 2005). Thus, vinculin makes minor yet significant contributions to the overall strength of adhesion.

#### 4.1.3. Force transmission

The transmission of force requires focal adhesion complexes that link the extracellular matrix on the outside of the cell to the actin cytoskeleton on the inside of the cell. In motile cells, at least two distinct types of force must be generated (Ridley et al., 2003; Stricker et al., 2010). One is provided by actin polymerization and is the protrusive force needed to extend lamellipodia or filopodia (Pantaloni et al., 2001; Pollard and Borisy, 2003). The other is myosin dependent and leads to rearrangement of the actin cytoskeleton (Ridley et al., 2003). This second force was originally thought to generate the contraction needed to move the cell body forward (Maciver, 1996; Verkhovsky et al., 1999), but more recent work suggests that it is not required for migration (Lombardi et al., 2007).

Focal adhesions assemble and enlarge when force increases and shrink or disassemble when force decreases. This unique property allows cells to respond appropriately to external and internal forces. Several lines of evidence indicate that vinculin regulates the transmission of force between the

extracellular matrix and the actin cytoskeleton. For example, cells lacking vinculin exert lower traction forces and are less stiff than their wild-type counterparts (Alenghat et al., 2000; Mierke et al., 2008), and the application of external or internal force increases vinculin recruitment to cell–matrix adhesion sites (Galbraith et al., 2002; Gallant et al., 2005) in a myosin II-dependent manner (le Duc et al., 2010). These findings led to the idea that vinculin recruitment to focal adhesions is force dependent. Using a biosensor that measures force across vinculin, the Schwartz lab showed that vinculin is recruited to focal adhesions and remains in the open conformation under conditions that reduce myosin-dependent contractility (i.e., treatment with Rho kinase inhibitors or reduction of myosin II expression) (Grashoff et al., 2010). Moreover, in migrating cells, the force across vinculin was found to be high in nascent adhesions and to decrease toward moderate levels as the focal adhesions enlarge, with force across vinculin remaining low or decreasing slightly as focal adhesions disassemble (Grashoff et al., 2010). Taken together, these findings indicate that vinculin recruitment and force bearing are independent and that the ability of vinculin to bear force determines whether adhesions assemble or disassemble under force.

How might vinculin regulate the transmission of force? The connection between the actin cytoskeleton and cell adhesions is not rigid, but rather involves points where slippage occurs. Consequently, cell adhesion has been likened to a molecular clutch (Hu et al., 2007). When the clutch is engaged, there is no slippage between adhesion and the cytoskeleton, and movement is productive. When the clutch is disengaged, however, polymerization pressure at the membrane and myosin-dependent contraction cause actin to slip backward, a process known as retrograde flow. Vinculin is a key component of this molecular clutch, and its interaction with F-actin is required for its effects in this context (Hu et al., 2007; Humphries et al., 2007). Moreover, the vinculin-containing clutch colocalizes with areas of high force during lamellipodia protrusion (Ji et al., 2008). These data indicate that in protruding regions, transient binding of vinculin to F-actin is important for force transduction.

#### 4.1.4. Linkages between the extracellular matrix and actin cytoskeleton

**4.1.4.1. Requirement of talin in linking vinculin to mechanical stimuli** One means by which vinculin could potentially link the integrins to extracellular matrix complexes to strengthen adhesion is by binding to talin. Recent biochemical and structural studies have provided new insights into the molecular details of the vinculin–talin interaction. Talin is an elongated and flexible antiparallel dimer, whose small globular head is connected to an extended rod (Isenberg and Goldmann, 1998; Winkler et al., 1997). Talin uses an N-terminal FERM domain (residues 86–400) to bind to the NPxY motif in the  $\beta$ -integrin cytoplasmic tail (Garcia-Alvarez



et al., 2003). The talin rod contains a second integrin-binding site (residues 1984–2541) of lower affinity (Tremuth et al., 2004; Xing et al., 2001), a C-terminal actin-binding site (residues 2345–2541) (Hemmings et al., 1996; McCann and Craig, 1997), and at least 11 vinculin-binding sites (Gingras et al., 2005; Hemmings et al., 1996).

Crystal (Izard and Vorrhein, 2004; Izard et al., 2004) and NMR structures (Fillingham et al., 2005) of vinculin D1 complexed with various talin peptides that contain one or more vinculin-binding sites have been solved, revealing that both molecules must undergo a conformational change to interact. Izard et al. first demonstrated that vinculin D1 must undergo a conformational change before talin can bind to it (Izard and Vorrhein, 2004; Izard et al., 2004). Specifically, all four  $\alpha$ -helices in the N-terminal bundle of D1 rearrange into a five-helix bundle to accommodate the vinculin-binding-site peptide. Interestingly, the structural changes to D1 that are induced by different vinculin-binding sites in talin appear to be quite similar (Izard and Vorrhein, 2004; Izard et al., 2004). Of the vinculin-binding sites in talin, only one is exposed on its surface in the basal state; the others become accessible only when structural rearrangements occur. In support of a requirement for a talin conformation change, studies show that although isolated talin peptides bind vinculin with high affinity, full-length talin binds only weakly (Bass et al., 2002; Izard and Vorrhein, 2004; Johnson and Craig, 1994; Patel et al., 2006). Also, the stability of the talin helical bundles negatively correlates with their ability to bind vinculin, a finding consistent with a conformational change (Patel et al., 2006). Most recently, NMR and electron paramagnetic resonance spectroscopy have enabled direct visualization of unfurling of the talin  $\alpha$ -helical bundles (Gingras et al., 2006; Papagrigoriou et al., 2004).

As talin must undergo a conformational change to bind vinculin, it is critical to determine how its vinculin-binding sites become exposed. The application of force using magnetic tweezers leads to unfolding of the talin rod and exposes cryptic binding sites for vinculin (del Rio et al., 2009). The number of vinculin molecules bound to talin in this context depends on the amount of force applied. Interestingly, findings from this analysis were consistent with the presence of three intermediate talin transition states (del Rio et al., 2009), as previously suggested based on a molecular simulation study (Hytonen and Vogel, 2008). Collectively, these studies establish mechanical force as an important determinant of vinculin binding to talin and in mechanosignaling transduction *in vivo*.

**4.1.4.2. Direct binding between vinculin and actin** The vinculin–actin interaction has long been studied from the perspective of vinculin. These works revealed vinculin is an actin-bundling protein. However, little else is known about the effects of vinculin on actin dynamics and filament structure. Many early studies that attempted to examine vinculin's effects on

actin were performed on vinculin preparations later found to be contaminated with actin and/or other proteins (Otto, 1986; Rosenfeld et al., 1985; Wilkins and Lin, 1982, 1986). We also now know that vinculin purified under the original conditions is in a closed autoinhibited conformation that binds actin with only very low affinity, probably accounting for the negative results obtained from the vast majority of these studies.

The advent of DNA technology allowed for the production of vinculin free of protein contaminants and facilitated exploration of vinculin's effects on actin. Although work as far back as the 1990s showed that vinculin binds actin directly (Johnson and Craig, 1995b), precisely where the actin-binding site lies remains a matter of debate (Table 5.1). Analysis of the vinculin protein sequence revealed putative consensus binding sites between helix 1 and helix 3 (H1–H3), and helix 1 and helix 4 (H1–H4) of D5. Although a more C-terminally located region (1016–1066) was also reported to be an actin-binding site (Huttelmaier et al., 1997; Johnson and Craig, 1995b), other binding studies showed that a fragment containing this region does not bind F-actin (Goldmann et al., 1998; Janssen et al., 2006). These differences may be explained in part by the fact that some of these residues are important for maintaining the vinculin head–tail interaction and by the finding that perturbing this interaction may impact actin binding.

It is well established that upon binding to actin vinculin dimerizes and assembles actin filaments into bundles (Janssen et al., 2006; Jockusch and Isenberg, 1981; Johnson and Craig, 1995b, 2000; Pardo et al., 1983a,b). However, less is known with respect to the effects of vinculin on actin

**Table 5.1** Putative actin-binding sites in vinculin

| Actin-binding sites                                         | Methods                                                                                                                | References                |
|-------------------------------------------------------------|------------------------------------------------------------------------------------------------------------------------|---------------------------|
| 940–1012, 1012–1066                                         | <i>In vitro</i> binding to GST fusion proteins                                                                         | Johnson and Craig (2000)  |
| 893–1016                                                    | Maltose-binding protein fused with vinculin fragments to cosediment with F-actin, and colocalization analysis in cells | Menkel et al. (1994)      |
| 893–985, 1016–1066                                          | Maltose-binding protein fused with vinculin fragments to cosediment with F-actin                                       | Huttelmaier et al. (1997) |
| 894–1012, no binding to 1012–1066                           | Stopped-flow and dynamic light scattering analysis                                                                     | Goldmann et al. (1998)    |
| 883–890, base of H3 and a stretch of residues in C-terminus | EM reconstruction                                                                                                      | Janssen et al. (2006)     |

filament formation and structure. The earliest detectable actin-associated adhesions are “dots or doublets of actin dots.” These plaques are highly enriched for integrins, paxillin, and vinculin (Zimmerman et al., 2004), suggesting that one of these proteins may have the capability to initiate actin filament formation. This possibility stimulated renewed interest in studying the effects of vinculin on actin assembly and/or dynamics. Our study of the association of the vinculin tail with monomeric and filamentous actin has defined two novel effects of vinculin on actin (Wen et al., 2009). The vinculin tail binds to monomeric G-actin, in which case it forms a nucleus from which genuine actin filament bundles assemble; the characteristics of filaments formed under these conditions are similar to those of filaments assembled under physiological conditions. The vinculin tail also binds to existing filaments and alters their structure. Hence, vinculin has two novel effects on actin: it recruits G-actin to form a nucleus for actin polymerization and it modifies the structure of existing actin filaments.

**4.1.4.3. Linkage of vinculin and actin via the Arp2/3 complex** We (DeMali et al., 2002) and others (Moese et al., 2007; Nolz et al., 2007; Schindeler et al., 2005) have shown that vinculin binds and recruits the Arp2/3 complex. In migrating cells, the interaction between vinculin and the Arp2/3 complex occurs transiently in response to signals that trigger membrane protrusion. The interaction is regulated by phosphatidylinositol-3-kinase and Rac1 activity and is sufficient to recruit the Arp2/3 complex to new sites of integrin clustering (DeMali et al., 2002). Vinculin with point mutations that disrupt the Arp2/3 complex binding site fail to restore cell spreading and lamellipodia formation to the same extent as wild-type vinculin when transfected into vinculin-null cells, in spite of the fact that the encoded proteins are targeted to focal adhesions and mediate adhesion (DeMali et al., 2002). These observations indicate that the interaction between the Arp2/3 complex and vinculin promotes the extension of lamellipodia and cell spreading. Further, they support a model whereby nascent adhesion receptors are linked to the existing actin cytoskeleton via vinculin and the Arp2/3 complex.

The current data support the existence of two vinculin-dependent mechanisms for linking nascent adhesions to the actin cytoskeleton: (1) vinculin itself triggers filament formation and (2) vinculin recruits the Arp2/3 complex, which in turn nucleates filament formation. It is not readily apparent why there is a need for two vinculin-dependent mechanisms that trigger filament formation, but the most straightforward explanation is that vinculin might act alone when physiological conditions dictate the need for a bundled actin filament, but operate in concert with the Arp2/3 complex when a branched actin network, such as those that are present in lamellipodia, is needed. The other possibility is that vinculin itself may

nucleate polymerization to link nascent adhesions to the actin cytoskeleton, and the vinculin:Arp2/3 complex interaction might be required to allow for further protrusion for these adhesion sites (DeMali and Burridge, 2003). More work is needed to establish the physiological conditions under which each mechanism operates and to fully understand how nascent adhesions form during cell migration, as well as how they are linked to the actin cytoskeletal network that underlies this process.

## 4.2. Modulation of apoptosis

Loss of vinculin has been correlated with tumorigenesis (Kawahara et al., 1999; Lifschitz-Mercer et al., 1997; Meyer and Brinck, 1997; Sadano et al., 1992; Somiari et al., 2003). This observation can be explained, in part, by vinculin's role in regulating cell adhesion, migration, and invasion (Mierke et al., 2010; Ziegler et al., 2006). However, emerging evidence suggests that vinculin also plays a key role in regulating apoptosis. For example, vinculin-null F9 cells are resistant to caspase-3 activation under conditions that would normally trigger a massive apoptotic response (Subauste et al., 2004). It appears that this modulation of the apoptotic response by vinculin is due to its ability to compete with FAK for paxillin binding. Evidence for this comes from the finding that in cells lacking vinculin, more paxillin than usual is available to bind FAK and to regulate downstream cell-survival signaling. In contrast, when vinculin, or a vinculin fragment containing residues 811–1066, is expressed in vinculin null cells, the paxillin-FAK interaction is inhibited and the apoptotic response is rescued (Subauste et al., 2004). These results suggest that vinculin may regulate cell survival by modulating interactions between paxillin and FAK. Interestingly, a vinculin phosphorylation mutant, Y822F, does not restore the apoptotic response in vinculin-null cells. How this mutation affects vinculin function has not been explored.

## 4.3. Regulation of bacterial entry

Vinculin has been implicated in facilitating the invasion of pathogenic bacteria and their propulsion through the host-cell cytoplasm. This phenomenon is best characterized in the case of the gram-negative bacterium *Shigella*. Upon contact with the intestinal epithelium, *Shigella* secretes at least four invasins (IpaA, IpaB, IpaC, and IpaD) and induces robust rearrangements in the host cytoskeleton that produce a phagocytic cup that engulfs the bacterium. Entry is abolished by deletion of the genes encoding *ipaB*, *ipaC*, or *ipaD* and is inhibited tenfold by inactivation of *ipaA* (Menard et al., 1993; Tran Van Nhieu et al., 1997). This ability to reduce invasion reflects a requirement for IpaB-D in formation of

the phagocytic cup; IpaA, in contrast, induces the rearrangement of actin networks present in and around the cup.

The mechanism underlying IpaA-induced host cell rearrangements involves vinculin. The C-terminus of IpaA contains two *bona fide* binding sites and a third, putative, binding site (Izard et al., 2006). The first two of these sites are required for vinculin binding and recruitment to the site of bacterial entry. Once IpaA is bound to the vinculin head, the vinculin tail is free to associate with F-actin and to trigger a loss of filamentous actin (Bourdet-Sicard et al., 1999; Tran Van Nhieu et al., 1997).

There is some controversy as to how IpaA–vinculin binding triggers rearrangement of actin filaments at the site of *Shigella* entry. Polymerization experiments showed that IpaA binding uncovers a site in vinculin that allows it to partially cap the barbed ends of actin filaments, resulting in an overall net loss of filamentous structures (Ramarao et al., 2007). While this mechanism has received the most attention, it is unlikely that partial capping of the filament ends alone accounts for the instantaneous loss of actin filaments observed in the host cell upon contact with *Shigella*. In further support of this notion, the deletion of a single vinculin-binding site in IpaA completely ablated the partial capping activity of vinculin, but only slightly reduced the invasive potential of *Shigella*. Hence, it appears that the IpaA C-terminus (which contains the vinculin-binding sites) modestly contributes to bacterial invasion (Izard et al., 2006).

We have examined the mechanism for the effects of IpaA on the actin cytoskeleton and found other regions of importance. The IpaA-induced loss of actin stress fibers and cell rounding in cells exposed to IpaA does not require an intact vinculin-binding site on IpaA or vinculin (DeMali et al., 2006). Rather, we find that cells expressing IpaA exhibit elevated Rho activity and increased myosin light chain phosphorylation. In addition, IpaA decreases integrin's affinity for extracellular matrix ligands by interfering with talin recruitment to the integrin cytoplasmic tail. The combination of these two effects, namely weakened adhesion and increased contractility, accounts for the loss of actin stress fibers and cell rounding observed in cells exposed to IpaA. Taken together, these results and previous work suggest a model whereby IpaA binding to vinculin localizes IpaA to adhesion sites. In this locale, IpaA can interfere with the actin cytoskeleton by unmasking the barbed-end capping activity of vinculin and by perturbing talin's interaction with vinculin and integrins. These combined effects would result in a massive loss of F-actin at the site of *Shigella* entry.

Vinculin has also been implicated in the pathogenesis of *Helicobacter pylori*, but less is known about its role in this context. Like *Shigella*, *H. pylori* initiates pathogenesis by translocating bacterial proteins to the host cell cytoplasm. The translocation of one such protein, CagA, into gastric epithelial cells has been linked to an increased risk for peptic ulcers and gastric carcinoma, and this has been shown to be a consequence of its ability to

deregulate intercellular signal transduction pathways. Upon *H. pylori* infection, CagA becomes phosphorylated by the Src family kinases and then binds to and activates/inactivates multiple signaling proteins, including (but not limited to) other kinases and phosphatases. Numerous adhesion and cytoskeletal proteins such as vinculin are also affected; vinculin, in particular, undergoes dramatic dephosphorylation at tyrosine residues (Moese et al., 2007) which prevents it from binding to the Arp2/3 complex. Consequently, nascent adhesions do not link to the underlying actin cytoskeleton, and the number of focal complexes that anchor the gut epithelium to the underlying basement membrane is greatly reduced. Taken together with the findings from *Shigella* studies, these discoveries demonstrate that bacteria such as *Shigella* and *H. pylori* hijack the normal functions of vinculin in a cell to circumvent some of the constraints to bacterial entry. While these bacteria share a common target in vinculin, it is important to note that these effects occur via vastly different mechanisms. Moreover, these effects appear to be limited to a subset of bacteria, as vinculin accumulates only modestly at the entry site of the gram-negative bacterium *Salmonella* (Finlay et al., 1991), and its inhibition does not affect bacterial invasion. Likewise, vinculin is not present at the site of enteropathogenic *Escherichia coli* entry into cells (Finlay et al., 1992).

## 5. MODES OF VINCULIN REGULATION

### 5.1. Regulation of conformational changes: Tyrosine phosphorylation

Vinculin was identified as the first substrate of the Src tyrosine kinase nearly 30 years ago (Sefton et al., 1981), yet the consequences of its phosphorylation remain poorly understood. Early studies correlated alterations in tyrosine phosphorylation on vinculin with a loss of cell–matrix and cell–cell adhesion (Ayalon and Geiger, 1997; Halebouga, 1987; Tidball and Spencer, 1993; Vostal and Shulman, 1993), but many of those were performed using tyrosine kinase inhibitors that alter the phosphorylation states of other proteins in addition to vinculin (Ayalon and Geiger, 1997). More recently, the Haimovich laboratory identified tyrosines Y100 and Y1065 as the major sites of tyrosine phosphorylation in platelets (Zhang et al., 2004). In the full-length crystal structure, Y100 is fully exposed, whereas Y1065 is occluded by the proline-rich linker domain (Fig. 5.1C) (Bakolitsa et al., 2004; Borgon et al., 2004). Tyrosine to phenylalanine mutations at Y100 and Y1065 inhibit cell spreading (Zhang et al., 2004), and a single substitution at Y1065 leads to decrease traction (Diez et al., 2009). The mechanism for the latter effect likely results from uncontrolled exchange of vinculin in and out

of adhesion sites (Kupper et al., 2010; Mohl et al., 2009). Collectively, these findings suggest that Y1065 plays an important role in regulating adhesion dynamics.

How tyrosine phosphorylation regulates vinculin function remains to be fully explored. Phosphorylation at Y1065 reduces head–tail interactions, suggesting that vinculin activation might be affected by this modification (Zhang et al., 2004). Consistent with this notion, the Arp2/3 complex cannot bind the vinculin strap in cells expressing a mutant version of vinculin with a Y1065F substitution (Moese et al., 2007). A loss of vinculin binding to the Arp2/3 complex results in a decrease in the association of nascent focal adhesion complexes with the underlying actin cytoskeleton (DeMali et al., 2002), which might explain the decrease in cell spreading and traction observed in the presence of Y1065F. If tyrosine phosphorylation at Y1065 does regulate head–tail interactions, it seems unlikely that all the active vinculin in a cell is phosphorylated at Y1065; if it were, the amount of tyrosine-phosphorylated vinculin should reflect the amount of active vinculin in a cell, yet in cells transformed with the rous sarcoma virus, only 2% of the total vinculin is phosphorylated (Sefton et al., 1981; Zhang et al., 2004), whereas the amount of active vinculin in a cell is much greater. Hence, it is unlikely that tyrosine phosphorylation of vinculin strictly mirrors vinculin activation. An alternative possibility is that only a subset of the active vinculin is phosphorylated. Consistent with this notion, the Craig lab elegantly demonstrated heterogeneity in the vinculin conformation that is present in focal adhesions, and that the ratio of the different conformers correlates with adhesion dynamics. It is also plausible that phosphorylation is an important step in the pathway to activation. For example, phosphorylation may be requisite for anchorage of vinculin to the lipid membrane (Diez et al., 2009). A scenario such as the latter would imply that the activation state of vinculin is tightly regulated by phosphorylation. A complete understanding of this phenomenon awaits the identification of the phosphatase that dephosphorylates vinculin.

## 5.2. Regulation of vinculin expression

While it has been appreciated for some time that vinculin function is regulated by conformational changes and posttranslational modification(s), recent work indicates that vinculin function may also be highly regulated at the expression level (Babic et al., 2009). Specifically, the 3' untranslated region of vinculin binds polypyrimidine tract-binding protein (PTB), a widely expressed RNA-binding protein with roles in splicing, polyadenylation, mRNA stability, and translation initiation (Auweter and Allain, 2008; Sawicka et al., 2008). PTB function is regulated by a combination of events,

including its subcellular distribution (it shuttles from the nucleus to the cytoplasm) and its interaction with additional proteins (Sawicka et al., 2008). In most cells in culture, PTB localizes to the nucleus. However, in cells undergoing adhesion and spreading, PTB transiently shifts to the cytoplasm where it concentrates in nascent adhesions and membrane protrusions (Babic et al., 2009). In these regions, it colocalizes with and binds to the vinculin mRNA. This interaction appears to be essential for vinculin expression at adhesion sites, as RNA interference-mediated PTB inhibition reduced the amounts of both the vinculin-encoding mRNA and vinculin protein localized to cell-matrix adhesions (Babic et al., 2009). In further support of the essential nature of the interaction between these proteins, cells lacking PTB exhibit many of the same phenotypes as cells devoid of vinculin: they are more rounded, have smaller focal adhesions, and reduced membrane protrusions. Hence, PTB is required for efficient expression of vinculin in nascent adhesions and for the adhesion assembly (Fig. 5.4).

Raver1 is another protein that likely plays a role in vinculin expression at cell adhesion sites. It is a heterogeneous nuclear ribonucleoprotein that was first identified as a vinculin tail binding protein in a yeast two-hybrid screen (Huttelmaier et al., 2001). It has three N-terminal RNA recognition motifs (RRM1-3), the first of which directly binds to the vinculin tail domain with micromolar affinity (Lee et al., 2009). In addition, it has two nuclear localization signals and one nuclear export sequence, which allow it to shuttle between the nucleus and the cytoplasm. When in the nucleus, raver1 interacts with PTB to regulate mRNA processing, but during cell differentiation it redistributes to the cytoplasm where it colocalizes with and

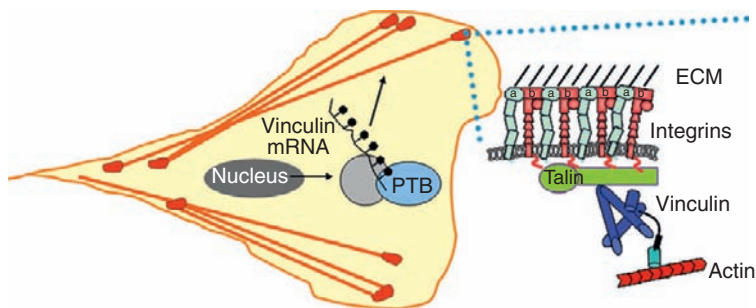


**Figure 5.4** *Vinculin mRNA translation is regulated spatiotemporally at sites of adhesion.* In response to migratory cues, vinculin mRNAs are transported to sites of membrane protrusion to allow for localized protein translation and the assembly of focal adhesions (dark circles). The delivery of mRNAs is likely regulated by a number of proteins including PTB and other unidentified proteins (gray circle).



binds to vinculin in focal adhesions, adherens junctions, and costameres (Huttelmaier et al., 2001). A recent crystal structure of RRM1–3 of raver1 bound to the isolated vinculin tail reveals that raver1 has the potential to bind RNA and vinculin simultaneously (Lee et al., 2009). Moreover, even in complex with vinculin, raver1 is able to interact with actin filaments. A possible role for the raver1–vinculin complex in cell adhesions has been proposed based on these findings (Lee et al., 2009). Specifically, active vinculin binds to the raver1 RRM1 domain, which may or may not already be bound to, or subsequently bind to, mRNA cargo, resulting in localization of the raver1–RNA complex to sites of cell adhesion where the vinculin–raver1 complex could engage the actin cytoskeleton. The raver1–vinculin interaction may thus play a dominant role in targeting bound vinculin mRNAs to adhesions to promote the localized translation of constituent proteins. Validation of this model awaits direct experimental evidence for simultaneous binding of the raver1 N-terminus to both vinculin and mRNAs.

While the studies carried out to date have provided significant insight into how vinculin expression is regulated, the connection, if any, between the PTB and raver1 pathways in this context has not been explored. Interestingly, raver1 colocalizes with and binds to PTB in the nucleus, and both proteins can translocate to cytoplasm (Huttelmaier et al., 2001; Sawicka et al., 2008). These findings raise the possibility that these proteins act in concert to regulate the expression of vinculin (and that of other focal adhesion proteins) (Huttelmaier et al., 2001). In support of this notion, the binding sites for vinculin and PTB on raver1 appear to be distinct, with vinculin binding to the raver1 N-terminus and PTB to the C-terminus (Babic et al., 2009; Huttelmaier et al., 2001; Lee et al., 2009). However, other evidence suggests that PTB can act independently of raver1 in some circumstances. For example, Babic et al. (2009) found that while PTB translocates to the cytoplasm during cell spreading and adhesion, raver1 remains in the nucleus. Whether this phenomenon is universal remains to be determined, as it is unknown if PTB remains in the nucleus under conditions that promote shuttling of raver1 to the cytoplasm.



## **6. EMERGING THEMES AND CONCEPTS**

### **6.1. Vinculin in adherens junctions**

#### **6.1.1. A key member of the cadherin–adhesion complex**

Since the identification and localization of vinculin to focal adhesions and cell–cell adhesions over 30 years ago, its presence in focal adhesions has commanded more attention. Thus, relatively little is known about its

function in cell–cell junctions. Several specialized cell–cell attachment sites were originally defined as morphologically distinct structures by electron microscopy: tight junctions, adherens junctions, and desmosomes (Obrink, 1986). In the adherens junctions, the major cell–surface adhesion receptors are the cadherins, but the nectins are also present (Niessen and Gottardi, 2008; Nishimura and Takeichi, 2009; Ogita and Takai, 2008). The extracellular domain of cadherins mediate strong cell–cell adhesion by binding to cadherins on an adjacent cell; the cytoplasmic tail of cadherin interacts with several proteins, including  $\beta$ -catenin (via the distal portion of the cadherin cytoplasmic tail) and p120-catenin (via a more proximal region of the cadherin cytoplasmic tail; Perez-Moreno and Fuchs, 2006).  $\beta$ -Catenin in turn binds  $\alpha$ -catenin, and both  $\beta$ - and  $\alpha$ -catenin bind the vinculin head. The interaction between  $\beta$ -catenin and vinculin requires residues in the  $\beta$ -catenin N-terminus; key among these is methionine 8, which when mutated to a proline residue blocks vinculin binding, both *in vitro* and in cells (Peng et al., 2010). The  $\alpha$ -catenin binding site for vinculin remains unclear, with several groups having shown that vinculin binds to  $\alpha$ -catenin residues 273–510 (or smaller fragments, 326–510 amino acids) (Bakolitsa et al., 2004; Imamura et al., 1999; Watabe-Uchida et al., 1998; Yonemura et al., 2010), and others report that vinculin binds to  $\alpha$ -catenin 697–906 (Weiss et al., 1998).

With regard to functional relevance, all the evidence to date suggests that vinculin is required to maintain the integrity of adherens junctions. The first hint of vinculin's importance came from the observation that cell–cell adhesion is lost in numerous cancer cells during the initial stages of tumor formation, at the time when vinculin becomes mislocalized (Kawahara et al., 1999; Lifschitz-Mercer et al., 1997; Meyer and Brinck, 1997; Sadano et al., 1992; Somiari et al., 2003). Later it was found that defects in mice lacking vinculin were consistent with a role for vinculin in regulating adherens junction function (discussed in detail later). However, one limitation to interpreting vinculin's importance using these approaches is that vinculin function at cell–matrix adhesions is also perturbed. Thus, it is impossible to draw definitive conclusions about the contribution of vinculin specifically to adherens junctions. Similarly, overexpression studies are uninformative as overexpressed vinculin neither integrates readily into preexisting cell–cell adhesions nor turns over in a manner consistent with cadherin–catenin dynamics (Yamada et al., 2005). Given that vinculin's affinity for cell–matrix adhesions is higher than its affinity for cell–cell adhesions, and that only a small amount of vinculin is required to maintain cell–matrix adhesions (Bakolitsa et al., 2004; Xu et al., 1998a,b), it seemed likely that vinculin could be preferentially depleted from adherens junctions by RNA interference. Indeed, it is possible to disrupt vinculin colocalization with  $\beta$ -catenin and its binding to cadherin adhesion complexes through this approach, and the outcome is loss of epithelial morphology,

adhesion to cadherin extracellular domains, and junctional integrity (Maddugoda et al., 2007; Peng et al., 2010). Moreover, these effects could be specifically attributed to the pool of vinculin in adherens junctions, as the residual vinculin localized to focal adhesions, and cell adhesion to the extracellular matrix was maintained at wild-type levels (Peng et al., 2010).

### 6.1.2. Roles for vinculin in adherens junctions

Although vinculin had been identified as an integral component of adherens junctions in various tissues throughout the years, it was only recently that attention was focused on understanding its role at this site (Bloch and Hall, 1983; Drenckhahn and Franz, 1986; Drenckhahn and Mannherz, 1983; Geiger et al., 1981; Koteliensky and Gneushev, 1983; Massa et al., 1995; Opas et al., 1985; Pardo et al., 1983a). These efforts have uncovered three roles for vinculin.

One line of evidence suggests that vinculin acts downstream of myosin VI, a minus end-directed motor necessary for the E-cadherin-dependent process of border-cell migration (Maddugoda et al., 2007). Depletion of myosin VI in epithelial cells resulted in a loss of vinculin binding to E-cadherin, and in a disruption of the actin cytoskeletal network. This observation, combined with the fact that cells devoid of vinculin (Watabe-Uchida et al., 1998) share phenotypes with cells lacking myosin VI, led to the idea that vinculin may be responsible for the effects of myosin VI. To test this possibility, it was determined if vinculin could rescue the phenotype of myosin VI knockdown cells using chimeras of the vinculin head or tail fused to the N-terminal region of  $\alpha$ -catenin to overcome the potential complication of vinculin autoinhibition. Interestingly, both transgenes rescue the junctional defects induced by a loss of myosin VI. These observations suggest that vinculin acts downstream of myosin VI; this idea is confirmed by the observation that exogenous myosin VI could not rescue the effects induced by a loss of myosin VI in the absence of vinculin expression (Maddugoda et al., 2007).

The second reported role for vinculin in cadherin-based adhesion is the regulation of E-cadherin surface expression. We found that in the absence of vinculin, the expression of E-cadherin at the cell surface was significantly reduced, whereas the total E-cadherin levels remained unchanged (Peng et al., 2010). This defect could be rescued by wild-type vinculin, but not by a mutant (A50I) form. Biochemical analysis showed that the A50I mutation blocked vinculin binding to  $\beta$ -catenin while maintaining the  $\alpha$ -catenin–vinculin interaction, suggesting that the interaction between vinculin and  $\beta$ -catenin may account for the decreased expression of E-cadherin at the cell surface. Indeed, a  $\beta$ -catenin point mutant that specifically blocks vinculin binding recapitulated the loss of surface E-cadherin expression phenotype.

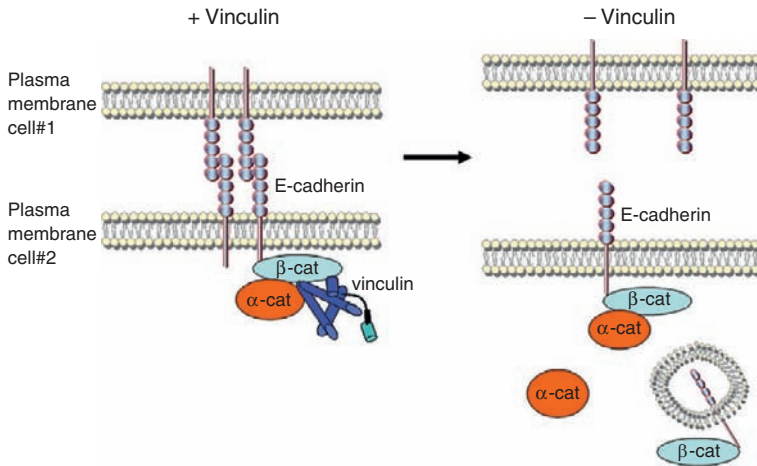


**Figure 5.5** *Vinculin is required for proper cell–cell adhesion.* In the presence of vinculin (left panel), E-cadherin is stably expressed at the cell surface and strong adhesions are formed between neighboring cells. Upon the loss of vinculin (right panel), cell–cell adhesions disassemble, and E-cadherin is lost from the cell surface and is internalized.

Thus, vinculin regulates surface E-cadherin dynamics via its interaction with β-catenin (Fig. 5.5).

Third, vinculin has been reported to play a role in the mechanosensory response of E-cadherin (le Duc et al., 2010). In F9 cells, cadherin-mediated junctional stiffness increases in proportion to the applied stress, providing direct evidence that reinforcement of E-cadherin adhesion is dependent on force (le Duc et al., 2010). This response requires the contractile actin cytoskeleton, as treatment with latrunculin B, cytochalasin D, and blebbistatin largely ameliorated this effect. In the search for the protein(s) that transmit force between the cadherin complex and the actin cytoskeleton, vinculin was found to be recruited to cell–cell junctions in a myosin II-dependent manner (le Duc et al., 2010; Yonemura et al., 2010). More importantly, cells lacking vinculin had a ~50% reduction in stiffness and exhibited a dramatic decrease in the recruitment of phosphorylated myosin light chains (a downstream mediator of tension) to cell–cell junctions when stimulated with hepatocyte growth factor. Further, α-catenin binding to vinculin was recently reported to be dependent upon myosin II activity (Yonemura et al., 2010). This effect is similar to what has been observed when force is applied to talin (del Rio et al., 2009).

## 6.2. Vinculin recruitment to adhesion sites

### 6.2.1. Vinculin recruitment to focal adhesions

Talin has long been thought to be the protein that recruits vinculin to focal adhesions due to its early engagement with integrin (Horwitz et al., 1986). However, recent studies have shown that the above-mentioned vinculin mutant, A50I, which blocks talin binding is nevertheless able to localize to focal adhesions, leaving the question of how vinculin is recruited unanswered (Bakolitsa et al., 2004; Cohen et al., 2006; Humphries et al., 2007; Peng et al., 2010). Some evidence suggests that paxillin may be responsible for this recruitment, via its ability to bind both integrins and vinculin directly. Indeed, Pasapera et al. (2010) proposed a model for vinculin recruitment to focal adhesions. According to this model nascent adhesions are bound to talin and paxillin, an increase in myosin II-mediated FAK phosphorylation results in elevated paxillin phosphorylation, and phosphorylated paxillin promotes vinculin recruitment to the adhesion site (Pasapera et al., 2010). The observation that paxillin and vinculin have different dynamics in mature focal adhesions (Hu et al., 2007; Humphries et al., 2007), together with the finding that vinculin localizes to large and stable adhesions at times when FAK expression is inhibited, suggests that vinculin recruitment is more complicated than what this model predicts (Pasapera et al., 2010). Consistent with this notion, vinculin fragments that lack an intact paxillin binding site still localizes to focal adhesions (Humphries et al., 2007).

### 6.2.2. Vinculin recruitment to adherens junctions

How vinculin is recruited to adherens junctions is controversial. Historically,  $\alpha$ -catenin has been thought to recruit vinculin to intercellular junctions because it is lost from adherens junctions in cancer cells and hearts lacking  $\alpha$ -catenin (Sheikh et al., 2006; Watabe-Uchida et al., 1998). However, in some cancer cell lines that lack  $\alpha$ -catenin, vinculin can be coimmunoprecipitated with  $\beta$ -catenin–E-cadherin complexes (Hazan et al., 1997). We too have found that  $\beta$ -catenin is required for vinculin localization, based on two observations. The first is that a mutant version of vinculin (A50I) that retains the ability to bind  $\alpha$ -catenin, but not  $\beta$ -catenin, is impaired in junctional localization. Second, shRNA-mediated inhibition of  $\beta$ -catenin expression results in a phenotype reminiscent of those obtained in vinculin knockdown cells; importantly, this phenotype could not be rescued by a mutant version of  $\beta$ -catenin that cannot bind vinculin (Peng et al., 2010). One possible explanation for these differences is that, in some contexts, the influence of  $\alpha$ -catenin on vinculin is due to its effects on  $\beta$ -catenin. This notion is supported by the observation that the form of  $\beta$ -catenin that binds preferentially to cadherin also binds  $\alpha$ -catenin, and that

preassociation of recombinant  $\alpha$ -catenin with  $\beta$ -catenin leads to enhanced binding of  $\beta$ -catenin to cadherin (Castano et al., 2002).  $\alpha$ -Catenin expression is not disturbed in our vinculin knockdown cell lines, and the mutant version of  $\beta$ -catenin that fails to bind vinculin associates with  $\alpha$ -catenin at wild-type levels (Peng et al., 2010). These observations indicate that if  $\alpha$ -catenin is required for vinculin localization, it is secondary to  $\beta$ -catenin or is part of a molecular complex that contains  $\beta$ -catenin and is important for vinculin localization.

Myosin VI has also been implicated in vinculin recruitment to cell–cell junctions. Specifically, myosin VI is necessary for the incorporation of vinculin into stable cadherin-containing adhesions (Maddugoda et al., 2007). In the study that made this observation, it was noted that vinculin is recruited to cell–cell adhesions before myosin VI is detected at these sites (Maddugoda et al., 2007). This observation, in combination with our finding that vinculin recruitment requires  $\beta$ -catenin, suggests the intriguing possibility that the initial recruitment of vinculin to cell–cell adhesions is mediated by  $\beta$ -catenin, and that myosin VI is dominant at a later stage.

### 6.2.3. Different modes of recruitment

One question with respect to vinculin function that has remained unanswered for a number of years is how vinculin is differentially recruited to focal adhesions versus cell–cell adhesions. The vinculin mutant A50I which fails to localize to cell–cell adhesions is nevertheless able to localize to focal adhesions suggesting that ligand binding to this residue is dispensable for vinculin recruitment to cell–matrix adhesions (Bakolitsa et al., 2004; Cohen et al., 2006; Humphries et al., 2007; Peng et al., 2010). Hence, recruitment to different adhesions likely arises from differential binding to this amino acid residue. Future studies examining the mechanism of vinculin localization to focal adhesions and to adherens junctions will provide insight into how vinculin is directed to one site versus the other under distinct physiological conditions.



## 7. INTERPLAY BETWEEN CELL–CELL AND CELL–MATRIX ADHESION: VINCULIN IN DEVELOPMENT AND CARDIOMYOPATHY

Cell adhesions are pivotal in many morphogenic processes, including cell sorting, cell rearrangement, and cell movement (Gumbiner, 2005). Thus, it is not surprising that the disruption of cell adhesion components, such as vinculin, occurs in numerous diseased states. For example, vinculin

expression is commonly lost in cancers (Kawahara et al., 1999; Lifschitz-Mercer et al., 1997; Meyer and Brinck, 1997; Sadano et al., 1992; Somiari et al., 2003), and mutations in vinculin are linked to a variety of cardiomyopathies (Maeda et al., 1997; Olson et al., 2002; Vasile et al., 2006a,b,c). Efforts to better understand the role of vinculin in these and other diseased states have included the development of animal models in which to study vinculin function. This work has confirmed and expanded our knowledge of vinculin's role in cell-cell and cell-matrix adhesions and has underscored the importance of vinculin *in vivo*.

As described above, the loss of vinculin leads to the disruption of cell adhesion and cell migration, both of which are processes crucial to embryonic development. Therefore, it seemed likely that disrupting vinculin expression would lead to developmental abnormalities. To test this directly, homologous recombination was used to delete the vinculin gene in mouse (Xu et al., 1998a). Vinculin inactivation resulted in lethality at embryonic day E10, with abnormalities first observed as early as E8. The most prominent defect in the whole-mount animal was failure of the neural folds and head structures to fuse in the ventral cranial midline (Xu et al., 1998a). Another defect, and the most likely cause of lethality, was malformation of the heart (Xu et al., 1998a). At stage E10, a functional heart becomes very important because developing organs require the efficient vascular delivery of nutrients and the removal of waste. In the vinculin null embryo, the heart is only about half the size of that in normal littermates and is surrounded by a dilated pericardial cavity. The walls are thin, with too few cardiomyocytes in what should be the dense layer (Xu et al., 1998a). The endocardium is present, but the valves never form, and the heart never contracts (Xu et al., 1998a). The somites and limbs of the vinculin null embryos are also greatly reduced in size and retarded in development (Xu et al., 1998a). All these defects could potentially arise from improper adhesion and actin remodeling. These experiments suggest that these phenotypes may reflect a critical role for vinculin in mammalian embryogenesis, owing to its effects on cell-cell and cell-matrix adhesion.

The global vinculin knockout provides key insights into vinculin function and suggests that vinculin plays a crucial role in the regulation of heart function. In cardiac myocytes, vinculin is detected at the intercalated disks and costameres (Geiger et al., 1985; Koteliansky and Gneushev, 1983; Terracio et al., 1990; Volk and Geiger, 1984). The latter are heart-specific structures similar to cell-matrix adhesions and circumferentially align with the Z disk of the myofibrils (Samarel, 2005). They share many components of focal adhesions, including integrins, talin, vinculin,  $\alpha$ -actinin, and focal adhesion kinase, among others. Like focal adhesions, costameres organize myofilaments, which consist primarily of actin, into a three-dimensional structure and link them to the extracellular matrix. Costameres are also sites that transduce mechanical information across the cell membrane.

Intercalated disks, however, resemble intercellular junctions, such as the adherens junctions, desmosomes, and gap junctions (Noorman et al., 2009). These structures connect neighboring myocytes in a staggered fashion and are important for the mechanical and electrical coupling of cardiac myocytes. At both sites, vinculin is a major component of the mechanical transduction system, as its expression is upregulated in response to loading, and its localization in costameres is disrupted upon the unloading of mechanic force (Sharp et al., 1997).

As the vinculin homozygous knockout mouse fails to develop fully (Xu et al., 1998a), it has not been possible to use this model to study vinculin function in the adult heart. Fortunately, the vinculin hemizygous knockout mouse (vinculin<sup>+/-</sup>) develops normally (Zemljic-Harpe et al., 2004), and this mouse model system has been used to study the effects of diminished vinculin expression on the structural and functional integrity of the heart (Zemljic-Harpe et al., 2004). In the basal state, the vinculin<sup>+/-</sup> hearts are histologically and functionally normal, with the exception of small differences in conduction. The fact that bigger differences were not observed is somewhat surprising, given that the intercalated disks of vinculin<sup>+/-</sup> hearts are disrupted and the myofibrils are not properly anchored in the intercalated disks and Z-lines (Zemljic-Harpe et al., 2004). Whether the disrupted ultrastructure of the vinculin<sup>+/-</sup> hearts reduces function was tested by measuring tolerance to pressure loading induced by transverse aortic constriction (a commonly used operation to experimentally induce cardiac hypertrophy and heart failure). Thirty-three percentage of the vinculin<sup>+/-</sup> mice died immediately following surgery, and many of the remaining mice later developed progressive left-ventricular dysfunction and subsequently died (Zemljic-Harpe et al., 2004).

The Ross lab investigated whether the defects in vinculin<sup>+/-</sup> hearts are caused by a loss of cardiac myocyte function, using mice harboring a tissue-specific deletion of the vinculin gene (Zemljic-Harpe et al., 2007). Although the vinculin knockout mice appeared healthy initially, 50% died suddenly before reaching 14 weeks of age, due to ventricular tachycardia and disruptions in electrical conductance (Zemljic-Harpe et al., 2007). An analysis of tissues harvested prior to the loss of ventricular function showed highly serrated intercalated disks that were detached from the myofibrils (Zemljic-Harpe et al., 2007). The disruptions in intercalated disks arose from a loss of cadherin from this site, a phenomenon that is recapitulated in epithelial cells in which vinculin expression silenced (Peng et al., 2010). In addition, localization of connexin 43, a gap junction protein that is important for the electrical coupling of myocytes, was disrupted and is likely the cause of spontaneous arrhythmias that developed in these mice. Taken together, these findings demonstrate that vinculin is essential for proper heart function, owing to its effects on cell-cell adhesion in the intercalated disk.



## 8. CONCLUSIONS

Much progress has been made in our understanding of vinculin since its identification over 30 years ago. Recent advances in vinculin biology—specifically, elucidation of the full-length crystal structure and of the mechanisms, whereby vinculin regulates focal adhesion assembly and adherens junction function—will be critical in deciphering the function of vinculin at the organismal level and in disease. Accomplishing this task will require additional information about how these events are regulated in a cell. Specifically, the signal transduction pathways that control vinculin activation/inactivation, as well as those that trigger its incorporation into and dissociation from adhesions, will have to be elucidated. These feats will rely heavily upon technological advances. Mass spectrometry analyses will undoubtedly allow the full repertoire of vinculin binding partners to be uncovered, and high resolution imaging in combination with FRET should reveal how these interactions occur in a spatial and a temporal manner. A better understanding of these events will bring the scientific community one step closer to fully understanding how vinculin coordinates cell–matrix and cell–cell adhesion.

## ACKNOWLEDGMENTS

This work is supported by National Institutes of Health Grant # 1K01CA111818 and American Cancer Society Research Scholar Grant # 115274 to K. A. D. and American Heart Association Predoctoral Fellowship # 0910127G to X. P. The UI Interdisciplinary Training Grant in Molecular Biology (NIH Grant #5T32GM073610) supported E. N.

## REFERENCES

- Adey, N.B., Kay, B.K., 1997. Isolation of peptides from phage-displayed random peptide libraries that interact with the talin-binding domain of vinculin. *Biochem. J.* 324 (Pt. 2), 523–528.
- Alenghat, F.J., Fabry, B., Tsai, K.Y., Goldmann, W.H., Ingber, D.E., 2000. Analysis of cell mechanics in single vinculin-deficient cells using a magnetic tweezer. *Biochem. Biophys. Res. Commun.* 277, 93–99.
- Auweter, S.D., Allain, F.H., 2008. Structure–function relationships of the polypyrimidine tract binding protein. *Cell. Mol. Life Sci.* 65, 516–527.
- Ayalon, O., Geiger, B., 1997. Cyclic changes in the organization of cell adhesions and the associated cytoskeleton, induced by stimulation of tyrosine phosphorylation in bovine aortic endothelial cells. *J. Cell Sci.* 110 (Pt. 5), 547–556.
- Babic, I., Sharma, S., Black, D.L., 2009. A role for polypyrimidine tract binding protein in the establishment of focal adhesions. *Mol. Cell. Biol.* 29, 5564–5577.
- Bakolitsa, C., de Pereda, J.M., Bagshaw, C.R., Critchley, D.R., Liddington, R.C., 1999. Crystal structure of the vinculin tail suggests a pathway for activation. *Cell* 99, 603–613.

- Bakolitsa, C., Cohen, D.M., Bankston, L.A., Bobkov, A.A., Cadwell, G.W., Jennings, L., et al., 2004. Structural basis for vinculin activation at sites of cell adhesion. *Nature* 430, 583–586.
- Bass, M.D., Patel, B., Barsukov, I.G., Fillingham, I.J., Mason, R., Smith, B.J., et al., 2002. Further characterization of the interaction between the cytoskeletal proteins talin and vinculin. *Biochem. J.* 362, 761–768.
- Berrier, A.L., Yamada, K.M., 2007. Cell-matrix adhesion. *J. Cell. Physiol.* 213, 565–573.
- Bloch, R.J., Hall, Z.W., 1983. Cytoskeletal components of the vertebrate neuromuscular junction: vinculin, alpha-actinin, and filamin. *J. Cell Biol.* 97, 217–223.
- Bois, P.R., Borgon, R.A., Vornrhein, C., Izard, T., 2005. Structural dynamics of alpha-actinin–vinculin interactions. *Mol. Cell. Biol.* 25, 6112–6122.
- Bois, P.R., O'Hara, B.P., Nietlispach, D., Kirkpatrick, J., Izard, T., 2006. The vinculin binding sites of talin and alpha-actinin are sufficient to activate vinculin. *J. Biol. Chem.* 281, 7228–7236.
- Borgon, R.A., Vornrhein, C., Bricogne, G., Bois, P.R., Izard, T., 2004. Crystal structure of human vinculin. *Structure* 12, 1189–1197.
- Bourdet-Sicard, R., Rudiger, M., Jockusch, B.M., Gounon, P., Sansonetti, P.J., Nhieu, G.T., 1999. Binding of the *Shigella* protein IpaA to vinculin induces F-actin depolymerization. *EMBO J.* 18, 5853–5862.
- Brindle, N.P., Holt, M.R., Davies, J.E., Price, C.J., Critchley, D.R., 1996. The focal-adhesion vasodilator-stimulated phosphoprotein (VASP) binds to the proline-rich domain in vinculin. *Biochem. J.* 318 (Pt. 3), 753–757.
- Burridge, K., Feramisco, J.R., 1980. Microinjection and localization of a 130K protein in living fibroblasts: a relationship to actin and fibronectin. *Cell* 19, 587–595.
- Burridge, K., Mangeat, P., 1984. An interaction between vinculin and talin. *Nature* 308, 744–746.
- Calderwood, D.A., Zent, R., Grant, R., Rees, D.J., Hynes, R.O., Ginsberg, M.H., 1999. The talin head domain binds to integrin beta subunit cytoplasmic tails and regulates integrin activation. *J. Biol. Chem.* 274, 28071–28074.
- Carisey, A., Ballestrem, C., 2010. Vinculin, an adapter protein in control of cell adhesion signalling. *Eur. J. Cell Biol.* 90, 157–163.
- Castano, J., Raurell, I., Piedra, J.A., Miravet, S., Dunach, M., Garcia de Herreros, A., 2002. Beta-catenin N- and C-terminal tails modulate the coordinated binding of adherens junction proteins to beta-catenin. *J. Biol. Chem.* 277, 31541–31550.
- Ceccarelli, D.F., Song, H.K., Poy, F., Schaller, M.D., Eck, M.J., 2006. Crystal structure of the FERM domain of focal adhesion kinase. *J. Biol. Chem.* 281, 252–259.
- Chandrasekar, I., Stradal, T.E., Holt, M.R., Entschladen, F., Jockusch, B.M., Ziegler, W.H., 2005. Vinculin acts as a sensor in lipid regulation of adhesion-site turnover. *J. Cell Sci.* 118, 1461–1472.
- Chen, H., Cohen, D.M., Choudhury, D.M., Kioka, N., Craig, S.W., 2005. Spatial distribution and functional significance of activated vinculin in living cells. *J. Cell Biol.* 169, 459–470.
- Chen, H., Choudhury, D.M., Craig, S.W., 2006. Coincidence of actin filaments and talin is required to activate vinculin. *J. Biol. Chem.* 281, 40389–40398.
- Cohen, D.M., Chen, H., Johnson, R.P., Choudhury, B., Craig, S.W., 2005. Two distinct head-tail interfaces cooperate to suppress activation of vinculin by talin. *J. Biol. Chem.* 280, 17109–17117.
- Cohen, D.M., Kutscher, B., Chen, H., Murphy, D.B., Craig, S.W., 2006. A conformational switch in vinculin drives formation and dynamics of a talin–vinculin complex at focal adhesions. *J. Biol. Chem.* 281, 16006–16015.
- Coll, J.L., Ben-Ze'ev, A., Ezzell, R.M., Rodriguez Fernandez, J.L., Baribault, H., Oshima, R.G., et al., 1995. Targeted disruption of vinculin genes in F9 and embryonic

- stem cells changes cell morphology, adhesion, and locomotion. *Proc. Natl. Acad. Sci. USA* 92, 9161–9165.
- Coutu, M.D., Craig, S.W., 1988. cDNA-derived sequence of chicken embryo vinculin. *Proc. Natl. Acad. Sci. USA* 85, 8535–8539.
- del Rio, A., Perez-Jimenez, R., Liu, R., Roca-Cusachs, P., Fernandez, J.M., Sheetz, M.P., 2009. Stretching single talin rod molecules activates vinculin binding. *Science* 323, 638–641.
- DeMali, K.A., Burridge, K., 2003. Coupling membrane protrusion and cell adhesion. *J. Cell Sci.* 116, 2389–2397.
- DeMali, K.A., Barlow, C.A., Burridge, K., 2002. Recruitment of the Arp2/3 complex to vinculin: coupling membrane protrusion to matrix adhesion. *J. Cell Biol.* 159, 881–891.
- DeMali, K.A., Jue, A.L., Burridge, K., 2006. IpaA targets beta1 integrins and rho to promote actin cytoskeleton rearrangements necessary for *Shigella* entry. *J. Biol. Chem.* 281, 39534–39541.
- Diez, G., Kollmannsberger, P., Mierke, C.T., Koch, T.M., Vali, H., Fabry, B., et al., 2009. Anchorage of vinculin to lipid membranes influences cell mechanical properties. *Biophys. J.* 97, 3105–3112.
- Drenckhahn, D., Franz, H., 1986. Identification of actin-, alpha-actinin-, and vinculin-containing plaques at the lateral membrane of epithelial cells. *J. Cell Biol.* 102, 1843–1852.
- Drenckhahn, D., Mannherz, H.G., 1983. Distribution of actin and the actin-associated proteins myosin, tropomyosin, alpha-actinin, vinculin, and villin in rat and bovine exocrine glands. *Eur. J. Cell Biol.* 30, 167–176.
- Eimer, W., Niermann, M., Eppe, M.A., Jockusch, B.M., 1993. Molecular shape of vinculin in aqueous solution. *J. Mol. Biol.* 229, 146–152.
- Fillingham, I., Gingras, A.R., Papagrigoriou, E., Patel, B., Emsley, J., Critchley, D.R., et al., 2005. A vinculin binding domain from the talin rod unfolds to form a complex with the vinculin head. *Structure* 13, 65–74.
- Finlay, B.B., Ruschkowski, S., Dedhar, S., 1991. Cytoskeletal rearrangements accompanying salmonella entry into epithelial cells. *J. Cell Sci.* 99 (Pt. 2), 283–296.
- Finlay, B.B., Rosenshine, I., Donnenberg, M.S., Kaper, J.B., 1992. Cytoskeletal composition of attaching and effacing lesions associated with enteropathogenic *Escherichia coli* adherence to HeLa cells. *Infect. Immun.* 60, 2541–2543.
- Galbraith, C.G., Yamada, K.M., Sheetz, M.P., 2002. The relationship between force and focal complex development. *J. Cell Biol.* 159, 695–705.
- Gallant, N.D., Michael, K.E., Garcia, A.J., 2005. Cell adhesion strengthening: contributions of adhesive area, integrin binding, and focal adhesion assembly. *Mol. Biol. Cell* 16, 4329–4340.
- Garcia-Alvarez, B., de Pereda, J.M., Calderwood, D.A., Ulmer, T.S., Critchley, D., Campbell, I.D., et al., 2003. Structural determinants of integrin recognition by talin. *Mol. Cell* 11, 49–58.
- Geiger, B., 1979. A 130 K protein from chicken gizzard: its localization at the termini of microfilament bundles in cultured chicken cells. *Cell* 18, 193–205.
- Geiger, B., Tokuyasu, K.T., Dutton, A.H., Singer, S.J., 1980. Vinculin, an intracellular protein localized at specialized sites where microfilament bundles terminate at cell membranes. *Proc. Natl. Acad. Sci. USA* 77, 4127–4131.
- Geiger, B., Dutton, A.H., Tokuyasu, K.T., Singer, S.J., 1981. Immunoelectron microscope studies of membrane-microfilament interactions: distributions of alpha-actinin, tropomyosin, and vinculin in intestinal epithelial brush border and chicken gizzard smooth muscle cells. *J. Cell Biol.* 91, 614–628.
- Geiger, B., Volk, T., Volberg, T., 1985. Molecular heterogeneity of adherens junctions. *J. Cell Biol.* 101, 1523–1531.

- Gilmore, A.P., Burridge, K., 1996. Regulation of vinculin binding to talin and actin by phosphatidyl-inositol-4-5-bisphosphate. *Nature* 381, 531–535.
- Gingras, A.R., Ziegler, W.H., Frank, R., Barsukov, I.L., Roberts, G.C., Critchley, D.R., et al., 2005. Mapping and consensus sequence identification for multiple vinculin binding sites within the talin rod. *J. Biol. Chem.* 280, 37217–37224.
- Gingras, A.R., Vogel, K.P., Steinhoff, H.J., Ziegler, W.H., Patel, B., Emsley, J., et al., 2006. Structural and dynamic characterization of a vinculin binding site in the talin rod. *Biochemistry* 45, 1805–1817.
- Goldmann, W.H., Guttenberg, Z., Tang, J.X., Kroy, K., Isenberg, G., Ezzell, R.M., 1998. Analysis of the F-actin binding fragments of vinculin using stopped-flow and dynamic light-scattering measurements. *Eur. J. Biochem.* 254, 413–419.
- Grashoff, C., Hoffman, B.D., Brenner, M.D., Zhou, R., Parsons, M., Yang, M.T., et al., 2010. Measuring mechanical tension across vinculin reveals regulation of focal adhesion dynamics. *Nature* 466, 263–266.
- Groesch, M.E., Otto, J.J., 1990. Purification and characterization of an 85 kDa talin-binding fragment of vinculin. *Cell Motil. Cytoskeleton* 15, 41–50.
- Gumbiner, B.M., 2005. Regulation of cadherin-mediated adhesion in morphogenesis. *Nat. Rev. Mol. Cell Biol.* 6, 622–634.
- Halegoua, S., 1987. Changes in the phosphorylation and distribution of vinculin during nerve growth factor induced neurite outgrowth. *Dev. Biol.* 121, 97–104.
- Hamiaux, C., van Eerde, A., Parsot, C., Broos, J., Dijkstra, B.W., 2006. Structural mimicry for vinculin activation by IpaA, a virulence factor of *Shigella flexneri*. *EMBO Rep.* 7, 794–799.
- Hazan, R.B., Kang, L., Roe, S., Borgen, P.I., Rimm, D.L., 1997. Vinculin is associated with the E-cadherin adhesion complex. *J. Biol. Chem.* 272, 32448–32453.
- Hemmings, L., Rees, D.J., Ohanian, V., Bolton, S.J., Gilmore, A.P., Patel, B., et al., 1996. Talin contains three actin-binding sites each of which is adjacent to a vinculin-binding site. *J. Cell Sci.* 109 (Pt. 11), 2715–2726.
- Horwitz, A., Duggan, K., Buck, C., Beckerle, M.C., Burridge, K., 1986. Interaction of plasma membrane fibronectin receptor with talin—a transmembrane linkage. *Nature* 320, 531–533.
- Hu, K., Ji, L., Applegate, K.T., Danuser, G., Waterman-Storer, C.M., 2007. Differential transmission of actin motion within focal adhesions. *Science* 315, 111–115.
- Humphries, J.D., Wang, P., Streuli, C., Geiger, B., Humphries, M.J., Ballestrem, C., 2007. Vinculin controls focal adhesion formation by direct interactions with talin and actin. *J. Cell Biol.* 179, 1043–1057.
- Huttelmaier, S., Bubeck, P., Rudiger, M., Jockusch, B.M., 1997. Characterization of two F-actin-binding and oligomerization sites in the cell-contact protein vinculin. *Eur. J. Biochem.* 247, 1136–1142.
- Huttelmaier, S., Mayboroda, O., Harbeck, B., Jarchau, T., Jockusch, B.M., Rudiger, M., 1998. The interaction of the cell-contact proteins VASP and vinculin is regulated by phosphatidylinositol-4, 5-bisphosphate. *Curr. Biol.* 8, 479–488.
- Huttelmaier, S., Illenberger, S., Grosheva, I., Rudiger, M., Singer, R.H., Jockusch, B.M., 2001. Raver1, a dual compartment protein, is a ligand for PTB/hmRNPI and microfilament attachment proteins. *J. Cell Biol.* 155, 775–786.
- Huveneers, S., Danen, E.H., 2009. Adhesion signaling—crosstalk between integrins, Src and Rho. *J. Cell Sci.* 122, 1059–1069.
- Hytonen, V.P., Vogel, V., 2008. How force might activate talin's vinculin binding sites: SMD reveals a structural mechanism. *PLoS Comput. Biol.* 4, e24.
- Imamura, Y., Itoh, M., Maeno, Y., Tsukita, S., Nagafuchi, A., 1999. Functional domains of alpha-catenin required for the strong state of cadherin-based cell adhesion. *J. Cell Biol.* 144, 1311–1322.

- Isenberg, G., Goldmann, W.H., 1998. Peptide-specific antibodies localize the major lipid binding sites of talin dimers to oppositely arranged N-terminal 47 kDa subdomains. *FEBS Lett.* 426, 165–170.
- Isenberg, G., Leonard, K., Jockusch, B.M., 1982. Structural aspects of vinculin-actin interactions. *J. Mol. Biol.* 158, 231–249.
- Izard, T., Vornrhein, C., 2004. Structural basis for amplifying vinculin activation by talin. *J. Biol. Chem.* 279, 27667–27678.
- Izard, T., Evans, G., Borgon, R.A., Rush, C.L., Bricogne, G., Bois, P.R., 2004. Vinculin activation by talin through helical bundle conversion. *Nature* 427, 171–175.
- Izard, T., Tran Van Nhieu, G., Bois, P.R., 2006. *Shigella* applies molecular mimicry to subvert vinculin and invade host cells. *J. Cell Biol.* 175, 465–475.
- Janssen, M.E., Kim, E., Liu, H., Fujimoto, L.M., Bobkov, A., Volkmann, N., et al., 2006. Three-dimensional structure of vinculin bound to actin filaments. *Mol. Cell* 21, 271–281.
- Ji, L., Lim, J., Danuser, G., 2008. Fluctuations of intracellular forces during cell protrusion. *Nat. Cell Biol.* 10, 1393–1400.
- Jockusch, B.M., Isenberg, G., 1981. Interaction of alpha-actinin and vinculin with actin: opposite effects on filament network formation. *Proc. Natl. Acad. Sci. USA* 78, 3005–3009.
- Johnson, R.P., Craig, S.W., 1994. An intramolecular association between the head and tail domains of vinculin modulates talin binding. *J. Biol. Chem.* 269, 12611–12619.
- Johnson, R.P., Craig, S.W., 1995a. The carboxy-terminal tail domain of vinculin contains a cryptic binding site for acidic phospholipids. *Biochem. Biophys. Res. Commun.* 210, 159–164.
- Johnson, R.P., Craig, S.W., 1995b. F-actin binding site masked by the intramolecular association of vinculin head and tail domains. *Nature* 373, 261–264.
- Johnson, R.P., Craig, S.W., 2000. Actin activates a cryptic dimerization potential of the vinculin tail domain. *J. Biol. Chem.* 275, 95–105.
- Kawahara, E., Tokuda, R., Nakanishi, I., 1999. Migratory phenotypes of HSC-3 squamous carcinoma cell line induced by EGF and PMA: relevance to migration of loosening of adhesion and vinculin-associated focal contacts with prominent filopodia. *Cell Biol. Int.* 23, 163–174.
- Kioka, N., Sakata, S., Kawauchi, T., Amachi, T., Akiyama, S.K., Okazaki, K., et al., 1999. Vinexin: a novel vinculin-binding protein with multiple SH3 domains enhances actin cytoskeletal organization. *J. Cell Biol.* 144, 59–69.
- Kotliansky, V.E., Gneushev, G.N., 1983. Vinculin localization in cardiac muscle. *FEBS Lett.* 159, 158–160.
- Kroemker, M., Rudiger, A.H., Jockusch, B.M., Rudiger, M., 1994. Intramolecular interactions in vinculin control alpha-actinin binding to the vinculin head. *FEBS Lett.* 355, 259–262.
- Kupper, K., Lang, N., Mohl, C., Kirchgessner, N., Born, S., Goldmann, W.H., et al., 2010. Tyrosine phosphorylation of vinculin at position 1065 modifies focal adhesion dynamics and cell tractions. *Biochem. Biophys. Res. Commun.* 399, 560–564.
- le Duc, Q., Shi, Q., Blonk, I., Sonnenberg, A., Wang, N., Leckband, D., et al., 2010. Vinculin potentiates E-cadherin mechanosensing and is recruited to actin-anchored sites within adherens junctions in a myosin II-dependent manner. *J. Cell Biol.* 189, 1107–1115.
- Lee, J.H., Rangarajan, E.S., Yogesha, S.D., Izard, T., 2009. Raver1 interactions with vinculin and RNA suggest a feed-forward pathway in directing mRNA to focal adhesions. *Structure* 17, 833–842.
- Lifschitz-Mercer, B., Czernobilsky, B., Feldberg, E., Geiger, B., 1997. Expression of the adherens junction protein vinculin in human basal and squamous cell tumors: relationship to invasiveness and metastatic potential. *Hum. Pathol.* 28, 1230–1236.

- Lombardi, M.L., Knecht, D.A., Dembo, M., Lee, J., 2007. Traction force microscopy in *Dictyostelium* reveals distinct roles for myosin II motor and actin-crosslinking activity in polarized cell movement. *J. Cell Sci.* 120, 1624–1634.
- Lotz, M.M., Burdsal, C.A., Erickson, H.P., McClay, D.R., 1989. Cell adhesion to fibronectin and tenascin: quantitative measurements of initial binding and subsequent strengthening response. *J. Cell Biol.* 109, 1795–1805.
- Maciver, S.K., 1996. Myosin II function in non-muscle cells. *Bioessays* 18, 179–182.
- Maddugoda, M.P., Crampton, M.S., Shewan, A.M., Yap, A.S., 2007. Myosin VI and vinculin cooperate during the morphogenesis of cadherin cell cell contacts in mammalian epithelial cells. *J. Cell Biol.* 178, 529–540.
- Maeda, M., Holder, E., Lowes, B., Valent, S., Bies, R.D., 1997. Dilated cardiomyopathy associated with deficiency of the cytoskeletal protein metavinculin. *Circulation* 95, 17–20.
- Mandai, K., Nakanishi, H., Satoh, A., Takahashi, K., Satoh, K., Nishioka, H., et al., 1999. Ponsin/SH3P12: an I-afadin- and vinculin-binding protein localized at cell-cell and cell-matrix adherens junctions. *J. Cell Biol.* 144, 1001–1017.
- Massa, R., Silvestri, G., Sancesario, G., Bernardi, G., 1995. Immunocytochemical localization of vinculin in muscle and nerve. *Muscle Nerve* 18, 1277–1284.
- McCann, R.O., Craig, S.W., 1997. The I/LWEQ module: a conserved sequence that signifies F-actin binding in functionally diverse proteins from yeast to mammals. *Proc. Natl. Acad. Sci. USA* 94, 5679–5684.
- Menard, R., Sansonetti, P.J., Parsot, C., 1993. Nonpolar mutagenesis of the ipa genes defines IpaB, IpaC, and IpaD as effectors of *Shigella flexneri* entry into epithelial cells. *J. Bacteriol.* 175, 5899–5906.
- Menkel, A.R., Kroemker, M., Bubeck, P., Ronsiek, M., Nikolai, G., Jockusch, B.M., 1994. Characterization of an F-actin-binding domain in the cytoskeletal protein vinculin. *J. Cell Biol.* 126, 1231–1240.
- Meyer, T., Brinck, U., 1997. Immunohistochemical detection of vinculin in human rhabdomyosarcomas. *Gen. Diagn. Pathol.* 142, 191–198.
- Mierke, C.T., Kollmannsberger, P., Zitterbart, D.P., Smith, J., Fabry, B., Goldmann, W.H., 2008. Mechano-coupling and regulation of contractility by the vinculin tail domain. *Biophys. J.* 94, 661–670.
- Mierke, C.T., Kollmannsberger, P., Zitterbart, D.P., Diez, G., Koch, T.M., Marg, S., et al., 2010. Vinculin facilitates cell invasion into three-dimensional collagen matrices. *J. Biol. Chem.* 285, 13121–13130.
- Milam, L.M., 1985. Electron microscopy of rotary shadowed vinculin and vinculin complexes. *J. Mol. Biol.* 184, 543–545.
- Miller, G.J., Dunn, S.D., Ball, E.H., 2001. Interaction of the N- and C-terminal domains of vinculin. Characterization and mapping studies. *J. Biol. Chem.* 276, 11729–11734.
- Moese, S., Selbach, M., Brinkmann, V., Karlas, A., Haimovich, B., Backert, S., et al., 2007. The *Helicobacter pylori* CagA protein disrupts matrix adhesion of gastric epithelial cells by dephosphorylation of vinculin. *Cell. Microbiol.* 9, 1148–1161.
- Mohl, C., Kirchgessner, N., Schafer, C., Kupper, K., Born, S., Diez, G., et al., 2009. Becoming stable and strong: the interplay between vinculin exchange dynamics and adhesion strength during adhesion site maturation. *Cell Motil. Cytoskeleton* 66, 350–364.
- Molony, L., Burridge, K., 1985. Molecular shape and self-association of vinculin and metavinculin. *J. Cell. Biochem.* 29, 31–36.
- Niessen, C.M., Gottardi, C.J., 2008. Molecular components of the adherens junction. *Biochim. Biophys. Acta* 1778, 562–571.
- Nishimura, T., Takeichi, M., 2009. Remodeling of the adherens junctions during morphogenesis. *Curr. Top. Dev. Biol.* 89, 33–54.

- Nolz, J.C., Medeiros, R.B., Mitchell, J.S., Zhu, P., Freedman, B.D., Shimizu, Y., et al., 2007. WAVE2 regulates high-affinity integrin binding by recruiting vinculin and talin to the immunological synapse. *Mol. Cell Biol.* 27, 5986–6000.
- Noorman, M., van der Heyden, M.A., van Veen, T.A., Cox, M.G., Hauer, R.N., de Bakker, J.M., et al., 2009. Cardiac cell-cell junctions in health and disease: electrical versus mechanical coupling. *J. Mol. Cell. Cardiol.* 47, 23–31.
- Obrink, B., 1986. Epithelial cell adhesion molecules. *Exp. Cell Res.* 163, 1–21.
- Ogita, H., Takai, Y., 2008. Cross-talk among integrin, cadherin, and growth factor receptor: roles of nectin and nectin-like molecule. *Int. Rev. Cytol.* 265, 1–54.
- Ohmori, T., Kashiwakura, Y., Ishiwata, A., Madoiwa, S., Mimuro, J., Honda, S., et al., 2010. Vinculin activates inside-out signaling of integrin  $\alpha$ IIb $\beta$ 3 in Chinese hamster ovary cells. *Biochem. Biophys. Res. Commun.* 400, 323–328.
- Olson, T.M., Illenberger, S., Kishimoto, N.Y., Huttelmaier, S., Keating, M.T., Jockusch, B.M., 2002. Metavinculin mutations alter actin interaction in dilated cardiomyopathy. *Circulation* 105, 431–437.
- Opas, M., Turksen, K., Kalnins, V.I., 1985. Adhesiveness and distribution of vinculin and spectrin in retinal pigmented epithelial cells during growth and differentiation in vitro. *Dev. Biol.* 107, 269–280.
- Otto, J.J., 1986. The lack of interaction between vinculin and actin. *Cell Motil. Cytoskeleton* 6, 48–55.
- Pantaloni, D., Le Clainche, C., Carlier, M.F., 2001. Mechanism of actin-based motility. *Science* 292, 1502–1506.
- Papagrigoriou, E., Gingras, A.R., Barsukov, I.L., Bate, N., Fillingham, I.J., Patel, B., et al., 2004. Activation of a vinculin-binding site in the talin rod involves rearrangement of a five-helix bundle. *EMBO J.* 23, 2942–2951.
- Pardo, J.V., Siliciano, J.D., Craig, S.W., 1983a. A vinculin-containing cortical lattice in skeletal muscle: transverse lattice elements (“costameres”) mark sites of attachment between myofibrils and sarcolemma. *Proc. Natl. Acad. Sci. USA* 80, 1008–1012.
- Pardo, J.V., Siliciano, J.D., Craig, S.W., 1983b. Vinculin is a component of an extensive network of myofibril-sarcolemma attachment regions in cardiac muscle fibers. *J. Cell Biol.* 97, 1081–1088.
- Pasapera, A.M., Schneider, I.C., Rericha, E., Schlaepfer, D.D., Waterman, C.M., 2010. Myosin II activity regulates vinculin recruitment to focal adhesions through FAK-mediated paxillin phosphorylation. *J. Cell Biol.* 188, 877–890.
- Patel, B., Gingras, A.R., Bobkov, A.A., Fujimoto, L.M., Zhang, M., Liddington, R.C., et al., 2006. The activity of the vinculin binding sites in talin is influenced by the stability of the helical bundles that make up the talin rod. *J. Biol. Chem.* 281, 7458–7467.
- Peng, X., Cuff, L.E., Lawton, C.D., DeMali, K.A., 2010. Vinculin regulates cell-surface E-cadherin expression by binding to beta-catenin. *J. Cell Sci.* 123, 567–577.
- Perez-Moreno, M., Fuchs, E., 2006. Catenins: keeping cells from getting their signals crossed. *Dev. Cell* 11, 601–612.
- Pokutta, S., Drees, F., Takai, Y., Nelson, W.J., Weis, W.I., 2002. Biochemical and structural definition of the  $\beta$ -catenin- and actin-binding sites of  $\alpha$ -catenin. *J. Biol. Chem.* 277, 18868–18874.
- Pollard, T.D., Borisy, G.G., 2003. Cellular motility driven by assembly and disassembly of actin filaments. *Cell* 112, 453–465.
- Pruzman, K.C., Gao, G., King, M.L., Iyer, V.V., Mueller, G.A., Schaller, M.D., et al., 2004. The focal adhesion targeting domain of focal adhesion kinase contains a hinge region that modulates tyrosine 926 phosphorylation. *Structure* 12, 881–891.
- Ramarao, N., Le Clainche, C., Izard, T., Bourdet-Sicard, R., Ageron, E., Sansonetti, P.J., et al., 2007. Capping of actin filaments by vinculin activated by the *Shigella* IpaA carboxyl-terminal domain. *FEBS Lett.* 581, 853–857.

- Ridley, A.J., Schwartz, M.A., Burridge, K., Firtel, R.A., Ginsberg, M.H., Borisy, G., et al., 2003. Cell migration: integrating signals from front to back. *Science* 302, 1704–1709.
- Rodriguez Fernandez, J.L., Geiger, B., Salomon, D., Sabanay, I., Zoller, M., Ben-Ze'ev, A., 1992. Suppression of tumorigenicity in transformed cells after transfection with vinculin cDNA. *J. Cell Biol.* 119, 427–438.
- Rosenfeld, G.C., Hou, D.C., Dingus, J., Meza, I., Bryan, J., 1985. Isolation and partial characterization of human platelet vinculin. *J. Cell Biol.* 100, 669–676.
- Sadano, H., Inoue, M., Taniguchi, S., 1992. Differential expression of vinculin between weakly and highly metastatic B16-melanoma cell lines. *Jpn. J. Cancer Res.* 83, 625–630.
- Samarel, A.M., 2005. Costameres, focal adhesions, and cardiomyocyte mechanotransduction. *Am. J. Physiol. Heart Circ. Physiol.* 289, H2291–H2301.
- Saunders, R.M., Holt, M.R., Jennings, L., Sutton, D.H., Barsukov, I.L., Bobkov, A., et al., 2006. Role of vinculin in regulating focal adhesion turnover. *Eur. J. Cell Biol.* 85, 487–500.
- Sawicka, K., Bushell, M., Spriggs, K.A., Willis, A.E., 2008. Polypyrimidine-tract-binding protein: a multifunctional RNA-binding protein. *Biochem. Soc. Trans.* 36, 641–647.
- Schindeler, A., Lavulo, L., Harvey, R.P., 2005. Muscle costameric protein, Chisel/Smpx, associates with focal adhesion complexes and modulates cell spreading in vitro via a Rac1/p38 pathway. *Exp. Cell Res.* 307, 367–380.
- Schwartz, M.A., DeSimone, D.W., 2008. Cell adhesion receptors in mechanotransduction. *Curr. Opin. Cell Biol.* 20, 551–556.
- Schwienbacher, C., Jockusch, B.M., Rudiger, M., 1996. Intramolecular interactions regulate serine/threonine phosphorylation of vinculin. *FEBS Lett.* 384, 71–74.
- Sefton, B.M., Hunter, T., Ball, E.H., Singer, S.J., 1981. Vinculin: a cytoskeletal target of the transforming protein of Rous sarcoma virus. *Cell* 24, 165–174.
- Sharp, W.W., Simpson, D.G., Borg, T.K., Samarel, A.M., Terracio, L., 1997. Mechanical forces regulate focal adhesion and costamere assembly in cardiac myocytes. *Am. J. Physiol.* 273, H546–H556.
- Sheikh, F., Chen, Y., Liang, X., Hirschy, A., Stenbit, A.E., Gu, Y., et al., 2006. Alpha-E-catenin inactivation disrupts the cardiomyocyte adherens junction, resulting in cardiomyopathy and susceptibility to wall rupture. *Circulation* 114, 1046–1055.
- Somiari, R.I., Sullivan, A., Russell, S., Somiari, S., Hu, H., Jordan, R., et al., 2003. High-throughput proteomic analysis of human infiltrating ductal carcinoma of the breast. *Proteomics* 3, 1863–1873.
- Steimle, P.A., Hoffert, J.D., Adey, N.B., Craig, S.W., 1999. Polyphosphoinositides inhibit the interaction of vinculin with actin filaments. *J. Biol. Chem.* 274, 18414–18420.
- Stricker, J., Falzone, T., Gardel, M.L., 2010. Mechanics of the F-actin cytoskeleton. *J. Biomech.* 43, 9–14.
- Subauste, M.C., Pertz, O., Adamson, E.D., Turner, C.E., Junger, S., Hahn, K.M., 2004. Vinculin modulation of paxillin-FAK interactions regulates ERK to control survival and motility. *J. Cell Biol.* 165, 371–381.
- Takahashi, H., Mitsushima, M., Okada, N., Ito, T., Aizawa, S., Akahane, R., et al., 2005. Role of interaction with vinculin in recruitment of vinexins to focal adhesions. *Biochem. Biophys. Res. Commun.* 336, 239–246.
- Terracio, L., Simpson, D.G., Hilenski, L., Carver, W., Decker, R.S., Vinson, N., et al., 1990. Distribution of vinculin in the Z-disk of striated muscle: analysis by laser scanning confocal microscopy. *J. Cell. Physiol.* 145, 78–87.
- Tidball, J.G., Spencer, M.J., 1993. PDGF stimulation induces phosphorylation of talin and cytoskeletal reorganization in skeletal muscle. *J. Cell Biol.* 123, 627–635.
- Tran Van Nhieu, G., Ben-Ze'ev, A., Sansonetti, P.J., 1997. Modulation of bacterial entry into epithelial cells by association between vinculin and the *Shigella* IpaA invasin. *EMBO J.* 16, 2717–2729.



- Tremuth, L., Kreis, S., Melchior, C., Hoebeke, J., Ronde, P., Plancon, S., et al., 2004. A fluorescence cell biology approach to map the second integrin-binding site of talin to a 130-amino acid sequence within the rod domain. *J. Biol. Chem.* 279, 22258–22266.
- Turner, C.E., Glenney Jr., J.R., Burridge, K., 1990. Paxillin: a new vinculin-binding protein present in focal adhesions. *J. Cell Biol.* 111, 1059–1068.
- Vasile, V.C., Edwards, W.D., Ommen, S.R., Ackerman, M.J., 2006a. Obstructive hypertrophic cardiomyopathy is associated with reduced expression of vinculin in the intercalated disc. *Biochem. Biophys. Res. Commun.* 349, 709–715.
- Vasile, V.C., Ommen, S.R., Edwards, W.D., Ackerman, M.J., 2006b. A missense mutation in a ubiquitously expressed protein, vinculin, confers susceptibility to hypertrophic cardiomyopathy. *Biochem. Biophys. Res. Commun.* 345, 998–1003.
- Vasile, V.C., Will, M.L., Ommen, S.R., Edwards, W.D., Olson, T.M., Ackerman, M.J., 2006c. Identification of a metavinculin missense mutation, R975W, associated with both hypertrophic and dilated cardiomyopathy. *Mol. Genet. Metab.* 87, 169–174.
- Verkhovskiy, A.B., Svitkina, T.M., Borisy, G.G., 1999. Network contraction model for cell translocation and retrograde flow. *Biochem. Soc. Symp.* 65, 207–222.
- Volberg, T., Geiger, B., Kam, Z., Pankov, R., Simcha, I., Sabanay, H., et al., 1995. Focal adhesion formation by F9 embryonal carcinoma cells after vinculin gene disruption. *J. Cell Sci.* 108 (Pt. 6), 2253–2260.
- Volk, T., Geiger, B., 1984. A 135-kd membrane protein of intercellular adherens junctions. *EMBO J.* 3, 2249–2260.
- Vostal, J.G., Shulman, N.R., 1993. Vinculin is a major platelet protein that undergoes calcium ion-dependent tyrosine phosphorylation. *Biochem. J.* 294, 675–680.
- Watabe-Uchida, M., Uchida, N., Imamura, Y., Nagafuchi, A., Fujimoto, K., Uemura, T., et al., 1998. alpha-Catenin-vinculin interaction functions to organize the apical junctional complex in epithelial cells. *J. Cell Biol.* 142, 847–857.
- Weekes, J., Barry, S.T., Critchley, D.R., 1996. Acidic phospholipids inhibit the intramolecular association between the N- and C-terminal regions of vinculin, exposing actin-binding and protein kinase C phosphorylation sites. *Biochem. J.* 314 (Pt. 3), 827–832.
- Weiss, E.E., Kroemker, M., Rudiger, A.H., Jockusch, B.M., Rudiger, M., 1998. Vinculin is part of the cadherin-catenin junctional complex: complex formation between alpha-catenin and vinculin. *J. Cell Biol.* 141, 755–764.
- Wen, K.K., Rubenstein, P.A., DeMali, K.A., 2009. Vinculin nucleates actin polymerization and modifies actin filament structure. *J. Biol. Chem.* 284, 30463–30473.
- Wilkins, J.A., Lin, S., 1982. High-affinity interaction of vinculin with actin filaments in vitro. *Cell* 28, 83–90.
- Wilkins, J.A., Lin, S., 1986. A re-examination of the interaction of vinculin with actin. *J. Cell Biol.* 102, 1085–1092.
- Winkler, J., Jockusch, B.M., 2001. 3-Dimensional organization of the N-terminal vinculin head fragment. *Eur. J. Cell Biol.* 80, 201–206.
- Winkler, J., Lunsdorf, H., Jockusch, B.M., 1996. The ultrastructure of chicken gizzard vinculin as visualized by high-resolution electron microscopy. *J. Struct. Biol.* 116, 270–277.
- Winkler, J., Lunsdorf, H., Jockusch, B.M., 1997. Energy-filtered electron microscopy reveals that talin is a highly flexible protein composed of a series of globular domains. *Eur. J. Biochem.* 243, 430–436.
- Wood, C.K., Turner, C.E., Jackson, P., Critchley, D.R., 1994. Characterisation of the paxillin-binding site and the C-terminal focal adhesion targeting sequence in vinculin. *J. Cell Sci.* 107 (Pt. 2), 709–717.
- Xing, B., Jedsadayamata, A., Lam, S.C., 2001. Localization of an integrin binding site to the C terminus of talin. *J. Biol. Chem.* 276, 44373–44378.

- Xu, W., Baribault, H., Adamson, E.D., 1998a. Vinculin knockout results in heart and brain defects during embryonic development. *Development* 125, 327–337.
- Xu, W., Coll, J.L., Adamson, E.D., 1998b. Rescue of the mutant phenotype by reexpression of full-length vinculin in null F9 cells; effects on cell locomotion by domain deleted vinculin. *J. Cell Sci.* 111 (Pt. 11), 1535–1544.
- Yamada, S., Pokutta, S., Drees, F., Weis, W.I., Nelson, W.J., 2005. Deconstructing the cadherin-catenin-actin complex. *Cell* 123, 889–901.
- Yang, J., Dokurno, P., Tonks, N.K., Barford, D., 2001. Crystal structure of the M-fragment of alpha-catenin: implications for modulation of cell adhesion. *EMBO J.* 20, 3645–3656.
- Ylanne, J., Scheffzek, K., Young, P., Saraste, M., 2001. Crystal structure of the alpha-actinin rod reveals an extensive torsional twist. *Structure* 9, 597–604.
- Yonemura, S., Wada, Y., Watanabe, T., Nagafuchi, A., Shibata, M., 2010. alpha-Catenin as a tension transducer that induces adherens junction development. *Nat. Cell Biol.* 12, 533–542.
- Zemljic-Harpe, A.E., Ponrartana, S., Avalos, R.T., Jordan, M.C., Roos, K.P., Dalton, N.D., 2004. Heterozygous inactivation of the vinculin gene predisposes to stress-induced cardiomyopathy. *Am. J. Pathol.* 165, 1033–1044.
- Zemljic-Harpe, A.E., Miller, J.C., Henderson, S.A., Wright, A.T., Manso, A.M., Elsherif, L., et al., 2007. Cardiac-myocyte-specific excision of the vinculin gene disrupts cellular junctions, causing sudden death or dilated cardiomyopathy. *Mol. Cell Biol.* 27, 7522–7537.
- Zhang, Z., Izaguirre, G., Lin, S.Y., Lee, H.Y., Schaefer, E., Haimovich, B., 2004. The phosphorylation of vinculin on tyrosine residues 100 and 1065, mediated by SRC kinases, affects cell spreading. *Mol. Biol. Cell* 15, 4234–4247.
- Ziegler, W.H., Tigges, U., Zieseniss, A., Jockusch, B.M., 2002. A lipid-regulated docking site on vinculin for protein kinase C. *J. Biol. Chem.* 277, 7396–7404.
- Ziegler, W.H., Liddington, R.C., Critchley, D.R., 2006. The structure and regulation of vinculin. *Trends Cell Biol.* 16, 453–460.
- Zimmerman, B., Volberg, T., Geiger, B., 2004. Early molecular events in the assembly of the focal adhesion–stress fiber complex during fibroblast spreading. *Cell Motil. Cytoskeleton* 58, 143–159.

This page intentionally left blank

# NUCLEAR PORE COMPLEX: BIOCHEMISTRY AND BIOPHYSICS OF NUCLEOCYTOPLASMIC TRANSPORT IN HEALTH AND DISEASE

T. Jamali, Y. Jamali, M. Mehrbod, *and* M.R.K. Mofrad

## Contents

|                                                    |     |
|----------------------------------------------------|-----|
| 1. Introduction                                    | 234 |
| 2. What Drives Cargo Transport Through the NPC?    | 240 |
| 2.1. Cargo complex association                     | 242 |
| 2.2. Transport of cargo complex across the channel | 247 |
| 2.3. Cargo complex dissociation                    | 249 |
| 2.4. Karyopherin recycling                         | 254 |
| 2.5. Ran cycle                                     | 258 |
| 3. Nucleocytoplasmic Transport Pathway             | 265 |
| 4. NPC and Diseases                                | 267 |
| 4.1. Cancer                                        | 267 |
| 4.2. Autoimmune diseases                           | 270 |
| 4.3. Nervous system diseases                       | 270 |
| 4.4. Cardiac disease                               | 272 |
| 4.5. Infectious diseases                           | 272 |
| 4.6. Other disorders                               | 275 |
| 5. Conclusion                                      | 276 |
| Acknowledgments                                    | 276 |
| References                                         | 277 |

## Abstract

Nuclear pore complexes (NPCs) are the gateways connecting the nucleoplasm and cytoplasm. These structures are composed of over 30 different proteins and 60–125 MDa of mass depending on type of species. NPCs are bilateral pathways that selectively control the passage of macromolecules into and out of the nucleus. Molecules smaller than 40 kDa diffuse through the NPC passively while larger molecules require facilitated transport provided by their attachment to karyopherins. Kinetic studies have shown that approximately 1000 translocations occur per second per NPC. Maintaining its high selectivity while

Department of Bioengineering, University of California, Berkeley, California, USA

*International Review of Cell and Molecular Biology*, Volume 287  
ISSN 1937-6448, DOI: 10.1016/B978-0-12-386043-9.00006-2

© 2011 Elsevier Inc.  
All rights reserved.

allowing for rapid translocation makes the NPC an efficient chemical nanomachine. In this review, we approach the NPC function via a structural viewpoint. Putting together different pieces of this puzzle, this chapter confers an overall insight into what molecular processes are engaged in import/export of active cargos across the NPC and how different transporters regulate nucleocytoplasmic transport. In the end, the correlation of several diseases and disorders with the NPC structural defects and dysfunctions is discussed.

**Key Words:** Nuclear pore complexes, Nucleocytoplasmic transport, Karyopherins, Importin, Exportin, Ran, Infectious disease, Cancer. © 2011 Elsevier Inc.

## 1. INTRODUCTION

The nucleus and cytoplasm are home to a myriad of processes vital to the cell. These processes are dependent upon shuttling of various macromolecules between these two environments (Kau et al., 2004). Such transport phenomena occur through nanopores called nuclear pore complexes (NPCs). NPCs are embedded in the nuclear envelop (NE), where the internal and external membranes fuse (Fig. 6.1) (Peters, 2009a).

Different studies have shown that the NPC structure resembles an hourglass (Peters, 2009a) or a donut (Stoffler et al., 2003) shape but has an octagonal radial symmetry around its central axis (Frenkiel-Krispin et al., 2010; Miao and Schulten, 2009; Wolf and Mofrad, 2008; Yang and Musser, 2006) as well as a pseudo-twofold symmetry across the NE (Frenkiel-Krispin et al., 2010; Miao and Schulten, 2009). This structure comprises eight centered cylindrical frameworks, each called a spoke, which enclose a central channel. This channel is sandwiched between the cytoplasmic and nuclear rings (Fig. 6.1; Akey and Radermacher, 1993; Wolf and Mofrad, 2008). In addition, eight cytoplasmic filaments emanate from the cytoplasmic ring to the cytoplasm and eight nuclear filaments, which are branched from the nuclear ring, join each other in the nuclear side of the NPC, shaping a basket-like structure known as the nuclear basket (Fig. 6.1; Elad et al., 2009). Various microscopic studies have shown that the overall length of the NPC including its extended cytoplasmic and nuclear filaments reaches 150–200 nm, while its external diameter is around 100–125 nm. The radius of the cytoplasmic and nuclear sides of this channel is 60–70 nm, and it narrows to about 25–45 nm at the center (Adam, 2001; Brohawn and Schwartz, 2009; DeGrasse et al., 2009; Kau et al., 2004; Schwartz, 2005; Stoffler et al., 2003; Yang and Musser, 2006) (Fig. 6.1). Nevertheless, the opening diameter of this channel has been estimated to be approximately 10 nm (Shulga and Goldfarb, 2003). In addition to the central channel, some peripheral channels with diameters of about 8 nm reportedly exist,

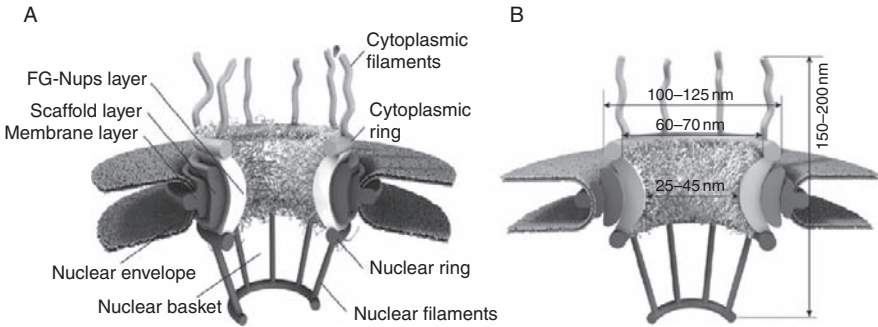


**Figure 6.1** (A) The NPC structure resembles an hourglass (Peters, 2009a) or donut (Stoffler et al., 2003). This channel is sandwiched between the cytoplasmic and nuclear rings (Akey and Radermacher, 1993; Wolf and Mofrad, 2008). In addition, eight cytoplasmic filaments emanate from the cytoplasmic ring to the cytoplasm and eight nuclear filaments, which are branched from the nuclear ring, join each other in the nuclear side of the NPC, shaping a basket-like structure known as the nuclear basket (Elad et al., 2009). The structure of the NPC is composed of three concentric layers (Lusk et al., 2007; Suntharalingam and Wentz, 2003; Walde and Kehlenbach, 2010): (1) The FG repeat layer is the innermost layer of the NPC and is directly exposed to cargo undergoing transport. (2) The membrane layer is the outermost layer that anchors the NPC to the NE. (3) The scaffold layer is located between the above-mentioned layers, forming the structure of the NPC (Lusk et al., 2007). (B) The overall length of the NPC including its extended cytoplasmic and nuclear filaments reaches 150–200 nm, while its external diameter is around 100–125 nm. The radius of the cytoplasmic and nuclear sides of this channel are 60–70 nm, with the radius narrowing to about 25–45 nm at the center (Adam, 2001; Brohawn and Schwartz, 2009; DeGrasse et al., 2009; Kau et al., 2004; Schwartz, 2005; Stoffler et al., 2003; Yang and Musser, 2006).

which contribute to transport of ions and small proteins (Frenkiel-Krispin et al., 2010; Kramer et al., 2007; Stoffler et al., 2003).

The NPC, as the largest nanomachine of the cell, is a bilateral, selective filter for a variety of molecules, transporting them quite rapidly without completely opening or closing the gateway structure (Kapon et al., 2008). Small molecules and ions ( $M_r \sim 20\text{--}40$  kDa, diameter  $\sim 5\text{--}9$  nm) travel through the NPC via passive diffusion, whereas larger molecules ( $M_r > 40$  kDa up to  $\sim 25$  MDa, diameter of up to  $\sim 40$  nm) such as ribosomes, RNAs, and some proteins can only be transported through an active mechanism regulated by transporters (Miao and Schulten, 2009; Yang and Musser, 2006). It is observed that the size of the entering molecule affects the transport rate through the NPC (Moussavi-Baygi et al., 2011). A sharp drop in the transport rate is expected for cargo complexes with radii larger than the channel radius (Peters, 2005). Some researchers reported that passive diffusion and facilitated transport are not coupled and occur through different pathways (Naim et al., 2007). Nevertheless, recent studies provided evidence to refute this hypothesis, suggesting that passive and

facilitated transports take place through the same channel in the NPC (Mohr et al., 2009). Studies of microscopy indicate that the NPC structure dynamically changes its conformation in response to chemical or physical effectors, such as alterations in calcium ion concentration,  $\text{CO}_2$ , and ATP in the cell environment (Erickson et al., 2006; Oberleithner et al., 2000; Rakowska et al., 1998).

Proteomics analyses show that the NPC is a supra molecule made up of approximately 30 types of proteins named nucleoporins (Nups) (Fig. 6.2) (Hetzer, 2010; Walde and Kehlenbach, 2010). Due to the eightfold symmetry of the NPC structure, Nups have been observed in sets of multiple (8–48) copies in yeast and mammalian cells (Bednenko et al., 2003b). Therefore, the total number of Nups per NPC is estimated to be approximately 500–1000 (Peters, 2005; Sorokin et al., 2007). Some Nups are symmetrically found in both cytoplasmic and nuclear sides, some are only present on one side, and others make up the central framework (Strawn et al., 2004; Zeitler and Weis, 2004). This structure also possesses some mobile Nups that have different activities during each period of the cell cycle (Hou and Corces, 2010; Terry and Wentz, 2009; Walde and Kehlenbach, 2010). The structure of the NPC is composed of three concentric layers (Fig. 6.1; Lusk et al., 2007; Suntharalingam and Wentz, 2003; Walde and Kehlenbach, 2010): (1) The *FG repeat layer* is the innermost layer

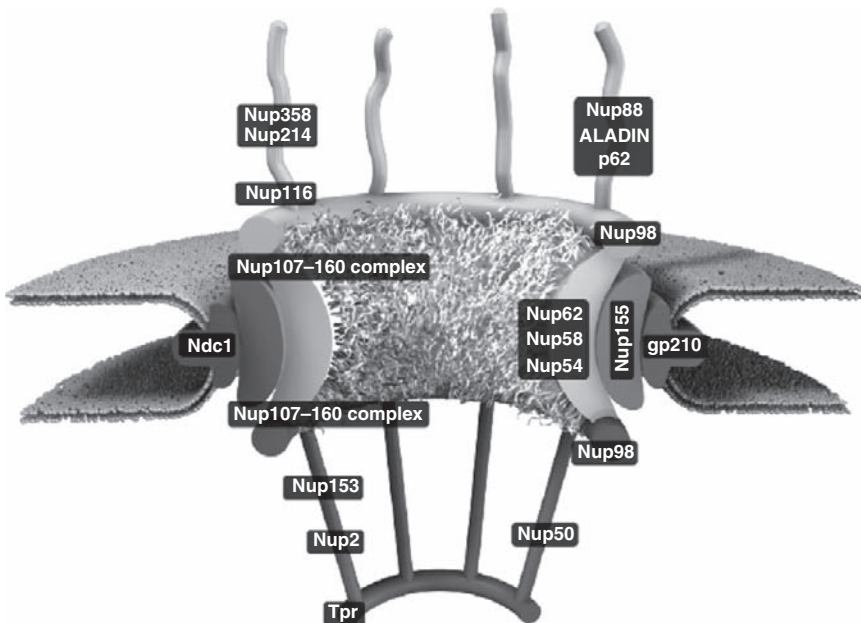


**Figure 6.2** The overall structure of NPC along with some important Nups shown at their approximate positions.

of the NPC and is directly exposed to cargo undergoing transport; this layer coats the channel, facilitating the active transport of cargos (Terry and Wentz, 2009). (2) The *membrane layer* is the outermost layer that anchors the NPC to the NE. (3) The *scaffold layer* is located between the above-mentioned layers, forming the structure of the NPC (Lusk et al., 2007). These layers are composed of various Nups (Fig. 6.2). The first layer is composed of phenylalanine–glycine–rich repeat domains such as FxFG, GLFG, PxFG, and SxFG. These Nups have flexible structures and are spread over the peripheral and central parts of the NPC (Denning et al., 2003; Peleg and Lim, 2010; Zeitler and Weis, 2004) (Fig. 6.1). It is reported that FG domains include some one-third of the Nups, and FG repeat domains account for 12–20% of the NPC mass (Devos et al., 2006; Frey and Gorlich, 2007). Although the cargo complex transport mechanism through the NPC remains unsolved, several models, such as virtual gate, selective phase, reduction of dimensionality, reversible FG, and forest model (Frenkiel-Krispin et al., 2010; Moussavi-Baygi et al., 2011; Peleg and Lim, 2010; Suntharalingam and Wentz, 2003), have been proposed, each elucidating a transport mechanism through this proteinaceous structure in a distinct way.

The flexible domains of these Nups play a key role in the passage of cargos along the nucleotransport pathway via their low affinity with cargo. Molecules that travel through the NPC by binding to FG repeats have significantly higher transport rates than those without attachment to FG repeats, given their similar size and shapes (Ribbeck and GoËrlich, 2001). Additionally, FG-Nups are equipped with coiled coil domains, which anchor them to the NPC bulk (Devos et al., 2006). The membrane layer of the NPC is composed of integral membrane proteins, which have transmembrane helices. Generally, these structures are equipped with  $\alpha$ -helical domains to anchor them to the NE and with Cadherin-fold domains to reinforce the NE against excessive lateral movements. The only nondynamic Nups of the NPC are those existing in the membrane layer (Bednenko et al., 2003b). Aside from Nups containing FG, coiled coil, and transmembrane domains, all other Nups are part of the scaffold (the third) layer and include approximately 1/2 of all Nups (Walde and Kehlenbach, 2010). These Nups have  $\beta$ -propeller and  $\alpha$ -solenoid structures and a significant percentage of the NPC mass is composed of these Nups, with approximately one-third of Nups containing  $\alpha$ -solenoid domains (Devos et al., 2006; Rout et al., 2000). In addition, some Nups include specific structural motifs such as “Zinc finger domains” and motifs connected to RNA (Cassola and Frasch, 2009; Yaseen and Blobel, 1999).

Generally, the number of NPCs on the NE is independent of the nucleus’ surface area and DNA volume. The number of NPCs per nucleus varies significantly for different species, environmental conditions, cell activities, and periods of the cell life cycle (Gerace and Burke, 1988).













For example, yeast barely have 200 NPCs per nucleus, while the number of NPCs per nucleus for vertebrates is on average 2000–5000 ( $10\text{--}20$  pores/ $\mu\text{m}^2$ ) (Fabre and Hurt, 1997). Large nuclei of *Xenopus oocytes* are home to as many as  $5 \times 10^7$  NPCs (over  $60$  pores/ $\mu\text{m}^2$ ) (Gorlich and Kutay, 1999). While NPCs are seen to exist throughout the cell cycle, the number of these pores doubles in dividing cells during interphase and before mitosis and they reach a maximum number in the S-phase of the cell cycle (D'Angelo et al., 2006). It has also been shown that some hormones increase the number and density of NPCs (Miller et al., 1991). Apparently, an increased number of NPCs provides some cells with resistance to chemotherapy (Lim et al., 2008). Experiments clearly indicate an increase in the number of NPCs in embryonic stem cells (ES) as they differentiate into proliferative cardiomyocytes. Therefore, differentiation of embryonic stem cells could be traced to changes in the number of NPCs. Differentiation of ES in cardiac progeny is likely associated with the structural and functional remodeling of the NPC (Lim et al., 2008; Perez-Terzic et al., 2007). A comparison between isolated cardiomyocytes from heart and ES-originated cells indicates no difference in dimensions of the NPCs. Nonetheless, it is reported that the number of NPCs in cells isolated from the heart is greater than those originating from stem cells. Also, increased transport activity of the NPC is reportedly observed in stem cell-derived cardiomyocytes (Perez-Terzic et al., 2003).

The overall architecture of the NPC is conserved among the eukaryotic cells (Brohawn and Schwartz, 2009) and this conservation is established in the last eukaryotic common ancestor (DeGrasse et al., 2009). It is likely that the NPC has been a structural part of another organism like archaea (Bapteste et al., 2005). Also, it is speculated that NPCs are the chimaeras from endomembrane and mitosis-related chromatin-associated proteins (Cavalier-Smith, 2010). Investigations conducted on yeast and mammalian cells indicate that functions and localization of their NPCs are similar even though their sequences are not exactly conserved (Bapteste et al., 2005; Kiseleva et al., 2004; Neumann et al., 2006; Yasuhara et al., 2009). Interestingly, a large number of Nups are conserved among all known eukaryotic cells, but many of them are specific to certain cells (Frenkiel-Krispin et al., 2010; Neumann et al., 2006). As a result, it is claimed that the overall shape and size of the NPC has been conserved through evolution (Alber et al., 2007; Yasuhara et al., 2009); however, some structural distinctions are observable among NPCs of different species (Elad et al., 2009). Structural analyses illustrate some differences in the location of Nups as well as their number of copies among the NPCs of different species. In contrast to related species, though, NPCs of distinct species have low structural homology (Frenkiel-Krispin et al., 2010).

Indeed, transport through the NPC and the NPC components provides a broad range of vital functions for the cell. Comparative proteomic analysis of

the NPC predicts some unexpected functions for this massive complex (Elad et al., 2009). Generally, this structure could affect indispensable cellular functions, such as gene expression, DNA damage and repair, aging, apoptosis, and even determination of cell differentiation and fate (Batrakou et al., 2009; Mishra et al., 2010; Nagai et al., 2008; Nakano et al., 2010; Yasuhara et al., 2007, 2009; Wolf and Mofrad, 2009). As a result, any structural defect or malfunction in this key regulator could cause different diseases or even death. Since understanding the NPC structure is essential to deciphering its function, many scientists have been engaged in structural studies of this large complex during the past few years and various approaches have been exploited to investigate the role of the NPC in different diseases with the hope to find remedial solutions. In this review, we first examine and discuss how different molecules are transported through the NPC while the dysfunctions caused by the NPC structural defects will be described at the end.

This review is composed of two major parts. In the first part (Sections 2 and 3), we will discuss briefly how different molecules (Fig. 6.3) orchestrate the exquisite process of nucleocytoplasmic transport (NCT). Since some cargos need to form complexes with specific molecules, termed transporters, in order to be able to pass through the NPC, we will first explain the definition of transporters along with signal sequences on the cargo transporter proteins required to identify a protein. Section 2.1 will focus mainly on the structure of important transporters, such as importin  $\alpha$  ( $\text{imp}\alpha$ ) and importin  $\beta$  ( $\text{imp}\beta$ ), and interactions between cargos and these transporters, which lead to the formation of a nucleus entering cargo complex in the

| Human        | Yeast | Involve in                                                        | Mw(KD) | Shape                                                                               | Human       | Yeast    | Involve in | Mw(KD) | Shape                                                                                |
|--------------|-------|-------------------------------------------------------------------|--------|-------------------------------------------------------------------------------------|-------------|----------|------------|--------|--------------------------------------------------------------------------------------|
| Imp $\alpha$ | Kap60 | Cargo complex association/disassociation<br>Karyopherin recycling | 60     |  | NTF2/P10    | NTF2/P10 | Ran cycle  | 28     |  |
| Imp $\beta$  | Kap95 | Cargo complex association/disassociation                          | 95     |  | RanGAP      | Ran1     | Ran cycle  | 58–60  |  |
| Nup50        | Nup2  | Cargo complex disassociation                                      | 50     |  | RanBP2      | -        | Ran cycle  | 358    |  |
| CAS          | Cse1  | Karyopherin recycling                                             | 100    |  | RanBP1      | Yrb1     | Ran cycle  | 23     |  |
| Ran          | Gsp1  | Cargo complex disassociation<br>Ran cycle                         | 24     |  | RanGEF/RCC1 | Prp20    | Ran cycle  | 45     |  |

**Figure 6.3** Some important molecules of nucleocytoplasmic transport.

cytoplasm. In Section 2.2, we will follow the pathway of a typical active cargo through the NPC, while Section 2.3 will take a glance at some newly deciphered molecular structures, such as Ran, Nup50 (Nup2p), and their interaction with the entering cargo complexes, which leads to dissociation of the complex in the nuclear basket. Next, in Section 2.4, the recycling pathway of transporters to the cytoplasm and the molecular structure of cellular apoptosis susceptibility molecule (CAS), which is highly engaged in this process, will be explained. Section 2.5 will examine the Ran cycle (hydrolysis process of GTP of RanGTP and replacement of GTP with GDP in RanGDP), the molecules involved in this cycle, and their contribution to NCT. Finally, in Section 3, we conclude this part of the review by summarizing the nucleocytoplasmic pathway mechanism. The second part of this review is dedicated to diseases and disorders linked to NPC structural and functional defects, for example cancer, nervous system and autoimmune disorders, and cardiac and infectious diseases will be discussed.

## 2. WHAT DRIVES CARGO TRANSPORT THROUGH THE NPC?

The major task of the NPC is control and regulation of the traffic of macromolecules into and out of the nucleus. When considering the bidirectional transport of cargos from the cytoplasm to the nucleus and vice versa, on average, as many as 1000 transports are observed through an NPC per second (Fahrenkrog et al., 2004; Peters, 2005), with this high-throughput rate of cargo translocation achieved via transporters. The most important category of transporters is known as the  $\beta$  karyopherin family, which we call the karyopherin family hereinafter for the sake of simplicity (Cook and Conti, 2010; Fiserova and Goldberg, 2010; Pemberton and Paschal, 2005; Peters, 2009b). Members of this family are engaged in regulation of the NE and NPC assembly as well as the replication phenomenon (Mosammaparast and Pemberton, 2004). Karyopherins are possibly conserved through evolution and they are developed from a common ancestor. While the molecular weight of karyopherins is quite similar, they share no more than 20% common sequences (Mosammaparast and Pemberton, 2004). These large proteins ( $\sim 100$  kDa) are generally divided into two groups: importins and exportins. As their names suggest, importins control import of materials from the cytoplasm to the nucleus, while exportins help macromolecules exit the nucleus. Currently, 14 members of the karyopherin family in yeast and 20 of them in human cells have been identified. In human cells, 10 of these macromolecules belong to importins; however, only two groups are known to have a significant contribution to the transport phenomena and are more commonly called  $\text{imp}\alpha$  and  $\text{imp}\beta$ .

Also, seven types of exportins have been discovered, which include Crm1, exp-t, and CAS. Some karyopherins such as importin13 in human and msn5p in yeast are involved in import and export of materials across the NPC (Chumakov and Prasolov, 2010; Dorfman and Macara, 2008; Mosammaparast and Pemberton, 2004; Pemberton and Paschal, 2005; Strom and Weis, 2001). Additionally, there are other transporters, such as Tap/Mex67 and Calreticulin, that play critical roles in the transport process, yet they do not belong to the karyopherin family (Holaska et al., 2001; Tartakoff and Tao, 2010; Wentz, 2000).

Members of the karyopherin family have three major characteristics. First, they need to bind to cargos to carry them. Second, if they are to pass through the NPC they must interact with FG repeats, which line the inner face of the NPC. Finally, they need a supply of energy for continued transport, which is provided via interactions with GTP-bound Ran (Ran is a member of Ras family GTPase) (Moore and Blobel, 1994). This trait has a central effect on the regulation of cargo transport. The affinity of karyopherins to Ran varies among members of the karyopherin family. Some karyopherins bind to Ran molecules with high affinities ( $k_d \sim \text{nM}$ ), whereas some others have low affinities to Ran (Macara, 2001). Further, evidence exists on the affinity of karyopherins to GDP-bound Ran and it is known that the  $\text{imp}\beta\text{-RanGDP}$  bond is four orders of magnitude weaker than the  $\text{imp}\beta\text{-RanGTP}$  bond (Lonhienne et al., 2009). However, karyopherins are capable of attaching to cargos which facilitates their passage through the channel. Some results indicate collisions and interactions of import transporters with cytoplasmic compounds slow down movement of the transporters. Nonetheless, the binding of transporters to cargos disrupts these interactions and expedites the transport process (Wu et al., 2009). It has been reported that karyopherins undergo post-translational modification, which also helps regulate the import and export of cargos (Mosammaparast and Pemberton, 2004).

Importins and exportins bind to certain sequences of the cargo termed nuclear localization sequences (NLSs) and nuclear export sequences (NESs), respectively. NLSs are divided into classic and nonclassic groups. Classic NLSs (cNLSs) contain basic charged amino acids like arginine and lysine, as opposed to nonclassic NLSs (ncNLS), which lack basic amino acid residues. There are two types of classic NLSs: monopartites contain a single basic amino acid stretch, while bipartites possess a couple of those stretches. This sequence, for instance, looks like “ $^{126}\text{PKKKRK}^{132}$ ” in Simian Virus40 (SV40) T antigen, forming a monopartite NLS. In nucleoplasmin, the NLS can be shown as “ $^{155}\text{KRPAATKKAGQAKKKK}^{170}$ ,” having two stretches of basic amino acids 10–12 amino acids apart from each other and forming a bipartite NLS (Fontes et al., 2000, 2003; Lam and Dean, 2010; Lange et al., 2007). It was observed recently that length of the linker between two basic amino acid groups may vary depending on amino acid

compositions and reach to even 29 amino acids (Lange et al., 2010). Exported cargos are decorated with NESs usually having Leu-rich or the hydrophobic amino acids. Computational alignment studies show that most NESs have sequences like the following:  $\varphi$ -X<sub>(2-3)</sub>- $\varphi$ -X<sub>(2-3)</sub>- $\varphi$ -X- $\varphi$  (where  $\varphi$  is one of the hydrophobic amino acids, M, F, V, L, and J, and X could be any arbitrary amino acid) (Kutay and Güttinger, 2005; La Cour et al., 2004; Lui and Huang, 2009).

## 2.1. Cargo complex association

### 2.1.1. Importin $\beta$

Imp $\beta$  is a 95-kDa flexible super-helix, which can take different conformations. Like other members of the karyopherin family, its flexibility facilitates the formation of complexes with different cargo sizes and shapes. It is capable of interacting reversibly with crucial transport molecules such as cargo, FG-Nups, and RanGTP (Cook et al., 2007) (Fig. 6.4). This super-helix is composed of 19 tandem HEAT repeats (Huntingtin, elongation factor 3 [EF3], protein phosphatase 2A [PP2A], and the yeast PI3-kinase TOR1) (Fig. 6.5). HEAT repeat motifs exist in structures of imp $\beta$ , CAS, and other importins and exportins. These repeats only have about 20% of their sequences in common with each other. However, they are mostly similar in their N-terminus, which is a binding site for Ran. HEAT repeats include 39 amino acid motifs and are composed of antiparallel A and B  $\alpha$ -helices (Fig. 6.5). These A and B helices build two C-like arches, which connect to each other by a turn. These  $\alpha$ -helices are stacked so that they construct a spring-like helicoidal structure. A-helices construct the convex side of imp $\beta$ , while its concave side is composed of B-helices (Lee et al., 2005; Stewart, 2006; Strom and Weis, 2001; Zachariae and Grubmuller, 2008).

In the free condition, imp $\beta$  has an S-shaped open conformation. It then closes when attached to the importin  $\beta$  binding (IBB) domain of imp $\alpha$ , RanGTP, and Nups (Fig. 6.4). In other words, its helical pitch reduces upon attachment, like a snake wrapping around its “prey.” Simulations indicate that imp $\beta$  is curved when bound to a ligand and it opens up and elongates once it is released (Bednenko et al., 2003a; Cingolani et al., 1999; Conti et al., 2006).

### 2.1.2. Importin $\alpha$

Imp $\alpha$  is a 55-kDa protein that acts as an adaptor to connect classic NLSs to imp $\beta$ . It is decorated with Arm repeats (Armadillo), which are related to imp $\beta$ -producer HEAT repeats (Goldfarb et al., 2004) (Fig. 6.6). The Arm repeat is a 40 amino acid motif composed of three  $\alpha$ -helices called H1, H2, and H3 (Tewari et al., 2010). These  $\alpha$ -helices are mounted together in a right-handed super-helix, building a banana-like shape (Fig. 6.6). Analyses show that imp $\alpha$  is composed of three major parts. Its N-terminus is

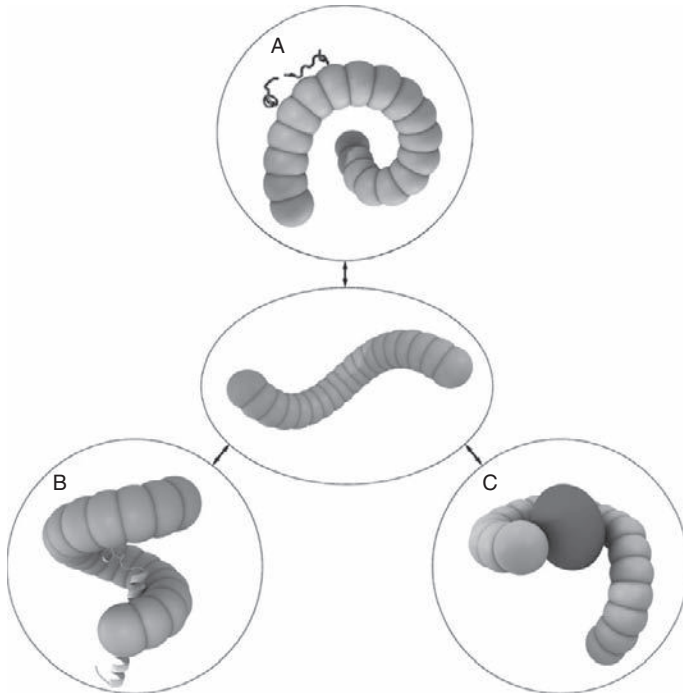


**Figure 6.4** Imp $\beta$  is a flexible super-helix that can take different conformations. This flexibility helps form complexes with a variety of cargo sizes and shapes. In its free condition (central figure), importin- $\beta$  has an S-shaped open conformation. It closes when attached to Nups (A), the IBB domain of importin- $\alpha$  (B), or RanGTP (C). Its helical pitch reduces upon attachment, similar to a snake wrapping around its “prey” (Bednenko et al., 2003a; Cingolani et al., 1999; Conti et al., 2006).

composed of 40 amino acids referred to as the importin  $\beta$  binding (IBB) domain and is the imp $\beta$  binding site (Fig. 6.6); its central part, which has Arm repeats, is able to bind to NLSs; and last, the C-terminus part with the 10th Arm repeat, which binds to CAS (Goldfarb et al., 2004; Stewart, 2006) (Fig. 6.6).

### 2.1.3. Interactions engaged in NLS-imp $\alpha$ -imp $\beta$ complex formation

The NLS-imp $\alpha$ -imp $\beta$  complex is known to assemble via two major processes. In the first mechanism, imp $\alpha$  binds to the NLS and afterward to imp $\beta$ . In the second process, which is actually more probable to occur, imp $\alpha$  primarily binds to imp $\beta$  and after that this complex binds to the NLS (Goldfarb et al., 2004). The IBB domain in imp $\alpha$  has a basic L-shaped structure including an extended section bound to HEAT repeats 7–10 of imp $\beta$  (Fig. 6.7). In this zone, the IBB interacts with an acidic loop

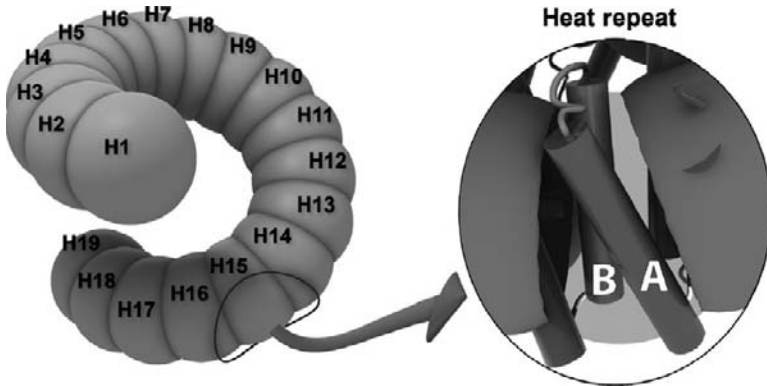


**Figure 6.5** Importin- $\beta$ : this super-helix is composed of 19 tandem HEAT repeats. HEAT repeat motifs exist in structure of imp $\beta$ , CAS, and other importins and exportins. HEAT repeats include 39 amino acid motifs and are composed of antiparallel A and B  $\alpha$ -helices. These A and B helices form two C-like arches, which connect to each other by a turn. These  $\alpha$ -helices are piled so that they construct a spring-like helicoidal structure. A-helices construct the convex side of imp $\beta$ , while its concave side is composed of B-helices (Lee et al., 2005; Stewart, 2006; Strom and Weis, 2001; Zachariae and Grubmuller, 2008).

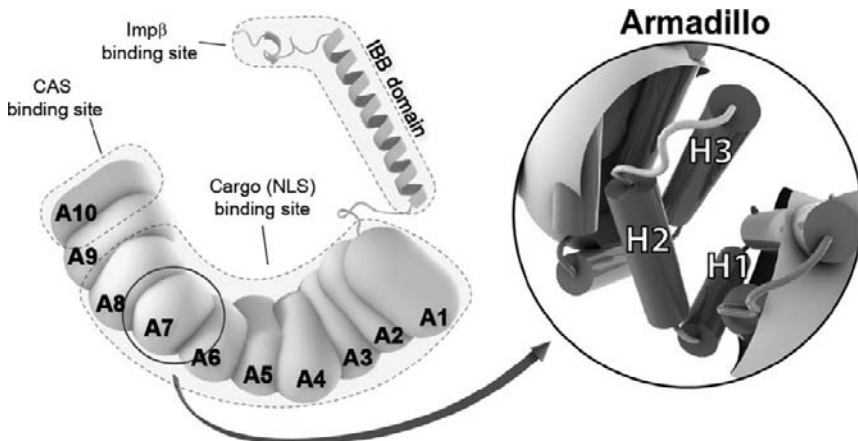


**Figure 6.6** Imp $\alpha$  is a 55-kDa protein that acts as an adaptor to connect classic NLSs to imp $\beta$ . It is decorated with Arm repeats (Armadillo). Arm repeat is a 40 amino acid motif made up of three  $\alpha$ -helices called H1, H2, and H3 (Tewari et al., 2010). These  $\alpha$ -helices are stacked together in a right-handed super-helix, building a banana-like shape. The concave inner part of imp $\alpha$  is made out of H3  $\alpha$ -helices. Analyses show that imp $\alpha$  is composed of three major parts. First, the N-terminus part composed of 40 amino acids that is called IBB domain (importin  $\beta$ -binding domain) and is the imp $\beta$  binding site. Second, the central part equipped with Arm repeats, which are able to bind to NLSs, and lastly, the C-terminus part with the 10th Arm repeat, which binds to CAS (Goldfarb et al., 2004; Stewart, 2006).

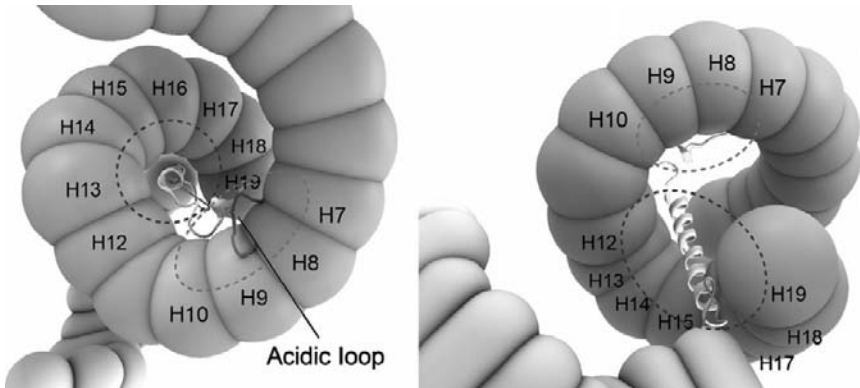


**Figure 6.7** Importin  $\alpha$ - $\beta$  complex: the IBB domain in  $\text{imp}\alpha$  (lighter color) has a basic L-shaped structure including an extended section bound to HEAT repeats 7–10 of  $\text{imp}\beta$  (darker color). In this zone, the IBB interacts with an acidic loop located on the HEAT repeat 8. The IBB structure is also composed of  $\alpha$ -helices attaching to HEAT repeats 12–19. The inner surface of  $\text{imp}\beta$  contains acidic residues that interact with positively charged IBB domain residues.

(DDDDW) located on HEAT repeat 8 (Fig. 6.7). The IBB structure is also composed of  $\alpha$ -helices attaching to HEAT repeats 12–19 (Fig. 6.7). In fact, the inner surface of  $\text{imp}\beta$  contains acidic residues that interact with positively charged IBB domain residues. As many as 40 different contacts including electrostatic, Van der Waals, and hydrophobic ones come together to attach the IBB domain to  $\text{imp}\beta$  (Cingolani et al., 1999; Madrid and Weis, 2006; Stewart, 2003; Zachariae and Grubmuller, 2008).

The concave inner part of  $\text{imp}\alpha$  comprises H3  $\alpha$ -helices (Fig. 6.6). This part has two binding sites for NLSs (Fig. 6.8). The first one is a major groove, which presents a larger area of binding between Arm repeats 2 and 4 and is closer to the  $\text{imp}\alpha$  N-terminus. The major groove attaches to the monopartite NLS and the larger basic cluster of the bipartite NLS. The second bond is the minor groove located between Arm repeats 7 and 8, forming a smaller area of binding (Fig. 6.8). This groove binds to the smaller cluster of the basic bipartite NLS residue and also to the monopartite NLS. Interaction between Asn, Trp, and acidic amino acids of  $\text{imp}\alpha$  with the basic ones of the NLS leads to this attachment (Fig. 6.8), and various sets of electrostatic, hydrophobic, and hydrogen bonds give rise to a firm  $\text{imp}\alpha$ -NLS attachment (Fontes et al., 2000; Yang et al., 2010).

The IBB domain has autoinhibitory characteristic, meaning that it competes with the NLS to attach to  $\text{imp}\alpha$ , and this is a result of resemblance of the NLS and the IBB domain amino acids. Typically, affinity of  $\text{imp}\alpha$  to the NLS is higher than its affinity to IBB domain; however, when the IBB is



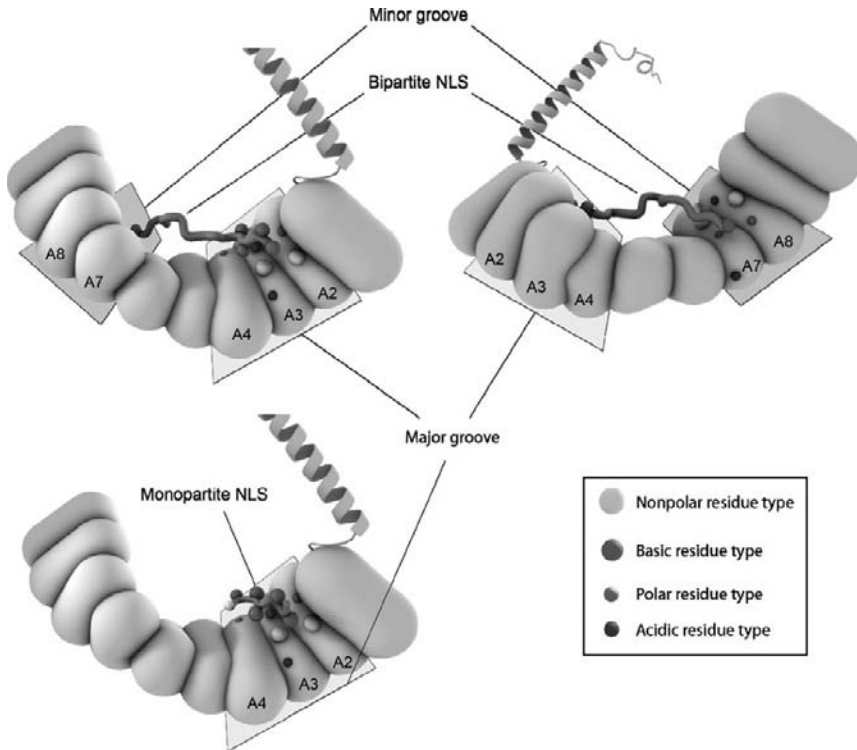


**Figure 6.8** NLS– $\text{imp}\alpha$  complex: the concave inner part of  $\text{imp}\alpha$  has two binding sites for NLSs. The first one is a major groove, which prepares a larger area of binding between Arm repeats 2 and 4, and is closer to the  $\text{imp}\alpha$  N-terminus. The major groove attaches to the monopartite NLS (bottom) and the larger basic cluster of the bipartite NLS (top). The second bond is the minor groove, located between Arm repeats 7 and 8, making a smaller area of binding. This groove binds to the smaller cluster of the basic bipartite NLS residue and also monopartite NLS. Interaction of Asn, Trp, and acidic amino acids of  $\text{imp}\alpha$  with the basic ones of NLS causes this attachment. Various sets of electrostatic, hydrophobic, and hydrogen bonds give rise to a firm  $\text{imp}\alpha$ –NLS attachment (Fontes et al., 2000; Yang et al., 2010).

attached to  $\text{imp}\beta$ , the NLS bond to  $\text{imp}\alpha$  is stronger and no autoinhibitory activity exists in the IBB domain. Interestingly, NLS affinity remains unchanged for  $\text{imp}\alpha$  without the IBB domain and  $\text{imp}\alpha$  bound to  $\text{imp}\beta$  ( $\sim 10$  nM). It seems that the entrance rate of cargos into the nucleus is correlated with NLS– $\text{imp}\alpha$  bond strength (Catimel et al., 2001; Fanara et al., 2000; Lange et al., 2007; Stewart, 2007; Zilman et al., 2007).  $\text{Imp}\alpha$  has a homolog structure in mouse and yeast, and as there are different NLS types working in cells, the NLS recognition mechanisms should have been conserved (Conti and Kuriyan, 2000).

Despite the important role of the IBB domain in the formation of  $\text{imp}\beta$ – $\text{imp}\alpha$ –NLS complex, some cargos carrying ncNLSs simply bind to  $\text{imp}\beta$  directly. These cargos, equipped with ncNLS motifs, resemble the IBB domain. For example, the structure of HIV-1, Rev, and Tat proteins includes Arg motifs that shape a helical secondary structure and imitate the IBB domain function (Truant and Cullen, 1999). It is yet to be determined if  $\text{imp}\beta$  includes a secondary binding site (other than the domain bound to the IBB) for  $\text{imp}\alpha$ -independent cargos, or if an  $\text{imp}\beta$ -targeting NLS facilitates forming a direct bond to  $\text{imp}\beta$  (Cingolani et al., 2002).

## 2.2. Transport of cargo complex across the channel

After the cargo–carrier complex is formed, it passes across the NPC channel. During the passage, FG-Nups, which are speculated to occlude the central channel, interact weakly with  $\text{imp}\beta$  (Fig. 6.9). This interaction with  $\mu\text{M}$ -range affinity is the key corner stone for the selective transport. Each FG-Nup is composed of 20–30 FG-rich domains, such as FG, GLFG, FxFG (where x could be any amino acid) (Fig. 6.9; Frey and Gorlich, 2007, 2009). In fact, FxFG repeats are separated from each other by Thr- and Ser-rich spacer sequences; however, spacer sequences between GLFG repeats have

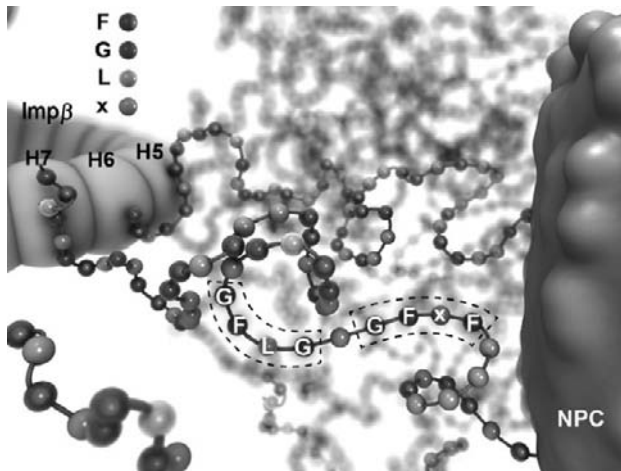


**Figure 6.9** FG-Nups: after the cargo–carrier complex is formed, it passes through the NPC. During the passage, FG-Nups, which are speculated to occlude the central channel, interact weakly with  $\text{imp}\beta$ . Each FG-Nup is composed of 20–30 FG-rich domains, such as FG, GLFG, FxFG (x could be any amino acid), and so on (Frey and Gorlich, 2007, 2009). FG-Nups hold hydrophobic interactions on the convex face of  $\text{imp}\beta$ . These Nups bind  $\text{imp}\beta$  somewhere between HEAT repeats 5 and 7 (Bayliss et al., 2002). Also, another binding site has been recognized on HEAT14–16 of importin- $\beta$ .

abundant amounts of Gln and Asn and no acidic residues are observed in these sequences (Terry and Wente, 2009). GLFG and FxFG Nups bind to overlapping sites on Imp $\beta$ , somewhere between HEAT repeats 5 and 7 (Fig. 6.9; Bayliss et al., 2002). FG-Nups are distributed over the internal face of the central channel as well as nuclear and cytoplasmic sides of the NPC. FG domains of these Nups have flexible structures, and some of them, such as Nup153 and Nup214, are even able to move from one side of the channel all the way to the other side of the channel (Paulillo et al., 2006). On average, 3500 FG repeats exist per NPC (Miao and Schulten, 2009; Strawn et al., 2004).

It is reported that removing up to 50% of FG motifs does not significantly affect the transport process or cell life. However, removing specific FG motifs, such as those in Nup116 (Fig. 6.2), would be fatal to the cell (Stewart, 2007; Strawn et al., 2004). Generally, removing the symmetric-about-NE-planar-axis FG-Nups does have a significant effect on transport. This is because certain combinations of FG domains of symmetric FG-Nups, especially GLFGs, are critical to transport. However, some types of transport processes remain unchanged even after removal of the symmetric FG-Nups, which clearly proves distinct transport pathways exist for different carriers (Strawn et al., 2004; Zeitler and Weis, 2004). Experimental studies and simulations show an attachment between imp $\beta$  and Nups occurs via some hydrophobic binding spots, meaning that FG-Nups hold hydrophobic interactions on the convex face of imp $\beta$  (Fig. 6.9). During the primary interaction, the hydrophobic side chain of Phe in GLFG and FxFG domains penetrates the hydrophobic pocket of imp $\beta$  involving HEAT repeats 5–7. Additionally, another FG-Nup binding site has been recognized on HEAT repeats 14–16 of imp $\beta$  (Bednenko et al., 2003a; Zeitler and Weis, 2004). Experiments show that bonds between FG domains and transporters are sensitive to the number of FG motifs and amino acids located right after them. In other words, the tendency of each FG-Nup to interact with a carrier protein depends on how many FG repeats exist in its proximity, while interaction strength might be modulated by the linkers between the consecutive FG-Nups (Patel and Rexach, 2008; Stewart, 2007). It turns out that Phe located in FG motifs plays the major role in making the connection between imp $\beta$  and FG repeats. Substituting Phe on an FG motif with Ser or Ala residues prevents the transport from happening, and replacing Phe with aromatic Tyr or Trp residues reduces the binding strength. The amino acid that plays the central role in GLFG sequence is Leu. This amino acid is not present in the hydrophobic pocket of imp $\beta$ ; rather by protecting Phe from the solvent, it appears to affect the stability of the imp $\beta$ –Nup bond (Patel and Rexach, 2008). It is hypothesized that some pockets on imp $\beta$  have similar affinities to FG-Nups, even though affinities of other sites are different. Experiments illustrate a positive affinity gradient of Nups to imp $\beta$  from the cytoplasmic to the nuclear side of

the NPC (Ben-Efraim and Gerace, 2001; Ben-Efraim et al., 2009). For instance, the affinity of  $\text{imp}\beta$  for Nup153 on the nuclear side is 20 times stronger than that of Nup358 on the cytoplasmic side (Fahrenkrog and Aebi, 2003). This characteristic makes the entering complex travel from low-affinity Nups to middle-affinity and finally to high-affinity ones unidirectionally, and this, as a result, enhances the transport efficiency (Ben-Efraim and Gerace, 2001). Recently, evidence confirming that the IBB domain modulates the avidity of  $\text{imp}\beta$  to Nups in the NPC channel was provided (Lott et al., 2010). Additionally, the bond between the RanGTP molecule and  $\text{imp}\beta$  in the nucleoplasm affects binding pockets on  $\text{imp}\beta$ , reducing the affinity of  $\text{imp}\beta$  to FG-Nups (Otsuka et al., 2008).

Other reports about distribution of transporter binding sites in the NPC suggest that attachment of transporters is localized around the channel entrance, though others reported a uniform distribution of transporter binding sites along the channel length (Fiserova and Goldberg, 2010; Kahms et al., 2009). In addition to known hydrophobic interactions between transporters and FG-Nups, more recent data suggest that electrostatic interaction between the transport receptors, which are highly negatively charged, and NPC compounds, which are positively charged, facilitates the selective transport across the NPC (Colwell et al., 2010).

## 2.3. Cargo complex dissociation

### 2.3.1. Nup50

Nup50 and its yeast homolog, Nup2p, are located on the nuclear basket (Fig. 6.2). These Nups are able to detach from the nuclear basket and shuttle between the nucleus and cytoplasm (Dilworth et al., 2001; Ogawa et al., 2010). Nup50 (Nup2p) is composed of an N-terminus domain, FG repeats, and a C-terminus domain (Fig. 6.10). Its N-terminus domain has affinity to the  $\text{imp}\alpha$  C-terminus and its NLS-binding site, and the FG repeat domain of this Nup, like other FG-Nups, has affinity to  $\text{imp}\beta$  (Fig. 6.10). The C-terminal domain contains a Ran-binding domain (RBD), having a weak affinity for RanGTP on the order of micromolar. Structural traits of these Nups give rise to a higher tendency of cargo-carrier complexes binding to them, more than any other nuclear basket Nup. These Nups increase the density of carriers in the proximity of their sites on the nuclear basket, thereby boost the probability of impacts needed for assembly/disassembly interactions. Hence, these Nups provide appropriate disassembly sites for imported complexes as well as assembly sites for exported cargos (Denning et al., 2002; Matsuura and Stewart, 2005; Matsuura et al., 2003; Swaminathan and Melchior, 2002).

Other Nups are also reported to mediate disassembly of imported cargos. For instance, Nup153, located on the nuclear ring, is capable of binding to RanGTP, via its Zinc Finger, and increasing RanGTP concentration in its

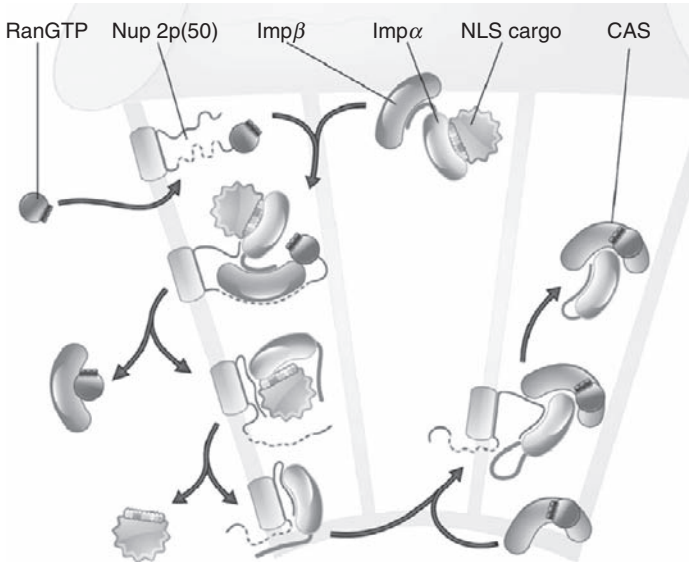


**Figure 6.10** When the cargo complex enters the nucleocytoplasmic part and is bound to the Nup50 (Nup2p) FG repeat, the weak bond between RanGTP and Nup50 (Nup2p) breaks apart, releasing RanGTP to attach to *impβ* (Gilchrist and Rexach, 2003). Nup50 (Nup2p) primarily binds to the *impα* C-terminus with a high affinity. Following that, through a mechanism similar to that of IBB, it breaks the bond between NLS and *impα*, and finally, NLS detaches from *impα*, and Nup50 (Nup2p) substitutes it. Once the disassembly process takes place, *impβ* through binding to RanGTP easily recycles back to the cytoplasm, while *impα* requires another molecule termed CAS to exit (Cse1p). After Nup50 is bound to *impα* and NLS is detached from *impα*, CAS, which is attached to RanGTP, detaches Nup50 (Nup2p) from the *impα* C-terminus. Upon breakage of Nup50 (Nup2p), the IBB domain occupies the second binding site of Nup50 (Nup2p) to *impα*, which has lower affinity to *impα*, and is the NLS binding site. This is required to form the CAS–RanGTP–*impα* complex, and ultimately, Nup50 (Nup2p) detaches from the complex.

propinquity. As a result, Nup153 enhances impact probability of RanGTP and entering cargo complexes, and thereby it is highly involved in the cargo complex dissociation process (Schrader et al., 2008).

### 2.3.2. Ran

Ran is a 24-kDa member of the RAS family GTPase. Members of this family could attach either to GTP (guanosine-5'-triphosphate) or GDP (guanosine-5'-diphosphate). Ran has a core or G domain (guanine nucleotide-binding domain) including a p-loop, Switch I and II, and a 40-amino acid C-terminal extension (conserved across all Ran orthologs) consisting of a linker, an  $\alpha$ -helix, and an acidic tail (DEDDDL) (Fig. 6.11).

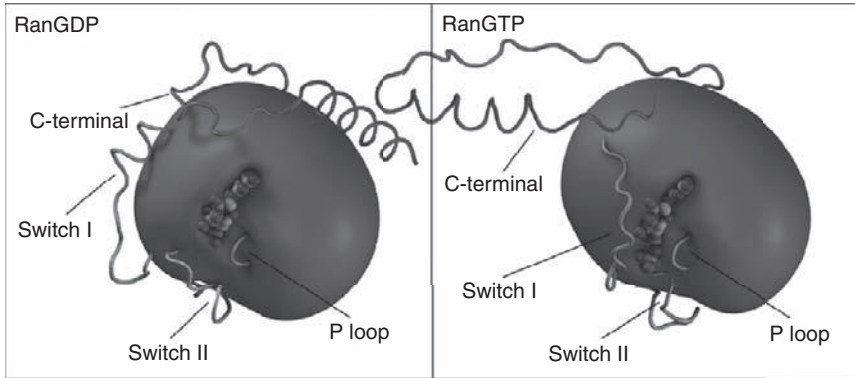


**Figure 6.11** Ran: the overall structure of Ran remains somehow unchanged when it attaches to GTP or GDP, except in Switch I and II regions. In addition, the Ran C-terminus remodels upon its attachment to a nucleotide. The Ran C-terminus is disordered in the RanGTP complex (right) and is extended away from the complex core, whereas this extended portion touches the core in RanGDP at a few locations (left) (Fahrenkrog and Aebi, 2003; Lui and Huang, 2009; Rush et al., 1996; Scheffzek et al., 1995; Yudin and Fainzilber, 2009).

The overall structure of Ran remains almost unchanged when it attaches to GTP or GDP, except in Switch I and II regions, and in addition, the Ran C-terminus remodels upon its attachment to a nucleotide (Fig. 6.11). The Ran C-terminus is disordered in the RanGTP complex and is extended away from the complex core, whereas this extension touches the core in the RanGDP structure (Fig. 6.11; Fahrenkrog and Aebi, 2003; Lui and Huang, 2009; Neuwald et al., 2003; Rush et al., 1996; Scheffzek et al., 1995; Yudin and Fainzilber, 2009). This helical conformation obstructs the RanGDP-karyopherin attachment, while RanGTP is capable of binding to karyopherin members like  $\text{imp}\beta$ . Interestingly, it has been shown recently that  $\text{kap95p}$  and RanGDP are able to form a stable complex, which is capable of being unbound by  $\text{imp}\alpha$ . In  $\text{kap95p}$ -RanGDP complex,  $\text{kap95p}$  induces a conformational change in the RanGDP Switch I and II that makes conformation of these switches resemble those of RanGTP (Forwood et al., 2008).

### 2.3.3. Interactions that lead to the cargo complex disassembly

Disassembly of an entering complex could occur independent of Nup50 (Nup2p) presence. When a cargo complex enters the nucleoplasm, RanGTP can directly interact with  $\text{imp}\beta$  in absence of Nup50 (Nup2p). Such attachments release other factors in the complex of  $\text{imp}\beta$  via a conformational change. In other words, attachment of RanGTP to  $\text{imp}\beta$  induces a conformational change in  $\text{imp}\beta$  that unbinds its other partners

from it. Hence, the RanGTP–imp $\beta$  bond is necessary to detach cargo–imp $\alpha$  complex from imp $\beta$ . The interaction between RanGTP and imp $\beta$  occurs in three regions: at the first site, Switch II loop of RanGTP attaches to CRIME motif (CRM1, imp $\beta$ , etc.), located in the imp $\beta$  N-terminus on HEAT repeats 1–4 (Fig. 6.12). This bond exists in all members of the karyopherin family, as this site is similar in imp $\beta$ , transportin, and Cse1p. At the second site, a basic part on the surface of the RanGTP G domain holds an electrostatic interaction with amino acids of the HEAT repeat 8 acidic loop in imp $\beta$  (Fig. 6.12), thereby releasing the IBB domain from the imp $\beta$  HEAT repeat 8 region. Finally, at the third site, the Switch I loop and some parts of the amino acids of the RanGTP core interact with HEAT repeats and residues 12–15 on imp $\beta$ . This local attachment is required to change the conformation, increase the helical pitch in the imp $\beta$ , and eventually, detach the IBB domain.

It seems that Lys37 and Lys152 on RanGTP interact with the HEAT repeat 14 via electrostatic bonds. Mutations in Lys37 or Lys152 prevent the conformational change, thus obstruct the IBB detachment. Hydrogen bonds also have been observed in this site between Arg29, Arg154, and Arg156 on Ran and imp $\beta$  amino acids. Also, evidence shows Phe35 and

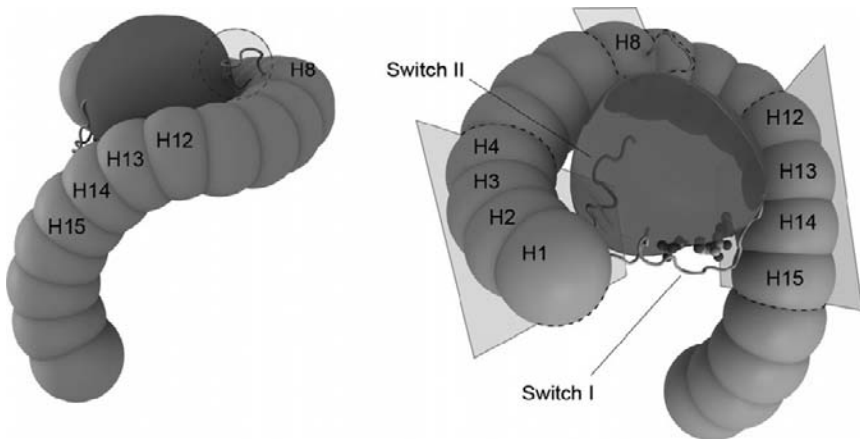


**Figure 6.12** Imporin- $\beta$ –RanGTP complex: the interaction between RanGTP and imp $\beta$  occurs in three regions: at the first site, the Switch II loop of RanGTP attaches to amino acids located in the imp $\beta$  N-terminus on HEAT repeats 1–4. At the second site, the basic part on the surface of the RanGTP G domain holds an electrostatic interaction with amino acids of the HEAT repeat 8 acidic loop in imp $\beta$  thereby, releasing the imp $\beta$  IBB domain on the HEAT8 region. Finally, at the third site, the Switch I loop and some parts of the amino acids of RanGTP core interact with residues of HEAT repeats 12–15 on imp $\beta$ . This local attachment is required to change the conformation, increase the helical pitch in the imp $\beta$ , and eventually detach the IBB domain.

Phe157 amino acids hide together with imp $\beta$  Phe613 and Leu563. Once imp $\beta$ –RanGTP bond is formed, this complex is recycled back to the cytoplasm.

When the cargo–imp $\alpha$  complex dissociates from imp $\beta$ , the IBB domain is released and competes with the NLS for attachment to the binding site on imp $\alpha$  through an autoinhibitory mechanism. It reduces the NLS–imp $\alpha$  bond strength and eventually detaches the NLS. Following that, imp $\alpha$  and imp $\beta$  are exported to the cytoplasm separately from one another (Cook et al., 2007; Lee et al., 2005; Stewart, 2006, 2007; Xu and Massagué, 2004). Nevertheless, the NLS–imp $\alpha$  bond has a high affinity of around 10 nM and is not easy to break apart, although Nup50 (Nup2p) helps alleviate this process (Fig. 6.10). In Nup50-dependent disassembly, when the imported cargo complex enters the nucleocytoplasmic part and is bound to a Nup FG repeat, the weak bond between RanGTP and Nup50 (Nup2p), which has a high dissociation rate ( $K_{\text{off}}$ ), breaks apart, releasing RanGTP to let it attach to imp $\beta$  (Fig. 6.10) (Gilchrist and Rexach, 2003). This newly formed complex detaches from the entering complex and is exported to the cytoplasm.

Kinetic studies indicate that Nup50 (Nup2p) in addition to increasing RanGTP and cellular apoptosis susceptibility (CAS) protein concentration in the nuclear basket causes active detachment of the NLS from imp $\alpha$  (Fig. 6.10). Nup50 (Nup2p) primarily binds to the imp $\alpha$  C-terminus with a high affinity. Following that, using a mechanism similar to that of the IBB, it breaks the bond between the NLS and imp $\alpha$ , and finally, NLS detaches from imp $\alpha$  and Nup50 (Nup2p) substitutes it (Fig. 6.10). Nup50 (Nup2p)–imp $\alpha$  affinity at this binding site is higher than the affinity at the imp $\alpha$ . Moreover, these Nups bind to imp $\alpha$  with higher affinities than do NLSs, through their electrostatic, hydrophobic, and hydrogen bonds. The Nup2p N-terminus attaches to kap60p without IBB with an affinity of about 2.4 nM, while the NLS attaches to the kap60p without IBB domain with an affinity of approximately 10–30 nM, resulting in kap60p binding more firmly to Nup2p than it is doing to the NLS. Presence of Nup50 increases the NLS dissociation rate from imp $\alpha$  by an order of magnitude relative to the spontaneous NLS dissociation rate in the absence of Nup50. The Nup50-dependent pathway is crucial for the detachment of the bipartite NLS as the IBB is not able to conduct this process on its own.

In general, Nup50 facilitates the NLS detachment in two ways: Nup50 is able to interact with imported imp $\alpha$ –imp $\beta$ –NLS complex and once the NLS is released, RanGTP detaches imp $\beta$  from the complex. At the end, RanGTP–CAS complex releases Nup50 and recycles imp $\alpha$  back to the cytoplasm. The alternate way to expedite the NLS detachment reaction is Nup50 coming into play immediately after imp $\beta$  is detached by RanGTP (Matsuura and Stewart, 2005; Matsuura et al., 2003; Moore, 2003; Sun et al., 2008).



Since Nup50 structure is capable of binding to  $\text{imp}\alpha$ ,  $\text{imp}\beta$ , and RanGTP, and it is a dynamic protein, a model based upon the presence of Nup50 as an entering complex has also been suggested. In this model, Nup50 is able to bind to both  $\text{imp}\alpha$  (attached to the NLS) and  $\text{imp}\beta$  in the cytoplasm and thereby increases assembly of the entering quadruple complex. This complex passes across the central channel and enters the nuclear basket, where binding of RanGTP to Nup50 initiates a complex disassembly process, and eventually, two triple complexes, i.e. Nup50–RanGTP– $\text{imp}\beta$  and  $\text{imp}\alpha$ –CAS–RanGTP, are formed and transported back to the cytoplasm (Moore, 2003; Swaminathan and Melchior, 2002). It has been discovered recently that two Nup50 isoforms, called Npap60s and Npap60l, regulate nuclear import of proteins. In other words, alterations in the expression level of these two Nups, which act in opposite ways to release the NLS in the nuclear basket, control efficiency of the nuclear import. This phenomenon confirms the role of Nups in regulating the import efficiency (Ogawa et al., 2010).

## 2.4. Karyopherin recycling

Once the disassembly process takes place  $\text{imp}\beta$  easily recycles back to the cytoplasm via binding to RanGTP; however,  $\text{imp}\alpha$  requires a CAS molecule to exit the nucleus (Fig. 6.10). After Nup50 is bound to  $\text{imp}\alpha$  and the NLS is detached from  $\text{imp}\alpha$ , CAS (Cse1p), which is attached to RanGTP, detaches Nup50 (Nup2p) from the  $\text{imp}\alpha$  C-terminus (Fig. 6.10). Upon breakage of Nup50 (Nup2p) strong bonds, the IBB domain occupies the second binding site of Nup50 (Nup2p) to  $\text{imp}\alpha$ , which has lower affinity to  $\text{imp}\alpha$  and in fact is the NLS binding site. This is required to form the CAS–RanGTP– $\text{imp}\alpha$  complex (Fig. 6.13), and ultimately, Nup50 (Nup2p) detaches from this complex. Nup50 (Nup2p) attachment to  $\text{imp}\alpha$ , its detachment by CAS (Cse1p), and the strong binding of CAS to  $\text{imp}\alpha$  guarantee that  $\text{imp}\alpha$  returns to the cytoplasm only after cargo is already released (Matsuura and Stewart, 2004, 2005).

### 2.4.1. CAS (Cse1p)

Cse1p is made up of 20 HEAT repeats that are stacked up. HEAT repeat motifs of CAS (Cse1p) are composed of 40 amino acids. These HEAT repeats comprise two antiparallel  $\alpha$ -helices called A and B, shaping up the internal and external faces of Cse1p, respectively. A and B helices are connected by a tiny loop in all HEAT repeats except in the HEAT repeat 19 helices, where they are connected by a long loop. Also, in HEAT repeat 8 helices, an intrarepeat connection replaces the tiny connection loop. Not only does RanGTP cause dissociation of importins and their partners in the nucleus, but also it mediates the CAS attachment to  $\text{imp}\alpha$ . Therefore, these

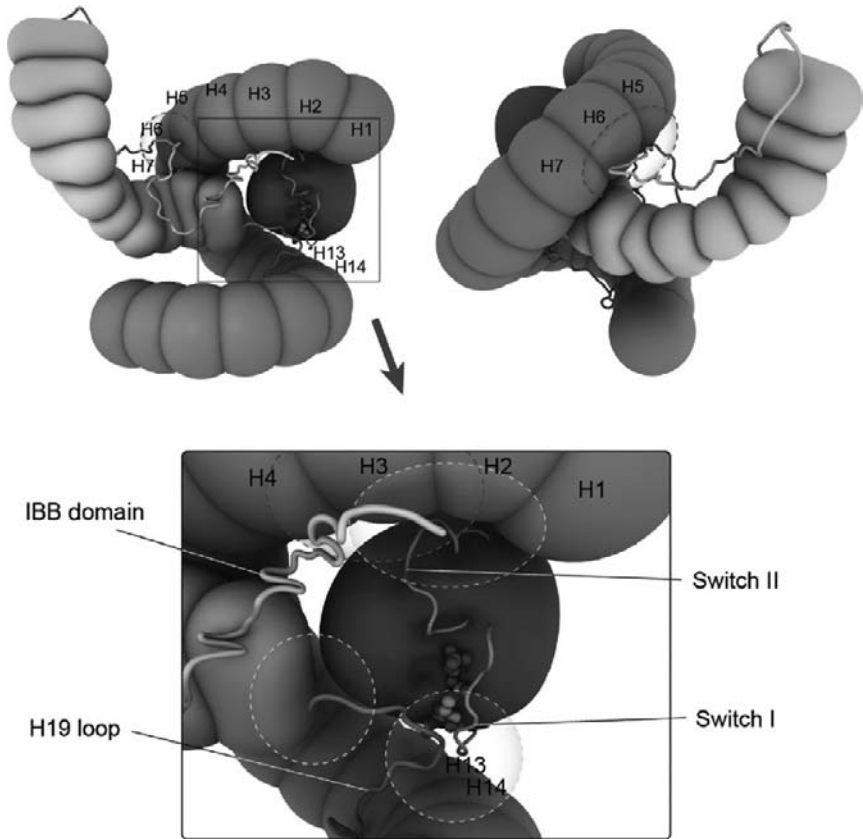


**Figure 6.13** Cse1p–kap60p–RanGTP complex: when kap60p is absent RanGTP only possesses a single binding site on Cse1p (its HEAT 1–3) through Arg76 and Asp77 on the Switch II loop. In presence of kap60p, Cse1p distorts and RanGTP binds to the second binding site on Cse1p, i.e. HEAT 13–14 and the long loop of HEAT 19 via its Lys37 on the Switch I loop and Lys152, which strengthens the RanGTP–Cse1p bond. Hence, in Cse1p, Ran is located around the center, surrounded from two sides by arch-like structures of HEAT repeats 1–3 and HEAT repeats 13–14, and it interacts with HEAT19. Other than being a mere binding site, HEAT19 acts to prevent detachment of guanine nucleotide. Upon the binding of kap60p to the Cse1p–RanGTP complex the IBB N-terminus interacts with Cse1p HEAT 2–4 and so does a tiny portion of the IBB middle part with the HEAT 5–7 external surface. This way, IBB is engaged in forming the kap60p–RanGTP–Cse1p triple complex. Moreover, the only part of Cse1p that is forming bonds with both RanGTP and kap60p in the Cse1p–RanGTP complex is HEAT 19.

processes orchestrate an on-time association/dissociation via regulating the affinity of  $\text{imp}\beta$  and CAS to their partners (Matsuura and Stewart, 2004; Zachariae and Grubmüller, 2006).

### 2.4.2. Interactions forming a recycling complex

When kap60p is absent RanGTP possesses a single binding site on Cse1p (its HEAT 1–3) through Arg76 and Asp77 on the Switch II loop. In presence of kap60p, Cse1p distorts and RanGTP binds to the second binding site on Cse1p, i.e. HEAT repeats 13–14 and the long loop of the HEAT repeat 19, via its Lys37 on the Switch I loop and Lys152, and this strengthens the RanGTP–Cse1p bond (Fig. 6.13). Hence, in Cse1p, Ran is located around the center surrounded from two sides by arch-like structures of HEAT repeats 1–3 and HEAT repeats 13–14, and it interacts with the HEAT repeat 19 (Fig. 6.13). In addition to being a binding site, HEAT repeat 19 acts to prevent detachment of guanine nucleotide. Upon the binding of kap60p to the Cse1p–RanGTP complex, the IBB N-terminus interacts with Cse1p HEAT repeats 2–4 and so does a tiny portion of the IBB central region with the HEAT repeats 5–7 external surface, this way IBB is engaged in forming the kap60p–RanGTP–Cse1p triple complex (Fig. 6.13). Moreover, the kap60p C-terminus is involved in an interaction with Cse1p and RanGTP, and the only part of Cse1p engaged in bonds with both RanGTP and kap60p in the Cse1p–RanGTP complex is HEAT repeat 19 (Fig. 6.13). RanGTP amino acids Arg95, Lys99, Lys130, and Lys134 are essential to its interaction with kap60p (Matsuura and Stewart, 2004). When Ran is absent because of ineffectiveness of collisions, no bonds form during the CAS interaction with  $\text{imp}\alpha$ .

CAS has a closed conformation in its free state and a decreased helical pitch as opposed to  $\text{imp}\beta$  (Fig. 6.14). CAS takes on an open conformation when it connects to a cargo, and this conformational change (open-to-closed) is caused by bonds forming between CAS N-terminus residues and a region close to its C-terminus and central region (Fig. 6.14; Conti et al., 2006; Stewart, 2006). Molecular dynamics (MD) simulations indicate that the Cse1 structure collapses spontaneously via electrostatic interactions during extremely short-time scales (10 ns), forming a close cytoplasmic structure. Moreover, MD studies conducted on mutations of these electrostatic interactions revealed their significance in triggering a conformational change from open to closed (Zachariae and Grubmüller, 2006). During the bonding process, the HEAT repeat 14 moves along relative to HEAT repeats 1–3, forming a cluster of acidic residues of Glu652, Asp653, and Glu656 on HEAT repeat 14 with a charged chain of Lys21, Lys30, Arg25, and Arg28 on HEAT repeats 1–2. Moreover, HEAT repeats 2–3 loop amino acids (i.e., Glu72 and Asp71) hold an electrostatic interaction with HEAT repeats 15–16 amino acids (i.e., Arg728 and Lys695, Lys733). Simulations suggest CAS conformational closing occurs as a result of formation of an interaction between HEAT repeats 1 and 3 and HEAT repeats 14 and 17 residues after they move toward each other (Fig. 6.14; Zachariae and Grubmüller, 2006). Altogether with some other polar interactions, these bonds hide the Ran-binding site considerably. The HEAT repeat 19

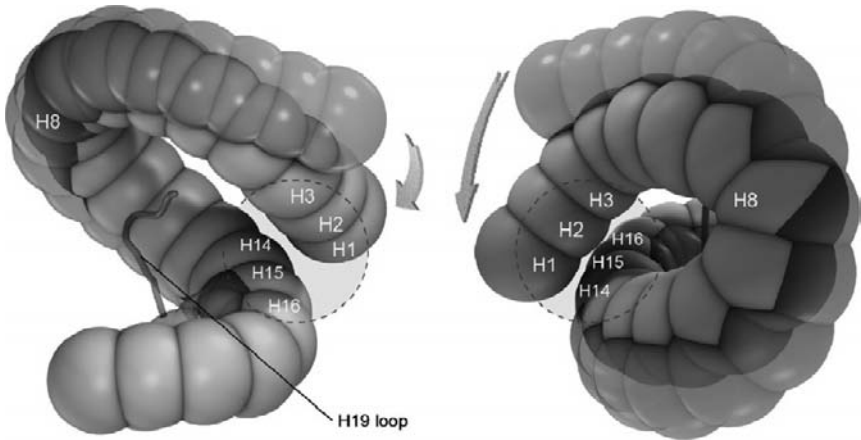


**Figure 6.14** CAS (Cse1p) conformation: CAS has a closed conformation in free state and a decreased helical pitch as opposed to  $\text{imp}\beta$ . It (the transparent one) opens its conformation when it connects to a cargo. The conformational change (open-to-closed) is caused by bonds between CAS N-terminus residues and a region close to the C-terminus and the center. During the bonding process, HEAT repeat 14 moves along relative to HEAT repeats 1–3, forming a cluster of acidic residues on HEAT repeat 14 with a charged chain on HEAT repeats 1–2. Moreover, HEAT repeats 2–3 loop amino acids hold an electrostatic interaction with HEAT repeats 15–16 amino acids. HEAT repeat 19 loop, which mediates the attachment of  $\text{imp}\alpha$  and RanGTP to CAS while forming free CAS, changes its conformation as a result of its clash with the N-terminus so that protease could affect it and cut it off, and hence, free CAS lacks HEAT repeat 19 loop. In closed-to-open conformational change, the most important rearrangement region is located on HEAT repeat 8. This HEAT repeat is in fact a hinge region, and having a conserved insertion, it acts like a switch. It causes conformational opening by allowing the interaction between RanGTP,  $\text{imp}\alpha$ , and CAS to occur.

loop, which mediates the attachment of  $\text{imp}\alpha$  and RanGTP to CAS while forming free CAS, changes its conformation as a result of its clash with the N-terminus so that protease could affect it and cut it off, and hence, the free CAS lacks the HEAT repeat 19 loop (Fig. 6.14). This conformational change is a regulatory mechanism to prevent  $\text{imp}\alpha$  from binding to CAS at a wrong time and keeps CAS and  $\text{imp}\alpha$  bound to each other in the nucleus. In the closed-to-open conformational change, the most important rearrangement region is located on HEAT repeat 8 (Fig. 6.14). This HEAT repeat is in fact a hinge region and having a conserved insertion, it acts like a switch. It causes a conformational opening by allowing the interaction between RanGTP,  $\text{imp}\alpha$ , and CAS to occur. In the closed conformation, the  $\text{imp}\alpha$  binding site is rearranged and RanGTP is closed. During the closed-to-open conformational change a movement around the hinge zone (i.e., the HEAT repeat 8) exposes some of the binding sites of RanGTP on HEAT repeat 19 of CAS to an interaction. This enables  $\text{imp}\alpha$  to gain access

to some binding sites, especially the CAS N-terminus. After the  $\text{imp}\alpha$ -RanGTP-CAS complex forms, it is transported to the cytoplasm. In this pathway, the complex is propelled in channel by hydrophobic interactions of FG-Nups with CAS. Once it reaches the cytoplasm, the complex attaches to RanBP1 or RanBP2, RanGAP (these proteins will be explained in Section 2.5), catalyzes the hydrolysis of RanGTP, and in the end, the complex disassembles, separating  $\text{imp}\alpha$  and CAS from each other and preparing them for the next transport cycle (Zachariae and Grubmüller, 2006). In addition to these models, single molecule fluorescence resonance energy transfer (FRET) studies showed that  $\text{imp}\alpha$ -cargo complex disassembly takes place in the NPC channel in presence of CAS and RanGTP, and afterward, most of the dissociated molecules penetrate the nucleus while nondissociated complexes return to the cytoplasm (Sun et al., 2008).

## 2.5. Ran cycle

Ran and its regulators are key components of the nucleocytoplasmic pathway and most of other vital pathways of the cell, such as RNA synthesis, mitosis, etc. This small molecule exists in both import and export pathways and indeed, it determines the transport direction. In the nucleus, RanGTP substitutes RanGDP and travels back to the cytoplasm by attaching to the export complex. In the cytoplasm, however, RanGTP is hydrolyzed, providing RanGDP again for further use. The rate of Ran export from the nucleus is extraordinarily high ( $10^5$  copies per second) (Batrakou et al., 2009; Lui and Huang, 2009; Yasuhara et al., 2009; Yudin and Fainzilber, 2009). In fact, RanGTP (active form of Ran) is a nucleocytoplasmic pathway controller and its nuclear concentration is higher than that of RanGDP (inactive form of Ran), as opposed to its cytoplasmic concentration. This concentration gradient provides the energy required to regulate and direct transport (GoËrlich et al., 2003). *In vitro* studies confirmed that reversing the RanGTP concentration gradient leads to a reversal in the transport direction. Thus, it could be stated that the RanGTP/RanGDP gradient controls the transport direction and it provides a driving force for transport across the NPC (GoËrlich et al., 2003).

RanGAP (Ran GTPase activating protein) and RanGEF (Ran guanine nucleotide exchange factor) mediate the formation of a vital switch between RanGTP and RanGDP. In the cytoplasm, RanGAP catalyzes hydrolysis of GTP, which exists in RanGTP along with RanBP1 or RanBP2 factors and finally, produces RanGDP via imposing conformational changes to Ran (Figs. 6.15 and 6.16). In the nucleus, RanGEF with intervention of RanBP3 separates GDP nucleotide from Ran. It stabilizes the Ran and eventually replaces GDP with GTP and thereby causes RanGTP to accumulate in the nucleus via RanGEF (Fig. 6.19). There are approximately  $3 \times 10^5$  RanGAP copies and almost the same number of Rcc1 (regulator of

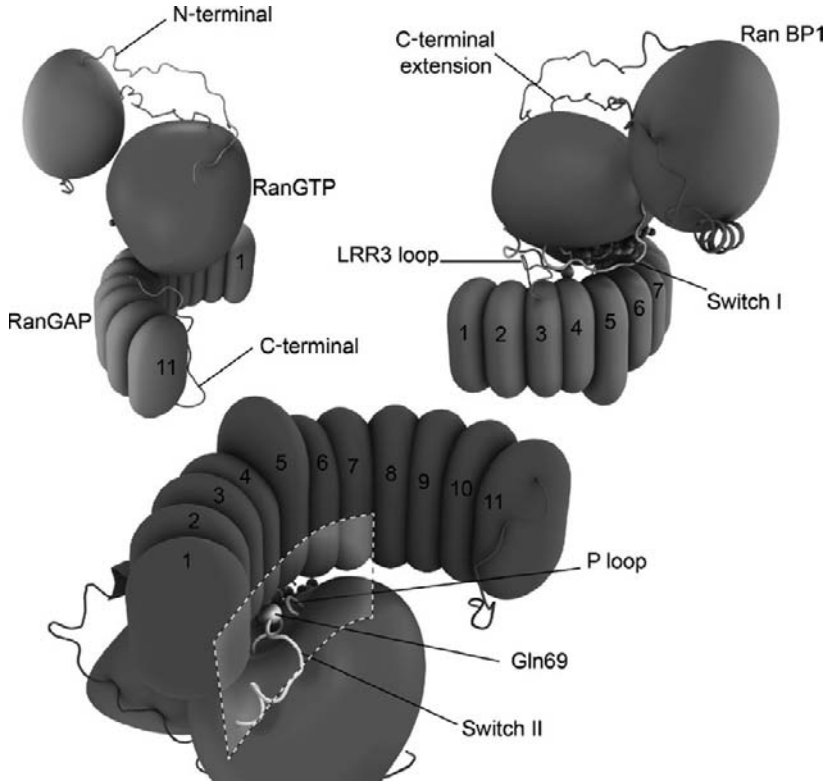


**Figure 6.15** RanBP1–RanGTP–RanGAP complex: in this complex, RanGAP and RanBP1 bind to opposite sides of Ran resulting in no interaction between these two agents, plus RanGAP is located on the edge of RanGTP. Therefore, RanBP1 excites RanGAP indirectly by affecting Ran. The Ran acidic C-terminal extension wraps around the basic RanBD patch. The acidic hand on the RanBD N-terminus stretches across to attach to the basic patch on Ran. Hence, the body of the RanBD is held closely against the switch I region and against other residues in the C-terminal half of the Ran protein (Bischoff and Gorlich, 1997; Lounsbury and Macara, 1997; Saric et al., 2007; Seewald et al., 2003). RanGTP holds electrostatic interactions with residues of seven Leu-rich repeats (LRR) of RanGAP. A grown loop in the third LRR acts as a footrest, stabilizing the Switch II region of Ran. RanGAP stimulates RanGTPase activity by stabilizing the Switch II and correcting orientation of catalytic glutamine of Ran. In fact, when RanGAP touches the Ran Switch II and p-loop, it induces an alteration in orientation of one of their amino acids, i.e. Gln69 (Cook et al., 2007; Madrid and Weis, 2006; Seewald et al., 2002).

chromosome condensation1: mammalian RanGEF) copies in a single cell, hence, the hydrolysis capacity of GTP is balanced with its exchange capacity (Bos et al., 2007; Lui and Huang, 2009; Macara, 2001; Nishimoto, 2000; Rush et al., 1996).

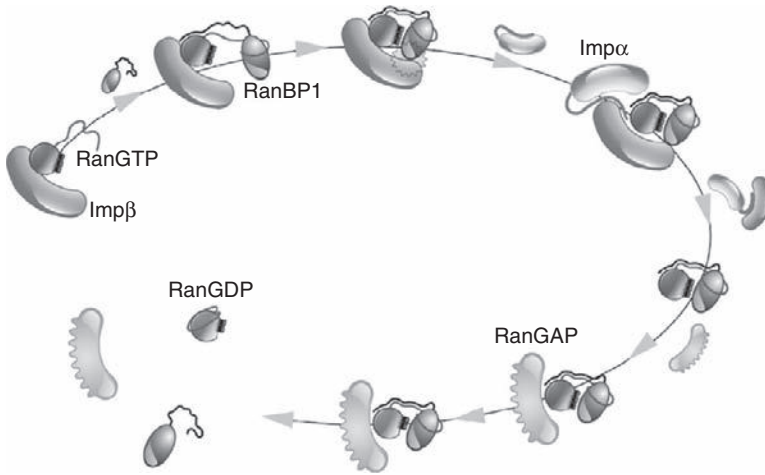


**Figure 6.16** In the triple RanBD–RanGTP–imp $\beta$  complex, the extension of the Ran C-terminus in the karyopherin–RanGTP complex suggests that RanBD is able to access the Ran C-terminus. The Ran acidic C-terminal extension with the DEDDDL motif wraps around the basic RanBD patch. Upon the binding of RanBD to the imp $\beta$ –RanGTP complex, clash of RanBD to imp $\beta$  (sterical hindrance) facilitates imp $\beta$  detachment, and it eventually dissociates in the presence of imp $\alpha$ . Afterward, the acidic hand on the RanBD N-terminus stretches across to attach to the basic patch on Ran. This interaction obstructs rebinding of imp $\beta$  to the RanBD–RanGTP complex and is essential for the detachment to occur. Hence, RanBD is held closely against the Switch I region and against other residues in the C-terminal portion of the Ran protein. At this time, RanGAP comes into play and provokes RanGTP hydrolysis by binding to the RanBD–RanGTP complex. The RanBD connection to the Ran–importin complex pulls the Ran C-terminus aside, facilitating the RanGAP attachment to RanGTP (Bischoff and Gorlich, 1997; Lounsbury and Macara, 1997; Petersen et al., 2000; Saric et al., 2007; Seewald et al., 2002, 2003). So, is RanGAP able to interact with RanGTP, forming a quadruple complex along with RanBD and imp $\beta$ , or is imp $\beta$  released first and then RanGAP fulfills its job? (Melchior and Gerace, 1998).

### 2.5.1. Ran's GTP hydrolysis

The hydrolysis rate of RanGTP with Ran is low ( $k_{\text{cat}} = 1.8 \times 10^{-5} \text{ s}^{-1}$ ). However, RanGAP increases this rate up to  $k_{\text{cat}} = 2\text{--}10 \text{ s}^{-1}$ . Hence, RanGAP is able to increase the RanGTP hydrolysis rate by as much as  $10^5$ -fold up to 5 RanGTP/Sec. RanGAP is composed of a symmetric structure of 11 Leu-rich repeats (LRR) (Fig. 6.15). This crescent-like structure is a compound of a number of helices and hairpins. RanGAPs of different species share the same catalytic N-terminal domain. Further, the RanGAP C-terminus, which has 230 amino acids, is conserved among some species of eukaryotes (Fig. 6.15). In budding yeast, the RanGAP NLS and NESs facilitate its transport into and out of the nucleus. In vertebrates, SUMO modification (a polypeptide dependent on ubiquitin)

occurs on the RanGAP C-terminus covalently. This increases the tendency of RanGAP to interact with RanBP2/Nup358 which is a component of cytoplasmic fibrils (Fig. 6.2), and this finally expedites the hydrolysis rate. In fact, Nup358 modifies RanGAP through the activity of its Sumo E3 ligase, while RanGAP diffuses in the yeast cytoplasm, since it lacks a RanBP2/Nup358 homolog (Seewald et al., 2002).

Recent works also indicate that Nup358–RanGAP complex plays a crucial role in  $\text{imp}\alpha/\beta$ -dependent nuclear import and disassembly of the export complex. Generally speaking, two pathways are proposed in this regard. The first one suggests disassembly of the RanGTP– $\text{imp}\beta$  complex, which has entered the cytoplasm from the nucleus, and the formation of a new  $\text{imp}\beta$ – $\text{imp}\alpha$ –NLS imported complex by mediation of soluble RanGAP and RanBP1 (Fig. 6.19). The second pathway is based on the interaction of recycled-to-the-cytoplasm RanGTP– $\text{imp}\beta$  with Nup358/RanBP2, which is in contact with RanGAP. Following this event, RanGTP is hydrolyzed and a new entering complex is formed through the attachment of  $\text{imp}\alpha$  and NLS (Fig. 6.19; Hutten et al., 2008; Nishimoto, 2000).

In fact, RanGTP should be protected against GTP hydrolysis caused by RanGAP and against the exchange caused by Rcc1, and this task is performed by karyopherins. Basically, karyopherins when bound to RanGTP block the access of RanGAP to the RanGTP Switch II (Figs. 6.15 and 6.16), and this prevents RanGAP from binding to RanGTP while it is carrying a karyopherin. Instead, RanBP2 or RanBP1 is able to bind to Ran in this case. In vertebrates, interactions of importin with Nup358/RanBP2 increase off rate of RanGTP from importins. RanBP2 has four RanBDs (Ran-binding domains), and structural investigations of RanGTP while bound to the first and second RanBD of RanBP2 showed RanBD has a Pleckstrin Homology fold domain (PH domain), which stretches up to the Ran Switch I and its N-terminus loops around RanGTP. Additionally, the RanGTP C-terminus wraps around RanBD and these factors cooperate to hydrolyze RanGTP to RanGDP in the cytoplasm (Geyer et al., 2005; Petersen et al., 2000).

RanBP1 is a 23-kDa protein factor equipped with RanBD (Fig. 6.15). RanBD binds to RanGTP with a high affinity, increasing the activity of RanGAP to hydrolyze GTP by 10-fold (Madrid and Weis, 2006; Seewald et al., 2003). In the triple RanBD–RanGTP– $\text{imp}\beta$  complex, the RanBD binding site on RanGTP does not overlap with the  $\text{imp}\beta$  binding site on RanGTP. Also, the extension of the Ran C-terminus in the karyopherin–RanGTP complex suggests that RanBD is able to access the Ran C-terminus. The Ran acidic C-terminal extension with the DEDDDL motif wraps around the basic RanBD patch (Fig. 6.16). Upon the binding of RanBD to the  $\text{imp}\beta$ –RanGTP complex, collisions of RanBD to  $\text{imp}\beta$  (sterical hindrance) facilitate  $\text{imp}\beta$  detachment and it eventually dissociates in the presence of  $\text{imp}\alpha$  (Fig. 6.16). Afterward, the acidic hand on the N-terminus of



RanBD stretches across to attach to the basic patch on Ran. This interaction obstructs rebinding of  $\text{imp}\beta$  to the RanBD–RanGTP complex and is essential for the detachment to occur (Fig. 6.16). Hence, RanBD is held closely against the Switch I region and against other residues in the C-terminal portion of the Ran protein. At this time, RanGAP comes into play and excites RanGTP hydrolysis by binding to the RanBD–RanGTP complex (Fig. 6.16). The RanBD connection to the Ran–importin complex pulls the C-terminus of Ran aside, facilitating the RanGAP attachment to RanGTP (Bischoff and Gorlich, 1997; Lounsbury and Macara, 1997; Petersen et al., 2000; Saric et al., 2007; Seewald et al., 2002, 2003). So, is RanGAP able to interact with RanGTP, forming a quadruple complex along with RanBD and  $\text{imp}\beta$ , or is  $\text{imp}\beta$  released first and followed by that RanGAP fulfills its task? This question calls for further investigation through this intricate biochemical machine (Melchior and Gerace, 1998).

In the CAS– $\text{imp}\alpha$ –RanGTP complex exiting the nucleus, the RanBD–RanGTP connection causes the detachment of CAS from RanGTP and the binding of RanGAP to the complex (Bischoff and Gorlich, 1997). In the RanBP1–RanGTP–RanGAP complex (Fig. 6.15), RanGAP and RanBP1 bind to opposite sides of Ran which results in no interaction between these two agents; moreover, RanGAP is located on the edge of RanGTP. Therefore, RanBP1 excites RanGAP indirectly by affecting Ran. RanGTP holds electrostatic interactions with residues of seven Leu-rich repeats (LRR) of RanGAP. A grown loop in the third LRR acts as a footrest, stabilizing the Switch II region of Ran (Fig. 6.15). In other small GTPases, GAP-assisted GTP hydrolysis is mediated by an Arg residue of GAP, while the Arg finger is not observed in the RanGTP–RanBP1–RanGAP complex. RanGAP stimulates RanGTPase activity through stabilizing the Switch II and correcting orientation of catalytic glutamine of Ran. In fact, when RanGAP touches the Ran Switch II and p-loop, it induces an alteration in orientation of one of their amino acids, i.e. Gln69. A mutation in Gln69 reduces the RanGAP activity thus, declines the GTP hydrolysis rate in RanGTP (Fig. 6.15) (Cook et al., 2007; Madrid and Weis, 2006; Seewald et al., 2002). It is known that in the nucleus, Tyr39 on Ran holds Gln69 of Ran, protecting this amino acid from water molecule invasion. Conversely, in the cytoplasm, Asn133 of RanGAP interacts with Gln69 of Ran thereby, enables the correct position and water invasion via displacing Tyr39 (Brucker et al., 2010).

### 2.5.2. NTF2

Nuclear transport factor2 (NTF2) is a dedicated carrier for RanGDP shuttling back and forth from the cytoplasm to the nucleus. NTF2 is a barrel-like homodimer that is conserved among all eukaryotes and has two hydrophobic pockets. RanGDP can attach to these pockets with its Switch I and Switch II, in a large contact interface. During its transport through the

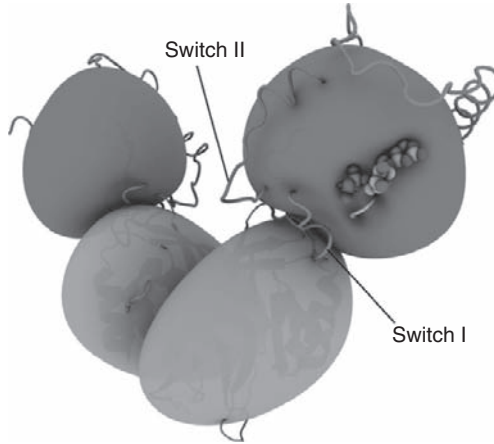


**Figure 6.17** NTF2 (lighter color) is a homodimer molecule that has two hydrophobic pockets. RanGDP can attach to these pockets with its Switch I and Switch II, in a large contact interface. During its transport through the NPC, NTF2 interacts with FG repeats via its hydrophobic end. These FG repeats bind to two symmetric hydrophobic binding sites on the interface of the two dimers (Madrid and Weis, 2006).

NPC, NTF2 interacts with FG repeats from its hydrophobic end. FG repeats bind to two symmetric hydrophobic binding sites on the interface of the two dimers (Madrid and Weis, 2006). However, simulations identify six adjacent binding spots for FG repeats on NTF2 import and export complexes (Fig. 6.17) (Isgro and Schulten, 2007). Rcc1 releases RanGDP from NTF2 in the nucleus and consequently, NTF2 returns to the cytoplasm. The comparison between the RanGDP–NTF2 and Ran–Rcc1 complexes shows that Ran cannot bind to NTF2 and Rcc1 simultaneously. This is consistent with the fact that NTF2 obstructs dissociation of Ran and GDP by Rcc1. Hence, it suggests that RanGDP should detach from NTF2 before the nucleotide exchange occurs (Fig. 6.17) (Chumakov and Prasolov, 2010; Madrid and Weis, 2006; Renault et al., 2001).

### 2.5.3. Ran's nucleotide exchange

RanGEF (see Fig. 6.18) has a donut-like structure composed of seven bladed propellers at the periphery and a hole near its center. It possesses an acidic residue that interacts with one of Lys' on Ran. This structure is attached at one end to Ran and at the other to chromatin. It is speculated that RanGEF is bound to H2A and H2B of nucleosomes with a high affinity. However, it is also likely that RanGEF is rather bound to an internucleosome-exposed zone. Although RanBP3 is necessary to activate

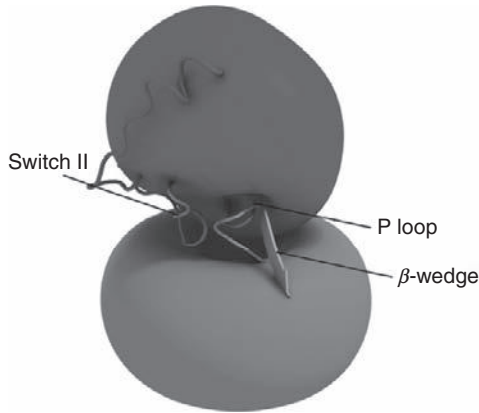


**Figure 6.18** Rcc1 (lighter) has a donut-like structure that induces disorder in the acidic Ran C-terminus. Therefore, it takes part in the detachment of GDP from RanGDP. Rcc1 inserts its  $\beta$ -hairpin, which acts as a  $\beta$ -wedge, into the Switch II and Ran p-loop, which is the nucleotide-binding site. Therefore, causes the GDP separation; a conformational change different from that occurs to Ran during its attachment to GDP and GTP.

RanGEF, it is observed that histones could even double the activity of RanGEF. Attachment of Rcc1 to chromatin is necessary for NCT and cell mitosis to occur (Chumakov and Prasolov, 2010; Fuller, 2010; Madrid and Weis, 2006; Yudin and Fainzilber, 2009). Metazoan and yeast RanGEFs are called Rcc1 and prp20, respectively. Rcc1 is a 45-kDa structure that induces disorder in the Ran acidic C-terminus. Therefore, it takes part in the detachment of GDP from RanGDP. Rcc1 inserts its  $\beta$ -hairpin, located on its third blade propeller which acts as a  $\beta$ -wedge, into the Switch II and Ran p-loop, which is the nucleotide-binding site and in so doing causes the GDP separation; a conformational change different from that occurs to Ran during its attachment to GDP and GTP (Fig. 6.18). Briefly, Rcc1 destabilizes the Ran-GDP complex by inducing a conformational change in Switch II, p-loop, and the RanGDP C-terminus. After GDP is separated, since the concentration of GTP is higher than that of GDP and Rcc1 expression is increased, GDP is replaced with GTP readily via Rcc1 mediation. This interaction progresses very slowly in the absence of Rcc1 (Bos et al., 2007; Lui and Huang, 2009; Renault et al., 2001; Vetter and Wittinghofer, 2001).

Apparently, the attachment of RanGEF to Histones enhances RanGEF activity up to twice as much. This bond induces a mild conformational change in the Rcc1 binding site to His. This conformational change propagates toward the nucleotide-binding site of Ran through the  $\beta$ -wedge of Rcc1, and therefore, Rcc1 attachment to the nucleosome increases the guanine nucleotide exchange. Further, a model has been proposed

suggesting a direct bond between Ran and both Rcc1 and nucleosome (England et al., 2010).

The effect of Rcc1 is to such a degree that guanine nucleotide exchange reaction occurs  $10^5$  times faster in the presence of Rcc1. Moreover, the spontaneous dissociation half-life of GDP from Ran is around 2 h at 25 °C, which could be further shortened by Rcc1 facilitation (Klebe et al., 1995). Rcc1 has an NLS on its N-terminus and rides on importins to enter the nucleus. An accompanying importin is, however, not a requirement for entrance, and substitute pathways potentially exist.

Recently, a model has been suggested in which imp $\beta$  works in Ran as the exchanging factor of GTP to GDP. In this model, the RanGDP–RanBP1–imp $\beta$ –imp $\alpha$ –NLS complex forms in the cytoplasm and NTF2 facilitates its passage across the channel. Also, presence of NTF2 protects the complex against GDP nucleotide exchange. Upon passing across the channel, NTF2 is separated by an unknown factor and GDP is replaced with GTP. In fact, Ran affinity to GTP when bound to imp $\beta$  is more than that to GDP, and this is the key factor that makes the nucleotide exchange possible. Once RanGTP is formed and a strong interaction with imp $\beta$  occurs, imp $\alpha$  and NLS are detached from the complex (Lonhienne et al., 2009).

### 3. NUCLEOCYTOPLASMIC TRANSPORT PATHWAY

The main NCT pathways are shown in Fig. 6.19. Nuclear pore complexes mediate bidirectional transport of various macromolecules. At first, in the cytoplasm, the NLS-carrying cargo through interaction with imp $\alpha$  binds to the imp $\alpha$ /imp $\beta$  complex to form an import complex, which then docks the cytoplasmic filaments. This complex passes across the NPC toward the nucleus via weak interactions with FG-Nups. Inside the nucleus, the imported complex attaches to the nuclear basket Nups such as Nup50 (Nup2). After binding of import complex to Nup50 occurs, RanGTP, which is in high concentration near the nuclear basket, dissociates imp $\beta$  from the cargo complex and the new RanGTP–imp $\beta$  complex is recycled back to the cytoplasm. Subsequently, cargo detaches from imp $\alpha$  via a connection of Nup50 to imp $\alpha$ . Then, imp $\alpha$  in the presence of a CAS molecule, in a complex with RanGTP, is detached from Nup50, and finally is exported back to the cytoplasm, attaching to the CAS–RanGTP complex. In the cytoplasm, the imp $\alpha$ –CAS–RanGTP and RanGTP–imp $\beta$  complexes should be disassembled into their components.

Disassembly of the RanGTP–imp $\beta$  complex may occur by intervention of soluble RanGAP and RanBP1 (Fig. 6.19), or Nup358/RanBP2, which is in contact with RanGAP; RanGTP is hydrolyzed later on (Fig. 6.19; Hutten et al., 2008; Nishimoto, 2000). In fact, once attachment of this

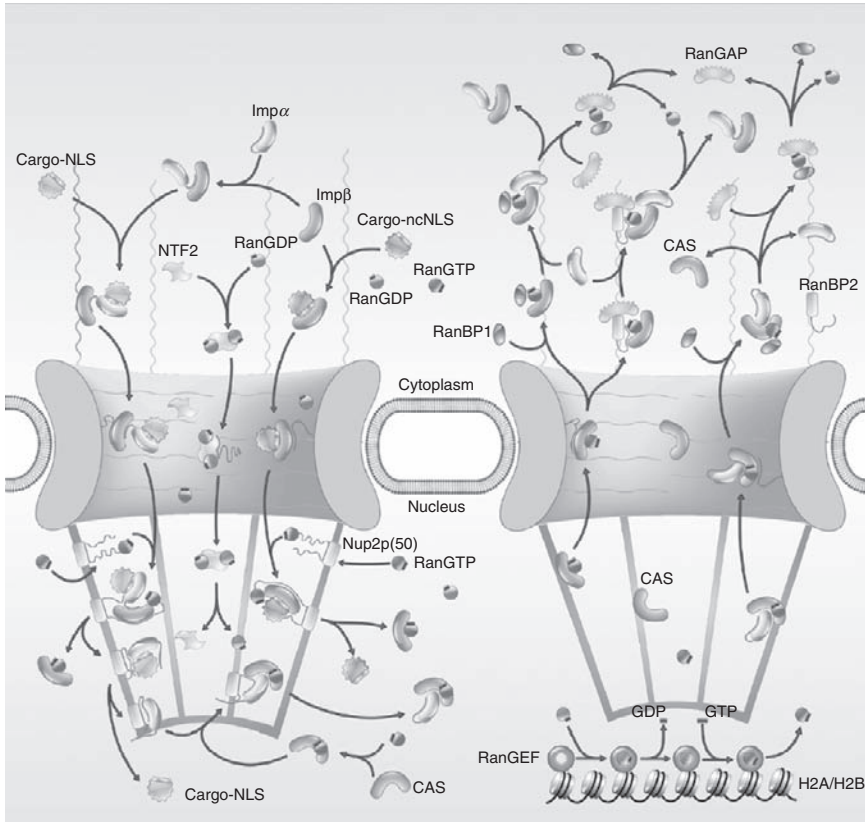


**Figure 6.19** The nucleocytoplasmic transport (NCT) pathways.

complex to RanBP1 takes place, in the presence of  $\text{imp}\alpha$ ,  $\text{imp}\beta$  is released. RanGAP through binding to RanGTP excites the GTP-to-GDP hydrolysis. Ultimately, the RanGAP–RanGTP–RanBD complex dissociates upon formation of RanGDP. However, the  $\text{imp}\beta$ –RanGTP complex through binding to RanBP2/Nup358, which is connected to RanGAP, forms a quadruple complex. Afterward, the presence of  $\text{imp}\alpha$  helps destabilize the complex– $\text{imp}\beta$  interaction and enables RanGAP to bind to RanGTP and provoke its hydrolysis.  $\text{imp}\beta$  and  $\text{imp}\alpha$  detach from the complex when the RanGTP hydrolysis is over. Indeed, it is not known whether RanGAP comes into play immediately after the complex enters the cytoplasm and causes its disassembly via provoking RanGTP hydrolysis, or  $\text{imp}\beta$  detaches from the complex prior to the action of RanGAP.

While the CAS– $\text{imp}\alpha$ –RanGTP complex is exiting the nucleus, the RanBD–RanGTP connection causes the detachment of CAS from RanGTP, and eventually, the hydrolysis of RanGTP is catalyzed by the

binding of RanGAP to the complex (Bischoff and Gorlich, 1997). However, some researchers believe RanBP1 and RanGAP together attach to the CAS–imp $\alpha$ –RanGTP complex, and after the hydrolysis of GTP, because CAS does not have a high affinity to RanGDP, the complex is disassembled (Kutay et al., 1997).

Cargos carrying an NES attach to the exportin–RanGTP complexes, such as Crm1–RanGTP and return to the cytoplasm. The abovementioned hydrolysis process gives rise to RanGTP conversion into RanGDP and releases the cargo. However, NTF2 is in charge of carrying RanGDP from the cytoplasm to the nucleus. In the nucleus, NTF2 detaches from RanGDP, and RanGEF catalyzes the replacement of GDP by GTP, preparing the environment for recycling of the complexes to the cytoplasm. Therefore, interactions of a variety of molecules result in the accumulation of cargo molecules inside the nucleus via the import pathway and their removal via their export to the cytoplasm.

## 4. NPC AND DISEASES

Structural changes in Nups and carriers or defects in transport pathways leading to nuclear or cytoplasmic overaccumulation of materials are correlated with a number of diseases, such as cancer, immune system disorders, and nervous system diseases. Sometimes, an alteration in the transport mechanism is the reason behind these types of diseases; while they could also be caused by conformational changes or malfunctions appear as a result of an NPC disorder. A thorough understanding of the relation between NPC function and these diseases is a stepping stone toward the development of treatments for them.

### 4.1. Cancer

Overexpression of at least one of the NPC protein decoder genes likely induces cancer. For instance, overexpression of Nup88 (Fig. 6.2) located on the cytoplasmic side of the NPC is observed in breast and ovarian tumors (Cronshaw and Matunis, 2004). This Nup has cell-specific activities and its failure to control specific signal translocation pathways in human cells potentially gives rise to tumor formation. This Nup anchors Nup214 (Fig. 6.2) to the NPC and facilitates the export of NES-bearing cargos. Overexpression of Nup88 in cancerous cells decreases the NF $\kappa$ B export (i.e., the transcription factor involved in apoptosis, cancer, and immune responses) thereby, causes NF $\kappa$ B accumulation in the nucleus. This

increased concentration of NF $\kappa$ B in human cell nuclei, such as colon carcinoma, breast, and pancreas, induces a detrimental upregulation of target genes (Kohler and Hurt, 2010; Xu and Powers, 2009).

However, the NCT patterns are altered in tumor cells. The expression level of transporters, presumably affecting the transport patterns, also changes in cancer cells. Any mutation or expression level changes in transport receptors or RanGTP/RanGDP gradient results in changes the distribution of factors like tumor suppressors or oncoproteins (Chahine and Pierce, 2009). Overexpression of CAS is observed in many types of cancers, such as liver neoplasm, breast, and colon cancers. This overexpression increases nuclear concentration of imp $\alpha$ , which introduces a redistribution of tumor suppressors and oncoproteins and thereby, an enhanced cell proliferation and resistance against apoptosis. An increase in concentration of CAS obstructs the import of P53 by imp $\alpha$  (Chahine and Pierce, 2009; Kau et al., 2004). Yet it is not known whether this overexpression induces cancer via changes in the distribution of imp $\alpha$ -dependent cargoes, like P53 (a tumor suppressor protein), or it is due to a secondary role of CAS independent of its participation in transport phenomena as an exportin.

A specific form of imp $\alpha$  is observed in ZR-75-1 breast cancer cells, which lacks the NLS-binding domain. In such cells, because of imp $\alpha$  structural defects, the nuclear import level of P53 is reduced and P53 remains in the cytoplasm. Accumulation of the cytoplasmic P53 was observed in 40% of breast cancer cases (Kim et al., 2000). In these cells, in addition to P53, other suppressors are likely to be affected by inappropriate localizations.

Upregulation of Ran occurs in prostate, breast, colon, kidney, ovarian, sarcoma, and nasopharyngeal carcinoma cancers. While a small magnitude of Ran suffices viability of normal cells, a significant increase in the amount of Ran concentration causes tumorigenesis. Abnormalities in Ran-gradient-regulating enzymes during oxidative stress have been observed in breast cancer. In other words, oxidants eventually destroy the Ran gradient pattern and nuclear import of proteins (Chahine and Pierce, 2009).

In "familial adenomatous polyposis" (a dominant autosomal disease characterized by development of colon carcinoma) due to defects in the adenomatosis polyposis coli gene, which induces CRM1-mediated- $\beta$ catenin export,  $\beta$ -catenine piles in the nucleus abnormally and consequently leads to the activation of transforming genes (Faustino et al., 2007; Henderson, 2000). In some cancerous cells, accumulation of cargoes in the nucleus or cytoplasm is caused by alterations in cargo NLSs or NESs, such as NF $\kappa$ B, whose activation induces tumorigenesis and cancers like Hodgkin's lymphoma. In healthy cells, NF $\kappa$ B joins a complex with I $\kappa$ B inhibitor, which masks NLS of NF $\kappa$ B to block its way to the nucleus. When I $\kappa$ B is phosphorylated and degraded, NLS of NF $\kappa$ B is unmasked and allows NLS to enter the nucleus. Hence, defects in NF $\kappa$ B regulators cause

upregulation of tumorigenesis target genes (Chahine and Pierce, 2009). Several cases of such inappropriate crowds of cancerous cells have been observed.

Genes of several Nups, which produce “oncogenic fusion proteins” (i.e., a protein made from a fusion gene when parts of two different genes join), are known to contribute to some types of cancers. For example, translocation of Nup98 gene (i.e., the movement of Nup98 gene fragment from one chromosomal location to another) is related to hematological malignancies, especially in acute myeloid leukemia (AML). Nup98 gene could fuse to at least 14 other genes. This Nup has an FG repeat sequence at the end of its N-terminus, which is the Rae1 binding site responsible for RNA export and the mitotic checkpoint activation. This part of Nup98 fuses to its partners, most importantly the homeobox family of transcription factors (HOX). A chromosomal rearrangement following that produces oncogenic fusion proteins, which induce tumorigenesis and cancer. These proteins potentially cause deficiency in the transport of materials, leading to leukemogenesis. It is also possible that Nup98 FG repeats randomly, via interaction with transcriptional coactivators, excite transcription of some leukemogenesis-related genes. Since Rae1 (a protein bound to Nup98) is a regulator of mitotic checkpoint activation, any deficiency of Rae1 could lead to a disturbance in the cell mitosis and thereby, leukemogenesis. Multiple mechanisms are speculated to engage in this transformation process. In some cancers, such as myeloid leukemia, fusion of Nup214 gene (an FG-Nup located on the cytoplasmic side of the NPC) (Fig. 6.2) has been reported. Nup214 gene could fuse to coder genes of DNA-associated proteins like DEK and SEK, generating new chromosomal translocations. Also, Nup214 FG repeat probably causes activation of other genes related to leukemia. Nup98 and Nup214 fusion proteins remain in the cytoplasm and preserve their capability of binding to soluble factors (Cronshaw and Matunis, 2004; Kohler and Hurt, 2010; Xu and Powers, 2009).

Sequestration of karyopherins obstructs their active participation in the transport cycle. Tpr is a 265-kDa Nup located on the nuclear side of the NPC and is a compound of the nuclear basket (Fig. 6.2). Tpr contributes to the export of RNA and proteins from the nucleus and regulates Mad1 and Mad2 checkpoints of the mitosis spindle. Biochemical studies show that the N-terminal coiled coil domain of this Nup fuses to kinase proteins such as MET, RAF, and TRK, and it mediates protein polymerization, activates protein kinases in cellular transformation, and plays a role in the occurrence of cancer (Kohler and Hurt, 2010; Xu and Powers, 2009). Another Nup that might be involved in chromosomal translocation is Nup358. This Nup could fuse its N-terminus to the kinase protein domain Alk and by activating Alk induce cell transformation (Ma et al., 2003).



As opposed to other fusion proteins, which are separate from the NPC, this oncogenic fusion protein is localized on the NPC.

## 4.2. Autoimmune diseases

In some autoimmune diseases (e.g., primary biliary, symmetric lupus erythroid, etc.), anti-NPC autoantibodies attach to some Nups, such as Nup62, Nup153, Nup358, gp210, and Tpr (Fig. 6.2). In primary biliary cirrhosis (PBC), bile ducts deteriorate gradually, resulting in the development of liver cirrhosis. Autoantibodies for gp210 and Nup-p62 (Fig. 6.2) recognized in patients suffering from these diseases, especially during the advanced stages, could be markers of how severely the disease has developed. However, looking at the strong correlation between the concentration of these antibodies and development of the disease, some researchers proposed that these antibodies themselves cause the disease, which still remains unverified (Cronshaw and Matunis, 2004; Tsangaridou et al., 2010).

## 4.3. Nervous system diseases

Central nervous system (CNS) selective effects of RanBP2 could prepare pathogenesis background for specific neuropathies, such as Parkinson. In this CNS disease, mutated Parkin protein has E3 ubiquitin ligase activity. It targets RanBP2 and the attached ubiquitin to RanBP2, and protosomal degeneration occurs in RanBP2 (Aslanukov et al., 2006; Um et al., 2006). Acute necrotizing encephalopathy (ANE) is another CNS disease that is diagnosed in young children usually after an influenza type A or B viral infection. It is suggested that this disease develops as a result of a mutation in RanBP2 (Gika et al., 2010; Huang et al., 2004; Neilson et al., 2009).

Recently, conducted studies on relations of NPC proteins and Alzheimer (a fatal brain disorder) reveal that a nuclear irregularity occurs in the NPC and Tau proteins (usually in association with neurofibrillary tangles). In addition, a cytoplasmic accumulation of NTF2 in hippocampal neurons (with or without tangles) is observed in Alzheimer, indicating the inharmonicity of the transport. Also, disruptions in the distribution pattern of some karyopherins like  $\text{imp}\alpha 1$  are reported in Alzheimer (Lee et al., 2006; Sheffield et al., 2006; Yadirgi and Marino, 2009).

Triple A syndrome (also called as Allgrave syndrome) is an autosomal recessive disorder characterized by adrenal failure, achalasia of the cardia, alacrima (absence of tears), and neurological defects. Triple A syndrome is a consequence of a mutation in ALADIN (alacrima achalasia adrenal insufficiency neurological disorder) gene, a part (Nup) of the NPC

structure. However, recent investigations indicate that ALADIN integration in the NPC occurs via the NDC1 transmembrane Nup. Since reduction of the ALADIN integration is a major mechanism for triggering and the development of Triple A syndrome, it is suggested that the interaction between these two Nups might play a role in pathogenesis and its elimination might be important in development of the disease. An initial defect in ALADIN protein disrupts the karyopherin  $\alpha/\beta$ -mediated import pathway and hence, blocks the nuclear import of DNA report proteins like aparataxin and DNA ligase I. This makes DNA damage and cellular death under the oxidative stress highly probable. Further, as a result of ALADIN Nup defects, nuclear import of Ferritin heavy chain, which is the DNA protector, is disrupted, making the cell more prone to the oxidative damage. Engagement of adrenal and CNS is clearly observed in this disease (Kind et al., 2009; Kiriyama et al., 2008; Storr et al., 2009; Yamazumi et al., 2009).

Mutation in Nup62 gene, which is the coder gene of one of Nups called p62, gives rise to a disease named infantile bilateral striatal necrosis (IBSN) that is a neurodegenerative disorder, and CNS is engaged in this disorder in the same way as it is in Triple A syndrome. p62 taking part in the NCT plays a cell type-specific role in basal ganglia degradation (a group of nuclei in vertebrate brains). Reportedly, mutations of protein gene do not affect its localization in the NPC and they are cell-type-specific mechanisms caused by these mutations that induce the disease. However, this is a matter of controversy and various hypotheses, such as partial abnormality of the NPC structure, detrimental disorders in transport pathways of proteins involved in neural cells in basal ganglia, and alteration in chromatin localization in some specific cells, exist on trigger of this disease (Basel-Vanagaite et al., 2006; Chahine and Pierce, 2009).

Amyotrophic lateral sclerosis (ALS) is an incurable progressive disease affecting a group of motor neurons in the brain and spinal cord, resulting in neurodegradation as well as muscle degradation. Studies on the cells suffering from this disease, i.e. anterior horn cells (AHC), show irregularities of nuclear contours along with an inefficient distribution of transporters along the channel. Lack of  $\text{imp}\beta$  and irregularity in Nup62 in a subset of these cells suggested that a detrimental dysfunctional NCT occurs in these cells. Again, like Triple A syndrome, disruptions in transport activities of the NPC most probably hinder a successful entry of a regeneration signal to the nucleus, facilitating the neurodegradation and taking part in the ALS pathogenesis in this way. Transactivation response DNA binding protein 43 (TDP43), which typically exists in the nucleus, has been observed only in the cytoplasm of diseased cells. It is assumed that their disease is caused by the NPC dysfunction and is related to the ALS pathogenesis (Kinoshita et al., 2009).

#### 4.4. Cardiac disease

A direct link between the NPC machine and heart disease was recognized first in arterial fibrillation (AF), which is a cardiac dysrhythmia. Further studies revealed that mutations in Nup155 coder gene (a Nup involved in transport of mRNA and proteins) lead to the development of this disease and early sudden cardiac death. Decrease of Nup155 interrupts export of HSP70 mRNA and import of HSP70, which is a vital protein for the cell, to the nucleus. Therefore, it is suggested that Nup155 plays a key role in regulating HSP70 gene expression and mutation in this gene causes cardiac death. In addition, recent studies focusing on the influence of heart failure (HF) on the NPC in human cardiomyocytes indicated high levels of importins, exportins, Ran regulators like RanGAP, and p62, whereby density of NPCs did not show any significant change (Cortes et al., 2010; Zhang et al., 2008).

#### 4.5. Infectious diseases

Another category of diseases that could be stemmed from the NPC and its function is infectious diseases. Generally, viruses fall into two categories of those including DNA genome and those including RNA genome, each of which deals with the NPC in a distinct way to cause the disease.

##### 4.5.1. Viruses with DNA genome

Viruses encapsulating DNA genome, after entering the cytoplasm, should pass through the NPC to access the nucleus to fuse their genes to the host cell genes and proliferate. The major obstacle on their way to the nucleus is the small diameter of the NPC. Small viruses, such as hepatitis-B virus (HBV) and parvovirus (MVM), easily travel through the NPC with their whole viral capsid, but larger ones, like herpes simplex virus (HSV), need to disassemble their viral capsid to be able to pass across the NPC (Chowdhury, 2009; Greber and Fornerod, 2005; Puntener and Greber, 2009).

Transport of HBVs through the NPC is facilitated by phosphorylation of their capsids during maturity, which are actually their NLSs. This change in the viral capsid eases access of NLS to  $\text{imp}\alpha$  and  $\text{imp}\beta$ . In the nuclear basket, upon interaction between  $\text{imp}\beta$  and Nup153, the entering complex is stopped whereby RanGTP unbinds the transporter ( $\text{imp}\beta$ ) and recycles it back to the cytoplasm. When the transporter is unbound, viral capsids attach to the Nups 150 times stronger than  $\text{imp}\beta$  does. Thereafter, mature capsids become disassembled and capsid subunits and viral DNAs leave the nuclear basket and get released in the nucleus, while immature capsids are trapped in the nuclear basket, waiting for further maturation (Schmitz et al., 2010). Large viruses like HSV or adenovirus particles primarily attach to cytoplasmic fibers. Docking of HSV through the NPC relies on the presence of

imp $\beta$ , and once inside the nucleus, HSV releases its DNA (Lee and Chen, 2010; Rixon, 2010). However, adenovirus capsids in the cytoplasm bind to CAN/Nup214 directly. These viruses trap necessary factors for their capsid disassembly, such as Hsc70, histone H1, and transport factors of imp $\beta$  and importin7 (Greber and Fassati, 2003), and finally release their DNA into the NPC to travel all the way to the nucleus (Russell, 2009; Trotman et al., 2001). Recent studies suggested that protein VII and its receptor, transportin, mediate import of DNA (Hindley et al., 2007). Also, polyomaviruses like SV40 undergo changes before reaching the nucleus. These viruses release their DNA containing subviral particles in the cytosol by passing through the endoplasmic reticulum, which causes exposure of some capsid protein NLSs, and these NLSs enter the nucleus by mediation of imp $\alpha$  and imp $\beta$  (Puntener and Greber, 2009). Papillomaviruses are another category of viruses that become uncoated in the endoplasmic network prior to entering the nucleus and they need importins to be transported to the nucleus because of their large size (Sapp and Day, 2009).

#### 4.5.2. Viruses with RNA genome

Viruses with RNA, for example, picornaviruses (polioviruses, rhinoviruses) and rhabdoviruses, proliferate in the cytoplasm of their host cells and they do not need to reach the nucleus. Nevertheless, cells infected by these viruses experience NPC structural and functional nucleocytoplasmic disorders. For instance, infection by polioviruses or rhinoviruses causes certain nuclear proteins, such as Sam68, La, and nucleolin, to become jammed in the cytoplasm (Hiscox, 2003; Weidman et al., 2003). These proteins induce virus replication upon reacting with its RNA. In fact, these viruses inhibit active import by the proteolytic degradation of Nups, especially Nup62, Nup153, and Nup98, and thereby weaken the host cell's immune response against the virus (Gustin and Sarnow, 2002; Park et al., 2008). Most probably, the overall activity of the NPC continues after infection because certain imports and exports keep occurring even while the cell is infected (Lin et al., 2009).

Vesicular stomatitis virus (VSV) includes an important protein called M-protein. This protein induces some alterations in the NPC and the transport pathways. It is thought to interact with Nup98 on the nuclear side of the NPC and is capable of dissociating Rae1 from Rae1–Nup98 complex and inhibiting the mRNA export process. It also obstructs nuclear import processes and the export of UsnRNA, rRNA, and snRNA. During the antiviral response via interferon signaling, Nup98 becomes upregulated thereby, releases M-protein and commences the export process (Cronshaw and Matunis, 2004; Ren et al., 2010; von Kobbe et al., 2000).

Although retroviruses are mostly able to proliferate in dividing cells, which lack a nuclear envelope, a group of them called lentiviruses (including HIV) proliferate in nondividing cells as well, because these viruses gain

access to their host cell DNA upon passing across the NPC. These viruses lose their capsid in the host cell cytoplasm and consequently, their RNA genome is reverse-transcribed into a complementary DNA (cDNA). This cDNA along with cellular and viral protein factors forms a complex termed preintegration complex (PIC), which enters the nucleus through the NPC and obtains proliferation capability. This complex contains matrix protein (MA), Vpr, integrase (IN), and DNA flap which are able to mediate the DNA nuclear import either directly or by means of karyopherins, such as  $\text{imp}\alpha$ ,  $\text{imp}\beta$ ,  $\text{imp}7$ , and transportin, or by means of different Nups, such as Nup98, Nup358, Nup153, and RanBP2. It has been shown recently that a direct interaction between integrase and Nup153 takes part in the PIC nuclear import (Woodward et al., 2009). It appears that MA, Vpr, and IN proteins enter the nucleus via interaction with importins and Nups (Aida and Matsuda, 2009; Suzuki and Craigie, 2007; Suzuki et al., 2009). Most likely, central DNA flap plays a more important role in the import process than do other elements (De Rijck and Debyser, 2006; Riviere et al., 2010). Interestingly, it is suggested that HIV docks to cytoplasmic fibers on the NPC by its capsid upon arriving in the cytoplasm and the reverse-transcription on its RNA confers a cDNA, and finally, upon formation of a DNA flap, PIC enters the nucleus after removal of the viral capsid. In other words, in this model, the viral capsid has the central role in the cDNA nuclear import (Arhel et al., 2007; Suzuki and Craigie, 2007; Zennou et al., 2000).

Avian sarcoma virus (ASV), which is an alpharetrovirus, is able to penetrate cycle-arrested cell nuclei. Apparently, this virus enters its host cell nucleus by a protein on its integrase. Studies indicate the ASV integrase import occurs without a classic binding to  $\text{imp}\alpha$  but depends on soluble cellular factors. Integrase enters the nucleus by exploiting one or a few soluble cellular factors responsible for transport of histone H1 (Anderson and Hope, 2005; Andrade et al., 2008; Chowdhury, 2009).

Influenza virus is an Orthomyxovirus containing eight genomic ribonucleoproteins (RNPs), including RNA and nucleoprotein (NP). This virus is equipped with RNA-dependent RNA polymerase, which is an enzyme for replication and transcription. In a certain level of infection, RNPs and some other viral proteins are released in the cytoplasm, whereas they need to enter the nucleus to be able to proliferate. Generally, during an influenza infection, several nuclear imports and exports occur. In primary levels of infection, incoming VRNPs wandering in the cytoplasm enter the nucleus, and afterward, synthesized transcripts of the virus are exported from the nucleus. Then, newly synthesized proteins, NPs and RdRp subunits (PA, PB1, and PB2), enter the nucleus via their specific NLSs, and finally, Crm1 helps assembled VRNPs exit the nucleus. RNA to be transported to the nucleus is dependent upon the presence of  $\text{imp}\alpha$ ,  $\text{imp}\beta$ , and Ran, as well as a coating with nontypical NLS-carrying NPs. It is yet to be known that whether these specific NLSs bind directly to RNA or they attach

to the transporters. Recently, a lot of attention has been paid to investigating the nuclear transport mechanism of influenza virus proteins. For instance, it was determined recently that in influenza A virus (a specific type of influenza virus), PB1 and PA forming a dimer, enter the nucleus via importin5 factor. PB2 separately penetrates the nucleus and attaches to PA–PB1 dimer in the nucleus. A mutation in the PB2 NLS subunit hinders its nuclear import, leading to the formation of an abnormal polymerase in the cytoplasm. Additionally, in influenza A virus, two NLSs (NLS1 and NLS2) on the NP facilitate the transport of RNPs into the nucleus. Studies show that for incoming VRNPs and newly distributed NPs, to enter the nucleus, their NLS is exposed to the interaction. After the NPs entered the nucleus, RNP assembly occurs and RNPs are exported from the nucleus and these RNPs are no longer able to enter the nucleus. Among these RNPs, it is observed that NLS1 is hidden and thus, it is suggested that NLS1 hides in the NPs prior to the RNP assembly. Nonetheless, another model states that NLS1 hides after the NPs are assembled to form the RNP. Experiments indicated that the NP oligomerization is not the reason behind this NLS masking, rather it happens because of a past modification, binding to cellular proteins or the NP conformational change. Therefore, NLSs play a significant role in the function of these viruses and they regulate the nuclear transport directionality of their genome via selective exposure of NLSs (Whittaker et al., 1996; Wu and Pante, 2009).

Basically, each cell shows a specific reaction when it faces a virus attack. For this response to develop, transcription factors should enter the nucleus and activate some particular genes. A group of alphaviruses take a smart action to prevent the host cell from showing this response, that is, blocking the NCT pathway. Venezuelan equine encephalitis virus (VEEV) blocks the NPC central channel to stop the import of gene transcription factors needed to induce the response against the virus. The capsid of this virus binds simultaneously to Crm1 exportin,  $\text{imp}\alpha$ , and  $\text{imp}\beta$  in the cytoplasm, forming an abnormal tetrameric complex. Also, these capsids are able to make dimeric complexes with Crm1 and attach to Nup358 and finally, they form a tetrameric complex with  $\text{imp}\alpha$  and  $\text{imp}\beta$ . This odd complex settles at the NPC central pore and blocks import of crucial factors to the nucleus, though small proteins can still shuttle into and out of the nucleus. Using this strategy, the virus stops the cell antiviral response and increases its ability to proliferate (Atasheva et al., 2010).

#### 4.6. Other disorders

Cell stressors such as UV irritation, oxidative stress, and heat shock stress induce diseases like schema, HF, hypertension, diabetes, and cancer by mislocalizing transport receptors like  $\text{imp}\alpha$  (Chahine and Pierce, 2009; Miyamoto et al., 2004). Additionally, Ran overexpression interrupting

nuclear retention of important transcription factors engaged in activation of T-cells potentially causes defected responses in these cells (Qiao et al., 2010).

In addition to the aforementioned disorders, an import pathway has been discovered that participates in determining the sex by gender determination transporting transcription factors. This conserved pathway among eukaryotes is mediated by  $\text{Ca}^{2+}$ /calmodulin and is independent of Ran. It is known that defects in this NPC pathway due to stopping transit of some factors such as SRY and SOX9 in sertoli cells could cause human sex reversal diseases like campomelic dysplasia and sywer syndrome (Hanover et al., 2009).

## 5. CONCLUSION

The purpose of this review was to examine the nucleocytoplasmic pathways, interaction of molecules taking part in transport processes, and NPC-related diseases. In the past few years, major scientific efforts have been made to express and analyze the sophisticated structure of the NPC, the bilateral NPC pathways, and the roles played by molecules involved in the NCT process, which are critical to understanding how this super-efficient nanomachine works and how it may potentially control the mechanobiology of the cell (Wolf and Mofrad, 2009). These studies, conferring an overall insight of the NPC function, have set the stage for us to move on to more detailed investigations in this field. Several diseases such as cancer, neural and immune system, and infectious diseases have been associated with NPC structural disorders and NCT disruptions. Further study of this dependence can shed light into the mechanism of this complicated system, and once this mechanism is deciphered, we will be able to predict and control transport of macromolecules more accurately to come up with affordable treatments for such diseases. In other words, on one hand, knowledge of the NPC structure and function paves the way toward understanding diseases and thereby discovering efficient treatment methods for them, while on the other hand, study of diseases increases our understanding of the NPC.

## ACKNOWLEDGMENTS

The authors thank members of Molecular Cell Biomechanics Laboratory, especially Dr. Mohammad Azimi, for fruitful discussions and editorial assistance.

## REFERENCES

- Adam, S.A., 2001. The nuclear pore complex. *Genome Biol* 2, reviews0007.1–reviews0007.6.
- Aida, Y., Matsuda, G., 2009. Role of Vpr in HIV-1 nuclear import: therapeutic implications. *Curr. HIV Res.* 7, 136–143.
- Akey, C.W., Radermacher, M., 1993. Architecture of the *Xenopus* nuclear pore complex revealed by three-dimensional cryo-electron microscopy. *J. Cell Biol.* 122, 1–19.
- Alber, F., Dokudovskaya, S., Veenhoff, L.M., Zhang, W., Kipper, J., Devos, D., et al., 2007. The molecular architecture of the nuclear pore complex. *Nature* 450, 695–701.
- Anderson, J.L., Hope, T.J., 2005. Intracellular trafficking of retroviral vectors: obstacles and advances. *Gene Ther* 12, 1667–1678.
- Andrake, M.D., Sauter, M.M., Boland, K., Goldstein, A.D., Hussein, M., Skalka, A.M., 2008. Nuclear import of Avian Sarcoma Virus integrase is facilitated by host cell factors. *Retrovirology* 5, 1–14.
- Arhel, N.J., Souquere-Besse, S., Munier, S., Souque, P., Guadagnini, S., Rutherford, S., et al., 2007. HIV-1 DNA Flap formation promotes uncoating of the pre-integration complex at the nuclear pore. *EMBO J.* 26, 3025–3037.
- Aslanukov, A., Bhowmick, R., Guruju, M., Oswald, J., Raz, D., Bush, R.A., et al., 2006. RanBP2 modulates Cox11 and hexokinase I activities and haploinsufficiency of RanBP2 causes deficits in glucose metabolism. *PLoS Genet.* 2, 1653–1665.
- Atasheva, S., Fish, A., Fornerod, M., Frolova, E.I., 2010. Venezuelan equine Encephalitis virus capsid protein forms a tetrameric complex with CRM1 and importin alpha/beta that obstructs nuclear pore complex function. *J. Virol.* 84, 4158–4171.
- Baptiste, E., Charlebois, R.L., MacLeod, D., Brochier, C., 2005. The two tempos of nuclear pore complex evolution: highly adapting proteins in an ancient frozen structure. *Genome Biol.* 6, R85.1–R85.15.
- Basel-Vanagaite, L., Muncher, L., Straussberg, R., Pasmanik-Chor, M., Yahav, M., Rainshtein, L., et al., 2006. Mutated nup62 causes autosomal recessive infantile bilateral striatal necrosis. *Ann. Neurol.* 60, 214–222.
- Batrakou, D.G., Kerr, A.R., Schirmer, E.C., 2009. Comparative proteomic analyses of the nuclear envelope and pore complex suggests a wide range of heretofore unexpected functions. *J. Proteomics* 72, 56–70.
- Bayliss, R., Littlewood, T., Strawn, L.A., Wenthe, S.R., Stewart, M., 2002. GLFG and FxFG nucleoporins bind to overlapping sites on importin-beta. *J. Biol. Chem.* 277, 50597–50606.
- Bednenko, J., Cingolani, G., Gerace, L., 2003a. Importin beta contains a COOH-terminal nucleoporin binding region important for nuclear transport. *J. Cell Biol.* 162, 391–401.
- Bednenko, J., Cingolani, G., Gerace, L., 2003b. Nucleocytoplasmic transport: navigating the channel. *Traffic* 4, 127–135.
- Ben-Efraim, I., Frosst, P.D., Gerace, L., 2009. Karyopherin binding interactions and nuclear import mechanism of nuclear pore complex protein Tpr. *BMC Cell Biol.* 10, 1–9.
- Ben-Efraim, I., Gerace, L., 2001. Gradient of increasing affinity of importin beta for nucleoporins along the pathway of nuclear import. *J. Cell Biol.* 152, 411–417.
- Bischoff, F.R., Gorlich, D., 1997. RanBP1 is crucial for the release of RanGTP from importin beta-related nuclear transport factors. *FEBS Lett.* 419, 249–254.
- Bos, J.L., Rehmann, H., Wittinghofer, A., 2007. GEFs and GAPs: critical elements in the control of small G proteins. *Cell* 129, 865–877.
- Brohawn, S.G., Schwartz, T.U., 2009. Molecular architecture of the Nup84–Nup145C–Sec13 edge element in the nuclear pore complex lattice. *Nat. Struct. Mol. Biol.* 16, 1173–1177.
- Brucker, S., Gerwert, K., Kotting, C., 2010. Tyr39 of ran preserves the Ran-GTP gradient by inhibiting GTP hydrolysis. *J. Mol. Biol.* 401, 1–6.



- Cassola, A., Frasch, A.C., 2009. An RNA recognition motif mediates the nucleocytoplasmic transport of a trypanosome RNA-binding protein. *J. Biol. Chem.* 284, 35015–35028.
- Catimel, B., Teh, T., Fontes, M.R., Jennings, I.G., Jans, D.A., Howlett, G.J., et al., 2001. Biophysical characterization of interactions involving importin- $\alpha$  during nuclear import. *J. Biol. Chem.* 276, 34189–34198.
- Cavalier-Smith, T., 2010. Origin of the cell nucleus, mitosis and sex: roles of intracellular coevolution. *Biol. Direct* 5, 1–78.
- Chahine, M.N., Pierce, G.N., 2009. Therapeutic targeting of nuclear protein import in pathological cell conditions. *Pharmacol. Rev.* 61, 358–372.
- Chowdhury, E.H., 2009. Nuclear targeting of viral and non-viral DNA. *Expert Opin. Drug Deliv.* 6, 697–703.
- Chumakov, S.P., Prasolov, V.S., 2010. [Organization and regulation of nucleocytoplasmic transport]. *Mol. Biol. (Mosk)* 44, 211–228.
- Cingolani, G., Bednenko, J., Gillespie, M.T., Gerace, L., 2002. Molecular basis for the recognition of a nonclassical nuclear localization signal by importin beta. *Mol. Cell* 10, 1345–1353.
- Cingolani, G., Petosa, C., Weis, K., Muller, C.W., 1999. Structure of importin-beta bound to the IBB domain of importin-alpha. *Nature* 399, 221–229.
- Colwell, L.J., Brenner, M.P., Ribbeck, K., 2010. Charge as a Selection Criterion for Translocation through the Nuclear Pore Complex. *PLoS Comput. Biol.* 6, 1–8.
- Conti, E., Kuriyan, J., 2000. Crystallographic analysis of the specific yet versatile recognition of distinct nuclear localization signals by karyopherin alpha. *Structure* 8, 329–338.
- Conti, E., Muller, C.W., Stewart, M., 2006. Karyopherin flexibility in nucleocytoplasmic transport. *Curr. Opin. Struct. Biol.* 16, 237–244.
- Cook, A., Bono, F., Jinek, M., Conti, E., 2007. Structural biology of nucleocytoplasmic transport. *Annu. Rev. Biochem.* 76, 647–671.
- Cook, A.G., Conti, E., 2010. Nuclear export complexes in the frame. *Curr. Opin. Struct. Biol.* 20, 247–252.
- Cortes, R., Rosello-Lleti, E., Rivera, M., Martinez-Dolz, L., Salvador, A., Azorin, I., et al., 2010. Influence of heart failure on nucleocytoplasmic transport in human cardiomyocytes. *Cardiovasc. Res.* 85, 464–472.
- Cronshaw, J.M., Matunis, M.J., 2004. The nuclear pore complex: disease associations and functional correlations. *Trends Endocrinol. Metab.* 15, 34–39.
- D'Angelo, M.A., Anderson, D.J., Richard, E., Hetzer, M.W., 2006. Nuclear pores form de novo from both sides of the nuclear envelope. *Science* 312, 440–443.
- De Rijck, J., Debyser, Z., 2006. The central DNA flap of the human immunodeficiency virus type 1 is important for viral replication. *Biochem. Biophys. Res. Comm.* 349, 1100–1110.
- DeGrasse, J.A., DuBois, K.N., Devos, D., Siegel, T.N., Sali, A., Field, M.C., et al., 2009. Evidence for a shared nuclear pore complex architecture that is conserved from the last common eukaryotic ancestor. *Mol. Cell Proteomics* 8, 2119–2130.
- Denning, D.P., Patel, S.S., Uversky, V., Fink, A.L., Rexach, M., 2003. Disorder in the nuclear pore complex: the FG repeat regions of nucleoporins are natively unfolded. *Proc. Natl. Acad. Sci. USA* 100, 2450–2455.
- Denning, D.P., Uversky, V., Patel, S.S., Fink, A.L., Rexach, M., 2002. The *Saccharomyces cerevisiae* nucleoporin Nup2p is a natively unfolded protein. *J. Biol. Chem.* 277, 33447–33455.
- Devos, D., Dokudovskaya, S., Williams, R., Alber, F., Eswar, N., Chait, B.T., et al., 2006. Simple fold composition and modular architecture of the nuclear pore complex. *Proc. Natl. Acad. Sci. USA* 103, 2172–2177.
- Dilworth, D.J., Suprpto, A., Padovan, J.C., Chait, B.T., Wozniak, R.W., Rout, M.P., et al., 2001. Nup2p dynamically associates with the distal regions of the yeast nuclear pore complex. *J. Cell Biol.* 153, 1465–1478.

- Dorfman, J., Macara, G.I., 2008. STRADalpha regulates LKB1 localization by blocking access to importin-alpha, and by association with Crm1 and exportin-7. *Mol. Biol. Cell* 19, 1614–1626.
- Elad, N., Maimon, T., Frenkiel-Krispin, D., Lim, R.Y., Medalia, O., 2009. Structural analysis of the nuclear pore complex by integrated approaches. *Curr. Opin. Struct. Biol.* 19, 226–232.
- England, J.R., Huang, J., Jennings, M.J., Makde, R.D., Tan, S., 2010. RCC1 uses a conformationally diverse loop region to interact with the nucleosome: a model for the RCC1-nucleosome complex. *J. Mol. Biol.* 398, 518–529.
- Erickson, E.S., Mooren, O.L., Moore, D., Krogmeier, J.R., Dunn, R.C., 2006. The role of nuclear envelope calcium in modifying nuclear pore complex structure. *Can. J. Physiol. Pharmacol.* 84, 309–318.
- Fabre, E., Hurt, E., 1997. Yeast genetics to dissect the nuclear pore complex and nucleocytoplasmic trafficking. *Annu. Rev. Genet.* 31, 277–313.
- Fahrenkrog, B., Aebi, U., 2003. The nuclear pore complex: nucleocytoplasmic transport and beyond. *Nat. Rev. Mol. Cell Biol.* 4, 757–766.
- Fahrenkrog, B., Koser, J., Aebi, U., 2004. The nuclear pore complex: a jack of all trades? *Trends Biochem. Sci.* 29, 175–182.
- Fanara, P., Hodel, M.R., Corbett, A.H., Hodel, A.E., 2000. Quantitative analysis of nuclear localization signal (NLS)-importin alpha interaction through fluorescence depolarization – Evidence for auto-inhibitory regulation of NLS binding. *J. Biol. Chem.* 275, 21218–21223.
- Faustino, R.S., Nelson, T.J., Terzic, A., Perez-Terzic, C., 2007. Nuclear transport: target for therapy. *Clin. Pharmacol. Ther.* 81, 880–886.
- Fiserova, J., Goldberg, M.W., 2010. Nucleocytoplasmic transport in yeast: a few roles for many actors. *Biochem. Soc. Trans.* 38, 273–277.
- Fontes, M.R., Teh, T., Jans, D., Brinkworth, R.I., Kobe, B., 2003. Structural basis for the specificity of bipartite nuclear localization sequence binding by importin-alpha. *J. Biol. Chem.* 278, 27981–27987.
- Fontes, M.R., Teh, T., Kobe, B., 2000. Structural basis of recognition of monopartite and bipartite nuclear localization sequences by mammalian importin-alpha. *J. Mol. Biol.* 297, 1183–1194.
- Forwood, J.K., Lonhienne, T.G., Marfori, M., Robin, G., Meng, W., Guncar, G., et al., 2008. Kap95p binding induces the switch loops of RanGDP to adopt the GTP-bound conformation: implications for nuclear import complex assembly dynamics. *J. Mol. Biol.* 383, 772–782.
- Frenkiel-Krispin, D., Maco, B., Aebi, U., Medalia, O., 2010. Structural analysis of a metazoan nuclear pore complex reveals a fused concentric ring architecture. *J. Mol. Biol.* 395, 578–586.
- Frey, S., Gorlich, D., 2007. A saturated FG-repeat hydrogel can reproduce the permeability properties of nuclear pore complexes. *Cell* 130, 512–523.
- Frey, S., Gorlich, D., 2009. FG/FxFG as well as GLFG repeats form a selective permeability barrier with self-healing properties. *EMBO J.* 28, 2554–2567.
- Fuller, B.G., 2010. Self-organization of intracellular gradients during mitosis. *Cell Div.* 5, 1–21.
- Gerace, L., Burke, B., 1988. Functional organization of the nuclear envelope. *Annu. Rev. Cell Biol.* 4, 335–374.
- Geyer, J.P., Doker, R., Kremer, W., Zhao, X., Kuhlmann, J., Kalbitzer, H.R., 2005. Solution structure of the Ran-binding domain 2 of RanBP2 and its interaction with the C terminus of Ran. *J. Mol. Biol.* 348, 711–725.
- Gika, A.D., Rich, P., Gupta, S., Neilson, D.E., Clarke, A., 2010. Recurrent acute necrotizing encephalopathy following influenza A in a genetically predisposed family. *Dev. Med. Child. Neurol.* 52, 99–102.

- Gilchrist, D., Rexach, M., 2003. Molecular basis for the rapid dissociation of nuclear localization signals from karyopherin alpha in the nucleoplasm. *J. Biol. Chem.* 278, 51937–51949.
- Goërllich, D., Seewald, M., Ribbeck, K., 2003. Characterization of Ran-driven cargo transport and the RanGTPase system by kinetic measurements and computer simulation. *EMBO J.* 22, 1088–1100.
- Goldfarb, D., Corbett, A., Mason, D., Harreman, M., Adam, S., 2004. Importin: a multi-purpose nuclear-transport receptor. *Trends Cell Biol.* 14, 505–514.
- Gorlich, D., Kutay, U., 1999. Transport between the cell nucleus and the cytoplasm. *Annu. Rev. Cell Dev. Biol.* 15, 607–660.
- Greber, U.F., Fassati, A., 2003. Nuclear import of viral DNA genomes. *Traffic* 4, 136–143.
- Greber, U.F., Fornerod, M., 2005. Nuclear import in viral infections. *Curr. Top Microbiol. Immunol.* 285, 109–138.
- Gustin, K.E., Sarnow, P., 2002. Inhibition of nuclear import and alteration of nuclear pore complex composition by rhinovirus. *J. Virol.* 76, 8787–8796.
- Hanover, J.A., Love, D.C., Prinz, W.A., 2009. Calmodulin-driven nuclear entry: trigger for sex determination and terminal differentiation. *J. Biol. Chem.* 284, 12593–12597.
- Henderson, B.R., 2000. Nuclear-cytoplasmic shuttling of APC regulates beta-catenin subcellular localization and turnover. *Nat. Cell Biol.* 2, 653–660.
- Hetzer, M.W., 2010. The nuclear envelope. *Cold Spring Harb. Perspect Biol.* 2, 1–16.
- Hindley, C.E., Lawrence, F.J., Matthews, D.A., 2007. A role for transportin in the nuclear import of adenovirus core proteins and DNA. *Traffic* 8, 1313–1322.
- Hiscox, J.A., 2003. The interaction of animal cytoplasmic RNA viruses with the nucleus to facilitate replication. *Virus Res.* 95, 13–22.
- Holaska, J.M., Black, B.E., Love, D.C., Hanover, J.A., Leszyk, J., Paschal, B.M., 2001. Calreticulin is a receptor for nuclear export. *J. Cell Biol.* 152, 127–140.
- Hou, C., Corces, V.G., 2010. Nups take leave of the nuclear envelope to regulate transcription. *Cell* 140, 306–308.
- Huang, S.M., Chen, C.C., Chiu, P.C., Cheng, M.F., Lai, P.H., Hsieh, K.S., 2004. Acute necrotizing encephalopathy of childhood associated with influenza type B virus infection in a 3-year-old girl. *J. Child Neurol.* 19, 64–67.
- Hutten, S., Flotho, A., Melchior, F., Kehlenbach, R.H., 2008. The Nup358-RanGAP complex is required for efficient importin alpha/beta-dependent nuclear import. *Mol. Biol. Cell* 19, 2300–2310.
- Isgro, T., Schulten, K., 2007. Association of nuclear pore FG-repeat domains to NTF2 import and export complexes. *J. Mol. Biol.* 366, 330–345.
- Kahms, M., Lehrich, P., Huve, J., Sanetra, N., Peters, R., 2009. Binding site distribution of nuclear transport receptors and transport complexes in single nuclear pore complexes. *Traffic* 10, 1228–1242.
- Kapon, R., Topchik, A., Mukamel, D., Reich, Z., 2008. A possible mechanism for self-coordination of bidirectional traffic across nuclear pores. *Phys. Biol.* 5, 036001.
- Kau, T., Way, J., Silver, P., 2004. Nuclear transport and cancer: from mechanism to intervention. *Nat. Rev. Cancer* 4, 1–12.
- Kim, I.S., Kim, D.H., Han, S.M., Chin, M.U., Nam, H.J., Cho, H.P., et al., 2000. Truncated form of importin alpha identified in breast cancer cell inhibits nuclear import of p53. *J. Biol. Chem.* 275, 23139–23145.
- Kind, B., Koehler, K., Lorenz, M., Huebner, A., 2009. The nuclear pore complex protein ALADIN is anchored via NDC1 but not via POM121 and GP210 in the nuclear envelope. *Biochem. Biophys. Res. Commun.* 390, 205–210.
- Kinoshita, Y., Ito, H., Hirano, A., Fujita, K., Wate, R., Nakamura, M., et al., 2009. Nuclear contour irregularity and abnormal transporter protein distribution in anterior horn cells in amyotrophic lateral sclerosis. *J. Neuropathol. Exp. Neurol.* 68, 1184–1192.

- Kiriyama, T., Hirano, M., Asai, H., Ikeda, M., Furiya, Y., Ueno, S., 2008. Restoration of nuclear-import failure caused by triple A syndrome and oxidative stress. *Biochem. Biophys. Res. Commun.* 374, 631–634.
- Kiseleva, E., Allen, T.D., Rutherford, S., Bucci, M., Wenthe, S.R., Goldberg, M.W., 2004. Yeast nuclear pore complexes have a cytoplasmic ring and internal filaments. *J. Struct. Biol.* 145, 272–288.
- Klebe, C., Bischoff, F.R., Ponstingl, H., Wittinghofer, A., 1995. Interaction of the nuclear GTP-binding protein Ran with its regulatory proteins RCC1 and RanGAP1. *Biochemistry* 34, 639–647.
- Kohler, A., Hurt, E., 2010. Gene regulation by nucleoporins and links to cancer. *Mol. Cell* 38, 6–15.
- Kramer, A., Ludwig, Y., Shahin, V., Oberleithner, H., 2007. A pathway separate from the central channel through the nuclear pore complex for inorganic ions and small macromolecules. *J. Biol. Chem.* 282, 31437–31443.
- Kutay, U., Bischoff, F.R., Kostka, S., Kraft, R., Gorlich, D., 1997. Export of importin alpha from the nucleus is mediated by a specific nuclear transport factor. *Cell* 90, 1061–1071.
- Kutay, U., Güttinger, S., 2005. Leucine-rich nuclear-export signals: born to be weak. *Trends in Cell Biol.* 15, 121–124.
- La Cour, T., Kiemer, L., Molgaard, A., Gupta, R., Skriver, K., Brunak, S., 2004. Analysis and prediction of leucine-rich nuclear export signals. *Protein Eng. Desig. & Select.* 17, 527–536.
- Lam, A.P., Dean, D.A., 2010. Progress and prospects: nuclear import of nonviral vectors. *Gene Ther* 17, 439–447.
- Lange, A., McLane, L.M., Mills, R.E., Devine, S.E., Corbett, A.H., 2010. Expanding the definition of the classical bipartite nuclear localization signal. *Traffic* 11, 311–323.
- Lange, A., Mills, R., Lange, C., Stewart, M., Devine, S., Corbett, A., 2007. Classical nuclear localization signals: definition, function, and interaction with importin {alpha}. *J. Biol. Chem.* 282, 5101–5105.
- Lee, C.P., Chen, M.R., 2010. Escape of herpesviruses from the nucleus. *Rev. Med. Virol.* 20, 214–230.
- Lee, H.G., Ueda, M., Miyamoto, Y., Yoneda, Y., Perry, G., Smith, M.A., et al., 2006. Aberrant localization of importin alpha1 in hippocampal neurons in Alzheimer disease. *Brain Res* 1124, 1–4.
- Lee, S., Matsuura, Y., Liu, S., Stewart, M., 2005. Structural basis for nuclear import complex dissociation by RanGTP. *Nature* 435, 693–696.
- Lim, R., Ullman, K., Fahrenkrog, B., 2008. Biology and biophysics of the nuclear pore complex and its components. *Int. Rev. Cell Mol. Biol.* 267, 299.
- Lin, J.Y., Chen, T.C., Weng, K.F., Chang, S.C., Chen, L.L., Shih, S.R., 2009. Viral and host proteins involved in picornavirus life cycle. *J. Biomed. Sci.* 16, 103.
- Lonhienne, T.G., Forwood, J.K., Marfori, M., Robin, G., Kobe, B., Carroll, B.J., 2009. Importin-beta 1s a GDP-to-GTP exchange factor of Ran implications for the mechanism of nuclear import. *J. Biol. Chem.* 284, 22549–22558.
- Lott, K., Bhardwaj, A., Mitrousis, G., Pante, N., Cingolani, G., 2010. The importin beta binding domain modulates the avidity of importin beta for the nuclear pore complex. *J. Biol. Chem.* 285, 13769–13780.
- Lounsbury, K.M., Macara, I.G., 1997. Ran-binding protein 1 (RanBP1) forms a ternary complex with Ran and karyopherin beta and reduces Ran GTPase-activating protein (RanGAP) inhibition by karyopherin beta. *J. Biol. Chem.* 272, 551–555.
- Lui, K., Huang, Y., 2009. RanGTPase: A Key Regulator of Nucleocytoplasmic Trafficking. *Mol. Cell. Pharmacol.* 1, 148–156.
- Lusk, C.P., Blobel, G., King, M.C., 2007. Highway to the inner nuclear membrane: rules for the road. *Nat. Rev. Mol. Cell Biol.* 8, 414–420.

- Ma, Z., Hill, D.A., Collins, M.H., Morris, S.W., Sumegi, J., Zhou, M., et al., 2003. Fusion of ALK to the Ran-binding protein 2 (RANBP2) gene in inflammatory myofibroblastic tumor. *Genes Chromosomes Cancer* 37, 98–105.
- Macara, I., 2001. Transport into and out of the nucleus. *Microbiol. Mol. Biol. Rev.* 65, 570–594.
- Madrid, A.S., Weis, K., 2006. Nuclear transport is becoming crystal clear. *Chromosoma* 115, 98–109.
- Matsuura, Y., Lange, A., Harreman, M., Corbett, A., Stewart, M., 2003. Structural basis for Nup2p function in cargo release and karyopherin recycling in nuclear import. *EMBO J.* 22, 5358–5369.
- Matsuura, Y., Stewart, M., 2004. Structural basis for the assembly of a nuclear export complex. *Nature* 432, 872–877.
- Matsuura, Y., Stewart, M., 2005. Nup50/Npap60 function in nuclear protein import complex disassembly and importin recycling. *EMBO J.* 24, 3681–3689.
- Melchior, F., Gerace, L., 1998. Two-way trafficking with Ran. *Trends Cell. Biol.* 8, 175–179.
- Miao, L., Schulten, K., 2009. Transport-related structures and processes of the nuclear pore complex studied through molecular dynamics. *Structure* 17, 449–459.
- Miller, M., Park, M.K., Hanover, J.A., 1991. Nuclear pore complex: structure, function, and regulation. *Physiol. Rev.* 71, 909–949.
- Mishra, R.K., Chakraborty, P., Arnaoutov, A., Fontoura, B.M.A., Dasso, M., 2010. The Nup107-160 complex and gamma-TuRC regulate microtubule polymerization at kinetochores. *Nat. cell biol.* 12, 164–169.
- Miyamoto, Y., Saiwaki, T., Yamashita, J., Yasuda, Y., Kotera, I., Shibata, S., et al., 2004. Cellular stresses induce the nuclear accumulation of importin alpha and cause a conventional nuclear import block. *J. Cell Biol.* 165, 617–623.
- Mohr, D., Frey, S., Fischer, T., Guttler, T., Gorlich, D., 2009. Characterisation of the passive permeability barrier of nuclear pore complexes. *EMBO J.* 28, 2541–2553.
- Moore, M.S., 2003. Npap60: a new player in nuclear protein import. *Trends Cell Biol.* 13, 61–64.
- Moore, M.S., Blobel, G., 1994. A G protein involved in nucleocytoplasmic transport: the role of Ran. *Trends Biochem. Sci.* 19, 211–216.
- Mosammamarast, N., Pemberton, L.F., 2004. Karyopherins: from nuclear-transport mediators to nuclear-function regulators. *Trends Cell Biol.* 14, 547–556.
- Moussavi-Baygi, R., Jamali, Y., Karimi, R., Mofrad, M.R.K., 2011. Biophysical Coarse-Grained Modeling Provides Insights into Transport through the Nuclear Pore Complex. *Biophys. J.*
- Nagai, S., Dubrana, K., Tsai-Pflugfelder, M., Davidson, M.B., Roberts, T.M., Brown, G.W., et al., 2008. Functional targeting of DNA damage to a nuclear pore-associated SUMO-dependent ubiquitin ligase. *Science* 322, 597–602.
- Naim, B., Brumfeld, V., Kapon, R., Kiss, V., Nevo, R., Reich, Z., 2007. Passive and facilitated transport in nuclear pore complexes is largely uncoupled. *J. Biol. Chem.* 282, 3881–3888.
- Nakano, H., Funasaka, T., Hashizume, C., Wong, R.W., 2010. Nucleoporin translocated promoter region (Tpr) associates with dynein complex, preventing chromosome lagging formation during mitosis. *J. Biol. Chem.* 285, 10841–10849.
- Neilson, D.E., Adams, M.D., Orr, C.M., Schelling, D.K., Eiben, R.M., Kerr, D.S., et al., 2009. Infection-triggered familial or recurrent cases of acute necrotizing encephalopathy caused by mutations in a component of the nuclear pore, RANBP2. *Am. J. Hum. Genet.* 84, 44–51.
- Neumann, N., Jeffares, D.C., Poole, A.M., 2006. Outsourcing the nucleus: nuclear pore complex genes are no longer encoded in nucleomorph genomes. *Evol. Bioinform. Online* 2, 23–34.

- Neuwald, A.F., Kannan, N., Poleksic, A., Hata, N., Liu, J.S., 2003. Ran's C-terminal, basic patch, and nucleotide exchange mechanisms in light of a canonical structure for Rab, Rho, Ras, and Ran GTPases. *Genome Res.* 13, 673–692.
- Nishimoto, T., 2000. Upstream and downstream of ran GTPase. *Biol. Chem.* 381, 397–405.
- Oberleithner, H., Schillers, H., Wilhelmi, M., Butzke, D., Danker, T., 2000. Nuclear pores collapse in response to CO<sub>2</sub> imaged with atomic force microscopy. *Pflugers Arch.* 439, 251–255.
- Ogawa, Y., Miyamoto, Y., Asally, M., Oka, M., Yasuda, Y., Yoneda, Y., 2010. Two isoforms of npap60 (nup50) differentially regulate nuclear protein import. *Mol. Biol. Cell* 21, 630–638.
- Otsuka, S., Iwasaka, S., Yoneda, Y., Takeyasu, K., Yoshimura, S.H., 2008. Individual binding pockets of importin-β for FG-nucleoporins have different binding properties and different sensitivities to RanGTP. *Proc. Natl. Acad. Sci. USA* 105, 16101–16106.
- Park, N., Katikaneni, P., Skern, T., Gustin, K.E., 2008. Differential targeting of nuclear pore complex proteins in poliovirus-infected cells. *J. Virol.* 82, 1647–1655.
- Patel, S., Rexach, M., 2008. Discovering novel interactions at the nuclear pore complex using bead halo: a rapid method for detecting molecular interactions of high and low affinity at equilibrium. *Mol. Cell. Proteomics* 7, 121–131.
- Paulillo, S., Powers, M., Ullman, K., Fahrenkrog, B., 2006. Changes in nucleoporin domain topology in response to chemical effectors. *J. Mol. Biol.* 363, 39–50.
- Peleg, O., Lim, R.Y., 2010. Converging on the function of intrinsically disordered nucleoporins in the nuclear pore complex. *Biol. Chem.* 391, 719–730.
- Pemberton, L.F., Paschal, B.M., 2005. Mechanisms of receptor-mediated nuclear import and nuclear export. *Traffic* 6, 187–198.
- Perez-Terzic, C., Behfar, A., Mery, A., van Deursen, J.M.A., Terzic, A., Puceat, M., 2003. Structural adaptation of the nuclear pore complex in stem cell-derived cardiomyocytes. *Circ. Res.* 92, 444–452.
- Perez-Terzic, C., Faustino, R.S., Boorsma, B.J., Arrell, D.K., Niederlander, N.J., Behfar, A., et al., 2007. Stem cells transform into a cardiac phenotype with remodeling of the nuclear transport machinery. *Nat. Clin. Pract. Cardiovasc. Med.* 4 (Suppl 1), S68–76.
- Peters, R., 2005. Translocation through the nuclear pore complex: selectivity and speed by reduction-of-dimensionality. *Traffic* 6, 421–427.
- Peters, R., 2009a. Functionalization of a nanopore: the nuclear pore complex paradigm. *Biochim. Biophys. Acta* 1793, 1533–1539.
- Peters, R., 2009b. Translocation through the nuclear pore: Kaps pave the way. *Bioessays* 31, 466–477.
- Petersen, C., Orem, N., Trueheart, J., Thorner, J.W., Macara, I.G., 2000. Random mutagenesis and functional analysis of the Ran-binding protein. RanBP1. *J. Biol. Chem.* 275, 4081–4091.
- Puntener, D., Greber, U., 2009. DNA-tumor virus entry—From plasma membrane to the nucleus. *Semin. Cell. Develop. Biol.* 20, 631–642.
- Qiao, X., Pham, D.N., Luo, H., Wu, J., 2010. Ran overexpression leads to diminished T cell responses and selectively modulates nuclear levels of c-Jun and c-Fos. *J. Biol. Chem.* 285, 5488–5496.
- Rakowska, A., Danker, T., Schneider, S.W., Oberleithner, H., 1998. ATP-induced shape change of nuclear pores visualized with the atomic force microscope. *J. Membr. Biol.* 163, 129–136.
- Ren, Y., Seo, H.S., Blobel, G., Hoelz, A., 2010. Structural and functional analysis of the interaction between the nucleoporin Nup98 and the mRNA export factor Rae1. *Proc. Natl. Acad. Sci. USA* 107, 10406–10411.

- Renault, L., Kuhlmann, J., Henkel, A., Wittinghofer, A., 2001. Structural basis for guanine nucleotide exchange on Ran by the regulator of chromosome condensation (RCC1). *Cell* 105, 245–255.
- Ribbeck, K., Goërlich, D., 2001. Kinetic analysis of translocation through nuclear pore complexes. *EMBO J.* 20, 1320–1330.
- Riviere, L., Darlix, J.L., Cimarelli, A., 2010. Analysis of the viral elements required in the nuclear import of HIV-1 DNA. *J. Virol.* 84, 729–739.
- Rixon, F.J., 2010. Herpesviruses: an in-depth view. *Structure* 18, 2–4.
- Rout, M.P., Aitchison, J.D., Suprpto, A., Hjertaas, K., Zhao, Y., Chait, B.T., 2000. The yeast nuclear pore complex: composition, architecture, and transport mechanism. *J. Cell Biol.* 148, 635–651.
- Rush, M.G., Drivas, G., D'Eustachio, P., 1996. The small nuclear GTPase Ran: how much does it run? *Bioessays* 18, 103–112.
- Russell, W.C., 2009. Adenoviruses: update on structure and function. *J. Gen. Virol.* 90, 1–20.
- Sapp, M., Day, P.M., 2009. Structure, attachment and entry of polyoma- and papillomaviruses. *Virology* 384, 400–409.
- Saric, M., Zhao, X., Korner, C., Nowak, C., Kuhlmann, J., Vetter, I.R., 2007. Structural and biochemical characterization of the Importin-beta.Ran.GTP.RanBD1 complex. *FEBS Lett.* 581, 1369–1376.
- Scheffzek, K., Klebe, C., Fritz-Wolf, K., Kabsch, W., Wittinghofer, A., 1995. Crystal structure of the nuclear Ras-related protein Ran in its GDP-bound form. *Nature* 374, 378–381.
- Schmitz, A., Schwarz, A., Foss, M., Zhou, L., Rabe, B., Hoellenriegel, J., et al., 2010. Nucleoporin 153 arrests the nuclear import of hepatitis B virus capsids in the nuclear basket. *PLoS Pathog.* 6, 1–15.
- Schrader, N., Koerner, C., Koessmeier, K., Bangert, J.A., Wittinghofer, A., Stoll, R., et al., 2008. The crystal structure of the Ran-Nup153ZnF2 complex: a general Ran docking site at the nuclear pore complex. *Structure* 16, 1116–1125.
- Schwartz, T.U., 2005. Modularity within the architecture of the nuclear pore complex. *Curr. Opin. in Structural Biology* 15, 221–226.
- Seewald, M.J., Korner, C., Wittinghofer, A., Vetter, I.R., 2002. RanGAP mediates GTP hydrolysis without an arginine finger. *Nature* 415, 662–666.
- Seewald, M.J., Kraemer, A., Farkasovsky, M., Korner, C., Wittinghofer, A., Vetter, I.R., 2003. Biochemical characterization of the Ran-RanBP1-RanGAP system: are RanBP proteins and the acidic tail of RanGAP required for the Ran-RanGAP GTPase reaction? *Mol. Cell. Biol.* 23, 8124–8136.
- Sheffield, L., Miskiewicz, H., Tannenbaum, L., Mirra, S., 2006. Nuclear pore complex proteins in Alzheimer disease. *J. Neuropath. Exp. Neur.* 65, 45–54.
- Shulga, N., Goldfarb, D.S., 2003. Binding dynamics of structural nucleoporins govern nuclear pore complex permeability and may mediate channel gating. *Mol. Cell. Biol.* 23, 534–542.
- Sorokin, A., Kim, E., Ovchinnikov, L., 2007. Nucleocytoplasmic transport of proteins. *Biochemistry (Moscow)* 72, 1439–1457.
- Stewart, M., 2003. Structural biology. Nuclear trafficking. *Science* 302, 1513–1514.
- Stewart, M., 2006. Structural basis for the nuclear protein import cycle. *Biochem. Soc. T.* 34, 701–704.
- Stewart, M., 2007. Molecular mechanism of the nuclear protein import cycle. *Nature Reviews Molecular Cell Biol.* 8, 195–208.
- Stoffler, D., Feja, B., Fahrenkrog, B., Walz, J., Typke, D., Aebi, U., 2003. Cryo-electron tomography provides novel insights into nuclear pore architecture: implications for nucleocytoplasmic transport. *J. Mol. Biol.* 328, 119–130.

- Storr, H.L., Kind, B., Parfitt, D.A., Chapple, J.P., Lorenz, M., Koehler, K., et al., 2009. Deficiency of ferritin heavy-chain nuclear import in triple a syndrome implies nuclear oxidative damage as the primary disease mechanism. *Mol. Endocrinol.* 23, 2086–2094.
- Strawn, L., Shen, T., Shulga, N., Goldfarb, D., Wentz, S., 2004. Minimal nuclear pore complexes define FG repeat domains essential for transport. *Nat. Cell Biol.* 6, 197–206.
- Strom, A.C., Weis, K., 2001. Importin-beta-like nuclear transport receptors. *Genome Biol.* 2, reviews3008.1–reviews3008.9.
- Sun, C., Yang, W., Tu, L., Musser, S., 2008. Single-molecule measurements of importin / cargo complex dissociation at the nuclear pore. *Proc. Natl. Acad. Sci.* 105, 8613–8618.
- Suntharalingam, M., Wentz, S.R., 2003. Peering through the pore: Nuclear pore complex structure, assembly, and function. *Dev. Cell* 4, 775–789.
- Suzuki, T., Yamamoto, N., Nonaka, M., Hashimoto, Y., Matsuda, G., Takeshima, S.N., et al., 2009. Inhibition of human immunodeficiency virus type 1 (HIV-1) nuclear import via Vpr-Importin alpha interactions as a novel HIV-1 therapy. *Biochem. Biophys. Res. Commun.* 380, 838–843.
- Suzuki, Y., Craigie, R., 2007. The road to chromatin – nuclear entry of retroviruses. *Nat. Rev. Microbiol.* 5, 187–196.
- Swaminathan, S., Melchior, F., 2002. Nucleocytoplasmic transport: More than the usual suspects. *Dev. Cell* 3, 304–306.
- Tartakoff, A.M., Tao, T., 2010. Comparative and evolutionary aspects of macromolecular translocation across membranes. *Int. J. Biochem. Cell Biol.* 42, 214–229.
- Terry, L.J., Wentz, S.R., 2009. Flexible gates: dynamic topologies and functions for FG nucleoporins in nucleocytoplasmic transport. *Eukaryot. Cell* 8, 1814–1827.
- Tewari, R., Bailes, E., Bunting, K.A., Coates, J.C., 2010. Armadillo-repeat protein functions: questions for little creatures. *Trends Cell Biol.* 20, 470–481.
- Trotman, L.C., Mosberger, N., Fornerod, M., Stidwill, R.P., Greber, U.F., 2001. Import of adenovirus DNA involves the nuclear pore complex receptor CAN/Nup214 and histone H1. *Nat. Cell Biol.* 3, 1092–1100.
- Truant, R., Cullen, B.R., 1999. The arginine-rich domains present in human immunodeficiency virus type 1 Tat and Rev function as direct importin beta-dependent nuclear localization signals. *Mol. Cell Biol.* 19, 1210–1217.
- Tsangaridou, E., Polioudaki, H., Sfakianaki, R., Samiotaki, M., Tzardi, M., Koulentaki, M., et al., 2010. Differential detection of nuclear envelope autoantibodies in primary biliary cirrhosis using routine and alternative methods. *BMC Gastroenterol.* 10, 1–13.
- Um, J.W., Min, D.S., Rhim, H., Kim, J., Paik, S.R., Chung, K.C., 2006. Parkin ubiquitinates and promotes the degradation of RanBP2. *J. Biol. Chem.* 281, 3595–3603.
- Vetter, I.R., Wittinghofer, A., 2001. The guanine nucleotide-binding switch in three dimensions. *Science* 294, 1299–1304.
- von Kobbe, C., van Deursen, J.M., Rodrigues, J.P., Sitterlin, D., Bachi, A., Wu, X., et al., 2000. Vesicular stomatitis virus matrix protein inhibits host cell gene expression by targeting the nucleoporin Nup98. *Mol. Cell* 6, 1243–1252.
- Walde, S., Kehlenbach, R.H., 2010. The Part and the Whole: functions of nucleoporins in nucleocytoplasmic transport. *Trends Cell Biol.* 20, 461–469.
- Weidman, M.K., Sharma, R., Raychaudhuri, S., Kundu, P., Tsai, W., Dasgupta, A., 2003. The interaction of cytoplasmic RNA viruses with the nucleus. *Virus Res.* 95, 75–85.
- Wentz, S.R., 2000. Gatekeepers of the nucleus. *Science* 288, 1374–1377.
- Whittaker, G., Bui, M., Helenius, A., 1996. The role of nuclear import and export in influenza virus infection. *Trends Cell Biol.* 6, 67–71.
- Wolf, C., Mofrad, M.R., 2008. On the octagonal structure of the nuclear pore complex: insights from coarse-grained models. *Biophys. J.* 95, 2073–2085.



- Wolf, C., Mofrad, M., 2009. Mechanotransduction: role of nuclear pore mechanics and nucleocytoplasmic transport (Ch. 18). In: Mofrad, M., Kamm, R. (Eds.), *Cellular mechanotransduction: diverse perspectives from molecules to tissues*. Cambridge University Press, New York.
- Woodward, C.L., Prakobwanakit, S., Mosessian, S., Chow, S.A., 2009. Integrase interacts with nucleoporin NUP153 to mediate the nuclear import of human immunodeficiency virus type 1. *J. Virol.* 83, 6522–6533.
- Wu, J., Corbett, A.H., Berland, K.M., 2009. The intracellular mobility of nuclear import receptors and NLS cargoes. *Biophys. J.* 96, 3840–3849.
- Wu, W.W.H., Pante, N., 2009. The directionality of the nuclear transport of the influenza A genome is driven by selective exposure of nuclear localization sequences on nucleoprotein. *Virol. J.* 6, 1–12.
- Xu, L., Massagué, J., 2004. Nucleocytoplasmic shuttling of signal transducers. *Nature Rev. Mol. Cell Biol.* 5, 209–219.
- Xu, S., Powers, M.A., 2009. Nuclear pore proteins and cancer. *Semin. Cell Dev. Biol.* 20, 620–630.
- Yadirgi, G., Marino, S., 2009. Adult neural stem cells and their role in brain pathology. *J. Pathol.* 217, 242–253.
- Yamazumi, Y., Kamiya, A., Nishida, A., Nishihara, A., Iemura, S., Natsume, T., et al., 2009. The transmembrane nucleoporin NDC1 is required for targeting of ALADIN to nuclear pore complexes. *Biochem. Biophys. Res. Commun.* 389, 100–104.
- Yang, S.N., Takeda, A.A., Fontes, M.R., Harris, J.M., Jans, D.A., Kobe, B., 2010. Probing the specificity of binding to the major nuclear localization sequence-binding site of importin- $\alpha$  using oriented peptide library screening. *J. Biol. Chem.* 285, 19935–19946.
- Yang, W., Musser, S.M., 2006. Nuclear import time and transport efficiency depend on importin beta concentration. *J. Cell Biol.* 174, 951–961.
- Yaseen, N.R., Blobel, G., 1999. Two distinct classes of Ran-binding sites on the nucleoporin Nup-358. *Proc. Natl. Acad. Sci. USA* 96, 5516–5521.
- Yasuhara, N., Oka, M., Yoneda, Y., 2009. The role of the nuclear transport system in cell differentiation. *Semin. Cell Dev. Biol.* 20, 590–599.
- Yasuhara, N., Shibazaki, N., Tanaka, S., Nagai, M., Kamikawa, Y., Oe, S., et al., 2007. Triggering neural differentiation of ES cells by subtype switching of importin- $\alpha$ . *Nat. Cell Biol.* 9, 72–79.
- Yudin, D., Fainzilber, M., 2009. Ran on tracks—cytoplasmic roles for a nuclear regulator. *J. Cell Sci.* 122, 587–593.
- Zachariae, U., Grubmüller, H., 2008. Importin- $\beta$ : structural and dynamic determinants of a molecular spring. *Structure* 16, 906–915.
- Zachariae, U., Grubmüller, H., 2006. A highly strained nuclear conformation of the exportin Cse1p revealed by molecular dynamics simulations. *Structure* 14, 1469–1478.
- Zeitler, B., Weis, K., 2004. The FG-repeat asymmetry of the nuclear pore complex is dispensable for bulk nucleocytoplasmic transport in vivo. *J. Cell Biol.* 167, 583–590.
- Zennou, V., Petit, C., Guetard, D., Nerhbass, U., Montagnier, L., Charneau, P., 2000. HIV-1 genome nuclear import is mediated by a central DNA flap. *Cell* 101, 173–185.
- Zhang, X., Chen, S., Yoo, S., Chakrabarti, S., Zhang, T., Ke, T., et al., 2008. Mutation in nuclear pore component NUP155 leads to atrial fibrillation and early sudden cardiac death. *Cell* 135, 1017–1027.
- Zilman, A., Di Talia, S., Chait, B., Rout, M., Magnasco, M., 2007. Efficiency, selectivity, and robustness of nucleocytoplasmic transport. *PLoS Comput. Biol.* 3, 1281–1290.

# DYNAMIC MICROTUBULES AND THE TEXTURE OF PLANT CELL WALLS

Clive Lloyd

## Contents

|                                                                                                       |     |
|-------------------------------------------------------------------------------------------------------|-----|
| 1. Introduction                                                                                       | 288 |
| 1.1. The multinet-growth hypothesis and hoop reinforcement                                            | 289 |
| 1.2. Microtubule hoops                                                                                | 290 |
| 2. Microtubules                                                                                       | 294 |
| 2.1. Dynamic microtubules                                                                             | 294 |
| 2.2. Global organization emerges out of microtubule–microtubule interaction                           | 296 |
| 2.3. Rotating microtubule arrays explore all orientations                                             | 298 |
| 2.4. Microtubules do not always form circumferential hoops                                            | 300 |
| 2.5. Do microtubules behave differently in roots and shoots?                                          | 300 |
| 3. The Paradoxical Outer Epidermal Wall                                                               | 302 |
| 4. Microtubule Alignment and Twisted Growth                                                           | 304 |
| 5. Microtubule and Microfibril Coalignment                                                            | 306 |
| 5.1. Which orientates which?                                                                          | 306 |
| 5.2. The relationship of cellulose synthases with microtubules                                        | 308 |
| 5.3. Evidence from growth mutants                                                                     | 309 |
| 5.4. Non-elongating secondary cell walls provide clear examples of microtubule/cellulose co-alignment | 311 |
| 6. (Re)interpreting Wall Patterns                                                                     | 314 |
| 6.1. Steps between wall layers                                                                        | 314 |
| 6.2. Beyond microtubules: Post-cytoplasmic changes to wall texture                                    | 315 |
| 7. A New Dynamic Model for the Influence of Microtubules on the Texture of Plant Cell Walls           | 319 |
| 8. Concluding Remarks                                                                                 | 321 |
| Acknowledgments                                                                                       | 322 |
| References                                                                                            | 322 |

Department of Cell and Developmental Biology, John Innes Centre, Norwich, United Kingdom

*International Review of Cell and Molecular Biology*, Volume 287  
ISSN 1937-6448, DOI: 10.1016/B978-0-12-386043-9.00007-4

© 2011 Elsevier Inc.  
All rights reserved.

## Abstract

The relationship between microtubules and cell-wall texture has had a fitful history in which progress in one area has not been matched by progress in the other. For example, the idea that wall texture arises entirely from self-assembly, independently of microtubules, originated with electron microscopic analyses of fixed cells that gave no clue to the ability of microtubules to reorganize. Since then, live-cell studies have established the surprising dynamicity of plant microtubules involving collisions, changes in angle, parallelization, and rotation of microtubule tracks. Combined with proof that cellulose synthases do track along shifting microtubules, this offers more realistic models for the dynamic influence of microtubules on wall texture than could have been imagined in the electron microscopic era—the era from which most ideas on wall texture originate. This review revisits the classical literature on wall organization from the vantage point of current knowledge of microtubule dynamics.

*Key Words:* Microtubule dynamics, Microtubule rotation, Plant cell-wall texture, Multinet-growth hypothesis, Cellulose synthases. © 2011 Elsevier Inc.

## 1. INTRODUCTION

Ideas about wall lamellation have not really changed much over the past 50 years or so. Virtually, all the seminal ideas about wall construction originated in the electron microscopic era when the field divided between those who believed that layers of cellulose microfibrils were organized entirely by self-assembly principles (and may or may not be subsequently realigned by the forces of cell expansion) and those who believed that microtubules have some influence over the initial layering pattern. Heath's hypothesis that cellulose synthases move along microtubules was published nearly 40 years ago (Heath, 1974).

Since then, much has been learnt about dynamics, but this has been restricted to cytoplasmic and plasma membrane components rather than to the wall itself, which is still visualized with nondynamic methods with attendant problems of artifact and interpretation. Far more papers were published on the electron microscopic analysis of cell walls before the dynamic instability of microtubules was discovered in the 1980s than after. Obviously, such early wall studies were uninformed by advances in microtubule behavior and cellulose synthase movement, yet they continue to exert influence on ideas about wall texture. In this chapter, I shall rework concepts on wall organization from the predynamic era to show that they can be reconciled with what is now known about the dynamic microtubule template.

### 1.1. The multinet-growth hypothesis and hoop reinforcement

Long before microtubules were discovered, the fibrous texture of the cell wall was examined by polarized light microscopy. Using this technique, Van Iterson (1937) deduced that *Tradescantia* stamen hairs would have more or less transverse wall fibers. This is consistent with the biophysical explanation that transverse stress, which is twice the longitudinal force in an expanding cylinder, must be resisted by transverse hoop-reinforcement. This theoretical requirement for transverse reinforcement against the dominant tissue stress then became a recurring motif in early electron microscopic studies in which the alignment of cellulose microfibrils could be seen directly rather than inferred from polarization studies that deal in net alignment throughout the thickness of the wall. The pioneering electron microscopy (EM) of Roelofsen and Houwink (1951, 1953), demonstrated that cellulose microfibrils at the inner wall layer of *Tradescantia* stamen hairs were indeed arranged transversely around the cell. This prompted the multinet growth hypothesis (MGH), but it is important to remember that such observations, which influenced thinking about cell walls in complex tissues, were based on freely growing tubular cells (Roelofsen and Houwink, 1953).

In the MGH, it was suggested that layers of cellulose microfibrils were continuously applied to the inner surface of the wall (adjacent to the plasma membrane) as transverse helices with a flat, shallow pitch. In the original MGH, the microfibrils within one layer were pictured as a sheaf or bundle of fishing nets. In the net, microfibrils were woven but their alignment could be changed as the net was pulled this way or that according to the dominant growth axis. By this means, as the previous layer was displaced outward by a new layer of essentially transverse microfibrils applied at the plasma membrane, the strands in the older part of the wall were thought to become passively realigned by extension (Fig. 7.1). As newer layers took the dominant transverse stress, the older layers were hypothesized to succumb gradually to the next dominant stress of longitudinal tension. Over time, a gradient developed throughout the thickness of the wall in which microfibrils were transverse upon the plasma membrane, oblique in intermediate layers, and longitudinal in the outermost. This multinet-compatible arrangement was confirmed by Green (1960). However, Preston (1982) proposed a modified version of the MGH in which he corrected the idea that a single layer of microfibrils formed a literal net. He suggested that sheets of microfibrils (lamellae) responded passively to the forces of realignment. This modified MGH or passive realignment model retained the key concept that lamellae were laid down essentially transversely and then reoriented by extension toward the longitudinal axis as the layer journeyed outward along a force gradient.

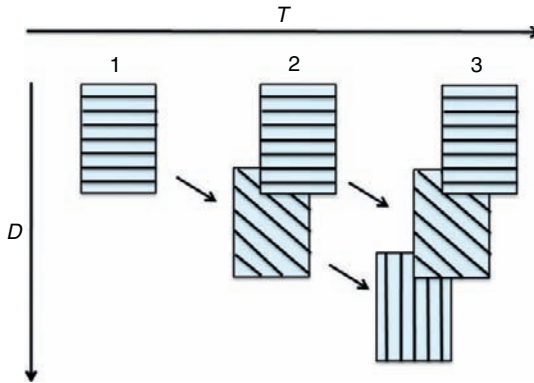


**Figure 7.1** *The modified multinet growth, or passive realignment, model.* According to this model, each new lamella applied to the plasma membrane is composed of transverse cellulose microfibrils. As the newer transverse lamella 2 is deposited at the plasma membrane, its predecessor 1 moves out radially and its microfibrils are passively realigned by the forces of cell expansion, first to an oblique orientation and then toward a longitudinal alignment as in 3.  $T$  = time;  $D$  = distance from the plasma membrane.

## 1.2. Microtubule hoops

Green (1962) prepared the way for a cytoplasmic template for wall organization when he published his mechanism for the control of cylindrical form in plants. Working on the tubular cells of the filamentous alga, *Nitella*, he described how strong transverse reinforcement was provided by cellulose microfibrils that were likened to “hoops on a barrel.” Because this transverse reinforcement could be disrupted by colchicine, with a consequent disturbance of cylindrical form, he predicted that the transverse axis would be maintained by cytoplasmic elements composed of “spindle fiber protein.” This was on the basis that colchicine—whose precise molecular action was not then known—could be seen to dissolve the birefringence of the mitotic spindle apparatus. In a landmark EM study of the following year, it was reported that “cytotubules” or “microtubules,” just beneath the plasma membrane, mirrored the orientation of cellulose microfibrils in the cell wall (Ledbetter and Porter, 1963). The microtubules were seen to be oriented circumferentially and were famously analogized to “hundreds of hoops around the cell.” The idea of hoop reinforcement, derived from algal filaments and backed by biophysical theory, therefore appeared to be vindicated by work on the complex tissues of higher plants.

### 1.2.1. Challenges to the multinet growth hypothesis

The MGH had a dominant influence on thinking about how the cell wall is organized. Its fundamental tenet, supported by biomechanical theory, was that innermost microfibrils of elongating cells circumnavigated the cell in

transverse “hoops.” However, as early as the 1950s, Roelofsen had to address observations from a range of higher plant cells that cellulose microfibrils are not always transverse; that is, perpendicular to the growth axis (Roelofsen, 1958). In the same year, Setterfield and Bayley concluded that throughout cell elongation, the primary wall of parenchyma cells of *Avena* coleoptiles contained layers of transverse and longitudinal microfibrils separated by microfibrils of intermediate orientation (Setterfield and Bayley, 1958). Their key observation was, “. . . that the form of the primary wall is not primarily a passive result of external forces but is precisely determined as part of specific cell differentiation.” In other words, the MGH was too simple to account for all observed patterns.

Crossed-helical wall patterns had already been shown in EM studies on filamentous green algae where layers of almost-transverse microfibrils alternated with layers of almost-longitudinal microfibrils (Frei and Preston, 1961). This formed alternating steeply pitched and flat-pitched helices around the cell, with a third set of microfibrils holding an intermediate alignment. In higher plants, too, there were clear examples of innermost cellulose microfibrils being deposited in non-transverse alignments as shown in a series of papers from Chafe’s laboratory (Chafe and Chauvet, 1974; Chafe and Doohan, 1972; Chafe and Wardrop, 1972; Wardrop et al., 1979).

In epidermal cells of four species of growing plant, cellulose microfibrils were found to be laid down in alternating transverse and longitudinal layers, although these could also be alternatively interpreted as flat and steeply pitched helices (Chafe and Wardrop, 1972). And in freeze-etch studies on elongating parenchyma cells from three angiosperm species, wall layers were seen to form a “crossed-polylamellate” or “crossed-fibrillar” pattern, where alignment alternated between near-transverse and near-longitudinal alignments without decreasing pitch from the inner to the outer layers (Itoh, 1975; Itoh and Shimaji, 1976). This finding of non-transverse microfibrils *at the plasma membrane* directly challenged the MGH and the concept of simple, transverse hoop reinforcement. With longitudinal microfibrils found near to, and transverse ones distant from, the plasma membrane, it was not really possible to see how such radically alternating young layers could be explained by a model in which initially transverse microfibrils were supposed to be pulled toward a longitudinal orientation by progressive displacement from the plasma membrane.

### 1.2.2. The Ordered fibril hypothesis favored non-transverse alignments

This growing challenge to the MGH, as it applied to higher plant tissues, culminated in a new model by Roland et al. (1975). Using a silver proteinate method to label fibrillar material (presumed to be cellulose microfibrils) remaining in the wall after extraction of matrix materials, transverse “fibrils” were observed not only at the plasma membrane but also in layers

throughout the thickness of the growing primary cell wall. Fibrils were seen to be deposited in alternating transverse and longitudinal “criss-cross” layers according to what was called the ordered fibril hypothesis (Roland et al., 1982; Fig. 7.2). These strata could be separated by others with intermediate angles and it was concluded that, “in successive strata the fibril direction is rotated through an angle intermediate between orthogonal directions” (Roland et al., 1977). This suggested that the pattern of deposition did not alternate discontinuously (criss-cross) between left-hand oblique and right-hand oblique, and so on but changed more progressively, with the angle of each layer being regularly offset from its predecessor. The distinctive feature of this helicoidal pattern was that where the transitional strata could clearly be seen in section, the layers formed regular, rhythmic, bow-shaped arcs (Fig. 7.3).

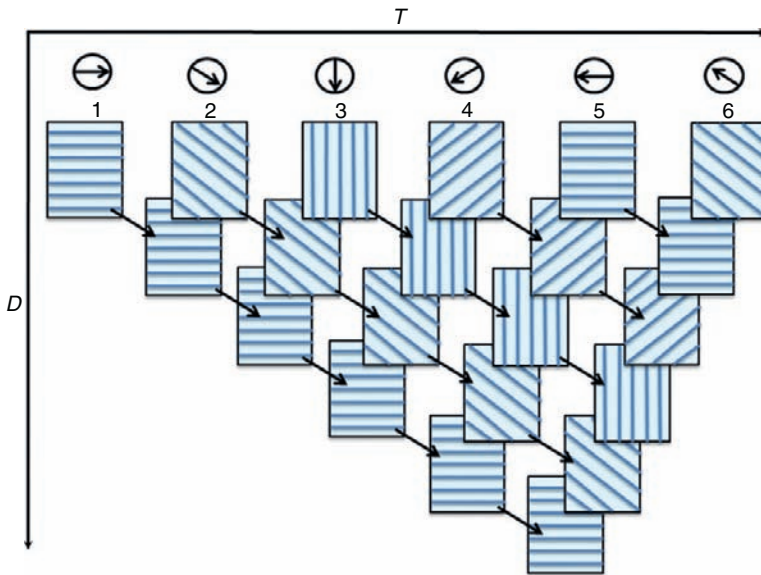


**Figure 7.2** *The ordered fibril or ordered subunit model.* In contrast to the passive realignment model, the OFH recognized that microfibrils are not just deposited at the plasma membrane in transverse alignment but that each new layer rotates in an often rhythmic way. Reading the diagram horizontally, from 1 to 6, each new layer laid at the plasma membrane rotates clockwise with respect to its predecessor. Read vertically, the diagram shows that each lamella retains its birth alignment as it is displaced by newer layers. In this way, a cross section of the wall represents a sedimentary rock record. For example, the horizontal alignment in 1 is preserved when it becomes the sixth layer. Still further away from the plasma membrane, and not represented here, organization was said in this model to become dissipated in the outermost part of the wall.  $T$  = time;  $D$  = distance from the plasma membrane.

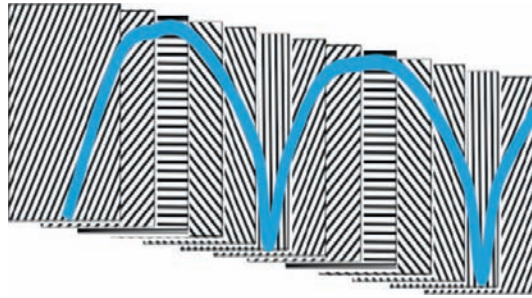


**Figure 7.3** *Bow-shaped arcs.* As envisaged in the ordered fibril model, the alignment of each lamella rotates with respect to its predecessor to form the helicoidal wall. When cross-sectioned and tilted, the differently angled microfibrils from each lamella give the illusion of joining up to form bow-shaped arcs.

However, because of their thinness, these intermediate layers were reportedly difficult to visualize, in which case the major criss-crossing layers adopted the herringbone appearance of the crossed-fibrillar pattern (as defined by Chafe and Wardrop, 1972). The Roland laboratory then extracted components from cell walls to see if they could be made to reproduce *in vitro* the patterns seen in EM sections (Roland et al., 1977). Although regenerated cellulose itself tended to reform in parallel strands, the hemicelluloses formed fairly ordered layers whose orientation changed from layer to layer, not too dissimilar to the rotating pattern seen in the wall. In view of this, they suggested that layer-to-layer shifts in fibrillar alignment could form by purely physicochemical processes within the wall itself, without any directional input from the cytoplasm, that is, microtubules.

### 1.2.3. Origins of self-assembly models for wall texture

In 1976, Neville and his colleagues put forward a new model for cellulose architecture that was based on the cell walls of oospores of the alga, *Chara vulgaris*, but was said to be applicable to higher plant cells (Neville et al., 1976). This “helicoidal” model, which is complementary to that of Roland and Vian (Roland et al., 1975, 1977, 1982), described the progressive shifts in fibrillar alignment, from layer to layer, as being like the steps of a spiral staircase. In such a rotating plywood, the pitch of the helical angle advances in regular steps from transverse through oblique then longitudinal, then onto oblique again but with the opposite helical sign. This was pictured like the moving hands of a clock, where the angle of each new lamella advanced regularly with time (Vian and Roland, 1987). Such regular rotary shifts of alignment from one layer to another are also seen in cholesteric liquid crystals ([http://en.wikipedia.org/wiki/Cholesteric\\_liquid\\_crystal](http://en.wikipedia.org/wiki/Cholesteric_liquid_crystal)).

The structure of insect cuticles (based on chitin, a polymer of *N*-acetylglucosamine embedded in a protein matrix, often calcified) is also



described as helicoidal. Crab shells, which are similarly based on chitin, are also said to have such a rotating arrangement of layers (Neville et al., 1976). Human bone, which is based on the fibrous protein, type 1 collagen, and a crystalline form of a calcium salt, has also been interpreted as having helicoidal layers of collagen fibrils although there is much discussion about this and the precise pattern is quite complex (Ascenzi et al., 2003). The common feature of the ideas of Neville, and of Roland and Vian, was that a liquid crystal-like, self-assembling process was at work in organizing the plant cell wall into helicoids. Historically, these ideas can be seen as a reaction against the strictures of the MGH. Prior to the discovery of microtubule dynamics, it is easy to see why microtubules and their biomechanically predicated transverse hoops were perceived as being too static to account for the more dynamic-seeming gyrations of the cell wall as it moved through non-transverse alignments. It was perhaps inevitable that the role of microtubules was downgraded or even ignored.

---



## 2. MICROTUBULES

### 2.1. Dynamic microtubules

In an attempt to retain the idea of a microtubular template in the face of complex, non-transverse orientations of cellulose, I proposed a dynamic helical model in which cortical microtubules were wrapped around the cell, not in transverse hoops, but in helices of variable pitch that matched the helices of wall microfibrils (Lloyd, 1984). The advantage of the helix is that a flat-pitched transverse helix can be transformed into steeper oblique and longitudinal alignments, that is, in all the orientations displayed by microtubules and microfibrils. The problem was that microtubules were conceived at that time to be like scaffold rods, providing a stiff and static framework. However, our immunofluorescence studies on elongated carrot suspension cells undergoing cellulase treatment showed that the array must be flexible (Lloyd et al., 1980). As these elongated cells were converted to spherical protoplasts, they increased their circumference severalfold yet at all stages an interconnected microtubule network reorganized itself to conform to the changing shape of the cell. The inescapable conclusion was that microtubules must be capable of moving relative to each other and to the plasma membrane to which they were attached.

At that time, the only known mechanism for microtubule movement was the dynein-based sliding of neighboring microtubules observed within the axonemal bundle of cilia and flagella as they waved and so it was speculated that stable microtubules might similarly slide past one another in plant cells to explain the change in helical angle of the dynamic array. This, however, was incorrect for in 1984 our understanding of microtubules

was revolutionized by Mitchison and Kirschner's description of the dynamic instability of animal microtubules (Mitchison and Kirschner, 1984). They saw that microtubules were not static entities but underwent stochastic shifts between periods of steady growth and catastrophic depolymerization. At that time, it was far from obvious that microtubules in non-motile plant cells would share these dynamic features of mobile animal cells. A decade later, Peter Hepler and his colleagues overcame the technical problems of microinjecting fluorescent tubulin across the thick wall of plant cells and showed that plant microtubules also displayed dynamic instability (Hush et al., 1994). In fact, plant microtubules were found to recover from fluorescence photobleaching four times faster than animal microtubules (and later corroborated by Shaw et al., 2003). It may seem paradoxical that immobile plants should have a more dynamic cytoskeleton than fast-migrating animal cells (Lloyd, 1994), but studies on microtubules assembled from isolated plant tubulin show they have a greater intrinsic dynamicity than microtubules made from animal tubulin (Moore et al., 1997).

By microinjecting fluorescent brain tubulin, which incorporates into plant microtubules, we were able to visualize the spontaneous reorientation of microtubules from transverse to longitudinal in pea epidermal cells (Yuan et al., 1994). The process was observed in living cells at intervals of several minutes, from which it was possible to see that the microtubules did not smoothly reorient from one alignment to another as originally conceived by the dynamic helical model, nor did microtubules in one alignment depolymerize while a new set polymerized in the final direction. Instead, the realignment was mediated by patches of what we termed "discordant" microtubules that appeared in the new direction before the array underwent a smoothing process in which microtubules progressively conformed to the new alignment (Lloyd, 1994; Yuan et al., 1994). Groups of discordant microtubules were also seen in living cells to mediate the reverse transition in which gibberellic acid induced longitudinal microtubules to switch to the transverse orientation.

The involvement of new patches of discordant microtubules was also observed in the gravity-induced reorientation of microtubules in maize coleoptiles (Himmelspach et al., 1999). In line with this, discordant microtubules have been seen to mediate reorientation in living *Arabidopsis* root cells expressing a GFP-tagged microtubule protein (Granger and Cyr, 2001).

Dynamic studies therefore provided the temporal dimension missing from the preceding fixation studies and illustrated how changing growth rates—either endogenously triggered or induced by external agents—could induce microtubules to switch between different orientations. Exogenous auxin and gibberellic acid were known to promote the alignment of transverse microtubules beneath the outer epidermal cell wall (Duckett

and Lloyd, 1994; Ishida and Katsumi, 1991, 1992; Mita and Shibaoka, 1984; Takeda and Shibaoka, 1981), while ethylene (Lang et al., 1982; Roberts et al., 1985) and abscisic acid (Ishida and Katsumi, 1992) promoted longitudinal microtubule alignment (Shibaoka, 1994). Takesue and Shibaoka (1998) assimilated this experimentally induced reorientation into a mechanism for the physiological cycling of microtubules between these two extremes. The key features of this oscillatory model were that it recognized the role of hormones in (re)orienting microtubules and accounted for the alternating crossed-fibrillar texture of the outer epidermal cell wall. In this model derived from fixed cells (Takesue and Shibaoka, 1998), the intermediate patches of discordant microtubules previously seen in living cells (Yuan et al., 1994) were suggested to constitute the transitional phases between the transverse and longitudinal alignments.

## 2.2. Global organization emerges out of microtubule–microtubule interaction

The subsequent use of GFP fusion proteins continues to provide a much fuller picture of how microtubules behave in forming a cortical template. By labeling cortical microtubules in *Arabidopsis* epidermal cells with GFP-tubulin, it was possible to conclude that microtubules move by a modified form of treadmilling where the plus end grows faster than the opposite end shrinks (Shaw et al., 2003). Since a photobleached mark on the microtubule stayed in the same position relative to the cell while the microtubule moved away, it appeared that single cortical microtubules were not sliding but using the power of opposite end assembly/disassembly (treadmilling) for translocation. In these studies, microtubules were seen to arise upon the inner surface of the plasma membrane at scattered points termed “sites of apparent microtubule initiation” (Shaw et al., 2003).

Microtubules also arise upon existing microtubules at branch points containing  $\gamma$ -tubulin (Murata et al., 2005). The fact that nascent microtubules branch off mother microtubules at approximately  $45^\circ$  demonstrates that nucleation is not random and implies that the nucleating material is sterically constrained upon the mother microtubule. This hypothesis is supported by studies on  $\gamma$ -tubulin complex proteins. microRNA inhibition of GCP4 expression decreases the angle with which microtubules are nucleated off existing microtubules (Kong et al., 2010). Complementary to this, a partial loss-of-function mutation of *Arabidopsis* GCP2 increases the range of angles at which newly nucleated microtubules diverge from the mother microtubule (Nakamura and Hashimoto, 2009). Using GFP-EB1 to label microtubule comets, it has also been shown that microtubules can branch at a range of angles, both left and right, from sites containing the  $\gamma$ -tubulin-interacting protein, NEDD1 (Chan et al., 2009). Using plus-tip markers such as SPR1 and EB1, which reveal the polarity of the mother

microtubule, this study indicated that outgrowth is biased toward the plus end of the mother microtubule with relatively few newly nucleated microtubules angled backward toward the minus end.

Further, about 40% of the newly nucleated microtubules did not branch but grew along the axis of the mother microtubule. In other words, some microtubules are born prealigned and perpetuate the bundle axis. Microtubule nucleation is therefore polarized and may depend on the steric interaction of  $\gamma$ -tubulin complexes with the microtubule lattice (Chan et al., 2009). In their investigations with fluorescently tagged GCP2 and GCP3, Nakamura and colleagues found that complexes attached to existing microtubules were more likely to nucleate microtubules than complexes located elsewhere (Nakamura et al., 2010). They also reported that microtubules are freed from the nucleation site by the severing activity of katanin, consistent with previous studies showing the transcript level of katanin increases during the reorientation of microtubules induced by hypergravity (Soga et al., 2009). Branching off the mother microtubule provides an explanation for the longer-term interchange between neighboring groups (“domains”) seen in time-lapse movies, showing how microtubule tracks merge and demerge over time (Chan et al., 2007). This view of the nucleation of microtubules from extant microtubules agrees with the prediction that microtubules would branch from nucleation sites to form fractal trees (Wasteneys, 2002). Future studies will undoubtedly address the second part of this model that the nucleating material moves along microtubules by plus-end directed motors.

Order, then, can be implicit in the way that nucleating material binds extant microtubules. Order can also emerge from the way that mobile microtubules interact after this initial nucleation event. An incoming microtubule colliding with another at a shallow angle alters its angle of growth so that the two become coaligned and “zipper-up” (Dixit and Cyr, 2004). Coaligned microtubules may then be susceptible to cross-bridging by the cross-linking protein MAP65 (Chan et al., 1999; Gaillard et al., 2008; Smertenko et al., 2004), although recent evidence suggests that being in a bundle offers no protection against depolymerization (Shaw and Lucas, 2011). At steeper angles, the contacting microtubule has been reported to depolymerize (Dixit and Cyr, 2004), to cross over (Chan et al., 2007; Shaw et al., 2003), or to sever at the crossover point, leading to the depolymerization of the lagging end (Wightman and Turner, 2007). New microtubules also arise at crossover points where they tend to follow one of the paths defined by the crossing microtubules (Chan et al., 2009).

Microtubules treadmill along tracks or bundles (Chan et al., 2007; Dhonukshe et al., 2005; Shaw et al., 2003) and the tendency of these tracks to converge and diverge in one fluid, interconnected network has been seen in long-term movies (over several hours) made from projections of microtubules labeled with AtEB1a-GFP (Chan et al., 2007). In light-grown

epidermal cells of *Arabidopsis* hypocotyls, these tracks could be seen to be sustained beyond the lifetime of individual microtubules both by addition of colliding microtubules and the birth of new microtubules upon the mother microtubule(s) (Chan et al., 2009). There are mechanisms, therefore, that tend to bring microtubules together while the otherwise inevitable convergence into a giant bundle is counteracted by the tendency of a proportion of nascent microtubules and microtubule tracks to branch.

### 2.3. Rotating microtubule arrays explore all orientations

Interestingly, over longer periods than required to see microtubule treadmilling, patches or domains of microtubule tracks could be seen to veer sideways, causing the array to rotate upon the outer cell surface of hypocotyl epidermal cells (Chan et al., 2007; Fig. 7.4). Note that individual microtubules do not rotate but the tracks along which they treadmill do rotate over the longer period. Rotations were followed for one or more complete  $360^\circ$  turns, either in one direction, clockwise or anticlockwise, or they could reverse and go the opposite way (Chan et al., 2007). Illuminated cells, like these under the confocal microscope, do not elongate as rapidly as they do under etiolated conditions (Gendreau et al., 1997) but cells were elongating nonetheless. Rotation stopped as the growth rate declined, the microtubules switching to oblique/longitudinal.

Domains, which creep forward in the direction of the majority of microtubules that pass through them, seem to correspond to the patches of discordant microtubules seen in our earlier microinjection studies (Himmelspach et al., 1999; Lloyd et al., 1996; Yuan et al., 1994). Different domains were seen to move in different directions in different parts of the same cell surface and in places to form collision fronts where movement was temporarily impeded until a new organization was sorted out (Chan et al., 2007). The swirling movement was not inhibited by latrunculin B,

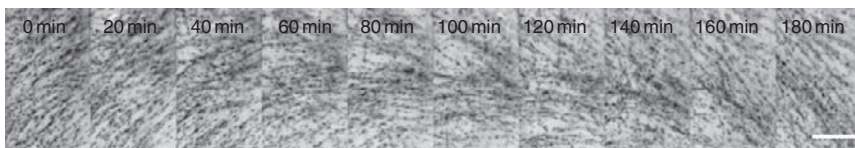


**Figure 7.4** *Rotation of microtubule tracks.* Using *Arabidopsis* seedlings expressing the plus end microtubule marker GFP-EB1, time-lapse movies are made at 20-min intervals as described by Chan et al. (2007). At each interval, the images are projected to show the movement of microtubule tracks over the outer epidermal surface. Over 180 min, the microtubule tracks can be seen to rotate through  $180^\circ$ , from right-hand oblique to left-hand oblique. Microtubule tracks can rotate through  $360^\circ$ , travel clockwise or anticlockwise, and can reverse direction. Scale bar = 10  $\mu\text{m}$ .

indicating that F-actin does not power movement. Neither did the cellulose synthesis inhibitor, 2,6-dichlorobenzonitrile (dichlobenil), prevent microtubule rotation. Instead—and this is a crucial point—rotation was stopped by microtubule-stabilizing taxol. If there were a two-way feedback between microtubule alignment and the self-organizing properties of the wall, it is difficult to see why microtubule rotation did not continue in the still-growing cells in which the cellulose synthases continued to move in linear tracks. This lack of rotation in the presence of taxol strongly suggests that the dynamicity of microtubules drives their rotation rather than feedback from the self-assembling properties of cellulose and its associated wall polymers.

Why do microtubule domains rotate? First, it needs to be said that rotation is only one option. Arrays can oscillate rather than fully rotate or they can hold metastable transverse, oblique, or longitudinal alignments. Rotation might result from a bias in the direction in which microtubules branch off the mother microtubule, adding up over time to a tendency for adjacent, interconnected groups of tracks to veer slowly to one side (Chan et al., 2009). A contributory factor might be the sensitivity of rotation to the particular shape of the cell and/or to the elongation rate, for these light-grown cells are much smaller than cells from etiolated *Arabidopsis* seedlings (Gendreau et al., 1997; Le et al., 2005). Due to the constraints of geometry, it is not possible to wrap parallel lines around the 11-sided (average) irregular polyhedron that is the epidermal cell (Lewis, 1926) without forming discontinuities where the lines stop or cross over, providing an explanation for the collision fronts between different domains of microtubules (Chan et al., 2007).

In previous immunofluorescence studies on elongated *Datura* epidermal cells, microtubules were seen to describe parallel helical arrays around the long axis, postponing the inevitable discontinuities to the radial end walls (Flanders et al., 1989). However, in isodiametric *Datura* epidermal cells, which formed regular hexagons in surface view, microtubules were seen to be arranged in organized parallel groups along the six radial/anticlinal side-walls but when they emerged upon the outer epidermal they overlapped in a criss-cross, discordant fashion (Flanders et al., 1989) suggestive of the collisions seen between domains in living cells (Chan et al., 2007). It is possible, therefore, that rotation is promoted by the competition between mobile domains that is more apparent in cells that are not highly elongated. In other words, a component of the rotary process could be due to dynamic microtubules trying to find the best fit according to shape and growth rate. However, such behavior is unlikely to be entirely autonomous but varied according to physiological conditions and the rate of expansion driven by hormonal signals. It has been known for some time that exogenous hormones shift the alignment of microtubules: these include ethylene (Roberts et al., 1985; Shibaoka, 1994), auxin (Shibaoka, 1994), gibberellic acid

(Duckett and Lloyd, 1994; Lloyd et al., 1996), abscisic acid (Shibaoka, 1994), and jasmonic acid (Shibaoka, 1994). From such experiments, hormonal flux was previously suggested to coordinate endogenous cycles of microtubule reorientation (Lloyd, 1994; Mayumi and Shibaoka, 1996; Takesue and Shibaoka, 1998). This can now be reinterpreted according to current ideas on microtubule dynamics where changing concentrations of hormones can, via MAPs and/or nucleation sites, modulate the behavior of microtubules and, thereby, the kinds of array that emerge from microtubule–microtubule interaction.

## 2.4. Microtubules do not always form circumferential hoops

In discussing the concept of microtubule alignment, we almost always refer to the orientation of microtubules at the outer epidermal wall of either roots or shoots, as this is the most accessible surface, yet microtubule alignment appears to be different in roots and shoots. In addition, a variety of observations on different tissues under different conditions tend to be reduced to the one-size-fits-all textbook view that microtubules form transverse, circumferential, hoop-like arrays in elongating cells. However, microtubule orientation can be distinctly different, even on different surfaces of the same cell (Busby and Gunning, 1983; Flanders et al., 1989; Hejnowicz et al., 2000; Ishida and Katsumi, 1992; Yuan et al., 1995). In particular, these papers show that microtubules can be transverse down the radial/anticlinal wall and inner periclinal epidermal walls yet—as shown by 3D reconstruction of confocal sections (Flanders et al., 1989; Yuan et al., 1995)—continuous with differently aligned tubules on the external periclinal wall. The epidermal cell is an irregular polygon with an average of 10 internal faces pressing against neighboring cells with the one external face, which is unfaceted by contact, tending to bulge outward. Microtubules do not therefore form simple hoops around these irregular bodies so that transverse microtubules on one face need not necessarily be matched by coaligned microtubules on the other faces of the same cell.

## 2.5. Do microtubules behave differently in roots and shoots?

The paradigmatic organ for microtubule alignment is probably the root where development is blocked out in zones from the apical meristem back: zone of division, zone of elongation, and zone of differentiation. In *Arabidopsis* roots, microtubules are generally transverse in the zone of elongation (Baskin et al., 1999; Granger and Cyr, 2001; Liang et al., 1996; Sugimoto et al., 2000) before reorienting toward oblique and longitudinal as the growth rate declines. Granger and Cyr (2001) inspected living *Arabidopsis* roots specifically for the kind of transverse-to-longitudinal-and-back-again reorientation that Mayumi and Shibaoka (1996) had deduced from fixed

images to occur in azuki bean shoot epidermal cells but they were not able to see this kind of cyclic reorientation (which represents oscillation rather than rotation).

The absence of microtubule rotation and the presence of an apparently more predictable realignment as microtubules adopt transverse, oblique, and longitudinal alignments, in that order, as they transit through a well-defined zone of elongation (Liang et al., 1996), seems to make roots quite different to shoots. But, rotation apart, is this really the case? There are several studies on *Arabidopsis* root epidermal cells that suggest the linkage between microtubule alignment and growth rate is not as tight as generally conceived. Tobias Baskin and colleagues, for instance, noted that reorientation of microtubules from transverse to oblique occurred *after* the rate of elongation had already undergone a significant decline (Baskin et al., 1999). Also, according to the Wasteney's laboratory, microtubules in *Arabidopsis* root epidermal cells are only transverse in the first part of the elongation zone (Sugimoto et al., 2000). Transverse orientations have been reported to occur over a range of rates, demonstrating that the exact angle of microtubules is not so tightly tied to growth (Granger and Cyr, 2001).

By comparison with this somewhat more relaxed standard for microtubule alignment in the root, the *Arabidopsis* shoot may not be that different. In the dark, the hypocotyl grows 10 times longer than in the light, so it is important to differentiate between the illuminated and the etiolated hypocotyl (Gendreau et al., 1997). Under etiolated conditions, elongation starts at the base and passes up the axis to a small region beneath the hook. In the dark, transverse microtubules have been found in elongating cells, switching to longitudinal when growth stops (Le et al., 2005). In the light, however, the elongation zone appears to become delocalized (Gendreau et al., 1997) and under these conditions, transverse, oblique, and longitudinal arrays occur simultaneously across the tissue (Buschmann et al., 2004; Chan et al., 2007; Le et al., 2005). The general correlation of transverse alignment with more rapid elongation may not therefore be so different in roots and in shoots—at least in the dark. In the light, however, the growth rate is suppressed and the elongation zone dispersed, making it difficult to compare the dark-grown root with the light-grown hypocotyl. These factors probably explain why nontransverse microtubule alignments have been reported with such frequency in stem epidermal cells (Buschmann et al., 2004; Chan et al., 2007; Duckett and Lloyd, 1994; Flanders et al., 1989; Furutani et al., 2000; Hejnowicz et al., 2000; Ishida and Katsumi, 1992; Ishida et al., 2007; Le et al., 2005; Lloyd et al., 1996; Mayumi and Shibaoka, 1996; Paolillo, 2000; Sawano et al., 2000; Takesue and Shibaoka, 1998; Yuan et al., 1994, 1995; Zandomeni and Schopfer, 1993). To take one example, Sawano et al. (2000) reported seeing equal proportions of transverse, oblique, or longitudinal arrays in epidermal cells of growing azuki bean epicotyls, with transverse arrays becoming scarce when the growth rate declined. [A caveat from



live-cell studies is that what may appear in fixed cells to be a mixture of alignments (Hejnowicz, 2005) can be seen in living cells to be stages of the rotary process (Chan et al., 2007)].

A key difference between roots and shoots is their response to illumination and some of the variation between different studies might be attributable to the experimental lighting conditions. This is well illustrated by a study on maize hypocotyl cells where blue light induced within 10 min a realignment to longitudinal while red light induced microtubules to change to transverse (Zandomeni and Schopfer, 1993). This effect of blue light illumination has been exploited to trigger transverse microtubules in *Arabidopsis* hypocotyl epidermal cells to switch to longitudinal, demonstrating that cellulose synthase trajectories follow microtubule realignment (Paredes et al., 2006).

Some images of epidermal cells show fields of uniformly transverse microtubules in *Arabidopsis* hypocotyls grown under etiolated conditions (Ehrhardt and Shaw, 2006). While we have reported seeing fields of cells containing uncoordinated microtubule alignments in light-grown *Arabidopsis* hypocotyls (Chan et al., 2007), we have also observed coordinated areas of nonrotating transverse arrays (Chan et al., 2010). This shows that zones of coordinated transverse alignment can, in particular circumstances, exist in the light.

### 3. THE PARADOXICAL OUTER EPIDERMAL WALL

One school of thought suggests that variable microtubule alignment on the outer wall of the shoot epidermis derives from the very uniqueness of this surface—the only one without an external neighbor. The idea that the circumferential patchwork of outer epidermal walls joins up to form an “organ wall” analogous to the tubular wall of giant algal cells used in pioneering studies (Green, 1960) may be overly simple, for instead of the directionality of growth being controlled by the outermost surface, it has been argued that this role is fulfilled by the hydrostatically inflated inner core tissues of stems (Baskin, 2005; Peters and Tomos, 2000). Bergfeld et al. (1988) suggested that the inner tissues exhibit transverse hoop reinforcement and dictate growth anisotropy, while the outer epidermal wall has an isotropic organization that resists expansion without affecting the direction of growth (Baskin, 2005; Schopfer, 2006). Baskin, 2005 referred to this as “the paradoxical behavior of the stem epidermis.” Stem segments from which the epidermis has been peeled expand while the peeled epidermis itself contracts (Kutschera et al., 1987; Schopfer, 2006). This demonstrates that the outer layer, which is under higher longitudinal tension, compresses the turgid, expanding inner tissues. Schopfer (2006) suggested that it is

generally the inner tissues of elongating organs that best demonstrate hoop reinforcement (and growth anisotropy), while the outer epidermal wall with its isotropically deposited wall layers “provides the major resistance to expansion without affecting the directions of growth” (see also Baskin, 2005). Stress from the inner tissues is transmitted outward, radially, until it meets the last surface without external neighbors—the outer epidermal wall. Consistent with a special biophysical role, this bulging outer epidermal wall is thicker than the other walls of the same cell and contains up to half of the total cell-wall material of the hypocotyl (Derbyshire et al., 2007; Kutschera, 2001). From their work on sunflower hypocotyl epidermal cells, Hejnowicz’s group argues that these differences in tissue stresses explain, “. . . *the mysterious differences in orientation of CMTs (cortical microtubules) underlying different walls in the same epidermal cell*” (Hejnowicz et al., 2000).

These authors further suggested that the variability of microtubule orientation reflects an underlying cyclic reorientation that is preserved in the helicoidal structure of the wall (Hejnowicz et al., 2000). This instability in microtubule alignment was suggested to be due to an oscillation between the maximal longitudinal tensile stress of the unpeeled epidermis, which has to be relaxed to allow elongation, and the maximal transverse stress of the individual turgid cell. (This offers another possible explanation for microtubule reorientation/rotation.) In such an oscillatory cycle (Mayumi and Shibaoka, 1996; Takesue and Shibaoka, 1998), microtubules would reorient from transverse to longitudinal and then follow the same journey in reverse. But later, from his studies on fixed cells, Hejnowicz perceptively suggested that the changing angle of microtubules beneath the outer epidermal wall of sunflower hypocotyls was part of a continuous rotary cycle that moves in a defined clockwise or anticlockwise direction to explore all alignments around the clock, passing through both helical signs (Hejnowicz, 2005). This author stated that only the rotational cycle has a defined chirality by rotating either clockwise or anticlockwise. As described in Section 4, the chirality of the cortical microtubule array appears to be important in helical mutants that contain left-hand or right-hand oblique alignments, which accompany organ twisting in the contrary direction (Buschmann et al., 2004; Furutani et al., 2000; Ishida et al., 2007). However, it is not easy to understand how the chirality of microtubule rotation relates to the direction of twisted growth since both clockwise and anticlockwise rotations pass through left-handed and right-handed helical alignments, cancelling each other out. Regardless of the direction of travel, the result of rotation is essentially isotropic. Some bias in alignment (e.g., rotation “sticking” at some positions of the clock face) seems to be necessary if the direction of organ twisting is to be regulated by a rotary cycle. By contrast, a more limited 90° oscillatory cycle, flipping back and forth between transverse and longitudinal, only passes through one oblique alignment: either left-handed S-helical or right-handed Z-helical, but not both.

The idea of microtubule alignment being sensitive to a growth-based cycle is attractive. However, microtubules in fixed sunflower epidermal cells are reported to have different alignments in neighboring cells and even in different parts of the same cell (Burian and Hejnowicz, 2010; Hejnowicz et al., 2000). This has also been seen in living *Arabidopsis* hypocotyls where microtubule tracks rotate at different speeds, clockwise or anticlockwise, in adjacent cells (Chan et al., 2007). Such cell-to-cell variation could be due to genuine asynchrony or to the presence of uncoordinated “downtimes” between bouts of more rapid synchronized growth—a problem compounded by the possible delocalization of the growth zone in aerial parts. It is possible that even applied force may not be sufficient to make microtubules respond in a coordinated manner across the tissue. In their study on the *Arabidopsis* shoot apex where meristems were pinched between Teflon blades, Hamant et al. (2008) showed that although microtubules became aligned parallel to the maximal stress direction, the response was noisy, as neighboring cells had microtubules with radically different orientations. In roots, too, microtubule alignment varies considerably in adjacent cells (Sugimoto et al., 2000) and helices of opposite helical sign have been seen in the same zone of root cells (Baskin et al., 1999). If microtubule alignment is being coordinated by forces expressed at a tissue level, we have to ask why such forces do not impose a higher degree of coordination across fields of outer epidermal walls in the shoot epidermis. This returns us to the explanation that coordinated transverse alignment might only occur in a brief window when the elongation rate is maximal, as reported for the root (Granger and Cyr, 2001; Sugimoto et al., 2000).

To summarize, there are indications that microtubule alignment on the domed outer epidermal wall may not be so strictly aligned as appears to be the case for roots, although strictness of alignment may be confined to phases of rapid elongation. The situation is complicated by the fact that the zone of elongation is not so clearly demarcated in aerial organs and may be delocalized in the light. In future, it will be crucial to measure microtubule alignment in individual cells whose growth rate is being actively monitored.

#### 4. MICROTUBULE ALIGNMENT AND TWISTED GROWTH

Having just discussed cell-to-cell variation in microtubule orientation, it is important to note that tissues exhibiting helical growth appear to provide counterexamples where clear tendencies for net alignment do emerge out of what at first sight seems like a noisy process. In such tissues, the cells are not stacked vertically upon each other but twist around the axis like stripes on a barber’s pole. In addition to hypocotyl twisting, the helical phenotype encompasses root bending, rosette twisting, and chiral bending of trichome

branches. All can be traced in many helical mutants to a modification of a microtubule-associated protein or to just a single amino acid modification of a tubulin isoform (see below), providing one of the strongest causative links between cell morphology and the microtubule cytoskeleton.

In the *Arabidopsis spiral* mutant, *spr1*, the root twists to the right but microtubules form contrary, left-handed oblique helices (Furutani et al., 2000). Conversely, suppressor mutants, *lefty1* and *lefty2*, twist in the opposite direction, to the left and cortical microtubules beneath the outer epidermal walls of roots form right-handed oblique helices (Thitamadee et al., 2002). The fact that organs twist in the opposite direction to the microtubules on the outer epidermal wall seems counterintuitive. This has been explained on the basis that expansion is perpendicular to the microtubule/microfibril axis (Furutani et al., 2000). Hence, growth that is  $90^\circ$  to a  $+45^\circ$  helix should result in  $-45^\circ$  growth, that is, reverses the helical sign. Another explanation is that as certain springs are stretched, fixed marks on the surface can unwind in the opposite direction (Roelofsen, 1950). Applying this principle to cell walls with helically wound cellulose microfibrils, cell elongation may cause the organ to twist in the opposite direction (Buschmann et al., 2009; Lloyd and Chan, 2002).

The interesting thing about helical growth mutants is that some derive from single amino acid substitutions in tubulins (Buschmann et al., 2009; Ishida et al., 2007; Sunohara et al., 2009; Thitamadee et al., 2002) or from modifications to microtubule-associated proteins (Buschmann et al., 2004; Sedbrook et al., 2004; Shoji et al., 2004; Whittington et al., 2001). SPIRAL1 is now known to be a small protein associated with the plus tips of microtubules (Nakajima et al., 2006; Sedbrook et al., 2004). SPIRAL2 (*SPR2*), which is allelic to *TORTIFOLIA1* (*TOR1*) (Buschmann et al., 2004; Furutani et al., 2000; Shoji et al., 2004), also codes for a MAP that reportedly accumulates at plus ends (Yao et al., 2008). In addition to these microtubule mutants, similar twisting phenotypes can be expressed when microtubules are either stabilized with taxol or destabilized with antimicrotubule propyzamide (Furutani et al., 2000; Hashimoto, 2002; Thitamadee et al., 2002; Wasteneys and Williamson, 1989).

In these twisted mutants, the obliquity of the microtubules is not absolute, for while wild-type arrays have been generally summarized as “transverse” and mutant arrays “oblique,” there appears to be a fair degree of variation about the mean. Careful measurement of microtubule alignment in hypocotyl epidermal cells from the microtubule-associated protein mutant, *tor1/spr2*, illustrated this variability (Buschmann et al., 2004). Seven days after germination in soil, wild-type seedlings contained microtubules with a large bimodal distribution of angles within which were two peaks, representing left- and right-handed helices. In *tor1/spr2*, by contrast, the right-handed helices—although still present—were heavily suppressed in favor of a more prominent set of values around the left-handed

oblique mean. In a study on *spr2*, a broad range of angles, from transverse to oblique, was measured in agar-grown wild-type hypocotyls and in the mutant the average angle shifted to the left (Yao et al., 2008). So although microtubules may not be strictly and coordinately aligned in the wild-type hypocotyl, the net alignment is not so random that it cannot be shifted in a reproducible manner by mutations that affect microtubule dynamics.

## 5. MICROTUBULE AND MICROFIBRIL COALIGNMENT

### 5.1. Which orientates which?

Throughout the history of microtubule research, there has been uncertainty, not only about whether microtubules can really be responsible for the full variety of microfibril alignments, but also about the possibility of there being some form of feedback from the self-assembling wall upon microtubule alignment (Cyr, 1994). In promoting a self-assembly mechanism, Neville and Levy wrote that if a microtubule-based model, “. . . *was responsible for building a multi-turn helicoid, it would seem to involve an improbably large number of alternating depolymerizations and repolymerizations of fields of microtubules, each time they change direction*” (Neville and Levy, 1984). But it is now known that this is exactly what microtubules do: they undergo a large and entirely probable number of excursions between growth and shrinkage as they treadmill (Shaw et al., 2003) along tracks that can veer sideways, rotate clockwise, anticlockwise, reverse direction, and undergo discontinuous jumps (Chan et al., 2007). Now it is also known that cellulose synthases are inserted alongside microtubules and track along them (Crowell et al., 2009; Gutierrez et al., 2009; Paredez et al., 2006), extruding cellulose microfibrils as they go.

However, the idea that wall organization is entirely self-derived still has currency (Diotallevi et al., 2010). One conjecture is that the self-organization of hemicelluloses drives microtubule rotation rather than the other way around (Hejnowicz et al., 2000). Mulder and Emons’ geometrical model for wall architecture dispenses with the requirement for microtubules and suggests that the direction in which cellulose-synthesizing particles move is governed by their density in conjunction with their interaction with stiff cellulose microfibrils plus associated matrix materials, and the geometry of the cell (Mulder and Emons, 2001). This is a more refined version of an earlier conclusion by Vian and Roland whose own self-assembly model underlined the importance of “*events occurring in the periplasm, the space between the plasmalemma and the cell wall, where the secreted molecules are forced to re-orientate, to graft and to change their conformation*” (Vian and Roland, 1987).

The protoplast is not an autonomous unit; it is physically constrained by the wall it secretes and it would be surprising if there were no feedback from the wall to the cellulose-synthesizing machinery. However, this is a long way from saying that the global organization of the cytoskeleton is controlled by the self-organizing tendencies of wall polymers and particle rosettes.

Several experiments demonstrate that microtubules do influence wall texture. Investigations from the Shibaoka laboratory found that the normal crossed-polylamellate texture of the outer wall of azuki bean epidermal cells was perturbed by addition of antimicrotubule colchicine (Takeda and Shibaoka, 1981). The drug caused a thick band of wall to be deposited, containing lamellae that did not rotate as they would normally have done. A similar result was reported by Vian et al. (1982) who added colchicine to depolymerize microtubules or ethylene to reorient them to the longitudinal axis. In both cases, the helicoidal progression in wall lamellation did not continue unabated—as might be expected from their self-assembly model in which microtubules play no part—but was strongly retarded. The effects of colchicine were also tested on the texture of the epidermal wall of maize coleoptiles where the typical multilayered structure of the wall was found to be exchanged for a thick, essentially monotonous inner wall layer (Satiat-Jeunemaitre, 1984). All three studies indicate that the preexisting wall pattern is not sufficient to entrain the rhythmic layering of the wall in the absence of microtubules even though thickening indicates that fibrils are still being laid down in the wall.

These results might be contested on the basis that removal of microtubules has unintended consequences for vesicle production and targeting such that delivery of wall materials essential for self-assembly is compromised in the absence of microtubules. This is unlikely to apply to the effect of ethylene, which is to reorient rather than to depolymerize microtubules (Roberts et al., 1985). Also, in our own recent study on wall texture (Chan et al., 2010), the stabilization of microtubules with taxol produced the same outcome as the removal of microtubules with oryzalin. CESA3 tracks rotate around the outer epidermal wall (Fig. 7.5), as had been previously shown for microtubule tracks (Chan et al., 2007). Although taxol caused the microtubule tracks to stop rotating, particles containing GFP-CESA3 were still delivered to the plasma membrane where they moved along lines with the same velocity as in controls. Cellulose microfibrils were therefore still being deposited under taxol treatment except that in the absence of microtubule rotation, the thick inner layer had a monotonous texture. This strongly suggests that rhythmic changes of wall texture depend far more on the mobility of microtubules than on the self-assembling properties of wall components.

It is difficult to see how the rapid self-organization/crystallization of wall matrix polymers observed *in vitro* (Roland et al., 1977) provides a realistic model for the time-consuming, layer-by-layer accretion of the living cell wall, where cellulose synthase-containing vesicles are lined up for insertion

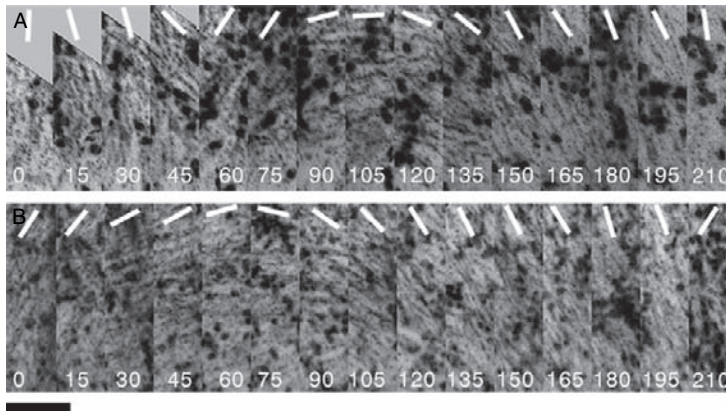


**Figure 7.5** *Rotation of cellulose synthase tracks.* In *Arabidopsis* seedlings expressing GFP-CESA3, cellulose synthase tracks rotate through  $180^\circ$ . The dotted gray lines are the synthase tracks; the darker spots are Golgi bodies. Reprinted from Chan et al. (2010). Scale bar =  $15\ \mu\text{m}$ .

into the plasma membrane by microtubules (Crowell et al., 2009; Gutierrez et al., 2009) that provide tracks for movement of synthases along the plasma membrane (Paredez et al., 2006).

The mechanism for constructing the plant cell wall has also been analogized to the self-assembly of cholesteric liquid crystals believed to explain the self-organization of other extracellular matrices in animals and lower plants (Neville et al., 1976). But the extracellular matrices of plants and animals are different in significant ways. The major fibril of animal matrices—the protein collagen—is secreted in the form of procollagen that is then assembled in the extracellular space. By contrast, the major load-bearing fibrils of the plant cell wall—the carbohydrate cellulose—are extruded from plasma membrane-embedded sites in contact with a cytoskeleton that determines the initial direction of travel. In experiments to investigate the relative contributions of wall and cytoskeleton to the directionality of microtubule tracks, Chan et al. (2007) inhibited cellulose biosynthesis with dichlobenil. This failed to stop microtubule rotation, suggesting that the ability of microtubules to undergo dramatic realignments is independent of the act of cellulose biosynthesis and, it follows, of feedback from the preceding wall layer(s).

## 5.2. The relationship of cellulose synthases with microtubules

Recent observations on living cells show that cellulose-synthesizing particles (labeled with YFP-CESA6) move along microtubules (labeled with CFP-tubulin; Paredez et al., 2006); that synthases are inserted into the plasma membrane where Golgi vesicles pause (Crowell et al., 2009); and that these

sites of insertion coincide with underlying microtubules (Crowell et al., 2009; Gutierrez et al., 2009). This underlines the importance of microtubules during the aligned insertion of mobile synthases and their travel along the plasma membrane. Consistent with this, when microtubules were induced to reorient from transverse to longitudinal by exposure to blue light, the assembly of new microtubule tracks was seen to precede the appearance of synthesizing particles in the new alignment (Paredes et al., 2006). In wild-type *Arabidopsis* plants, CESA particles move at similar speeds on either side of a microtubule. Site-directed mutagenesis of CESA1 phosphorylation sites caused antiparallel particles to move at different speeds but this asymmetry was removed by depolymerizing microtubules with oryzalin (Chen et al., 2010). Mutation resulted in cell swelling, which was explained in terms of changes to the structural nature of the cellulose polymer. This and the foregoing studies demonstrate that changes to microtubules, or to the microtubule-tracking movement of cellulose synthase particles, have a direct impact upon the wall and directional cell expansion.

The requirement for CESA particles to move along microtubules is not, however, absolute since particles continue to translocate for a short while along the original trajectory after spontaneous depolymerization of the coaligned microtubule(s) (Paredes et al., 2006). It is possible that once complexes are aligned and set in motion the rigidity of the crystalline microfibril is sufficient to maintain the original trajectory. A limited degree of self-organization of the synthases was also found after a 7.6-h treatment with oryzalin caused a “near-complete” loss of cortical microtubules. In this case, the synthase particles moved along parallel tracks set at an oblique angle to the cell axis (Emons et al., 2007; Paredes et al., 2006). It therefore appears that in the presence of antimicrotubule drug (and it needs to be verified that the residual microtubule fragments have no influence; Gardiner et al., 2003), the cellulose-synthesizing particles are arranged into a fixed oblique alignment. Although this could mean that particles have a limited capacity for self-organization, there is no evidence that CESA tracks can rotate and build up a rhythmically changing polylamellate wall texture without these cytoskeletal elements.

### 5.3. Evidence from growth mutants

Counterarguments against the idea that microtubules help regulate cell shape by regulating cellulose alignment have come from studies on radial swelling mutants. In the temperature-sensitive *Arabidopsis* mutants *radially swollen 4* and *radially swollen 7*, it was initially reported that cellulose microfibrils and microtubules were not disoriented despite the swollen phenotype (Wiedemeier et al., 2002). The conclusion was that cell anisotropy does not depend on the involvement of microtubules but depends on the self-ordering of microfibrils. However, this conclusion was revoked by



studies from the Baskin laboratory showing that *rsw7*, which produces a defect in a kinesin-5 motor protein, does result in microtubule disorganization (Bannigan et al., 2007). Similarly, *rsw4*—a mutant of a chromatid separase—was also found to have a disruptive effect on the cortical array (Wu et al., 2010). That is, radial swelling does appear to be linked to microtubule disorganization.

Microtubules are also disorganized in the temperature-sensitive *Arabidopsis* mutant, *mor1-1*, which produces radially swollen cells at the restrictive temperature (Whittington et al., 2001). MOR1 is a 215-kDa microtubule-associated protein whose mutation causes the shortening of microtubules, resulting in a less well-organized cortical array (Twel et al., 2002; Whittington et al., 2001). Despite the cytoskeletal perturbation, cellulose microfibrils still appeared to be well organized and perpendicular to the root axis and so it was concluded that cellulose microfibrils “*largely self-align in the absence of functional cortical microtubules*” (Sugimoto et al., 2003). Rather than dismiss a role for microtubules in cellulose synthesis, Wasteneys used these observations to hypothesize that microtubules regulate the length of co-aligned microfibrils (Wasteneys, 2004). According to this model, disorganization (and presumably shortening) of microtubules would lead to short and/or weak cellulose chains. Although such microfibrils may still be transversely oriented, they would be less able to resist isotropic separation of adjacent microfibrils and therefore tend to swell. Hence, alignment is not everything; the duration and quality of the interaction of the cellulose-synthesizing machinery with the microtubule may be crucial. General support for this idea comes from studies on the phospho-mutagenesis of CESA1 (Chen et al., 2010) in which asymmetry of particle velocity either side of a microtubule resulted in cell swelling—an effect ascribed to differences in the length of oppositely oriented cellulose microfibrils.

Twisted mutants provide another strong argument that microtubules are essential for regulating the direction of growth and, by implication, the organization of the wall. Several laboratories have screened for helical growth phenotypes and the overwhelming majority of resulting loci point toward an underlying defect in microtubule proteins rather than the cell wall (Buschmann et al., 2004, 2009; Perrin et al., 2007; Sedbrook et al., 2004). There are examples of helical mutants that differ from wild type by only a single amino acid in one of the tubulins. By examining several dozen tubulin mutants, Ishida et al. (2007) showed that there was a strong correlation between the primary sequence of  $\alpha$  or  $\beta$  tubulins, whether the cortical arrays were left- or right-handed helices, and the direction of helical growth. Single amino acid changes in the tubulin lattice therefore have a magnified effect on organ growth. If tissue stresses or wall self-assembly were feeding back on microtubules to cause their (re)alignment, it would be difficult to understand why mutant microtubules should respond any differently since they are electron microscopically indistinguishable from

wild-type microtubules, containing 13 protofilaments. A reasonable explanation is that the alignment of microtubules, and hence the direction of growth, is influenced by the structure of the microtubule lattice and the stereospecificity of its interactors.

Another argument against microtubule alignment being governed by wall—in this case, bands of secondary cell wall—comes from work on cellulose synthase mutants in *Arabidopsis* xylem cells (Gardiner et al., 2003) and this is described in Section 5.4.

#### 5.4. Non-elongating secondary cell walls provide clear examples of microtubule/cellulose co-alignment

The very dynamicity of cortical microtubules during primary wall growth combined with the complexity of wall lamellation patterns has meant that interpretation of the effects of microtubules on microfibrils is not straightforward, especially when different techniques have been used to visualize the two elements in separately prepared samples subject to separate experimental artifacts. By contrast, differentiated cells can form characteristic ornamentations of the secondary wall that, undistorted by cell elongation, have a more readily decipherable connection with the underlying microtubules. For example, in tension wood (layers of wall deposited in response to tension stress), highly oriented cellulose microfibrils are laid down in sequence in an S1 layer in a flat helix, an S2 layer with an oblique helix, and a longitudinal gelatinous layer. The alignment of microtubules corresponds with the microfibrils except where the microtubules reorient in advance of the next wall layer (Fujita et al., 1974).

Probably, the best example of the tight relationship between dynamic microtubules and the secondary cell wall is seen during the differentiation of xylem tracheary elements. These cells undergo programmed cell death and form the hollow tubes that conduct sap from root to shoot. Just before the cell dies, the cortical microtubules aggregate into thick bundles. Normally, the cortical microtubules of elongating cells are numerous and evenly distributed over the cortex but in tracheary elements, the heavily bundled microtubules form a limited number of bands in fixed patterns that provide a template for the overlying secondary wall. The great advantage of this bunching of wall and cytoskeleton is that the overall pattern formed by both elements can be seen within the same cell at low magnification (Fig. 7.6), side-stepping much of the ambiguity associated with microtubules and their templated microfibrils in the primary wall. In the protoxylem, which forms early on in primary meristems, the bands of microtubules and secondary wall are spiral or annular. Later on, and in secondary meristems, the microtubules and wall thickenings describe reticulate or pitted patterns in metaxylem. This close relationship between microtubules and the sculptured secondary cell wall was first seen in the EM (Hepler and Newcomb, 1964),

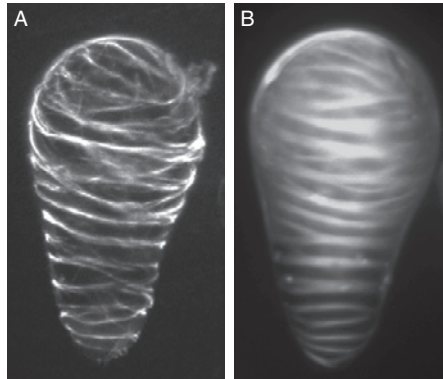


**Figure 7.6** Microtubules provide the template for secondary thickening in tracheary elements. In an *Arabidopsis* suspension cell triggered to form a tracheary element, the microtubules, labeled by GFP-tubulin, bunch up to form a “spiral” array (A). In (B), the same cell stained with the cellulose-binding dye Calcofluor White shows that the secondary wall conforms to the pattern of underlying microtubules. Courtesy of Edouard Pesquet.

but pioneering immunofluorescence studies on *Zinnia* mesophyll cells (Falconer and Seagull, 1985a), which could be induced to transdifferentiate into tracheary elements *in vitro*, demonstrated the vital relationship between microtubule dynamics and the final pattern of secondary thickening. When microtubule-stabilizing taxol was added, the microtubule bundles were fixed in abnormal longitudinal patterns making a 1:1 match with the atypical ribs of secondary wall (Falconer and Seagull, 1985b). Microtubules have also been shown to match xylem wall patterns *in planta*. In differentiating conifer tracheids, the microfibrils were concluded to rotate in a clockwise fashion from a flat left-handed, to a steep right-handed, back to a flat left-handed helix and microtubules were found in complementary patterns (Abe et al., 1995).

Apart from the fact that different trios of CESA isoforms are used in primary versus secondary growth, the fundamental process of cellulose deposition appears generically similar and it seems likely that lessons learned from one can be applied to the other. In the protoxylem of living *Arabidopsis* roots, all three species of CESA protein are required for the proper localization of cellulose-synthesizing particles with microtubules (Gardiner et al., 2003). When microtubules were depolymerized, the CESA particles that had initially colocalized with the microtubule bundles lost their tightly banded distribution. This indicates that the continual presence of microtubules is essential for maintaining CESA organization. Interestingly, in CESA mutants *irx3-1* and *irx5-1*, the microtubules bundled normally despite the fact that cellulose-synthesizing complexes failed to form, with a consequent shutdown of cellulose biosynthesis. As these authors

concluded, this illustrates that microtubules can self-organize in the absence of the cellulose-synthesizing machinery, arguing against its involvement in a hypothetical feedback loop from the wall (see Section 5.3).

Our own work on tracheary elements induced in an *Arabidopsis* cell suspension underlines the role of microtubule-associated proteins in patterning the secondary cell wall (Pesquet et al., 2010). Upon induction, the xylem-specific MAP, AtMAP70-5, was the only one among more than 200 microtubule-interacting proteins to be specifically upregulated when tracheary elements form (Pesquet et al., 2010). AtMAP70-5 is concentrated along the edges of the microtubule bands that underlie xylem thickenings. AtMAP70-5 also decorates microtubules that form curved “spacers” between adjacent thickenings. When expression of this protein, or of its binding partner AtMAP70-1, was reduced by RNAi, ribs of secondary wall surrounded by cortical microtubules detached from the primary wall and were displaced into the cell’s interior. The level of protein expression also affects the overall kind of wall patterning. Spiral thickenings, typical of protoxylem, tend to have clearly delineated thickenings with well-defined spaces between. In pitted thickenings, typical of metaxylem, the bands are broader and fused, leaving only small eyelets or pits. Overexpression of either of these MAPs resulted in an increase in the proportion of spiral thickenings in culture and a decrease in pitted thickenings. By contrast, RNAi caused an increase in pitted and a decrease in spiral thickenings. *In planta*, gene silencing of AtMAP70-5 caused a halving in the number of vascular bundles and a reduction in stem height (Pesquet et al., 2010).

Related to this, a newly discovered MAP has been shown to regulate pit formation in induced *Arabidopsis* tracheary elements (Oda et al., 2010). The microtubule depletion domain 1 (MIDD1) protein anchors to the plasma membrane where it encourages localized depolymerization of microtubules and formation of pits. RNA interference of this MAP caused formation of secondary walls without pits. Microtubule bundles, and the “negative” space between microtubule bundles, are therefore carefully regulated during xylem differentiation.

MAP65 is known to form regularly spaced cross-links between co-aligned microtubules *in vitro* (Chan et al., 1999). Transient overexpression of *Zinnia elegans* ZeMAP65-1 in uninduced *Arabidopsis* suspension cells was found to cause the evenly distributed cortical microtubules to aggregate into thick bundles, phenocopying the bundles seen in differentiated xylem cells (Mao et al., 2006).

Yet another example of the relationship between microtubule proteins and the wall with plant morphology is provided by interfascicular fibers—highly elongated fibrous cells that increase the mechanical strength of the growth axis. As the mutant’s name suggests, the inflorescence stem of *fragile fiber 2* plants is more fragile and this has been attributed to shorter cells with thinner walls (Burk et al., 2001). FRA2 is a katanin, which is a protein that

severs microtubules. In *fra2* plants, cortical microtubules were disorganized, cellulose microfibrils were also disorganized, and the thickness of primary and secondary cell walls was decreased (Burk and Ye, 2002). As with the spiral mutants, these studies on katanin illustrate that fundamental aspects of plant morphology appear to be governed by microtubules and their associated proteins via their effects on the cell wall. Collectively, the case for microtubules having a controlling role in the overall patterning of cellulose and other polymers in secondary cell walls is overwhelming.

## 6. (RE)INTERPRETING WALL PATTERNS

Before combining ideas on wall lamellation with what is now known about the dynamic microtubule template, it is worth briefly recapping the various descriptions of wall patterns.

### 6.1. Steps between wall layers

Alternating layers of cellulose microfibrils have been variously described as forming a herringbone, cross-ply, or crossed-polylamellate wall pattern, where successive lamellae criss-cross, that is, overlap at  $90^\circ$ . Chafe and Chauret (1974) proposed that “crossed-polylamellate” be used to describe the structure of plant cell walls in general. Such a structure implies steep crossing angles (around  $90^\circ$ ) between lamellae that could mean alternation either between  $+45^\circ$  and  $-45^\circ$  helices or between near-transverse flat helices (ca  $0^\circ$ ) and near-longitudinal alignments (ca  $90^\circ$ ; Chafe and Wardrop, 1972). Such patterns, if interpreted correctly, imply that nascent microfibrils are laid at a distinctly different angle (and perhaps even helical sign) to the preceding layer. However, there is evidence that in some walls the lamellae cross at less disparate angles. For example, Itoh’s (1975) freeze-fracture study on *Morus* parenchyma cells concluded that lamellae cross at angles between  $90^\circ$  and  $40^\circ$ .

Atomic force microscopy studies on maize parenchymal cells indicate that microfibrils in one layer rotate approximately  $50^\circ$  to the next (Ding and Himmel, 2006). The smaller the change of angle, the smoother the rotation through the thickness of the wall. Helicoidal progression implies steps less than  $90^\circ$  between successive lamellae, but it is worth remembering that the texture of the prototypical mung bean hypocotyl wall was at one time described as an “acute herringbone” (Reis et al., 1982), that is, undergoing radically alternating changes between left- and right-hand oblique helices, rather than smoother, more progressive changes of angle. This may be because the transitional strata that are necessary to make a more progressive rotating pattern were reportedly difficult to see in section because of their

thinness (Roland et al., 1977). In the collenchyma of *Apium*, microfibrils were seen to alternate between longitudinal and transverse but freeze-fracture revealed lamellae of transitional alignment of  $50^\circ$  to the long axis (Wardrop et al., 1979). Further, these freeze-fracture images showed transverse fibrils appearing to curve toward the more longitudinal alignment, suggestive of reorientation during the course of elongation.

The way the pattern is described may also depend upon the angle in which the section is cut (Vian et al., 1982). Indeed, the intermediately angled fibrils that have the appearance of separating longitudinal from transverse elements in the helicoidal wall are seen to best advantage by cutting the shoot, not transversely, but at  $45^\circ$ , as this provides a wider section that “opens up” the thickness of the wall. As these data show, even apparently quite different wall textures may be the expressions of the same twisted system (Vian et al., 1982).

Although there may be a common rotary mechanism underlying a wide spectrum of wall patterns, it is important to establish whether the angular progression between lamellae is small and may therefore give rise to smooth arcing patterns in transverse section, or occurs in larger jumps, giving rise to more discontinuous sectional patterns. This information will be pivotal in deciding the extent to which the contribution of microtubules to cellulose alignment is subsequently readjusted in the life history of the microfibril beyond the microtubule (see Section 7).

## 6.2. Beyond microtubules: Post-cytoplasmic changes to wall texture

In considering how microtubule patterns relate to wall patterns, a further layer of complexity is added by the fact that the microtubule-influenced alignment of cellulose microfibrils might be changed either naturally, as the cell continues to expand, or artifactually during processing for microscopy.

### 6.2.1. Experimental changes to wall texture

Sections swell when hemicelluloses and pectins are extracted from the matrix with alkali (Reis et al., 1982). In our hands, the methylamine extraction step that precedes silver proteinate (PATAg) staining increases cell-wall thickness in sunflower hypocotyls by 35% (Buschmann and Lloyd, unpublished). In addition, in removing noncrystalline wall components, the extraction procedures used for transmission EM may cause the residual fibers to aggregate. From high-resolution atomic force microscopy studies of nonextracted samples, it has been proposed that the 36-polymer “elementary microfibril”—the product of a single cellulose-synthesizing complex—hydrogen bonds with other simultaneously formed elementary microfibrils to generate a macrofibril that splits to form parallel microfibrils that later become coated with other matrix polymers (Ding and Himmel,

2006). These investigators suggested that the “treated microfibril” seen in extraction studies may not be the same as the actual elementary fibril. As they concluded, “*To characterize the native cell wall structure, traditional extraction processes must be eliminated to minimize possible cell wall modifications during sample preparation.*”

An area for concern about the PATAg method for enhancing the contrast of the polysaccharide fibril is that patterns obtained when the film of silver proteinate dries have been considered to be an artifact that may not faithfully reflect the organization of underlying fibrils (Wardrop et al., 1979). For these reasons, freeze fracture might be expected to provide a more authentic record of the change in alignment between layers but such studies have been rare. One such study on mung bean (Satiat-Jeunemaitre et al., 1992), which was the tissue used for the Roland group’s studies on the helicoidal wall (Reis et al., 1982; Roland et al., 1975, 1977, 1982, 1992; Vian et al., 1982), reported seeing the “three main directions,” implying jumps of ca 45° that separate transverse, oblique, and longitudinal alignments. The bow-shaped arcs drawn onto images of transverse sections of PATAg-stained walls (e.g., Fig. 11 in Roland et al., 1982) may therefore be implying a smoother, more continuous rotation than actually exists.

In passing, this freeze-fracture study (Satiat-Jeunemaitre et al., 1992) shows microfibrils fanning-out over about 45°. Provided the fracture plane represents a single lamella, this angular dispersion is rather different from the strict linear parallelism that is usually conceived. Such variation of cellulose alignment within a lamella suggests that cross sectioning should reveal different patterns in different parts of the wall. Consistent with this, whorls or eddies have been reported when even the apparently well-organized inner wall layers of mung bean are sectioned (Roland et al., 1992). In other words, lamellation does not proceed uniformly along the length of the cell but displays local turbulence. Such turbulence might now be reinterpreted as resulting from domains of microtubules that move in different directions in different parts of the same cell surface (Chan et al., 2007).

### 6.2.2. Growth-induced changes to wall texture

Another problem in back-extrapolating the perceived organization of the wall to the organization of microtubules is that layers of microfibrils may not necessarily remain in their birth alignment once they become distanced from the plasma membrane by younger microfibrils. Indeed, the basis of the multinet growth/passive realignment hypothesis (Preston, 1982; Roelofs, 1958; Roelofs and Houwink, 1951, 1953) was that microfibrils would become reoriented by cell expansion as the wall layer readjusted to accommodate increasing cell size. The ordered fibril or ordered subunit hypothesis (Roland et al., 1982; Vian and Roland, 1987; Vian et al., 1982), however, is based on the assumption that the wall represents a sedimentary “rock

record” that faithfully preserves the original alignment of each layer as deposited upon the plasma membrane (until, at least, it becomes “dissipated” in the outermost wall layers).

The difficulty in deciding between these opposing ideas is that there has been no dynamic method for following possible changes in microfibril alignment. However, promising studies on *Arabidopsis* roots with a cellulose-binding dye, Pontamine Fast Scarlet 4B, have shown that it is feasible to follow dynamic changes in the wall of living epidermal cells (Anderson et al., 2009). In this investigation, the relatively large confocal  $z$ -steps used to optically section the wall encompass several layers of wall rather than single lamellae; nonetheless, through-focusing shows that in elongating cells, the fibrillar angle changes from transverse in the inner layers to longitudinal in the outer layers. In living cells, the fibrillar angle within one focal plane could also be seen to rotate toward the longitudinal angle over a 20-min period of observation. This suggests that the passive realignment aspect of the MGH may be correct, although, as much of the foregoing discussion indicates, any successful model should also account for the deposition of nontransverse microfibrils upon the plasma membrane and not just for their realignment to that angle at some distance from the plasma membrane. Because they saw no reorientation of the innermost microfibrils when segments of expansin-treated cucumber hypocotyls were placed under 20–30% extension strain, Marga et al. (2005) suggested that cell walls extend by creep rather than passive realignment. Such a mechanism might not, however, be incompatible with the passive realignment model provided it is only the older layers that become reoriented.

With all of these complexities in mind, the paper by Roland’s group provides a good example of the various problems in interpreting wall lamellation patterns in sections (Roland et al., 1982). In that study, the organization of wall was investigated along the growth gradient of the mung bean hypocotyl. In order to address the “unavoidable swelling” of walls caused by chemical extractions, they used unextracted tissue to measure the thickness of wall at various levels. With conventional heavy metal staining the wall in section presented only a simple layered texture, said to be based on the alternation of “polysaccharides” between transverse and longitudinal alignments. Inspection of their Fig. 7.5, however, indicates these alternating light and dark layers to be thicker than can be explained by criss-crossing layers one microfibril thick. When sections were extracted either with DMSO or methylamine prior to staining with silver proteinate, details of organization were said to become revealed.

At the apex of the hook, this alternating pattern started to give way to a bow-shaped pattern indicating the appearance of alignments intermediate to the orthogonal transverse and longitudinal layers. This kind of bow-shaped ordering was, however, confined to only that quarter of the



hypocotyl's length where extension was maximal. Order was also confined to the inner part of the wall abutting the cytoplasm since order in the outer layers became more dissipated as extension proceeded. Others have also seen that the wall is initially thick but then thins during a phase of rapid elongation, as if the young shoot lays down a store of wall in readiness for fast expansion (Derbyshire et al., 2007; Refregier et al., 2004). In fact, in dark-grown *Arabidopsis* hypocotyls, only the first slow phase of growth when a thick polylamellate wall is deposited is sensitive to the cellulose synthesis inhibitor isoxaben, in contrast to the insensitivity of the rapid growth phase when the wall is thinned (Refregier et al., 2004). According to one paper, it is this thinning during expansion that degrades order in the outer part of the wall, leaving the regular bow-shaped arcs in the inner part untouched (Roland et al., 1982). One wonders, though, whether the inner layers really are entirely immune from the forces of expansion and whether some of that inner patterning could not have been readjusted during rapid elongation. The fact that bow-shaped arcs become more apparent after extraction of matrix materials causes the sectioned organ to expand—the reverse of what happens *in vivo*—might suggest some portion of the newly revealed order to be experimentally induced.

### 6.2.3. Reconciling the ordered fibril and passive realignment models

In considering the possible realignment of cellulose microfibrils, Sargent proposed a mechanism to reconcile the crossed-fibrillar with the orderly helical view of lamellation (Fig. 7.7A and B; Sargent, 1978). She found that the outer epidermal wall of barley was not helicoidal in the strict sense of Neville et al. (1976) but more resembled the crossed-fibrillar texture advocated by Chafe and Wardrop (1972), with the exception that intermediately aligned fibrils could be seen between the alternating transverse and longitudinal fibrils. Finding that these intermediate oblique fibrils did not undergo the illusory reversal when sections were tilted, which is a characteristic of helicoids, she suggested this texture was “derived from secondary reorientation of initially perpendicular fibrils in response to extension strain.” Sargent (1978) hypothesized that microfibrils are deposited in orderly helical angles as in the helicoidal model (Vian and Roland, 1987) but are then passively realigned as in the MGH (Roelofsen and Houwink, 1951) toward transverse or longitudinal, depending on which of these two crossed-extension vectors is dominant. In this way, nascent fibrils deposited in intermediate angles would be readjusted toward whichever of the two orthogonal strains was the greater local attractor but transverse and longitudinal fibrils already oriented along one of these strain vectors would not be realigned (Fig. 7.7C and D).

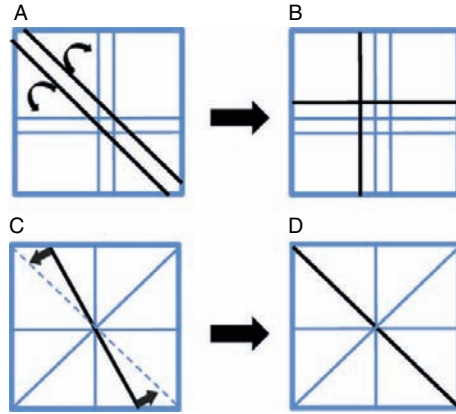


**Figure 7.7** *Realignment of microfibrils after deposition.* Sargent (1978) tried to reconcile the multinet/passive realignment (see Fig. 7.1) and the ordered fibril hypotheses (see Fig. 7.2) by introducing crossed-extension vectors to a basically helicoidal mechanism. Microfibrils were conceived as being initially deposited in an orderly rotary fashion but then realigned toward the transverse or longitudinal extension vectors. This is illustrated in (A–B) where microfibrils deposited obliquely during the rotary cycle are subsequently realigned toward one of the two major axes to produce a simplified, alternating lamellation pattern. However, microfibrils have often been seen in intermediate alignments that might be more stable than the transient forms envisaged by Sargent. (C–D) illustrate how a microfibril laid in an intermediate alignment may be reoriented by passive realignment toward the oblique, producing smoother rotating steps between wall layers.

## 7. A NEW DYNAMIC MODEL FOR THE INFLUENCE OF MICROTUBULES ON THE TEXTURE OF PLANT CELL WALLS

The strength of Sargent's model was that it addressed both the observed nontransverseness of some inner wall layers and the subsequent readjustment of fibril alignment suggested by several studies (Sargent, 1978). Her model did not encompass microtubules but a new model can be proposed that accommodates dynamic changes both to the cytoplasmic template in laying down the microfibril and to the microfibril after it has been deposited. A downside of the Sargent model was that in supporting the crossed-fibrillar view of lamellation it assumed microfibrils are subsequently realigned toward just two main vectors: transverse and longitudinal. Yet if we consider organization from the microtubular perspective, a large amount of subsequent research has shown that oblique microtubules occur in cell populations as frequently as do transverse and longitudinal microtubules and are therefore unlikely to be unstable intermediates (Buschmann et al., 2004;

Duckett and Lloyd, 1994; Takeda and Shibaoka, 1981). Certainly, in the case of helical mutants, the oblique microtubule array can even be the most highly represented form (Buschmann et al., 2004; Furutani et al., 2000; Thitamadee et al., 2002). Although she did not investigate oblique or any kind of microtubule(s), Sargent (1978) did see oblique microfibrils but explained these away as being “dynamically derived” intermediates caught in the process of realignment. However, freeze fracture (Itoh, 1975; Satiat-Jeunemaitre et al., 1992; Wardrop et al., 1979) and atomic force microscopy (Ding and Himmel, 2006) studies suggest that oblique microfibrils may occur more commonly in the wall than Sargent thought and are therefore not easily dismissed as transient forms. If passive realignment does readjust microfibrils, then it may rectify microfibrils that are deposited with an initially nonorthogonal alignment, not just to the transverse or longitudinal, but to the oblique saddle between them, or indeed to any other energetically favorable alignment (Fig. 7.7 C and D).

Thin sectioning is best at reading fibrils parallel to the plane of section and far less good at determining the alignment of cross-sectioned fibrils in all other orientations and, as described above, it has been difficult to determine the exact rhythm of wall deposition without experimental distortion. Determining alignment is especially difficult for thinly populated lamellae of the kind we might expect to be influenced by a rapidly moving cytoplasmic template. Improved methods will be needed to establish whether successive lamellae are laid down in small increments or in steps separated by tens of degrees. But, regardless of the extent to which the birth alignment of microfibrils may be readjusted in the growing cell wall, the ability of microtubule tracks to rotate smoothly around the clock demonstrates they form a versatile template capable of aligning cellulose synthase tracks in all possible orientations (Chan et al., 2010; Fig. 7.4).

Based on a synthesis of the preceding discussion, I propose a new microtubule-based realignment model in which microtubules exert a major influence upon the alignment of nascent cellulose microfibrils and recognizes that this alignment can continue to be adjusted throughout growth. The basis of the model is that the global organization of the array depends heavily upon the dynamicity of the microtubules and the ways that they can interact. The main force for microtubule reorientation is provided by the polymerization and depolymerization of microtubules combined with nucleation. The microtubule machine is not, however, autonomous: it is responsive, integrating a variety of signals that influence its ability to self-organize. Organization of the array will be affected by changes to the microtubule lattice, microtubule nucleation sites, MAPs, as well as growth regulators that initiate signaling cascades for which these proteins are targets. Changes initiated by photo- and gravi-perception will alter the nucleation, stability, interaction, and alignment of microtubules. By guiding the cellulose synthesizing rosette’s direction of travel, the changeable microtubule

template will have a major initial influence over the gross alignment of nascent cellulose microfibrils. That is not the only influence for the model recognizes the role that expansion plays in the continuing evolution of wall architecture. Upon extrusion, the nascent microfibril will physically and molecularly integrate with other molecules in that part of the wall immediately adjacent to the plasma membrane. Such local “bedding-in” interactions with other wall molecules (e.g., other microfibrils, xyloglucans, and pectin) may cause nascent microfibrils to deviate, to an extent, from the path followed by its synthesizing rosette. Biophysical forces might also rectify alignment of microfibrils within a lamella toward the dominant operating vector. However, since microtubules are seen here as having a primary role in determining the rhythm of wall deposition, any local inertia offered by the preexisting wall organization will be overridden by accumulating shifts in microtubule orientation that advance the lamellation pattern. Explicitly, it is the larger shifts in microtubule alignment (both discontinuous “jumps” and more continuous rotations/reorientations) that orchestrate the larger changes in lamellation angle and switches in helical sign. Over the longer term, this supralamellar pattern will continue to evolve beyond the microtubule as the cell elongates and the wall changes to accommodate this. In this case, secondary factors (e.g., biophysical forces of expansion in conjunction with wall-loosening agents; Pelletier et al., 2010) will continue to remodel the texture of the elongating cell’s wall that was first rough-mapped by microtubule alignment.



## 8. CONCLUDING REMARKS

One of the next challenges will be to determine how microtubules self-organize to form particular patterns, not just within the cell in isolation but within the larger developmental context. The fact that helical mutant phenotypes are based on subtle changes in microtubule-related proteins does seem to imply that the particular pattern adopted by the array is an emergent property of microtubule interactions, though how this can favor left- or right-handed helices is not yet known. If the answer does not lie with the chiral properties of the tubulin lattice itself, and this has to be determined, then it may depend upon the steric interaction of the assembling microtubule with other molecules (e.g., microtubule nucleating factors and MAPs) that might bias microtubule branching to one side or another. A further unknown is how light, gravity, and hormones feed into microtubule organization to generate arrays of a particular orientation, for this is the way that plants steer their growth relative to directional cues from the environment. Not only do hormones initiate signaling cascades that can modify microtubules and their associated proteins, but they also

provide spatial information (in terms of tissue specificity and apical/basal flux) from which microtubules can take compass readings. The nonexpanding end walls perpendicular to the apical/basal axis are self-evidently different from the elongating side walls; this is reflected in the polarized distribution of actin-binding proteins (Reichelt et al., 1999) and this may turn out to be the case for microtubule proteins making elongation-promoting arrays. Biophysical stresses are also inherently associated with cell shape and directional expansion. There is evidence that such forces might be important in aligning microtubules (Hamant et al., 2008) and more work is needed in this important area. Another major gap in our knowledge is what happens to microfibrils once they are displaced from the plasma membrane by newer layers. Of the three components of the transmembrane machinery, it is now possible to obtain dynamic images for the microtubules and the membrane-bound synthase complexes, but it is to the dynamic properties of the third element—the wall—that we must now pay attention if we are to understand how microfibril alignment evolves beyond the microtubular phase.

## ACKNOWLEDGMENTS

I would like to thank my colleagues Ming Yuan and Jordi Chan for the insights provided by their work on microtubule reorientation and microtubule rotation, respectively. I am grateful to Edouard Pesquet for supplying figure 7.6. I also thank Henrik Buschmann for careful reading of the chapter and his incisive comments. I am grateful to the BBSRC for the project grants that supported original work cited in this chapter.

## REFERENCES

- Abe, H., Funada, R., Imaizumi, H., Ohtani, J., Fukazawa, K., 1995. Dynamic changes in the arrangement of cortical microtubules in conifer tracheids during differentiation. *Planta* 197, 418–421.
- Anderson, C.T., Carroll, A., Akhmetova, L., Somerville, C., 2009. Real-time imaging of cellulose reorientation during cell wall expansion in *Arabidopsis* roots. *Plant Physiol.* 152, 787–796.
- Ascenzi, M.G., Ascenzi, A., Benvenuti, A., Burghammer, M., Panzavolta, S., Bigi, A., 2003. Structural differences between “dark” and “bright” isolated human osteonic lamellae. *J. Struct. Biol.* 141, 22–33.
- Bannigan, A., Scheible, W.R., Lukowitz, W., Fagerstrom, C., Wadsworth, P., Somerville, C., et al., 2007. A conserved role for kinesin-5 in plant mitosis. *J. Cell Sci.* 120, 2819–2827.
- Baskin, T.I., 2005. Anisotropic expansion of the plant cell wall. *Annu. Rev. Cell Dev. Biol.* 21, 203–222.
- Baskin, T.I., Meekes, H.T., Liang, B.M., Sharp, R.E., 1999. Regulation of growth anisotropy in well-watered and water-stressed maize roots. II. Role of cortical microtubules cellulose microfibrils. *Plant Physiol.* 119, 681–692.

- Bergfeld, R., Speth, V., Schpfer, P., 1988. Reorientation of microfibrils and microtubules at the outer epidermal wall of maize coleoptiles during auxin-mediated growth. *Bot. Acta* 101, 57–67.
- Burian, A., Hejnowicz, Z., 2010. Strain rate does not affect cortical microtubule orientation in the isolated epidermis of sunflower hypocotyls. *Plant Biol. Stuttg.* 12, 459–468.
- Burk, D.H., Ye, Z.H., 2002. Alteration of oriented deposition of cellulose microfibrils by mutation of a katanin-like microtubule-severing protein. *Plant Cell* 14, 2145–2160.
- Burk, D.H., Liu, B., Zhong, R., Morrison, W.H., Ye, Z.H., 2001. A katanin-like protein regulates normal cell wall biosynthesis and cell elongation. *Plant Cell* 13, 807–827.
- Busby, C.H., Gunning, B.E.S., 1983. Orientation of microtubules against transverse cell walls in roots of *Azolla pinnata* R. Br. *Protoplasma* 116, 78–85.
- Buschmann, H., Fabri, C.O., Hauptmann, M., Hutzler, P., Laux, T., Lloyd, C.W., et al., 2004. Helical growth of the *Arabidopsis* mutant *tortifolia1* reveals a plant-specific microtubule-associated protein. *Curr. Biol.* 14, 1515–1521.
- Buschmann, H., Hauptmann, M., Niessing, D., Lloyd, C.W., Schaffner, A.R., 2009. Helical growth of the *Arabidopsis* mutant *tortifolia2* does not depend on cell division patterns but involves handed twisting of isolated cells. *Plant Cell* 21, 2090–2106.
- Chafe, S.C., Chauret, G., 1974. Cell wall structure in the xylem parenchyma of trembling aspen. *Protoplasma* 80, 129–147.
- Chafe, S.C., Doohan, M.E., 1972. Observations on the ultrastructure of the thickened sieve cell wall in *Pinus strobus* L. *Protoplasma* 75, 67–78.
- Chafe, S.C., Wardrop, A.B., 1972. Fine structural observations on the epidermis. I. The epidermal cell wall. *Planta* 107, 269–278.
- Chan, J., Jensen, C.G., Jensen, L.C., Bush, M., Lloyd, C.W., 1999. The 65-kDa carrot microtubule-associated protein forms regularly arranged filamentous cross-bridges between microtubules. *Proc. Natl. Acad. Sci. USA* 96, 14931–14936.
- Chan, J., Calder, G., Fox, S., Lloyd, C., 2007. Cortical microtubule arrays undergo rotary movements in *Arabidopsis* hypocotyl epidermal cells. *Nat. Cell Biol.* 9, 171–175.
- Chan, J., Sambade, A., Calder, G., Lloyd, C., 2009. *Arabidopsis* cortical microtubules are initiated along, as well as branching from, existing microtubules. *Plant Cell* 21, 2298–2306.
- Chan, J., Crowell, E., Eder, M., Calder, G., Bunnewell, S., Findlay, K., et al., 2010. The rotation of cellulose synthase trajectories is microtubule-dependent and influences the texture of epidermal cell walls in *Arabidopsis* hypocotyls. *J. Cell Sci.* 123, 3490–3495.
- Chen, S., Ehrhardt, D.W., Somerville, C.R., 2010. Mutations of cellulose synthase (CESA1) phosphorylation sites modulate anisotropic cell expansion and bidirectional mobility of cellulose synthase. *Proc. Natl. Acad. Sci. USA* 107, 17188–17193.
- Crowell, E.F., Bischoff, V., Desprez, T., Rolland, A., Stierhof, Y.D., Schumacher, K., et al., 2009. Pausing of Golgi bodies on microtubules regulates secretion of cellulose synthase complexes in *Arabidopsis*. *Plant Cell* 21, 1141–1154.
- Cyr, R.J., 1994. Microtubules in plant morphogenesis: role of the cortical array. *Annu. Rev. Cell Biol.* 10, 153–180.
- Derbyshire, P., Findlay, K., McCann, M.C., Roberts, K., 2007. Cell elongation in *Arabidopsis* hypocotyls involves dynamic changes in cell wall thickness. *J. Exp. Bot.* 58, 2079–2089.
- Dhonukshe, P., Mathur, J., Hulskamp, M., Gadella Jr., T.W., 2005. Microtubule plus-ends reveal essential links between intracellular polarization and localized modulation of endocytosis during division-plane establishment in plant cells. *BMC Biol.* 3, 11.
- Ding, S.Y., Himmel, M.E., 2006. The maize primary cell wall microfibril: a new model derived from direct visualization. *J. Agric. Food Chem.* 54, 597–606.
- Diotallevi, F., Mulder, B.M., Grasman, J., 2010. On the robustness of the geometrical model for cell wall deposition. *Bull. Math. Biol.* 72, 869–895.

- Dixit, R., Cyr, R., 2004. Encounters between dynamic cortical microtubules promote ordering of the cortical array through angle-dependent modifications of microtubule behavior. *Plant Cell* 16, 3274–3284.
- Duckett, C.M., Lloyd, C.W., 1994. Gibberellic acid-induced microtubule reorientation in dwarf peas is accompanied by rapid modification of an  $\alpha$ -tubulin isotype. *Plant J.* 5, 363–372.
- Ehrhardt, D.W., Shaw, S.L., 2006. Microtubule dynamics and organization in the plant cortical array. *Annu. Rev. Plant Biol.* 57, 859–875.
- Emons, A.M.C., Hofte, H., Mulder, B., 2007. Microtubules and cellulose microfibrils: how intimate is their relationship? *Trends Plant Sci.* 12, 279–281.
- Falconer, M.M., Seagull, R.W., 1985a. Immunofluorescent and calofluor white staining of developing tracheary elements in *Zinnia elegans* L. suspension cultures. *Protoplasma* 125, 190–198.
- Falconer, M.M., Seagull, R.W., 1985b. Xylogenesis in tissue culture: taxol effects on microtubule reorientation and lateral association in differentiating cells. *Protoplasma* 128, 157–166.
- Flanders, D.J., Rawlins, D.J., Shaw, P.J., Lloyd, C.W., 1989. Computer-aided 3-D reconstruction of interphase microtubules in epidermal cells of *Datura stramonium* reveals principles of array assembly. *Development* 106, 531–541.
- Frei, E., Preston, R.D., 1961. Cell wall organization and wall growth in the filamentous green algae *Cladophora* and *Chaetomorpha*. II. Spiral structure and spiral growth. *Proc. Roy. Soc. Lond. B* 155, 55–77.
- Fujita, M., Saiki, H., Harada, H., 1974. Electron microscopy of microtubules and cellulose microfibrils in secondary wall formation of poplar tension wood fibers. *Mokuzai Gakkaishi* 20, 147–156.
- Furutani, I., Watanabe, Y., Prieto, R., Masukawa, M., Suzuki, K., Naoi, K., et al., 2000. The SPIRAL genes are required for directional control of cell elongation in *Arabidopsis thaliana*. *Development* 127, 4443–4453.
- Gaillard, J., Neumann, E., Van Damme, D., Stoppin-Mellet, V., Ebel, C., Barbier, E., et al., 2008. Two microtubule-associated proteins of *Arabidopsis* MAP65s promote antiparallel microtubule bundling. *Mol. Biol. Cell* 19, 4534–4544.
- Gardiner, J.C., Taylor, N.G., Turner, S.R., 2003. Control of cellulose synthase complex localization in developing xylem. *Plant Cell* 15, 1740–1748.
- Gendreau, E., Traas, J., Desnos, T., Grandjean, O., Caboche, M., Hofte, H., 1997. Cellular basis of hypocotyl growth in *Arabidopsis thaliana*. *Plant Physiol.* 114, 295–305.
- Granger, C.L., Cyr, R.J., 2001. Spatiotemporal relationships between growth and microtubule orientation as revealed in living root cells of *Arabidopsis thaliana* transformed with green-fluorescent-protein gene construct GFP-MBD. *Protoplasma* 216, 201–214.
- Green, P.B., 1960. Multinet growth of the cell wall of *Nitella*. *J. Biophys. Biochem. Cytol.* 7, 289–296.
- Green, P.B., 1962. Mechanism for plant cellular morphogenesis. *Science* 138, 1404–1405.
- Gutierrez, R., Lindeboom, J.J., Paredez, A.R., Emons, A.M., Ehrhardt, D.W., 2009. *Arabidopsis* cortical microtubules position cellulose synthase delivery to the plasma membrane and interact with cellulose synthase trafficking compartments. *Nat. Cell Biol.* 11, 797–806.
- Hamant, O., Heisler, M.G., Jonsson, H., Krupinski, P., Uyttewaal, M., Bokov, P., et al., 2008. Developmental patterning by mechanical signals in *Arabidopsis*. *Science* 322, 1650–1655.
- Hashimoto, T., 2002. Molecular genetic analysis of left–right handedness in plants. *Philos. Trans. R. Soc. Lond. B* 357, 799–808.
- Heath, I.B., 1974. A unified hypothesis for the role of membrane bound enzyme complexes and microtubules in plant cell wall synthesis. *J. Theor. Biol.* 48, 445–449.

- Hejnowicz, Z., 2005. Autonomous changes in the orientation of cortical microtubules underlying the helicoidal cell wall of the sunflower hypocotyl epidermis: spatial variation translated into temporal changes. *Protoplasma* 225, 243–256.
- Hejnowicz, Z., Rusin, A., Rusin, T., 2000. Tensile tissue stress affects the orientation of cortical microtubules in the epidermis of sunflower hypocotyl. *J. Plant Growth Regul.* 19, 31–44.
- Hepler, P.K., Newcomb, E.H., 1964. Microtubules and microfibrils in the cytoplasm of coleus cells undergoing secondary wall deposition. *J. Cell Biol.* 20, 529–532.
- Himmelspach, R., Wymer, C.L., Lloyd, C.W., Nick, P., 1999. Gravity-induced reorientation of cortical microtubules observed in vivo. *Plant J.* 18, 449–453.
- Hush, J.M., Wadsworth, P., Callaham, D.A., Hepler, P.K., 1994. Quantification of microtubule dynamics in living plant cells using fluorescence redistribution after photobleaching. *J. Cell Sci.* 107 (Pt. 4), 775–784.
- Ishida, K., Katsumi, M., 1991. Immunofluorescence microscopical observation of cortical microtubule arrangement by gibberellin in  $d_5$  mutant of *Zea mays* L. *Plant Cell Physiol.* 32, 409–417.
- Ishida, K., Katsumi, M., 1992. Effects of gibberellin and abscisic acid on the cortical microtubule orientation in hypocotyl cells of light-grown cucumber seedlings. *Int. J. Plant Sci.* 153, 155–163.
- Ishida, T., Thitamadee, S., Hashimoto, T., 2007. Twisted growth and organization of cortical microtubules. *J. Plant Res.* 120, 61–70.
- Itoh, T., 1975. Cell wall organization of cortical parenchyma of angiosperms observed by the freeze etching technique. *Bot. Mag. Tokyo* 88, 145–156.
- Itoh, T., Shimaji, K., 1976. Orientation of microfibrils and microtubules in cortical parenchyma cells of poplar during elongation growth. *Bot. Mag. Tokyo* 89, 291–308.
- Kong, Z., Hotta, T., Lee, Y.R., Horio, T., Liu, B., 2010. The  $\gamma$ -tubulin complex protein GCP4 is required for organizing functional microtubule arrays in *Arabidopsis thaliana*. *Plant Cell* 22, 191–204.
- Kutschera, U., 2001. Stem elongation and cell wall proteins in flowering plants. *Plant Biol.* 3, 466–480.
- Kutschera, U., Bergfeld, R., Schopfer, P., 1987. Cooperation of epidermis and inner tissues in auxin-mediated growth of maize coleoptiles. *Planta* 170, 168–180.
- Lang, J.M., Eisinger, W.R., Green, P.B., 1982. Effects of ethylene on the orientation of microfibrils of pea epicotyl cells with polylamellate cell walls. *Protoplasma* 110, 5–14.
- Le, J., Vandenbussche, F., De Cnodder, T., Van der Straten, D., Verbelen, J.-P., 2005. Cell elongation and microtubule behavior in the *Arabidopsis* hypocotyl: responses to ethylene and auxin. *J. Plant Growth Regul.* 24, 166–178.
- Ledbetter, M.C., Porter, K.R., 1963. A “microtubule” in plant cell fine structure. *J. Cell Biol.* 19, 239–250.
- Lewis, F.T., 1926. The effect of cell division on the shape and size of hexagonal cells. *Anat. Rec.* 33, 331–355.
- Liang, B.M., Dennings, A.M., Sharp, R.E., Baskin, T.I., 1996. Consistent handedness of microtubule helical arrays in maize and *Arabidopsis* primary roots. *Protoplasma* 190, 8–15.
- Lloyd, C.W., 1984. Toward a dynamic helical model for the influence of microtubules on wall patterns in plants. *Int. Rev. Cytol.* 86, 1–51.
- Lloyd, C., 1994. Why should stationary plant cells have such dynamic microtubules? *Mol. Biol. Cell* 5, 1277–1280.
- Lloyd, C., Chan, J., 2002. Helical microtubule arrays and spiral growth. *Plant Cell* 14, 2319–2324.
- Lloyd, C.W., Slabas, A.R., Powell, A.J., Lowe, S.B., 1980. Microtubules, protoplasts and plant cell shape. *Planta* 147, 500–506.



- Lloyd, C.W., Shaw, P.J., Warn, R.M., Yuan, M., 1996. Gibberellic-acid-induced reorientation of cortical microtubules in living plant cells. *J. Microsc.* 181, 140–144.
- Mao, G., Buschmann, H., Doonan, J.H., Lloyd, C.W., 2006. The role of MAP65-1 in microtubule bundling during *Zinnia* tracheary element formation. *J. Cell Sci.* 119, 753–758.
- Marga, F., Grandbois, M., Cosgrove, D.J., Baskin, T.I., 2005. Cell wall extension results in the coordinate separation of parallel microfibrils: evidence from scanning electron microscopy and atomic force microscopy. *Plant J.* 43, 181–190.
- Mayumi, K., Shibaoka, H., 1996. The cyclic reorientation of cortical microtubules on walls with crossed polylamellate structure: effects of plant hormones and an inhibitor of protein kinases on the progression of the cell cycle. *Plant Cell Physiol.* 36, 173–181.
- Mita, T., Shibaoka, H., 1984. Gibberellin stabilizes microtubules in onion leaf sheath cells. *Protoplasma* 119, 100–109.
- Mitchison, T., Kirschner, M., 1984. Dynamic instability of microtubule growth. *Nature* 312, 237–242.
- Moore, R.C., Zhang, M., Cassimeris, L., Cyr, R.J., 1997. In vitro assembled plant microtubules exhibit a high state of dynamic instability. *Cell Motil. Cytoskeleton* 38, 278–286.
- Mulder, B.M., Emons, A.M., 2001. A dynamical model for plant cell wall architecture formation. *J. Math. Biol.* 42, 261–289.
- Murata, T., Sonobe, S., Baskin, T.I., Hyodo, S., Hasezawa, S., Nagata, T., et al., 2005. Microtubule-dependent microtubule nucleation based on recruitment of gamma-tubulin in higher plants. *Nat. Cell Biol.* 7, 961–968.
- Nakajima, K., Kawamura, T., Hashimoto, T., 2006. Role of the SPIRAL1 gene family in anisotropic growth of *Arabidopsis thaliana*. *Plant Cell Physiol.* 47, 513–522.
- Nakamura, M., Hashimoto, T., 2009. A mutation in the *Arabidopsis* gamma-tubulin-containing complex causes helical growth and abnormal microtubule branching. *J. Cell Sci.* 122, 2208–2217.
- Nakamura, M., Ehrhardt, D.W., Hashimoto, T., 2010. Microtubule and katanin-dependent dynamics of microtubule nucleation complexes in the acentrosomal *Arabidopsis* cortical array. *Nat. Cell Biol.* 12, 1064–1070.
- Neville, A.C., Levy, S., 1984. Helicoidal orientation of cellulose microfibrils in *Nitella opaca* internode cells: ultrastructure and computed theoretical effects of strain reorientation during wall growth. *Planta* 162, 370–384.
- Neville, A.C., Gubb, D.C., Crawford, R.M., 1976. A new model for cellulose architecture in some plant cell walls. *Protoplasma* 90, 307–317.
- Oda, Y., Iida, Y., Kondo, Y., Fukuda, H., 2010. Wood cell-wall structure requires local 2D-microtubule disassembly by a novel plasma membrane-anchored protein. *Curr. Biol.* 20, 1197–1202.
- Paolillo, D.J., 2000. Axis elongation can occur with net longitudinal orientation of wall microfibrils. *New Phytol.* 145, 449–455.
- Paredes, A.R., Somerville, C.R., Ehrhardt, D.W., 2006. Visualization of cellulose synthase demonstrates functional association with microtubules. *Science* 312, 1491–1495.
- Pelletier, S., Van Orden, J., Wolf, S., Vissenberg, K., Delacourt, J., Ndong, Y.A., et al., 2010. A role for pectin de-methylesterification in a developmentally regulated growth acceleration in dark-grown *Arabidopsis* hypocotyls. *New Phytol.* 188, 726–739.
- Perrin, R.M., Wang, Y., Yuen, C.Y., Will, J., Masson, P.H., 2007. WVD2 is a novel microtubule-associated protein in *Arabidopsis thaliana*. *Plant J.* 49, 961–971.
- Pesquet, E., Korolev, A.V., Calder, G., Lloyd, C.W., 2010. The microtubule-associated protein AtMAP70-5 regulates secondary wall patterning in *Arabidopsis* wood cells. *Curr Biol.* 20, 744–749.

- Peters, W.S., Tomos, A.D., 2000. The mechanic state of "inner tissue" in the growing zone of sunflower hypocotyls and the regulation of its growth rate following excision. *Plant Physiol.* 123, 605–612.
- Preston, R.D., 1982. The case for multinet growth in growing walls of plant cells. *Planta* 155, 356–363.
- Refregier, G., Pelletier, S., Jaillard, D., Hofte, H., 2004. Interaction between wall deposition and cell elongation in dark-grown hypocotyl cells in *Arabidopsis*. *Plant Physiol.* 135, 959–968.
- Reichelt, S., Knight, A.E., Hodge, T.P., Baluska, F., Samaj, J., Volkmann, D., et al., 1999. Characterization of the unconventional myosin VIII in plant cells and its localization at the post-cytokinetic cell wall. *Plant J.* 19, 555–567.
- Reis, D., Mosiniak, M., Vian, B., Roland, J.-C., 1982. Cell walls and cell shape. Changes in texture correlated with ethylene-induced swelling. *Ann. Des Sci. Nat. Bot. Paris* 4, 115–133.
- Roberts, I.N., Lloyd, C.W., Roberts, K., 1985. Ethylene-induced microtubule reorientations: mediation by helical arrays. *Planta* 164, 439–447.
- Roelofsen, P.A., 1950. Cell-wall structure in the growth-zone of *Phycomyces* sporangiophores. 1. Model experiments and microscopical observations. *Biochim. Biophys. Acta* 6, 340–356.
- Roelofsen, P.A., 1958. Cell-wall structure as related to surface growth. Some supplementary remarks multinet growth. *Acta. Bot. Neerl.* 7, 77–89.
- Roelofsen, P.A., Houwink, A.L., 1951. Cell wall structure of staminal hairs of *Tradescantia virginica* and its relation with growth. *Protoplasma* 40, 1–22.
- Roelofsen, P.A., Houwink, A.L., 1953. Architecture and growth of the primary cell wall in some plant hairs and *Phycomyces* sporangiophores. *Acta Bot. Neerl.* 2, 218–225.
- Roland, J.C., Vian, B., Reis, D., 1975. Observations with cytochemistry and ultracytometry on the fine structure of the expanding walls in actively elongating plant cells. *J. Cell Sci.* 19, 239–259.
- Roland, J.-C., Vian, B., Reis, D., 1977. Further observations on cell wall morphogenesis and polysaccharide arrangement during plant growth. *Protoplasma* 91, 125–141.
- Roland, J.-C., Reis, D., Mosiniak, M., Vian, B., 1982. Cell wall texture along the growth gradient of the mung bean hypocotyl: ordered assembly and dissipative processes. *J. Cell Sci.* 56, 303–318.
- Roland, J.-C., Reis, D., Vian, B., 1992. Liquid crystal order and turbulence in planar twist of the growing plant cell walls. *Tissue Cell* 24, 335–345.
- Sargent, C., 1978. Differentiation of the crossed-fibrillar outer epidermal wall during extension growth in *Hordeum vulgare* L. *Protoplasma* 95, 309–320.
- Satiat-Jeuemaitre, B., 1984. Experimental modifications of the twisting and rhythmic pattern in the cell walls of maize coleoptiles. *Biol. Cell* 51, 373–380.
- Satiat-Jeuemaitre, B., Martin, B., Hawes, C., 1992. Plant cell wall architecture. *Protoplasma* 167, 33–42.
- Sawano, M., Shimmen, T., Sonobe, S., 2000. Possible involvement of 65 kDcans MAP in elongation growth of azuki bean epicotyls. *Plant Cell Physiol.* 41, 968–976.
- Schopfer, P., 2006. Biomechanics of plant growth. *Am. J. Bot.* 93, 1415–1425.
- Sedbrook, J.C., Ehrhardt, D.W., Fisher, S.E., Scheible, W.R., Somerville, C.R., 2004. The *Arabidopsis* sku6/spiral1 gene encodes a plus end-localized microtubule-interacting protein involved in directional cell expansion. *Plant Cell* 16, 1506–1520.
- Setterfield, G., Bayley, S.T., 1958. Arrangement of cellulose microfibrils in walls of elongating parenchyma cells. *J. Biophys. Biochem. Cytol.* 4, 377–382.
- Shaw, S.L., Lucas, J., 2011. Intrabundle microtubule dynamics in the *Arabidopsis* cortical array. *Cytoskeleton (Hoboken)*. 68, 56–67.

- Shaw, S.L., Kamyar, R., Ehrhardt, D.W., 2003. Sustained microtubule treadmilling in *Arabidopsis* cortical arrays. *Science* 300, 1715–1718.
- Shibaoka, H., 1994. Plant hormone-induced changes in the orientation of cortical microtubules. *Ann. Rev. Plant Physiol. Plant Mol. Biol.* 45, 527–544.
- Shoji, T., Narita, N.N., Hayashi, K., Asada, J., Hamada, T., Sonobe, S., et al., 2004. Plant-specific microtubule-associated protein SPIRAL2 is required for anisotropic growth in *Arabidopsis*. *Plant Physiol.* 136, 3933–3944.
- Smertenko, A.P., Chang, H.Y., Wagner, V., Kaloriti, D., Fenyk, S., Sonobe, S., et al., 2004. The *Arabidopsis* microtubule-associated protein AtMAP65-1: molecular analysis of its microtubule bundling activity. *Plant Cell* 16, 2035–2047.
- Soga, K., Kotake, T., Wakabayashi, K., Kamisaka, S., Hoson, T., 2009. The transcript level of katanin gene is increased transiently in response to changes in gravitational conditions in azuki bean epicotyls. *Biol. Sci. Space* 23, 23–28.
- Sugimoto, K., Williamson, R.E., Wasteneys, G.O., 2000. New techniques enable comparative analysis of microtubule orientation, wall texture, and growth rate in intact roots of *Arabidopsis*. *Plant Physiol.* 124, 1493–1506.
- Sugimoto, K., Himmelspach, R., Williamson, R.E., Wasteneys, G.O., 2003. Mutation or drug-dependent microtubule disruption causes radial swelling without altering parallel cellulose microfibril deposition in *Arabidopsis* root cells. *Plant Cell* 15, 1414–1429.
- Sunohara, H., Kawai, T., Shimizu-Sato, S., Sato, Y., Sato, K., Kitano, H., 2009. A dominant mutation of TWISTED DWARF 1 encoding an alpha-tubulin protein causes severe dwarfism and right helical growth in rice. *Genes Genet. Syst.* 84, 209–218.
- Takeda, K., Shibaoka, H., 1981. Effects of gibberellin and colchicine on microfibril arrangement in epidermal cell walls of *Vigna angularis* Ohwi et Ohashi epicotyls. *Planta* 151, 393–398.
- Takesue, K., Shibaoka, H., 1998. The cyclic reorientation of cortical microtubules in epidermal cells of azuki bean epicotyls: the role of actin filaments in the progression of the cycle. *Planta* 205, 539–546.
- Thitamadee, S., Tsuchihara, K., Hashimoto, T., 2002. Microtubule basis for left-handed helical growth in *Arabidopsis*. *Nature* 417, 193–196.
- Twell, D., Park, S.K., Hawkins, T.J., Schubert, D., Schmidt, R., Smertenko, A., et al., 2002. MOR1/GEM1 has an essential role in the plant-specific cytokinetic phragmoplast. *Nat. Cell Biol.* 4, 711–714.
- Van Iterson, G., 1937. A few observations on the hairs of the stamens of *Tradescantia virginica*. *Protoplasma* 27, 190–211.
- Vian, B., Roland, J.-C., 1987. The helicoidal cell wall as a time register. *New Phytol.* 105, 345–357.
- Vian, B., Mosiniak, M., Reis, D., Roland, J.-C., 1982. Dissipative process and experimental retraction of the twisting in the growing plant cell wall. Effect of ethylene-generating agent and colchicine: a morphogenetic reevaluation. *Biol. Cell.* 46, 301–310.
- Wardrop, A.B., Wolters-Arts, M., Sassen, M.M.A., 1979. Changes in microfibril orientation in the walls of elongating plant cells. *Acta. Bot. Neerl.* 28, 313–333.
- Wasteneys, G.O., 2002. Microtubule organization in the green kingdom: chaos or self-order? *J. Cell Sci.* 115, 1345–1354.
- Wasteneys, G.O., 2004. Progress in understanding the role of microtubules in plant cells. *Curr. Opin. Plant Biol.* 7, 651–660.
- Wasteneys, G.O., Williamson, R.E., 1989. Reassembly of microtubules in *Nitella tasmanica*: quantitative analysis of assembly and orientation. *Eur. J. Cell Biol.* 50, 76–83.
- Whittington, A.T., Vugrek, O., Wei, K.J., Hasenbein, N.G., Sugimoto, K., Rashbrooke, M.C., et al., 2001. MOR1 is essential for organizing cortical microtubules in plants. *Nature* 411, 610–613.

- Wiedemeier, A.M., Judy-March, J.E., Hocart, C.H., Wasteneys, G.O., Williamson, R.E., Baskin, T.I., 2002. Mutant alleles of *Arabidopsis* *RADIALLY SWOLLEN 4* and *7* reduce growth anisotropy without altering the transverse orientation of cortical microtubules or cellulose microfibrils. *Development* 129, 4821–4830.
- Wightman, R., Turner, S.R., 2007. Severing at sites of microtubule crossover contributes to microtubule alignment in cortical arrays. *Plant J.* 52, 742–751.
- Wu, S., Scheible, W.R., Schindelasch, D., Van Den Daele, H., De Veylder, L., Baskin, T.I., 2010. A conditional mutation in *Arabidopsis thaliana* separase induces chromosome non-disjunction, aberrant morphogenesis and cyclin B1;1 stability. *Development* 137, 953–961.
- Yao, M., Wakamatsu, Y., Itoh, T.J., Shoji, T., Hashimoto, T., 2008. *Arabidopsis* *SPIRAL2* promotes uninterrupted microtubule growth by suppressing the pause state of microtubule dynamics. *J. Cell Sci.* 121, 2372–2381.
- Yuan, M., Shaw, P.J., Warn, R.M., Lloyd, C.W., 1994. Dynamic reorientation of cortical microtubules, from transverse to longitudinal, in living plant cells. *Proc. Natl. Acad. Sci. USA* 91, 6050–6053.
- Yuan, M., Warn, R.M., Shaw, P.J., Lloyd, C.W., 1995. Dynamic microtubules under the radial and outer tangential walls of microinjected pea epidermal cells observed by computer reconstruction. *Plant J.* 7, 17–23.
- Zandomeni, K., Schopfer, P., 1993. Reorientation of microtubules at the outer epidermal wall of maize coleoptiles by phytochrome, blue-light photoreceptor, and auxin. *Protoplasma* 173, 103–112.

This page intentionally left blank

# Index

## A

- Acute myeloid leukemia (AML), 113, 269
- Adherens junctions, vinculin
  - cadherin–adhesion complex
    - $\beta$ -catenin dynamics, 215
    - cell–cell junctions, 214–215
    - epithelial morphology, 215–216
    - recruitment to adhesion sites, 218–219
    - roles, 216–217
- Afadin
  - adherens junctions formation, 116
  - knockout, 116–117
  - nectin-and F-actin formation, 115
  - tyrosine phosphatase SHP-2, 115
- AML. *See* Acute myeloid leukemia
- AMP-activated protein kinase (AMPK)
  - canonical phosphorylation, 48
  - cellular stresses, 66
  - hyperosmolar stress, 59
  - placental lactogen 1 (PL1) promoter, 50
- AMPK. *See* AMP-activated protein kinase
- Anterior horn cells (AHC), 271
- AQP4-based orthogonal arrays
  - agrin and blood–brain barrier
    - cell culture experiments, 23
    - interface, neuroglial *vs.* vascular compartment, 22
    - perfusion parameters, 21
    - perivascular basal lamina, 22
  - and brain tumor, 26–27
  - dystrophin–dystroglycan complex, 24
  - and inflammation, 27–28
  - inside central nervous system
    - in vitro* mammalian astrocytes, 17–20
    - in vivo* mammalian astrocytes, 13–17
  - loss of polarity, 20–21
  - outside central nervous system
    - cochlear duct, 12
    - rat ciliary epithelium, 11
    - skeletal muscle cells, 8–9
    - tracheal epithelium cells, 9–11
    - urinary system, 9
- properties
  - BBB, 7–8
  - CHO cells, 3–4
  - freeze–fracture replica, 4
  - M1 and M23 isoform, 5
  - membrane topology, 6

- palmitoylation, 6–7
- quantum dot single particle tracking, 5
- tetrameric protein complex formation, 4
- water flux in brain, 25–26

## B

- BBB. *See* Blood–brain barrier
- Biological functions, vinculin
  - apoptosis modulation, 209
  - bacterial entry regulation
    - dephosphorylation, 211
    - host–cell cytoplasm, 209
    - intercellular signal transduction pathways, 210–211
  - IpaA binding, 210
  - phagocytic cup formation, 209–210
- cell adhesion and migration
  - description, 201
  - extracellular matrix and actin cytoskeleton, 205–209
  - force transmission, 204–205
  - integrin clustering, 202–204
  - strength, 204
- Blood–brain barrier (BBB)
  - astrocytes, 22
  - dystrophin, 7–8
  - integrin, 22–23
  - leukocyte entry, 27

## C

- Cell adhesion molecules
  - afadin, 115–117
  - nectins, 112–115
- Cell–cell and cell–matrix adhesion
  - cardiac myocyte function, 221
  - components, 219
  - description, 219–220
  - embryonic development, 220
  - mechanical transduction system, 221
  - role, heart function, 220
- Cell movement
  - behaviors, 99
  - leading edge structures
    - adhesions, focal, 105–106
    - cellular traction, 100
    - filopodia, 101–103
    - focal complexes, 104–105

- Cell movement (*cont.*)  
 lamellipodia, 103–104  
 membrane ruffles, 104  
 Rho family, 100–101  
 WASP, 101  
 motile responses, 99  
 random, chemokinesis, 100  
 types  
 chemokinesis, 100  
 chemotaxis, 100  
 haptotaxis, 100
- Chemokinesis  
 cell movement, 98–99  
 definition, 100
- Chemotaxis  
 cell movement, 100  
 PI3-kinase signaling pathway, 123  
 polarity, cell, 123  
 vascular endothelial cells, 110
- D**
- Directional cell migration  
 cell–ECM adhesion  
 immature, 99  
 mature, 99  
 cell motility, 98  
 cell movement  
 fundamental behaviors, 99  
 leading edge structures, 100–106  
 motile responses, 99  
 types, 100  
 cells sense and responses, 98  
 cellular events, 99  
 growth factor receptors and integrins  
 adhesive interactions, 119  
 integrated cellular response, 119–120  
 Necl-5 role, 120–122  
 molecular mechanisms, 129  
 nectins, Necls and afadin  
 cell adhesion molecules, 111  
 cellular functions, 111  
 related molecules, 112–117  
 roles, 117–119  
 regulation  
 afadin, 124–125  
 cell polarity proteins, 123–124  
 mechanisms, 129  
 Necl-5 and microtubules, 125  
 PI3-kinase, 123  
 Rho family, 99  
 small G proteins and leading edge structures  
 act as biotimers, 106  
 Cdc42, 109  
 cyclical activation and inactivation,  
 125–128  
 GDIs, 106–107  
 monomeric proteins, 106  
 Rac, 108–109  
 Rap, 109–111  
 Rho, 107–108
- E**
- Embryonic stem cells (ESCs)  
 polycomb, 79  
 SAPK/JNK, 80  
 SCNT and iPS cells, 61  
 stem cell accumulation rates, 50  
 stress response, 57
- Extracellular matrix (ECM) and actin  
 cytoskeleton  
 Arp2/3 complex, 208–209  
 vinculin–actin interaction  
 actin-associated adhesions, 207–208  
 actin-bundling protein, 206  
 DNA technology, 207  
 vinculin to mechanical stimuli  
 crystal and NMR structures, 206  
 talin, 205–206
- F**
- Fungi, RNA import  
*Harpochytrium*, 161  
 lack tRNA genes, 161  
 nuclear-encoded, *Saccharomyces cerevisiae*  
 selectivity, tRNA<sup>Lys</sup>, 163–164  
 targeting and translocation, 164–166  
 tRK1 function, 162–163  
*Spizellomyces punctatus*, 161
- G**
- GDP dissociation inhibitors (GDIs)  
 hydrophobic pocket, 107  
 small G proteins, 106
- GTP hydrolysis  
 CAS–imp $\alpha$ –RanGTP complex, 262  
 GAP-assisted, 262  
 imp $\beta$ –RanGTP complex, 261–262  
 Leu-rich repeats (LRR), 260  
 Nup358–RanGAP complex, 261  
 RanBP1, 261
- H**
- Haptotaxis movement, 100
- I**
- Importin– $\alpha$   
 Arm repeat, 244  
 banana-like shape, 242, 244  
 defined, 240  
 NLSs, 242  
 structure, 239
- Importin– $\beta$   
 binding (IBB) domain

- autoinhibitory characteristics, 245
  - basic L-shaped structure, 243–244
  - Cse1p HEAT 2–4, 255
  - Nup50, 254
  - roles, 247
  - structure, 245
  - cargo sizes and shapes, 243
  - defined, 240
  - 95-kD $\alpha$  flexible super-helix, 242
  - S-shaped open conformation, 242
  - structure, 239
- Integrins**
  - activation, 110
  - clustering
    - cell–matrix adhesions, 202
    - molecular mechanisms, 202
    - vinculin, 202–204
  - cytoplasmic tails, 201
  - focal complexes, 105
  - growth factor receptors
    - adhesive interactions, 119
    - integrated cellular response, 119–120
    - Necl-5 role, 120–122
  - interaction, 117
  - signals, 108
- J**
- JunC terminal kinase (JNK)
  - ESC, 80
  - polycomb loss and stem cells, 79
- M**
- Macromolecule import, natural mechanisms to
  - potential application
  - cell viability, 173
  - DNA
    - antisense DNA sequences import, 176–177
    - DQAsomes, 177–178
    - transcription, *in vitro*, 178
    - translation, exogenous genes, 178–179
  - mitochondrial biogenesis, 173
  - protein
    - coding gene mutation, 173
    - mRNA translation, 175
    - mutated DNA accumulation, 176
    - nuclear transgene expression, 175
    - nucleic acids import techniques, 174
    - organellar genomes maintenance, 176
    - respiratory chain function, 175–176
  - RNA
    - disorders, 179
    - human PNPASE, 180
    - Leishmania*, 180
    - MERRF syndrome, 179–180
    - mRNAs electroporation, 180
    - tRNA structure, 180
- Mammalian astrocytes
  - in vitro*
    - absence, basal lamina, 18–19
    - morphological difference, 17–18
    - stability, 19–20
  - in vivo*
    - extracellular matrix, 13
    - freeze-fracture replica, 14
    - macroglial cells, 16
    - OAP appearance, 14–15
    - occurrence in different tissues, 17
    - retinal Müller cells, 13–14
- Mammalian embryos and stem cells
  - analysis, 80
  - cyclic nature, 80
  - diagnosing stress, 47
  - flexible and inflexible stem cells, 81
  - IVF/ART, 82
  - kinetics and substrate enzyme, 81
  - low and high dose stress, 82
  - optimized embryo media, 82
  - prioritized and compensatory differentiation, 81
  - protein kinases, 47
  - strategies key aspects, 80
  - strategy and molecular mechanisms, 47
  - stress and enzymes
    - contradictory signals, 61–64
    - definition, 47–51
    - developmental effects, 70–71
    - homeostatic set points, 64
    - IVF/ART, 67–70
    - kinetics responses, 66–67
    - maladaptive responses, 65–66
    - null mutants, developmental events
  - stress models and lessons
    - enzymes and epigenetic memory, 79–80
    - “idling car” hypothesis, 72–73
    - mechanisms, 78–79
    - organismal survival mechanisms, 77–78
    - preimplantation embryo model, 74–77
    - proliferative stem cells, 73–74
  - stress responses
    - cellular and essential events, 52–53
    - dose-dependence, 53–58
    - pluripotent stem cells, 60–61
    - time dependence, 58–60
  - stress stimuli, 80
  - testing, 80
- Metazoa
  - mammalian, 5S rRNA
    - cytosolic role, 167
    - detection, 166–167
    - in vivo*, 167–168
    - regulation, PNPASE, 170
    - rhodanese identification, 168
    - secondary structure, 168
    - systematic model, 169
    - trafficking, 169–170



- Metazoa (*cont.*)  
 miRNA, 172–173  
 RNase MRP and RNase P  
   H1 RNA, 170  
   *in vitro* assays, 172  
   PNPASE depletion, 171–172  
   proposal, 171  
   proteome analysis, 170–171  
   single protein (PRORP1), 171  
 5S rRNA import mechanism, 167–170  
 tRNAs import, 166
- MGH. *See* Multinet growth hypothesis
- Microtubules  
 alignment and twisted growth  
   cell morphology, 304  
   cell-to-cell variation, 304  
   helical growth mutants, 305  
   microtubule-associated protein mutant, 305  
 arrays  
   *Datura* epidermal cells, 299  
   endogenous cycles, 300  
   hormonal signals, 299–300  
   hypocotyl epidermal cells, 298  
   microinjection studies, 298  
   stabilizing taxol, 299  
 circumferential hoops, 300  
 dynamic  
   animal, instability, 295  
   dynein-based sliding, 294  
   elongated carrot suspension cells, 294  
   gravity-induced reorientation, 295  
   outer epidermal cell wall, 295–296  
   physiological cycling, 296  
 hoops  
   multinet growth hypothesis, 290–291  
   ordered fibril hypothesis, 291–293  
   tubular cells, 290  
   wall texture, self-assembly models,  
     293–294  
 interaction  
   *Arabidopsis* hypocotyls, 297–298  
   plus-end directed motors, 297  
    $\gamma$ -tubulin complex proteins, 296  
 and microfibril coalignment  
   cellulose synthase track rotation, 307–308  
   cellulose-synthesizing particles, 306,  
     308–309  
   cholesteric liquid crystals, 308  
   crossed-polylamellate texture, 307  
   growth mutants, 309–311  
   non-elongating secondary cell walls,  
     311–314  
   self-assembling wall, 306  
 roots and shoots  
   nontransverse alignments, 301  
   paradigmatic organ, 300  
   predictable realignment, 301  
   response to illumination, 302
- Mitochondrial RNA import  
 classical mitochondria, 146  
 cytosolic RNAs, 148  
 developments, 148  
 fungi, *Saccharomyces cerevisiae*  
   tRK1 function, 162–163  
   tRK1 targeting and translocation steps,  
     164–166  
   tRNA<sup>Gln</sup>, 162  
   tRNA<sup>Lys</sup>, 163–164  
 macromolecule and potential applications  
   DNA, 176–179  
   protein, 173–176  
   RNA, 179–180  
 metazoa  
   human, RNase MRP and RNase P, 170–172  
   mammalian, 5S rRNA, 166–170  
   miRNA, 172–173  
   tRNA, 166  
 mitochondria, 146–147  
 plants  
   evolutionary aspects and translation,  
     157–158  
   tRNA mechanism, 158–161  
   tRNA population determination, 156–157  
 proto-mitochondria, 147  
 protozoa  
   extent of process, 150–152  
   import tRNAs, 149  
   tRNA mechanisms, 152–155  
   tRNA characterizing, 147–148
- Multinet growth hypothesis (MGH)  
 cellulose microfibrils, 289–290  
 and hoop reinforcement, 289–290  
 passive realignment model, 289
- N**
- Nectins  
 independent immunoglobulin, 112  
 members, 112  
 molecules  
   members, 114  
   roles, 114–115  
   structure, 114  
 mutations, 113  
 splicing variants, 112  
 Tactile/CD96 and DNAM-1/CD226,  
 112–113
- NPCs. *See* Nuclear pore complexes
- NTF2. *See* Nuclear transport factor2
- Nuclear export sequences (NESs)  
 alignment studies, 242  
 exportin–RanGTP complexes, 267  
 importins and exportins, 241
- Nuclear localization sequences (NLSs)  
 binding sites, 249  
 detachment, 253

- imp $\alpha$  bond strength, 253
  - imp $\alpha$ –imp $\beta$  complex formation
    - autoinhibitory activity, 245–246
    - H3  $\alpha$ -helices, 245
    - IBB domain, 243–245
  - imp $\beta$ , 242
  - importins and exportins bind, 241
  - types, 241
  - Nuclear pore complexes (NPCs)
    - autoimmune diseases, 270
    - cancer diseases
      - hematological malignancies, 269
      - imp $\alpha$  structural defects, 268
      - karyopherins, 269
      - protein decoder genes, 267
      - transport receptors, 268
    - cardiac disease, 272
    - cargo complex across the channel
      - FG domains and transporters, 248
      - FG-Nups, 247
      - impb–Nup bond, 248
      - transporter binding sites, 249
      - types, transport process, 248
    - cargo complex association
      - importin  $\alpha$ , 242–243
      - importin  $\beta$ , 242
      - NLS–imp $\alpha$ –imp $\beta$  complex formation, 243–247
    - cargo complex dissociation
      - interactions, 251–254
      - Nup50, 249–250
      - Ran, 250–251
    - imp $\alpha$  and imp $\beta$  defined, 240–241
    - infectious diseases
      - viruses with DNA genome, 272–273
      - viruses with RNA genome, 273–275
    - $\beta$  karyopherin family
      - characteristics, 241
      - defined, 240
    - karyopherin recycling
      - CAS, 256
      - Cse1p–kap60p–RanGTP complex, 254–255
      - HEAT repeat, 257
      - molecular dynamics (MD) simulations, 256
      - RanGTP amino acids, 256
      - RanGTP–CAS complex forms, 258
    - nervous system diseases
      - ALADIN protein, 271
      - anterior horn cells (AHC), 271
      - cell-type-specific mechanisms, 271
      - RanBP2, 270
      - triple A syndrome, 270–271
    - nucleocytoplasmic transport pathway
      - CAS–imp $\alpha$ –RanGTP complex, 266–267
      - exportin–RanGTP complexes, 267
      - imp $\alpha$ /imp $\beta$  complex, 265
      - RanGAP and RanBP1, 265–266
  - Ran cycle
    - GTP hydrolysis, 260–262
    - Nuclear transport factor2 (NTF2), 262–263
    - nucleocytoplasmic pathway components, 258
    - nucleotide exchange, 263–265
    - RanBD–RanGTP–impb complex, 259–260
    - RanBP1–RanGTP–RanGAP complex, 259
    - RanGAP and RanGEF, 258–259
  - Nuclear transport factor2 (NTF2)
    - eukaryotes, 262
    - homodimer molecules, 262–263
    - symmetric hydrophobic binding sites, 263
- O**
- Orthogonal arrays of intramembranous particles (OAPs). *See* AQP4-based orthogonal arrays
- P**
- Plant cell walls
    - microtubule hoops
      - fibril hypothesis, 291–293
      - multinet growth hypothesis, 290–291
      - self-assembly models, texture, 293–294
    - microtubules
      - alignment and twisted growth, 304–306
      - arrays, 298–300
      - circumferential hoops, 300
      - dynamic, 294–296
      - and microfibril coalignment, 306–314
      - microtubule interaction, 296–298
      - roots and shoots, 300–302
    - multinet–growth hypothesis and hoop reinforcement, 289–290
    - new dynamic model
      - biophysical forces, 321
      - cross-sectioned fibrils alignment, 320
      - fibril alignment, 319
      - nascent cellulose microfibrils, 320–321
      - polymerization and depolymerization, 320
    - paradoxical outer epidermal wall
      - helicoidal structure, 303
      - oblique alignments, 303
      - shoot epidermis, 304
      - sunflower epidermal cells, 304
      - transverse hoop reinforcement, 302
    - reinterpreting wall patterns
      - experimental changes, 315–316
      - fibril and passive realignment models, 318–319
      - growth-induced changes, 316–318
      - layers, steps, 314–315
      - self-assembly principles, 288
  - Polypyrimidine tract-binding protein (PTB)
    - mRNAs delivery, 213

## Polypyrimidine tract-binding protein (PTB)

*(cont.)*

- raver1 pathways, 214
- vinculin, 212

## Protozoa

- bioinformatic analysis, 149
- cytosolic tRNAs delivery, 149
- imported tRNAs, 149
- selection and process extension
  - steady-state level, 152
  - Tetrahymena brucei* mitochondria, 150–151
  - tRNA classification, 151–152
  - tRNA<sup>Gln</sup>, 150
  - tRNA<sup>Trp</sup>, *Leishmania tarentolae*, 151
- tRNAs import mechanism
  - aminoacylated import, 154
  - pretreatment, 155
  - protein import controversial data, 152–153
  - RIC subunits, 155
  - schematic model, 154
  - surface targeting, 155
  - targeting and translocation, 153
  - tRNA<sup>Gln</sup>, 153
  - tRNA<sup>Lys</sup>, 155
  - tRNA<sup>Meti</sup> and tRNA<sup>Sec</sup>, 153

PTB. *See* Polypyrimidine tract-binding protein**R**

## Ran cycle

- GTP hydrolysis
  - CAS–imp $\alpha$ –RanGTP complex, 262
  - GAP-assisted, 262
  - imp $\beta$ –RanGTP complex, 261–262
  - Leu-rich repeats (LRR), 260
  - Nup358–RanGAP complex, 261
  - RanBP1, 261
- NTF2
  - eukaryotes, 262
  - homodimer molecules, 262–263
  - symmetric hydrophobic binding sites, 263
- nucleocytoplasmic pathway components, 258
- nucleotide exchange, 263–265
- RanBD–RanGTP–imp $\beta$  complex, 259–260
- RanBP1–RanGTP–RanGAP complex, 259
- RanGAP and RanGEF, 258–259

## Regulation modes, vinculin

- expression
  - conformational changes and
    - posttranslational modification, 212
  - mRNA translation, 213
  - PTB, 214
  - raver1–RNA complex, 211
- tyrosine phosphorylation
  - head–tail interactions, 212
  - Src tyrosine kinase, 211
  - Y100 and Y1065 inhibit cell spreading, 211–212

**S**

- SAPK. *See* Stress-activated protein kinase
- Sargent's model, 319
- Small G proteins and leading edge structures
  - act as biotimers, 106
  - afadin role, 118–119
  - GDI, 106–107
  - GDP exchange, 106
  - nectins and Necl5 cell movement, 117–118
  - nonomeric, 106
  - Rho family
    - actin reorganization and cell movement, 108
    - Cdc42, 109
    - Rac, 108–109
    - Rap, 109–111
    - regulate actin cytoskeleton, 107–108
    - ROCK I isoform, 108
- Stress-activated protein kinase (SAPK)
  - activation, 65
  - AMP/ATP levels, 49
  - catalytic subunits, 48
  - cell cycle, 55
  - contradictory signals, 61
  - embryonic development, 69
  - FGF4 signaling, 62
  - inhibitors, 69–70
  - levels, 62–63
  - mitochondrial activity, 50
- Stress and enzymes
  - contradictory signals and stem cells detection
    - implanting conceptus, 62–63
    - IVF embryo culture, 64
    - milieu, 61
    - Normoxia stem cells, 63
    - optimal culture conditions, 63–64
    - SAPK activation, 62
    - signals removal, 62
    - TSC isolation, 61–62
  - definition
    - activation, 50
    - cellular stress and effects, 47
    - characteristics and actions, 48
    - classes, 48
    - interactive and functions, 49–50
    - null mutants, developmental events, 51–52
    - protein kinases, 47–48
    - role, 48–49
    - transcription factors review, 50–51
  - developmental effects, 70–71
  - homeostatic set points, 64
  - IVF/ART, 67–70
  - kinetics responses, 66–67
  - maladaptive responses, 65–66
- Stress models and lessons
  - "idling car" hypothesis, 72–73
  - mechanisms, 78–79
  - organismal survival mechanisms, 77–78

- preimplantation embryo model, 74–77
  - proliferative stem cells, 73–74
  - stress enzymes and epigenetic memory, 79–80
  - Stress responses
    - activity, 59
    - cellular and essential events, 52–53
    - dose-dependence
      - effects, 54
      - high doses stress induce, 55
      - low-zone stress, 53
      - nil–low stress threshold, 55–56
      - Serum deprivation, 56
      - threshold conversion, 56
      - TSC and ESC, 57–58
    - mediate compensatory differentiation, 59
    - pluripotent stem cells, 60–61
    - time dependence
      - activity, 59
      - in adults, 60
      - global mRNA, 58
      - kinetics compensatory differentiation, 58
      - mediate compensatory differentiation, 59–60
- T**
- tRNA mechanism
    - membrane identification, 158–159
    - mutant tRNA, 159–161
    - selectivity process, *in vivo*, 159
    - sequence exchanges, 161
    - steady-state level, 161
    - tranlocase outer membrane, 159
  - Trophoblast stem cells (TSC)
    - accumulation rates, 50
    - blastocyst, 55
    - endocrine hormones, 59–60
    - Hand1 upregulation, 67
    - Id2 protein loss, 57
    - kinetic response, 83
    - lineage determination and differentiation, 65
    - mRNA stress response, 58
    - pluripotency, 61–62, 65–66
  - TSC. *See* Trophoblast stem cells

**V**

- Vinculin
  - activation
    - combinatorial, 198–199
    - in vivo*, 200–201
    - by IpaA, 200
    - by single ligand, 199–200
  - autoinhibited conformation, 196–198
  - biological functions
    - apoptosis modulation, 209
    - bacterial entry regulation, 209–211
    - cell adhesion and migration, 201–209
  - cell–cell and cell–matrix adhesion
    - cardiac myocyte function, 221
    - components, 219
    - description, 219–220
    - embryonic development, 220
    - mechanical transduction system, 221
    - role, heart function, 220
  - description, 192–193
  - regulation modes
    - expression, 212–214
    - tyrosine phosphorylation, 211–212
  - structure
    - description, 193
    - head domain, 195
    - helical bundles, 193–194
    - proline-rich linker, 196
    - tail domain, 196
    - types, 193
  - themes and concepts
    - in adherens junctions, 214–217
    - adhesion sites, 218–219

**W**

- Wiskott–Aldrich syndrome protein (WASP)
  - Arp2/3 complex, 109
  - description, 101
  - subfamily, 102